Georgia Institute of Technology

School of Civil and Environmental Engineering

Structural Engineering, Mechanics and Materials
Research Report No. 02-5

Transfer and Development Length of High Strength Lightweight Concrete Precast Prestressed Bridge Girders

Task 5 Report

Prepared for

Office of Materials and Research
Georgia Department of Transportation

GDOT Research Project No. 2004

by

Karl F. Meyer, Lawrence F. Kahn
James S. Lai, and Kimberly E. Kurtis

June 2002

20020604 069

Contract Research
GDOT Research Project No. 2004

Behavior of High-Strength/High-Performance Lightweight Concrete
Prestressed Girders

Prepared for

Office of Materials and Research
Georgia Department of Transportation

by

Karl F. Meyer, Lawrence F. Kahn
James S. Lai, and Kimberly E. Kurtis

June 2002

EXECUTIVE SUMMARY

This report presents the findings of a study that developed and tested high-strength lightweight concrete (HSLC) mixes having strengths from 8,000 psi to 12,000 psi made using slate lightweight aggregate. Based on optimized mix designs, 6 pretensioned AASHTO Type II girders were constructed using 8,000 psi and 10,000 psi slate HSLC and were prestressed using 0.6-inch diameter LOLAX strands tensioned to 75% of strand ultimate stress. The strands received no special preparation prior to girder casting.

After initial curing for approximately 24 hours, transfer length measurements were taken from time of release until the beams reached an age of 14 days. The current AASHTO and ACI code provisions conservatively predicted transfer length for slate HSLC; modification of the current code specifications for transfer length was not necessary for slate HSLC.

A direct pullout test was performed on both concrete design strengths to determine the bond between the slate lightweight concrete and the prestressing strand. A somewhat lower bond stress developed between the prestressing strand and the lightweight concrete when compared to similar strengths of normal-weight concrete. However, the average pullout strength for both series exceeded the minimum required value for 0.6-inch diameter strand of 43.2 kips.

Tests were conducted on each girder end to determine development length characteristics. The distance from the girder end to the load point was varied from

between 70 and 100 percent of the AASHTO specified development length. Strand slip was measured on each test. The current AASHTO and ACI code provisions conservatively predicted development length for slate HSLC; modification of the current code specifications for development length was not necessary for slate HSLC.

Tests were conducted on the center span of each girder to examine shear characteristics of HSLC. The combined center span and girder end shear results showed the current AASHTO Standard specification provided a conservative prediction of concrete and ultimate shear capacity when shear steel capacity was capped at a yield strength of 60 ksi. The alternate design procedure listed in ACI-318 Section 11.4.2.2 for predicting concrete shear strength produced some unconservative predictions for concrete compressive strengths over 10,000 psi. The current AASHTO LRFD specification provided a conservative prediction of ultimate shear capacity for slate HSLC.

An evaluation of girder flexural behavior showed the current prediction of cracking stress and cracking moment, when examined for slate HSLC, showed indications of becoming unconservative as concrete compressive strengths approached 11,000 psi. The use of a lambda factor (λ) of 0.85 for slate HSLC produced conservative results on average for compressive strengths below 11,000 psi. The modulus of rupture test, ASTM C 78, did not accurately predict the cracking stress of HSLC girders. The current AASHTO procedure for ultimate moment calculation was conservative for slate HSLC girders with normal weight concrete decks having a compressive strength under 6,000 psi.

ACKNOWLEDGEMENTS

TABLE OF CONTENTS

vi

LIST OF TABLES

LIST OF FIGURES

xx

NOTATION

Report	ACI 318-99	AASHTO Standard	Description
A_c	--	--	Cross sectional area of composite girder (combined area of girder and deck)
A_{nc}	--	--	Cross sectional area of girder
AASHTO	--	--	American Association of State Highway and Transportation Officials
A_{ps}	A_{ps}	A_s*	Cross sectional area of prestressing strand
A_{pse}	--	--	Effective area of prestressed reinforcement adjusted inside the transfer or development length regions
BCL	--	--	Distance from bottom of girder to center line of bottom row of prestressing strands
CM	--	--	Cementitious Materials
CSS	--	--	Concrete Surface Strain
DAQ	--	--	Data Acquisition
d_b	d_b	D	Diameter of prestressing strand
DEMEC	--	--	Detachable Mechanical Strain Gage
d_p	d_p	d	Distance from compression fiber to centroid of prestressed reinforcement
E_c	E_c	E_c	Modulus of elasticity of concrete based on 6 x 12 cylinder
E_{ci}	--	--	Modulus of elasticity of concrete based on 6 x 12 cylinder at strand release
f_c'	f_c'	f_c'	Concrete compressive strength at specified time
f_{ci}'	f_{ci}'	f_{ci}'	Concrete compressive strength at strand release
f_r	f_r	f_r	Modulus of rupture of concrete
f_{pc}	f_{pc}	f_{pc}	Resultant compressive stress at the centroid of the composite section or at the junction of the web and flange when the centroid lies within the flange due to both prestress and moments resisted by the precast member acting alone.
f_{ps}	f_{ps}	$f_{su}*$	Stress in prestressed reinforcement at nominal strength of member
f_{pt}	--	--	Stress in prestressing strand just prior to strand release
f_{pu}	f_{pu}	f_s'	Specified tensile strength of prestressed reinforcement
f_{se}	f_{se}	f_{se}	Effective prestressing stress after losses
f_{si}	--	--	Stress in prestressing strand just after strand release
f_y	f_y	f_{sy}	Specified yield strength of non-prestressed reinforcement

Report	ACI 318-99	AASHTO Standard	Description
h	h	h	Overall depth of the composite girder
I_c	--	--	Moment of inertia of composite girder (girder and deck)
I_{nc}	--	--	Moment of inertia of girder
l_d	l_d	--	Development length of prestressing strand (In AASHTO Standard, l_d refers to non-prestressed reinforcement development length)
l_{fb}	--	--	Flexural bond length. Additional length over which the strand should be bonded so the stress f_{ps} may develop in the strand at the nominal strength of the member.
l_t	--	--	Transfer length of prestressing strand
LOLAX	--	--	Low relaxation loss prestressing strand
M_{DL}	--	--	Moment due to Dead Load
n	n	--	Modular Ratio
S_{top-nc}	--	--	Top section modulus for non-composite girder
S_{bot-nc}	--	--	Bottom section modulus of non-composite girder
S_{top-c}	--	--	Top section modulus for composite girder
S_{bot-c}	--	--	Bottom section modulus for composite girder
TCL	--	--	Distance from top of girder to center line of top row of prestressing strands
W/CM	--	--	Water to Cementitious Materials Ratio
V_c	V_c	V_c	Nominal shear strength provided by concrete
V_{ci}	V_{ci}	V_{ci}	Nominal shear strength provided by concrete when diagonal cracking results from combined shear and moment
V_{cw}	V_{cw}	V_{cw}	Nominal shear strength provided by concrete when diagonal cracking results from excessive principal tensile stress in the web
V_s	V_s	V_s	Nominal strength provided by shear reinforcing steel
VWSG	--	--	Vibrating Wire Strain Gage

CHAPTER I

INTRODUCTION

Advances in concrete quality and engineering practices have enabled the design and construction of precast prestressed concrete bridge girders that approach 200 feet in length. Problems occur when trying to move and erect these long and heavy girders. In order to facilitate easier road movement and erection, high-strength lightweight concrete (HSLC) can be used to reduce member self-weight while still allowing a large load carrying capacity.

Previous research conducted relating to lightweight concrete (LWC) used in prestressed applications involved concrete with compressive strengths less than 7,500 psi. While this research is important and in most cases relevant, it does not verify current design procedures for use on higher strength lightweight concretes. There appears to have been little to no research conducted focusing on the use of HSLC for the construction of pretensioned bridge girders despite the fact that current articles indicate a belief that its use would be very beneficial.[1]

Additional research efforts are necessary in many areas before engineers can safely and confidently use HSLC in the design of pretensioned bridge girders.

1.1 Definitions

Transfer length is defined as the distance required to transfer the effective prestressing force from the strand to the surrounding concrete. Development length is defined as the sum of the "transfer length" and the "flexural bond length." The flexural bond length is the additional length of pretensioning strand beyond the transfer length over which bond is developed to allow the strand to reach the stress level f_{ps} at the nominal flexural strength of the member. Development length can also be defined as the minimum distance from the end of the member beyond which the application of a point load will result in a flexural failure. Transfer length and development length are covered in detail in Chapters 9 and 13.

1.2 Research Objectives

The research objectives of this project were as follows:

1. To determine the transfer length, l_t, characteristics of 0.6-in prestressing strand used with slate HSLC.

2. To determine the development length, l_d, characteristics of 0.6-in prestressing strand used with slate HSLC.

3. To verify current code provisions for transfer and development length as appropriate for use with slate HSLC and to suggest more appropriate equations if necessary.

4. To determine the effect of shear reinforcement spacing on strand slip, development length, and shear capacity of pretensioned slate HSLC

5. To determine the shear strength, V_c, of pretensioned slate HSLC.

6. To verify current code provisions for shear strength of slate HSLC.

7. To verify the current code-specified reduction factor, λ, for sand lightweight concrete as related to concrete tensile strength, and suggest a more appropriate factor if necessary.

1.3 Need for Research

This research was necessary because girders constructed with slate HSLC with a strength approaching 12,000 psi and 0.6-in pretensioning strand had not been tested previously. The Georgia Department of Transportation wanted to use precast prestressed bridge girders with spans of 150 ft and with gross weights less than 150 kips. To achieve such designs, concrete with strengths of about 10,000 psi and unit weights less and 125 pcf would be required. Neither the concrete materials nor behavior of girders made with such material shad been investigated previously.

1.4 Analytical and Experimental Program

The analytical and experimental program involved the following six phases:

1. Analytically evaluate if HSLC bridge girders using 0.6-in diameter strand could achieve the 150 ft and 150 kip gross weight requirements.

2. Develop slate HSLC mix designs to meet objective strengths of 8,000, 10,000 and 12,000 psi under laboratory conditions.

3. Produce the laboratory-developed HSLC mix designs in a field environment at a commercial concrete plant.

4. Determine the mechanical properties of the slate HSLC.

3

5. Design, construct, and test six full-scale AASHTO Type II pretensioned girders using the slate HSLC to determine transfer and development length, shear, and flexural behavior characteristics.

6. Evaluate the girder behavior with respect to current design specifications.

1.5 Organization of Report

This report begins with a background review in Chapter II that covers the manufacture of slate lightweight aggregate, the use and field production of HSLC, HSLC short and long-term properties, the origins of transfer and development length, and shear behavior in pretensioned girders.

Chapters III through VII focus on HSLC as a material. Chapter III provides an analytical investigation to determine required HSLC properties to construct the objective pretensioned bridge girders. Chapter IV provides information on the components of HSLC, moisture control, mixing, and preparation and testing of specimens. Chapter V discusses the development of HSLC mix designs. Chapter VI discusses the field production of HSLC mix designs in a commercial concrete plant. Chapter VII covers the mechanical properties of HSLC as required for the evaluation. Chapters VIII through XIII focus on construction and testing of the six HSLC girders. Chapter VIII provides details on the design and construction of the AASHTO Type II girders. Chapter IX covers the determination of transfer length, evaluation of current code provisions, and the development of a new equation to predict transfer length. Chapter X addresses the procedures for test set-up and conduct of the test. Chapter XI provides flexural behavior results of the 18 girder

4

behavior results to include an evaluation of current code provisions. Chapter XIII covers development length test results, examines the effect of cracking in the transfer region, examines current code provisions, and suggests a new equation to predict development length.

Chapter XIV provides conclusions and recommendations based upon this research project.

CHAPTER II

BACKGROUND REVIEW

2.1 Introduction

Much research has been published on lightweight concrete, however, only a small portion of it focuses on high-strength lightweight concrete used for pretensioned bridge girders. In most cases the research involved concrete with compressive strengths less than 7,500 psi. While this research is important and in most cases relevant, it does not verify current code provisions for use on higher strength lightweight concretes (HSLC) commercially available today. In addition, since the properties of lightweight aggregate (LWA) vary based on the raw material from which it is made and the production technique, a direct comparison is not always possible.

This review provides information on both HSLC and normal weight concrete. Initially, the review covers terms and definitions related to lightweight concrete. The production of slate lightweight aggregate is described and a review of the use of HSLC in prestressed bridge applications is provided. Previously developed HSLC mix designs are described and comments about their production in a field environment are discussed. The development of equations to predict transfer length in normal weight concrete is reviewed and current research on transfer length is summarized. Information on shear relating to findings in this research is provided as well as a review of other ongoing research. The

review culminates with a summary of the development of equations to predict prestressing strand development length as well as a review of other related research.

2.2 Terms and Definitions Related to Lightweight Concrete

The following terms are used throughout this report:

Lightweight Aggregate (LWA) – Aggregate with a dry, loose unit weight of 70 lb/ft^3 or less.[2]

Lightweight Concrete (LWC) - A general term that includes "all-lightweight concrete" and "sand-lightweight concrete" defined below.[2]

All-Lightweight Concrete (ALWC) - Concrete containing all lightweight aggregate and does not exceed 115 lb/ft^3.[2]

Sand-Lightweight Concrete (SLWC) - Lightweight concrete in which all the all of the fine aggregate consists of normal weight sand.[2]

Normal-Weight Concrete (NWC) - Concrete having a unit weight of approximately 145 lb/ft^3.

High-Performance Concrete (HPC) – Concrete having a strength over 6,000 psi and/or having durability characteristics in excess of minimally accepted standards.

High-Strength Lightweight Concrete (HSLC) - Concrete meeting the conditions of lightweight concrete and having a compressive strength greater than 6,000 psi.

2.3 Production of Slate Lightweight Aggregate

The expanded slate LWA used in this research is produced from argillite slate found in the foothills region of North Carolina east of Charlotte. Found in a geologic

formation known as the "Tillery Formation," the slate is a thinly laminated, fine-grained siltstone composed of clastic (transported) rock fragments. The slate was from rock fragments of volcanic ash origin, which were deposited in a water environment and later solidified into solid rock. Subsequent burial and tectonic pressure changed the rock into argillite slate. Currently, the Tillery Formation is the only source of slate used to produce expanded slate LWA.[3]

Expanded slate LWA is produced using a rotary kiln approximately 11 feet in diameter and 160 feet in length. The rotary kiln is constructed on a slight incline on large bearings. The inside of the kiln is lined with insulation and a refractory material to protect the thick outer steel casing. Raw slate enters the kiln through pre-heaters that slowly heat the rock. Once in the kiln, the raw slate slowly tumbles within as it moves down the slight incline towards the "burn zone" where the raw material ultimately reaches temperatures in excess of 2200 degrees Fahrenheit. The kilns are normally heated by injecting coal dust or natural gas at the low end. In the "burn zone" the slate becomes sufficiently plastic for small gas pockets within the slate to expand forming masses of small, unconnected cells. As the expanded slate cools, the cells remain providing the material its low unit weight and absorption characteristics. The expanded material called clinker, exits the kiln and is either air or water cooled depending on the manufacturing process and is then crushed to the desired gradations.[3]

2.4 Use of LWC for Prestressed Bridge Applications

The following comments describe many of the known uses of LWC and in some cases HSLC in bridge applications. Many of the applications were not in pretensioned

8

bridge girders, but demonstrate the feasibility of LWC and HSLC in prestressed construction.

Raithby and Lydon[4] described the use of LWC for highway bridges in North America and various countries in Europe. Their overall summary of said bridges was that performance was satisfactory and durability was at least as good as NWC. In cases where performance was not satisfactory, improper detailing or quality control was at fault. They describe several advantageous aspects of LWC including weight savings and reduced superstructure requirements, reduced cost of foundations, and reduced handling costs.

Bender[5] made many of the same conclusions as Raithby and Lydon after performing a cost analysis on the construction of a prestressed concrete bridge. His main assertion was that the reduced weight of LWC allowed the casting of fewer larger pieces thus less total pieces were required to be moved during construction.

Brown and Davis[6] conducted a study on the long-term performance of a prestressed LWC used in a bridge in Fanning Springs, Florida. Initially built in the early 1960s with 121.5-ft AASHTO Type IV girders using 6,500-psi concrete weighing 120 pcf; the bridge underwent a comprehensive load test in 1968 and again in 1992. In comparing data from the two tests, the deflections were very close. Taking into account a margin of error, there was no change in the deflection values. Overall, Brown and Davis felt the bridge performed very well.

Janssen[7] wrote about the Shelby Creek Bridge in Pike County, Kentucky. The use of 7,000 psi HSLC reduced hauling and lifting weights and reduced dead loads on the

structure. The post-tensioned girders were 8.5 feet deep and were made with SLWC having a unit weight of 130 pcf.

Roberts[8] reported on the use of LWC for bridges in California again emphasizing the importance of reduced weight. He noted that successful use of LWC demanded accurate knowledge of shrinkage, creep and modulus coefficients.

Murillo, Thoman and Smith[1] described the use of LWC for design on the Benicia-Martinez Bridge across San Pablo Bay, California. In addition to being the least expensive alternative, the reduced weight of the structure was also more appealing from the standpoint of seismic design.

A publication from the Expanded Shale, Clay and Slate Institute (ESCSI)[9] provided a listing of the most significant uses of LWC for bridges worldwide. Of particular note were three bridges using pretensioned bridge girders including the Coronado Bay Bridge in California, the Lewiston Pump-Generating Plant Bridge in New York, and the Sebastian Inlet Bridge in Florida. All constructed in the 1960s, the bridge girders used LWC with a compressive strength between 5,000 and 6,000 psi. When the publication was issued in 1994, all the bridges were reported to be in excellent condition.

Melby, Jordet and Hansvold[10] described the use of HSLC for long-span bridges in Norway. The authors commented that LWC has been used for bridges in Norway since 1987. Their recommendations focused on testing mix designs thoroughly and ensuring excellent quality control to obtain consistent properties. They stated that the use of LWC was economical for long span bridges, but that bridge geometry would determine the

amount of savings. Compressive strengths up to 8,700 psi with a unit weight of 125 pcf were successfully used to construct the Raftsundet Bridge.

Holm and Bremner[11] noted that LWC was a very promising alternative for the replacement of functionally obsolete bridges throughout the United States. In many cases, the use of LWC for deck replacement would allow upgrading bridge capacity based on lower deck dead load. The authors cited as an example the Woodrow Wilson Memorial Bridge in Washington, D. C. By replacing the bridge deck with LWC, engineers reduced the dead load on the structure and were able to add an additional lane of traffic without exceeding the load carrying capacity of the structure.

2.5 HSLC Mix Designs

2.5.1 Coarse Aggregate

Coarse aggregate is a primary factor in developing a mix design that is lightweight, high-strength, and cost effective. Manufactured lightweight coarse aggregates include expanded clays, expanded shales, expanded slates, expanded perlite, exfoliated vermiculite, and sintered fly ash. Lightweight coarse aggregates also occur naturally in the form of pumice and tuff. Depending on the source of the aggregate, the particle shape and surface texture vary significantly impacting all other aspects of the mix design and the placement characteristics of the concrete.[11] Numerous authors commented on the need for specifications by particular aggregate manufacturer or source with respect to design characteristics.[12,13,14]

The raw material from which the LWA is produced determines the strength of the aggregate and thus the strength that can be achieved in the concrete. Expanded slate aggregates are normally recognized as being one of the LWA products able to produce the highest compressive strength and modulus of elasticity.

The porosity of the LWA determines the degree to which the aggregate will absorb and release water and varies significantly between LWA types. Based on an absorption test using ASTM C 127[15] and ASTM C 128[16], the absorption of LWA can vary from 5 percent to over 25 percent moisture by mass of dry aggregate as compared to less than 2 percent for normal weight aggregate.[11] Knowledge of the exact absorption characteristics of the chosen LWA is important in properly batching LWC. In addition, handling and quality control must be more exact when working with LWA. Bremner and Newman[17] found that the internal microstructure of each type of LWA was independent of the source.

A reduction in the maximum size of coarse aggregate can increase compressive strength without increasing the cement content or reducing the water-cement ratio.[18]

2.5.2 Fine Aggregate

The addition of fine LWA to a mix design further lowers the unit weight of the concrete; however, other characteristics are impacted. In a study by Pfeifer,[19] various amounts of the lightweight fine aggregate fraction were replaced with normal weight sand. The results showed that increasing the proportion of normal weight sand increased both compressive strength and modulus of elasticity.

12

2.5.3 Portland Cement

In HSLC mixes, the cement paste matrix must carry a higher portion of the load imposed on the concrete. As the strength limit of the cement paste matrix is reached, strength of the aggregate and interface between the aggregate and cement paste become the limiting factors.[3]

The type of cement used in the mix determined its curing characteristics. Use of a Type I/II cement results in lower initial strengths, but slightly higher strengths after 28 days. The use of Type III cement yields higher compressive strengths initially, which was desirable for prestressed construction, but results in slightly lower strengths at 28 days compared to Type I/II.

2.5.4 Silica Fume

The inclusion of silica fume in LWC mix designs was reported to significantly improve strength and other performance characteristics. Fujii et al.[20] reported results of a study where they showed a silica fume blended cement to provide superior strength results compared to a belite-rich cement. In a study including high-strength NWC and HSLC, Leming[21] reported that silica fume was particularly effective in increasing the compressive strength of any concrete. Mor[22] reported the dramatically improved bond strength between LWC and reinforcing steel based on the use of silica fume, an occurrence that was verified during this research.

13

2.5.5 Moisture Content

Control of moisture in HSLC is critical. In order to produce concrete having the water to cementitious materials ratio desired, the exact absorbed (moisture within the pore structure of the LWA) and adsorbed (moisture on the outside surface of the LWA – free moisture) moisture of the aggregate must be known. The amount of absorbed moisture directly impacts the specific gravity of the LWA as proportioned and mixed. Smeplass[23] made this point very clear by stating "The consequence of this observation may be that the mix water absorption of LWA must be determined in the actual initial moisture condition, as under concrete production, and as often as necessary to detect variation."

Based on the porosity of LWA, the determination of absorbed moisture content and specific gravity must be handled differently than with normal weight aggregate. Holm and Valsangkar[24] suggested a 1-day soak of LWA prior to determining specific gravity using a pycnometer. After soaking the aggregate for 24 hours, the additional water absorbed in the pycnometer during specific gravity testing is minimal. Based on the then determined absorbed moisture content, the dry specific gravity could be determined by dividing the 24-hour soak specific gravity by (1 + absorbed moisture content).

2.5.6 Mix Proportioning

Mix proportioning of LWC is covered in ACI 211.2-91.[18] The current guide does not cover mix designs for concrete in excess of 6,000 psi strength.

2.6 Field Production of HSLC

Comments on field production of HSLC were limited. Holm and Bremner[11] suggested four basic principles including well-proportioned, workable mixtures that use a minimum amount of water, equipment capable of expeditiously moving the concrete, proper consolidation in the forms, and quality workmanship in finishing. If the concrete is to be pumped, they suggested insuring the aggregate absorbed moisture content was maintained at a high level by presoaking. In the event of low absorbed moisture, pumping could force mix water into the LWA pores reducing the workability of the mix.

Valum and Nilsskog[25] reported on field production of HSLC having a compressive strength of 8,700 psi for the construction of the Raftsundet Bridge in Norway. Field production included steps to insure expanded slate aggregate absorption was maintained at between 7 and 9 percent to prevent mix water absorption. The time from batching until concrete placement could be as long as 2 hours. In addition, bulk density and surface moisture were determined prior to each concrete placement to insure proper mix proportioning. Prior to a concrete truck leaving the batch plant, concrete temperature, slump, air content and wet density were checked for compliance with design specifications. Any results out of specification resulted in the mix being discarded. While these standards would be common for the production of normal weight HPC, the more exacting control of aggregate moisture content was evident for HSLC. In addition, exact control of moisture also enabled better control of unit weight.

Hoff[26] described field production of HSLC for offshore platform construction. Many of the same steps were followed as mentioned by Valum and Nilsskog. Hoff

15

reiterated the importance of moisture control and the impact it could have on slump loss

during placement and also commented that excessive moisture could result in unsuitable

resistance to freezing and thawing damage.

2.7 HSLC Short and Long-Term Material Properties

The following sections address specific material properties and material related

phenomenon where differences were noted between HSLC and NWC.

2.7.1 Modulus of Elasticity

An in-depth explanation of the determination of modulus of elasticity is covered

in Chapter 3, Analytical Investigation on HSLC for Pretensioned Bridge Girders.

The current ACI[2] equation for modulus of elasticity is:

$$E_c = 33 w_c^{1.5} \sqrt{f_c'} \tag{2.1}$$

An equation by Morales[27] (Equation 2.2) was suggested for use with lightweight

concrete.

$$E_c = (40{,}000 \sqrt{f_c'} + 1{,}000{,}000) \left(\frac{w_c}{145} \right)^{1.5} \tag{2.2}$$

16

Table 2.1 lists compressive strengths, dry (equilibrium) unit weights and modulus

values reported by various authors for slate HSLC mix designs having compressive

strengths between 6,000 and 12,000 psi.

Table 2.1 Reported Strength, Weight and Elasticity Modulus Values for Slate HSLC

Author(s) or Source	Compressive Strength f_c' (psi)	Dry Unit Weight w (pcf)	Modulus of Elasticity E_c (million psi)
Brown Davis[6]	6,500	120	3.90
Leming[28]	7,180	116.4	3.58
FIP Committee[29]	7,500	118.6	3.55
Harmon[3]	8,170	111.7	3.27
Bilodeau Chevrier Malhotra Hoff[30]	9,090	119.2	4.06
Valum Nilsskog[25]	9,550	123.0	3.41
Mor[22]	9,650	130.0	3.91
Holm Bremner[31]	9,856	117.0	3.50
Carolina Stalite Company[32]	10,281	126.0	4.10
Harmon[3]	10,980	119.2	3.95
Harmon[3]	11,500	134.0	4.40
Carolina Stalite Company[32]	11,588	132.0	4.40
Harmon[3]	11,850	122.0	4.56

2.7.2 Strength Ceiling

Harmon[3] discussed a strength ceiling for HSLC being in the region of 12,000 to

13,000 psi based on the limiting strength of the slate LWA. Holm[33] also discussed the

strength ceiling with respect to smaller maximum size of aggregate. As the maximum

size of aggregate is reduced, strength increases to some upper limit determined by the

strength ceiling. Beyond the strength ceiling, additional binder does not increase the concrete's strength.

Bremner and Holm[34] addressed the elastic mismatch between LWA and the high-strength cement paste matrix. As the HSLC strength increases, the difference between the elasticity modulus values becomes more pronounced. Under load, the "elastic mismatch" results in fracture that begins as transverse splitting of the LWA. This splitting action is indirectly responsible for the strength ceiling of HSLC.

Holm[33] also reported a tensile strength ceiling for LWC. Since the LWA is approximately one half voids, its tensile strength will be reduced in comparison to NWA. Holm suggested the LWA tensile strength ceiling might also be responsible for compression strength limitations.

2.7.3 Internal Curing

Internal curing results when absorbed water in the LWA provides an internal reservoir to enhance cement hydration and extend the curing process. Several authors have commented on this phenomenon as related to LWC and HSLC.[21,33,35] Bremner, Holm and Ries[36] performed a study in which LWA was added to NWC mixes to provide additional internal cure water in mixes having strengths from 6,400 psi to 8,700 psi. The internal curing is reported to not only add in strength gain, but positively impacts durability characteristics by providing a higher quality and denser matrix.

2.8 Transfer Length

Transfer length is defined as the distance required to transfer the effective prestressing force from the strand to the surrounding concrete. The transfer length is developed when the pretensioning strands are released by flame cutting or other method from the restraining abutments. Numerous factors are thought to contribute to determining the transfer length including size and surface condition of the prestressing strand, concrete strength and modulus of elasticity at time of strand release, level of prestressing in the strand, and the amount of confining steel and concrete consolidation in the transfer length region. Many experimental programs have focused on the above factors in determining a relation to predict transfer length.

The Master's Thesis by Chris Reutlinger,[37] "Direct Pull-Out Capacity and Transfer Length of 0.6-Inch Diameter Prestressing Strand in High Performance Concrete" provides very thorough coverage of the history and development of equations to predict transfer length. The following is a summary of current code provisions and other proposed equations as determined for NWC. There are no known proposed equations specifically addressing transfer length for HSLC.

2.8.1 Janney, 1954

Initial transfer length testing by Janney[38] in 1954 concluded that transfer length and the general shape of the stress transfer distribution were attributable to diameter and surface condition of the prestressing wire and concrete strength. Janney did not suggest a relation for predicting transfer length.

2.8.2 Hanson and Kaar, 1959

Although the focus of Hanson and Kaar's[39] work was on flexural bond, an appendix included comments on an assumed average transfer bond stress of 400 psi. Equation 2.3 was proposed as a way to determine the transfer bond stress.

$$u_t = \frac{A_{ps} f_{se}}{\Sigma_0 l_t} \tag{2.3}$$

A_{ps} is the area of prestressing strand, f_{se} is the effective prestressing stress at transfer, Σ_0 is the actual perimeter of the prestressing strand, l_t is the transfer length and u_t is the transfer bond stress.

2.8.3 Kaar, LaFraugh and Mass, 1963

Kaar et al.[37] concluded that transfer length varied directly based on strand diameter for ¼-inch and ½-inch strands but did not follow this same direct proportion for 0.6-inch strand. Kaar et al. found concrete strength did not impact transfer length, but affected the shape of the stress distribution. Higher concrete strength allowed the concrete to pick up stress more quickly when compared to lower strength specimens. Kaar et al. also reported differences in transfer length between "dead" and "cut" ends.

2.8.4 Mattock, 1963

In 1963, Mattock[37] used Equation 2.3 with an assumed average transfer bond

stress of 400 psi to derive the current ACI[2] equation for transfer length. The factors

0.725 and 4/3 were used to determine the actual area and perimeter respectively.

$$l_t = \frac{\left(0.725\dfrac{\pi\,d_b^2}{4}\right)f_{se}}{\left(\dfrac{4}{3}\pi\,d_b\right)0.4} = \frac{1}{2.94}f_{se}d_b \qquad (2.4)$$

Equation 2.4 was simplified to Equation 2.5, which is the current ACI[122] expression.

$$l_t = \frac{f_{se}d_b}{3} \qquad (2.5)$$

Mattock assumed the effective stress, f_{se}, for 250 ksi strand was 150 ksi and further

simplified Equation 2.5 to Equation 2.6, which was adopted by ACI in 1963 and

AASHTO[40] in 1973.

$$l_t = 50d_b \qquad (2.6)$$

Equation 2.6, currently maintained by AASHTO, is based on a limited number of tests

where strand ultimate strengths were less than products available today.[37]

2.8.5 Martin and Scott, 1976

Martin and Scott[41] re-evaluated previous testing by Hanson and Kaar based on prestressing strand having an ultimate strength, f_{pu}, of 270 ksi, and commonly encountered strand surface conditions, and they recommended the implementation of Equation 2.7.

$$l_t = 80 d_b \qquad (2.7)$$

2.8.6 Zia and Mostafa, 1977

Based on an extensive review of transfer length testing, Zia and Mostafa[42] proposed Equation 2.8 to account for the effects of strand diameter, initial level of prestress, and concrete strength at transfer. Equation 2.9 was reported to be applicable for concrete strengths from 2,000 to 8,000 psi. This evaluation is reported in Chapter 9.

$$l_t = 1.5 \frac{f_{si}}{f'_{ci}} d_b - 4.6 \qquad (2.8)$$

2.8.7 FHWA Memorandum, 1988

Based on testing at the University of North Carolina in 1986 where poor transfer and development length results were recorded, the FHWA issued a memorandum specifying four interim restrictions, one of which was the restriction from using 0.6-inch

prestressing strand.[37] This restriction prevented the prestressed concrete industry from fully utilizing the benefits of higher strength concretes in larger members. Several research programs were initiated based on the FHWA restrictions.

2.8.8 Deatherage, Burdette and Chew, 1989

Deatherage et al.[43] conducted experimental testing on 20 AASHTO Type I girders with varying strand diameters and spacings. Their conclusions were that 0.6-inch diameter strand should be allowed and that strand spacing of 1.75 inches should be allowed for ½-inch diameter strand. Equation 2.10 was suggested for the calculation of transfer length for ½-inch, ½-inch special and $^9/_{16}$-inch diameter prestressing strand. Equation 2.9 was conservative and acceptable for use on 0.6-inch strand, but further research was recommended.

$$l_t = \frac{f_{si} d_b}{3}$$ (2.9)

2.8.9 Russell, 1992

Russell[44] performed an extensive series of testing of rectangular, scale model AASHTO-type and full-sized Texas Type C cross sections as part of a PhD Thesis under the supervision of Dr. Ned Burns. The specimens were all prestressed with ½-inch or 0.6-inch strand spaced at 2 inches, except for three rectangular sections that were prestressed with 0.6-inch strand spaced at 2.25 inches. In many of the specimens, strands were debonded to various distances from the girder ends. Russell concluded that larger

23

cross sections had shorter transfer lengths, larger strand diameters required longer

transfer lengths, strand spacing greater than 2 inches for 0.6-inch strand was not required,

debonded strands had transfer lengths similar to fully bonded, strands and confining

reinforcement did not affect transfer length. Russell suggested Equation 2.10 for

predicting transfer length.

$$l_t = \frac{f_{se} d_b}{2}$$
(2.10)

2.8.10 Mitchell, Cook, Khan and Tham, 1993

Mitchell et al.[45] based their research on determining the effect of concrete strength

on transfer length. They examined strand diameters of 3/8-inch, 1/2-inch and 0.6-inch

used to prestress rectangular sections made using normal weight concretes having

strengths from 4,500 to 12,900 psi at 28 days. The method of strand release was gradual

which was reported to provide a better comparison to the sudden strand release used in

most prestressing operations. Based on their results, Mitchell et al. proposed Equation

2.11.

$$l_t = 0.33 f_{si} d_b \sqrt{\frac{3}{f'_{ci}}}$$
(2.11)

2.8.11 Buckner, 1994

Buckner[46] noted that inconsistencies existed between the methods used by various researchers to determine transfer length. After an evaluation of results, Buckner concluded that the 95 Percent Average Mean Strain (AMS) Method provided the best overall prediction of transfer length. Furthermore, he recommended Equation 2.12 for predicting transfer length. Buckner noted that $1250/E_{ci}$ was about 3 for compressive strengths greater than 3,500 psi; thus, his findings endorsed Equation 2.9 as well.

$$l_t = \frac{1250\, f_{si}\, d_b}{E_{ci}}$$
(2.12)

2.8.12 FHWA Study, 1996

In addition to the numerous studies aforementioned, the FHWA[47] also published findings from their own study addressing the bond of prestressing strand in NWC and HPC. The FHWA study addressed the following variables:

1. Concrete compressive strength at 28 days, f_c'

2. Square root of concrete compressive strength at 28 days, f_c'

3. Concrete compressive strength at transfer, f_{ci}'

4. Square root of concrete compressive strength at transfer, f_{ci}'

5. Concrete modulus of elasticity at 28 days, E_c

6. Concrete modulus of elasticity at transfer, E_{ci}

7. Prestressing strand diameter

8. Prestressing strand area

9. Stress in prestressing strand prior to transfer, f_{si}

10. Effective prestress, f_{se}

Based on FHWA results and their analysis of other research results, the restriction on the use of 0.6-inch strand was lifted. The FHWA proposed Equations 2.13 and 2.14 for "best-fit" and to provide a 95% confidence interval, respectively.

$$l_t = 4\frac{f_{pt}d_b}{f_c'} - 21 \qquad (2.13)$$

$$l_t = 4\frac{f_{pt}d_b}{f_c'} - 5 \qquad (2.14)$$

2.8.13 Summary of Transfer Length Review

Again, there are currently no equations specifically for predicting transfer length in girders made with LWC or HSLC. Chapter 9, Transfer Length, uses Equations 2.5 through 2.14 for an evaluation of transfer length results from this research program to determine which variables are most applicable for HSLC girders and to suggest a better equation for predicting transfer length.

2.9 Flexural Behavior

A review indicates that only limited research has been conducted on the flexural behavior of composite HSLC girders. Prior to the onset of flexural cracking and the

point at which flexural cracking occurs, the behavior of the HSLC is important. Beyond the cracking state, the behavior of the NWC deck is the governing concern. To the author's knowledge, no background information was available related to the findings and conclusions identified in this research for flexural behavior. The general flexural behavior of normal weight prestressed composite girders made with normal strength concrete is well understood and discussed in standard text books.[48,49,50]

2.10 Shear Behavior

Similar to flexural behavior, only a limited amount of research has been conducted on prestressed HSLC. Comments are provided for both HSLC and normal weight HPC as well as for LWC as applicable to this research.

2.10.1 Hanson, 1961

The origination of the lambda factor for use with LWC was based on work done by Hanson. Using the results of testing performed at PCA and at the University of Texas Hanson determined a good correlation between diagonal tensile strength in beams with the splitting tension test.[14] Hanson then determined that the ratio of splitting tension strength in lightweight concrete to that for normal weight concrete of the same compression strength was in general about 0.85 for concrete strengths below 5,000 psi. This relation was first reported in the 1963 ACI 318 Code. In the early 1970's, the reduction factor was formalized as lambda, λ, as 0.85 for sand LWC and 0.75 for all LWC. Based on the high degree of variability of LWA, concerns exist today that the lambda factors may become unconservative for concrete strengths over 5,000 psi.[51]

2.10.2 Johnson and Ramirez, 1989

Johnson and Ramirez[52] conducted research on non-prestressed beams, but made some observations that may be applicable for prestressed HSLC and normal weight HPC. One conclusion reached in their research was that in higher strength beams, shear reinforcement spacing was greater creating a deficiency in reserve shear strength. Once the upper limit of concrete shear capacity was exceeded, the shear force transferred to shear reinforcement would cause it to yield and rupture. They suggested applying either an upper limit to the term $(f_c')^{1/2}$ to limit the increase in V_c due to increasing f_c' or increasing the minimum shear reinforcement requirement as concrete strength increases. The 1989 ACI 318 code has included a specification reflecting this recommendation.[53]

2.10.3 Shahawy and Batchelor, 1996

Shahawy and Batchelor[54] conducted a research program examining the shear behavior of full-scale prestressed concrete girders made from 6,000 psi NWC. Of particular interest in their findings were comments that the AASHTO LRFD provisions for shear were very conservative and required modification to improve their reliability.

2.10.4 Barnes, Burns and Kreger, 1999

Barnes, Burns and Kreger[55] conducted an extensive research program at the University of Texas at Austin using 0.6-inch diameter prestressing strand in I-shaped prestressed girders made with normal weight HPC having strengths from 5,000 to 11,000 psi. The authors recommended limiting the principal tensile stress in the region from the composite section centroid to the extreme tensile fiber to $4(f_c')^{1/2}$. This recommendation

corresponds with ACI 318-99 Section 11.4.2.2[2] but extends the applicable area to include the section from the composite centroid to the extreme tension fiber.

2.10.5 Ma, Tadros and Baishya, 2000

Ma, Tadros, and Baishya[56] examined shear behavior in pretensioned I-girders made with 8,000 psi normal weight HPC. They concluded that both the AASHTO Standard and LRFD Specifications produced conservative predictions of girder shear capacity. When considering the results of their study, it must be recognized that prestressing strands were anchored in end diaphragms thus eliminating the possibility of slip and possibly increasing shear capacity at the girder ends.

2.10.6 Ramirez, Olek, Rolle, and Malone, 2000

Ramirez, Olek, Rolle, and Malone[57] conducted research on HSLC pretensioned girders made with ½-inch, and 0.6-inch diameter prestressing strands. The HSLC was made using expanded shale aggregate; the resulting concrete strengths ranged from 6,500 to 10,000 psi. The research at Purdue is thought to be the only other research conducted using 0.6-inch diameter prestressing strand in HSLC. As with Ma et al.,[56] an additional 1-meter anchorage was provided for the prestressing strand behind the center of bearing. Their conclusions related to shear were that the current AASHTO Standard and LRFD procedures were conservative for shear. Additionally they reported that the minimum amount of shear reinforcement for HSLC pretensioned girders must be further investigated based on a lower ratio of measured/calculated shear capacity with increased concrete strength.

2.10.7 ACI Committee 213, 2001

In a draft copy of Chapter 5, ACI 213,[58] shear and diagonal tension strength is covered in Section 5.8. Committee 213 reports that lightweight concrete members behave in fundamentally the same manner as normal weight concrete members. They recommend that the permissible shear capacity may be determined by substituting the splitting tensile strength, $f_{ct}/6.7$ for $(f_c')^{1/2}$ in the shear provisions of Chapter 11, ACI 318.[2]

2.11 Development Length

Development length of prestressing strands is the sum of the transfer length and the flexural bond length. Development length can be defined as the minimum distance from the end of the member beyond which the application of a point load will result in a flexural failure. As in transfer length, many factors are thought to affect development length. Many experimental programs have addressed development length resulting in suggested equations for its prediction.

The Master's Thesis by Chris Reutlinger,[37] "Direct Pull-Out Capacity and Transfer Length of 0.6-inch diameter Prestressing Strand in High Performance Concrete" provides very thorough coverage of the history and development of equations to predict development length. The following is a summary of current code provisions and other proposed equations as determined for NWC. The summary closely mirrors the development of transfer length equations. There are no known equations specifically addressing development length for HSLC.

30

2.11.1 Janney, 1954

Initial development length testing by Janney[38] in 1954 was based on the use of

5/16-inch wire having two different surface conditions prestressed to 0, 60, 120 and 165

ksi in beams made with NWC having strengths from 4,500 to 4,800 psi. Janney reported

a "wave of flexural bond stress concentration" and noted that once general bond slip

occurred, the beam failed shortly thereafter. Janney contributed bond in the transfer

region predominantly to the Hoyer effect, which was the confining pressure applied to the

wire by the concrete. Janney also reported improve bond characteristics for slightly

rusted wire.

2.11.2 Hanson and Kaar, 1959

Hanson and Kaar[39] conducted a study involving 47 small-scale concrete beams

reinforced with various sizes of Grade 250 stress-relieved strand. The tests focused on

five factors including strand diameter, embedment length, concrete strength, percentage

of reinforcement, and strand surface condition. All beams were loaded until failure.

Hanson and Kaar reported observations similar to those of Janney.[38] The results of

Hanson and Kaar's research were the basis for the current AASHTO development length

expression shown in Equation 2.16 and developed by Mattock.[37] Equation 2.15 simplifies

to Equation 2.16.

$$l_d = l_t + l_{fb} = \frac{f_{se}d_b}{3} + (f_{su}^* - f_{se})d_b \tag{2.15}$$

$$l_d = (f_{su}^* - \frac{2}{3}f_{se})d_b \qquad\qquad (2.16)$$

Shortly after the development of Equation 2.16 concerns developed based on the

introduction and common use of Grade 270 prestressing strand.[37]

2.11.3 Martin and Scott, 1976

Martin and Scott[41] re-evaluated the currently suggested equation (Equation 2.16)

and determined that inconsistencies may have been responsible for the collapse of a 20-ft

span slab under construction loads. They suggested two new equations that did not

determine development length, but specified a maximum strand stress based on a given

embedment length. The two equations are shown below for the given location l_x.

For l_x less than $80d_b$:

$$f_{su}^* \leq \frac{l_x}{80d_b}\left(\frac{135}{d_b^{\frac{1}{6}}}+31\right) \qquad\qquad (2.17)$$

For l_x greater than $80d_b$:

$$f_{su}^* \leq \frac{135}{d_b^{\frac{1}{6}}}+\frac{0.39l_x}{d_b} \qquad\qquad (2.18)$$

32

Equation 2.18 was rewritten in terms of l_x in Table 13.8 in order to determine its accuracy in predicting l_d.

2.11.4 Zia and Mostafa, 1977

Zia and Mostafa[42] also realizing the inconsistencies with Equation 2.16 suggested a new equation as well (Equation 2.19) which incorporated their suggested transfer length equation, Equation 2.8.

$$l_d = l_t + l_{fb} = \left(1.5\frac{f_{si}}{f_{ci}'}d_b - 4.6\right) + 1.25(f_{su}^* - f_{se})d_b \qquad (2.19)$$

2.11.5 FHWA Memorandum, 1988

Based on testing at the University of North Carolina in 1986 where poor transfer and development length results were recorded, the FHWA issued a memorandum specifying 4 interim restrictions as listed in Section 2.8.7.[37] Several research programs were initiated based on the FHWA restrictions.

2.11.6 Deatherage, Burdette and Chew, 1989

Deatherage et al.[43] conducted experimental testing on 20 AASHTO Type I girders with varying strand diameters and strand spacings and concrete design strengths of 5,000 psi. They suggested the flexural bond component suggested by AASHTO[40] should be increased by 50 percent as shown in Equation 2.20 below.

33

$$l_d = l_t + l_{fb} = \frac{f_{si}d_b}{3} + 1.50(f_{su}^* - f_{se})d_b \qquad (2.20)$$

2.11.7 Russell, 1992

Russell[44] performed an extensive series of testing of rectangular, scale model AASHTO-type and full-sized Texas Type C cross sections as part of a PhD Thesis under the supervision of Dr. Ned Burns. The specimens were all prestressed with ½-inch or 0.6-inch strand spaced at 2 inches except three rectangular sections that were prestressed with 0.6-inch strand spaced at 2.25 inches. In many of the specimens, strands were debonded to various distances from the girder ends. Russell concluded that "shear cracking through the transfer region will cause its bond to fail and that if cracks do not occur that the strand will develop is prestressing force plus any additional tension required by external loads."[44] To prevent cracking from occurring through the transfer region, Russell developed the criteria listed in Equation 2.21 where l_t was calculated using Equation 2.10.

$$M_{cr} > l_t V_u \qquad (2.21)$$

In addition, Russell specified that if $V_u > Vcw$ that vertical and longitudinal mild steel shear reinforcement should be provided to prevent web shear cracking from passing through the transfer region.

2.11.8 Mitchell, Cook, Khan and Tham, 1993

Mitchell et al.[45] based their research on determining the effect of concrete strength on develop length. They examined strand diameters of $^3/_8$-inch, ½-inch and 0.6-inch used to prestress rectangular sections made using concretes having strengths from 3,000 to 7,310 psi at release and from 4,500 to 12,900 psi at 28 days. Based on experimental results, Equation 2.22 was suggested.

$$l_d = 0.33 f_{si} d_b \sqrt{\frac{3}{f'_{ci}}} + (f_{su} - f_{se}) d_b \sqrt{\frac{4.5}{f'_c}}$$ (2.22)

2.11.9 Buckner, 1994

Buckner[46] noted that there was an interaction between transfer length, effective prestress and design stress. Buckner recommended using a procedure similar to that of Hanson and Kaar.[39] He also theorized that the development length expression should be based also on ultimate strain and suggested Equations 2.23 and 2.24.

$$l_d = l_t + l_{fb} = \frac{f_{si} d_b}{3} + \lambda (f^*_{su} - f_{se}) d_b$$ (2.23)

$$1.0 \le [\lambda = (0.6 + 40\varepsilon_{ps})] \le 2.0$$ (2.24)

In Equation 2.24, ε_{ps} is the strain corresponding with f_{su}*.

35

2.11.10 FHWA Study, 1996

In addition to the numerous studies aforementioned, the FHWA[47] also published findings from their own study addressing the bond of prestressing strand in NWC and HPC. The FHWA study addressed variables as specified previously in 2.8.12. Based on FHWA results and the results of other research programs, the restriction on the use of 0.6-inch strand was lifted. The FHWA proposed Equations 2.25 and 2.26 for "best-fit" or "mean" and to provide a "95% confidence interval," respectively.

$$l_d = l_t + l_{fb} = \left(4\frac{f_{pt} d_b}{f_c'} - 21 \right) + \left(\frac{6.4(f_{su} - f_{se})d_b}{f_c'} + 26 \right) \qquad (2.25)$$

$$l_d = l_t + l_{fb} = \left(4\frac{f_{pt} d_b}{f_c'} - 5 \right) + \left(\frac{6.4(f_{su} - f_{se})d_b}{f_c'} + 15 \right) \qquad (2.26)$$

2.11.11 Barnes, Burns and Kreger, 1999

Barnes, Burns and Kreger[55] tested 36 AASHTO Type I normal weight HPC girders having release strengths from 4,000 to 7,000 psi and strengths at testing from 5,700 to 11,000 psi. All prestressing strand was 0.6-inch diameter Grade 270 ksi LOLAX strand in either a "bright" or "rusted" surface condition. Included in the test program were girders with fully bonded strands and debonded strands. One of the outcomes of the research program was Equation 2.27 for predicting development length.

$$l_d = \frac{5}{4}\left(\frac{f_{pt}}{\sqrt{f'_{ci}}} + (f_{ps} - f_{pe})\right)d_b \qquad (2.27)$$

2.11.12 Peterman, Ramirez, Olek, 2000

Peterman, Ramirez, and Olek[59,60] conducted research on HSLC bridge girders as referenced in Section 2.10.5. Their research is the only other research known where HSLC girders using 0.6-inch diameter strands were tested. Their report indicated that all multiple strand specimens were reinforced with sufficient stirrups to prevent web-shear cracking at the member ends. The prevention of shear cracking in the transfer region has been shown to result in strand slip causing premature shear failure.

2.11.13 Kolozs, 2000

Kolozs,[61] under the supervision of Professors Ned Burns and John Breen, tested HSLC girders with strengths between 6,000 and 8,000 psi prestressed with ½-inch diameter Grade 270 LOLAX strand. Kolozs found the current AASHTO[40] equation for development length was conservative.

2.11.14 Summary of Development Length Review

Again, there are currently no specific equations for predicting development length for girders made with HSLC. Chapter 13, Development Length, uses Equations 2.16 through 2.20 and 2.22 through 2.27 for an evaluation of development length results from this research program to determine which variables are most applicable for HSLC girders and to suggest a better equation for predicting development length.

2.12 Elements of Bond

There are three mechanisms that allow the development of bond stress between the prestressing strand and the concrete to include adhesion, frictional bond due to Hoyer's effect, and mechanical interlock.[44] Slipping of the prestressing strand relative to the concrete is required to develop bond stress. In general, bond resistance of seven-wire prestressing strand remains constant or increases after initial slip.[62]

2.12.1 Adhesion

Adhesion occurs in a very thin layer at the interface between the concrete and prestressing strand. Acting like an "adhesive," adhesion exhibits rigid-brittle behavior preventing slip of the strand relative to the concrete up to a critical stress level. During the transfer of prestress or girder testing, adhesion is lost when the bond stress exceeds the critical stress level. Once the critical stress level is exceeded, the adhesion portion of bond is lost. In the case of seven-wire prestressing strand, the loss of adhesion is often replaced by other mechanisms of bond.[44] Because failure of the adhesive bond occurs at a very small displacement, the overall contribution of adhesion to bond is minor.[63]

2.12.2 Frictional Bond Due to Hoyer's Effect

Research by E. Hoyer in 1939 using small diameter smooth piano wire resulted in the identification of a mechanism of bond now known by his name.[44] When wire or prestressing strand is tensioned, Poisson effects cause the diameter to become smaller. After tensioning, concrete is cast around the strands and allowed to cure to some initial required strength. At strand release, the strand attempts to return elastically to its initial

38

length prior to tensioning.   As the strand becomes shorter, Poisson effects cause an

increase in strand diameter creating radial compression stress between the strand and

concrete.[63] The resulting increase in strand diameter upon release is most pronounced at

the free end of the strand and becomes less to a point where it becomes constant at a

distance approximately equal to the transfer length from the end of the member. After

initial end slip at strand release, the resulting frictional bond resistance and wedge action

shown in Figure 2.1 restrain the strand and maintain tension in it.
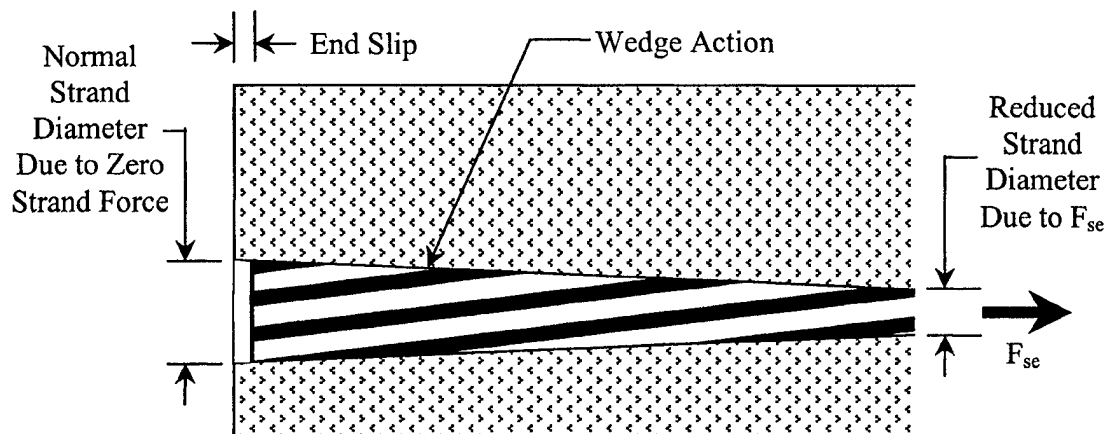
Figure 2.1 Wedge Action Resulting from Hoyer's Effect

During the application of load to a girder, the stress in the strand increases. At the

point where the stress exceeds the stress in the strand at transfer in the transfer region, the

wedge action begins to diminish.[44]

2.12.3 Mechanical Interlock

Standard seven-wire prestressing strand is manufactured by wrapping six wires around a seventh center wire in a helical pattern. Concrete placed around the strand fills the narrow spaces (interstices) between the individual wires completely encapsulating the strand. When the strand is prevented from twisting, the concrete ridges acting on the outside wires of the strand restrict movement by mechanical interlock. In order to prevent twisting, the wedge action created by Hoyer's effect must exist.[44] Mechanical interlock is reported to enhance the frictional bond component at strand release.[63]

CHAPTER III

ANALYTICAL INVESTIGATION OF HSLC FOR PRETENSIONED BRIDGE GIRDERS

3.1 Introduction

The potential advantages of using high strength HPC for precast prestressed bridge girders may be lost if those girders are too heavy to be transported. The advantages of using HPC for pretensioned girders presented by Kahn and Saber[64] included spans up to 40 percent longer than when normal strength (6 ksi) concrete was used, wider girder spacing and greater durability. Mr. Paul Liles, Georgia State Bridge Engineer, stated that the girders for spans over about 120 feet would weigh too much and that they would require a "super-load" permit for transportation. A gauge of the transportation problem is the necessity to obtain hauling permits or "super-load" permits.

In Georgia when the gross vehicle weight (GVW, weight of girder plus tractor-trailer rig) exceeds 150 kips, a "super permit" is required. This permit requires the hauler to obey certain additional restrictions that may include stopping before every bridge, proceeding over the bridge at a speed less than 5 miles per hour and that an escort vehicle lead and follow the truck. In addition, the state department of transportation must carefully review the route and evaluate the load capacity of each bridge. There may be no acceptable route. The slow rate over a bridge crossing can significantly disrupt traffic.

41

The established goal for this phase of the research was to achieve a 150 foot long pretensioned girder with a weight that when added to that of a tractor-trailer rig, was less than 150 kips; that is, create a 150-foot long girder that does not require a "super permit." A further goal was too have a minimum girder spacing of 7 feet for overall bridge efficiency. Use of either an all-lightweight or sand-lightweight concrete would be needed to achieve these goals. It was known from previous research[64] that AASHTO Type IV girders constructed with 15,000 psi NWC using 0.6-inch diameter prestressing strands and a girder spacing of 5 feet could achieve the span but with a GVW of about 185,000 lbs.

Therefore, the purpose of this analytical investigation was to determine if HSLC could be used to build pretensioned bridge girders with a length of 150 feet and girder spacing of 7 feet whose GVW did not exceed 150 kips. Standard AASHTO (American Association of State Highway and Transportation Officials) and AASHTO-PCI (Precast/Prestressed Concrete Institute) sections were considered. The range of girder strengths was 8, 10 and 12 ksi. The strength of the 7-inch thick, normal weight composite deck was 3,500 psi.

The scope of this study was limited to investigating AASHTO Type II-V and AASHTO-PCI Bulb-Tee 54, 63 and 72 sections (Standard and Modified) as shown in Figures 3.1, 3.2 and 3.3. For reference purposes, AASHTO-PCI Bulb-Tees were listed as "Bulb-Tees." A Modified AASHTO-PCI Bulb-Tee was listed as a "Modified Bulb-Tee."

Type II
I=50,980 in^4

Type III
I=125,390 in^4

Type IV
I=260,730 in^4

Type V
I=521.180 in^4
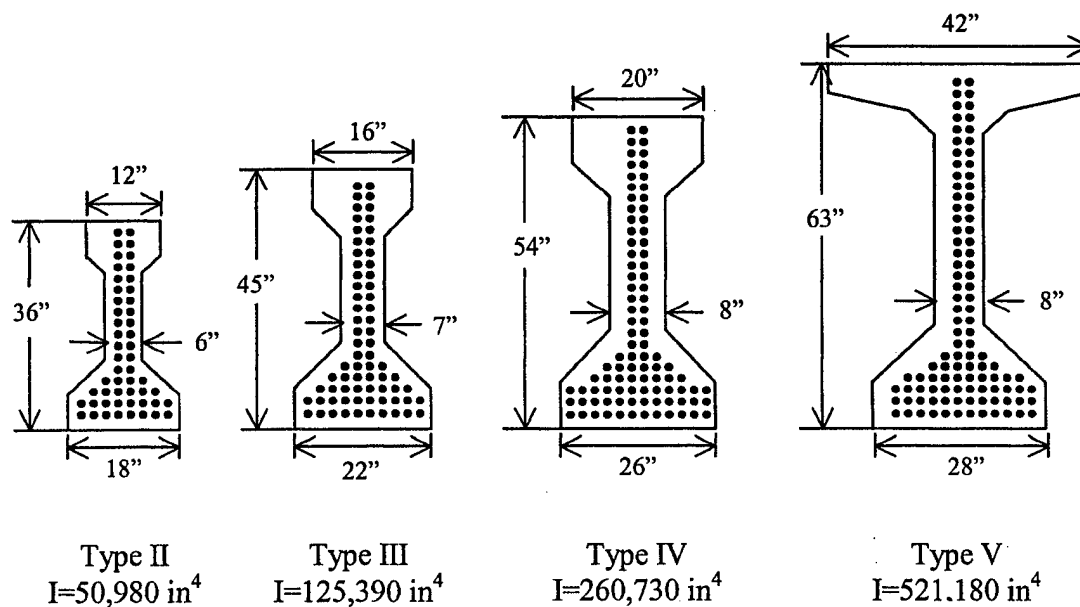
Figure 3.1 AASHTO Type II – V Sections

BT-54
I=268,077 in^4

BT-63
I=392.638 in^4

BT-72
I=545,894 in^4
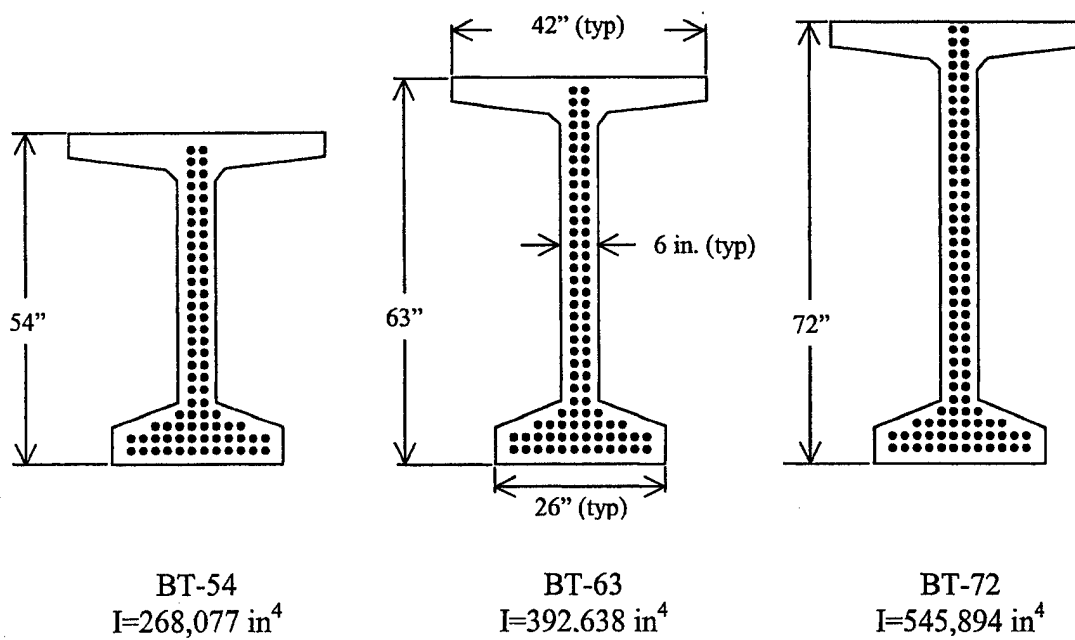
Figure 3.2 AASHTO-PCI Bulb Tee 54, 63 and 72 Shapes

43
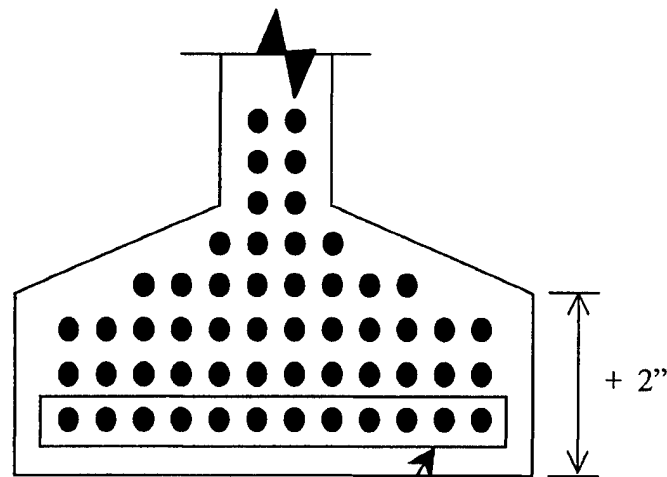
- One additional row of
  pre-tensioning strands
- 2 in (51 mm) deeper
  bottom flange

Moments of Inertia

54M – 308,318 in^4
63M – 446,700 in^4
72M – 616,067 in^4

Figure 3.3 Diagram of Bottom Flange of Modified Bulb Tee

The Modified Bulb-Tee sections consisted of a Standard Bulb-Tee with one

additional row of 12 strands added to the bottom flange. The additional row of 12 strands

added 2 inches to the depth of the member, all in the bottom flange. The inclusion of the

Modified Bulb-Tee sections was precipitated by discussions with Georgia precast

concrete producers who had previously constructed and recommended the section.

Prestressing strands were 0.6-inch diameter, 270 ksi low relaxation strands spaced at 2

inches.

The HSLC in this study assumed the use of regionally available expanded slate

LWA. Based on the requirement to produce concrete compressive strengths up to 12 ksi,

it was thought that the use of slate LWA would be necessary. Furthermore, available

HSLC test data indicating strengths upwards of 12 ksi predominantly used slate LWA.[3,12,21,31]

It was possible that HSLC using other types of LWA (expanded shale or clay) could achieve upwards of 12 ksi strength, but available data were limited. An extensive literature search focusing on HSLC used for prestressed applications indicated that neither shale nor clay LWA had been used where concrete strengths approached 12 ksi.[65]

3.2 Parametric Study

All girder designs in this research were based on the 16th Edition of the AASHTO Standard Specification for Highway Bridges[40] and used the Georgia DOT bridge design program with modification by the authors to enable the use of HSLC. A spreadsheet to create input files for the bridge program is shown in Appendix A. Several steps were necessary prior to using the program to design HSLC bridge girders.

It was assumed that prestress losses would be the same for HSLC as for normal strength concrete. Other ongoing research by the author indicates that for normal weight and lightweight HPC, the creep and shrinkage losses were less than for normal strength concretes. Yet, consideration of deflection was a major concern.

The parameters that were varied were concrete strength, unit weight, and girder type. Other variables that remained constant are listed in Table 3.1.

Table 3.1 Critical Girder Design Variables That Remained Constant.

Allowable top fiber tension stress at release	$3\sqrt{f_c'}$
Allowable final bottom fiber tension stress	$6\sqrt{f_c'}$
Release strength as percent of 28-day compressive strength	75 percent
Composite deck thickness	7 inches
Composite deck strength	3500 psi
Pretensioning strand diameter	0.6 inches
Pretensioning strand spacing	2 inches
Pretensioning strand ultimate strength, f_{pu}	270 ksi
Type of pretensioning strand	LOLAX
Percent of strand ultimate strength allowed at time of pretensioning	75 percent
Girder spacing	7 feet

3.3 Determination of Modulus of Elasticity

A critical requirement for design was to accurately predict the modulus of

elasticity at both the time of release (E_{ci}) and at 28 days (E_c) for HSLC made using slate

LWA. Accurate values of the modulus of elasticity were necessary to determine prestress

losses and girder deflections. Experimental data from thirteen mixes using slate LWA

were used to investigate the appropriate modulus values as shown in Table 2.1. The

current ACI[2] and AASHTO[40] equation for E_c is:

$$E_c = 33w_c^{1.5}\sqrt{f_c'}$$ (2.1)

When used with HSLC, Equation 2.1 was found to overpredict the modulus values for

strengths over 7,000 psi. The equation was specified for use on concretes having unit

weights between 90 and 155 pcf. Morales[27] proposed Equation 2.2 for use with LWC:

$$E_c = (40,000\sqrt{f_c'} + 1,000,000)\left(\frac{w_c}{145}\right)^{1.5} \qquad (2.2)$$

Equation 2.2 more closely predicted modulus values; however, when used with HSLC

made using slate LWA, the predicted values were low for strengths below 10 ksi and high

for strengths over 10 ksi when compared to experimental data. In order to more

accurately predict modulus values, Equation 3.1 was developed similar in form to the

Morales equation, but based on a "best fit" analysis of the experimental data from the

thirteen slate mixes.

$$E_c = (33,000\sqrt{f_c'} + 4,000,000)(w_c/242)^{0.9} \qquad (3.1)$$

Figures 3.4 and 3.5 plot the experimental data and the three equations for modulus of

elasticity versus compressive strength and versus unit weight, respectively. Equation 2.3

was used for all further analyses.

3.4 Girder Design

The computer program was used to find the maximum span length for each girder

type in the study. The variable parameters were concrete strength and concrete unit

weight. Other critical variables were kept constant at AASHTO[40] specified or other

values as shown in Table 3.1.
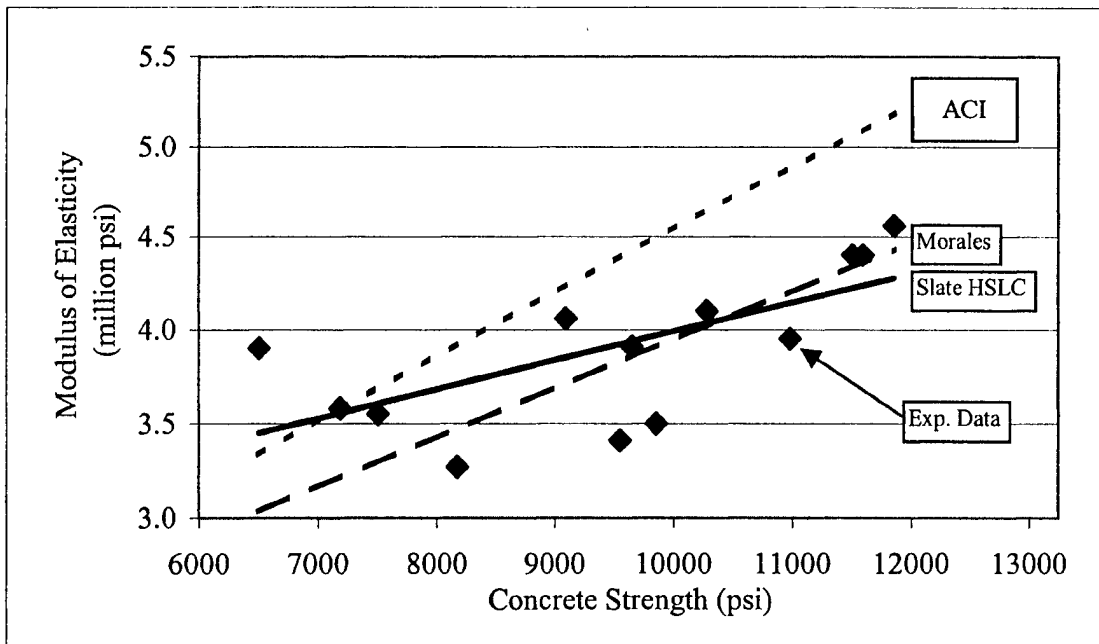
Figure 3.4 Modulus of Elasticity vs. Concrete Strength
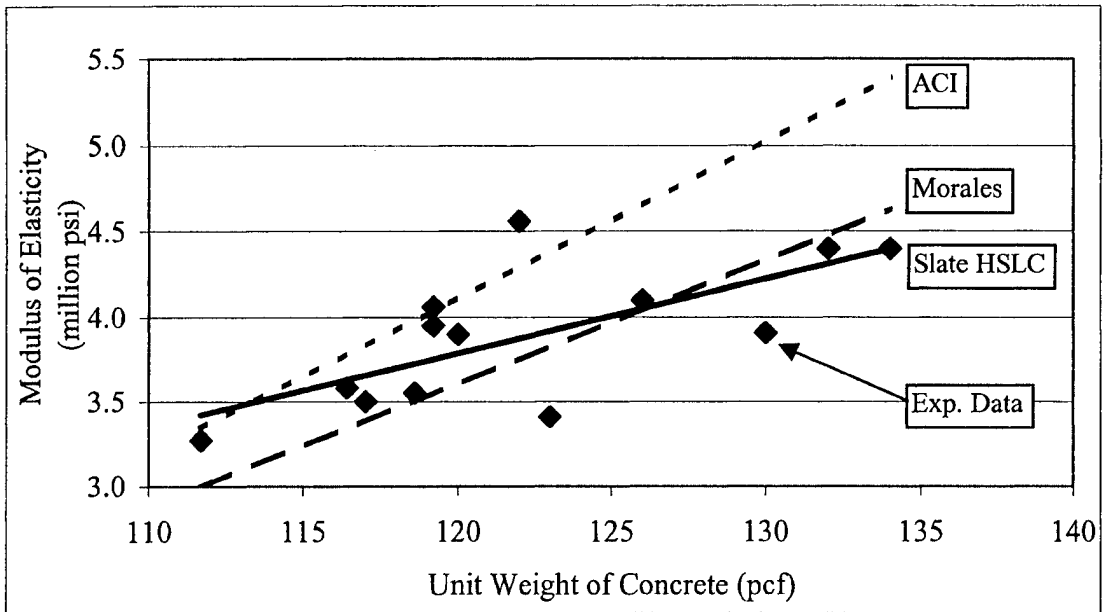
Figure 3.5 Modulus of Elasticity vs. Unit Weight of Concrete

48

The concrete strengths used were 8, 10 and 12 ksi.. When designing with high strength NWC, it was assumed the concrete weight was 150 pcf, and the modulus was determined with Equation 2.1 based upon previous high-strength NWC research in Georgia.[66] When using HSLC, Equation 2.3 was used with different unit weights.

Based on the study of the thirteen slate mixes, it was apparent that variations in unit weight existed for a given strength. A range of unit weights was established for each HSLC strength based on observed upper and lower limits. Table 3.2 shows the range of unit weights used in the study.

Table 3.2 Slate HSLC Unit Weight Values

Concrete strength f_c' (psi)		Unit Weight	
	Low (pcf)	Average (pcf)	High (pcf)
8,000	113	119	126
10,000	117	124	131
12,000	122	128	135

The variation in unit weights caused variations in modulus values as well as girder weights. Each bridge and girder design accounted for the differing modulus at release and final conditions. It is noted that of the strengths in Table 3.2, only the low unit weight 8,000 psi mix qualified as structural lightweight concrete according to the ACI definition.[2]

3.5 Analysis Results and Discussion

Figures 3.6 through 3.8 present the composite girder maximum simple-span length versus the girder's concrete compressive strength for AASHTO Type II through V sections, Bulb-Tee 54, 63 and 72 sections, and Modified Bulb-Tee 54, 63 and 72

49

sections. Shown in the figures are girders of high strength NWC and HSLC. The unit weights shown for HSLC are the "low" and "high" values listed in Table 3.2 to provide the range of results by concrete unit weight for each concrete strength.

3.5.1 Effect of Concrete Strength and Unit Weight on Girder Span Length

3.5.1.1 AASHTO Type II – V Sections

Girder span lengths using 8 ksi HSLC could be extended by up to about 4 percent (7 feet for 140-foot girders) as shown in Figure 3.6. The most significant length increases resulted from the use of the lightest concrete unit weight. The increase in length for Type II and III sections was less than for Type IV and V sections implying the use of HSLC provided the most significant benefit for girders with lengths over approximately 105 feet. Figure 3.6 also indicates there is little benefit to using concrete over 10 ksi strength in Type V sections. Length increase is proportional to the amount of reinforcement that can be located in the bottom flange.[64] At maximum lengths for Type V sections, the total strands possible were used in the bottom flange with 10 ksi concrete.

HSLC girder maximum live load deflections resulting from HS 20-44 loading increased between 15 and 22 percent on average when compared to girders of high-strength NWC. The lighter concrete unit weights experienced the greatest deflections; however, deflections were at most 85 percent of the AASHTO[40] maximum allowable L/800 requirement (where L is the span length) compared to 57 percent for high-strength NWC. Further, the natural period of vibration increased by less than 19 percent when HSLC was used compared to high-strength NWC for the 10 ksi Type IV girders.

50
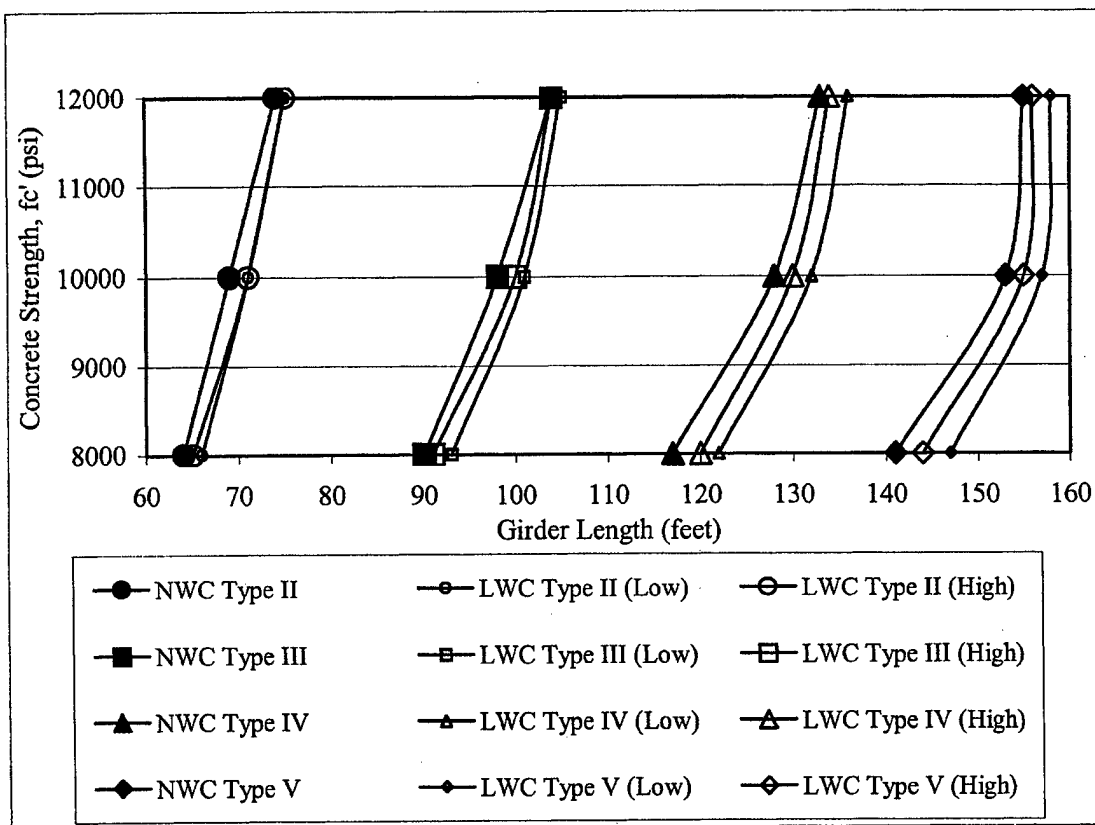
Figure 3.6 Concrete Strength vs. Maximum Length for AASHTO Girders

3.5.1.2 Bulb-Tee Sections

Figure 3.7 shows trends similar to those for AASHTO sections. HSLC with a strength of 8 ksi provided a length increase up to about 3 percent (3 feet for 110 foot girders). The major difference from AASHTO sections was that Bulb-Tee sections showed a consistent benefit from using concrete strengths up to 12 ksi. Based on the improved efficiency of the Bulb-Tee sections, there was not an observed plateau within the strength range investigated for the constant 7-foot girder spacing. Live load deflections of Bulb-Tee sections averaged at most 70 percent of the AASHTO maximum

51

allowable L/800. The natural period of vibration for a HSLC 135-foot, 63-inch deep

Bulb-Tee girder increased by less than 17 percent compared to that of a high-strength

NWC girder.
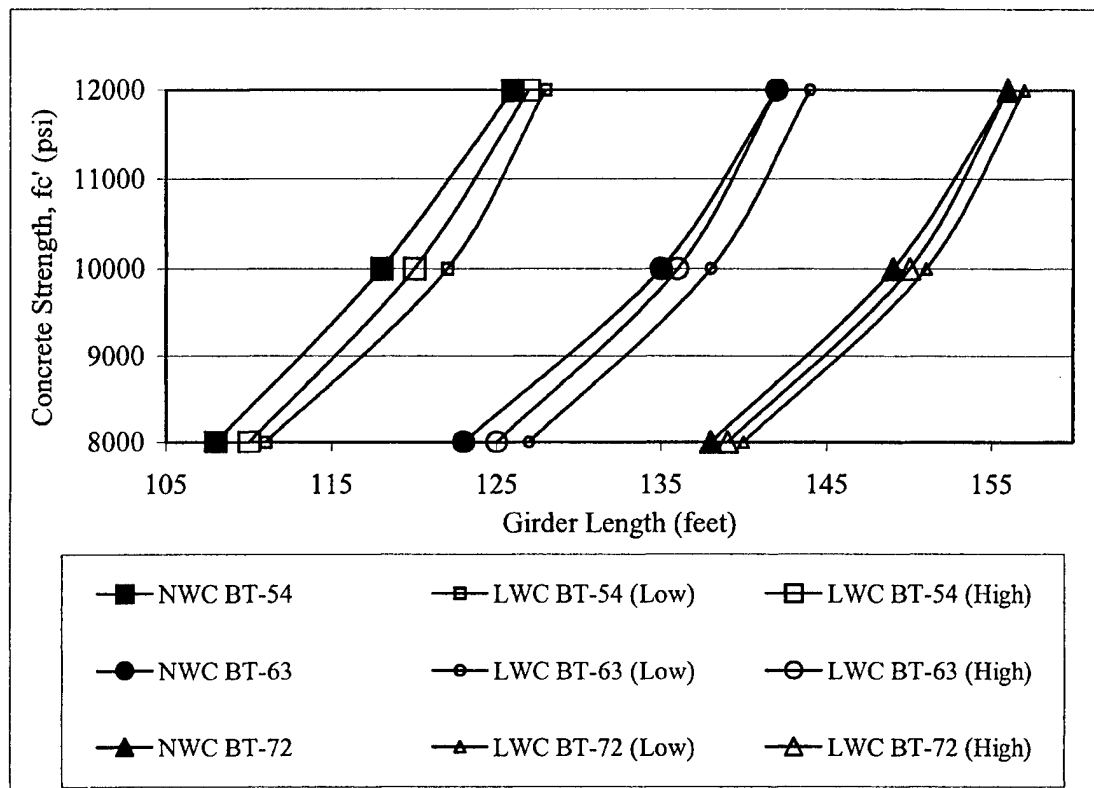
Figure 3.7 Concrete Strength vs. Maximum Length for Bulb-Tee Girders

3.5.1.3 Modified Bulb-Tee Sections

Figure 3.8 shows that Modified Bulb-Tee sections behaved in a similar manner to

the Standard Bulb-Tee sections. The greatest percent increase in length was gained with

8 ksi HSLC at about 3 percent (4 feet for 146-foot girders). The addition of a row of

pretensioning strands in the bottom flange allowed an increase in length of about 10 feet

at all strengths of concrete for all sections in comparison to Standard Bulb-Tee sections. Live load deflections were again well within the maximum allowable L/800 limit and averaged 64 percent of the allowable.

The additional strands and 2-inch increase in depth would allow designers to use a shallower section to reach lengths previously achievable only with the next larger size Bulb-Tee section. For the HSLC 156-foot, 65-inch deep Modified Bulb-Tee girders, the natural period of vibration increased by less than 15 percent compared to that of a high-strength NWC girder.

3.5.2 Weight Reduction Based on the Use of HSLC

The most significant advantage gained through the use of HSLC was overall girder weight reduction. Through the use of HSLC, it was possible to lower the GVW below the 150 kip threshold for the target 150-foot girder. The GVW was determined by adding the resulting girder weight to the estimated weight of an appropriate transport truck and trailer. Table 3.3 shows information related to Georgia permitting requirements for overweight cargo as provided by the Georgia DOT.
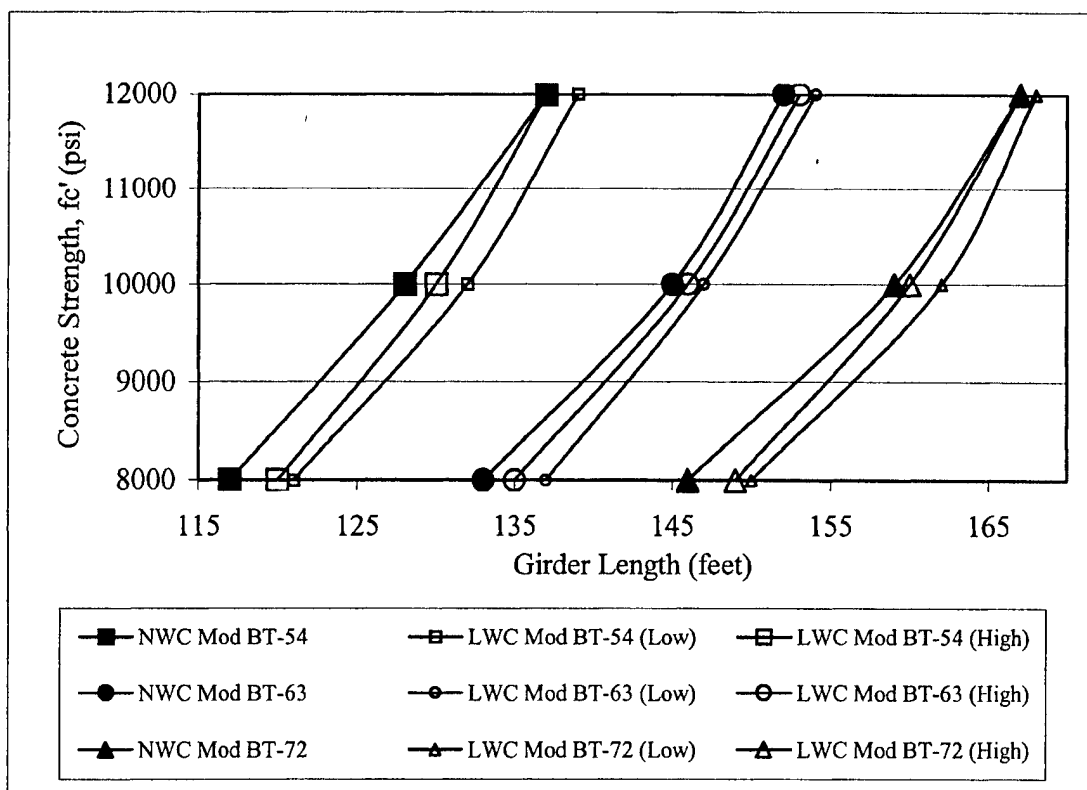
Figure 3.8 Concrete Strength vs. Maximum Length for Modified Bulb-Tee Girders

Table 3.3 Permitting Requirements for Overweight Cargo in Georgia.

Load category	Gross vehicle weight range (kips)	Estimated vehicle weight (kips)	Maximum girder weight (kips)	Permit type	No. of axles required
1	0 < GVW ≤ 80	40	40	None	NA
2	80 < GVW ≤ 125	40	85	Regular	6
3	125 < GVW ≤ 150	45	105	Regular	7
4	150 < GVW ≤ 160	50	110	Superload	8
5	160 < GVW ≤ 175	52.5	122.5	Superload	9
6	175 < GVW ≤ 180	55	125	Superload	10
7	180 < GVW	55+	125+	Superload	>10

Note: 1 kip = 454.5 kg.

54

It was difficult to provide exact data on weights and permitting requirements due to variations in tractor-trailer rig configurations and capabilities; however, Table 3.3 provides some average values that would be expected. Figure 3.9 illustrates the GVW for each of the maximum length girders for the ten sections using high-strength NWC at 8 ksi strength. Similar graphs were created for 10 and 12 ksi high-strength NWC and HSLC. The collective results of GVW, maximum girder length, and section type are shown in Figure 3.10. Since it was seen that AASHTO Type II and III girders showed little benefit from HSLC, they were not included in graph.
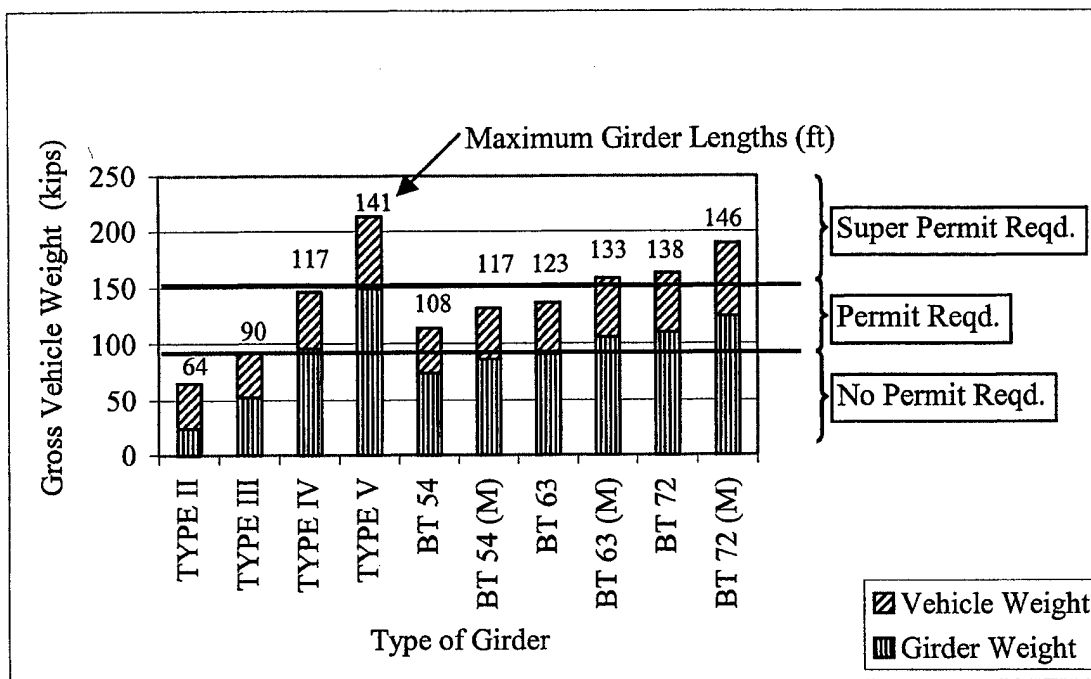
Figure 3.9 GVW by Girder Type, With Maximum Length Labeled, Based on 8 ksi NWC

Within Figure 3.10, there are three data points for each section listed. The three points correspond with the three strengths of concrete. In each case, the leftmost of the

55

three points represents 8 ksi. The center point represents 10 ksi, and the rightmost point

represents 12 ksi. The average unit weight given in Table 3.2 was used for the

lightweight (L) sections while a constant 150-pcf unit weight was used for the normal

weight (N) sections.
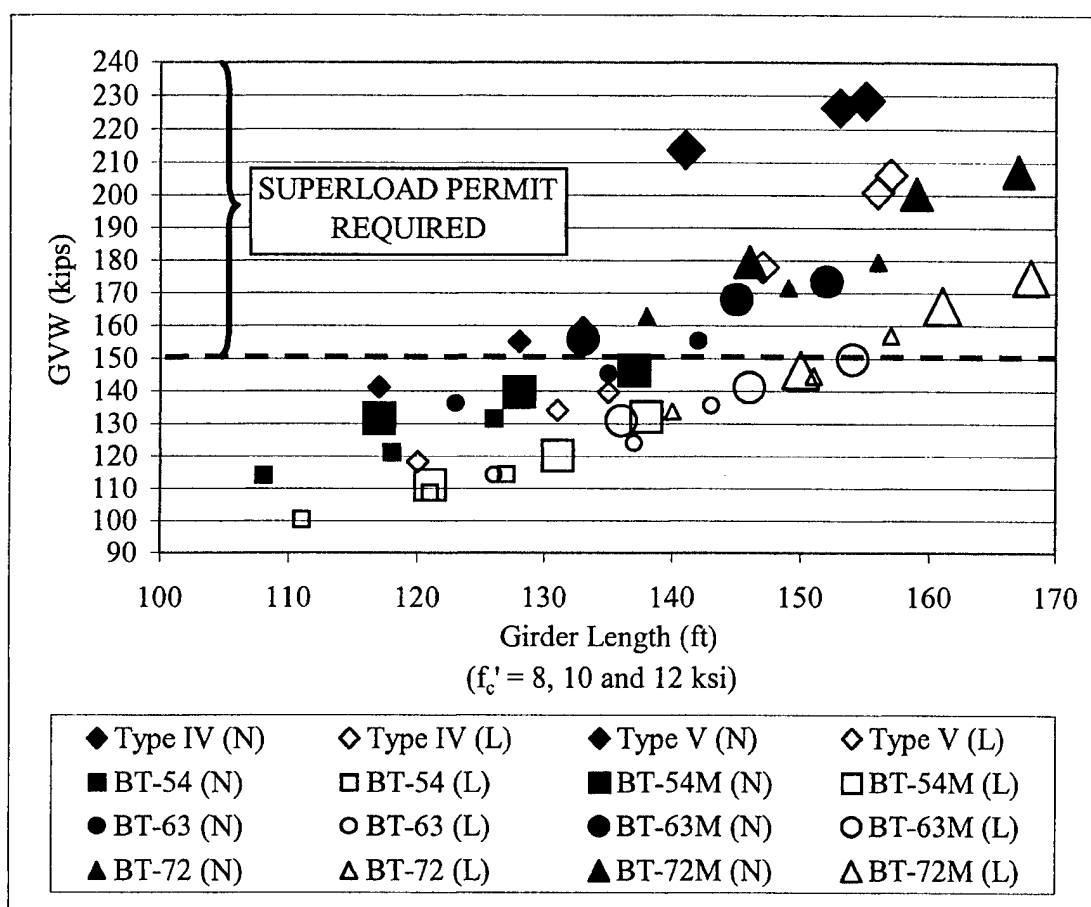
Figure 3.10 Gross Vehicle Weight vs. Maximum Girder Length

The most important finding was that it was possible to reach the target span of

150 feet without exceeding the 150 kip GVW limit through the use of HSLC. There were

three HSLC girders that satisfied the requirement: Modified BT-63 (12 ksi), BT-72 (10

ksi) and Modified BT-72 (8 ksi). Further economic analysis and a review of site constraints would be required to select the best possible alternative. For spans between 125 feet and 135 feet, Type IV lightweight girders were less than the 150 kip GVW while Type IV normal weight girders exceed the 150 kip GVW limit. Based on the parameters of this study, AASHTO Type IV and V sections were less efficient than similar height Bulb-Tee sections, both Standard and Modified.

If the AASHTO Type IV and V sections are removed from the chart, there are noticeable trendlines for the remaining normal weight and lightweight Bulb-Tee girders. The trendlines demonstrate the benefit in terms of GVW that result from the use of HSLC. The trendlines converge for girder lengths less than 105 ft (32 m) and diverge as girder lengths increase from that point.

3.6 Conclusions

Based on the results of this analytical investigation, the following conclusions were made:

The use of HSLC has the potential to increase the length of simple span AASHTO sections up to four percent and Bulb-Tee sections up to three percent.

For spans between 125 feet and 155 feet, the use of LWC can reduce the gross vehicle weight to less than 150 kips (68,200 kg) so that a superload permit is not required for transport of long span girders as compared to the need for a superload permit when normal weight concrete is used.

AASHTO Type II and III sections do not benefit appreciably from the use of HSLC. The Modified Bulb-Tee section extended the length of a Standard Bulb-Tee by 10 feet using 8, 10 and 12 ksi HSLC or high-strength NWC.

Bulb-Tee (Standard or Modified) sections provided longer spans at less weight for girders over 105 feet in length when compared to AASHTO sections.

CHAPTER IV

MATERIALS, MIXING AND TESTING OF HSLC

4.1 Introduction

The purpose of this chapter is to discuss the materials used, the methods of mixing, and the testing methods used in designing and then producing HSLC. Specific comments on mix design development, field production and material properties are addressed in Chapters 5, 6 and 7, respectively.

4.2 HSLC Components and Properties

4.2.1 Coarse Aggregate

The most important factor in creating a lightweight concrete that has high strength and high modulus of elasticity is the LWA. The coarse aggregate used during this project was a slate LWA provided by the Carolina Stalite Company, Salisbury, North Carolina. As described in Chapter 2, the Stalite LWA is a high-quality aggregate with a tight pore structure. Three different size gradations were used during this research including 3/8-inch, 1/2-inch and 3/4-inch. The 1/2-inch gradation was used predominantly during development and testing. The 3/8-inch aggregate was used in trying to exceed 12,000 psi strength. The 3/4-inch aggregate had a very limited use during this project because of its lower strength plateau.

When crushed, Stalite LWA takes on an angular appearance as shown in Figure

4.1. Figure 4.2 shows the LWA in clinker form, the way it appears upon exiting the

rotary kiln. Note the voids in the LWA clinker that reduce its weight and specific

gravity. Table 4.1 provides the specific gravity, weight, and gradation for the 3/8-inch

and 1/2-inch aggregate used during this research.
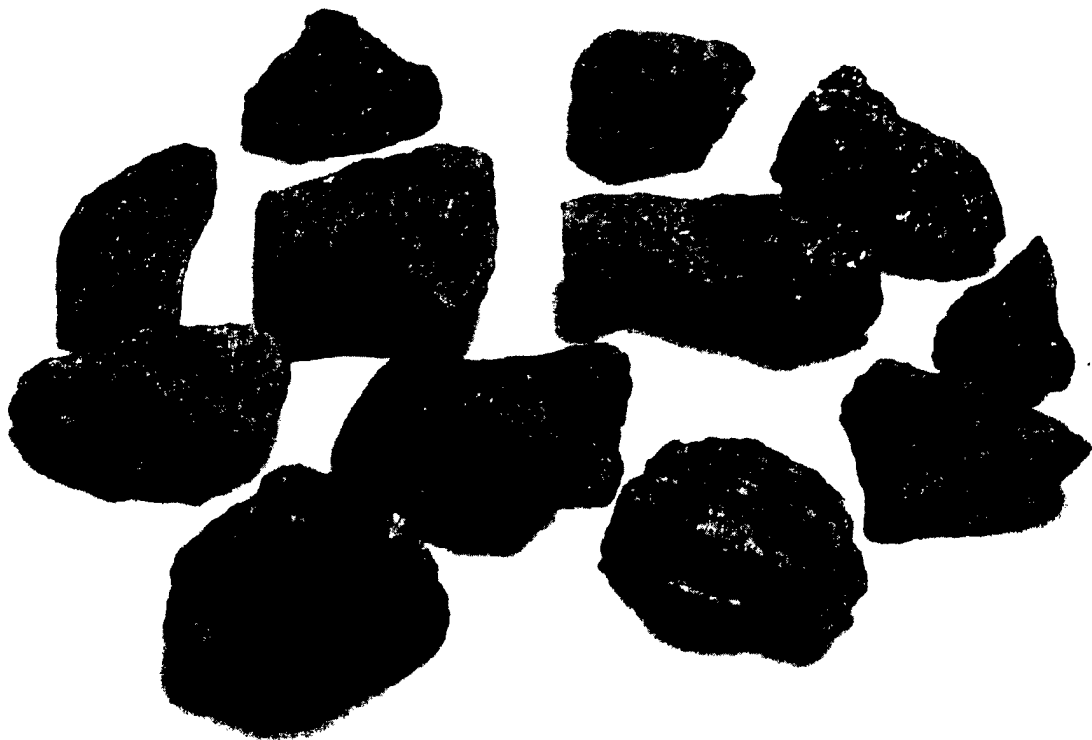
Figure 4.1 Crushed Slate LWA (3/4-inch Particles) From Carolina Stalite
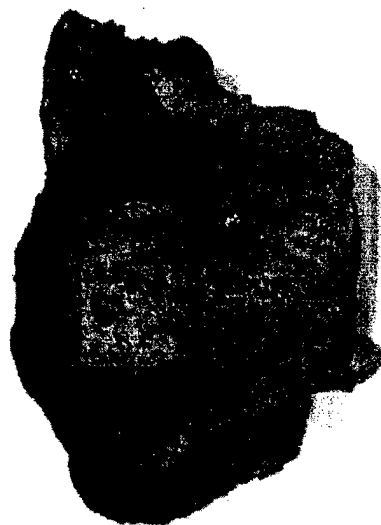
Figure 4.2 Close-up of Slate LWA Clinker Showing Voids

Table 4.1 Stalite LWA Specifications

Aggregate Size	3/8-inch		1/2-inch	
Oven Dry Specific Gravity	1.52		1.44	
Unit Weight Damp Loose (pcf)	50 - 54		48 – 52	
Absorption 24-hr Soak After Oven Dry (Maximum Absorption)	6 % (10 %)		6 % (10 %)	
Sieve Size	Percent Passing	ASTM[67] C 330 Specification	Percent Passing	ASTM[67] C 330 Specification
¾-inch	100	100	100	100
½-inch	100	100	90	90-100
³/₈-inch	100	75-100	53	40-80
#4	33	20-45	12	0-20
#8	3	0-15	5	0-10
#100	2	0-10	NA	NA

LWA specific gravity values were checked on several occasions using a technique outlined by Holm as addressed in Section 2.5.5.[24] For comparison purposes, normal weight aggregate has a specific gravity in the range of 2.60-2.65 and a maximum absorption of about 2 percent.

4.2.2 Fine Aggregate

Initially, lightweight fines were used in mix development. Low strength values and the inability to control water absorption resulted in termination of lightweight fines. Locally available normal weight fine aggregate known as Brown Brothers (BB) natural concrete sand was used. BB sand was approved for structural concrete use by GDOT and resulted in better strength and mixes that were easier to control. The BB sand had a fineness modulus of 2.36, which is low for use in structural concrete. Table 4.2 lists the specifications of BB sand and shows how the sand meets DOT specifications but fails to meet ASTM specification C 33.[68]

Table 4.2 Brown Brothers Natural Concrete Sand Specifications

Oven Dry Specific Gravity	2.62		
Fineness Modulus	2.36		
Percent Absorption	0.5 %		
Sieve Size	Percent Passing	ASTM C 33 Percent Passing	DOT 801.02D Percent Passing
# 4	100	95-100	95-100
# 8	98.6	80-100	
# 16	90.3	50-85 *	45-95
# 30	59.3	25-60	
# 50	14.8	10-30	8-30
# 100	1.3	2-10 *	1-10
Pass / Fail (*)		Fail	Pass

4.2.3 Overall Aggregate Gradation

Evaluations of the overall gradation of the coarse LWA and fine NWA combined indicated gaps in the grading for the # 8 and # 16 sieve sizes, but overages in the 3/8-inch, #4, and #50 sieve sizes.

4.2.4 Portland Cement

Type III cement supplied by Blue Circle Materials (now LaFarge) was used throughout mix design development based on the need to achieve early strength for prestressed girder construction. Type III cement has a higher Blaine fineness modulus than Type I and has higher contents of C_3S and C_3A causing hydration to occur more rapidly.[69]

The field-mixing phase (Chapter 6) of the research project was conducted at Tindall Concrete in Jonesboro, Georgia. Tindall used only Demopolis Type III Cement produced by CEMEX-Southdown Corporation. It was discovered that the Demopolis Type III provided better early strength than the Blue Circle – LaFarge Type III. Demopolis Type III cement was also used for girder production.

Cement grind specifications were not available for either brand of cement. Plant officials and quality control inspectors reported that the cements were ground in accordance with ASTM C 150.[70]

4.2.5 Mineral Admixtures

Silica fume and Class F fly ash were used in this research to improve concrete quality and durability, workability, and economy. The silica fume used in this project

was provided by Grace Construction Products under the name of Force 10,000. The silica fume had a specific gravity of 2.2 and was included in mix designs in amounts of 2 to 10 percent of total cementitious materials by weight.

Boral Material Technologies provided the Class F fly ash used in this project under the name of "Bowen" ash. The fly ash was produced at the Georgia Power Generating Plant located in Bowen, Georgia. The Bowen fly ash had a specific gravity of 2.28 and was included in mix designs as 15 percent of cementitious materials by weight. The fly ash satisfied the requirements of ASTM C 618.[71]

4.2.6 Chemical Admixtures

The chemical admixtures, all provided by Grace Construction Products, included ADVA Flow, a high-range water reducer (HRWR), WRDA 35, a water reducer/set retarder, and Daravair 1000, an air-entraining admixture (AEA). ADVA Flow satisfied the requirements of ASTM C 494[72] Type F; the WRDA 35 satisfied the requirements of ASTM C 494[72] Type A and D; the Daravair 1000 satisfied the requirements of ASTM C 260.[73]

4.3 Moisture Control

Control of moisture and accurate determination of moisture content were two of the most important steps involved in making high quality HSLC. Low absorbed moisture in the LWA can result in mix water being absorbed thus reducing workability and changing the water cement ratio. Excess adsorbed water that is not properly accounted for in the mix design also impacts the mix by affecting the aggregate proportion and also

64

the water cement ratio. The following sections describe steps taken during the project to insure moisture was properly controlled in the lab. Moisture control in the field is addressed in Chapter 6.

4.3.1 Laboratory Material Storage

The LWA was initially stored in large sacs in the lab. Prior to using the aggregate, it was soaked in buckets overnight to insure the absorbed moisture content was adequate. The trouble with soaking aggregate in buckets was that the method was not something possible under plant conditions for the production of large amounts of HSLC. If a method did not transfer to plant operations, it was not used in the lab.

Aggregate storage hoppers were procured and installed outside the lab facility. A misting device was installed in the top of each hopper and run continuously until the aggregate had adequate absorbed moisture. Adequate absorbed moisture was 6 percent; anything below 6 percent was unacceptable.

The initial stages of mix development were conducted during the winter months when outside temperatures often dipped well below freezing at night. Often times, the water misted onto the LWA froze requiring that it be chipped from inside the hoppers. In the event this occurred, the aggregate was allowed to warm inside the lab prior to mixing concrete. Later in the development phase, hoppers were installed inside the lab where the temperature was above 55 degrees Fahrenheit at all times. Figures 4.3, 4.4, and 4.5 show the aggregate hoppers (outside and inside) and the misting devices as installed inside the lab facility. The misting devices were constructed with nozzles having an output of approximately 3 gallons per hour. The water flow through the aggregate was minimized

to prevent segregation of fine particles from occurring. To reduce the gradient of free moisture inside the hoppers, the water was turned off 24 hours prior to concrete mixing. The normal weight BB sand was also stored inside the lab in a hopper.
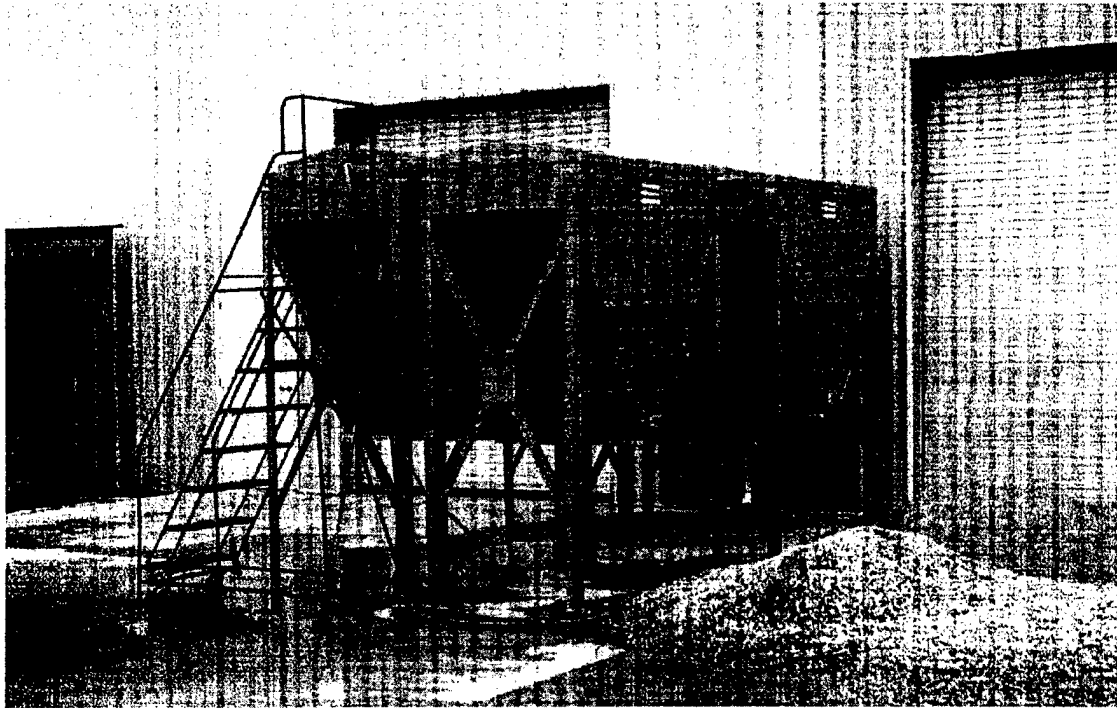
Figure 4.3 Exterior Aggregate Hoppers

Figure 4.4 Interior Aggregate Hoppers and Cement / Admixture Proportioning Station
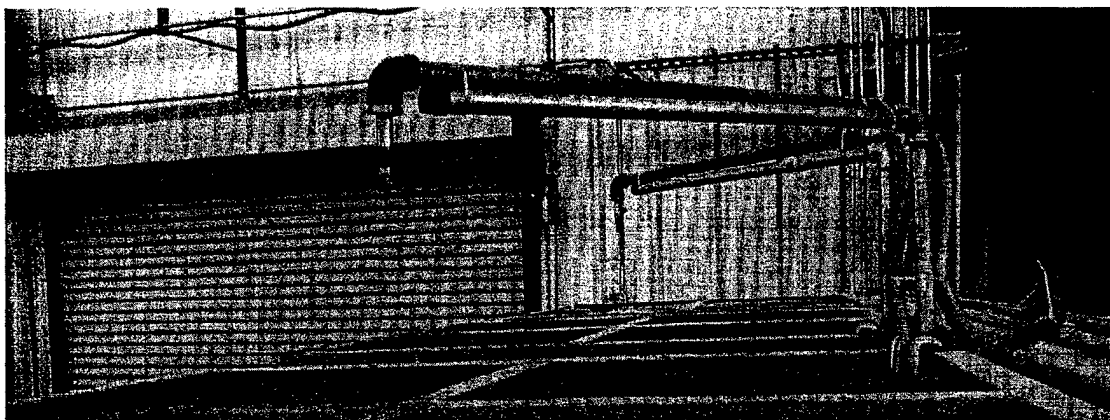
Figure 4.5 Misting Device Installed Over Interior Aggregate Hoppers

4.3.2 Determination of Moisture Content

Prior to mixing HSLC, a representative sample was taken from the aggregate hopper or stockpile. Moisture contents in the "as-is" and "saturated surface dry (SSD)" condition were determined from the representative sample by cooking the LWA over hotplates at a medium heat for approximately 1 hour or until all moisture had been removed. When LWA is heated, the internal pore water boils and explodes in a violent manner. To prevent flying aggregate particles from injuring people close by, screens were placed over top of the pan during cooking as shown in Figure 4.6.
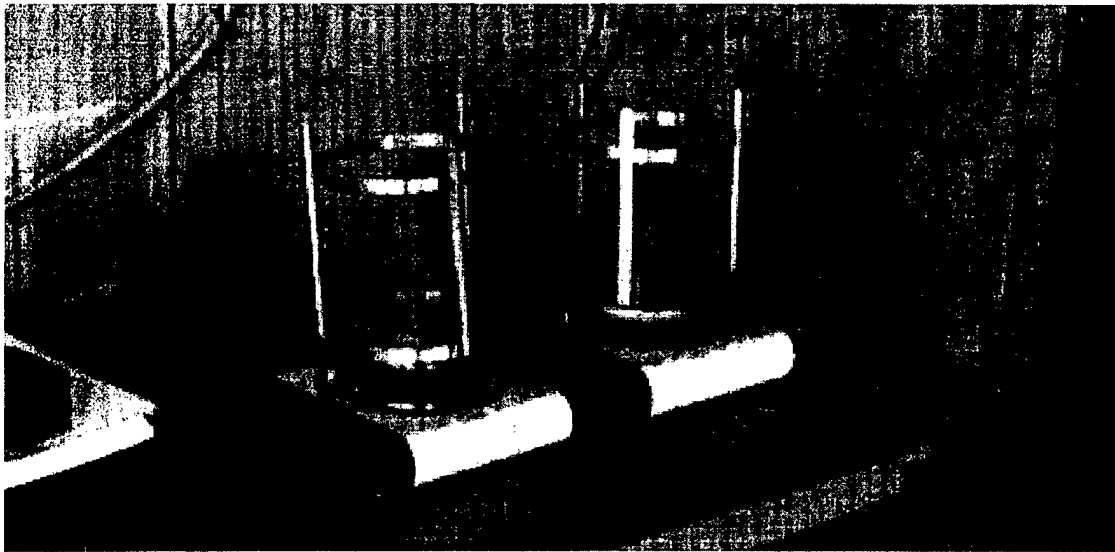
Figure 4.6 Screens Covering LWA During Moisture Test

When performing the "SSD" moisture check, the aggregate sample was placed on several layers of paper towels and patted dry prior to weighing. It was important to dry the aggregate sample to a point where there was no longer a shine on the surface.

Two methods were useful for determining when all moisture had been cooked

from the aggregate. If no moisture accumulated on a piece of glass held over the cooking

aggregate, it was dry. In addition, if the aggregate no longer "popped" it was considered

dry.

Moisture content checks were also performed on the BB sand whenever a mix

was made. Absorbed moisture was assumed to be 0.5 percent.

A material testing sheet was created as shown in Table 4.3 to simplify the testing

procedure and reduce chances for error. The moisture content calculation procedure is

explained on the sheet. Also covered in Table 4.3 is the determination of specific gravity

using a pycnometer, which is covered in ACI 211.2-91.[18]

4.4 HSLC Mix Designs

As addressed in Chapter 2, there was no method available "off-the-shelf" for

determining a mix design to achieve 12,000 psi HSLC. Previous mix designs and

guidance from Stalite representatives provided the initial HSLC mix designs in this

research. Based on suggestions from several sources, a mix design spreadsheet was

developed to automate the numerous calculations required for a HSLC mix design.

Appendix B provides an example of the spreadsheet and gives details on its use. The

development of mix designs is covered in detail in Chapter 5, Development of HSLC

Mix Designs.

Table 4.3 Material Testing Sheet

Lightweight Concrete Material Testing Sheet

Test Date / Location   _____

Technician Name   _____

Aggregate Moisture Content Testing

Time Test Started _____   Time Test Finished _____

Test Description   _____ _____ _____ _____

A – Weight of Wet Aggregate and Pan   _____ _____ _____ _____

B – Weight of Pan   _____ _____ _____ _____

C – Weight of Wet Aggregate (A – B)   _____ _____ _____ _____

D – Weight of Dry Aggregate and Pan   _____ _____ _____ _____

E – Weight of Dry Aggregate (D – B)   _____ _____ _____ _____

F – Weight of Water (C – E)   _____ _____ _____ _____

G – Percent Moisture (F / E) x 100   _____ _____ _____ _____

Aggregate Specific Gravity Testing

Time Test Started _____   Time Test Finished _____

Test Description   _____ _____ _____ _____

A – Wt. of Pycnometer w/Agg. & Water   _____ _____ _____ _____

B – Wt. of Pycnometer w/ Water   _____ _____ _____ _____

C – Wt. of Aggregate   _____ _____ _____ _____

SG = C / (C + B – A)   _____ _____ _____ _____

4.5 Concrete Mixer

The concrete mixer used for all laboratory mixes was a pan mixer, model 30 DP, manufactured by Lancaster and shown in Figure 4.7.
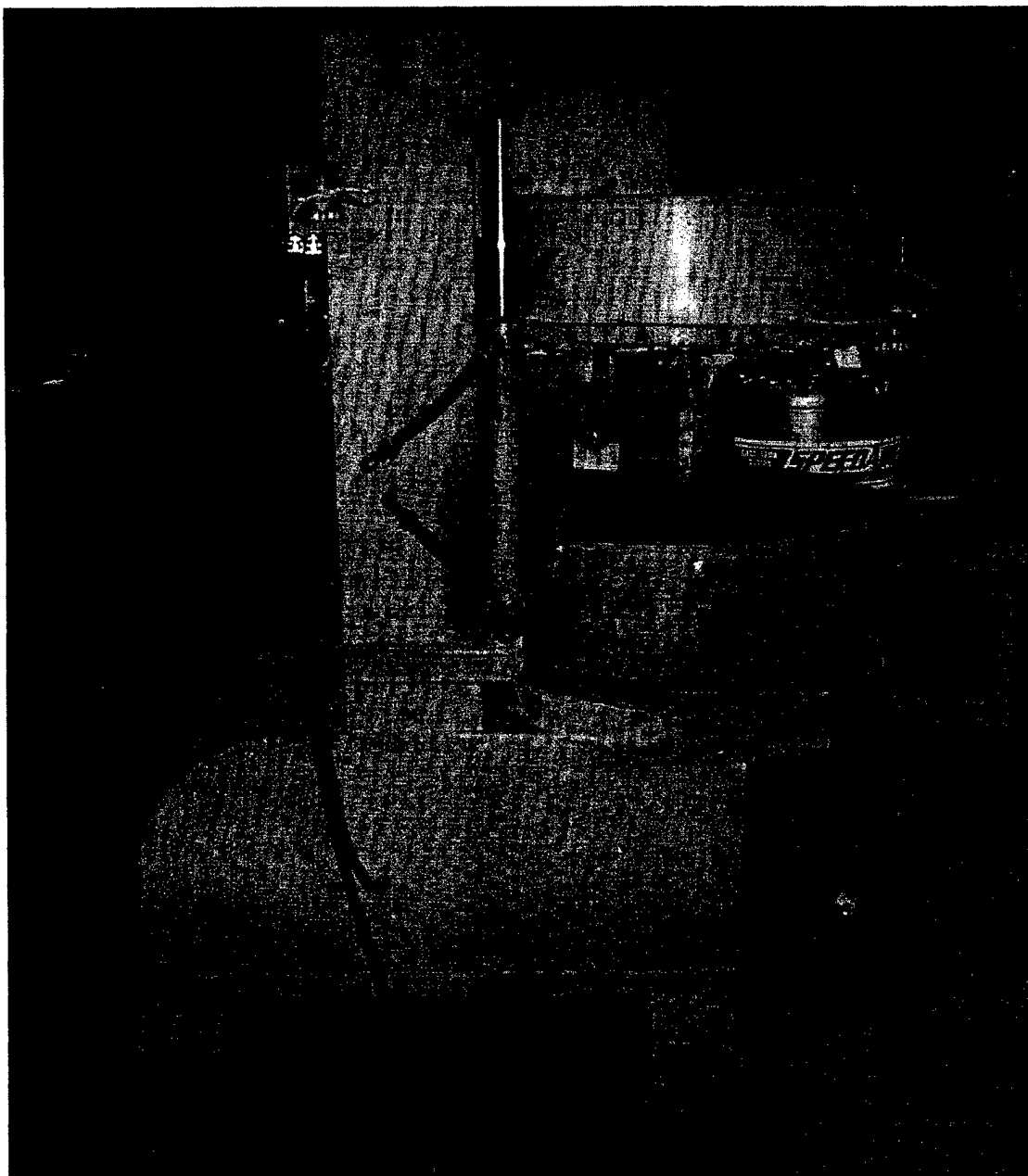
Figure 4.7 Lancaster Model 30 DP Pan Mixer

The Lancaster mixer operated with a shearing type action. The maximum amount of concrete that could be mixed in one batch was 1.75 cubic feet. Some trial mixes were made in a 4 cubic foot rotary mixer. The resulting mixes were poor; cylinder strengths were significantly lower than identical mixes made using the Lancaster mixer.

The concrete mixer used for field mixes is addressed in Chapter 6.

4.6 Order of Mixing

Components were added to the HSLC mixes in the following specific order. This order was developed over time and produced the best results.

1. Coarse Aggregate (Slate LWA)

2. Fine Aggregate (BB Natural Sand)

3. Approximately 2/3 of mix water combined with WRDA 35 (LRWR)

4. Daravair 1000 (AEA)

5. ADVA Flow (HRWR)

6. Type III Portland Cement

7. Class F Fly Ash

8. Remaining water / WRDA 35 mixture

9. Silica Fume

10. Additional ADVA Flow to achieve the desired workability

When mixing during the winter months, hot water (approximately 100 degrees F) was added to compensate for the cold aggregate to promote early strength gain. Steps 1-5

were performed immediately following each other. The components in the pan after step 5 were allowed to mix for one minute to insure consistent distribution of the AEA and water reducing admixtures. After the addition of the silica fume, the components were allowed to mix for approximately 2-3 minutes to insure thorough mixing. Additional ADVA (Step 10) was tracked on the mix design sheet for future reference. The same component addition sequence was used for lab and field mixing with good success.

4.7 HSLC Properties

After batching the HSLC, four properties of the concrete were tested. The slump was measured using a standard slump cone per ASTM C 143.[74] The unit weight was measured with a 1/4 cubic foot bucket per ASTM C 138.[75] The temperature of the concrete was measured using ASTM C 1064.[76] The air content was measured with a roll-a-meter per ASTM C 173.[77]

A common misconception is that air content can be determined for LWC with a pressure meter per ASTM C 231.[78] Since the LWA is a porous material, the pressure test can force water into the pore structure resulting in an incorrect (high) air content reading. Close examination of ASTM C 231 reveals that the test is not to be used for LWC.

4.8 Preparation of Specimens

Specimens were made per ASTM C 31.[79] Cylinders size 4 inches x 8 inches (4 x 8) were cast for determining compressive strength per ASTM C 39.[80] Cylinders size 6 inches x 12 inches (6 x 12) were cast for determining modulus of elasticity per ASTM C 469.[81] Beams size 4 inches x 4 inches x 14 inches (4 x 4 x 14) were cast to perform the

modulus of rupture test per ASTM C 78.[82] Cylinders size 4 inches in diameter x 15

inches with DEMEC gage inserts were cast in steel molds for creep testing per ASTM C

512.[83] Figures 4.8 and 4.9 show casting a beam and creep specimen molds, respectively.

Figure 4.8 Casting 4 x 4 x 14 Modulus of Rupture Specimens at Tindall Concrete Plant
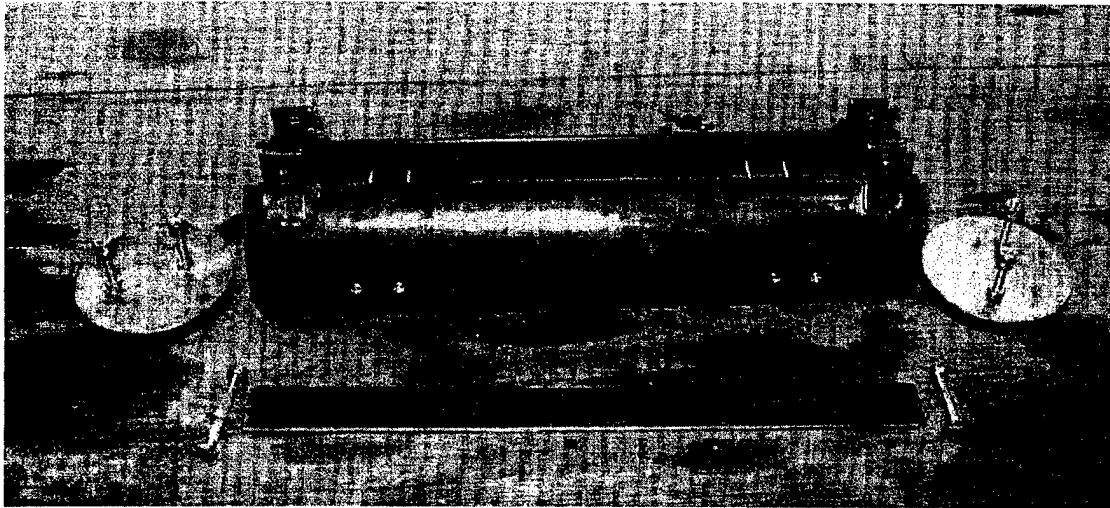
Figure 4.9 Specimen Mold for Creep and Shrinkage Testing

In addition to the standard specimen molds, a block measuring 24 inches x 12 inches x 36 inches was cast to allow coring cylinders for strength testing. During girder construction, a similar block 24 inches deep was cast to perform the prestressing strand direct pullout test. Figures 4.10 and 4.11 show construction of these two blocks.
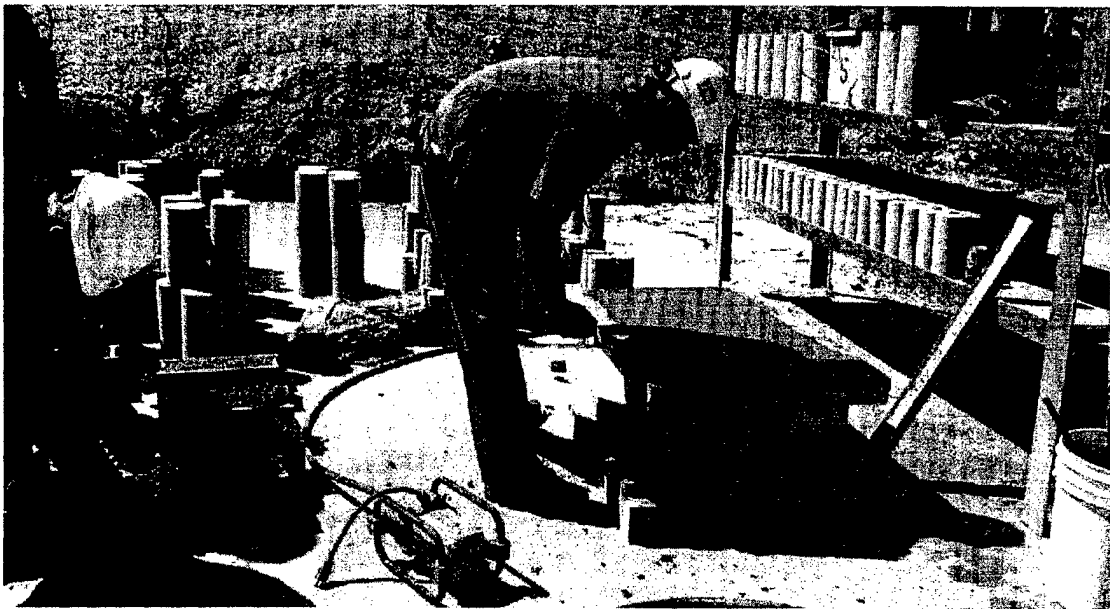
Figure 4.10 Construction of Block for Cored Cylinder Testing at Tindall Concrete Plant

Figure 4.11 Casting of Block for Direct Pullout Test at Tindall Concrete Plant

4.9 Specimen Curing

After casting specimens, the method of curing varied. Specimens were initially

cured either on site or in the lab as per ASTM C 31, or were placed in a curebox to retain

the heat of hydration. Accelerated curing using a curebox (Figure 4.12) was not covered

by any ASTM specification, but had been shown to closely replicate girder curing

conditions in previous research.[84] After 24 hours, all specimens (except cored cylinder

blocks and direct pullout test blocks which remained on site for 56 days) were removed

from molds and placed in a fog room for curing through the time of testing. The fog

room maintained 100 percent humidity and a temperature of approximately 73 degrees

Fahrenheit. Moduli of rupture specimens were cured in a lime bath in the fog room until

the time of testing.

76
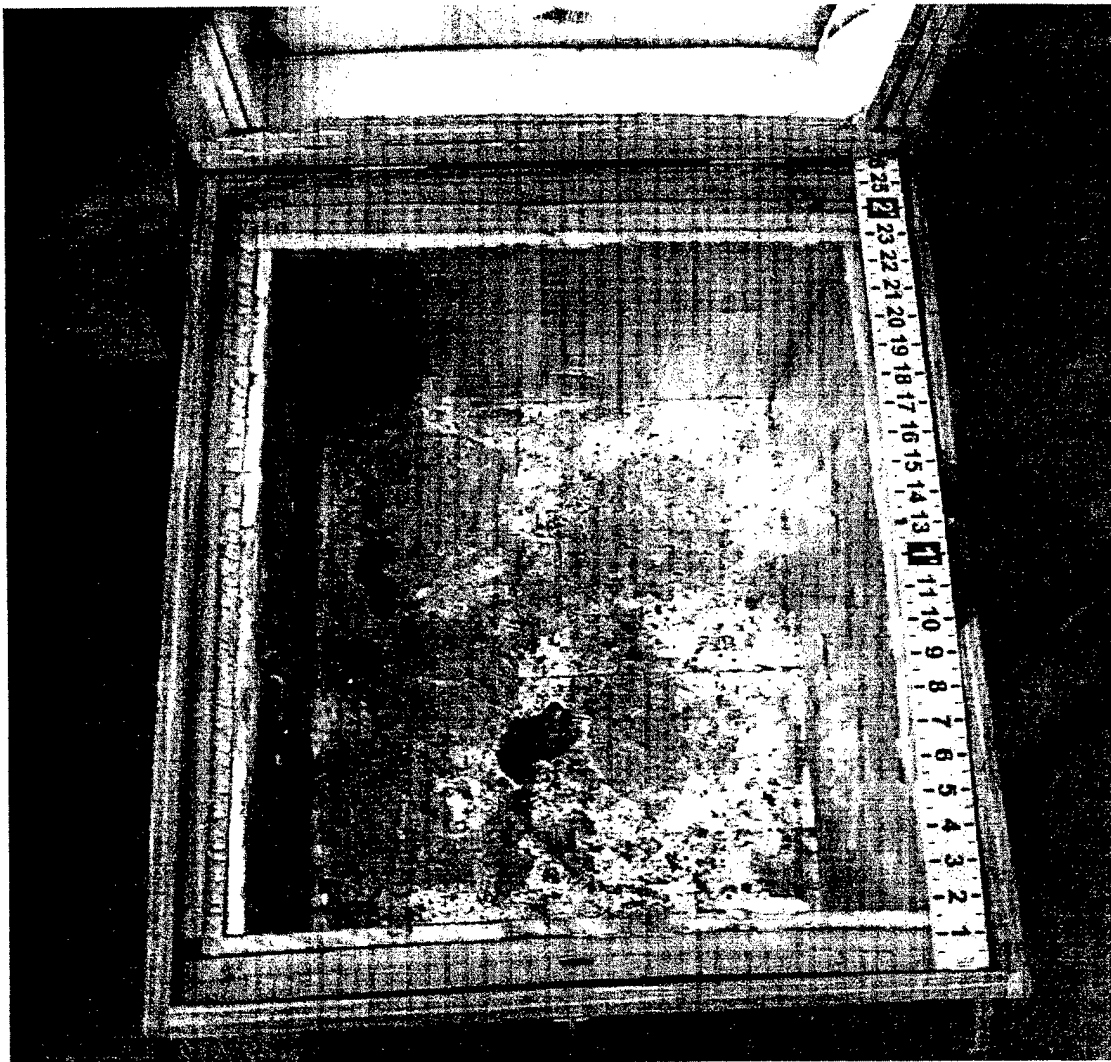
Figure 4.12 Insulated Curebox Used for Accelerated Curing

After placing specimens in the curebox, any remaining empty space around the specimens was filled with an insulating fabric.

4.10 Specimen Testing

Specimen testing was performed at specified times depending on the type of mix and phase of the research project. All tests were performed in accordance with the appropriate ASTM specification as follows.

4.10.1 Compressive Strength

Compressive strength testing was performed according to ASTM C 39[80] using hard rubber caps seated in steel end caps according to ASTM 1231.[85] The hard rubber caps were cut from 1/2-inch conveyor belt material and reused as long as the surface condition did not show signs of wear. Based on testing HSLC, a set of rubber caps could be used to test from 30 to 50 cylinders prior to replacement. Prior to testing, the cylinder ends were smoothed as necessary to remove ridges or bumps that could affect strength results.

4.10.2 Modulus of Elasticity

Modulus of elasticity testing was performed according to ASTM C 469[81] using 6 x 12 cylinders and hard rubber end caps as described in 4.10.1. Prior to performing the test, the average compressive strength of three 4 x 8 cylinders was determined. Based on the 4 x 8 strength, the predicted ultimate load was calculated for the 6 x 12 as well as 40 and 60 percent of the ultimate value. The modulus test frame (Figure 4.13) was installed on the 6 x 12 cylinder and the specimen placed in the 400-kip Baldwin load test machine. The specimen was initially loaded to 40 percent of ultimate to seat the cylinder and modulus test frame.
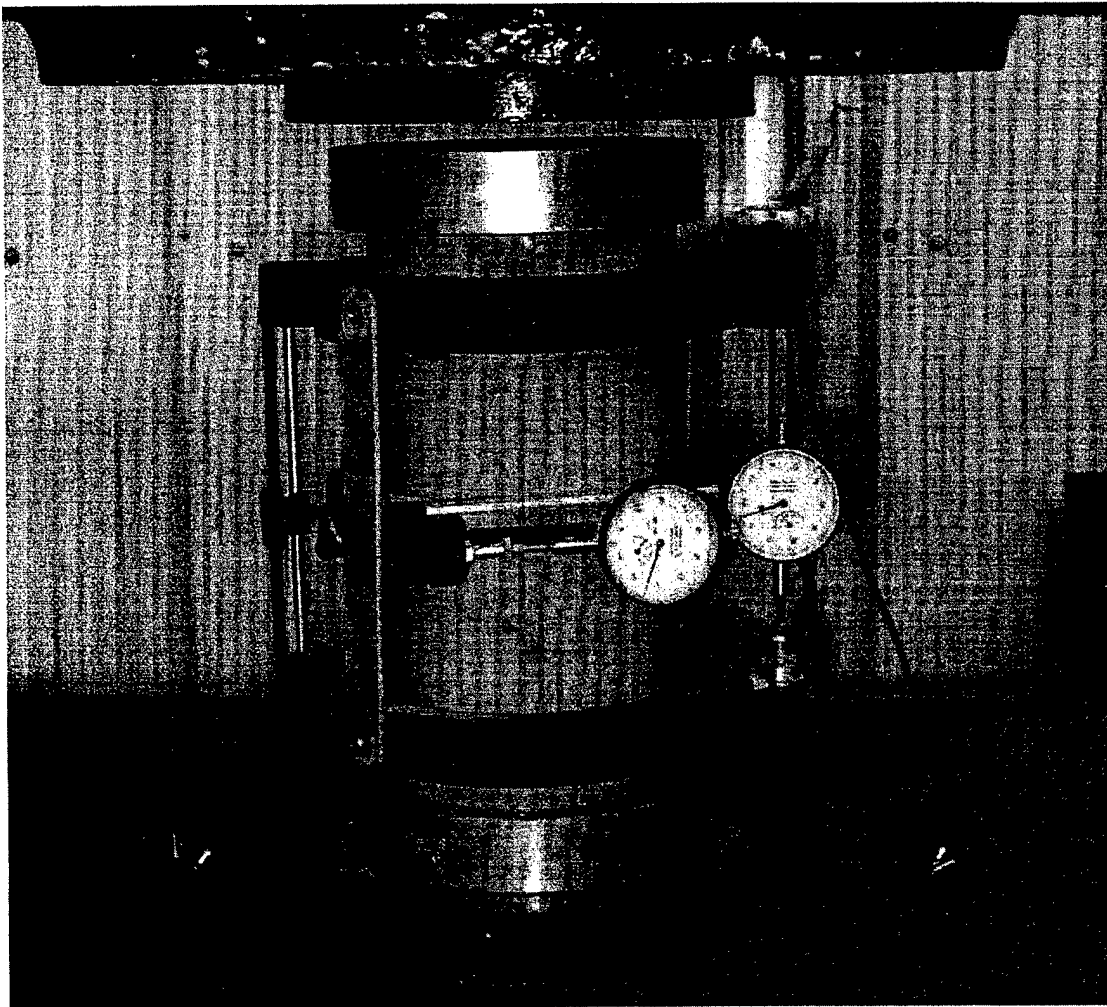
Figure 4.13 Modulus of Elasticity Testing Frame

After unloading the specimen, gages were zeroed and the specimen loaded to 60

percent of its ultimate strength. A data-taking sheet (Table 4.4) was created to simplify

the test procedure. Data from the sheet was entered into a spreadsheet, which then

determined the modulus of elasticity and Poisson's ratio. Critical to properly calculating

the modulus of elasticity and Poisson's ratio values were determination of lengths and

gage ratios from the test frame as per ASTM C 469.[81]

Table 4.4 Elasticity Modulus and Poisson's Ratio Test Data Sheet

Elasticity Modulus and Poisson's Ratio Data Sheet

Spec. Number _____ Date / Time _____ Est. Ult. _____ kips (4x8)

40% Est. Ult. _____ kips   60% Est. Ult. _____ kips   Ult. Load _____ kips (6x12)

Initial load to 40% of estimated ultimate accomplished to seat cylinder - yes / no.

Load cylinder (Tests A,B) to 60% of estimated ultimate while recording data below.

Longitudinal Gage Reading (inches)	Test A		Test B	
	Load (kips)	Lateral Gage Reading (inches)	Load (kips)	Lateral Gage Reading (inches)
0.00000				
0.0008				
0.001				
0.002				
0.003				
0.004				
0.005				
0.006				
0.007				
0.008				
0.009				
0.010				
0.011				
0.012				
0.013				
0.014				
0.015				
0.016				
0.017				
0.018				
0.019				
0.020				
0.021				
0.022				
0.023				
0.024				
0.025				
0.026				

4.10.3 Modulus of Rupture

The modulus of rupture was determined in accordance with ASTM C 78[82] using 4

x 4 x 14 beams tested using third-point loading. Figure 4.14 shows the modulus of

rupture test set-up.
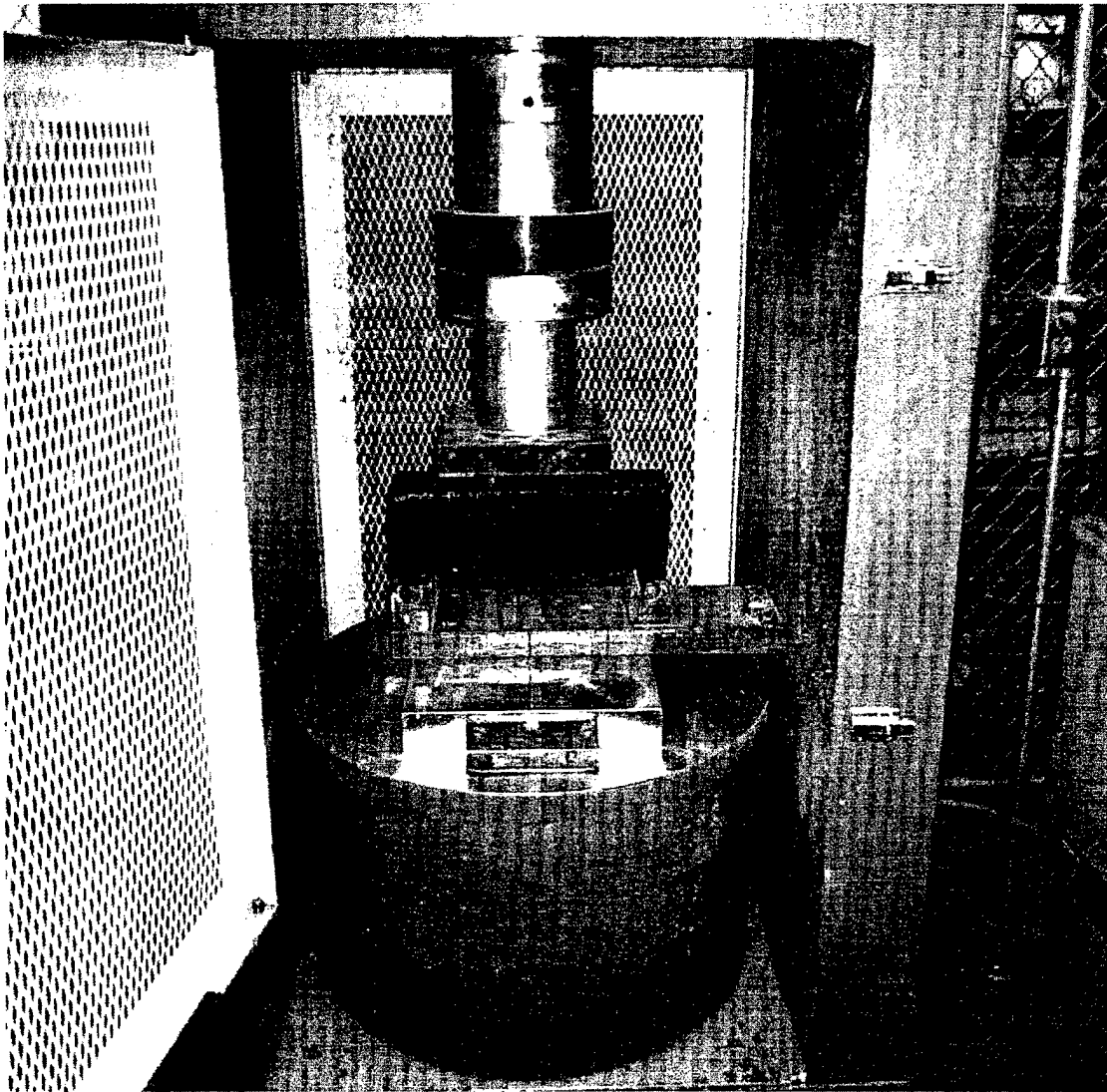
Figure 4.14 Modulus of Rupture Test Set-up

CHAPTER V

DEVELOPMENT OF HSLC MIX DESIGNS

5.1 Introduction

The purpose of this chapter is to discuss the laboratory development of the HSLC

mix designs that were later tested under field conditions and ultimately used to construct

pretensioned girders. The goal of this laboratory development phase was to configure

HSLC mix designs that would achieve 8, 10 and 12 ksi design compressive strengths at

28 days; the target mean compressive strengths were 1,400 psi greater than the design

strengths. In order to achieve those strengths, over 75 test mixes were batched and over

700 4 x 8 cylinders were tested.

5.2 Specimen and Curing Plan

The specimens cast during this phase predominantly 4 x 8 cylinders. The interest

initially was to configure mix designs to achieve the objective strengths. Thus, 9 each 4 x

8 cylinders were cast from each mix and cured initially in cureboxes. After 24 hours in

the curebox, 3 of the 9 cylinders were tested for compressive strength; the remaining 6

were placed in the fog room to continue curing for strength testing at 3 and 28 days.

5.3 Initial Mix Designs From Carolina Stalite

The starting points for the three objective HSLC mix design strengths were

suggested mix designs received from experts at Carolina Stalite and shown in Table 5.1.

Table 5.1 Initial HSLC Mix Designs from Carolina Stalite

Concrete Components to Produce 1 Cubic Yard of HSLC		Concrete Strength (psi)		
		8,000	10,000	12,000
1/2-inch Stalite LWA	(lbs)	950	950	950
Normal Weight Fine Aggregate	(lbs)	1221	1063	905
Class F Fly Ash	(lbs)	200	200	200
Silica Fume	(lbs)	35	45	56
Cement	(lbs)	500	650	800
Water	(gals)	32	33	34
Air Content	(percent)	4	4	4
Water / Cementitious Materials Ratio (W/CM)		0.36	0.31	0.27
Theoretical Equilibrium Unit Weight (pcf)		117.5	117.9	118.3

The coarse aggregate used in all initial mixes was the 1/2-inch Stalite LWA. Dosing on

chemical admixtures was not initially specified in the Stalite mixes. Literature from

Grace Construction Products and guidance from the local sales representative served as

starting points.

5.4 Plan for Mix Development

Below are listed the steps followed in determining the optimum HSLC mix

designs to meet the objective strengths.

1. Holding all other parameters steady, vary the ratio of coarse LWA to fine NWA

   over a wide range from approximately 1 to 2. Determine if an optimum coarse to

   fine aggregate ratio exists in that range.

83

2. Using the result of Step 1 and holding all other parameters steady, vary the percent cement paste in the mix from approximately 33 percent to 45 percent. Cement paste was defined as all components in the mix design except the aggregate. Determine if an optimum percent cement paste exists in that range.

3. Using the result of Steps 1 and 2 and holding all other parameters steady, vary the percent of silica fume in the mix from approximately 4 to 12 percent of the total cementitious materials (CM). Determine if an optimum percent silica fume exists in that range.

4. Using the results of Steps 1 – 3 (if possible), test the apparent optimum mix design with different size aggregates to determine the effect.

Based on the objective strength of 12,000 psi, a water to cementitious materials (W/CM) ratio of 0.23 was selected for mix proportioning.

5.4.1 Initial Mixes and Entrained Air

During the execution of Step 1, manufacturer suggested dose rates were followed for chemical admixtures. The first major problem encountered involved excessive air content. It became apparent over time that the air-entraining agent (AEA) was enhanced by the use of high-range water reducing (HRWR) admixture. In some cases, the resulting air contents approached 10 percent.

In order to determine specific details about the source of the air, and whether it was entrapped or entrained air, a study was conducted that was not part of the original development plan. The study involved making three batches of concrete as described in

Table 5.2. The 8,000 psi suggested mix design from Carolina Stalite was used for the test mixes.

Table 5.2 Air Content Study

Type of Coarse Aggregate	Admixtures Used	Resulting Percent Air Content
Normal Weight (Granite)	ADVA and WRDA 35	2.0
1/2-inch Stalite LWA	ADVA and WRDA 35	2.0
1/2-inch Stalite LWA	No Admixtures	2.0

The resulting air contents shown in Table 5.2 indicated that neither the use of LWA or the use of ADVA and WRDA 35 had an impact on air content. Since the air content was the same for each mix, it was apparent that the mix most likely had 2 percent "entrapped" air. In order to achieve 4 percent air content total, only 2 additional percent were required. This was an indication that most likely a small dose of AEA would result in 4% total air content. Future mixes were dosed with only 0.75 to 1.0 fluid ounces of Daravair 1000 (AEA) per 100 weight of cementitious materials. Since the HRWR enhanced the effectiveness of the AEA, less AEA was required at higher HRWR dose rates. Based on manufacturer literature, 0.75 fluid ounces per 100 weight of CM was the lowest recommended AEA dose rate.

5.4.2 Variation of Coarse to Fine Aggregate Ratio – Step 1

The coarse to fine aggregate ratio was defined as the volume of coarse aggregate divided by the volume of fine aggregate. The parameters in Table 5.3 were held constant throughout all mixes in Step 1:

Table 5.3 Parameters Held Constant in Step 1

Water / Cementitious Materials Ratio	0.23
Percent Cement Paste	39
Fly Ash as Percent of Total Cementitious Materials	15
Silica Fume as Percent of Total Cementitious Materials	8
Type III Cement as Percent of Total Cementitious Materials	77

The results of Step 1 are shown in Table 5.4 and graphed in Figure 5.1.

Table 5.4 Results of Varying Coarse to Fine Aggregate Ratio – Step 1

Coarse to Fine Aggregate Ratio By Volume	1-Day Compressive Strength (psi)	3-Day Compressive Strength (psi)	28-Day Compressive Strength (psi)
0.94	8,070	8,960	10,100
1.09	8,550	8,860	10,350
1.26	8,980	9,090	10,360
1.46	9,130	10,440	11,020
1.71	7,830	9,370	10,020
2.01	6,820	7,970	10,610

Figure 5.1 indicates that the optimum coarse to fine aggregate ratio using 1/2-inch

Stalite LWA was approximately 1.46. The resulting strengths did not vary significantly,

yet indicated a trend.

A similar study using 3/8-inch Stalite LWA showed the optimum ratio also to be

approximately 1.5.
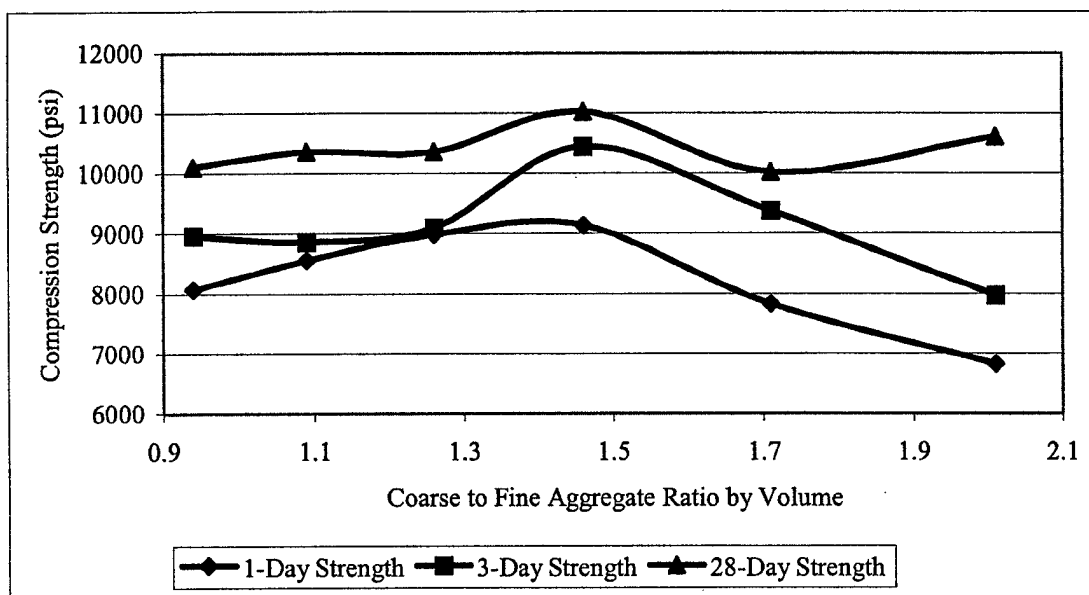
Figure 5.1 Results of Varying Coarse to Fine Aggregate Ratio

5.4.3 Variation of Percent Cement Paste – Step 2

Using the optimum coarse to fine ratio of 1.46 determined in Step 1, mixes were

configured for Step 2 where the percent cement paste was varied between 33 and 39

percent. For a well-graded aggregate profile, 33 percent cement paste was considered

optimum. The aggregate grading for this project contained gaps in the #8 and #16

particle sizes. Thus, it was thought that by examining the range from 33 to 39 percent

that the additional paste would effectively fill the gaps in the smaller particle sizes. The

parameters in Table 5.5 were held constant throughout all mixes in Step 2:

Table 5.5 Parameters Held Constant in Step 2

Water / Cementitious Materials Ratio	0.23
Coarse to Fine Aggregate Ratio by Volume	1.46
Fly Ash as Percent of Total Cementitious Materials	15
Silica Fume as Percent of Total Cementitious Materials	8
Type III Cement as Percent of Total Cementitious Materials	77

The results of Step 2 are shown in Table 5.6 and graphed in Figure 5.2.

Table 5.6 Results of Varying Percent Cement Paste – Step 2

Percent Cement Paste	1-Day Compressive Strength (psi)	3-Day Compressive Strength (psi)	28-Day Compressive Strength (psi)
33	6,760	7,880	9,420
35	8,950	9,350	8,360
37	8,810	9,420	10,280
39	8,920	9,360	10,550
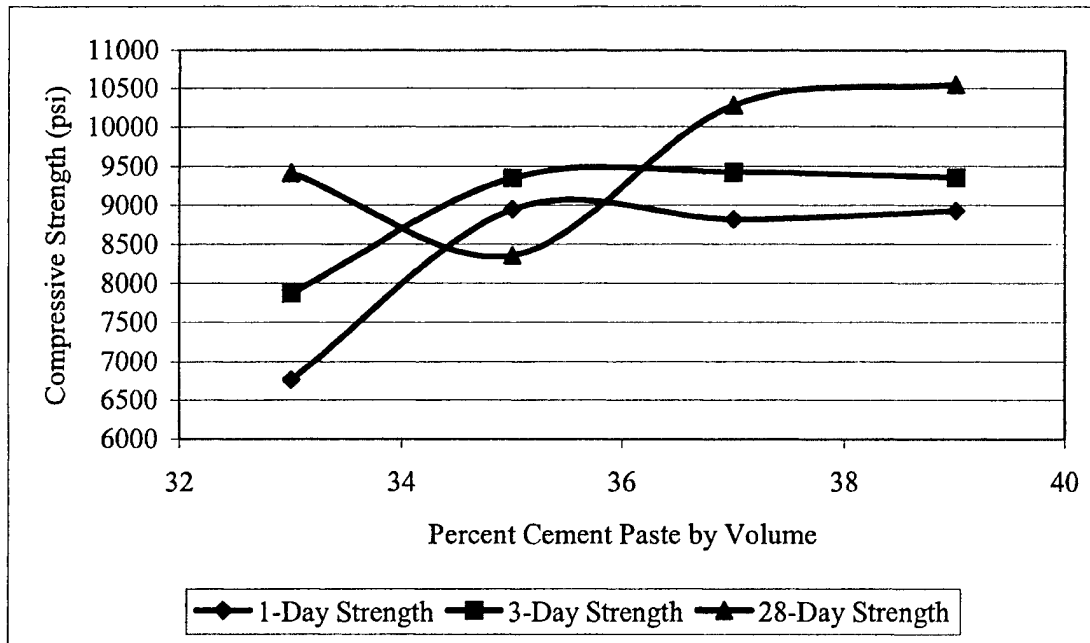
Figure 5.2 Results of Varying Percent Cement Paste

88

The results of Step 2 indicated the optimum percent cement paste was not at 33 percent based on the known gap grading in the aggregate profile. The need for additional cement paste appeared necessary. Figure 5.2 did not indicate an optimum value, but appeared to show a plateau that encompassed 39 percent based on 28-day strength. The drop in strength at 28 days for the 35 percent tests could not be explained. Thirty nine percent was chosen as the optimal percent cement paste value and was implemented in Step 3.

A similar study performed using 3/8-inch Stalite LWA and varying the percent cement paste from 35 to 45 percent also showed the optimum value to be around 39 percent. Based on gap grading in the overall aggregate profile considering 3/8-inch Stalite LWA and BB sand proportioned at a coarse to fine aggregate ratio of 1.5, this higher level of cement paste also was justifiable.

5.4.4 Variation of Percent Silica Fume– Step 3

Using the optimum coarse to fine ratio of 1.46 determined in Step 1, and the optimum percent cement paste of 39 percent determined in Step 2, mixes were configured for Step 3 where the percent silica fume was varied from 4 to 12 percent of total cementitious materials by weight. Based on the literature, it was thought that 8 percent silica fume was the upper limit for useful mix designs.[69] The parameters in Table 5.7 were held constant throughout all mixes in Step 3. Since the percent of silica fume varied during this step, the percent of cement had to vary as well in order to maintain a constant percent cement paste and W/CM ratio.

89

Table 5.7 Parameters Held Constant in Step 3

Water / Cementitious Materials Ratio	0.23
Coarse to Fine Aggregate Ratio by Volume	1.46
Percent Cement Paste by Volume	39
Fly Ash as Percent of Total Cementitious Materials	15

The results of Step 3 are shown in Table 5.8 and graphed in Figure 5.3.

Table 5.8 Results of Varying Percent Silica Fume – Step 3

Percent Silica Fume	1-Day Compressive Strength (psi)	3-Day Compressive Strength (psi)	28-Day Compressive Strength (psi)
4	8,540	8,710	10,660
6	8,920	9,470	10,550
8	8,820	9,400	10,930
10	10,620	11,190	11,330
12	10,200	10,500	11,080
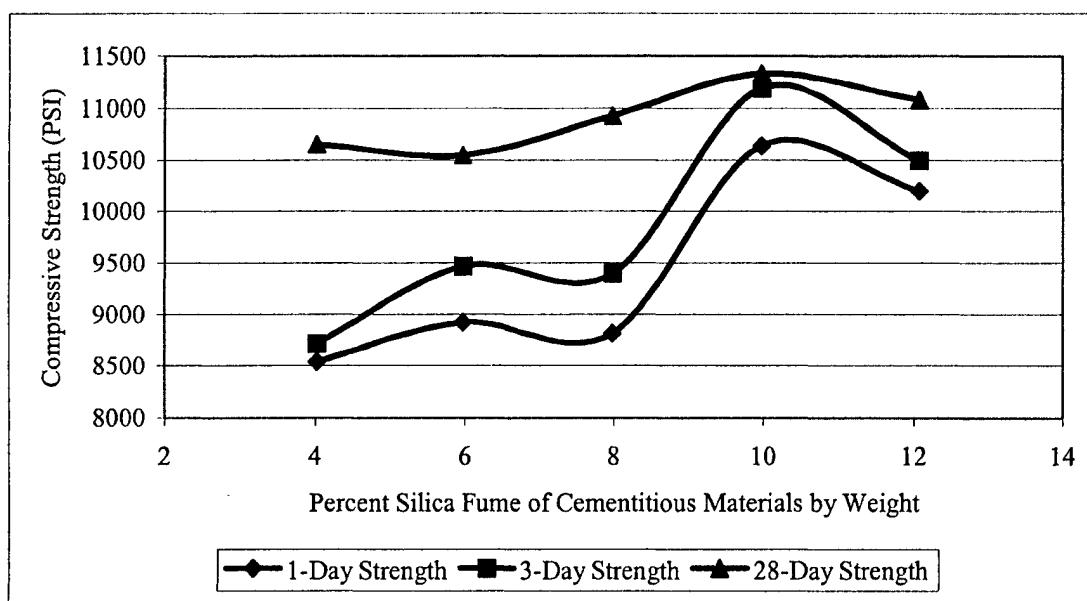
Figure 5.3 Results of Varying Percent Silica Fume

90

Figure 5.3 indicates that silica fume used as 10 percent of the total cementitious

materials by weight provided the best strength results at 1, 3 and 28 days.

The use of 10 percent silica fume required the use of additional HRWR to provide

necessary workability.

5.4.5 Strength Ceiling

The concept of a strength ceiling was discussed in Section 2.7.2. During mix

development, it was noticed that a reduction of the W/CM ratio below 0.23 did not result

in higher strengths. The strength ceiling also appeared to be inversely related to LWA

size. The use of smaller aggregate resulted in higher compressive strengths. In order to

investigate this phenomenon, a series of mixes was conducted as specified in Table 5.9.

The high-strength normal weight concrete (HSNWC) listed in Table 5.9 was used for two

sets of specimens. The first set incorporated all components in the mix design as listed.

The second set of specimens contained only the portion of the mix that would pass

through a 3/8-inch screen. The mix was screeded through a 3/8-inch screen in an attempt

to remove the larger size coarse aggregate for purposes of determining the strength of the

paste. While there may have been some small particles of the granite remaining in the

paste, the vast majority was removed during screeding. The volume of coarse aggregate

was identical for both mixes; the weight difference between the LWA and NWA is an

indication of the weight reduction achieved with HSLC.

91

Table 5.9 Mixes for "Strength Ceiling" Study

Concrete Components to Produce 1 Cubic Yard		HSLC	HSNWC
# 67 Crushed Granite	(lbs)	--	1,574
½-inch Stalite LWA	(lbs)	948	--
BB Sand	(lbs)	1100	1100
Class F Fly Ash	(lbs)	152	151
Silica Fume	(lbs)	101	101
Type III Cement	(lbs)	760	758
WRDA 35	(fl oz)	61	61
ADVA Flow	(fl oz)	132	173
Daravair 1000	(fl oz)	7.5	7.5
Water	(gal)	28.1	27.8

Slump	(inches)	4	5
Plastic Unit Weight	(pcf)	122.4	147.6
Temperature	(def F)	81	82

The results of the strength ceiling study are listed in Table 5.10. The HSNWC paste had the highest strength followed by the HSNWC then the HSLC. It would appear from the data that the strength ceiling for HSLC made with 1/2-inch Stalite LWA is around 11,400 psi. This result is in keeping with values estimated by Harmon.[45] Figure 5.4 shows a graph of the results in Table 5.10.

Table 5.10 Results of "Strength Ceiling" Study

Concrete Type	1-Day Strength (psi)	3-Day Strength (psi)	28-Day Strength (psi)
HSNWC Paste	11,780	13,160	13,380
HSNWC	11,740	12,050	13,060
HSLC	10,800	11,190	11,390
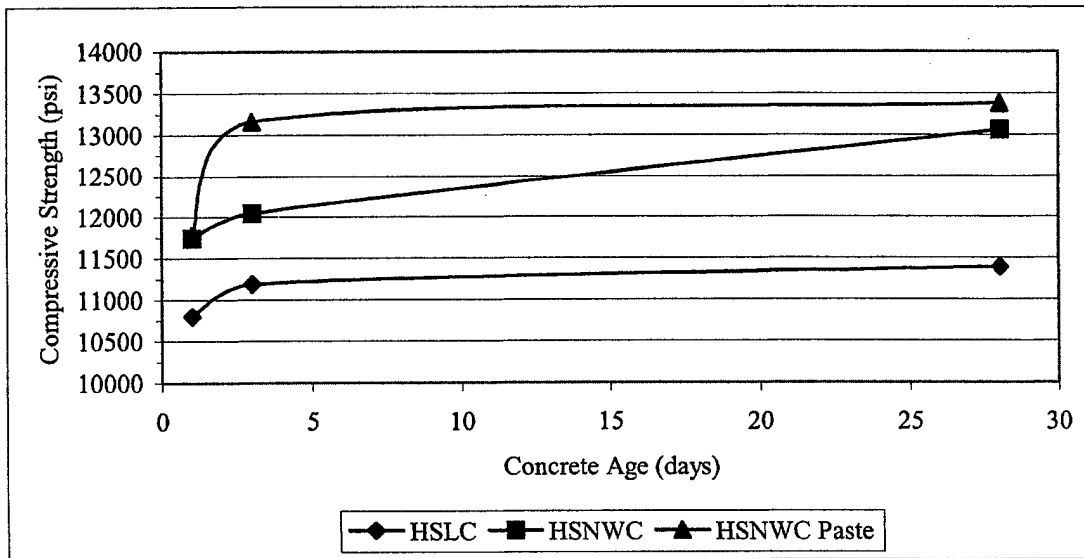
Figure 5.4 Results of "Strength Ceiling" Study

5.5 Final Mix Designs

Using the optimum values determined in Steps 1, 2 and 3 (1.46 coarse to fine

ratio, 39 percent cement paste, and 10 percent silica fume) and results of strength testing,

the mix designs shown in Table 5.11 were suggested for 8,000, 10,000, and 12,000-psi

strengths using 1/2-inch Stalite LWA. It was thought that the use of 1/2-inch aggregate

would be more readily accepted in the precast industry than the smaller 3/8-inch

aggregate. The mixes were configured by altering the content of CM based on W/CM

ratios deemed necessary for each concrete strength.

Strength results of laboratory mixes using the final mix designs are given in

Figure 5.5. The 12 mix underwent a drop in strength between 1 and 7 days, but increased

in strength between 7 and 28 days.

93

Table 5.11 Objective 8,000, 10,000, and 12,000 psi Mix Designs for Field Testing

Concrete Components to Produce 1 Cubic Yard of HSLC Aggregate Assumed to be at SSD		Concrete Mix Designation Objective Strength (psi)		
		8 Mix 8,000	10 Mix 10,000	12 Mix 12,000
1/2-inch Stalite LWA	(lbs)	1022	1030	1030
Normal Weight Fine Aggregate	(lbs)	947	955	955
Class F Fly Ash	(lbs)	142	145	150
Silica Fume	(lbs)	19	50	100
Type III Cement	(lbs)	783	765	740
WRDA 35	(fl oz)	57	58	59
ADVA Flow	(fl oz)	57	65	139
Daravair 1000	(fl oz)	9.4	9.6	7.5
Water	(gals)	32.1	29.9	27.3
Water / Cementitious Materials Ratio (W/CM)		0.28	0.26	0.23
Theoretical Equilibrium Unit Weight	(pcf)	115.6	116.2	116.6

Figure 5.5 Strength Results of Laboratory Developed HSLC Mix Designs

CHAPTER VI

FIELD PRODUCTION OF HSLC

6.1 Introduction

The purpose of this chapter is to describe the field production of the HSLC mix designs developed in the lab and discussed in Chapter 5. The goal of this phase of the research project was to verify that the HSLC mix designs and procedures determined and tested in the lab could be replicated under field conditions.

6.2 Concrete Plant Equipment Description

All field production testing was performed at the Tindall Concrete Plant in Jonesboro, Georgia. The plant (Figure 6.1) specialized in the construction of bridge girders for use on highway and rail applications and double-tee girders used for various applications.

Figure 6.1 Tindall Concrete Plant, Jonesboro, Georgia

Aggregate storage was in large bins behind the mixing tower. Aggregate dropped through control gates at the base of the bins to a conveyor belt, which transported the material into hoppers atop the mixing tower. The bin into which the 1/2-inch Stalite LWA was delivered (Figure 6.2) was equipped with a sprinkler to wet the aggregate prior to use.

Figure 6.2 Tindall Aggregate Storage Bin With Sprinkler

At delivery, the Stalite LWA had an absorbed moisture content of over 6 percent. In order to maintain and improve the level of absorbed moisture, the sprinkler was run continuously until 24 hours prior to concrete placement. At the time of placement, tested moistures indicated absorption levels of at least 7.5 percent, well above the minimum

96

allowable 6 percent standard established for producing HSLC. As in the lab, the reason for shutting off the sprinkler 24 hours prior to mixing was to reduce the moisture gradient throughout the stockpile. After 24 hours, the excess free water had drained leaving a fairly consistent level of free moisture on the aggregate.

The concrete mixer was a 3 cubic yard auger-style mixer as shown in Figure 6.3. The mixer was charged using conveyor belts for the aggregate and a chute for the cement. The mix tower was only equipped to dispense Portland cement; all silica fume and fly ash was added to the mixer manually as shown in Figure 6.4. After mixing, the concrete was dispensed through an opening in the side of the mixer to a chute that carried the concrete to the Tuckerbilt concrete transport vehicle shown in Figure 6.5.

Figure 6.3 Auger-Type Mixer at Tindall Concrete

97

Figure 6.4 Manual Addition of Fly Ash and Silica to Concrete Mixer at Tindall Concrete

6.3 Description of Materials Available at Tindall Concrete

The Tindall Plant used only Type III Cement manufactured by CEMEX-Southdown. The particular brand of cement was "Demopolis" named for the city near which it was manufactured in Alabama. The cement had a lower specific gravity (3.08) than the cement received from Blue Circle-LaFarge for mix development, which was about 3.15. The "Demopolis" Type III was reputed for producing exceptional high-early strength gain.
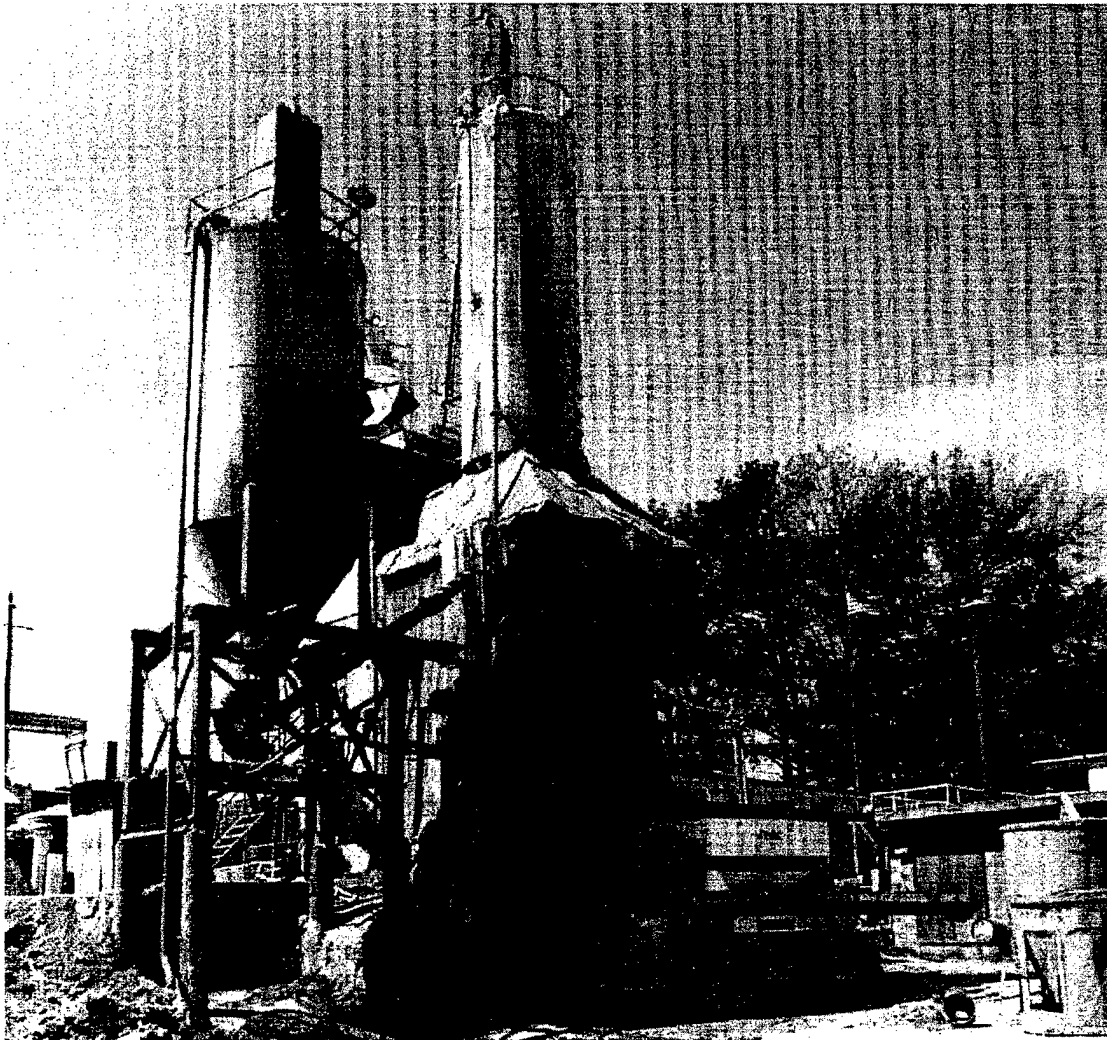
Figure 6.5 Mix Tower and Tuckerbilt Concrete Transport Vehicle

Tindall also used Brown Brothers sand, the same as used during HSLC mix development. Quality control checks on the sand indicated it had a specific gravity of 2.5 and a fineness modulus of 2.38.

Chemical admixtures available were from Grace Construction Products and matched those used during HSLC mix development. Chemical admixtures were dosed automatically from controls in the mix tower.

6.4 Area for Casting Specimens

The Tindall Plant Superintendent, Mr. Todd Davidson, was very accommodating during the field production testing phase. A large, flat area was provided for casting specimens and access was provided to quality control equipment. Figure 6.6 shows casting specimens outside the Tindall quality control shop.
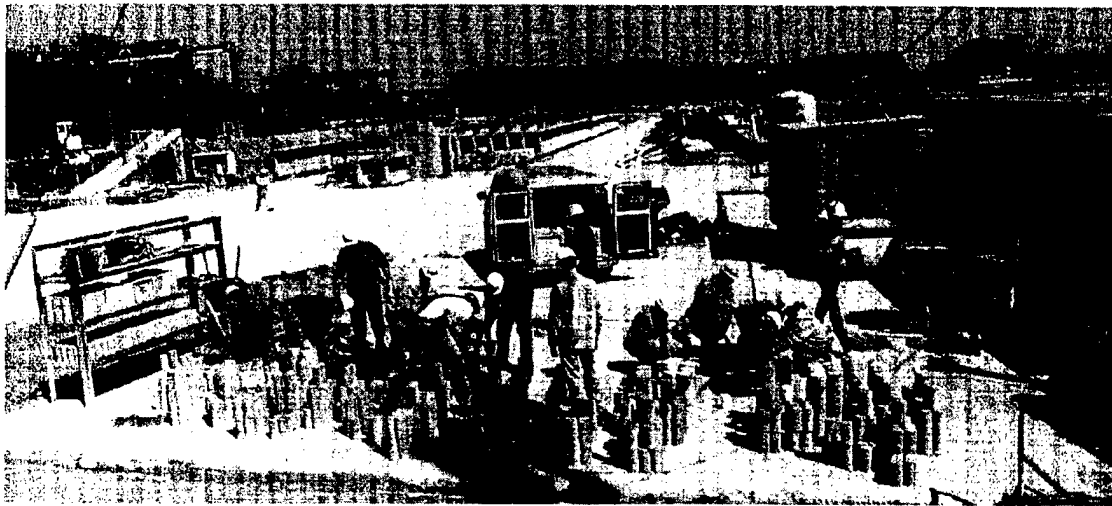
Figure 6.6 Casting Specimens at Tindall Concrete

6.5 Field Production of HSLC Mixes

The following sections address the field placements of the 8,000, 10,000 and 12,000 psi HSLC mixes identified as 8F, 10F and 12F, respectively. Several common actions occurred prior to mixing concrete to include positioning all molds and equipment in the casting area, performing quality control checks (moisture contents on LWA and NW sand), coordination with the plant manager, mix proportioning, and a briefing for student assistants on safety and the correct technique for casting specimens. The

specimens cast during each field-mixing test are specified in Table 6.1. Resulting

material properties are covered in Section 6.6.

Table 6.1 Number of Specimens Cast During Each Field Mixing Test

Specimen Type Curing Method Type of Test	Time of Testing After Placement (H=Hours, D=Days)						
	16H	20H	24H	7D	28D	56D	365D
4 x 8 Cylinder Curebox Compressive Strength	3	3	3	3	3	3	3
4 x 8 Cylinder ASTM Compressive Strength			3		3	3	3
6 x 12 Cylinder Curebox Modulus of Elasticity	3		3		3	3	
6 x 12 Cylinder ASTM Modulus of Elasticity						3	
4 x 4 x 14 Beam Curebox Modulus of Rupture			3			3	
4 x 8 Cylinder Curebox Chloride Permeability						3	3
20 x 36 x 12 Block ASTM Cored Cylinder Compressive Strength (3 Cores Tested)						1	

The 20 x 36 x 12 (W x L x H) block was cast to replicate curing conditions in the

bottom flange of a girder. In addition to the specimens listed above, extra specimens

were cast to the greatest extent possible based on space in cureboxes and availability of

molds. Extra specimens provided flexibility in the event a specimen was dropped, testing

was improperly conducted, or test results were irregular.

After casting, the specimens were covered with plastic lids or other suitable material to provide protection, and placed on a level surface. Thermocouples were inserted into select specimens to monitor the heat of hydration for each type of specimen. After reaching initial set (about 2-3 hours), those specimens identified as curebox specimens were placed into an insulated curebox as pictured in Figure 4.12. The cureboxes had been prepositioned in the back of a van prior to casting. ASTM specimens were placed in open containers and allowed to cure exposed to the ambient temperature. Approximately 12-14 hours after placement (after final set of the concrete), the specimens were transported back to the Georgia Tech Structures Lab and prepared for testing as necessary. The specimens were not removed from the curebox until their specified time of testing or until 24 hours had passed, whichever occurred first. Upon removal from the curebox, the specimen was demolded, labeled with its mix number, date and researchers initials, then either tested or placed in the fog room for additional curing through its time of testing.

6.5.1 Field Production Test # 1 – 8,000 PSI HSLC (Designation = 8F)

The first field production test was conducted on March 27, 2001. The weather was ideal for concrete placement with a temperature of 50° F, dry conditions, and no wind. Quality control tests on the aggregate resulted in "absorbed" and "as-is" moistures of 7.83 and 11.00 percent, respectively, for the Stalite LWA. The "as-is" moisture for the NW sand was 4.1 percent. The 8,000 psi mix "as batched" is listed in Table 6.2.

Mixing was initiated using a "buttering mix" to prepare the concrete mixer for future batches. The purpose of the buttering mix was to coat the mixer with cement paste

and prevent mix water from being pulled out of mixes to follow. The buttering mix was 1/4-cubic yard in size and had the same proportions as the mix planned for casting specimens. After buttering the mixer, the buttering mix was discarded.

Table 6.2 8,000 PSI (8F) Field Production Mix

Concrete Components to Produce 1 Cubic Yard		
1/2-inch Stalite LWA	(lbs)	978
Brown Brothers Sand	(lbs)	1062
Class F Fly Ash	(lbs)	142
Silica Fume	(lbs)	19
Type III Cement	(lbs)	785
WRDA 35	(fl oz)	57
ADVA Flow	(fl oz)	47+10
Daravair 1000	(fl oz)	9.5
Water	(gal)	23.9+0.5

Slump	(inches)	4
Planned Wet Unit Weight	(pcf)	118.1
Actual Wet Unit Weight	(pcf)	118.6
Temperature	(def F)	67.5
Air Content	(Percent)	3.5
Curing Start Time		3:00 pm

Mixing proceeded without any major problems. The components of the mix were added in the same order determined during laboratory mix development and listed in Section 4.6. An additional 10 fluid ounces of ADVA was added to provide the required workability. The additional water resulted from a valve that could not be closed completely. It was estimated that 1/2-gallon leaked into the mixer; however it was impossible to determine an exact value.

103

After mixing, the HSLC was dispensed into the Tuckerbilt and taken to the specimen casting area for quality control checks and then casting. Results of the quality control checks are listed at the bottom of Table 6.2. The resulting mix was within standard for all tests performed.

Several lessons were learned and noted for future placements. The most important issue of note was the valve that allowed water to leak into the concrete mixer. This leak made it impossible to determine the exact amount of water in the batch.

6.5.2 Field Production Test # 2 – 10,000 PSI HSLC (Designation = 10F)

The second field production test was conducted on April 3, 2001. The temperature was 62° F, but the weather was not ideal for concrete placement. Immediately after beginning to batch the concrete, heavy rain began to fall. The wind picked up to the point where it was raining almost horizontally. In anticipation of the rain, the molds had been moved under cover next to the casting area. Heavy rain continued through the conclusion of casting.

Earlier quality control tests on the aggregate resulted in "absorbed" and "as-is" moistures of 7.88 and 11.19 percent respectively for the Stalite LWA. The "as-is" moisture for the NW sand was 2.98 percent. The 10,000 psi mix as batched is listed in Table 6.3.

Mixing was again initiated using a 1/4-cubic yard "buttering mix.

During this mix, only 15 gallons of the planned 23.4 gallons were added. It appeared that the moisture content of the sand was much higher than determined earlier, which would have reduced the amount of required mix water. Since the aggregate

104

hoppers in the mix tower were covered, the rain was not the cause of the higher moisture contents.

Table 6.3 10,000 PSI (10F) Field Production Mix

Concrete Components to Produce 1 Cubic Yard		
1/2-inch Stalite LWA	(lbs)	984
Brown Brothers Sand	(lbs)	1055
Class F Fly Ash	(lbs)	146
Silica Fume	(lbs)	49
Type III Cement	(lbs)	765
WRDA 35	(fl oz)	57
ADVA Flow	(fl oz)	62+2
Daravair 1000	(fl oz)	9
Water	(gal)	23.4 (15)

Slump	(inches)	7.5
Planned Wet Unit Weight	(pcf)	118.7
Actual Wet Unit Weight	(pcf)	121.0
Temperature	(def F)	62
Air Content	(Percent)	3.8
Curing Start Time		2:00 pm

The components of the mix were added in the same order determined during laboratory mix development and listed in Section 4.6. An additional 2 fluid ounces of ADVA was added to provide the required workability.

Results of the quality control checks are listed at the bottom of Table 6.3. The resulting mix had a slump and unit weight that were higher than planned, but still acceptable.

Despite the rain and moisture control problems, the mix produced good results.

6.5.3 Field Production Test # 3 – 12,000 PSI HSLC (Designation = 12F)

The third and final field production test was conducted on April 10, 2001. The temperature was 90° F in the shade. Conditions were dry with no wind.

Quality control tests on the aggregate resulted in "absorbed" and "as-is" moistures of 7.69 and 11.12 percent respectively for the Stalite LWA. The "as-is" moisture content of the NW sand was 6.12 percent. The 12,000-psi mix "as batched" is listed in Table 6.4.

Mixing was again initiated using a 1/4-cubic yard "buttering mix.

During this mix, only 14 gallons of the planned 16.7 gallons were added. It appeared that the moisture content of the sand was slightly higher than tested earlier.

Table 6.4 12,000 PSI (12F) Field Production Mix

Concrete Components to Produce 1 Cubic Yard		
1/2-inch Stalite LWA	(lbs)	985
Brown Brothers Sand	(lbs)	1088
Class F Fly Ash	(lbs)	150
Silica Fume	(lbs)	100
Type III Cement	(lbs)	740
WRDA 35	(fl oz)	59
ADVA Flow	(fl oz)	129+8
Daravair 1000	(fl oz)	7
Water	(gal)	16.7 (14)

Slump	(inches)	4.5
Planned Wet Unit Weight	(pcf)	119.1
Actual Wet Unit Weight	(pcf)	124.2
Temperature	(def F)	86
Air Content	(Percent)	2.5
Curing Start Time		4:00 pm

The components of the mix were added in the same order determined during laboratory mix development and listed in Section 4.6. An additional 8 fluid ounces of ADVA was added to provide the required workability.

Results of the quality control checks are listed at the bottom of Table 6.4. The resulting mix had a low air content that was cause in part for the mix having a higher unit weight than anticipated. The 4.5-inch slump enabled easily casting the specimens. Despite the heat, the casting went well.

6.6 Results of Field Mixing

The combined results of field mixing are shown in Table 6.5 by specimen type, mix designation, and age of specimen. Each strength or modulus result shown is the average of three tests. The Masters Thesis by Brandon Buchberg,[86] "Investigation of Mix Design and Properties of High-Strength/High-Performance Lightweight Concrete" addresses chloride permeability, creep and shrinkage, coefficient of thermal expansion, and provides extensive detail on the results of each mix in this research project. Chapter 7 of this report compares the results of the field testing program (8F, 10F and 12F) with results achieved during a similar laboratory testing program using the same specified 8,000, 10,000, and 12,000 psi mixes (8L, 10L, and 12L) and with the 8,000 and 10,000 mixes (G1 and G2) used in girder construction.

There are several trends seen in Table 6.5 that are addressed further in the following sections.

Table 6.5 Results of Field Mixing

Specimen Curing Test	Units	Mix	Mean Strength or Modulus at Time of Testing (H=Hours, D=Days)						
			16H	20H	24H	7D	28D	56D	365D
4 x 8 Cyl Curebox Comp. Str.	psi	8F	7,920	8,470	8,870	9,570	9,830	10,600	10,830
		10F	7,710	9,070	9,750	10,010	10,430	11,170	11,520
		12F	10,990	10,500	11,490	11,250	11,460	11,550	12,140
4 x 8 Cyl ASTM Comp. Str.	psi	8F			6,760		10,250	11,090	11,800
		10F			6,200		11,140	11,300	11,680
		12F			9,330		11,550	11,620	12,280
6 x 12 Cyl Curebox Elast. Mod.	10^6 psi	8F	3.49		3.67		3.85	3.86	
		10F	3.48		3.75		4.22	4.08	
		12F	3.92		4.12		4.30	4.26	
6 x 12 Cyl ASTM Elast. Mod.	10^6 psi	8F						4.13	
		10F						4.26	
		12F						4.40	
4 x 4 x 14 Curebox Rupt. Mod.	psi	8F			788			1,089	
		10F			641			998	
		12F			761			1,014	
Block ASTM Comp. Str.	psi	8F						9,550	
		10F						10,270	
		12F						11,470	

6.6.1 Strength Gain of 4 x 8 Cylinders

For all three mixes, the 1-day curebox strengths showed remarkable early strength gain. The 8F mix continued to gain strength through 365 days ultimately achieving 10,830 psi and 11,800 psi for curebox and ASTM specimens, respectively. The 10F mix also showed remarkable early strength gain and continued to gain strength through 365 days. The 12F mix reached within 650 psi of its ultimate strength after 24 hours based on curebox specimen results. From that point through 365 days, the mix initially lost strength then rose again to reach 12,140 psi and 12,280 psi for curebox and ASTM specimens, respectively. The effect of the silica fume can be seen in mix 12F. After 24

hours, it had achieved a compressive strength 1,700 psi greater than the 10F mix and

2,600 psi greater than the 8F mix. The main differences between the mixes were the

silica fume content and W/C ratio. Figures 6.7 and 6.8 show plots of strength gain for the

three mixes through 56 and 365 days, respectively.
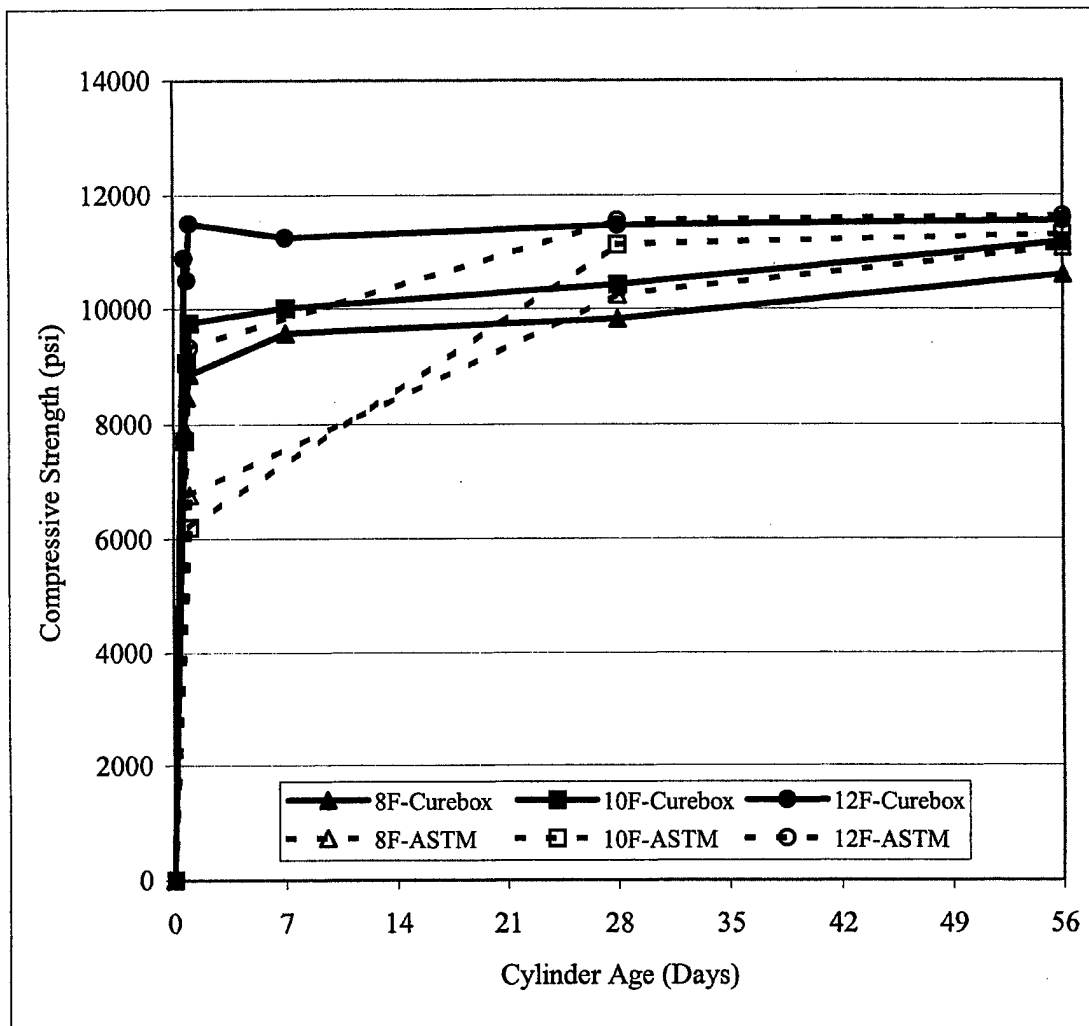
Figure 6.7 Strength Gain for 4 x 8 Curebox and ASTM Cylinders Through 56 Days
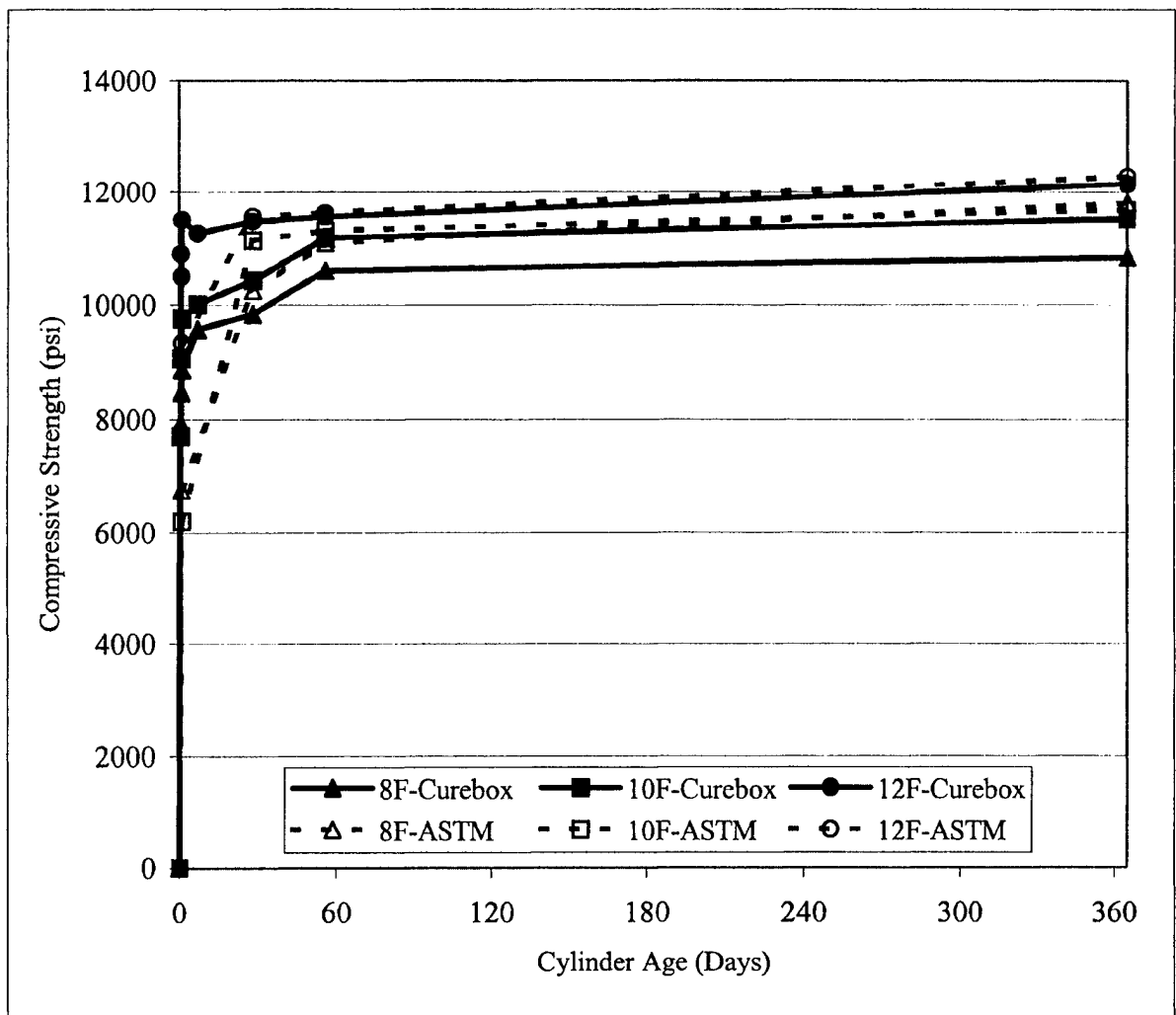
Figure 6.8 Strength Gain for 4 x 8 Curebox and ASTM Cylinders Through 365 Days

6.6.2 Curebox vs. ASTM 4 x 8 Cylinders

After 24 hours of curing, the curebox cylinders had reached a strength between

2,000 and 2,500 psi greater than the ASTM cured cylinders. The insulated cureboxes

held in the heat of hydration causing the curebox cylinders to hydrate more quickly and

achiever higher early strengths. After 56 days, the ASTM strengths were about 2 percent

greater than the curebox strengths for each mix. After 365 days, the 8F ASTM strengths

were about 9 percent greater than curebox strengths; the 10F and 12F ASTM strengths were less than 1 percent greater. Figures 6.7 and 6.8 show how the ASTM and curebox strength gains differed.

6.6.3 Strength Ceiling

The concept of a strength ceiling was discussed in Sections 2.7.2 and 5.4.5. Examination of Figure 6.8 reveals that an apparent strength ceiling exists at just above 12,000 psi, slightly higher than it was thought to be during the laboratory development phase. The 12F mix provides the best indication of a strength ceiling. After 24 hours, the 12F cylinders had practically reached their maximum strength at 11,490 psi. At 56 days, the 12F cylinders had effectively gained 60 psi strength. 60 psi could be considered as normal variation in testing between the two sets of cylinders. The 12F ASTM cylinders showed a similar trend gaining only 70 psi from 28 through 56 days. After 365 days, the curebox and ASTM cylinders had gained an additional 590 psi and 660 psi, respectively.

6.6.4 Modulus of Elasticity

The modulus of elasticity results showed a slight drop at 56 days for the 10F and 12F cylinders. The ASTM cylinders achieved about 5 percent higher modulus values on average at 56 days in comparison to the curebox cylinders. Further analysis of modulus of elasticity values is covered in Chapter 7, Short and Long-Term Properties.

6.6.5 Modulus of Rupture

Table 6.5 shows how the moduli of rupture results were unpredictable. As the compressive strength increased, the modulus of rupture was expected to have increased.

111

The 8F mix produced the highest modulus of rupture results of the three tests, but it had the lowest compressive strength. Based on these results it is hypothesized that there is an upper limit for f_r in HSLC. Chapter 7 compares these results with laboratory specimens and specimens created during girder construction.

6.6.6 Target Strengths

According to ACI 318, Section 5.3.2.2,[2] the required average compressive strength when data are not available to establish a standard deviation is the design strength + 1,400 psi for strengths over 5,000 psi. Table 6.6 outlines the test results for each mix and the allowable design strength based on 56-day results.

Table 6.6 Resulting Strengths and Allowable Design Strengths

Mix Designation	Average Curebox Strength (psi)	Average ASTM Strength (psi)	Maximum Specifiable Design Strength (psi)
8F	10,600	11,090	9,690
10F	11,170	11,300	9,900
12F	11,550	11,620	10,220

Based on ACI requirements, the maximum design strength achievable from the three mixes was 10,220 psi. The maximum specifiable design strength was based on the average ASTM strength results since they were greater. These results indicate that the existence of a strength ceiling at about 11,500 psi limits the specifiable design strength to just over 10,000 psi.

During girder construction, a series of cylinders was cast such that a statistical study could be performed. ACI 318[2] allows the use of statistical results to reduce the code specified 1,400-psi strength reduction. Chapter 7 includes discussion of the statistical study conducted for HSLC.

6.7 Conclusions

Mixing HSLC in a commercial plant can be accomplished with good success. The strength results in Table 6.5 indicate that with proper quality control that the same strengths can be achieved in the field as in the laboratory.

Moisture content in slate LWA can be adequately controlled in a field environment by sprinkling the aggregate continuously until just prior to mixing.

Curebox cured specimens achieved greater early strengths at 24 hours, but ultimately did not achieve the strengths reached by ASTM specimens at 56 days.

Moduli of elasticity values for ASTM cured specimens were greater than for curebox-cured specimens.

CHAPTER VII

MECHANICAL PROPERTIES OF HSLC

7.1 Introduction

The purpose of this chapter is to report and compare the mechanical properties

from all HSLC mixes determined and tested during this research project and to discuss

the aspects that relate directly to girder performance characteristics examined. Specific

batch information and test results including compression strength, modulus of elasticity,

and modulus of rupture are reported. The results of a statistical study are discussed. The

Masters Thesis by Brandon Buchberg[86] "Mix Design Performance of High Strength –

High Performance Lightweight Concrete" provides a more in-depth analysis of all

material property related data.

7.2 Overview of HSLC Material Testing Program

The mixing and testing of HSLC was accomplished in four phases with specimens

designated as shown in Table 7.1.

Table 7.1 HSLC Material Testing Program Specimen Designation

Objective Mix Design Strength (psi)	Phase 1 Mix Development In Laboratory	Phase 2 Field Production	Phase 3 Laboratory Verification	Phase 4 Girder Construction
8,000	8 Mix	8F	8L	G1
10,000	10 Mix	10F	10L	
12,000	12 Mix	12F	12L	G2

In Phase 1, mix designs labeled "8 Mix," "10 Mix," and "12 Mix" were developed in order to meet objective design strengths of 8,000, 10,000, and 12,000 psi as described in Chapter 5. A strength ceiling of approximately 12,200 psi prevented the 12,000 psi objective design strength from being reached; the designation was maintained for consistency of reference.

In Phase 2, the mix designs developed during Phase 1 underwent a field production test as described in Chapter 6; the Phase 2 mix designs and specimens were designated 8F, 10F, and 12F to signify the objective design strength of the mix and that it was field-produced at Tindall Concrete.

In Phase 3, the same mix designs developed in Phase 1 and field-produced in Phase 2 were more fully evaluated in the laboratory. The Phase 3 mix designs and specimens were designated 8L, 10L, and 12L to signify the objective strength of the mix and that they were produced in the laboratory. Many individual batches of concrete were required during Phase 3. Every attempt was made to maintain consistency between the batches.

In Phase 4, the same mix designs developed in Phase 1 and field-produced in Phase 2 were used to construct girders; only the 8,000 and 12,000 psi objective strength mixes were used for girder construction. During girder construction, the 8,000 psi mix design and specimens were labeled G1 indicating a Grade 1 concrete. The 12,000 psi objective strength mix design and specimens were labeled G2 indicating a Grade 2 concrete

7.3 Specimen Casting Plan

Table 6.1 listed the specimen casting plan used during each field-production test. Table 7.2 shows the specimen casting plan during laboratory evaluation (Phase 3). The number in parenthesis indicates the individual batch from which the specimens were cast. The 10L series of batches had only three matches (1-3) as explained in Section 7.5.3.

Table 7.2 Specimens Cast During Laboratory Verification Batches (Phase 3)

Specimen Type / Curing Method / Type of Test	Time of Testing After Placement (H=Hours, D=Days)						
	16H	20H	24H	7D	28D	56D	365D
4 x 8 Cylinder Curebox Compression Strength	3(4)	3(4)	3(4)	3(1)	3(1)	3(1)	3(1)
4 x 8 Cylinder ASTM Compression Strength			3(1)		3(1)	3(1)	3(1)
6 x 12 Cylinder Curebox Modulus of Elasticity	3(4)		3(4)			3(2)	
6 x 12 Cylinder ASTM Modulus of Elasticity						3(2)	
4 x 4 x 14 Beam Curebox Modulus of Rupture			3(3)			3(3)	
4 x 4 x 14 Beam ASTM Modulus of Rupture			3(3)			3(3)	
4 x 8 Cylinder Curebox Chloride Permeability						2(2)	2(2)
4 x 15 Cylinder Curebox Creep / Shrinkage	5(5)		5(5)				

Table 7.3 shows the specimen casting plan for girder construction (Phase 4). The first number listed is the number of specimens cast from the initial batch of concrete

116

(G1A1, G1B1, G2A1, G2B1) on each day girders were cast. The number in parenthesis is the number of specimens cast from all subsequent batches of concrete (G1A2-4, G1B2 3, G2A2-5, G2B2-4) on each day girders were cast. The direct pullout test block was only cast during placements G1A and G2A. Extra specimens were cast when possible.

Table 7.3 Specimens Cast During Girder Construction Batches (Phase 4)

Specimen Type Curing Method Type of Test	Time of Testing After Placement (D=Days)				
	1D	7D	28D	56D	Time Of Girder Testing
4 x 8 Cylinder Curebox Compression Strength	3(3)	3	3	3	3(3)
4 x 8 Cylinder ASTM Compression Strength	3	3	3	3(3)	3
6 x 12 Cylinder Curebox Modulus of Elasticity	3			3	
6 x 12 Cylinder ASTM Modulus of Elasticity				1(1)	
4 x 4 x 14 Beam Curebox Modulus of Rupture				3	
4 x 4 x 14 Beam ASTM Modulus of Rupture				1(1)	
4 x 15 Cylinder Curebox Creep / Shrinkage	6				
20 x 36 x 24 Block ASTM Direct Pullout Test				1	

7.4 Mix Designs as Determined in Phase 1

For reference, Table 7.4 lists the resulting mix designs from Phase 1.

Table 7.4 Objective 8,000, 10,000, and 12,000 psi Mix Designs from Phase 1

Concrete Components to Produce 1 Cubic Yard of HSLC Aggregate Assumed to be at SSD		Concrete Mix Designation Objective Strength (psi)		
		8 Mix 8,000	10 Mix 10,000	12 Mix 12,000
1/2-inch Stalite LWA	(lbs)	1,022	1,030	1,030
Normal Weight Fine Aggregate	(lbs)	947	955	955
Class F Fly Ash	(lbs)	142	145	150
Silica Fume	(lbs)	19	50	100
Type III Cement	(lbs)	783	765	740
WRDA 35 Low-Range Water Reducer (LRWR)	(fl oz)	57	58	59
ADVA Flow High-Range Water Reducer (HRWR)	(fl oz)	57	65	139
Daravair 1000 Air Entraining Agent (AEA)	(fl oz)	9.4	9.6	7.5
Water	(gals)	32.1	29.9	27.3
Water / Cementitious Materials Ratio	(W/CM)	0.28	0.26	0.23
Theoretical Wet Unit Weight	(pcf)	118.1	118.7	119.1
Theoretical Equilibrium Unit Weight	(pcf)	115.6	116.2	116.6

7.5 Mixes as Batched and Wet Concrete Properties

The following sections provide the "as batched" component listings for each

batch of concrete produced in Phases 2, 3 and 4. The components listed are based on

aggregate at the saturated surface dry (SSD) condition.

7.5.1 Girder Placement Dates, Times and Ambient Temperatures

Table 7.5 Girder Construction Batch Information

Girders	Batch Series	Date/Time	Ambient Temp. ^{0} F	Weather
G1A, G1B	G1A	9 July 01, 1800	87	Dry, Clear
G2A, G2B	G2A	12 July 01, 1000	88	Dry, Clear
G1C	G1B	17 July 01, 1700	90	Dry, Clear
G2C	G2B	17 July 01, 1600	92	Dry, Clear

7.5.2 8,000 psi HSLC Design Strength

Tables 7.6 and 7.7 show batching results for the 8,000 psi design strength mixes.

118

Table 7.6 8,000 psi HSLC Mixes (8F and 8L)

Concrete Components to Produce 1 Cubic Yard							
Component	Unit	8F	8L1	8L2	8L3	8L4	8L5
1/2-in LWA	Lbs	947	954	954	954	954	954
NW Sand	Lbs	1,022	1,029	1,029	1,029	1,029	1,029
Class F Fly Ash	Lbs	141	140	140	140	140	140
Silica Fume	Lbs	19	19	19	19	19	19
Type III Cement	Lbs	780	774	774	774	774	774
LRWR	fl oz	56	56	56	56	56	56
HRWR	fl oz	57	81	78	85	90	104
AEA	fl oz	9.4	9.3	9.3	9.3	9.3	9.3
Water	Gal	32.0	31.7	31.7	31.7	31.7	31.7

Slump	in	4.00	4.25	4.5	4.5	4.5	7
Wet Unit Wt	pcf	118.6	118.6	119.4	120.3	122.0	123.8
Batch Temp	^{0}F	68	90	89	90	88	89
Air Content	%	3.50	4.00	3.75	4.00	--	--

Table 7.7 8,000 psi HSLC Mixes (G1)

Concrete Components to Produce 1 Cubic Yard								
Component	unit	G1A1	G1A2	G1A3	G1A4	G1A5	G1B1	G1B2	G1B3
1/2-in LWA	lbs	944	937	925	925	925	941	960	941
NW Sand	lbs	1,018	1,011	999	999	999	1,029	1,050	1,030
Class F Fly Ash	lbs	141	140	138	138	138	143	146	143
Silica Fume	lbs	19	19	19	19	19	19	19	19
Type III Cement	lbs	780	774	765	765	765	788	804	788
LRWR	fl oz	56	56	55	55	55	57	58	57
HRWR	fl oz	64	64	63	63	63	58	53	58
AEA	fl oz	9.4	9.3	9.2	9.2	9.2	9.5	9.7	9.5
Water	gal	34.1	35.3	37.3	37.3	37.3	32.3	28.8	32.3

Slump	in	8.00	--	--	--	--	7.00	--	--
Wet Unit Wt	pcf	118.6	--	--	--	--	120.8	--	--
Batch Temp	^{0}F	85	--	--	--	--	86	--	--
Air Content	%	4.5	3.2	--	--	--	--	--	--

119

7.5.3 10,000 psi HSLC Design Strength

Table 7.8 shows batching results for the 10,000 psi design strength mixes. This mix design was only batched during the field production test (Phase 1) and the laboratory verification (Phase 3). No girders were cast with this mix design; thus only three batches of this mix design were made during the laboratory evaluation phase.

Table 7.8 10,000 psi HSLC Mixes (10F and 10L)

Concrete Components to Produce 1 Cubic Yard					
Component	unit	10F	10L1	10L2	10L3
1/2-inch LWA	lbs	955	952	952	952
NW Sand	lbs	1,030	1,027	1,027	1,027
Class F Fly Ash	lbs	146	146	146	146
Silica Fume	lbs	49	49	49	49
Type III Cement	lbs	765	762	764	764
LRWR	fl oz	58	57	58	58
HRWR	fl oz	64	88	88	88
AEA	fl oz	9.6	9.6	9.6	9.6
Water	gal	29.9	31.8	31.4	31.4

Slump	in	7.50	3.50	4.25	4.25
Wet Unit Weight	pcf	121.0	122.7	122.4	122.3
Temperature	^{0}F	62	92	91	92
Air Content	%	3.80	3.00	3.00	3.00

7.5.4 12,000 psi HSLC Design Strength

Tables 7.9 to 7.11 show batching results for the 12,000 psi objective mix design.

Table 7.9 12,000 psi HSLC Mixes (12F and 12L)

Concrete Components to Produce 1 Cubic Yard							
Component	Unit	12F	12L1	12L2	12L3	12L4	12L5
1/2-in LWA	Lbs	955	947	947	947	956	955
NW Sand	Lbs	1,029	1,021	1,021	1,021	1,026	1,024
Class F Fly Ash	Lbs	150	149	149	149	149	149
Silica Fume	Lbs	100	99	99	99	100	100
Type III Cement	Lbs	740	734	734	735	740	740
LRWR	fl oz	59	59	59	59	59	59
HRWR	fl oz	131	135	135	135	185	222
AEA	fl oz	9.9	7.4	7.4	7.4	9.9	9.9
Water	Gal	27.2	27.2	27.2	28.6	27.7	27.6

Slump	In	4.50	3.50	3.00	3.50	4.00	6.00
Wet Unit Wt	Pcf	124.0	121.2	121.7	120.9	122.8	123.2
Batch Temp	^{0}F	86	90	91	89	93	95
Air Content	%	2.50	3.50	3.00	3.50	--	--

Table 7.10 12,000 psi HSLC Mixes (G2A)

Concrete Components to Produce 1 Cubic Yard						
Component	Unit	G2A1	G2A2	G2A3	G2A4	G2A5
½-in LWA	lbs	968	949	940	939	945
NW Sand	lbs	1,039	1,018	1,009	1,007	1,014
Class F Fly Ash	lbs	151	148	147	147	148
Silica Fume	lbs	101	99	98	98	98
Type III Cement	lbs	746	732	725	724	728
LRWR	fl oz	60	59	58	58	58
HRWR	fl oz	148	150	146	144	144
AEA	fl oz	7.5	7.3	7.3	7.3	7.3
Water	gal	25.8	29.2	30.9	31.1	30.0

Slump	in	5.75	--	--	--	--
Wet Unit Wt	pcf	120.0	--	--	--	--
Batch Temp	^{0}F	86	--	--	--	--
Air Content	%	5.40	3.50	--	--	--

Table 7.11 12,000 psi HSLC Mixes (G2B)

Concrete Components to Produce 1 Cubic Yard					
Component	Unit	G2B1	G2B2	G2B3	G2B4
½-in LWA	lbs	956	933	933	945
NW Sand	lbs	1,025	1,001	1,001	1,014
Class F Fly Ash	lbs	149	146	146	148
Silica Fume	lbs	100	97	97	98
Type III Cement	lbs	737	719	719	729
LRWR	fl oz	59	58	58	59
HRWR	fl oz	147	145	145	146
AEA	fl oz	7.4	7.3	7.3	7.3
Water	gal	28.1	32.1	32.1	31.7

Slump	in	4.5	--	--	--
Wet Unit Wt	pcf	114.0	--	--	--
Batch Temp	^{0}F	86	--	--	--
Air Content	%	3.00	3.20	3.60	--

7.6 Compression Strength Results

Compression strength results are shown according to cylinder size, type of curing, and age of cylinder. The 6 x 12 compression strength results were determined when performing modulus of elasticity tests. A comparison between the 4 x 8 and 6 x 12 results is provided as are the results of a statistical study performed on specimens cast during batch series G2B.

7.6.1 4 x 8 Cylinder Compression Strength Results

The results of compression strength testing for all 4 x 8 cylinders are shown in Table 7.12. For field production and laboratory evaluation, the resulting strengths shown are the average of three compression strength tests. For girder construction batches, the values are the average of all cylinders made from the four or five batches in the batch

122

series. The number after the "Time of Test" strength is the average specimen age in

Days. Figures 7.1, 7.2 and 7.3 graph the strength vs. age of the 8,000, 10,000 and 12,000

psi concretes, respectively. The 1-day strength was not available for the 10L ASTM

specimen.

Table 7.12 Results of 4 x 8 Cylinder Compression Strength Testing

Objective Strength Curing	Batch #	Mean Cylinder Strength (psi) (H=Hours, D=Days, Y=Year)							
		16H	20H	24H	7D	28D	56D	Time Of Test	1Y
8,000 Curebox	8F	7,920	8,470	8,870	9,570	9,830	10,600		10,830
	8L	7,320	7,630	7,730	9,300	9,630	10,430		
	G1A			7,470	7,810	8,710	9,080	9,418	103D
	G1B			6,320	6,300	7,480	7,750	8,792	110D
8,000 ASTM	8F			6,760		10,250	11,090		11,802
	8L			6,300		9,830	10,520		
	G1A			5,740	7,320	8,840	9,350	10,229	103D
	G1B			5,400	5,890	7,600	8,460	9,118	110D
10,000 Curebox	10F	7,710	9,070	9,750	10,010	10,430	11,170		11,516
	10L				9,260	9,410	9,920		
10,000 ASTM	10F			6,200		11,140	11,300		11,675
	10L			6,950		10,360	11,040		
12,000 Curebox	12F	10,990	10,500	11,490	11,250	11,460	11,550		12,138
	12L	9,840	9,760	11,101	10,230	10,590	10,860		
	G2A			9,640	9,460	10,170	10,420	10,965	123D
	G2B			8,260	9,150	9,340	10,250	10,454	144D
12,000 ASTM	12F			9,330		11,550	11,620		12,278
	12L			6,890		10,600	11,480		
	G2A			9,290	9,460	10,120	10,820	11,012	123D
	G2B			6,550	8,070	9,810	10,510	10,868	144D
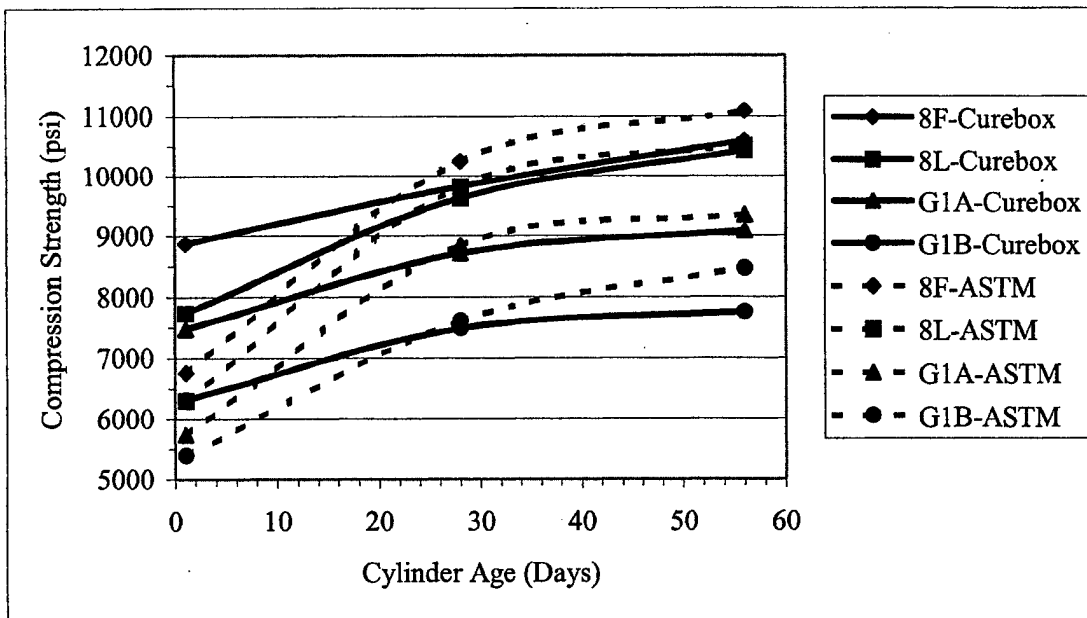
Figure 7.1 Compression Strength vs. Cylinder Age for 8,000 psi Mixes to 56 Days
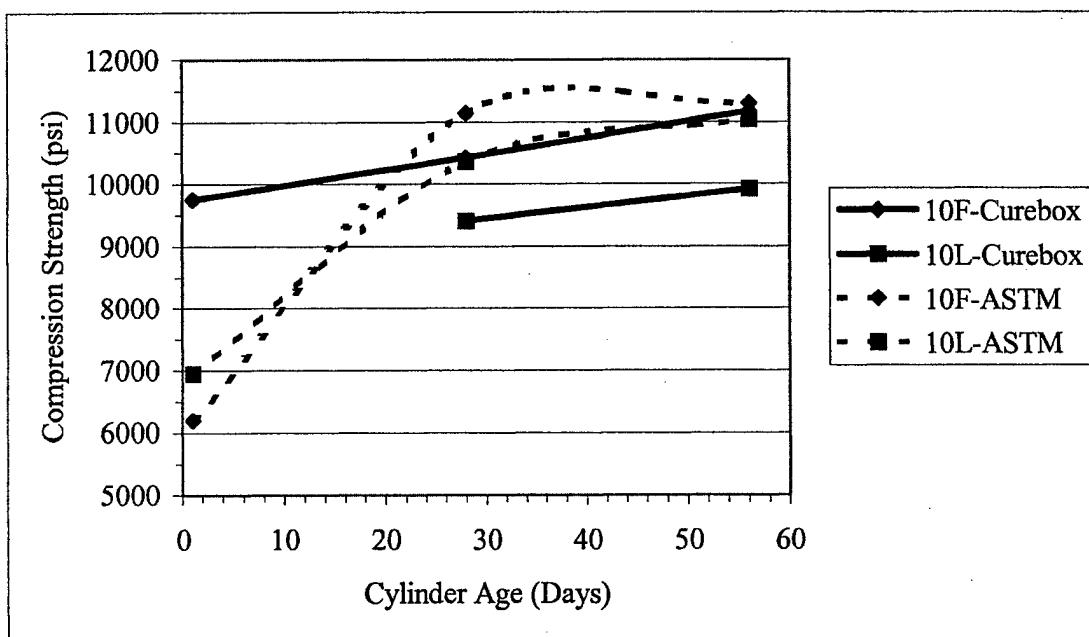
Figure 7.2 Compression Strength vs. Cylinder Age for 10,000 psi Mixes to 56 Days

124
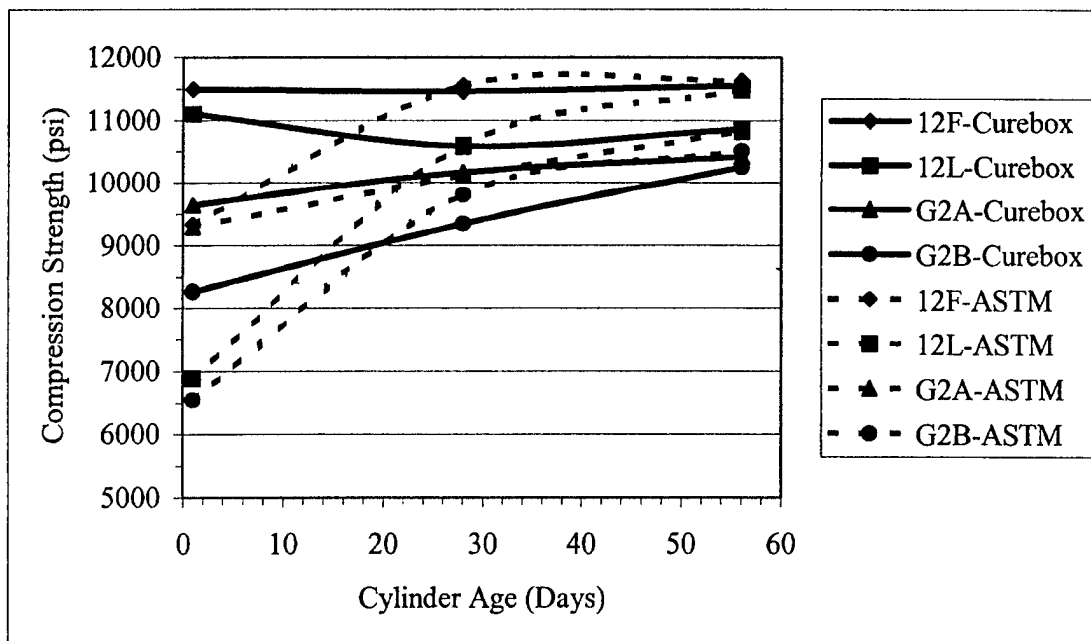
Figure 7.3 Compression Strength vs. Cylinder Age for 12,000 psi Mixes to 56 Days

Examination of Table 7.12 and Figures 7.1 through 7.3 show the difference between ASTM cylinder strengths and curebox strengths is significant at early ages and after 100 days. After 103 days, the G1A batch series ASTM specimens had about 800 psi greater strength than the curebox specimens. On average at the time of testing, ASTM specimens had about 4 percent greater strength than curebox specimens compared to 8 percent for the G1A batch series specimens.

Examination of results at the time of testing showed that strength gain continued from 56 days through the time of testing. The strength gain for the 8,000-psi batches was 729 psi on average, a gain of about 8.5 percent. The strength gain for the 12,000-psi batches was 324 psi on average, a gain of about 3 percent.

125

Examination of results after 365 days for the 8F, 10F and 12F showed that strength gain continued through 365 days. The 8F ASTM specimens had about 9 percent greater strength than the curebox specimens, but that ASTM specimens for the 10F and 12F mixes had less than 1 percent greater strength in comparison to the curebox specimens.

Comparison of the laboratory evaluation mixes with field-production test mixes shows that the field-production mixes had an average strength 3 percent greater than the corresponding laboratory mixes. When making the laboratory mixes, the same type of cement was used as during the field-production batches. The difference could be attributed to mix effort, age of cement, or the slightly different proportioning between the field and laboratory mixes.

The strength of girder mixes made on different days (G1A vs. G1B, G2A vs. G2B) were normally within 7%. In the case of batch series G1A vs. G1B, the difference was about 12 percent. The difference was most likely attributed to the water leak in the concrete mixer.

7.6.2 6 x 12 Cylinder Compression Strength Results

The results of 6 x 12 cylinder compression strength tests are shown in Table 7.13. All strengths are based on an average of three cylinder tests, except the ASTM values for batches G1A, G1B, G2A, and G2B were based on the average of tests of one cylinder from each of the four or five batches in the batch series.

Table 7.13 Results of 6 x 12 Cylinder Compression Strength Testing

Objective Strength Curing	Batch #	Mean Cylinder Strength (psi) (H=Hours, D=Days)			
		16H	24H	28D	56D
8,000 Curebox	8F	7,910	8,460	9,940	10,450
	8L	8,110	8,520		10,330
	G1A		7,890		9,420
	G1B		6,650		7,480
8,000 ASTM	8F				10,740
	8L				10,520
	G1A				9,350
	G1B				8,580
10,000 Curebox	10F	7,940	9,060	10,410	10,510
	10L				9,770
10,000 ASTM	10F				11,720
	10L				10,150
12,000 Curebox	12F	10,880	10,870	10,990	11,460
	12L	10,290	10,750		10,550
	G2A		9,270		10,240
	G2B		9,280		10,710
12,000 ASTM	12F				11,520
	12L				10,690
	G2A				10,660
	G2B				10,840

7.6.3 Comparison of 4 x 8 and 6 x 12 Cylinder Compression Strength Results

In cases where a comparison was possible, 4 x 8 compression strength results were compared to 6 x 12 compression strength results. Table 7.14 provides the percentage differences for the Phases 2, 3 and 4. The percent difference was calculated by subtracting the 6 x 12 value from the 4 x 8 value, dividing the result by the 6 x 12 value, and multiplying by 100. A negative value indicates the 4 x 8 compression strength was less than the 6 x 12 compression strength.

Table 7.14 Comparison of 4 x 8 to 6 x 12 Cylinder Compression Strengths

Objective Strength Curing	Batch #	Percent Difference (H=Hours, D=Days)			
		16H	24H	28D	56D
8,000 Curebox	8F	0%	5%	-1%	1%
	8L	-10%	-9%		1%
	G1A		-10%		-5%
	G1B		-11%		4%
8,000 ASTM	8F				3%
	8L				0%
	G1A				0%
	G1B				-6%
10,000 Curebox	10F	-3%	8%	0%	6%
	10L				1%
10,000 ASTM	10F				-4%
	10L				9%
12,000 Curebox	12F	1%	6%	4%	1%
	12L	-4%	-3%		3%
	G2A		6%		2%
	G2B		-10%		-4%
12,000 ASTM	12F				1%
	12L				7%
	G2A				1%
	G2B				-6%

Examination of Table 7.14 shows great variation from one strength group to another. For the 8,000 psi batches, early strength data (16H and 24H) indicate that 6 x 12 cylinders had greater strength than 4 x 8 cylinders on average. However, after 56 days, the resulting strengths were about the same on average. For the 10,000 psi batches, there is limited data on which to base a conclusion. For the 12,000 psi batches, results indicate 4 x 8 and 6 x 12 early strengths to be about the same on average. After 56 days, 4 x 8 cylinders had about 1.4% greater strength on average.

7.6.4 Statistical Study

A statistical study was conducted using 30 each 4 x 8 and 30 each 6 x 12 cylinders cast from batch series G2B.[86] Ten each 4 x 8 cylinders and 10 each 6 x 12 cylinders were taken from the three different batches of batch series G2B. The cylinders were allowed to cure under ASTM conditions for 56 days and tested for compression strength.

According to Chapter 5, ACI 318-99,[2] the testing of 100 or more specimens is desirable. However, based on the inherent uncertainty that like conditions will exist at the time test specimens are created and the time concrete is produced, a sample size of 30 is deemed adequate. The average required compressive strength, f_{cr}', was determined as the minimum of Equations 7.1 and 7.2 (ACI[2] Equations 5-1 and 5-2, respectively) below where "s" is the standard deviation.

$$f_{cr}' = f_c' + 1.34s \qquad (7.1)$$

$$f_{cr}' = f_c' + 2.33s - 500 \qquad (7.2)$$

Table 7.15 provides the results of the study.

Table 7.15 Results of Statistical Study

Batch #	4 x 8			6 x 12		
	Mean	Required Mean	Standard Deviation	Mean	Required Mean	Standard Deviation
G2B-1	10,717	10,730	528	10,930	10,300	224
G2B-2	10,464	10,740	532	10,349	10,428	319
G2B-3	10,703	10,214	160	10,106	10,557	416
G2B Overall	10,628	10,533	443	10,462	10,635	474

The results in Table 7.15 indicate that the three different batches were not statistically different and that based on 4 x 8 compression strength results the G2B batch series satisfied the requirements for being considered a 10,000 psi design strength mix. Based on 6 x 12 results, the batch series did not satisfy the requirements for being considered a 10,000 psi design strength mix, rather the design strength would be 9,988 psi.

In this research, 4 x 8 cylinders have been used to determine compression strength. Based on this statistical study, an average break strength for the G2 series batches over 10,533 psi indicates the batch series has a 10,000 psi design strength.

7.7 Modulus of Elasticity Results

Modulus of elasticity specimens were cast as specified in Tables 6.1, 7.2 and 7.3. Table 7.16 shows the combined results of all modulus of elasticity testing. Each value represents the average of 3 tests except the ASTM values for batches G1A, G1B, G2A, and G2B that are based on the average of tests on one cylinder from each of the four or five batches in the batch series.

Table 7.16 Modulus of Elasticity Results

Objective Strength Curing	Batch #	Mean Modulus of Elasticity (10^6 psi) (H=Hours, D=Days)			
		16H	24H	28D	56D
8,000 Curebox	8F	3.49	3.67	3.85	3.86
	8L	3.53	3.67		4.02
	G1A		3.57		3.86
	G1B		3.00		3.28
8,000 ASTM	8F				4.13
	8L				4.39
	G1A				3.83
	G1B				3.56
10,000 Curebox	10F	3.48	3.75	4.22	4.08
	10L				4.08
10,000 ASTM	10F				4.26
	10L				4.33
12,000 Curebox	12F	3.92	4.12	4.30	4.26
	12L	4.08	4.25		4.24
	G2A		3.55		3.93
	G2B		3.91		4.10
12,000 ASTM	12F				4.40
	12L				4.33
	G2A				4.06
	G2B				4.05

Examination of Table 7.16 shows that the modulus of elasticity increased with age. In two cases (10F and 12F curebox) the modulus dropped somewhat between 28 and 56 days. In general, it would not appear that significant gain in modulus of elasticity occurs after 28 days.

ASTM specimens produced higher modulus of elasticity results. On average, ASTM results were 5.6 percent higher for the 8,000 psi design strength batches and 1.9 percent higher for the 12,000 psi design strength batches. Percent difference was

calculated by subtracting the ASTM modulus value from the curebox value, dividing the result by the ASTM modulus value and multiplying the result by 100.

The 56-day results from girder construction tests (G1A, G1B, G2A, G2B) were on average 8.9 percent less than the corresponding field production and laboratory evaluation results. This same trend was evident in Table 7.12 with compression strength results. The suspected cause of the lower results for both strength and modulus was the water leak in the concrete mixer. Despite every effort to control moisture, the water leak allowed more water into the mixes than designed.

The results indicate good consistency between the field production (Phase 2) and laboratory evaluation (Phase 3) modulus of elasticity values.

The results from batch G1B indicate a very low modulus value. The cause of the low results could be poorly compacted cylinders or a higher W/CM ratio than anticipated. Cross-referencing the modulus of elasticity results with strength results in Table 7.12 indicates that a higher W/CM ratio was probably the cause.

Figures 7.4 and 7.5 plot the results of modulus of elasticity vs. equilibrium unit weight and modulus of elasticity vs. compression strength, respectively, from this research and from the data presented in Chapter 2 (Table 2.1). Linear trendlines representing the experimental data and the proposed equation (Equation 3.1) are plotted on each graph. The results from this research are based on 56-day tests; the exact age of data presented in Table 2.1 is unknown. Appendix C lists all modulus of elasticity values. Overall, Equation 3.1 conservatively predicted modulus of elasticity by 4.4 percent with a standard deviation of 6.2 percent.
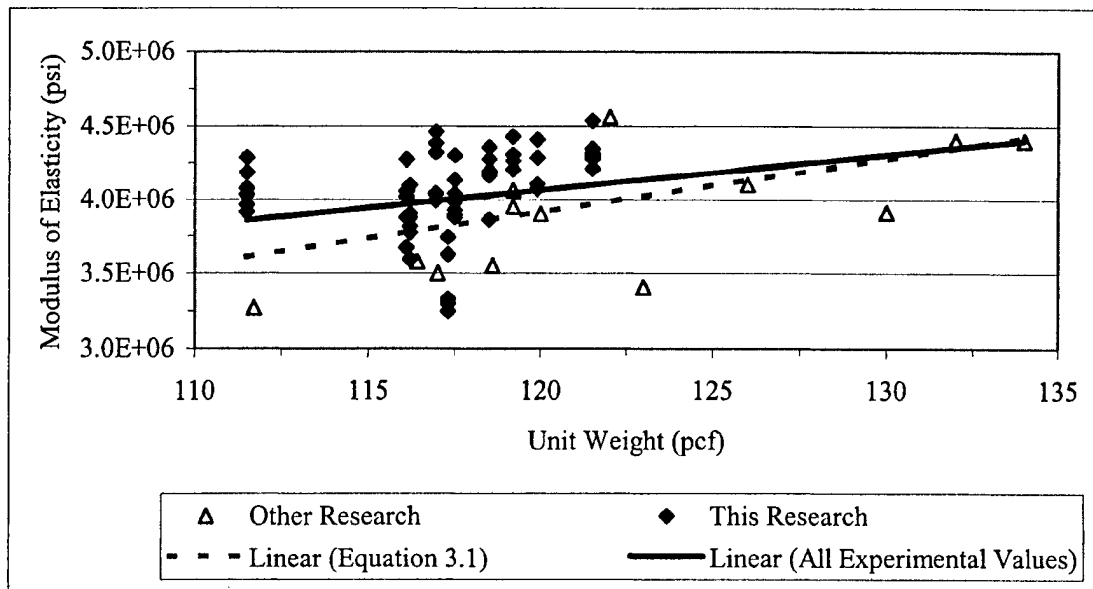
Figure 7.4 Modulus of Elasticity vs. Equilibrium Unit Weight
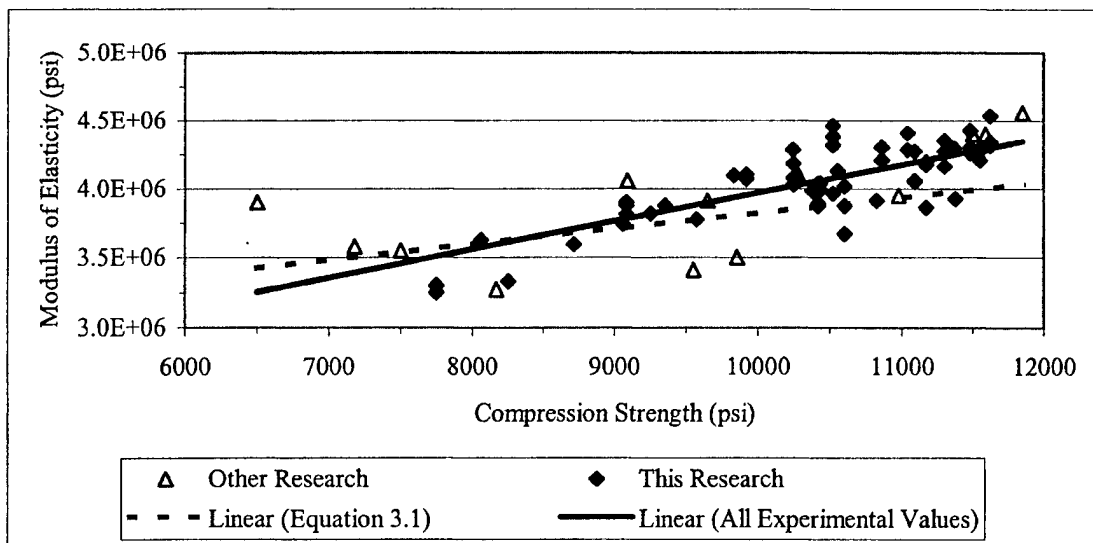
Figure 7.5 Modulus of Elasticity vs. Compression Strength

$$E_c = (33,000\sqrt{f_c'} + 4,000,000)(w_c/242)^{0.9}$$ (3.1)

For comparison, the same modulus of elasticity values used previously to evaluate

Equation 3.1 were used to evaluate the current equations (Equations 7.3 and 2.1) for

modulus of elasticity suggested in ACI 363[87] and by ACI 318[2], respectively.

$$E_c = (40,000\sqrt{f_c'} + 1,000,000)(w_c/145)^{1.5}$$ (7.3)

$$E_c = 33w_c^{1.5}\sqrt{f_c'}$$ (2.1)

On average, Equation 7.3 conservatively predicted the modulus of slate HSLC by about

9.5 percent with a standard deviation of 5.5 percent. On average, Equation 2.1 predicted

the modulus of slate HSLC by about 5.3 percent greater than that found experimentally

with a standard deviation of 4.6 percent.

In an attempt to better align the predicted modulus of elasticity values with the

experimental values, and to determine a simpler equation than Equation 3.1, a similar

investigation was done as detailed in Section 3.3 and shown in Figures 3.4 and 3.5.

The experimental modulus of elasticity values were normalized separately by

dividing by $(f_c')^{0.5}$, $(w_c)^{0.5}$, and $(w_c)^{1.5}$. The resulting plot normalized by $(f_c')^{0.5}$ is shown

in Figure 7.6.
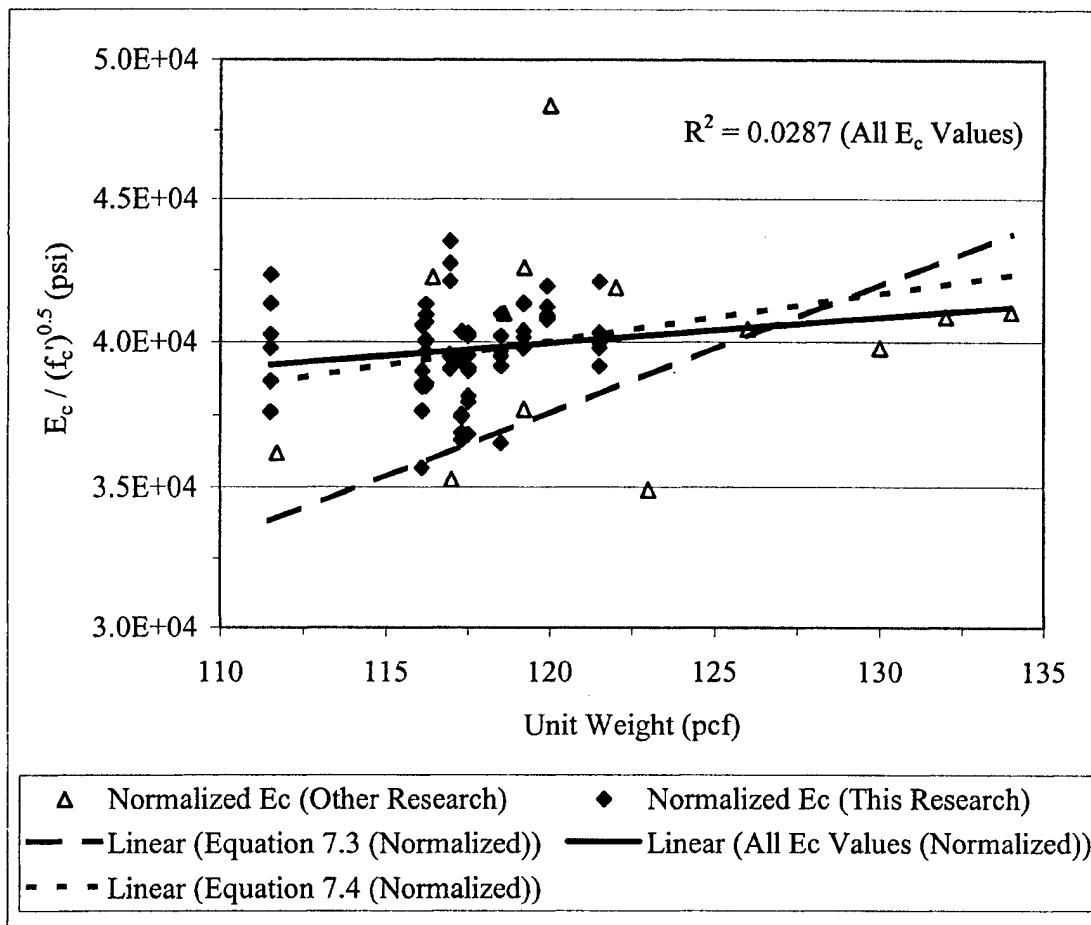
Figure 7.6 Experimental Modulus of Elasticity Values Normalized by $(f_c')^{0.5}$

An evaluation of the best-fit relation for "All E_c Values" (all experimental E_c values from this research and other research) showed that a linear trend line was as good or better than other possible curves. The R^2 value for the linear relation was 0.0287 for "All E_c Values." The indication in Figure 7.6 was that the roll of unit weight in determining modulus of elasticity was highly variable resulting in wide scatter and a low R^2 value. In other words, modulus of elasticity for slate HSLC showed little relation to w_c.

The linear trend resulting from Equation 7.3 used to predict modulus of elasticity, normalized by $(f_c')^{0.5}$, is also plotted in Figure 7.6. Equation 7.3 contains the term $w_c^{1.5}$, which emphasizes the effect of unit weight. The resulting linear trend does not compare favorably with the trend indicated by experimental values (all E_c values).

Similar evaluations with other variable forms indicated that $(f_c')^{0.5}$ was the variable that appeared most appropriate in predicting modulus of elasticity.

After examining several equation forms, Equation 7.4 was determined to be the equation that best predicted the modulus of elasticity of slate HSLC.

$$E_c = 44,000\sqrt{f_c'\frac{w_c}{145}} \tag{7.4}$$

Overall, Equation 7.4 provided a better prediction of modulus of elasticity for slate HSLC than the previously suggested Equation 3.1. Equation 7.4 conservatively predicted modulus of elasticity values by 0.2 percent on average with a standard deviation of 5.1 percent. The linear trend resulting from Equation 7.4 used to predict E_c values is also plotted in Figure 7.6. Since Equation 7.4 contains the term $w_c^{0.5}$, which de-emphasizes unit weight, the resulting linear trend compares more favorably with the trend indicated by the experimental values (all E_c values).

Low, mean, and high unit weight values of 111.5 pcf, 118.2 pcf, and 134 pcf, respectively, were determined from the 56-day experimental modulus of elasticity values from this research project and modulus of elasticity values from other research as listed in

Table 2.1. Figure 7.7 shows a plot of the above-mentioned values vs. compression

strength and also shows lines plotting the predicted modulus of elasticity using Equation

7.4 based on the low, mean and high unit weight values. Figure 7.7 shows that at a given

compressive strength, the variation in modulus of elasticity can be substantial. At a

compressive strength of approximately 10,600 psi, the modulus of elasticity varied from

approximately 3.65 million psi to 4.45 million psi.

Figures 7.8 and 7.9 show Equation 2.1 and Equation 7.3, respectively, evaluated

using the low, mean, and high unit weight values plotted over the same modulus of

elasticity values shown in Figure 7.7. Equation 2.1 unconservatively predicted modulus

of elasticity for slate HSLC; Equation 7.3 conservatively predicted modulus of elasticity

for slate HSLC.
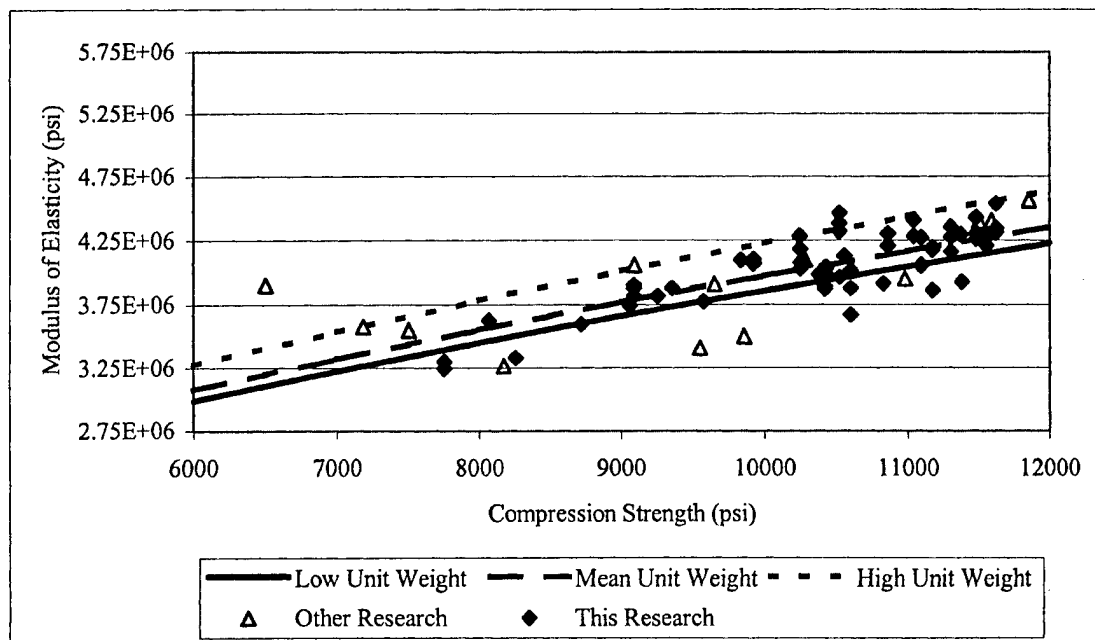
Figure 7.7 Low, Mean, and High Unit Weight Values Plotted Using Equation 7.4
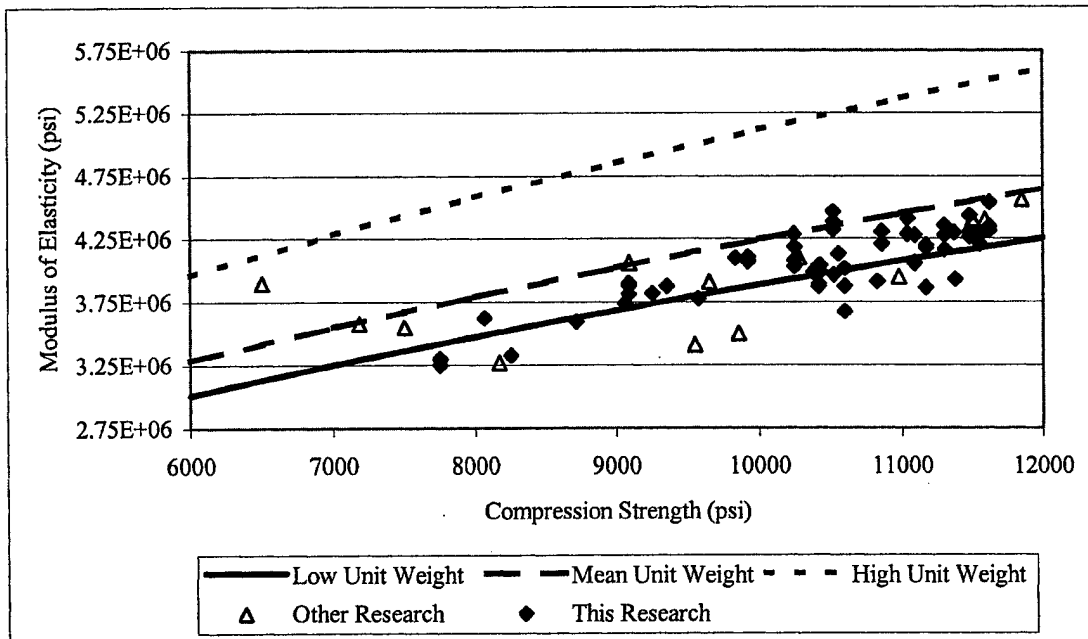
Figure 7.8 Low, Mean, and High Unit Weight Values Plotted Using Equation 2.1
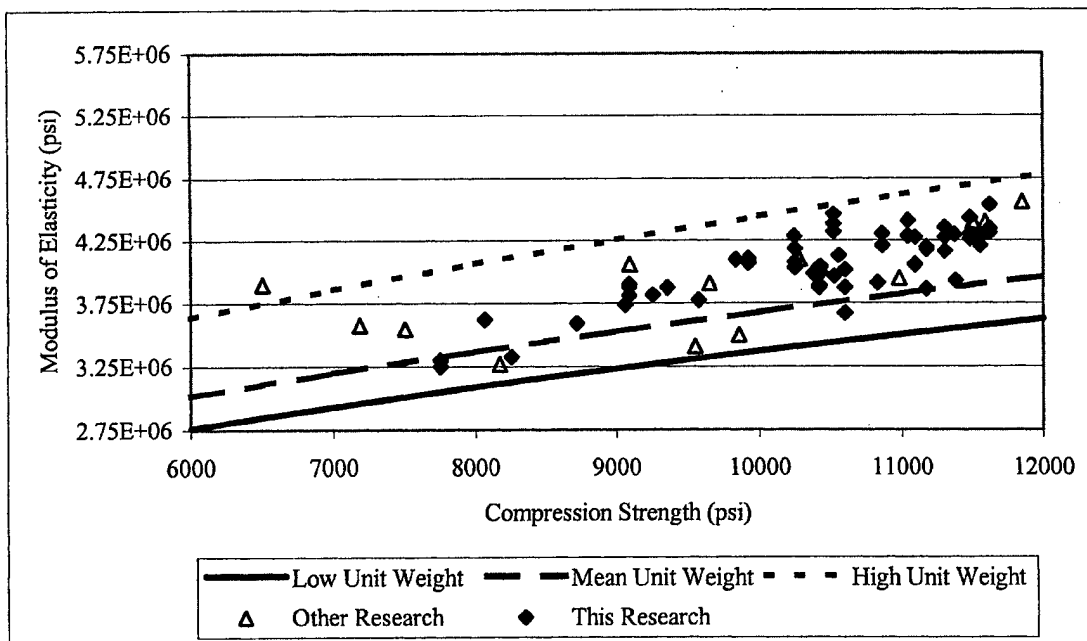
Figure 7.9 Low, Mean, and High Unit Weight Values Plotted Using Equation 7.3

138

7.8 Modulus of Rupture Results

Modulus of rupture specimens were cast as specified in Tables 6.1, 7.2 and 7.3. Table 7.17 shows the combined results of all modulus of rupture testing. Each value represents the average of 3 tests except the ASTM values for batches G1A, G1B, G2A, and G2B that are based on the average of tests on one specimen from each batch in the batch series. The 56-day normalized modulus of rupture value was calculated by dividing the 56-day modulus of rupture by λ and $(f_c')^{1/2}$.

Table 7.17 Modulus of Rupture (f_r) Results

Objective Strength Curing	Batch Series #	Mean Modulus of Rupture (H=Hours, D=Days) (psi)		$\dfrac{f_r}{\lambda\sqrt{f_c'}}$	Concrete Compressive Strength (psi)	Mean Normalized Values
		24H	56D	56D	56D	56D
8,000 Curebox	8F	788	1,089	12.43	10,160	12.20
	8L	649	1,077	12.40	10,430	
	G1A		1,042	12.86	9,080	
	G1B		830	11.09	7,750	
8,000 ASTM	8F					10.84
	8L	761	1,030	11.81	10,520	
	G1A		992	11.21	9,350	
	G1B		743	9.50	8,460	
10,000 Curebox	10F	641	998	11.10	11,170	12.42
	10L	670	1,164	13.74	9,920	
10,000 ASTM	10F					11.26
	10L	678	1,006	11.26	11,040	
12,000 Curebox	12F	761	1,014	11.10	11,550	12.10
	12L	645	926	10.45	10,860	
	G2A		1,283	14.79	10,420	
	G2B		1,038	12.06	10,250	
12,000 ASTM	12F					10.79
	12L	678	918	10.07	11,480	
	G2A		1,156	13.07	10,820	
	G2B		805	9.23	10,510	

The modulus of rupture results shown in Table 7.17 are difficult to interpret. Based on 56-day strengths, the specimens cured in insulated cureboxes produced higher rupture strengths than ASTM cured specimens. This trend is opposite of that seen for all other specimens where ASTM cured specimens resulted in higher strengths.

In examining specimens cast during field production, the specimens coming from batches with the highest compression strength produced the lowest modulus of rupture values on average for both 24-hour and 56-day data. In examining specimens cast during girder construction, the specimens coming from batches with the highest compression strength produced the highest modulus of rupture values on average.

ACI 318-99[2] specifies that rupture modulus, f_r, can be predicted using ACI Equation (9-9) shown in Equation 7.5 below.

$$f_r = 7.5\lambda\sqrt{f_c'}$$ (7.5)

The normalized values shown in Table 7.17 indicate good consistency between curebox and ASTM values. The average normalized curebox values are consistently higher than the average ASTM values. It would appear these values indicate a consistency of specimen casting and curing throughout all strengths and types of curing.

Other researchers[11,12,14] have commented on difficulties encountered in using modulus of rupture test results for predicting the cracking strength of concrete beams. They indicated the test is significantly impacted by the level of moisture during curing and indicated the splitting tension test per ASTM C 496[88] provided a better indication of

140

beam cracking strength. Nevertheless, the normalized values indicate that the "7.5" value used in Equation 7.5 is conservative.

7.9 Conclusions

Batching concrete in a mixer having a water leak will most likely produce more widely scattered test results.

For 4 x 8 cylinders cast during girder construction, substantial strength gain occurred between 56 days and the time of testing. For 4 x 8 cylinders cast as part of field production testing (8F, 10F, and 12F) strength gain continued through 365 days. It is likely that internal curing contributed to these gains.

As a general rule, for strength testing after 56 days, 4 x 8 cylinders provided on average about 1 percent higher strength values than 6 x 12 cylinders.

ASTM cylinders on average had about 4 percent higher strength than curebox cylinders at 56 days of age or later.

Modulus of elasticity tests on ASTM cylinders produced higher values than corresponding tests on curebox cylinders.

Equation 3.1 conservatively predicted modulus of elasticity results for slate HSLC. Equation 7.4 provided a better overall prediction that was still conservative. Equation 2.1 provided an unconservative prediction of modulus of elasticity. The modulus of elasticity for slate HSLC showed little relation to w_c.

The modulus of rupture test results indicated great variability and that the current ACI equation (Equation 7.5) conservatively predicts f_r.

CHAPTER VIII

DESIGN AND CONSTRUCTION OF HSLC PRETENSIONED BRIDGE GIRDERS

8.1 Introduction

The following objectives were established to serve as guidelines to prioritize and focus the experimental design and procedure.

1. To determine the transfer length, l_t, for 0.6-inch diameter prestressing strand used with slate HSLC.

2. To determine the development length, l_d, for 0.6-inch diameter prestressing strand used with slate HSLC.

3. To verify current code equations for l_t and l_d as appropriate for use with slate HSLC and suggest better equations if necessary.

4. To determine the effect of shear reinforcement spacing on strand slip, development length, and shear capacity of pretensioned slate HSLC girders.

5. To determine the shear strength, V_c, of prestressed slate HSLC.

6. To verify current code equations for shear strength of slate HSLC.

7. To verify the current code-specified reduction factor, λ, for SLWC as related to concrete tensile strength, and, suggest a more appropriate factor if necessary.

142

In order to achieve the seven experimental objectives, the following variables were altered in order to observe the results.

Concrete Compressive Strength, f_c'. Concrete design strengths of 8,500 and 10,000 psi were used for girder construction.

Shear Span to Depth Ratio, a/d. The "a" distance was varied from approximately 63 to 100 percent of the current code-specified l_d value.

Yield Strength of Shear Reinforcement Steel, f_y. Only Grade 60 # 4 bar stirrups were used. Values of f_y of 60 ksi (414 MPa) and the actual f_y value were used to determine whether an upper limit was appropriate for use with HSLC.

Spacing of Shear Reinforcement Steel, "s." The "s" distance was varied to determine the impact of A_v/s on l_d, strand slip, and shear strength.

Span Length of Tested Section, L_t. In order to achieve three tests per girder, the span length was varied to focus on specific sections of the girder for each test.

8.2 Design of Experiment

8.2.1 Type of Girders and Prestressing Strands

AASHTO Type II cross-sections were chosen for testing for several reasons. First, other recent experimental research on transfer and development length was done at Georgia Tech[84] and at the University of Texas at Austin[44] using AASHTO Type II girders. The ability to compare results was desirable. Second, Type II girders were more easily fabricated, transported and handled in the lab and were more economical to produce than larger sections. Third, the section was sufficiently deep to yield the

143

prestressing strands, which was required to investigate development length. By properly configuring the girder cross-section, it was possible to achieve applicable testing results and data.

The prestressing reinforcement chosen was 0.6-inch diameter, 270-ksi, 7-wire, low relaxation (LOLAX) strand provided by Insteel.

In order to produce the worst-case bond situation, the girders were configured with 8 each 0.6-inch diameter strands in the bottom row. In an AASHTO Type II girder, 8 strands constituted a full layer in the bottom flange. In the event of a severe bond failure, a horizontal crack would be induced across the full layer of prestressed reinforcement. The bottom strands were positioned at a distance 3 inches from the bottom of the girder as per GDOT standards and designed for prestressing to $0.75*f_{pu}$ or 203 ksi creating the worst-case bond situation.

In addition to the 8 bottom strands, 2 each 0.6-inch strands were placed 2.5 inches from the top of the girder. The purpose of these strands was to control tension stress at the top of the girder at time of strand release, and as a means to space and secure shear reinforcement. The top strands were also stressed to a level of $0.75*f_{pu}$ or 203 ksi.

8.2.2 Configuration of Girders for Testing

In previous work,[44,84] pretensioned girders were configured such that two tests per girder were possible; one test at each girder-end. In some cases, the center portion of the girder was left predominantly undamaged in the testing process. It was thought that a third test might be possible at the center of the girder with careful planning and proper design. There were two important reasons for wanting to test the center of the girder.

144

First, since girder cost was a major portion of the research budget, it was thought that by lengthening the girders it would be possible to achieve a third test at relatively little additional cost. Second, and more importantly, by testing the center portion of the girder, it would be possible to insure a fully developed strand and to more clearly focus on the shear characteristics of HSLC. When testing at the girder's ends, the data related to shear could possibly be skewed by less than fully developed pretensioning strands. Each of the six girders in this research project was configured to allow three tests per girder. This reduced the cost per test and provided substantially more data related to the shear strength of HSLC.

8.2.3 Prestressed Girder Design Spreadsheet

In order to facilitate the design of each girder, an EXCEL spreadsheet was developed to perform repetitive calculations related to the design of prestressed slate HSLC girders. The spreadsheet was very comprehensive and allowed the user to input numerous variables related to pretensioned girder design. Calculations within the spreadsheet were based on the 1996 AASHTO[40] Standard Specification. A complete description of the spreadsheet along with an example of the design of girder test G1C-West is presented in Appendix D.

8.2.4 Composite Girder Cross Section

It was desirable to construct the deck with a width as close to the width of the top flange of the girder as possible for ease of forming and testing. In addition, based on

previous research,[55,84] it was desirable to achieve a greater depth of composite girder to increase the strain at the level of the bottom strands.

The goal of the testing was to simulate the conditions seen in composite girders found in actual bridges. As such, it was desirable to replicate the moment arm "jd" in testing, as it would be encountered in actual bridge structures. An analysis was conducted assuming AASHTO Type II girders and deck thicknesses as specified by a standard GDOT deck design guide.[89] For girder spacings from 42" to 120", the minimum deck thickness varied from about 6.5 inches to 8.6 inches and jd varied from 31.65 to 34.74 inches with a jd of 33.75 inches for a 7-foot girder spacing

A deck thickness of 11.5 inches and width of 19 inches was selected. This combination produced a predicted internal moment arm of 33.61 inches, which closely matched the desired 7-foot girder spacing. In addition, a deck width of 19 inches meant simplified formwork for deck placement. Thus, by increasing the deck thickness to 11.5 inches, it was possible to increase the depth of the composite girder to increase strain demand on the bottom strands, simplify the formwork for casting of the deck, and closely replicate the moment arm "jd" encountered in standard bridge design.

8.2.5 Composite Girder Design

Having determined the configuration of the composite girder cross-section, it was possible to determine the layout of the girders for testing. In designing three tests per girder, it was important to insure that one test did not overly damage other future test areas on the girder.

146

8.2.5.1 Concept of Testing Sequence

Portion of Girder Damaged During Test # 1

Test # 1 on Composite Girder

Portion of Girder Damaged During Test # 2

Test # 2 on Composite Girder

Center
Of
Bearing

Center
Of
Bearing

L_2

L_1

L

Test # 3 on Composite Girder
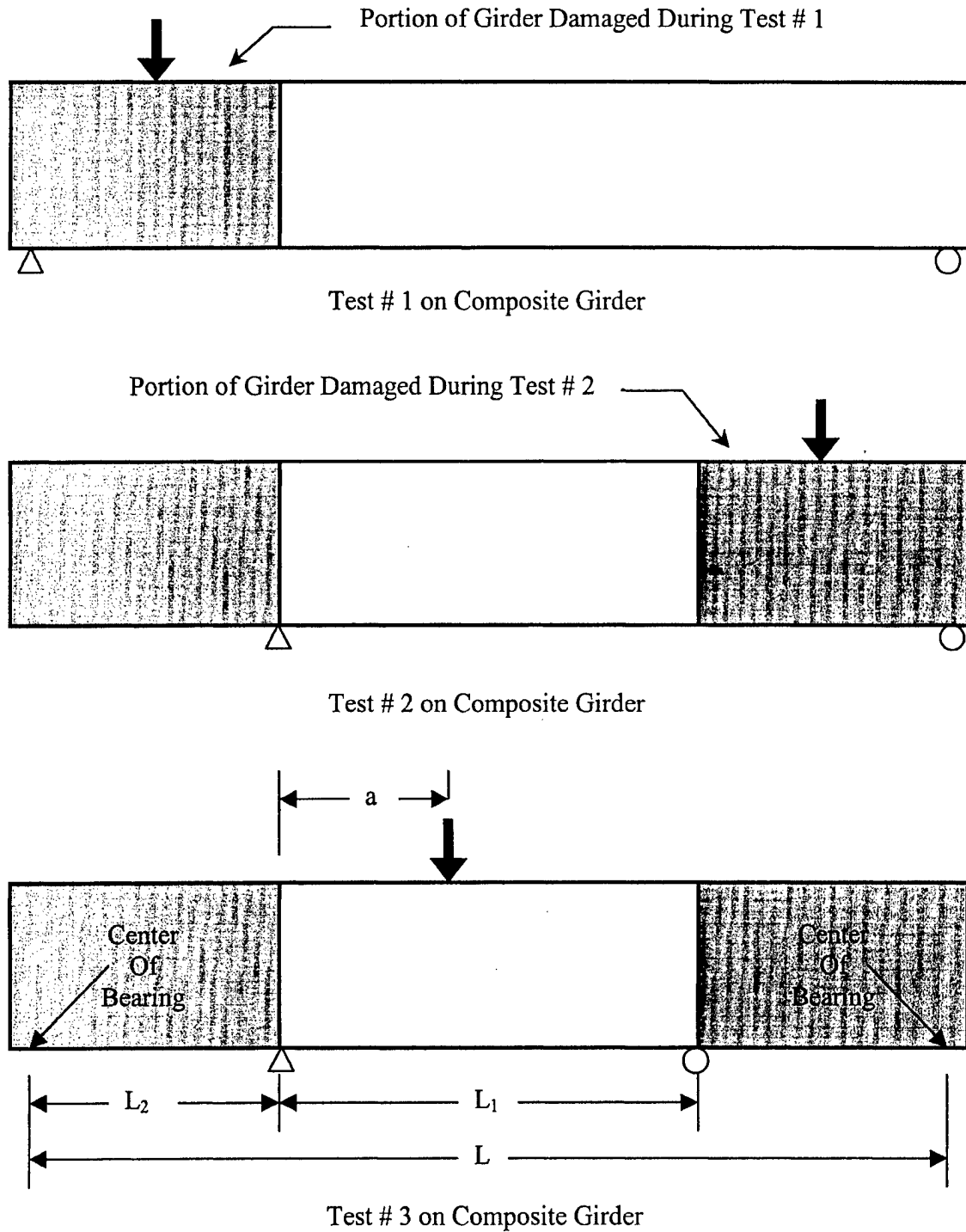
Figure 8.1 Concept of Girder Testing Sequence

147

The first test entailed supporting the girder over its entire length and testing one end. The second test involved moving the left support to a point inside any significant damage resulting from the first test, and testing the opposite end of the girder. The third test involved moving the right support to a point inside any significant damage resulting from the second test and testing the center portion of the girder. By using this sequence, it was possible to achieve three tests from one girder.

8.2.5.2 Experimental Objectives vs. Girder Design

The following guidelines were established for girder design to accomplish the objectives set in Section 8.2.

1. Install DEMEC gage points on the girder at the ends on both sides of the top flange (from girder-end to a distance of 30 inches) and bottom flange (from girder-end to a distance of 48 inches) to facilitate measurement of concrete surface strains and allow calculation of the transfer length, l_t. This action allowed achievement of research objective 1.

2. Install DEMEC gage points on the girder on both sides of the top and bottom flange at midspan over a distance of 24". This action allowed determination of the effective prestressing force at midspan which was essential information for the achievement of all objectives.

3. Apply a point load to the composite girder at approximately 70 percent, 85 percent, 95 percent and 100 percent of l_d where l_d was determined by the 1996 AASHTO[40] Standard Specification. The point at which the failure transitioned from a "shear-type" failure to a "flexural-type" failure was the point at which the

strand was considered fully developed. Shear reinforcement in these tests was in accordance with the 1996 AASHTO[40] Standard Specification. This action allowed achievement of research objectives 2 and 3 and partial achievement of objective 4.

4. Using double the amount of shear reinforcement required according to the 1996 AASHTO[40] Standard Specification together with applying a point load at approximately 70 percent and 85 percent of l_d allowed achievement of research objective 4, and partial achievement of objectives 5, 6 and 7.

5. Using varying amounts of shear reinforcement and loading the girder with varying a/d ratios allowed achievement of research objectives 5, 6 and 7.

8.2.5.3 Composite Girder Design Procedure

Three each Series G1 girders and three each Series G2 girders were designed with concrete design strengths, f_c', of 8,500 psi and 10,000 psi, respectively. Based on previous experiences, it was assumed the girder lengths would be in the range of 35-45 feet. Final design lengths were revised to accommodate the tests as needed. Three tests were planned for each of the six girders indicating 18 total tests. Since two concrete strengths were being investigated, there were 9 different test configurations that were performed on each series of girders. The prestressed girder design spreadsheet was used to iteratively design the tests to fit on the girders. The resulting tests were detailed in Table 8.1. The a/d ratio listed under "Point Load Placement Criteria" is the shear span to depth ratio where "d" is the total height of the composite girder.

149

Table 8.1 – Girder Test Configurations

Test Configuration	Stirrup Density	Point Load Placement Criteria	Shear Span "a" (inches)	Distance "L₁" (inches)	Distance "L₂" (inches)	Distance "L" (inches)
1	Single	l_d	90	456	0	456
2	Double	$0.70*l_d$	61	316	0	456
3	Double	$0.85*l_d$	75	456	0	456
4	Single	$0.95*l_d$	85	504	0	504
5	Single	$0.70*l_d$	61	321	0	456
6	Single	$0.85*l_d$	75	369	0	504
7	Minimum	a/d=2.28	82	185	140	456
8	Minimum	a/d=2.67	96	210	135	456
9	Minimum	a/d=3.33	120	244	135	504

d = 47.5 inches

The dimension "a" was the shear span. The dimension L_1 was the distance from the left support to the right support. The dimension L_2 was the distance from the left COB to the left support. The COB was the point a distance of 6 inches in from each girder-end that was assumed to be the girder's support point for curing. L_2 was used to signify a cantilever on the left girder-end. The dimension L was the distance from COB to COB. The dimensions "a," L_1, L_2 and L are shown in Figure 8.1.

Diagrams of the test configurations are depicted in Figures 8.2 through 8.10. Diagrams of the resulting three girders, configuration "A", "B" and "C", in each series, G1 and G2, are depicted in Figures 8.11 through 8.13. The testing sequence was alike for each girder with the left end tested first, the right end next, and the center section last.

150
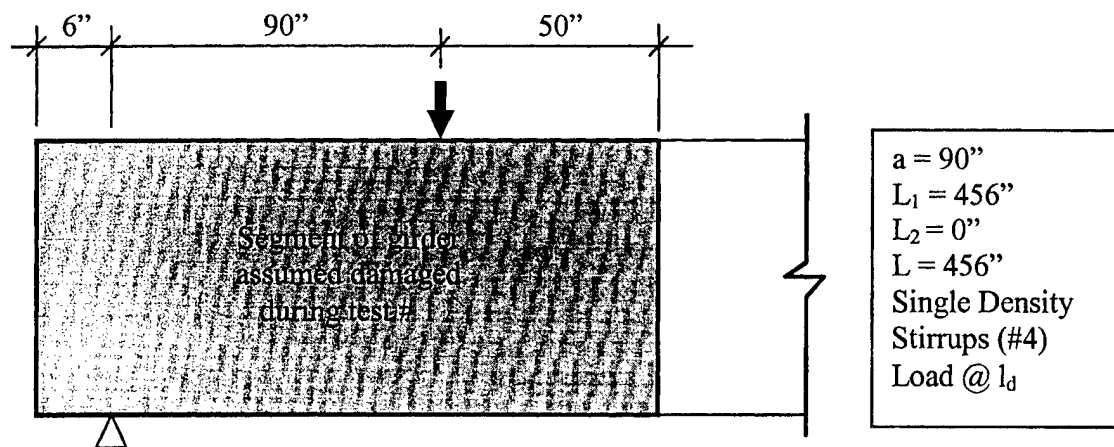
Figure 8.2 Test Configuration 1

a = 90"
L_1 = 456"
L_2 = 0"
L = 456"
Single Density
Stirrups (#4)
Load @ l_d
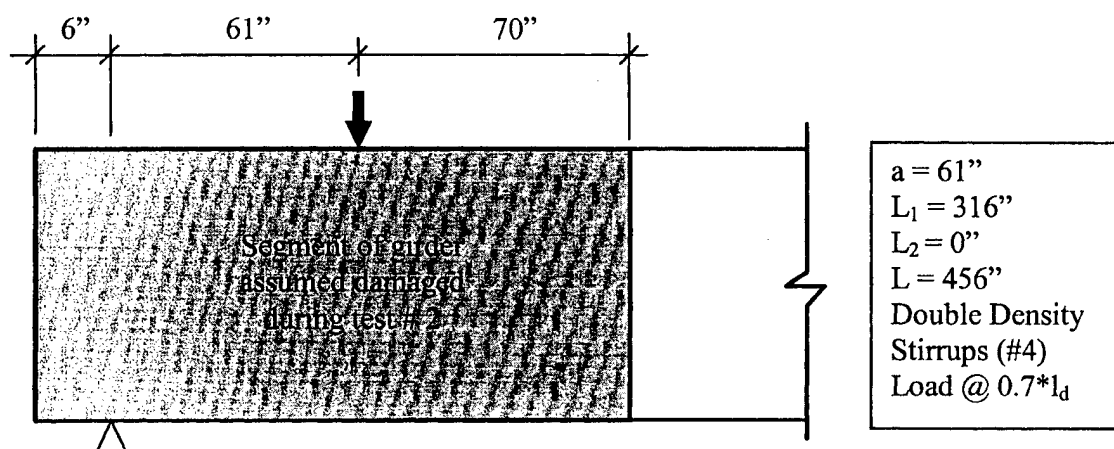
Figure 8.3 Test Configuration 2

a = 61"
L_1 = 316"
L_2 = 0"
L = 456"
Double Density
Stirrups (#4)
Load @ 0.7*l_d
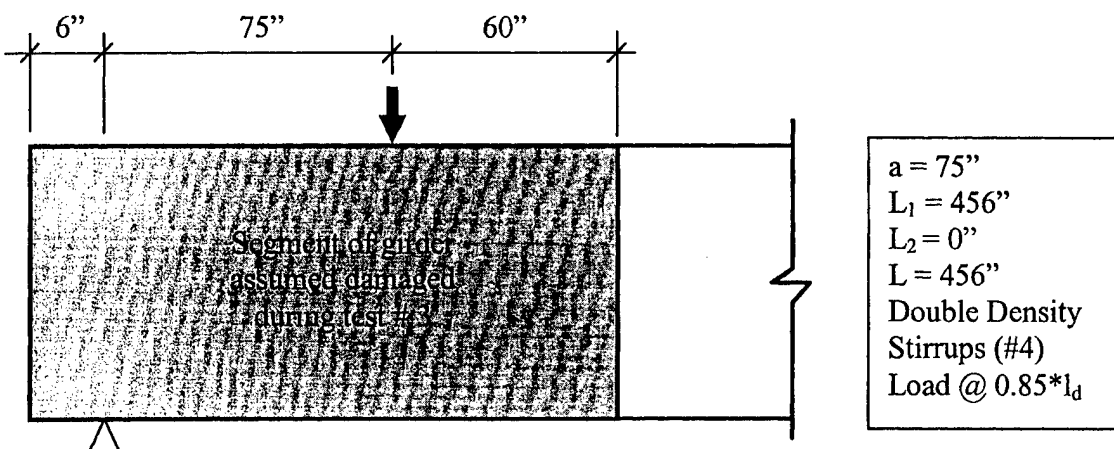
Figure 8.4 Test Configuration 3

a = 75"
L_1 = 456"
L_2 = 0"
L = 456"
Double Density
Stirrups (#4)
Load @ 0.85*l_d

151
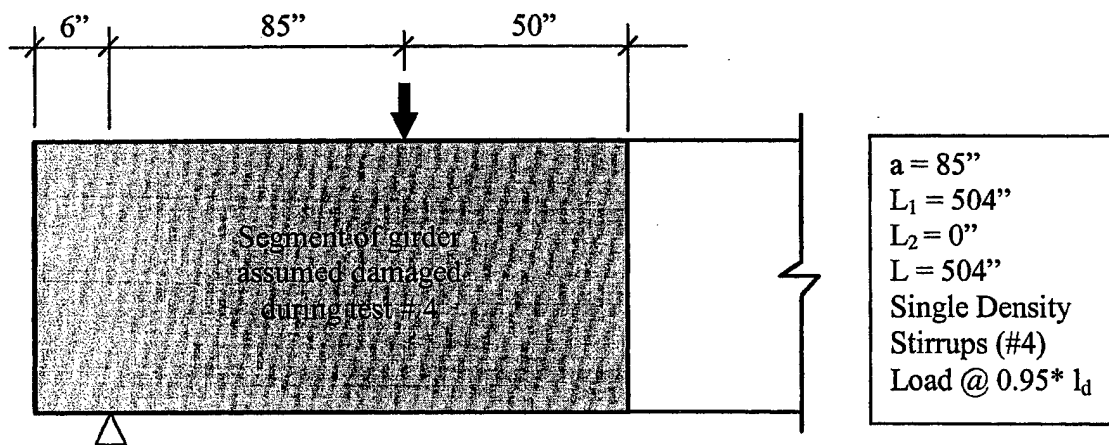
Figure 8.5 Test Configuration 4

| a = 85" |
| L_1 = 504" |
| L_2 = 0" |
| L = 504" |
| Single Density |
| Stirrups (#4) |
| Load @ 0.95* l_d |
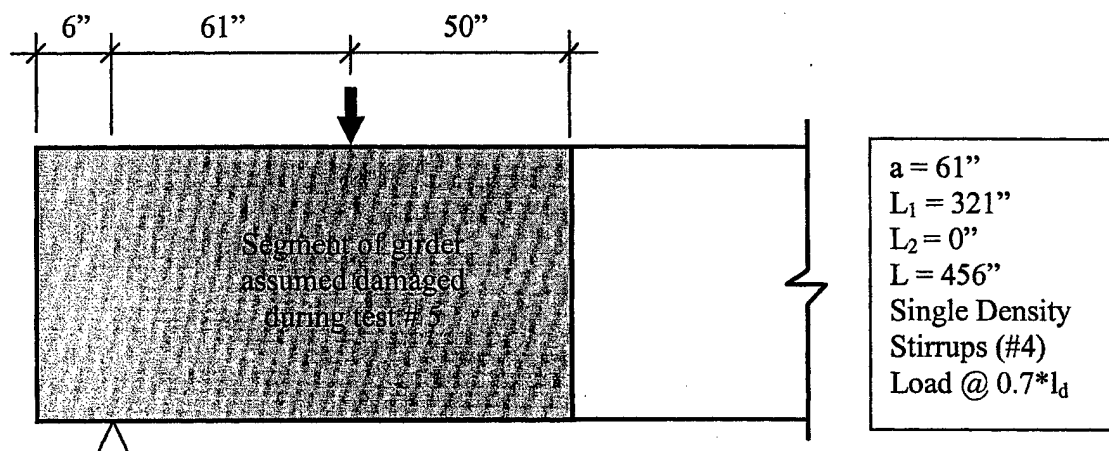
Figure 8.6 Test Configuration 5

| a = 61" |
| L_1 = 321" |
| L_2 = 0" |
| L = 456" |
| Single Density |
| Stirrups (#4) |
| Load @ 0.7*l_d |
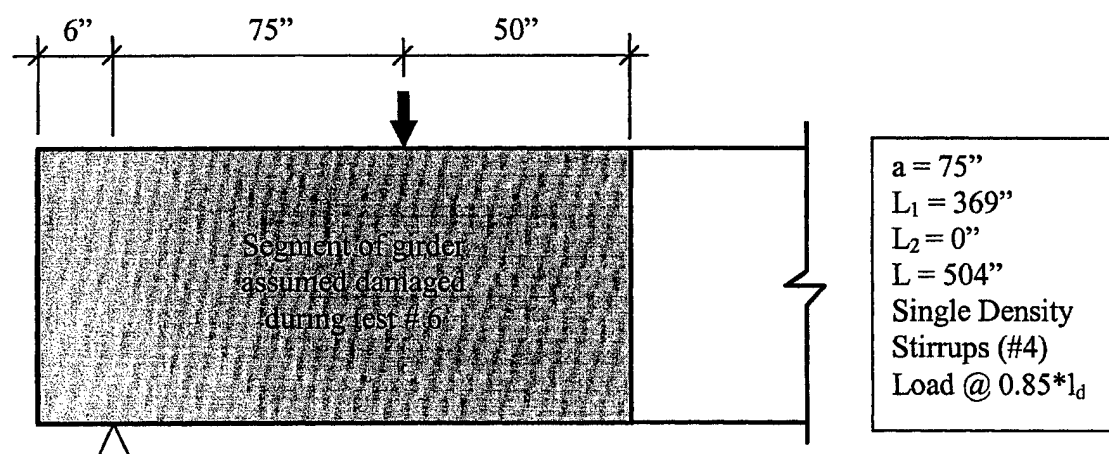
Figure 8.7 Test Configuration 6

| a = 75" |
| L_1 = 369" |
| L_2 = 0" |
| L = 504" |
| Single Density |
| Stirrups (#4) |
| Load @ 0.85*l_d |
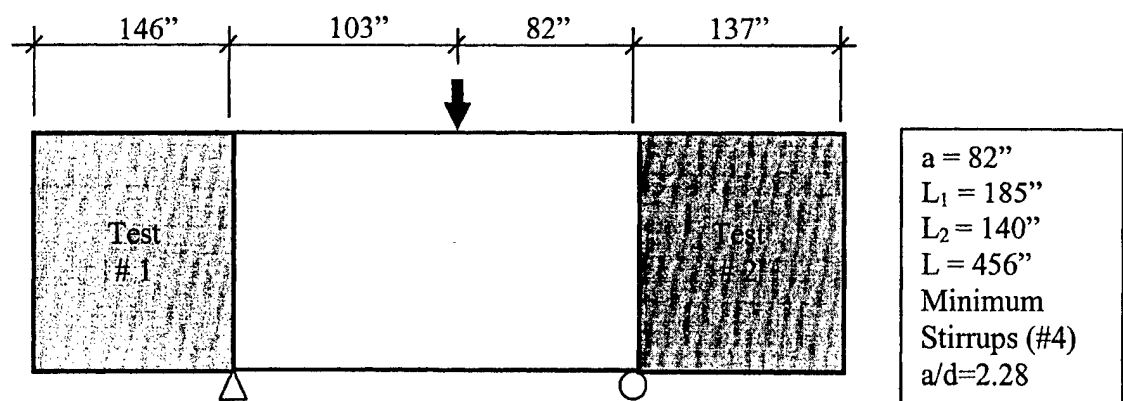
Figure 8.8 Test Configuration 7
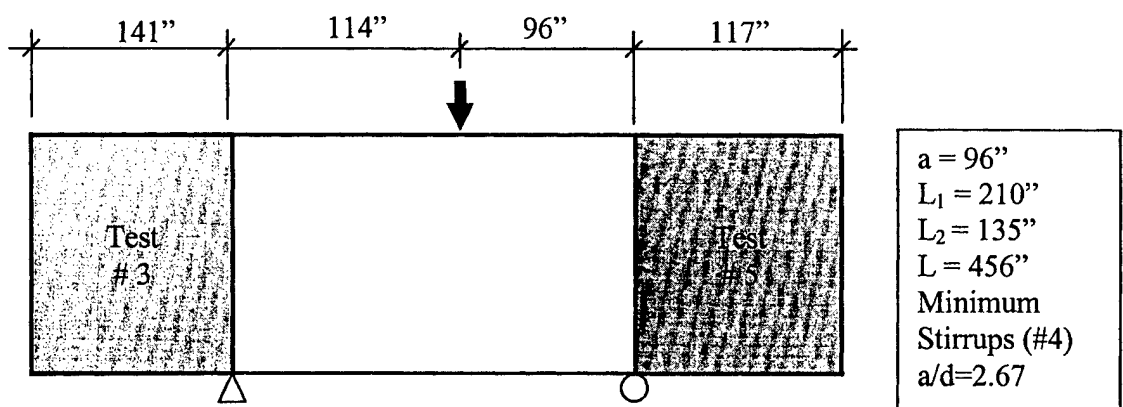
Figure 8.9 Test Configuration 8
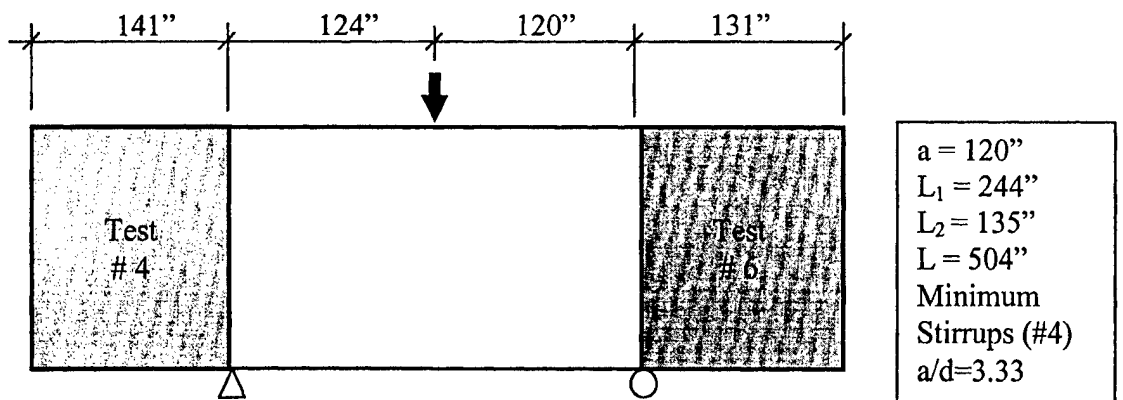
Figure 8.10 Test Configuration 9

153

|← 146" →|← 89" →|← 96" →|← 137" →|

Stirrups @ 24" Spacing

Test #1 | Test #7 | Test #2
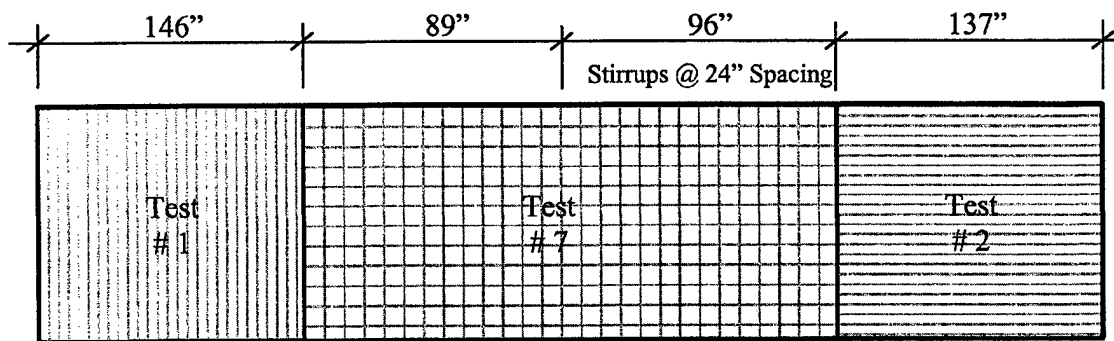
Figure 8.11 Girder Layout A

|← 141" →|← 114" →|← 96" →|← 117" →|

Stirrups @ 24" Spacing

Test #3 | Test #8 | Test #5
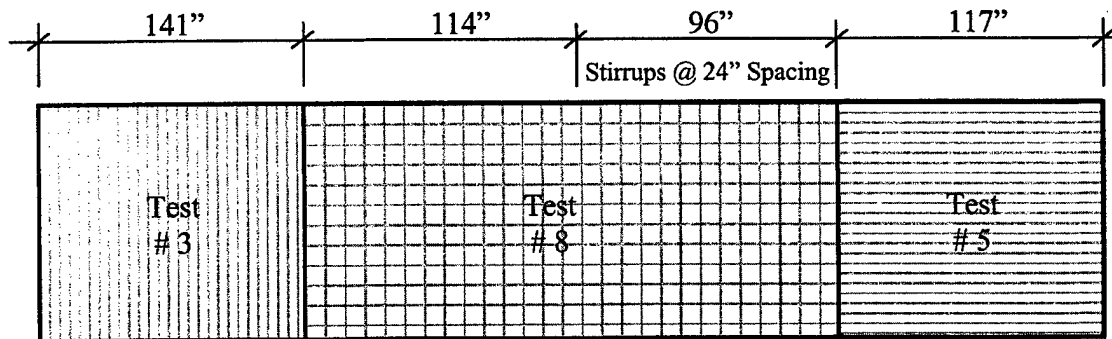
Figure 8.12 Girder Layout B

|← 141" →|← 124" →|← 120" →|← 131" →|

Stirrups @ 24" Spacing

Test #4 | Test #9 | Test #6
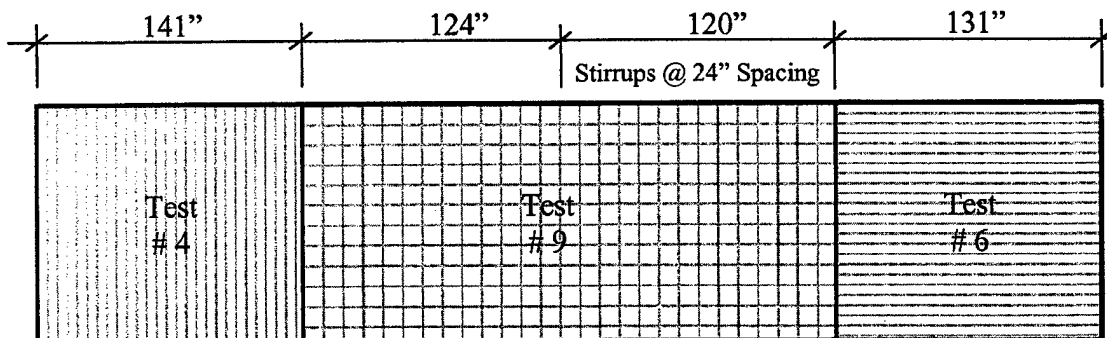
Figure 8.13 Girder Layout C

154

8.2.5.4 Design Considerations

In designing the test girders, it was necessary to assume a damaged area resulting from each test. In the case of tests 1 through 6, it was assumed that a distance equal to at least "d" away from the point of load application towards the center of the girder would be damaged in addition to the specific area of interest. In the case of girders having double the AASHTO specified amount of shear reinforcing steel, additional area was added for damage as a precaution.

Another consideration in configuring tests 2, 5 and 6 was the fact that a portion of the center of each girder was reinforced with only the minimum-specified 24" steel spacing as seen in Figures 8.8 through 8.10. This 24" spacing area would be used during tests 7 through 9 to specifically examine the shear capacity of the girders. In order to ensure that this area would not undergo significant damage other than minor flexural cracking, girder-bottom stresses were examined for tests 2, 5 and 6 in the area of 24" stirrup spacing. Tests 2, 5 and 6 were critical since the distance between supports would be less allowing a greater point load and thus a greater shear to develop. As long as the resulting bottom stresses were less than $12(f_c')^{1/2}$, it was assumed that resulting damage would not be a significant factor for center-girder tests. In all cases, the bottom stresses were below the critical level.

8.2.5.5 Final Girder Designs

In order to arrive at the final girder designs, tests 1-9 were configured into three girders such that consistent lengths could be achieved to the greatest extent possible. For each series, two each 39-foot girders and one 43-foot girder were configured. Based on

the closeness of the Series 1 and Series 2 concrete design strengths, the shear design

varied only slightly. Based on this closeness of design, it was decided to construct both

series of girders with the same shear reinforcement spacing.

As part of the final design, additional # 4 stirrups were positioned in the initial d/4

of the girder at both ends to control bursting forces as per AASHTO[40] Section 9.22.1.

Five # 3 "doghouse bars" were spaced at 12 inches on center in the bottom flange at both

ends of each girder to enclose the prestressing steel as per AASHTO[40] Section 9.22.2.

Figures 8.14 through 8.16 provide sketches of girders "A", "B", and "C." The

final designs were the same for both series of girders. These final designs were provided

to the fabricator for production of the girders.

5 each # 3 "doghouse" bars spaced at 12" (Typ both ends)

2" End Cover (Typ both ends)
4 Spaces @ 2" (Typ both ends)

18' – 9"
33 spaces
(7" max spacing)

8' – 0"
4 spaces
(24" max spacing)

10' – 7"
37 spaces
(3-1/2" max spacing)

39' – 0"

AASHTO Type II

f'_c = 8,500 psi (10,000 psi) (75% of f'_c at Release)

Strand = 0.6" 270 ksi LOLAX pulled to 75% of f_{pu}

Strand Spacing = 2"

Distance From Bottom to 1st Row of Strands = 3.0"

Distance From Bottom to TOP Row of Strands = 33.5"

Stirrup (# 4 Bars) Spacing Shown Above

Total Stirrups = 186 (2 at each location)

Total Doghouse Bars = 10

Beam top surface to be intentionally roughened (raked)

Drawn by: KFM Phone (404) 385-1429

Stirrup Detail

43-3/4"

7"

4

8-1/2"

Figure 8.14 Girder Layout A

157

Stirrup Detail

AASHTO Type II

f'_c = 8,500 psi (10,000 psi) (75% of f'_c at Release)

Strand = 0.6" 270 ksi LOLAX pulled to 75% of f_{pu}

Strand Spacing = 2"

Distance From Bottom to 1st Row of Strands = 3.0"

Distance From Bottom to TOP Row of Strands = 33.5"

Stirrup (# 4 Bars) Spacing Shown Above

Total Stirrups = 186 (2 at each location)

Total Doghouse Bars = 10

Beam top surface to be intentionally roughened (raked)

Drawn by KFM   Phone: (404) 385-1429

Figure 8.15 Girder Layout B

158

Stirrup Detail

5 each # 3 "doghouse" bars spaced at 12" (Typ both ends)

10' – 1"
18 spaces
(7" max spacing)

10' – 0"
5 spaces
(24" max spacing)

21' – 3"
37 spaces
(7" max spacing)

43' –

2" End Cover (Typ both ends)

4 Spaces @ 2" (Typ both ends)

43-3/4"

7

4

8-1/2"

AASHTO Type II

f'_c = 8,500 psi (10,000 psi) (75% of f'_c at Release)

Strand = 0.6" 270 ksi LOLAX pulled to 75% of f_{pu}

Strand Spacing = 2"

Distance From Bottom to 1st Row of Strands = 3.0"

Distance From Bottom to TOP Row of Strands = 33.5"

Stirrup (# 4 Bars) Spacing Shown Above

Total Stirrups = 138 (2 at each location)

Total Doghouse Bars = 10

Beam top surface to be intentionally roughened (raked)

Drawn by KFM   Phone: (404) 385-1429

Figure 8.16 Girder Layout C

159

8.3 Girder Instrumentation

During construction, instrumentation points were installed in each girder to allow measurement of concrete surface strains and deflections. The following sections describe the construction of devices to allow installation of the measurement points.

Concrete surface strain data were obtained using DEMEC gage points. The gage points were cast into each girder by attaching the points to steel strips, which were bolted to the steel girder forms. Figure 8.17 shows a diagram of the DEMEC inserts and the method used for embedding them in the girders. The embedment strips were constructed from steel bar 1½ inches wide by 1/4 inch thick. The DEMEC embedments were installed at a distance of 2 inches on center. The mounting screws were placed at a distance of approximately 10 to 12 inches apart to adequately affix the strips to the girder formwork. Distances greater than 12 inches resulted in the strips bowing away from the formwork. The wing nuts pictured in CUT A were the DEMEC embedments.

Mounting the strips to the formwork was accomplished as pictured in CUT B of Figure 8.17. The strips were placed as shown in Figure 8.18.
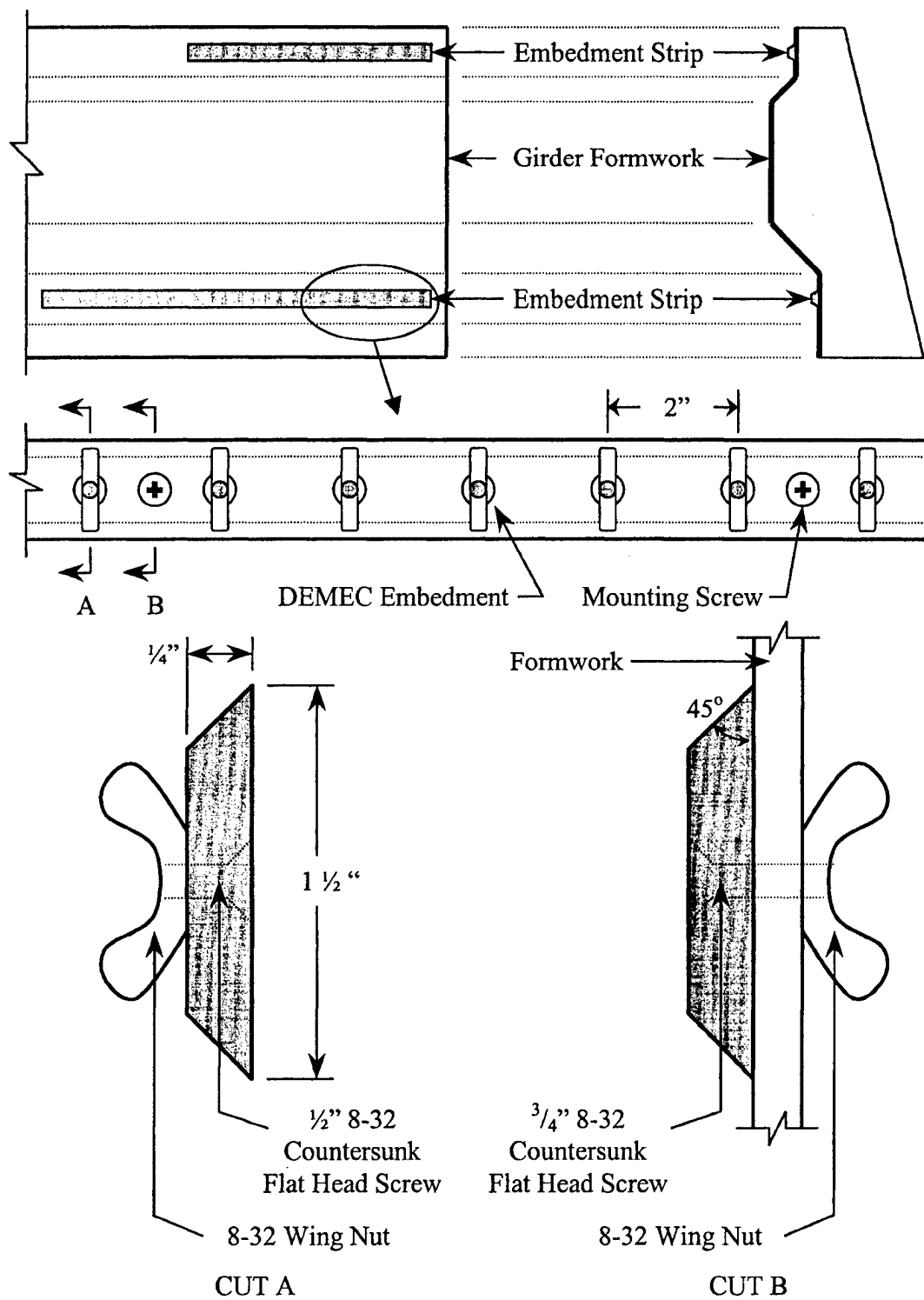
Figure 8.17 Diagram of DEMEC Embedment Strip Construction and Installation

30" Strip

C_L

48" Strip

24" Strip

1"
typical
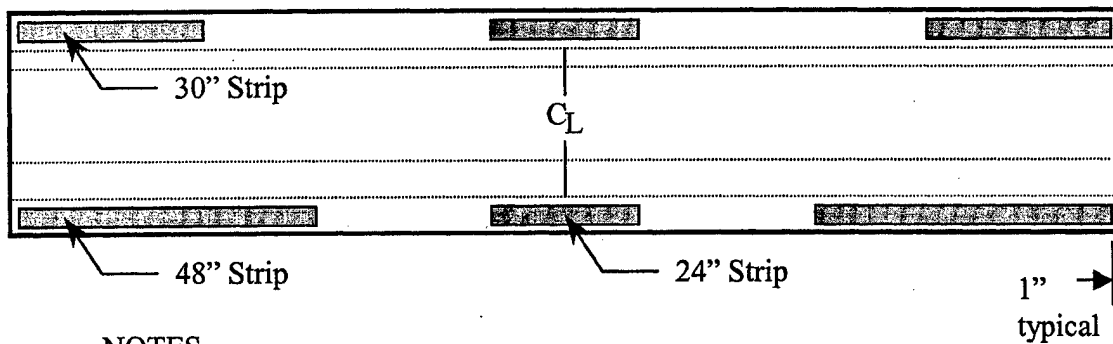
NOTES
1. Place embedment strips as close to end of girder as possible.
2. Place embedment strips such that embedments are at the same level as the prestressing strands.

Figure 8.18 DEMEC Embedment Strip Placement on Girder

C_L

Dead End

Pulley End

2"

6"

Pulley

¼" x 1¼" Bolt

¼" Nut

¼" Coupling Nut

¼" Washer

¼" x ½" Bolt

Cast into Girder

¼" x 1¼" Bolt

¼" Nut
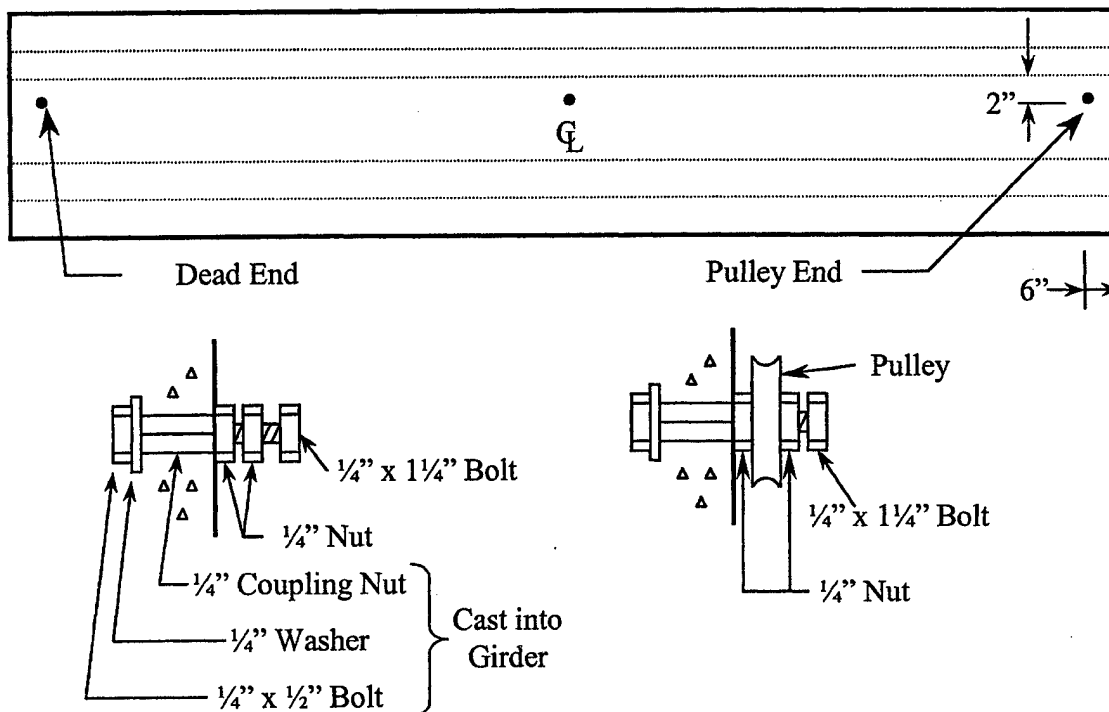
Figure 8.19 Attachment Points for Taut Wire

162

Deflection at midspan was measured using a piano wire stretched between a mounting post at one end and a pulley at the other as shown in Figure 8.19 A 10-pound weight was attached to the wire to keep it taut. At midspan, a metal ruler and mirror were affixed to the girder with epoxy. (Figure 8.20) The ruler enabled deflection measurement and the mirror prevented error due to parallax.

Figure 8.20 Use of Taut Wire for Deflection Measurement at Midspan

Vibrating wire strain gages (VWSG) with a 6-inch gage length were installed at midspan at the level of the bottom strands. (Figure 8.21)
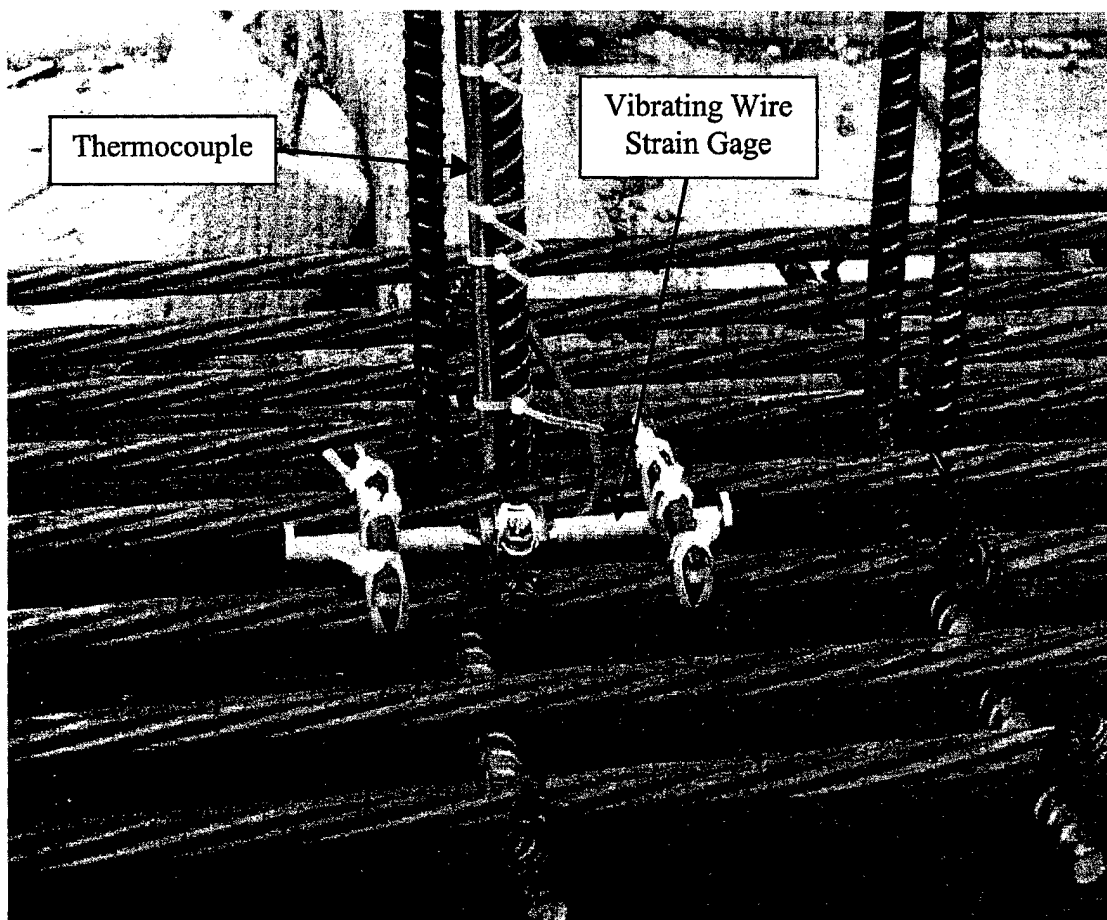
Figure 8.21 VWSG and Thermocouple Prior to Concrete Placement

Thermocouples were installed in each girder to measure heat of hydration during the curing process. The thermocouples were 6 inches long, ¼ inch in diameter, type K with 1-meter lead wires. The thermocouples were placed in the vicinity of the VWSGs as shown in Figure 8.21.

8.4 Girder Construction

The six girders were constructed at Tindall Corporation precast plant in Jonesboro, Georgia using plant personnel and standard precast plant procedures. The author together with Georgia Tech students and faculty installed and measured all instrumentation and fabricated all material test specimens. The girders were constructed in three identical sequences. During each sequence, two girders were constructed. During the first sequence, girders G1A and G1B were constructed. During the second sequence, girders G2A and G2B were constructed. During the third and final sequence, girders G1C and G2C were constructed.

8.4.1 DEMEC Gage Embedment and Taut Wire Insert Installation

Installation of the DEMEC gages was accomplished a few days in advance of the actual start of construction. Careful coordination with the concrete plant manager was essential to insure formwork was positioned to allow drilling holes and installation of the DEMEC gage embedment strips. Cordless drills with backup batteries and chargers, a good supply of back-up drill bits, cutting oil, grease pencils and measuring tapes were the keys to success.

Before the strips were attached, a layer of grease was spread across the back of the strip to fill the screw heads of the screws holding the wing nuts (embedments) in place on the strip. The backside of the strip was placed against the formwork. Once in place, any gap between the edge of the strip and the formwork was filled with grease to prevent concrete from getting behind the strip. In addition, the exposed portion of the

strip was coated with grease to prevent the strip from sticking to the girder. Grease was

kept from the wing nuts because their firm bond to the concrete was essential.

Connection points were also attached to the inside of the formwork to allow

installation of connections for the taut wire.

Prior to the formwork being moved into place for girder placement, it was sprayed

with form release oil. It was necessary to wipe any excess oil from the wing nuts before

the forms were lowered into position.

8.4.2 Strand Tensioning

After the prestressing strands were threaded through the bulkheads, load cells

were installed on the passive end to monitor the prestressing force. The load cells were

calibrated in advance of tensioning. Results of the calibration can be found in Appendix

E. Figure 8.22 shows the load cells in place.
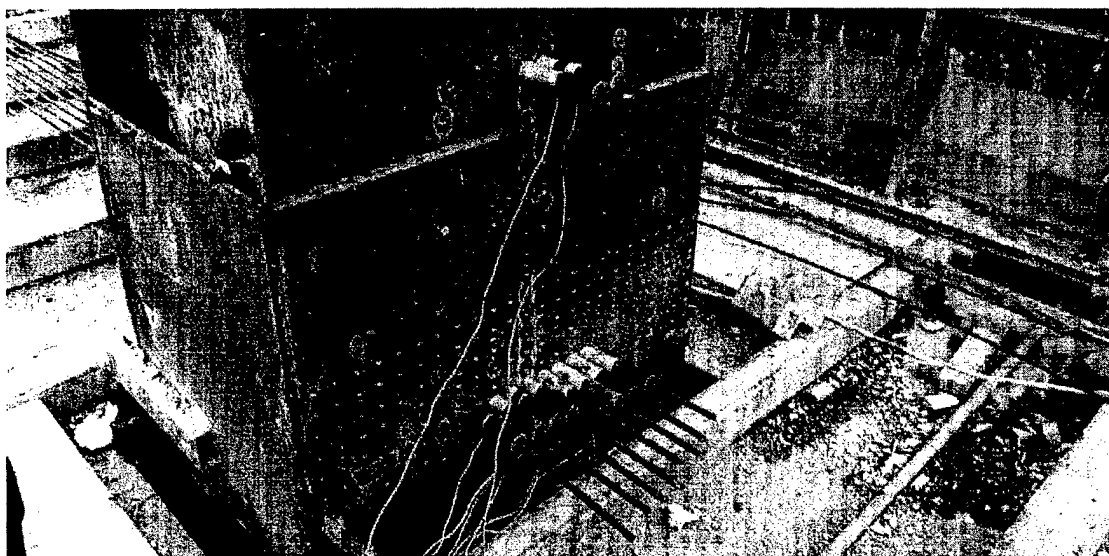
Figure 8.22 Strand Load Cells Installed at Passive End of Girder Line

The load cells were wired to a BLH 1225 Portable 10 Channel Switch and Balance Unit, which was then connected to a BLH 1200B Portable Digital Strain Indicator. The same units used during construction were also used during load cell calibration. Figure 8.22 shows the BLH 1225 and BLH 1200B.
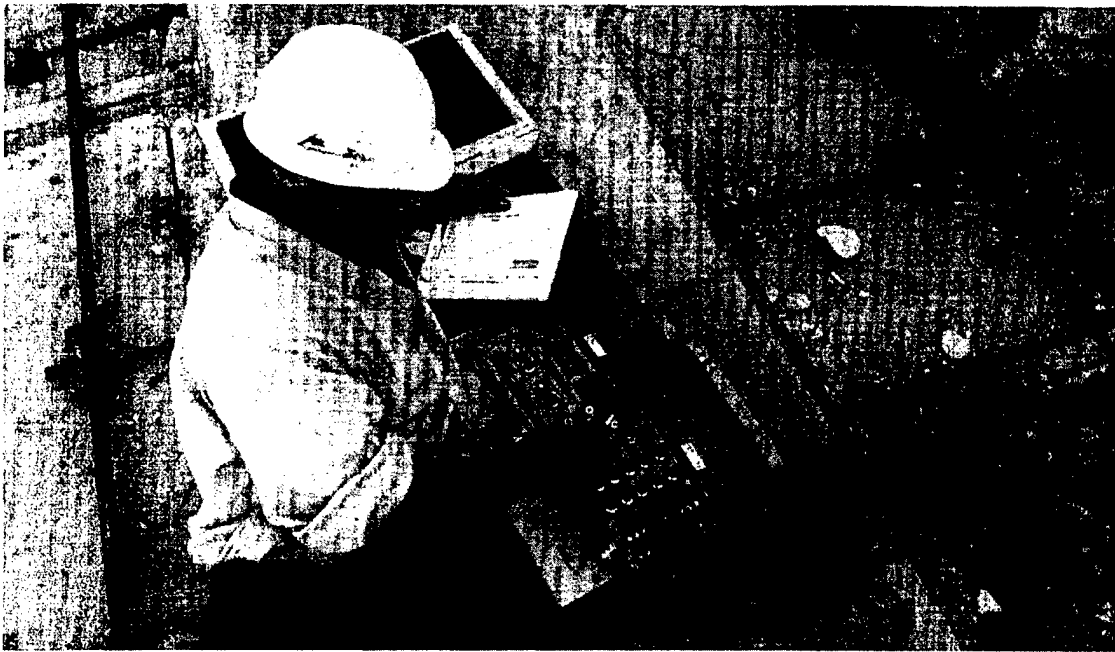
Figure 8.23 Strand Load Cell Monitoring Equipment

With the load cells connected and zeroed, plant personnel tensioned the strands using a Hercules hydraulic jack. Tensioning the 0.6-inch strands to 75 percent of f_{pu} or 203 ksi required a tension force of approximately 44.5 kips. All tensioning and strand elongation data can be found in Appendix H. For purposes of tensioning and tracking strand force, strands were numbered as shown in Figure 8.24. Figure 8.24 also provides the order in which the strands were released.
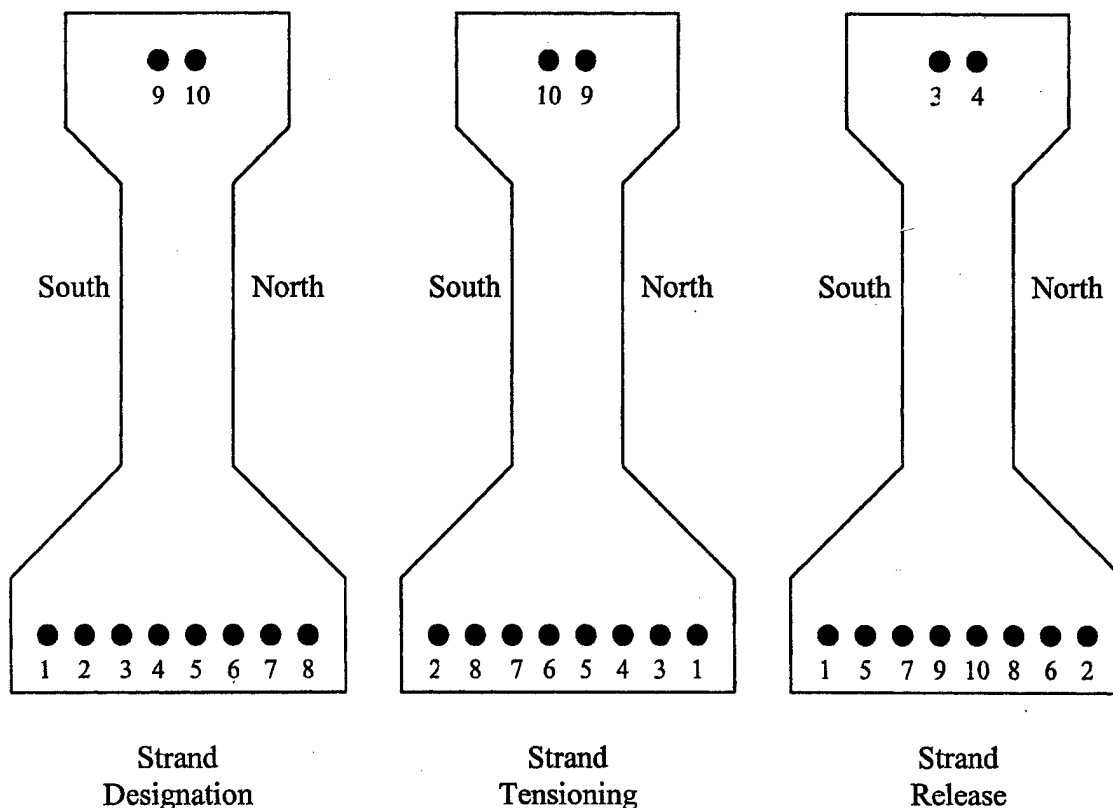
Figure 8.24 Strand Designation, Tensioning Order, and Release Order

The plant had trouble with their tensioning machine while tensioning the third

sequence of girders and had to replace the hydraulic ram. The Hercules tensioning

machine was designed for use on 0.5-inch strand and struggled to tension the 0.6-inch

strand. In comparing the reported strand tension values with the values recorded using

the strand load cells, the strand load cells reported tension values up to 20 percent less

than that reported by the hydraulic pump. Appendix F includes determination of

prestress force from the strand load cell reported strains and a comparison with plant

reported tension values. Load cell data were used for all subsequent analyses. Figures

8.25 and 8.26 show Tindall personnel tensioning the strands.

Figure 8.25 Tindall Personnel Operating Tensioning Machine

Figure 8.26 Jacking of Prestressing Strand

8.4.3 Installation of Shear Reinforcing Steel

Following the tensioning of prestressing strands, the shear reinforcing steel was installed per the sketches shown in Figures 8.14, 8.15 and 8.16. Georgia Tech personnel carefully checked stirrup locations to insure they were in accordance with the plans. Figure 8.27 shows the installation of shear reinforcing steel.

Figure 8.27 Installation of Shear Reinforcing Steel Near Girder End

8.4.4 Installation of VWSG and Thermocouples

The last step taken prior to installing the formwork was to attach the VWSG and thermocouple at midspan. As seen in Figure 8.21, the VWSG was firmly attached to the prestressing strand at the level of the bottom strands. The thermocouple was securely attached in the same vicinity as the VWSG.

8.4.5 Place Formwork

Prior to lifting the formwork into place, the forms were coated with a form release agent (form oil). It was necessary to recheck the DEMEC embedments and wipe any excess oil from the wing nuts prior to form installation. In a few cases, wing nuts had been knocked off the embedment strips and required replacement. Once properly aligned, the forms were locked into place by large threaded rods beneath the formwork and wishbone struts on top. Figures 8.28 and 8.29 show installation of the formwork.
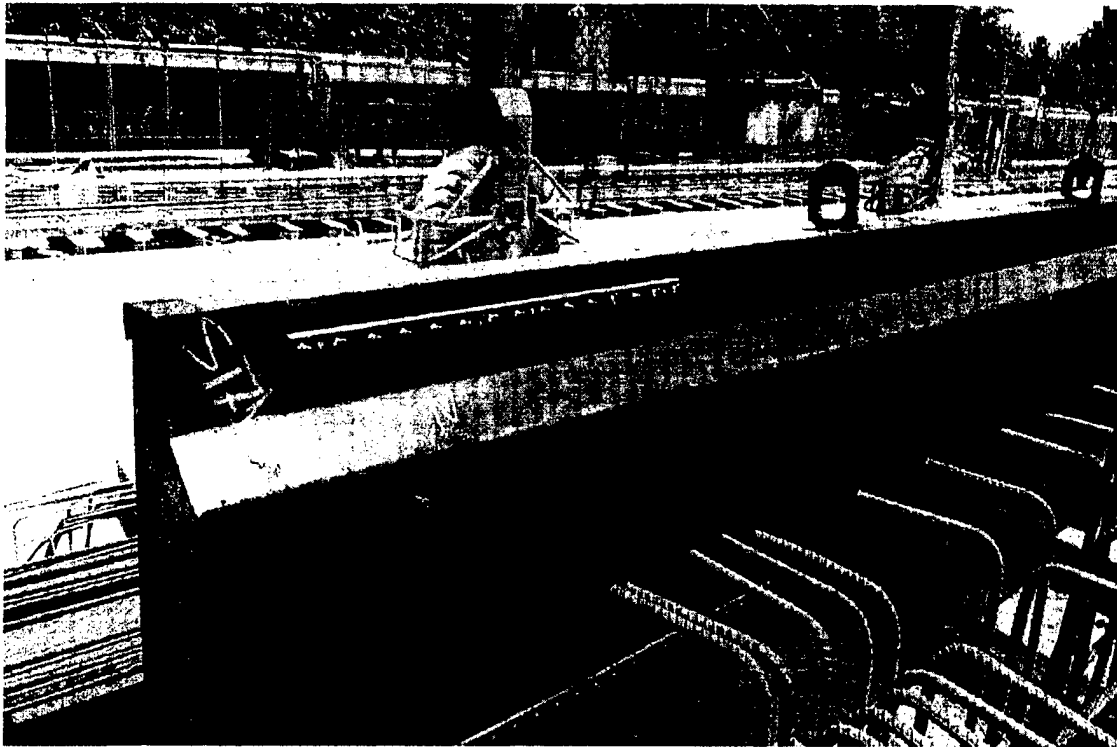
Figure 8.28 Formwork with DEMEC Embedment Strips Being Lifted Into Place

Figure 8.29 Tindall Supervisor Directing Placement of Formwork.

8.4.6 Batch and Place Concrete

Prior to batching the HSLC, moisture tests were conducted on the lightweight

aggregate and sand to determine the exact mix design. The moisture tests were started at

least two hours prior to placement to allow time to correctly dry the aggregate and

configure the mix design.

8.4.6.1 Mix Designs

Table 8.5 provides an overview of the mix design for each girder placement. The mix designs below were based on making 2 cubic yard batches. Each girder required approximately 3.5 cubic yards.

Table 8.2 Mix Designs for Girder Placements (2 cubic yard mix)

Girder #		G1A, G1B	G2A, G2B	G1C	G2C
Date of Placement		9 July 01	12 July 01	17 July	17 July 01
Lightweight Aggregate	(lbs)	1977	1958	1947	1995
Normal Weight Sand	(lbs)	2195	2173	2155	2165
Class F Fly Ash	(lbs)	284	300	284	300
Silica Fume	(lbs)	38	200	38	200
Type III Portland Cement	(lbs)	1570	1480	1570	1480
WRDA 35 (LRWR)	(fl oz)	114	119	114	119
Daravair 1000 (AEA)	(fl oz)	24	20	24	20
ADVA Flow (HRWR)	(fl oz)	95	258	95	258
Water	(gal)	39.5	36.7	44.8	33.1

8.4.6.2 Concrete Mixing

The concrete was mixed in a rotary auger-type mixer located in an elevated mix station approximately 200 feet from the prestressing bed. The mix station did not have a silo for fly ash or silica fume, thus those two components had to be added manually. The concrete components were added in a specific sequence for each batch of concrete. The lightweight and normal weight aggregates were added first with all the low range water reducer (LRWR), air entraining agent (AEA), high range water reducer (HRWR), and approximately half the mix water. Water was held out of the mix because Tindall's mixer had a water leak making exact determination of water added impossible. The initial components were allowed to mix for approximately 1 minute to insure thorough

dispersion of the chemical admixtures. Next, the Type III cement was added. Additional water was added as necessary to allow proper mixing of the cement. Next the Class F fly ash was added with additional water as required. Last, the silica fume was added. Any remaining water up to the specified mix design amount was added and the result observed. If the mix was still stiff, additional HRWR was added to bring the mix to a workable state.

When working with low water cement ratio mixes, water content is crucial. Noted variations in aggregate moisture content made a relatively large difference in the amount of added mix water required. During the batching process, water beyond the specified mix amount was added based on aggregate observed to be drier than measured during testing. While this may seem imprecise, experience with a particular mix design allows the person supervising the batch process to make adjustments and still achieve excellent results. In each batch process, water was added beyond the specified mix design with resulting strengths being in line with that expected. Without exact moisture control, such changes "on the fly" were unavoidable.

Figure 8.30 shows the elevated mix platform at Tindall Concrete. Concrete transport vehicles (Tuckerbilt) transport the concrete from the base of the platform to the girder line.

8.4.6.3 Material Testing

Upon batching of concrete, it was loaded into the transport vehicle and brought to the quality control station. Tindall personnel performed a slump test according to ASTM C231,[74] a unit weight test according to ASTM C138,[75] and recorded the temperature

174

according to ASTM C1064.[76] Georgia Tech personnel performed an air content test

using a roll-a-meter according to ASTM C173.[77] To the greatest extent possible, these

tests were performed on each batch of concrete.
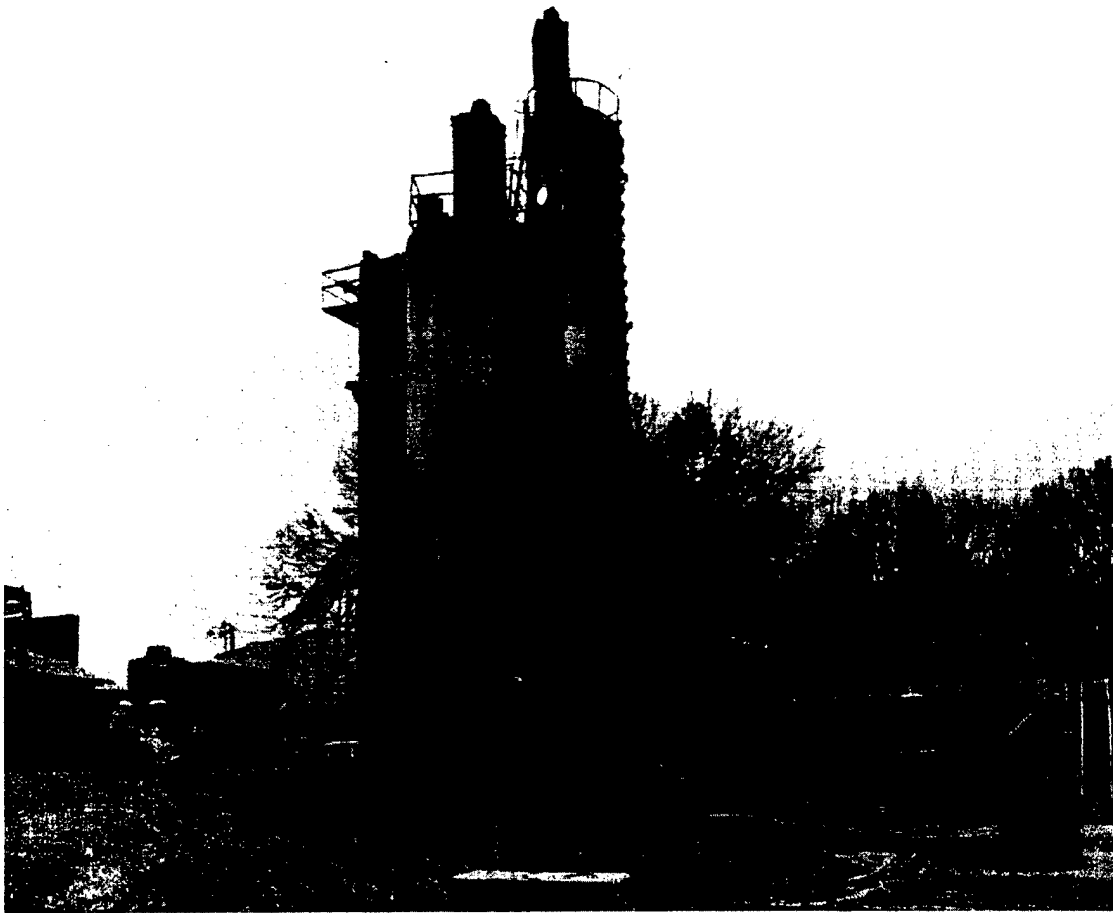
Figure 8.30 Elevated Mix Platform

A significant number of quality control specimens were cast during each girder

placement; many of the specimens were cured in insulated boxes. Based on previous

research at Georgia Tech,[84] cylinders cured in insulated boxes more closely matched

actual girder strengths for full-sized girders for the first 7 days. Temperature plots for cylinders cured in insulated boxes compared well to actual girder curing curves during this project.

During the third girder placement, cylinders were cast for a statistical study to determine the actual variation in placing HSLC.

8.4.6.4 Concrete Placement in Girders

After delivering concrete to the quality control station, the remaining concrete was transported to the girder line where it was placed into the forms. The Tindall concrete workers placed the concrete in lifts vibrating each lift with a spud vibrator. One Georgia Tech researcher was present on the girder line at all times during concrete placement to insure the concrete workers did not damage any instrumentation or DEMEC inserts. After all lifts of concrete were in place, the top of the girder was screeded and raked to give it the required 1/4-inch variation for good bond between the deck and girder. The girders were then covered with heavy plastic to protect them from rain and hold in heat during the curing process.

8.4.6.5 Comments on Placement Conditions

The girders in this project were placed during July when the ambient temperature reached well above 90 degrees Fahrenheit at mid-day. During the third concrete placement, events occurred at the plant that forced the placement time to be at about 3:00 pm, the hottest part of the day. The following key conditions existed that created placement problems.

1. The formwork had been exposed to direct sunlight throughout the day and was extremely hot to the touch.

2. The concrete transport vehicle had been sitting in the sun as well, and the metal hopper was hot.

3. The aggregate had been sitting in the silo above the elevated mix platform all day. In addition to being warm, the moisture content was probably not as high as that recorded from earlier testing.

The first batch of concrete mixed was for girder G2C. The water to cementitious materials ratio was 0.23. The batch was mixed as previous ones had been mixed. The consistency in the mixer appeared to have a slump of approximately 5-6 inches. When the concrete was released from the mixer into the transport vehicle, a flash set initiated when the concrete touched the hot metal in the hopper. Although not initially noticed, the problem became apparent when concrete was released for quality control checks. The slump was about 3 inches, the air content was about 3 percent and the unit weight was low at 114 pcf. It was decided to use the concrete because it still appeared workable enough to use in the girder. When the delivery vehicle began placing concrete into the girder, it was discovered that better than half the concrete in the vehicle had set in the hopper and could not be discharged into the formwork. In retrospect, the decision to use this initial batch of concrete was an error. At that point, Tindall personnel and volunteers worked quickly to remove the setting concrete from the hopper of the delivery vehicle. After about 30 minutes of effort, all the concrete had been removed.

In the mean time, the small amount of concrete placed in the girder was setting. Before another batch of concrete was mixed, the delivery vehicle was sprayed with cold water to lower the temperature of the hopper and coated with a lubricant to prevent the concrete from becoming bonded to the metal surface. The resulting girder, G2C was acceptable. There was no honeycombing and the cold joint did not appear to be a significant problem. As it turned out during testing, the particular girder end, G2C-West, performed acceptably.

The lessons learned in this event were numerous and related mostly to temperature. The formwork and equipment should have been kept cool prior to the placement. The aggregate should be kept cool to the greatest extent possible.

8.4.7 Concrete Curing

The girders were allowed to cure overnight. Temperature was monitored on each girder using the embedded thermocouple and a printing thermometer. A typical temperature curing curve for girder G1A is shown in Figure 8.31 together with the temperature in the curing box for test cylinders.

Tindall quality control personnel performed compressive strength tests on ASTM cured cylinders approximately 16 hours after casting. For comparison, curebox cylinders were also tested. The curebox cylinders always broke at a much higher strength than the ASTM cylinders. Table 8.3 provides times from concrete placement to form removal and release of prestress. The drop in the ambient temperature at 20 hours resulted from moving the cureboxes from outside into the laboratory.

178
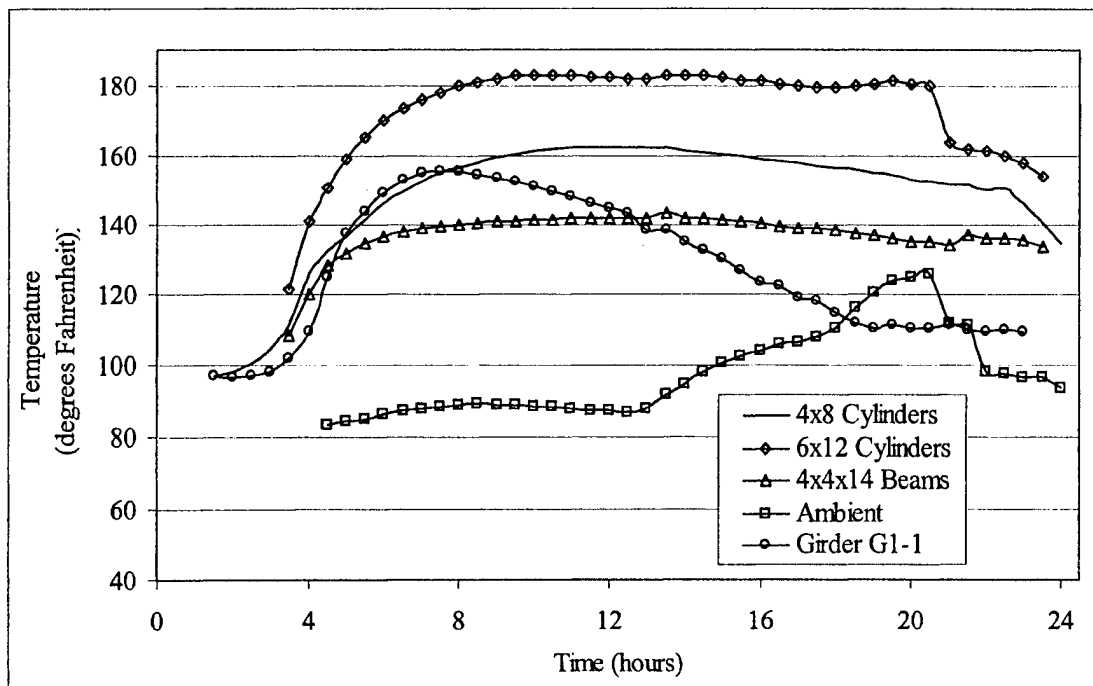
Figure 8.31 Typical Temperature Curing Curve for Girder G1A

Table 8.3 Concrete Placement Time; Hours Until Form Removal, Release of Prestress

Girder	Time/Date of Placement	Hours Until Form Removal	Hours Until Prestress Release
G1A	9 July 01, 1800	17.5	21.5
G1B	9 July 01, 1800	17.5	21.5
G1C	17 July 01, 1700	18	22
G2A	12 July 01, 1000	24	29
G2B	12 July 01, 1000	24	29
G2C	17 July 01, 1600	20.5	23

8.4.8 Formwork Removal, Embedment Preparation and Initial Readings

After the metal forms were removed, the DEMEC steel embedment strips were

unscrewed and stripped out (Figure 8.32). Once the embedments (wing nuts) were

exposed, "initial" DEMEC readings were taken as described in detail in Section 9.6.2.

179
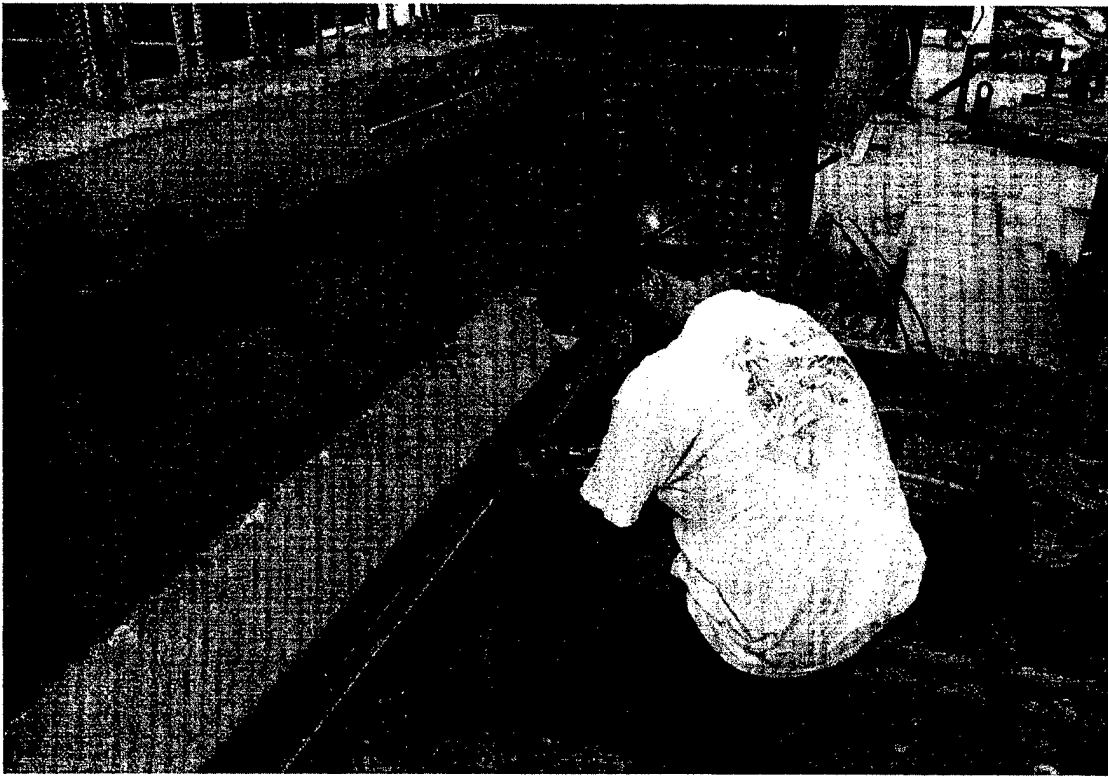
Figure 8.32 Removal of Screws from DEMEC Embedment Strips

The taut wire was also installed at this time. The mounting hardware as pictured in Figure 8.19 was installed, the wire stretched and the weight hung. The metal ruler was attached using 90-second epoxy at midspan such that two inches was exposed above the wire and 4 inches was exposed below the wire. The mirror was attached also using 90-second epoxy to the side of the ruler following the same spacing guidelines. After two sets of "initial" readings were taken using the DEMEC gage reader and the "initial" deflection was taken, the girder was ready for release of prestress.

8.4.9 Release of Prestress and "Release" Readings

Three Tindall workers using oxy-acetylene welding torches simultaneously flame cut the strands following the pattern identified in Figure 8.24 and shown in Figure 8.33. After all strands were cut, the "release" concrete surface strain, VWSG, and deflection readings and subsequent readings were recorded as outlined in Section 9.6.2.

Figure 8.33 Flame Cutting of Prestressing Strands with Oxy-Acetylene Welding Torch

8.4.10 Movement From Prestressing Bed to Temporary Storage Location

After prestress release, the girders were moved to a storage area and placed on wooden dunnage located at the centers of bearing (6 inches from each end). While in storage, Georgia Tech researchers took readings as outlined in Chapter 9 to examine

181

transfer length. Figure 8.34 shows the movement of a girder to the storage location using an overhead crane.
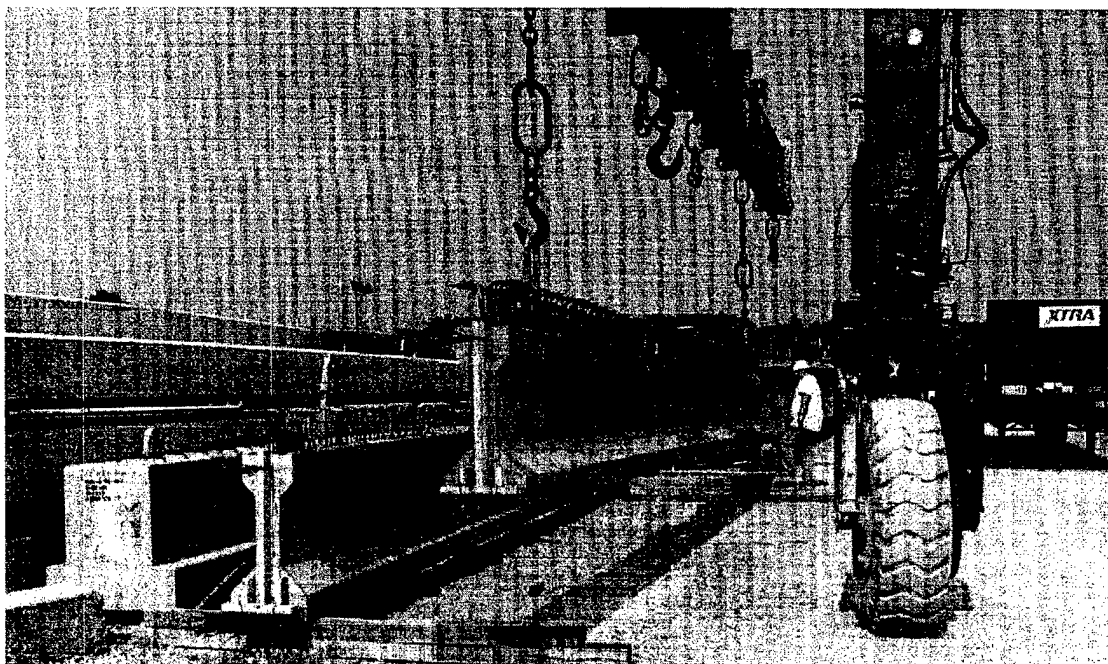
Figure 8.34 Movement of Girder to Storage Location Using Overhead Crane

8.4.11 Movement of Girders to Georgia Tech Structures Lab

After curing for approximately 3-4 weeks at the Tindall Plant, the girders were transported on flatbed trucks to the Georgia Tech Structures Lab. In the lab, the girders were stored as they had been at the concrete plant. One final set of surface strain, VWSG, and deflection readings were taken upon arrival and prior to beginning deck construction. Figure 8.35 shows girder delivery to the Georgia Tech Structures Lab.

182
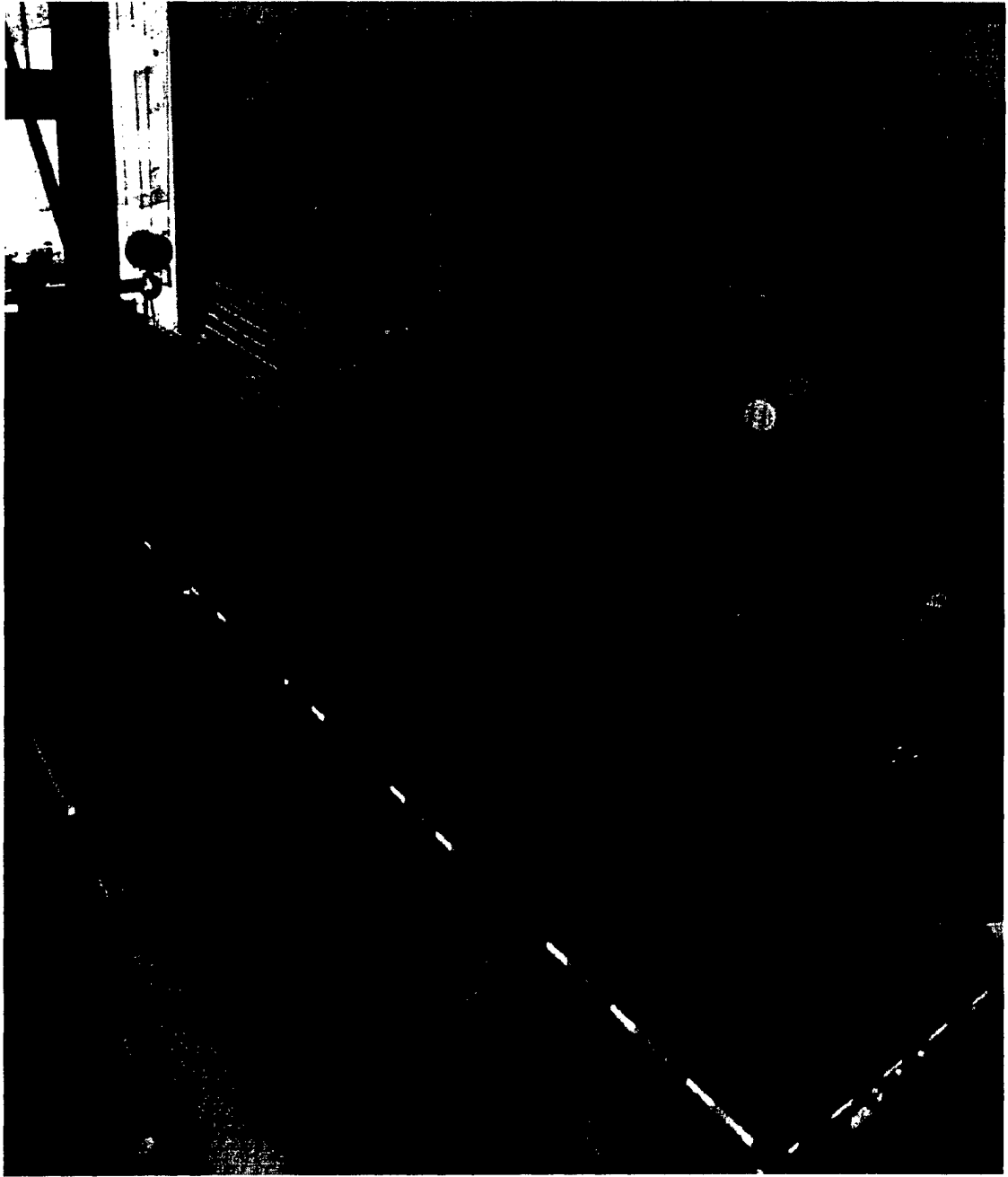
Figure 8.35 Delivery of Girders to Georgia Tech Structures Lab

8.5 Composite Deck Construction

Two weeks after the girders were delivered to the Georgia Tech Structures Lab, composite decks were cast on each girder. The concept for deck placement was to cast the entire deck on all six girders in one placement.

8.5.1 Formwork Construction

Figure 8.36 shows a cross section of the formwork used to place the composite decks.
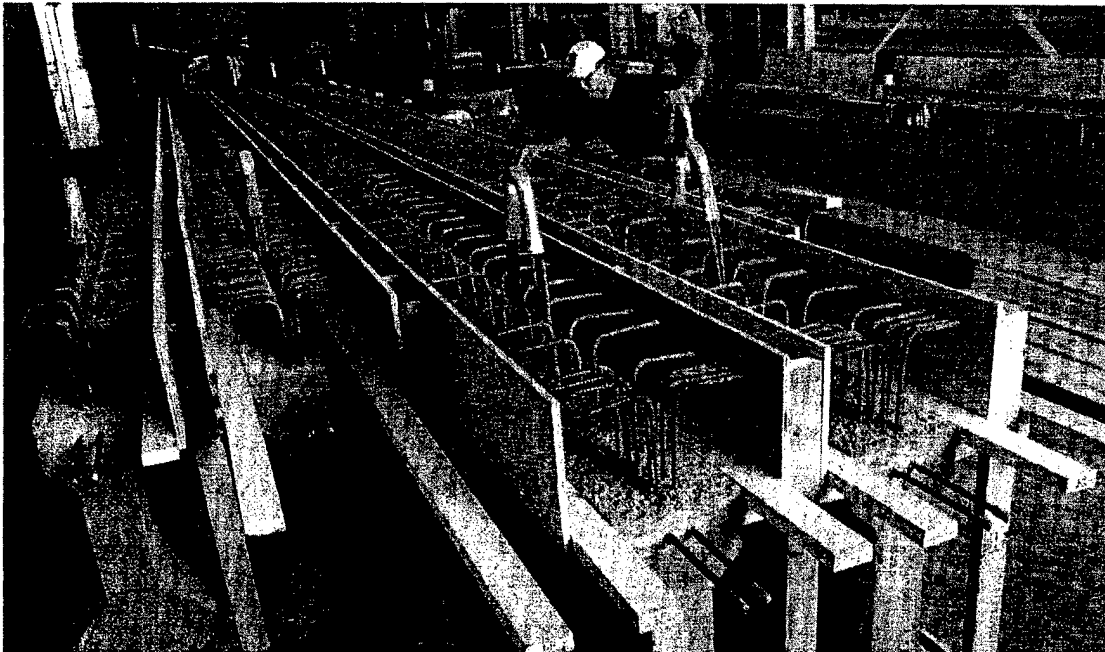
Figure 8.36 Formwork for Composite Deck

By placing the girders close together, it was possible to share formwork between two girders. Based on the selection of 19 inches for the deck width, a 2 x 4 (nominal 1.5 inches by 3.5 inches) was used to form the bottom underneath side of the deck. The side

of the deck was formed with ¾ inch plywood ripped into 13-inch widths and attached to the 2 x 4 boards with screws. The two "L" shaped pieces were then attached with screws to 2 x 4 uprights that ran to the floor for support. The upright lengths were adjusted as necessary to account for camber in the girders. The dead weight of the girders held the formwork in place nicely during deck placement.

Formwork for the outside of edge girders was held in place by ¼-inch threaded rods. Holes were drilled through the formwork through which the threaded rods were run. The rods were then bent around shear stirrups and secured with tie wire. Washers and nuts were installed on the threaded rod on the outside and tightened until the formwork was pulled snugly against the edge of the girder. The upright 2 x 4 boards of the outside edge formwork were held in place by a 2 x 4 that was bolted to the floor cover plates. The plates covered the tie-down locations and were conveniently placed at 4 feet on center. This detail can be seen in Figure 8.38.

8.5.2 Temperature and Shrinkage Steel

Temperature and shrinkage steel reinforcement consisting of two #4 bars was fastened to the shear stirrups at a distance of 3½ inches from the edge of the deck and approximately 2 inches down from the top surface. The bars came in 20-foot lengths and were overlapped by 18 inches as necessary. Figure 8.37 shows the temperature and shrinkage steel in place.
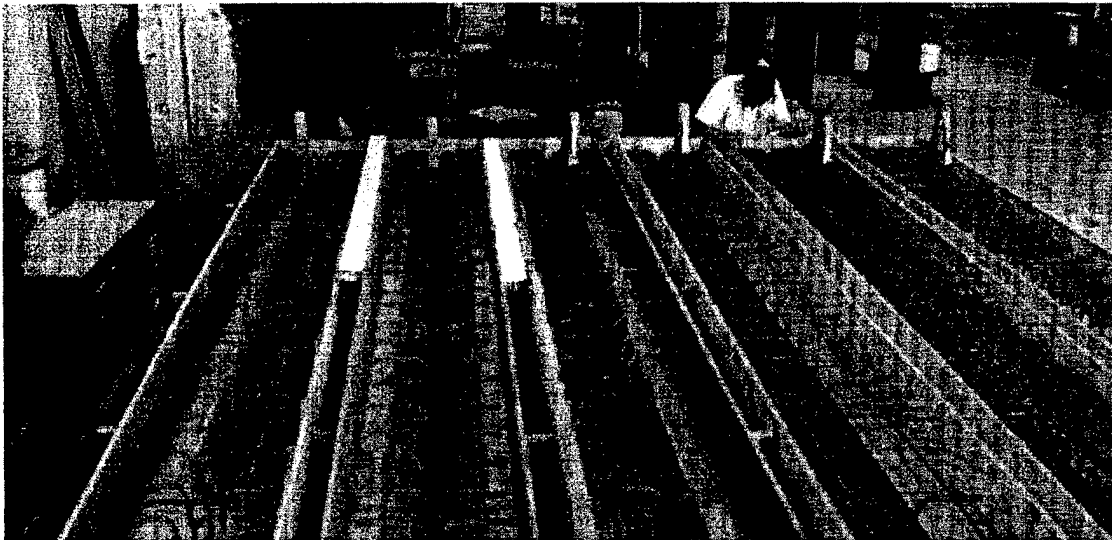
Figure 8.37 Formwork in Place with Temperature and Shrinkage Steel Installed
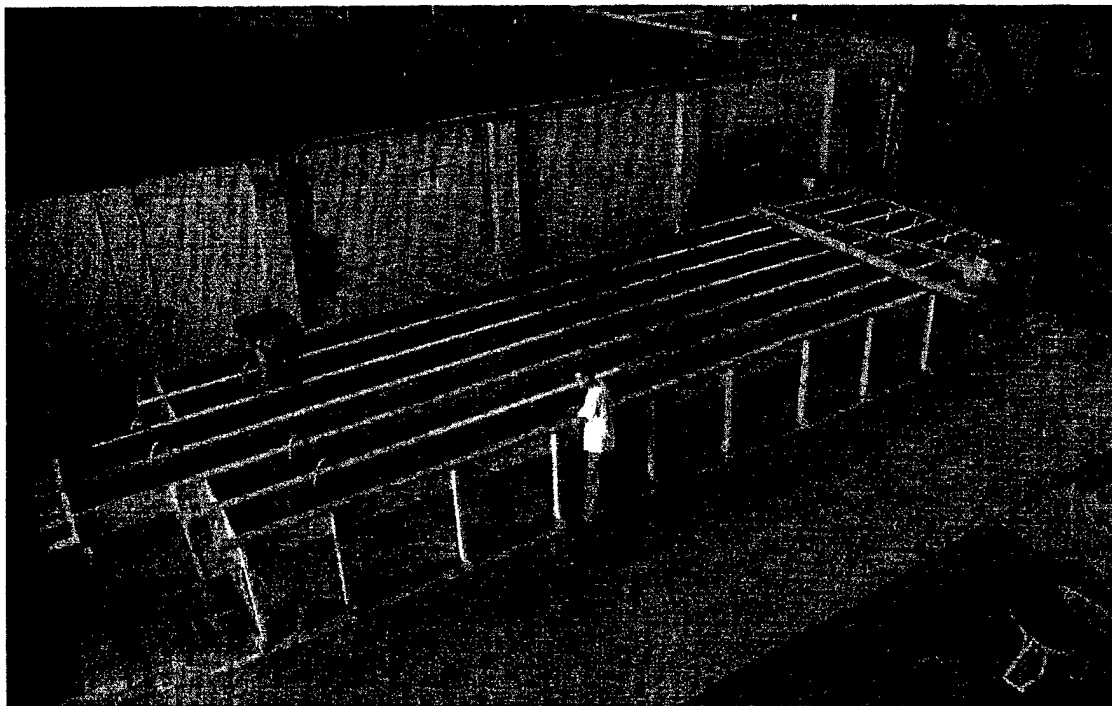
Figure 8.38 Formwork Ready for Concrete Placement

186

8.5.3 Concrete Placement

8.5.3.1 Type of Concrete

The type of concrete used for the composite deck was the standard Georgia Department of Transportation 3,500 psi normal weight bridge deck mix. Thomas Concrete, of Atlanta, Georgia delivered the concrete to the Structures Lab in readymix trucks.

8.5.3.2 Concrete Placement and Finishing

The readymix trucks were equipped with a concrete conveyor assembly as pictured in Figure 8.39.

Several Georgia Tech researchers assisted in the deck placement. One person operated the spud vibrator to insure good consolidation of the concrete into the forms and around the steel. Two other researchers used a large screed beam to smooth the top surface of the concrete. Two persons insured concrete from the chute was placed into the correct location.

In total, three readymix truckloads were required for completion of the deck. The first truckload was somewhat dry. Water was added on site to increase the slump to 6 inches. The second and third truckloads required no additional water; the measured slump was adequate upon arrival.

After the concrete began to set, the surface was finished with a trowel and then a broom surface was applied. The deck concrete was covered with plastic after initial set was reached. The deck was watered as necessary to keep it moist under the plastic.

187

After 7 days, the deck was uncovered and formwork removed. The formwork was completely disassembled, cleaned and stored for future use. Girder testing began approximately 52 days after the deck was cast.
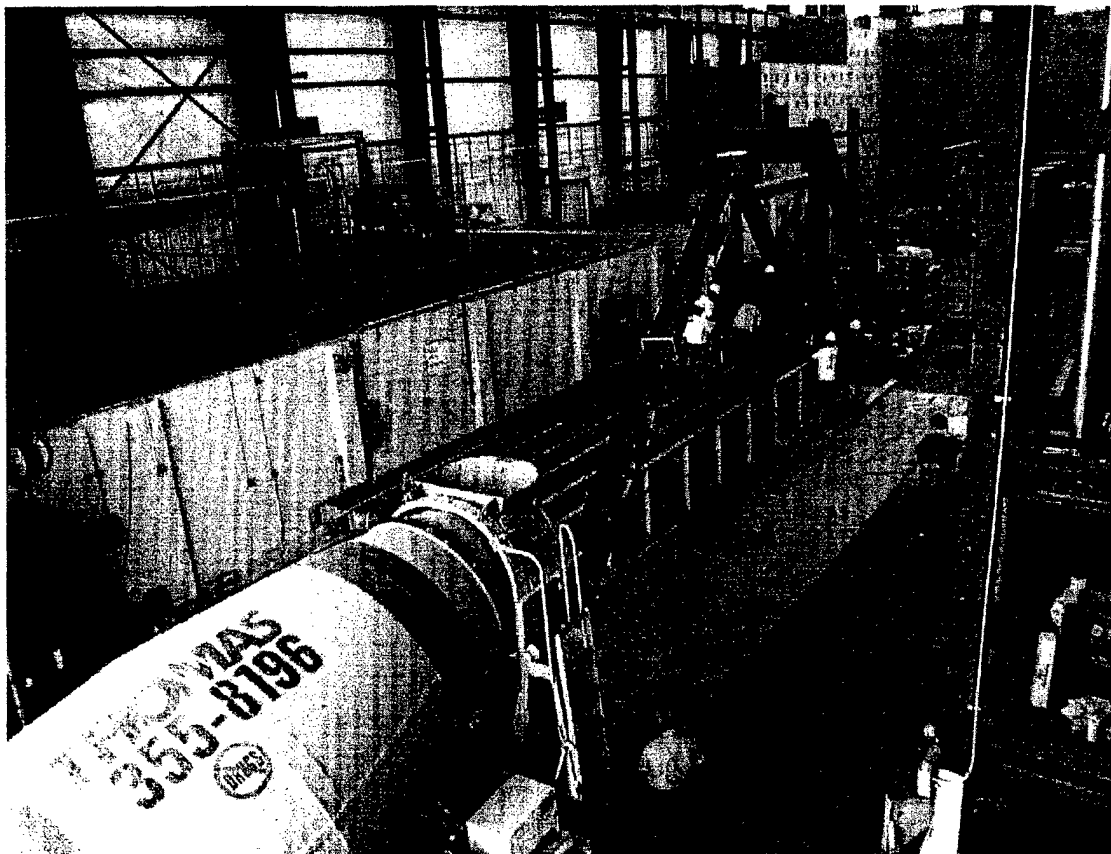
Figure 8.39 Readymix Truck with Conveyor Attachment

8.5.3.3 Materials Testing

Both 4 x 8 and 6 x 12 cylinders were cast for compressive strength and modulus of elasticity tests, respectively. The cylinders were cured under ASTM conditions for the first 24 hours then moved to the fog room for curing through the time at which the girders

were tested. The average strength of the deck concrete was 5,385 psi and the modulus of elasticity, E, was 3.37 million psi.

8.6 Direct Pull-Out Test

During girder placement, 24-inch x 36-inch x 24-inch specimen blocks were cast from the G1 and G2 series mixes for the "Mostafa", prestressing strand the direct pull-out test as shown in Figure 8.40.[90]

Figure 8.40 Mostafa Prestressing Strand Direct Pull-out Test

Each block had six, 48-inch segments of strand that were taken from the same reel used for girder construction. The segments were embedded 20 inches into the block with the top 2 inches being encased by PVC pipe as a bond breaker. The total embedded length

was 18 inches. The dimensions of the block were such that each strand had a free radius of at least 8 inches in all directions. Nominal reinforcing and lifting hooks made with #4 bars were placed in the block. Table 8.4 provides an overview of pull-out test results. The listed value is the load at which the strand underwent initial significant slip. Figures 8.41 and 8.42 provide plots of force vs. strand pull-out.

Table 8.4 Direct Pull-Out Test Results

Strand Test #	G1 Series (kips)	G2 Series (kips)
1	47.43	43.82
2	48.22	49.52
3	50.75	42.81
4	51.47	54.36
Average	49.47	47.63
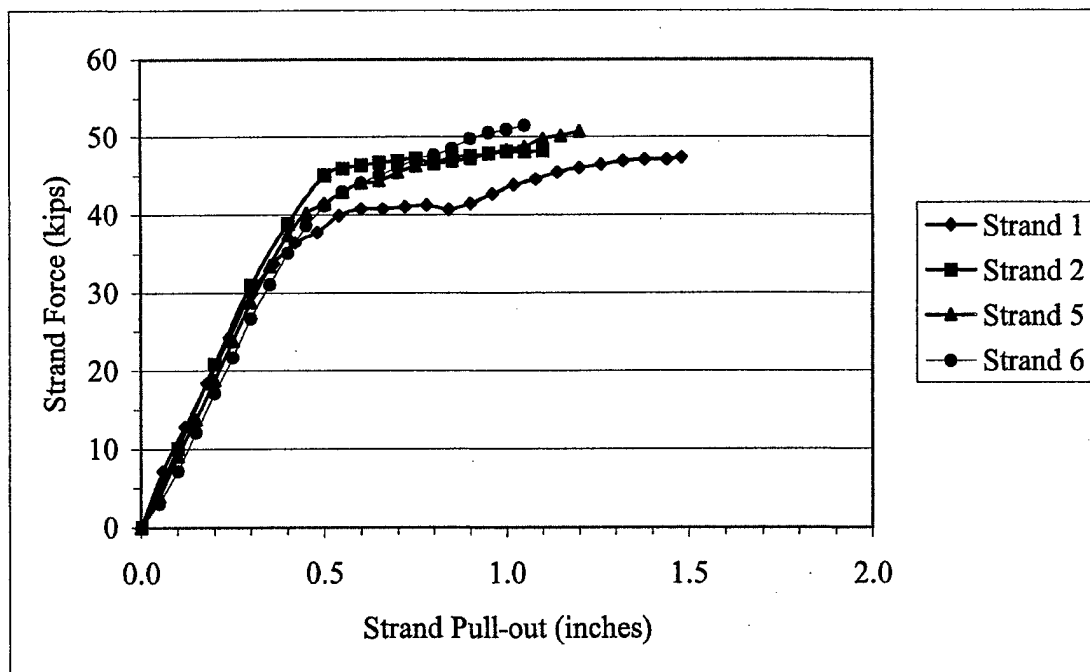
Figure 8.41 Direct Pull-Out Results for G1 Series HSLC
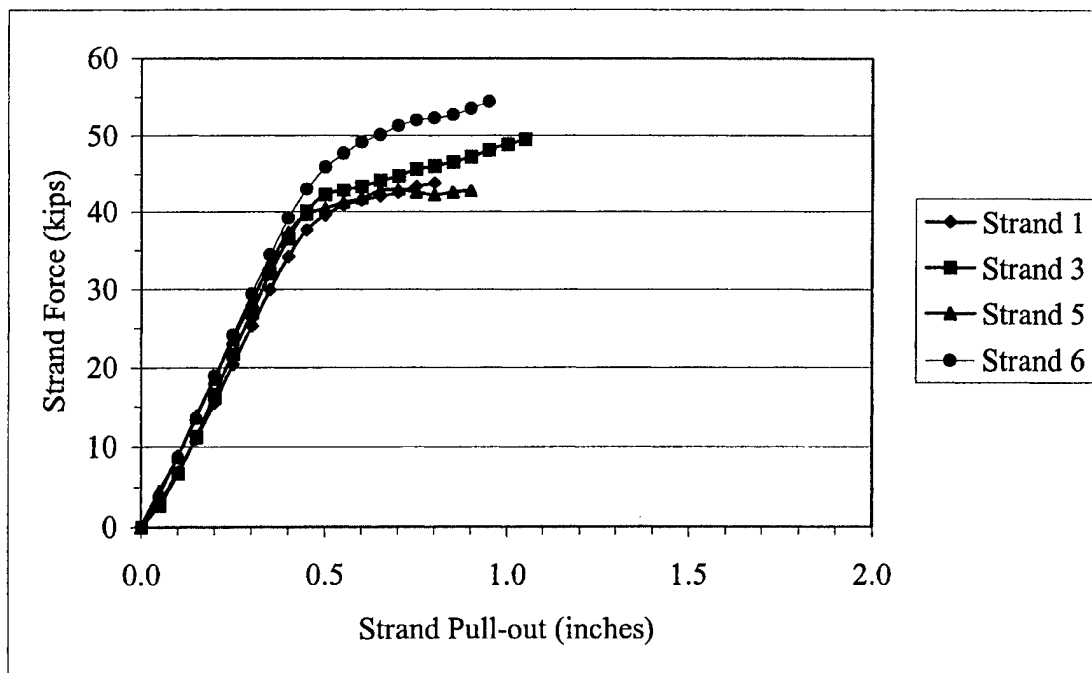
Figure 8.42 Direct Pull-Out results for G2 Series HSLC

Measurement of the load was accomplished using a strand load cell connected to the BLH 1200B. The same procedure was used as during girder construction. Load cell # 1 was used for this test. Force was calculated from the strain data using a direct relationship determined during the calibration process. Consult Appendix E for load cell calibration data.

The determination of pull-out capacity was based on the point at which the strand experienced increased slip with little or no increase in load or the point at which the strand underwent a sudden increase in slip and drop in load. This "popping" occurrence was common for all 8 tests performed. In Figures 8.41 and 8.42, the last data point shown was the point at which popping occurred.

Based on Logan's work, the minimum direct pull-out capacity for 0.6-inch diameter strand was 43.2 kips.[90] The average pull-out strength for both series exceeded the minimum value. One G2 test was slightly below the 43.2 kip minimum.

8.7 Material Properties

In order to evaluate the flexural performance of the girders, it was necessary to determine various material properties. The following sections provide material properties of the girders at the time of testing. Appendix C provides information on the reinforcing steel used for the shear stirrups and "doghouse" bars. Variations in concrete strength for the composite deck were the result of three different concrete deliveries during deck placement.

8.7.1 Girder Concrete Properties

Specimens were cast at the time of girder placement to allow determination of compressive strength, modulus of elasticity, and modulus of rupture strength at specific times. Table 8.5 lists the results of specimen testing with the range of test values listed.

The initial compressive strength values, f_{ci}', and modulus of elasticity values, E_{ci}, were based solely on curebox cured specimens and were tested at 24 hours, the approximate time of strand release. The compressive strength values, f_c', are based on an average of curebox and ASTM cured specimens tested just prior to girder testing approximately 3-4 months after casting. The moduli of elasticity values, E_c, are based on an estimate using the HSLC modulus equation. When compared with 56-day test values, the estimated values were in agreement. The E_c values listed for the G2C girders are the

56-day test values. Suspected inconsistencies in wet unit weight measurement at the time

of placement produced predicted values from the HSLC modulus equation that were less

than the known 56-day values. The modulus of rupture values, f_r, are based on an

average of curebox and ASTM cured specimens tested at 56 days.

Table 8.5 Girder Concrete Properties

Test #	f_{ci}' 24-hour Curebox (psi)	f_c' Time of Test Curebox & ASTM[79] (psi)	E_{ci} 24-hour Curebox (psi)	E_c Time of Test Estimated (psi)	f_r 56-day Curebox & ASTM[79] (psi)
G1A-E					
G1A-W					
G1A-C	7,465	9,580	3.47E+06	3.72E+06	1,010
G1B-E					
G1B-W					
G1B-C					
Range	6,753-8,689	8,702-10,640	3.39E+06-3.52E+06	NA	861-1,101
G1C-E					
G1C-W	6,315	8,911	3.00E+06	3.69E+06	796
G1C-C					
Range	5,444-7,666	8,001-9,450	2.98E+06-3.03E+06	NA	729-908
G2A-E					
G2A-W					
G2A-C	9,640	10,975	3.55E+06	3.88E+06	1,204
G2B-E					
G2B-W					
G2B-C					
Range	8,459-10,307	10,499-11,455	3.11E+06-3.79E+06	NA	1,024-1,352
G2C-E					
G2C-W	8,261	10,523	3.91E+06	4.08E+06	905
G2C-C					
Range	7,737-8,738	9,900-11,485	3.87E+06-3.96E+06	NA	744-1,086

8.7.2 Deck Concrete Properties

Specimens were cast during deck placement to allow determination of compressive strength and modulus of elasticity. Table 8.6 lists the results of testing with the range of test values listed.

Table 8.6 Deck Concrete Properties

Test #	f_c' Time of Test ASTM[79] (psi)	E_c Time of Test ASTM[79] (psi)
G1A-East		
G1A-West		
G1A-Center		
G1B-East		
G1B-West	5,384	3.35E+06
G1B-Center		
G1C-East		
G1C-West		
G1C-Center		
Range	4,848-5,929	3.24E+06-3.45E+06
G2A-East		
G2B-East	5278	3.45E+06
G2C-West		
Range	5,047-5,560	3.28E+06-3.55E+06
G2A-West		
G2A-Center		
G2B-West		
G2B-Center	5440	3.36E+06
G2C-East		
G2C-Center		
Range	4,975-6,109	3.32E+06-3.42E+06

Three batches of concrete were delivered to place the deck. The first batch encompassed all G1 series girders. The second batch encompassed all the G2 series

194

girder sections except G2A-East, G2B-East, and G2C-West, which were covered by the third and final batch delivered. The concrete compressive strength, f_c', and modulus of elasticity, E_c, values were determined by averaging the test results of specimens from each batch of concrete delivered for the deck. Although the girder tests encompassing a particular batch of deck concrete took place over a range of a few weeks, the strengths and moduli values recorded were in a tight range.

8.7.3 Prestressing Strand Properties

Manufacturer test results were received at the time of girder construction. Table 8.7 lists pertinent properties of the prestressing strand.

Table 8.7 Prestressing Strand Properties

0.6-inch Diameter Grade 270 ksi Low-Relaxation Strand		
Property	Value	Units
Strand Diameter, d_b	0.6	inches
Cross Sectional Area, A_{ps}	0.2183	inches^2
Modulus of Elasticity, E_{ps}	29,000	ksi
Yield Strain, ε_y	0.01	inch/inch
Yield Stress, f_y	259.6	ksi
Ultimate Strain, ε_{su}	0.065	inch/inch
Ultimate Stress, f_{su}	283.2	ksi

8.8 Effective Prestressing Stress and Losses

It was necessary to determine the strand effective prestressing stress, f_{se}, at the time transfer length was determined and at the time of testing. Two methods were used to determine f_{se} and the results compared. The first method made use of vibrating wire strain gages cast into the girders at midspan at the level of the bottom strands. The second method made use of concrete surface strain (CSS) data. One inherent difference

195

in these two methods was that the VWSG method read strain internal to the girder and the CSS method read surface strains. A second difference between the two methods was the gage length over which strain was determined. The VWSG had a 6-inch gage length; the CSS measurements were made over a 24-inch distance at midspan. The measurements made over a greater distance should have been more accurate.

Prior to release of prestress, the stress in the strands was known based on load cell readings. Refer to Appendix F for details on the determination of prestressing stress. At release, the known force was transferred to the girders. The elastic shortening of the girder reduced the effective stress in the prestressing strand. At the initial release of prestress, the VWSG and CSS values differed by almost 40 percent. At the time of testing, the measured strains differed by only about 7-9 percent indicating stabilization had occurred across the section.

When the initial prestressing stress was adjusted by the effect of the change in strain in the strand over time, the resulting effective stress values were within about 3 ksi. Force in the strand at a given strain was determined using Figure 8.43. Figure 8.43 was created using a manufacturer provided strand force vs. strand strain test plot.
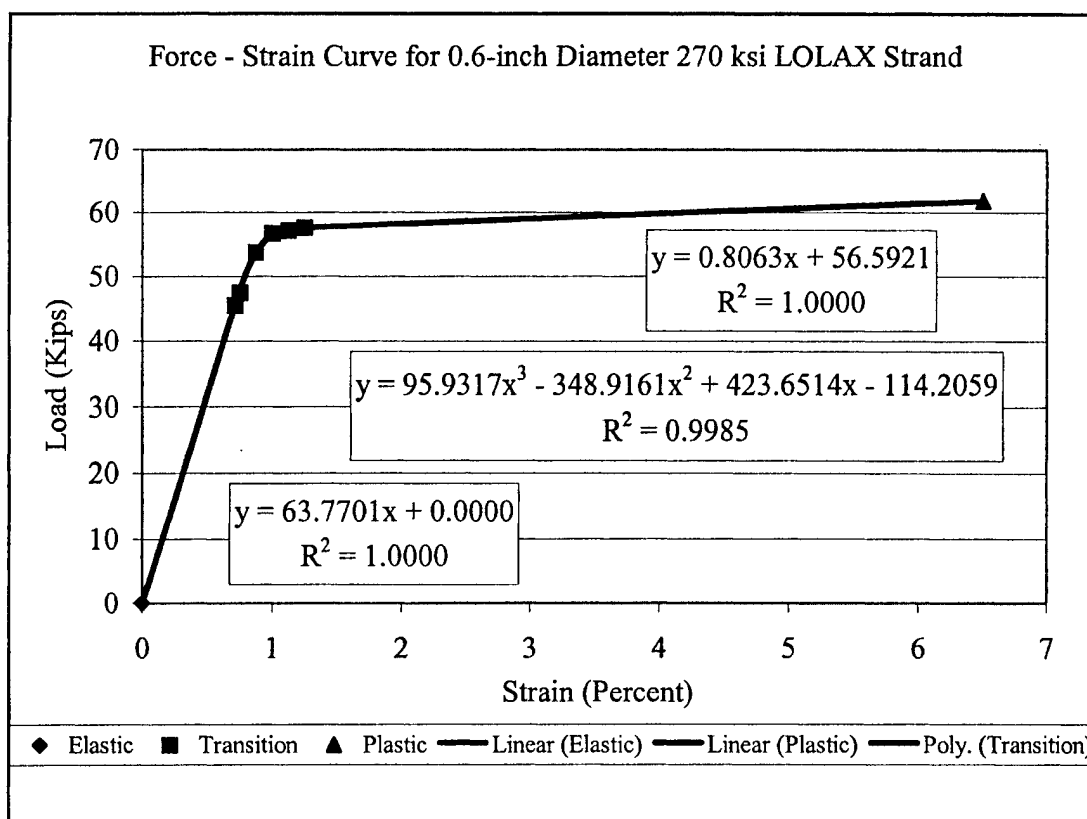
Figure 8.43 Force-Strain Curve for Prestressing Strand

Based on previous research that used VWSGs successfully, it was decided to use the VWSG indicated strain values to determine the effective prestressing stress. Table 8.8 provides details on the effective prestressing stress and losses determined experimentally and estimated using the AASHTO[40] procedure.

Although not a specific focus of this research, it is interesting to note the differences between AASHTO[40] estimated losses and experimentally measured losses. Table 8.9 lists the percent differences between the two values by batch number.

Table 8.8 Effective Prestressing Stress and Losses

Test #	Effective Prestressing Stress at Time of Test f_{se} (ksi)	Girder Age at Time of Test (days)	Batch #	AASHTO[40] Predicted Losses (ES,R,CR,SH) (ksi)	Experimentally Determined Losses (ES,R,CR,SH) (ksi)
G1A-East	153.7	111	1T1	34.6	25.4
G1A-West	152.3	106	1T1	34.6	26.8
G1A-Center	151.5	113	1T1	34.6	27.5
G1B-East	151.2	94	1T1	34.6	27.8
G1B-West	149.7	99	1T1	34.6	29.3
G1B-Center	149.4	101	1T1	34.6	29.7
G1C-East	149.0	110	1T2	35.7	30.2
G1C-West	147.6	107	1T2	35.7	31.5
G1C-Center	147.7	112	1T2	35.7	31.4
G2A-East	175.8	122	2T1	36.1	15.5
G2A-West	175.7	119	2T1	36.1	15.6
G2A-Center	175.0	124	2T1	36.1	16.3
G2B-East	176.2	131	2T1	36.1	15.1
G2B-West	175.6	126	2T1	36.1	15.8
G2B-Center	175.6	136	2T1	36.1	15.7
G2C-East	159.3	140	2T2	33.3	19.8
G2C-West	158.8	133	2T2	33.3	20.3
G2C-Center	157.7	142	2T2	33.3	21.5

Table 8.9 Comparison of AASHTO[40] Predicted Losses to Experimental Losses

Batch #	AASHTO Predicted Losses (ksi)	Experimental Losses (Average) (ksi)	Percent Difference By Batch	Percent Difference By Series
1T1	34.6	27.8	-19.8%	-17.6%
1T2	35.7	31.0	-13.1%	
2T1	36.4	15.7	-56.6%	-50.5%
2T2	33.3	20.5	-38.3%	

Batch 1T1 was the G1 series mix made during the "first" G1 series girder

placement session. Batch 1T2 was the G1 series mix made during the "second" G1 series

girder placement. The numbering for batches 2T1 and 2T2 follows the same rule. Although the mix designs were the same for both sessions, exact determination of water content was not possible due to a malfunctioning valve. The batches during both second sessions produced greater losses. The percent difference by series indicates the overall difference for all girders made from a particular mix design. The resulting losses for the G2 series girders differed significantly from the AASHTO[40] estimated values.

Further details on determination of the effective prestressing stress were included in Appendix F.

8.9 Girder Section Properties

The AASHTO Type II girders had section properties as listed in Table 8.10.

Table 8.10 AASHTO Type II Girder Section Properties (Non-Composite Girder)

Property	Non-Composite Value	Units
Moment of Inertia, I_{nc}	50,979	in^4
Cross Sectional Area, A_{nc}	369	in^2
Height, h_{nc}	36	in
Centroid to Girder Top, $y_{top\text{-}nc}$	20.17	in
Centroid to Girder Bottom, $y_{bot\text{-}nc}$	15.83	in
Top of Girder to Top Strands, TCL	2.5	in
Bot of Girder to Bot Strands, BCL	3	in

The resulting girder dimensions deviated slightly from the designed dimensions. Table 8.11 lists the resulting composite section dimensions and properties for each test.

199

Table 8.11 Composite Section Properties

Test #	Mod. Ratio η	Girder Height h_c (inches)	Moment Of Inertia I_c (inches)	Cross Section Area A_c (inches)	Centroid to Top y_{top-c} (inches)	Centroid to Bottom y_{bot-c} (inches)
G1A-East	0.900	48.00	145736	581	10.62	25.38
G1A-West	0.900	47.88	142657	572	10.90	25.10
G1A-Center	0.900	48.00	143768	574	10.82	25.18
G1B-East	0.900	48.00	144954	578	10.70	25.30
G1B-West	0.900	47.50	140492	570	11.04	24.96
G1B-Center	0.900	47.50	139730	567	11.12	24.88
G1C-East	0.907	47.75	143550	577	10.79	25.21
G1C-West	0.907	47.88	144285	578	10.74	25.26
G1C-Center	0.907	48.19	147106	583	10.52	25.48
G2A-East	0.890	47.75	140863	568	11.06	24.94
G2A-West	0.867	47.88	141167	567	11.05	24.95
G2A-Center	0.867	47.88	140391	565	11.13	24.87
G2B-East	0.890	48.00	143464	573	10.85	25.15
G2B-West	0.867	47.75	138916	561	11.25	24.75
G2B-Center	0.867	48.19	143919	572	10.84	25.16
G2C-East	0.824	48.00	137292	553	11.46	25.54
G2C-West	0.846	47.63	135266	551	11.59	24.41
G2C-Center	0.824	48.13	138744	556	11.34	24.66

200

CHAPTER IX

TRANSFER LENGTH TEST RESULTS AND DISCUSSION

9.1 Introduction

This chapter discusses transfer length in pretensioned girders. Definitions are provided, the importance and use of transfer length is discussed, current code provisions are presented and explained, and the results of the experimental program are presented. Based on experimentally measured transfer length values from this experimental program and others, current code provisions and equations previously suggested for predicting transfer length are evaluated. New equations for predicting transfer length are suggested based on experimental data.

9.2 Definition

Transfer length is the distance required to transfer the effective prestressing force from the strand to the surrounding concrete. Transfer length is developed when the pretensioning strands are released by flame cutting or other method from the restraining abutments. In order for the force transfer to take place, there must be sufficient bond between the pretensioning strand and the concrete. The transfer of force from the strand to the concrete is represented in Figure 9.1.[40]
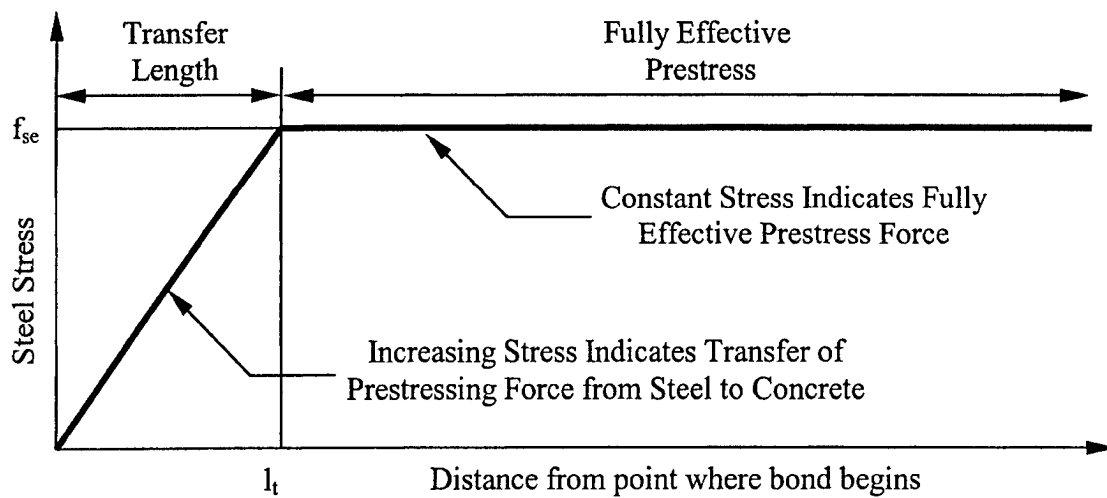
Figure 9.1 Diagram of f_{se} vs Distance From Girder End

The initial sloped portion of the diagram begins at a stress level of zero where bond

begins and is assumed to increase linearly over a distance equal to the transfer length.

The second horizontal portion of the diagram is the region where the strand has fully

transferred the effective prestress. The stress in the strand is assumed to remain constant

in this region.

9.3 Importance of Transfer Length

While in most cases, transfer length is not the governing design consideration in a

pretensioned bridge girder, its importance and implications must be understood. Of

greatest importance with regard to transfer length is the design of adequate confinement,

transverse steel to enclose the prestressing strands at the ends of the girder where initial

stress transfer occurs. The 1996 AASHTO[40] Standard Specification for Highway Bridges

Section 9.22.2 identifies the requirement to detail "nominal reinforcement" in the bottom

flange of the beam to enclose the strands over at least a distance "d" from the beam end. Without adequate steel present in the transfer region, cracking can occur around pretensioning strands effectively increasing the transfer length.

The elastic behavior of the beam also is affected by transfer length. As the stress in the strand increases from zero at the free-end of the beam to the level of effective prestress, f_{se}, at a distance equal to the transfer length from the girder end, the flexural stress required to cause cracking on the bottom surface of the beam also increases. Close to the end of the beam, the required cracking moment is less than that at a distance greater than the transfer length from the end of the girder. This change in cracking moment is important not only as a flexural design consideration but also for shear design, which is discussed in Chapter 11. Shear design within the transfer region must consider the reduced effective prestressing force.

9.4 Current Code Provisions

Current code provisions differ on the way transfer length is determined. Both the AASHTO and ACI techniques are conservative and produce similar results; but the two approach the phenomenon differently. AASHTO[40] Section 9.20.2.4 states the transfer length for prestressing strand shall be taken as 50 diameters ($50*d_b$) for strand and 100 diameters for single wire. Section R12.9 of the ACI 318[2] Commentary specifies that transfer length shall be determined using the equation 2.5.

$$l_t = \frac{f_{se}d_b}{3} \tag{2.5}$$

The value f_{se} is the effective stress in the prestressed reinforcement in ksi after allowance for all losses and d_b is the strand diameter in inches. The derivation of the ACI equation was covered in detail in Section 2.8. The current research program examined only 0.6-inch diameter, seven-wire, 270 ksi, low-relaxation pretensioning strand.

9.5 Test Specimens

Six full-scale AASHTO Type II girders were constructed for this research program. The cross section of each girder was identical; each used eight 0.6-inch Grade 270 low-relaxation strands in the bottom flange and two strands in the top flange. Both bottom and top strands were stressed to 75 percent of the strand ultimate strength, f_{pu}. The 28-day concrete design strengths, f_c', were 8,000 psi for the G1 series girders and 10,000 psi for the G2 series girders.

Transfer length data were taken on each girder end producing 12 sets of data. The girders were designated as described in Chapter 8 with a girder number (G1A, G1B, G1C, G2A, G2B and G2C) and end (East or West). Girder numbers were based on concrete design strength, girder length and reinforcement layout. Girder ends were designated based on their orientation in the precast plant at time of construction; i.e. west would indicate the beam end pointed in the westerly direction. For example, transfer length data are reported as G1A-West indicating information about the West end of girder G1A.

9.6 Measurement of Transfer Length Data

Transfer length data for the bottom prestressing strands were measured using the Concrete Surface Strain (CSS) method. As the prestressing strands transferred stress to the concrete, compressive stress and thus strain was induced in the concrete. Based on compatibility, the strain profile in the concrete should mirror the strain in the prestressing strand. Thus, the concrete strain profile should appear the same as the prestressing strand strain profile shown in Figure 9.1. The point at which the concrete strain reaches a maximum value and stabilizes at a constant strain level is the transfer length.

9.6.1 CSS Method

The CSS method of measuring strain in the concrete was accomplished through the use of a detachable mechanical strain gage known as a DEMEC gage. The DEMEC gage measured the distance between two points through the use of two conical points that were inserted into embedments on the surface of the concrete. A DEMEC gage is pictured in Figure 9.2; use of the DEMEC gage is pictured in Figure 9.3.
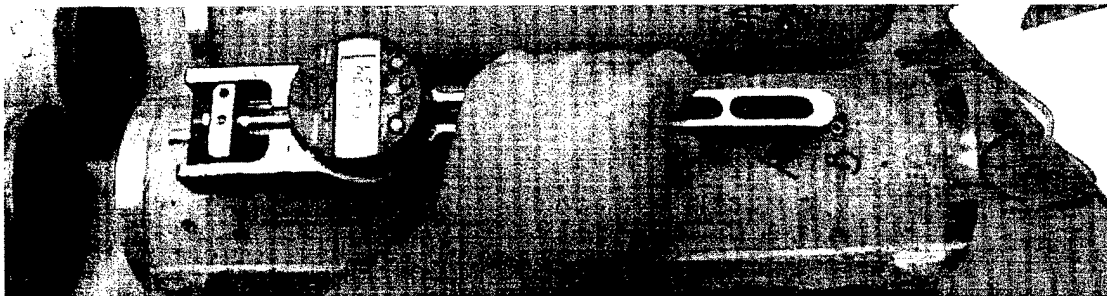
Figure 9.2 DEMEC Gage

Figure 9.3 DEMEC Gage in Use

The DEMEC gage was used to collect CSS data for determination of the transfer length,

development length, and level of prestressing in the strands. A thorough description of

construction and installation of the DEMEC gage embedments was covered in Chapter 8.

In order to collect transfer length data on the bottom strands, DEMEC gage

embedments were installed at the level of the bottom strands over a 48-inch distance from

each girder end on each side of the girder. Spacing on the embedments was set at two

inches to produce a well-defined strain profile over the transfer length region. The

distance between the conical inserts on the DEMEC gage was approximately 8 inches;

this distance varied slightly based on small variations in hole placement on the

embedment strips. On average, the 8-inch gage length coupled with the 0.0001-inch accuracy of the gage produced a sensitivity of 12.5 microstrains in the measurements.

9.6.2 Measurement of Surface Strains and Other Data

It is important to note that the DEMEC gage did not directly measure concrete strains. The readings from the DEMEC gage were distances between the embedments from which the strains could be calculated. The DEMEC gage readings were referred to as "CSS readings" throughout this report; calculations were necessary to determine the strain. The DEMEC gage measured distance over an 8-inch distance. Within that 8-inch distance were located four 2-inch segments. The reading over the 8-inch gage distance inherently averaged the strains over the four included segments.

CSS measurements were made at specified times in the life of each girder. A CSS data-recording sheet shown in Appendix G, Figure G.1 was created to facilitate organized and consistent collection of the thousands of CSS readings and other data. The following readings were taken on each of the six girders prior to strand release, just after strand release and 1, 2, 3, 7, and 14 days after strand release.

- Transfer length CSS readings

- Girder internal temperature and ambient temperature

- Vibrating Wire Strain Gage reading at level of bottom strands at midspan

- CSS readings at midspan used for prestress loss (not used for transfer length calculations)

- Girder midspan deflection (not used for transfer length calculations)

There were several important rules that were followed when making the CSS and other readings. First, the readings before strand release served as "initial" readings and were the basis for all strain calculations. If the initial readings were in error, all subsequent strain calculations would be flawed. Previous research showed that taking two sets of initial CSS readings and averaging the results provided a good indication of the initial distance between embedments.[37] Since some variation in the readings might occur based on operator inconsistency or environmental conditions, two initial readings helped to remove some of the inherent error. On subsequent readings, inconsistencies on data measurement would tend to average out and produce acceptable results.

Second, except for the "initial" and "just after release" readings, the time at which the CSS readings were taken was just prior to sunrise. Based on experience from previous research, it was found that temperature and solar radiation had a tremendous effect on surface strain.[37] In order to alleviate these effects to the greatest extent possible, CSS readings were made early in the morning before the girders were exposed to direct sunlight. Also based on previous research, transfer length CSS readings were only taken up through 14 days. After 14 days, the transfer length stabilized. Results in this research indicated stabilization of results occurred as soon as 7 days after release.

Third, when taking the CSS readings, it was essential to use the same DEMEC gage to make the readings each time. It was found that slight differences existed between the two gages that could impact the consistency of the readings. Two DEMEC gages were available; they were labeled #1 and #2. Likewise, the beam sides were labeled with #1 and #2, respectively, to insure the DEMEC gages were used on the same side for each

reading. In addition, two people were required to make the CSS readings. One person took readings while the other person recorded data. To the greatest extent possible, the same people were used to take CSS readings each time. Prior to using a DEMEC gage, it was zeroed to 8 inches between the conical points using a length "standard" bar.

VWSG readings at midspan, temperature readings, and other CSS readings at midspan and at other locations on the beam also were taken. The VWSG and CSS readings at midspan at the level of the bottom strands were used to determine the stress in the prestressing strand. Accurate knowledge of prestressing stress was necessary when evaluating existing transfer length equations and suggesting new ones. Differences occurred between strain readings using the VWSG and CSS methods. Just after release, there were significant differences in the strains that resulted between the two methods. As time progressed, the difference became less, but remained between 5 and 10 percent. Appendix F addresses the determination of prestressing force.

9.6.3 Reduction of Transfer Length Data

Determination of the transfer length was a several step process. An EXCEL spreadsheet was created such that raw transfer length data could be entered with the outcome being a smoothed strain profile for each girder end. The analysis process was broken into steps as listed below. A complete listing of the various worksheets in the spreadsheet to evaluate Girder G1C is provided in Appendix G and referenced below in STEPS 1-8.

STEP 1: Girder data with respect to strand tensioning, temperatures, VWSG readings, midspan deflections and times at which measurements were taken was entered into the "Data" worksheet (Table G.2).

STEP 2: Dimensions describing the location of embedment strips were entered into two worksheets titled "Gages-North" (Table G.3) and "Gages-South" (Table G.4). These dimensions allowed the calculation of exact strain measurement locations with respect to the girder ends. The figures indicate the location of each embedment strip on the particular side of the girder. For transfer length calculations, only data from the embedment strips at the bottom of the girder at each end were used.

STEP 3: CSS readings for each individual embedment strip were entered on the next series of 12 worksheets. Tables G.5 through G.16 show worksheets for each embedment strip on the girder. The location of the embedment strip is indicated by a shaded rectangle in the box below the header line. For example, a reading of -0156 on this sheet would indicate the distance between the measured embedments was 8"- 0.0156" or 7.9844". The "Initial" readings on this series of worksheets were averaged and used to determine the initial gage lengths on "Gages-North" and "Gages-South."

STEP 4: Tables G.17 and G.18 show worksheets "Raw-North" and "Raw-South" which subtracted initial CSS readings from subsequent readings and divided the result by the initial gage length. The resulting values were raw strains for both sides of the girder.

STEP 5: In order to smooth the CSS plots, values were averaged using a 3-point floating average as specified in equation 9.1.

$$\varepsilon_x = \frac{\varepsilon_{x-2} + \varepsilon_x + \varepsilon_{x+2}}{3} \tag{9.1}$$

The values ε_{x-2} and ε_{x+2} are the strains at 2 inches before and after the strain at "x" inches from the end of the girder. This floating 3-point average smoothed out the peaks and valleys in the CSS data to produce a strain plot that better facilitated determination of the transfer length. Tables G.19 and G.20 show worksheets "Smooth-North" and "Smooth-South." A comparison of the "smooth" and "raw" data demonstrates the smoothing effect. As with the "raw" data, this operation was performed for data from both sides of the girder.

STEP 6: Strains from the left and right sides were averaged and smoothed in Tables G.21 and G.22 respectively.

STEP 7: From the "Average Raw" and "Average Smooth" worksheets were plotted the CSS profiles just after release, and 1, 3, 7 and 14 days after release for both ends of the girder. Figure 9.4 shows a typical "raw" CSS plot for the East end of girder G1C. Figure 9.5 shows a typical "smooth" CSS plot for the same girder end. It was very useful to plot both average raw and average smooth data for error checking.
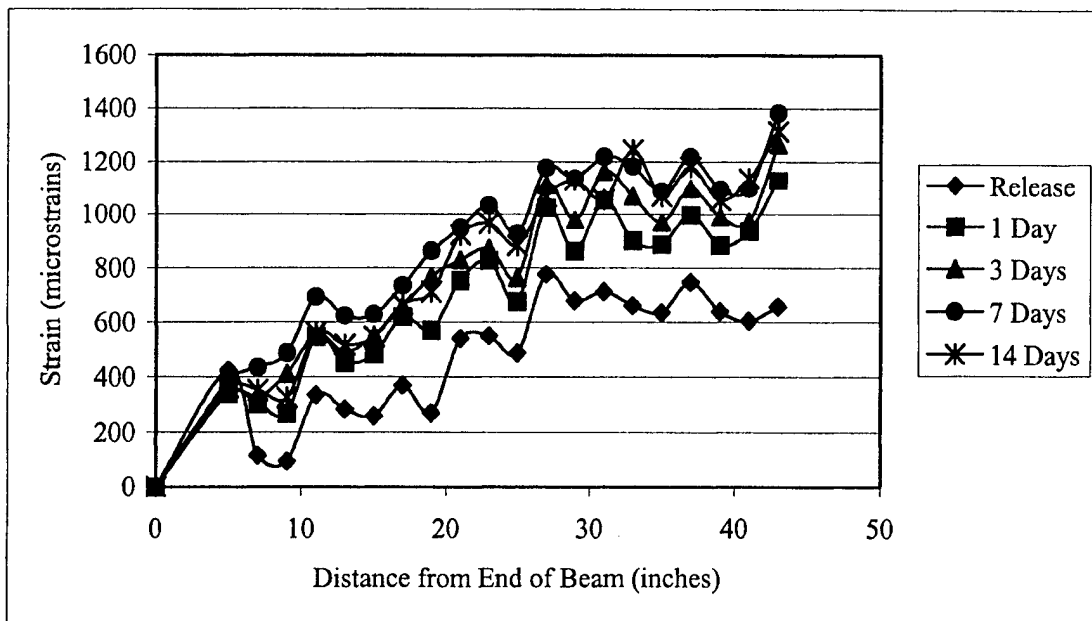
Figure 9.4 Raw CSS Plot for East End of Girder G1C
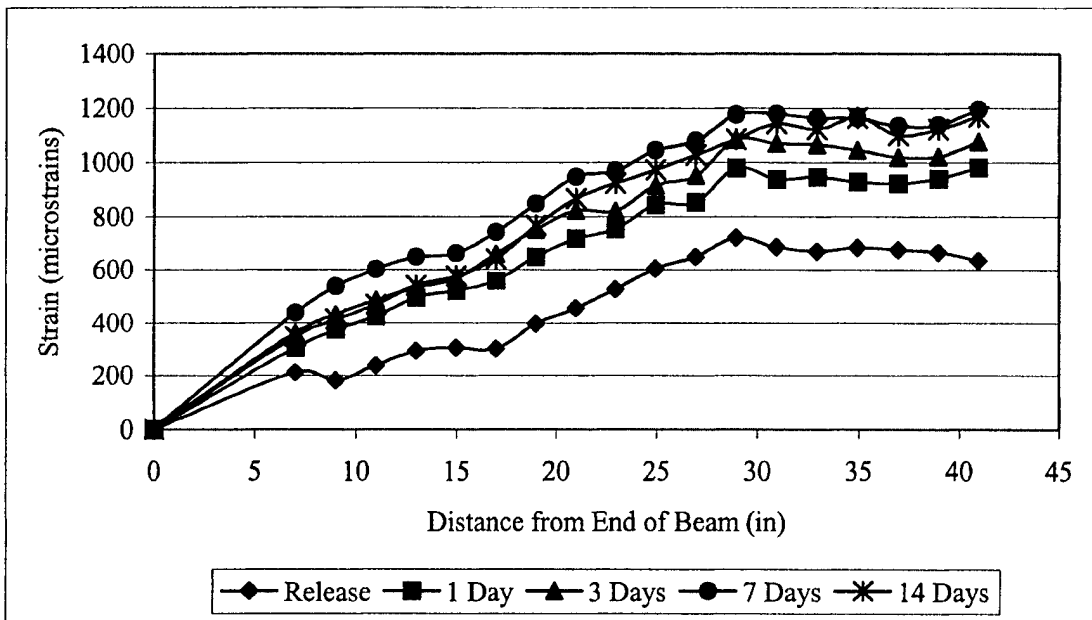
Figure 9.5 Smoothed CSS Plot for East End of Girder G1C

212

STEP 8: Examination of CSS profiles for each of the 12 girder ends and experience

from previous research showed that 14-day data provided an excellent prediction of

transfer length.[37] Based on this observation, two final plots were constructed, one for

each end of the girder. Figure 9.4 shows a typical 14-day smooth CSS plot for the East

end of girder G1C. The process for determining transfer length from the CSS plot is

covered in Section 9.6.4.
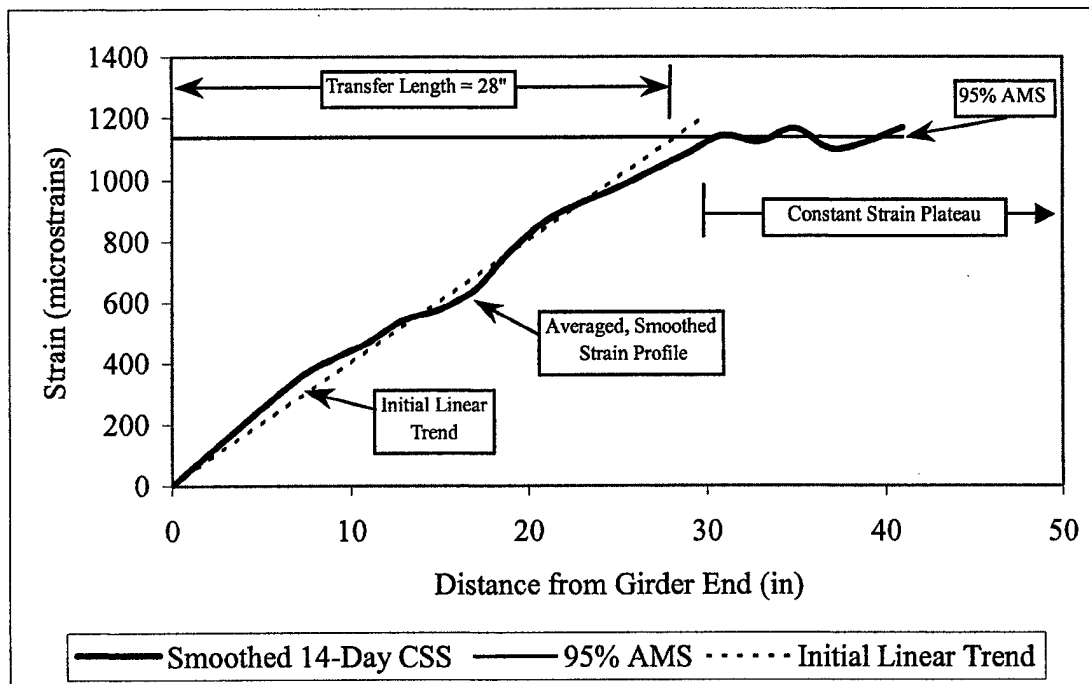
Figure 9.6 Transfer Length Determined Using 95 Percent AMS Method for G1C-East

9.6.4 Determination of Transfer Length

Transfer length was determined using the 95% Average Maximum Strain Method (95% AMS). Both Buckner[46] and Russell[44] recommended this method as a conservative and objective technique for determining transfer length.

9.6.4.1 95% Average Maximum Strain Line

Recalling Figure 9.1, which provided the idealized profile of stress in the prestressing strand, the second portion of the curve identifying the region of constant strand stress is analogous with the "Constant Strain Plateau." Determination of this region required identifying the point on the 14-day CSS plot where the transition to constant strain occurred. After evaluating the 12 girder-end CSS plots, it was determined that the constant strain plateau began at a point approximately 30 inches from the girder end in each case. The 30-inch distance was chosen for consistency and provided an excellent prediction overall of the strain plateau for all specimens. Referring to Table G.22, there is a column labeled 95%. The values in this column were calculated by taking 95% of the average of the strain values measured at greater than 30 inches from the girder end.

9.6.4.2 Initial Linear Trend Line

The "Initial Linear Trend" line shown in Figure 9.6 was determined in a much more subjective manner. Previous researchers took the intersection of the CSS plot with the constant strain plateau as the defined transfer length.[44] In many of the CSS plots in this project, the initial sloped portion of the plot was highly non-linear and undependable

for an accurate prediction of transfer length. It was decided to use a technique where a best-fit line was determined by visual inspection for the initial sloped portion of the CSS plot. After determining the approximate location of the line, the CSS data point marking the x-coordinate of the top end of the line was identified. Using the "trend line" option in EXCEL, the best-fit trend line passing through the origin was plotted. The intersection of the initial linear trend line with the 95% AMS line was identified as the transfer length.

9.6.5 CSS Transfer Length Results

Table 9.1 provides transfer length results after 14 days for the 12 girder-ends.

Table 9.1 – CSS Transfer Length Results (inches)

G1A		G1B		G1C		G2A		G2B		G2C	
East	West	East	West	East	West	East	West	East	West	East	West
19.5	18.75	25.00	18.75	28.00	21.50	17.50	13.25	13.00	13.00	19.00	18.00
		FREE		FREE		FREE					

9.6.6 Potential Sources of Error in CSS Transfer Length Results

As presented by Reutlinger[37], past work by Buckner and Deatherage pointed out that potential differences existed between transfer lengths of top and bottom strands. Buckner noted a study at the University of Illinois which reported a 25% decrease in bond strength for strands having 10 inches or more of concrete cast beneath them as compared to strands with only 2 inches of concrete below them. A study conducted by Deatherage on fully pretensioned top strands found that end slip for top strands was 1.5 to 5.2 times that for bottom strands. These results suggest that the transfer length of top

strands may be significantly longer than for bottom strands based on accumulation of excess water and air below the top strands.

Reutlinger[37] performed a parametric study to determine the potential effect of differences between the top and bottom strand transfer length on bottom strand transfer length calculations. Assuming that top-strand transfer lengths were between 1 and 5.5 times the bottom-strand transfer lengths, he determined that 95% AMS transfer lengths for the bottom strands could be unconservative by as much as 37%.

Transfer lengths were not determined for top strands in this research project. However, the concrete used had very little mix water and was dosed heavily with superplasticizers; no excess bleed water was observed at any time. It is very unlikely there was a difference between the top and bottom strand transfer lengths.

9.7 Discussion of Results

9.7.1 Effect of Girder Orientation

Chapter 8 provided details concerning girder construction. The girders were constructed in pairs: G1A and G1B, G2A and G2B and G1C and G2C. The pairs of girders had a combined length in each case at least 35 feet less than the length of the prestressing bed. This 35-foot difference meant there was 35 feet of free prestressing strand between the end of the second girder and the dead end of the prestressing bed. In Table 9.1, girder ends labeled "FREE" were the ends exposed to the excess strand. In each case, the transfer length was substantially longer than similar ends in the girder pairs. Other researchers also have reported this phenomenon.[44]

9.7.2 Effect of Concrete Grade

A single variable statistical analysis produced the results shown in Table 9.2 for

the two grades of concrete:

Table 9.2 Statistical Analysis of Transfer Length Data

Girder Series	f_c' Design Strength (psi)	Average f_{ci}' Actual Strength at 24 Hours (psi)	Average Transfer Length (in)	Standard Deviation (in)
G1	8,000	7,082	21.92	3.81
G2	10,000	9,180	15.63	2.83

The average transfer length for the G1 series girders was 6.29 inches longer than that of

the G2 series girders indicating a clear relation between concrete strength and transfer

length. The standard deviation was also significantly less for the G2 series girders

compared to the G1 series potentially indicating more consistent transfer lengths overall

for higher strength concrete.

In examining the relation between concrete strength and transfer length, it was

recognized that concrete strength affected material properties and the amount of change

in prestress from release until all losses had occurred. For the purpose of examining

transfer length, this study focused on concrete strength and modulus of elasticity.

Indirectly, however, the strength of concrete impacted the resulting initial level and

effective level of prestress. Initial elastic shortening was determined by the modulus of

elasticity of the concrete at release. Creep shortening over the period of time from

release until the transfer length was measured was directly related to the concrete grade; a

higher strength of concrete, in general, underwent less creep.

9.8 Comparison of Results with Code Provisions and Proposed Equations

This section compares the transfer length results from this research with transfer lengths predicted by code specified provisions and techniques proposed by other researchers. The goal of this comparison was to determine which variables provided the best prediction of transfer length. For comparison purposes, 12 transfer length values from this HSLC research were evaluated along with 8 values from a previous normal weight HPC study by Reutlinger[37] to determine what differences if any existed between HSLC and HPC. The transfer length tests in the HPC study were labeled in a manner similar to those in this research project. A transfer length test label of G4A-N indicated "grade 4" concrete, girder reinforcement pattern "A," and the "North" end of the girder. The 8 sets of normal weight HPC data were listed as the last 8 values in the tables. All the transfer length tests used 0.6-in diameter prestressing strand.

9.8.1 Material Properties

To evaluate current equations, a material property listing was composed. Table 9.3 shows concrete strengths at times from release through 56 days. The curing method was either accelerated using a curebox for the first 24 hours or by the ASTM[79] procedure

Table 9.3 Concrete Strength Data

Test #	l_t (in)	f_{ci}' 24-hour Curebox (psi)	f_{ci}' 24-hour ASTM (psi)	f_c' 28-Day Curebox (pse)	f_c' 28-Day ASTM (psi)	f_c' 56-Day Curebox (psi)	f_c' 56-Day ASTM (psi)
G1A-E	19.50	7465	5735	8711	8835	9084	9346
G1A-W	18.75	7465	5735	8711	8835	9084	9346
G1B-E	25.00	7465	5735	8711	8835	9084	9346
G1B-W	18.75	7465	5735	8711	8835	9084	9346
G1C-E	28.00	6315	5400	7478	7595	7750	8457
G1C-W	21.50	6315	5400	7478	7595	7750	8457
G2A-E	17.50	9640	9294	10166	10116	10418	10816
G2A-W	13.25	9640	9294	10166	10116	10418	10816
G2B-E	13.00	9640	9294	10166	10116	10418	10816
G2B-W	13.00	9640	9294	10166	10116	10418	10816
G2C-E	19.00	8261	6553	9344	9807	10249	10512
G2C-W	18.00	8261	6553	9344	9807	10249	10512
G2A-S	15.40	14989	10078	16513	17058	16770	18714
G2A-N	17.00	12379	7590	12939	14139	13430	15456
G2B-S	17.90	12379	7590	12939	14139	13430	15456
G2B-N	17.80	11721	7186	12251	13387	12716	14634
G4A-S	16.70	14675	9866	16166	16700	16418	18321
G4A-N	13.80	14395	9678	15858	16382	16105	17972
G4B-S	13.50	14395	9678	15858	16382	16105	17972
G4B-N	13.40	14610	9822	16094	16626	16345	18240

Table 9.4 lists modulus of elasticity values at release (24 hours) and after 56 days

Methods of curing were the same as for the concrete strength specimens.

219

Table 9.4 Modulus of Elasticity Data

Test #	l_t (in)	E_{ci} 24-hour Curebox (psi)	E_c 56-Day Curebox (psi)	E_c 56-Day ASTM (psi)
G1A-E	19.50	3.47E+06	3.86E+06	3.83E+06
G1A-W	18.75	3.47E+06	3.86E+06	3.83E+06
G1B-E	25.00	3.47E+06	3.86E+06	3.83E+06
G1B-W	18.75	3.47E+06	3.86E+06	3.83E+06
G1C-E	28.00	3.00E+06	3.28E+06	3.56E+06
G1C-W	21.50	3.00E+06	3.28E+06	3.56E+06
G2A-E	17.50	3.55E+06	3.93E+06	4.06E+06
G2A-W	13.25	3.55E+06	3.93E+06	4.06E+06
G2B-E	13.00	3.55E+06	3.93E+06	4.06E+06
G2B-W	13.00	3.55E+06	3.93E+06	4.06E+06
G2C-E	19.00	3.91E+06	4.10E+06	4.05E+06
G2C-W	18.00	3.91E+06	4.10E+06	4.05E+06
G2A-S	15.40	6.16E+06	5.58E+06	6.12E+06
G2A-N	17.00	5.78E+06	5.71E+06	5.61E+06
G2B-S	17.90	5.78E+06	5.71E+06	5.61E+06
G2B-N	17.80	5.78E+06	5.71E+06	5.61E+06
G4A-S	16.70	6.16E+06	5.58E+06	6.12E+06
G4A-N	13.80	6.16E+06	5.58E+06	6.12E+06
G4B-S	13.50	6.16E+06	5.58E+06	6.12E+06
G4B-N	13.40	6.16E+06	5.58E+06	6.12E+06

9.8.2 Prestressing Strand Stresses

Table 9.5 lists average prestressing strand stresses prior to release (f_{pt}), just after release (f_{si}), and after all losses (f_{se}). The strand tensioning stress, f_{pt}, was determined using strand load cells as described in Chapter 8. Both a CSS technique and VWSG output were used to determine stress in the strands. When strand stresses were required to predict transfer length, values from both techniques were used and the results

compared to measured values. CSS determined prestressing stress values were not

determined on the four normal weight HPC girders.

Table 9.5 Prestressing Levels

Test #	l_t (in)	f_{pt} (ksi)	f_{si} VWSG (ksi)	f_{si} CSS (ksi)	f_{se} VWSG 14-Days (ksi)	f_{se} CSS 14-Days (ksi)
G1A-E	19.50	179.06	161.73	167.40	154.74	152.20
G1A-W	18.75	179.06	161.73	167.40	154.74	152.20
G1B-E	25.00	179.06	160.90	167.94	153.34	153.04
G1B-W	18.75	179.06	160.90	167.94	153.34	153.04
G1C-E	28.00	179.11	162.11	159.52	153.65	146.76
G1C-W	21.50	179.11	162.11	159.52	153.65	149.76
G2A-E	17.50	191.30	178.66	181.52	176.52	171.14
G2A-W	13.25	191.30	178.66	181.52	176.52	171.14
G2B-E	13.00	191.30	178.94	181.28	176.52	169.92
G2B-W	13.00	191.30	178.94	181.28	176.52	169.92
G2C-E	19.00	179.11	164.64	161.87	159.82	161.87
G2C-W	18.00	179.11	164.64	161.87	159.82	156.14
G2A-S	15.40	190.86	178.13		169.75	
G2A-N	17.00	190.86	178.13		169.75	
G2B-S	17.90	190.86	177.24		168.72	
G2B-N	17.80	190.86	177.24		168.72	
G4A-S	16.70	190.86	179.31		170.62	
G4A-N	13.80	190.86	179.31		170.62	
G4B-S	13.50	190.86	179.14		169.90	
G4B-N	13.40	190.86	179.14		169.90	

9.8.3 Code and Suggested Transfer Length Equations

Transfer lengths were predicted using 20 equation variations. Included were

code-specified equations and equations suggested by researchers. Table 9.6 provides an

overview of the equations examined. The equation number listed refers to the discussion

of the equation in Chapter 2, Background Review.

Table 9.6 Summary of Transfer Length Equations

Source / Author of Equation	Transfer Length, l_t	Equation Number
AASHTO[40]	$50 d_b$	2.6
ACI[2]	$\dfrac{f_{se} d_b}{3}$	2.5
Zia and Mostafa[42]	$1.5 \dfrac{f_{si}}{f'_{ci}} d_b - 4.6$	2.8
Martin and Scott[41]	$80 d_b$	2.7
Deatherage et al.[43]	$\dfrac{f_{si} d_b}{3}$	2.9
Russell[44]	$\dfrac{f_{se} d_b}{2}$	2.10
Mitchell et al.[45]	$0.33 f_{si} d_b \sqrt{\dfrac{3}{f'_{ci}}}$	2.11
Buckner[46]	$\dfrac{1250 f_{si} d_b}{E_{ci}}$	2.12
Lane (Mean)[47]	$4 \dfrac{f_{pt} d_b}{f'_c} - 21$	2.13
Lane (95% Confidence)[47]	$4 \dfrac{f_{pt} d_b}{f'_c} - 5$	2.14

d_b Prestressing strand diameter

l_t Transfer length

f_{pt} Stress in prestressing strand prior to release

f_{si} Stress in prestressing strand immediately after release (f_{pt}-ES)

f_{se} Stress in prestressing strand after all losses (f_{pt}-ES-CR-SH)

ES   Prestress losses due to elastic shortening

CR   Prestress losses due to creep

SH   Prestress losses due to shrinkage

f'_{ci} Concrete compressive strength at release

f'_c Concrete compressive strength at 28 or 56 days

E_{ci} Concrete modulus of elasticity at release

In order to compare the experimentally measured transfer length values with code and suggested equation results, the following relationship was used to determine the average difference between equation and experimental results:

$$\frac{l_{t(Equation)} - l_{t(Experimental)}}{l_{t(Equation)}} \tag{9.2}$$

By performing the difference comparison in this manner, the code or suggested equation served as the accepted value.

9.8.4 Results of Comparison

Table 9.7 provides an overview of the results of a comparison of experimentally measured to predicted transfer lengths. The curing method and time of curing specified describe whether an accelerated (curebox) or ASTM curing procedure was used and the age of the specimen. The prestress stress measurement technique describes whether CSS readings or vibrating wire strain gage (VWSG) output was used. The "Max Over" column lists the predicted transfer length value with the largest percentage greater than the experimentally measured value. The "Max Under" column lists the predicted transfer length value with the largest percentage less than the experimentally measured value.

Table 9.7 Overview of Results Sorted by Equation Source

Equation Source & Designation	Equation Predicting l_t	Curing Method & Age	Prestress Stress Msmt. Technique	Overall Results		
				Avg Diff (%)	Max Over (%)	Max Under (%)
AASHTO	$50 d_b$	NA	NA	42%	57%	7%
ACI-a	$\dfrac{f_{se} d_b}{3}$	NA	VWSG	46%	63%	9%
ACI-b	$\dfrac{f_{se} d_b}{3}$	NA	CSS	40%	62%	5%
Buckner - a	$\dfrac{1250\, f_{si} d_b}{E_{ci}}$	Curebox-24	VWSG	41%	66%	22%
Buckner - b	$\dfrac{1250\, f_{si} d_b}{E_{ci}}$	Curebox-24	CSS	49%	66%	30%
Deatherage et al. - a	$\dfrac{f_{si} d_b}{3}$	NA	VWSG	49%	64%	14%
Deatherage et al. - b	$\dfrac{f_{si} d_b}{3}$	NA	CSS	44%	64%	12%
Lane - 95 - a	$4 \dfrac{f_{pt} d_b}{f'_c} - 5$	Curebox-28	NA	50%	68%	28%
Lane - 95 - b	$4 \dfrac{f_{pt} d_b}{f'_c} - 5$	ASTM-28	NA	48%	68%	26%
Lane - a	$4 \dfrac{f_{pt} d_b}{f'_c} - 21$	Curebox-28	NA	-7%	46%	-129%
Lane - b	$4 \dfrac{f_{pt} d_b}{f'_c} - 21$	ASTM-28	NA	-20%	47%	-163%
Martin, Scott	$80 d_b$	NA	NA	63%	73%	42%
Mitchell et al. - a	$0.33\, f_{si} d_b \sqrt{\dfrac{3}{f'_{ci}}}$	Curebox-24	VWSG	7%	34%	-27%
Mitchell et al. - b	$0.33\, f_{si} d_b \sqrt{\dfrac{3}{f'_{ci}}}$	ASTM-24	VWSG	19%	35%	-17%
Russell, Burns - a	$\dfrac{f_{se} d_b}{2}$	NA	VWSG	64%	75%	39%
Russell, Burns - b	$\dfrac{f_{se} d_b}{2}$	NA	CSS	60%	74%	36%
Zia, Mostafa - a	$1.5 \dfrac{f_{si}}{f'_{ci}} d_b - 4.6$	Curebox-24	VWSG	-66%	-7%	-161%
Zia, Mostafa - b	$1.5 \dfrac{f_{si}}{f'_{ci}} d_b - 4.6$	ASTM-24	VWSG	-10%	10%	-42%
Zia, Mostafa - c	$1.5 \dfrac{f_{si}}{f'_{ci}} d_b - 4.6$	Curebox-24	CSS	-28%	-5%	-60%
Zia, Mostafa - d	$1.5 \dfrac{f_{si}}{f'_{ci}} d_b - 4.6$	ASTM-24	CSS	-4%	14%	-35%

224

9.8.4.1 Results of Analysis Based on Average Difference

Analysis of Table 9.7 showed that Mitchell et al.–a produced the best overall estimate of transfer length. The Mitchell et al.-a equation would be considered a "best-fit" equation where a "best-fit" equation was defined as the equation having the lowest average difference between experimental and predicted values.

The use of initial concrete compressive strengths, f'_{ci}, based on curebox data produced better results overall than ASTM strengths. This occurrence was logical. A comparison of heat of hydration curves between girders and curebox specimens showed a close correlation.

The use of prestressing stresses based on CSS data seemed to produce slightly better results than VWSG data. However, the differences were small and results from Buckner's equation showed the opposite trend. Data from Reutlinger's[37] tests were based on VWSG data making it desirable to also base this current analysis on VWSG predicted prestress values. Based on the above, VWSG predicted prestress values were used for future analyses.

Although Mitchell et al.-a and Mitchell et al.-b were the best overall equations, there were cases where transfer lengths were underestimated by as much as 27%. Equations by Buckner, Deatherage, ACI and AASHTO always provided a conservative estimate of transfer length.

9.8.4.2 Results of Analysis Based on Maximum Underestimate

Analysis of Table 9.7 based on maximum underestimate showed equation ACI-b to provide a good overall estimate of transfer length without being overconservative.

225

ACI-b would be the best choice as a "design equation." A "design" equation was defined as the equation having the lowest positive maximum underestimate value without being overly conservative. Determination of the amount an equation was overconservative was based on the maximum overestimate value. The most favorable combination of these two values indicated the best "design" equation.

Table 9.7 also showed the AASHTO equation and the equation by Deatherage provided good conservative estimates without being overconservative. An interesting note concerning these five equations was that they did not include a term describing the properties of the concrete.

9.8.4.3 Evaluation of Top Five "Best-Fit" and "Design" Equations

In order to determine a strategy for improving current transfer length equations, Table 9.8 was created to show a listing of the top five equations in both the "best-fit" and "design" categories. From this table, it was possible to summarize which factors appeared to be important when predicting transfer length. It was obvious that strand diameter, d_b was a necessary equation variable. It appeared that f_{si} was a better variable for describing the impact of the level of prestress. The variable that appeared to best describe the concrete was f'_{ci}; Since the Mitchell et al. equations ranked highest with respect to "best-fit," f'_{ci} was considered an important variable. However, based on the use of HSLC and the effect reducing concrete unit weight has on modulus of elasticity, the consideration of E_{ci} was not discarded from further analysis.

226

Table 9.8 Review of Top Five "Best-Fit" and "Design" Equations

Best-Fit Equations								
Rank	Equation Source & Designation	Equation	Curing Method & Age	Equation Variables				
				d_b	f'_{ci}	E_{ci}	f_{si}	f_{se}
1	Mitchell et al. - a	$0.33\, f_{si} d_b \sqrt{\dfrac{3}{f'_{ci}}}$	Curebox-24	X	X		X	
2	Mitchell et al. - b	$0.33\, f_{si} d_b \sqrt{\dfrac{3}{f'_{ci}}}$	ASTM-24	X	X		X	
3	ACI-b	$\dfrac{f_{se} d_b}{3}$	NA	X				X
4	Buckner - a	$\dfrac{1250\, f_{si} d_b}{E_{ci}}$	Curebox-24	X		X	X	
5	AASHTO	$50 d_b$	NA	X				

Design Equations								
Rank	Equation Source & Designation	Equation	Curing Method & Age	Equation Variables				
				d_b	f'_{ci}	E_{ci}	f_{si}	f_{se}
1	ACI-b	$\dfrac{f_{se} d_b}{3}$	NA	X				X
2	AASHTO	$50 d_b$	NA	X				
3	ACI-a	$\dfrac{f_{se} d_b}{3}$	NA	X				X
4	Deatherage et al. - b	$\dfrac{f_{si} d_b}{3}$	NA	X			X	
5	Deatherage et al. - a	$\dfrac{f_{si} d_b}{3}$	NA	X			X	

9.9 Development of an Improved Transfer Length Equation

Table 9.8 helped focus efforts in determining an improved transfer length

equation. Using the base equations specified by AASHTO and ACI and the equations

suggested by Buckner, Deatherage et al., and Mitchell et al., numerous different equation

configurations were developed and evaluated. In evaluating the equation forms, the following values were used:

f'_{ci} Curebox (accelerated) 24-hour concrete compressive strength

E_{ci} Curebox (accelerated) 24-hour modulus of elasticity

f_{si} Initial prestressing force based on vibrating wire strain gage output

f_{se} Effective prestressing force based on vibrating wire strain gage output

For initial equation development, only the 20 sets of transfer length data (12 HSLC and 8 HPC) were used. For later development, more data from several other researchers was considered.

When determining the percent difference, a different method was used. During the evaluation of existing equations, the "accepted" value was taken as the "equation" value. While developing a new equation, the "accepted" value was the "measured" value. The percent difference was calculated using the following relation:

$$\frac{l_{t(Equation)} - l_{t(Experimental)}}{l_{t(Experimental)}} \tag{9.3}$$

9.9.1 Determination of Equation Variables

The first step taken in developing an improved equation was to identify the variable or variables that would best predict transfer length. Plots were created which singled out one variable and compared it to measured transfer length values. Figures 9.7 through 9.10 show plots involving f'_{ci} and E_{ci}.
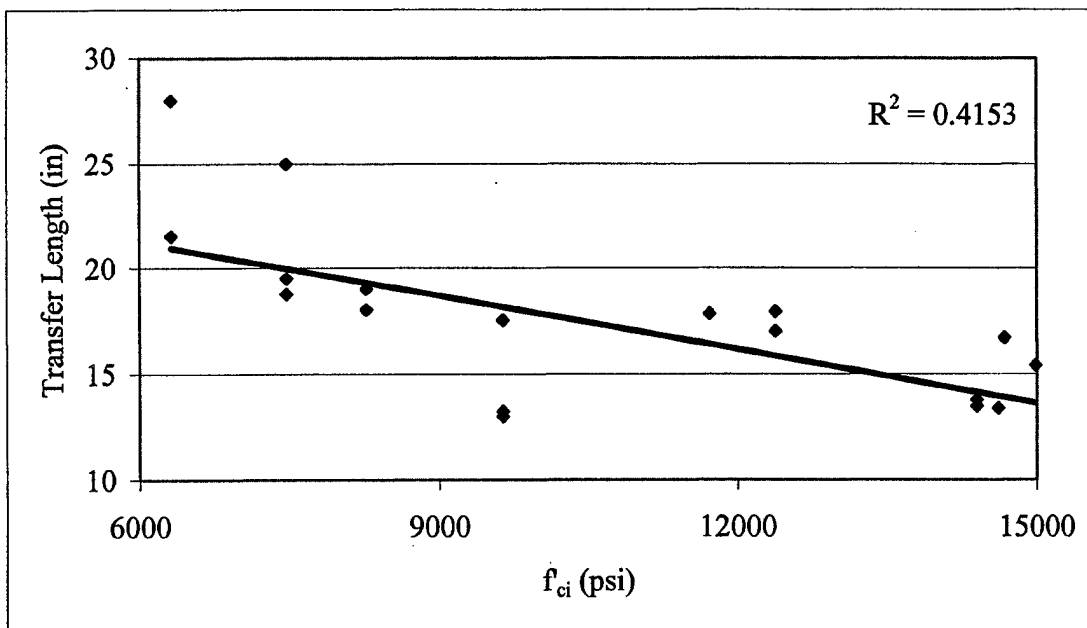
Figure 9.7 Transfer Length vs. f'ci
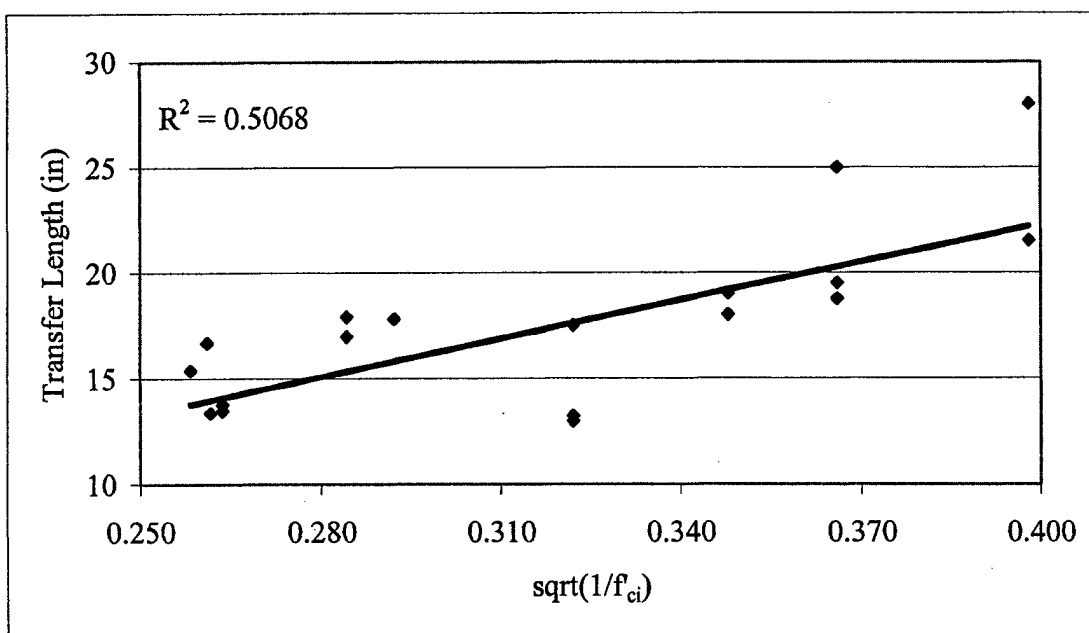
Figure 9.8 Transfer Length vs. $(1/f'_{ci})^{0.5}$

229
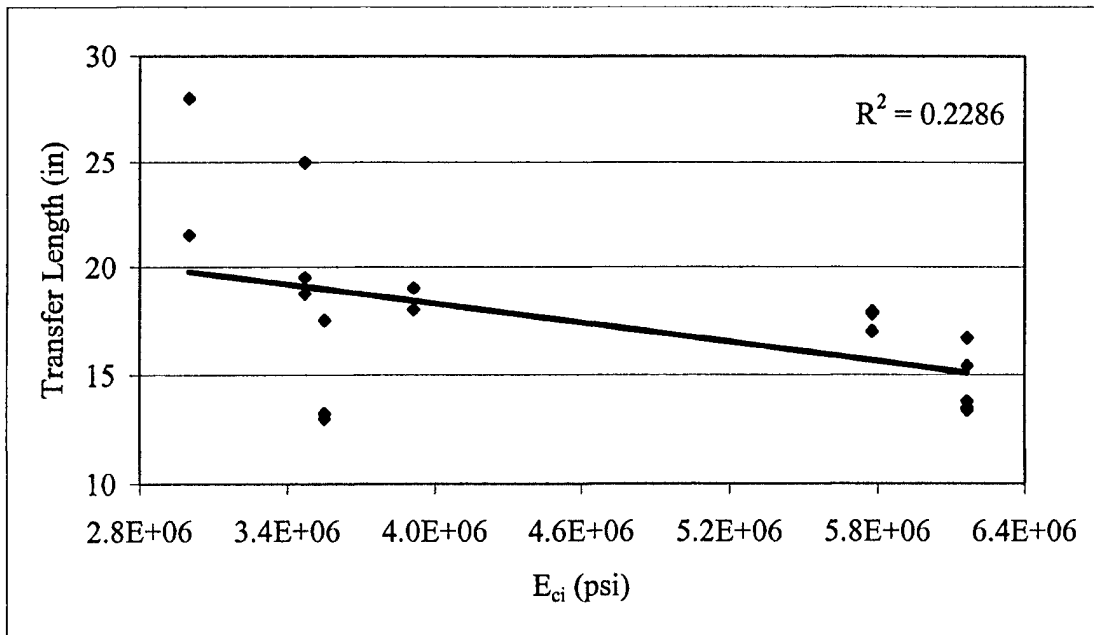
Figure 9.9 Transfer Length vs. E_{ci}
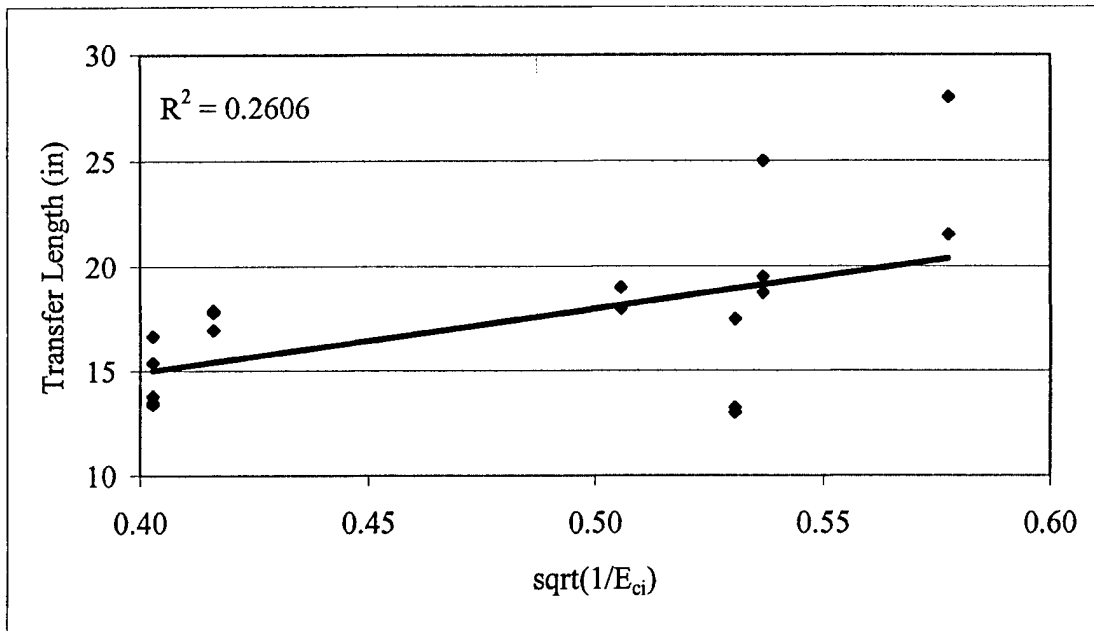
Figure 9.10 Transfer Length vs. $(1/E_{ci})^{0.5}$

230

In Figures 9.7 through 9.10, the data points are not separated by lightweight or normal weight concrete. Each point describes one of the 20 tests. In a few cases, two data points are at the same location. A trendline and R^2 values were plotted in each figure to provide an idea of which variable form might best fit the transfer length data.

The results of Figures 9.7 through 9.10 indicated the variable f'_{ci} was most likely a better predictor of transfer length than E_{ci}. The R^2 values for comparison of f'_{ci} related variables with transfer length were greater indicating better correlation than those for E_{ci}. As a note, the R^2 value provided an indication of the degree of fit of a series of data points to a line. In comparisons to f_c', a straight line was the best-fit line. In the comparisons involving E_{ci}, other curve forms provided only a very slight improvement in correlation. Overall, the straight line provided a good common basis of comparison.

9.9.2 Determination of Equation Forms

Figures 9.7 through 9.10 showed that f'_{ci} was most likely the material-related variable to predict transfer length. Based on the use of HSLC in this research, it was decided to consider both f'_{ci} and E_{ci}. Using these variables, existing code specified equations and equations seen in Table 9.8, 27 different equation forms were configured and evaluated using the 12 sets of HSLC transfer length data and the 8 sets of normal weight HPC transfer length data from Reutlinger.[37] The value f_{ci}' was based on 24-hour curebox specimens and prestress levels were based on measurements using VWSG data.

231

9.9.3 Results of Equation Analysis

The results of the equation analysis showed that the same equation form provided both the "best fit" and "design" equation. The definitions for "best fit" and "design" were defined previously in Sections 9.8.4.1 and 9.8.4.2. The only difference between the two equations was a constant value under the radical. Concrete strength values at release, f_{ci}', are in psi; transfer lengths are in inches.

The equation that provided the best fit was:

$$50 \, d_b \sqrt{\frac{3170}{f'_{ci}}} \qquad\qquad (9.4)$$

The best equation for design was:

$$50 \, d_b \sqrt{\frac{5500}{f'_{ci}}} \qquad\qquad (9.5)$$

Equation 9.4 was similar to one suggested by Mitchell for conservatively checking stress in concrete at the time of transfer. Mitchell's equation used 3000 as the constant in lieu of 3170. Mitchell did not recommend using the equation to calculate the transfer length portion of development length.[45]

9.9.4 Equation Verification with Transfer Length Data from other Researchers

To verify the applicability equations 9.4 and 9.5, transfer length data from several

other researchers were compiled into a database and evaluated. The data were based only

on 0.6-in diameter prestressing strand. In most cases, the tests involved I-shaped girders;

however, tests by Mitchell[45] and Russell[44] used rectangular cross sections. Table J.1 lists

data used in the verification.

Each set of transfer length datum was plotted on a graph with f'_{ci} on the X-axis

and transfer length on the Y-axis. Plotting the "best fit" and "design" equations specified

in Section 9.9.3 on the overall data plot was successful. However, by slightly increasing

the constant values under the radical as seen in equations 9.6 (best fit) and 9.7 (design)

below, the predicted plot line better fit the scatter of data points.

$$50 \, d_b \sqrt{\frac{4000}{f'_{ci}}} \qquad (9.6)$$

$$50 \, d_b \sqrt{\frac{6000}{f'_{ci}}} \qquad (9.7)$$

Figures 9.11 and 9.12 show equations 9.6 and 9.7 plotted respectively against the

experimental data points listed in Appendix J.

It is important to comment that the rectangular shapes tested by Russell[44] were released simultaneously by flame cutting. Specimens by Mitchell[45] were released gradually which was reported to more closely match transfer lengths recorded under similar conditions in I-shaped girders. When finally configuring the equations, the rectangular shapes from Russell's testing were not included.
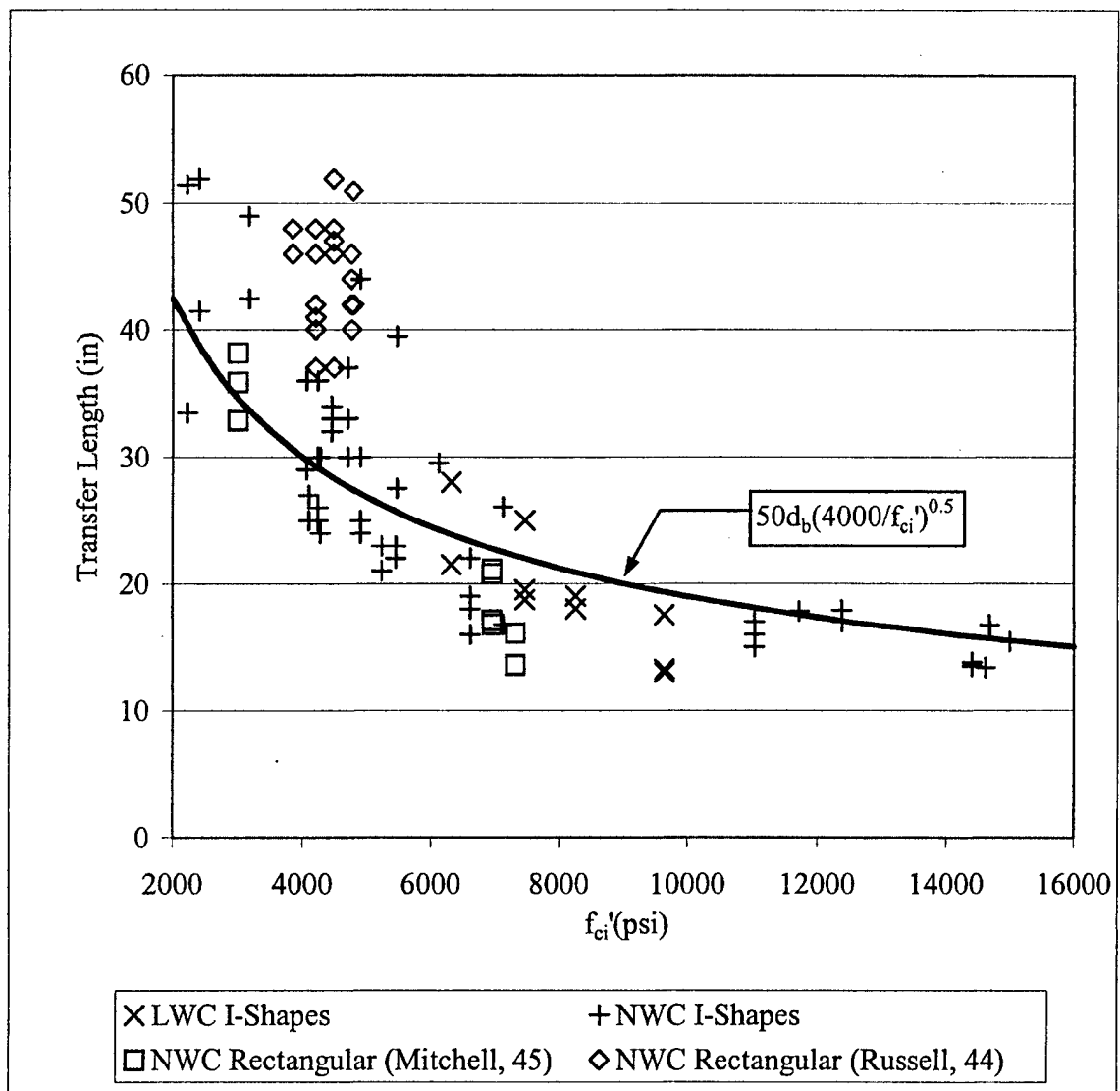
Figure 9.11 Proposed Best Fit Equation Plotted on Transfer Length Data
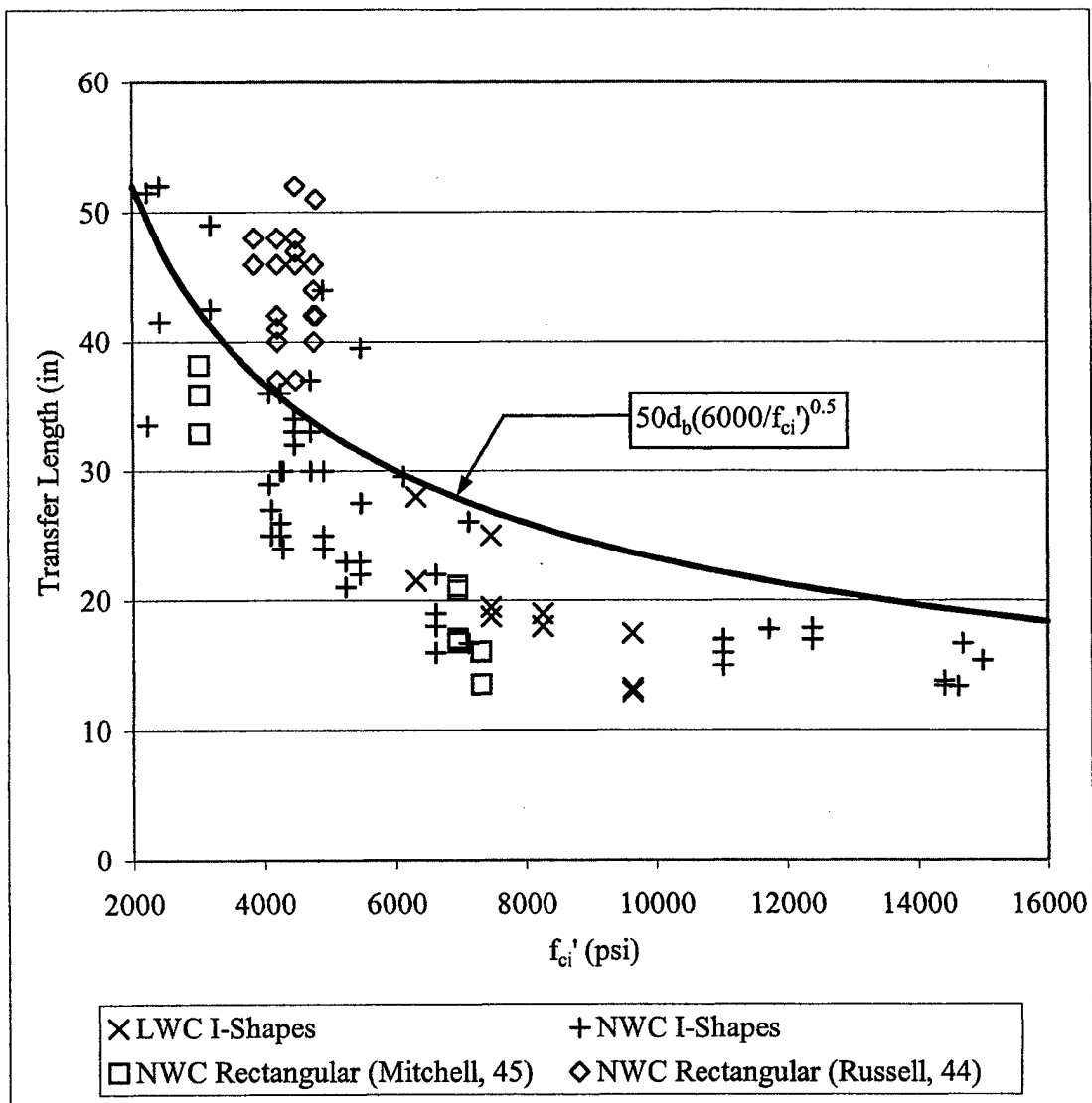
Figure 9.12 Proposed Design Equation Plotted on Transfer Length Data

Evaluation of the proposed equation for both "best fit" and "design" is shown in

Table 9.9 where f_{ci}' is in psi units. In the "Overall I Shape" category, comparison of both

the "Best Fit" and "Design" equations with the current AASHTO equation showed

favorable results.

Table 9.9 Results of Evaluation of the Proposed Equations

Basis Of Comparison	AASHTO CODE[40]	Proposed Design Equation	Proposed Best Fit Equation
	$50\,d_b$	$50\,d_b\sqrt{\dfrac{6000}{f'_{ci}}}$	$50\,d_b\sqrt{\dfrac{4000}{f'_{ci}}}$
Avg Diff (Overall I Shape)	33%	25%	2%
Max Over (Overall I Shape)	131%	82%	49%
Max Under (Overall I Shape)	-42%	-25%	-38%
Avg Diff (LWC I-Shape)	69%	44%	18%
Max Over (LWC I-Shape)	131%	82%	49%
Max Under (LWC I-Shape)	7%	4%	-15%
Avg Diff (NWC I-Shape)	27%	22%	0%
Max Over (NWC I-Shape)	124%	79%	46%
Max Under (NWC I-Shape)	-42%	-25%	-38%
Avg Diff (NWC Rect)	-10%	-1%	-19%
Max Over (NWC Rect)	121%	100%	63%
Max Under (NWC Rect)	-42%	-34%	-46%
Avg Diff (Overall)	21%	18%	-3%
Max Over (Overall)	131%	100%	63%
Max Under (Overall)	-42%	-34%	-46%

The reason the proposed equations provided a better estimate was found in the strength range below 6,000 psi. Examination of the equations shows that the constant term under the radical determines the point at which the equation begins to increase the predicted transfer length above the AASHTO suggested $50d_b$. In the case of the "best fit" form of the equation, strengths below 4,000 psi underwent an increase in predicted transfer length above $50d_b$. Examination of Figure 9.11 demonstrates this condition. In the case of the "design" form of the equation, strengths below 6,000 psi underwent an

increase in predicted transfer length above $50d_b$. Examination of Figure 9.12 demonstrates this condition.

In examining the results of 32 different equation forms, it was observed that equation forms based on the AASHTO $50d_b$ prediction of transfer length in all cases showed better accuracy than the same equation form based on the ACI prediction $f_{se}d_b/3$. For 0.6-inch strand, $50d_b$ is 30 inches. On average, f_{se} is about 165 ksi meaning $f_{se}/3$ would equal about 55. Heuristically speaking, it makes sense to include a term addressing the level of prestress; however, the results of this evaluation did not indicate it produced the most accurate prediction.

Further examination of Table 9.18 showed insignificant difference between transfer length results for HSLC and normal weight HPC. Figures 9.11 and 9.12 show how transfer lengths for HSLC plotted consistently with the normal weight HPC values. To the author's knowledge, there is no other transfer length data available for 0.6-inch prestressing strand used in lightweight concrete in this strength and unit weight range.

9.10 Conclusions

An evaluation of current code provisions using the 12 HSLC transfer lengths in this research and 8 normal weight HPC transfer lengths from Reutlinger[37] showed the current AASHTO[40] and ACI[2] equations to be conservative. The AASHTO equation overestimated transfer lengths by 42% on average and never underestimated transfer lengths. The ACI equation using VWSG data also overestimated transfer lengths by 46% and never underestimated transfer lengths. Use of either the AASHTO or ACI equations to predict transfer length for slate HSLC was conservative. Based on the concrete

237

strength range addressed in this research project, modification of the current code specifications for transfer lengths was not necessary for HSLC.

An evaluation of other suggested equations for predicting transfer length showed an equation by Mitchell et al.[45] to provide the best overall prediction of transfer length. Equations by Buckner[46] and Deatherage et al.[43] also produced good overall predictions. The above equations were applicable to both HSLC and normal weight HPC with good results.

An evaluation of the applicability of initial concrete compressive strength, f_{ci}', and initial modulus of elasticity, E_{ci}, and 32 possible equation forms showed that d_b and f_{ci}' were the best parameters for predicting transfer length. New equations for predicting transfer length based on "Best Fit" and "Design" produced more accurate results than current code equations.

There was no indication throughout this analysis that a need existed to differentiate between slate HSLC and normal weight HPC with regard to transfer length. For initial concrete strengths, f_{ci}', over 6,000 psi, the prediction of transfer length was the same for both lightweight and normal weight concrete.

CHAPTER X

GIRDER TEST SET-UP AND PROCEDURE

10.1 Introduction

This chapter provides a description of the set-up and procedure used to test the composite HSLC girders. Detail is provided on the site layout, data acquisition system, and conduct of the test.

10.2 Test Set-up

Figure 10.1 illustrates the overall test set-up. Figure 10.2 shows the test frame with the hydraulic ram attached. Details on pieces of the set-up were included in Figure 10.1.

10.3 Instrumentation

The load cell used to monitor the applied load was a Strainsert 700 kip load cell. The model number was (CLC-FB) Q14928. The voltage rating was 2.00-mv/V (Nom.). The load cell was a full-bridge configuration that required an excitation voltage of 10 volts direct current (DC).

The wire potentiometer used to measure deflection at the point of load application was a Rayelco Position Transducer, model P5-A, 10 volts DC excitation. In addition to the wire pot covered in Section 10.2.3, a dial gage was positioned at the point of load

application to verify wire pot output. The dial gage readings matched wire pot output during each girder test.

500 Ton Hydraulic Ram

Strainsert 700 kip Load Cell

W10x77 x 24" w/Stiffeners

1 $\frac{1}{8}$" ϕ x 18" Rollers

1" x 6" x 20" PL

$\frac{3}{8}$" x 5½" x 18" Pad

Strand Slip Indicators

1"

LVDT for Top Strain

LVDT Strain Rosette

LVDT for Bottom Strain

3"

Wire Potentiometer

Dial Gage To Measure Interface Slip

1" x 6" x 24" PL

2½" ϕ x 24" Pin Stitch Welded to PL

2¾" ϕ x 24" Roller

MC 6x12 x 24"

1½" x 6" x 24" PL

1" x 6" x 24" PL

7" x 9" x 30" Steel Support

Figure 10.1 Experimental Test Set-up
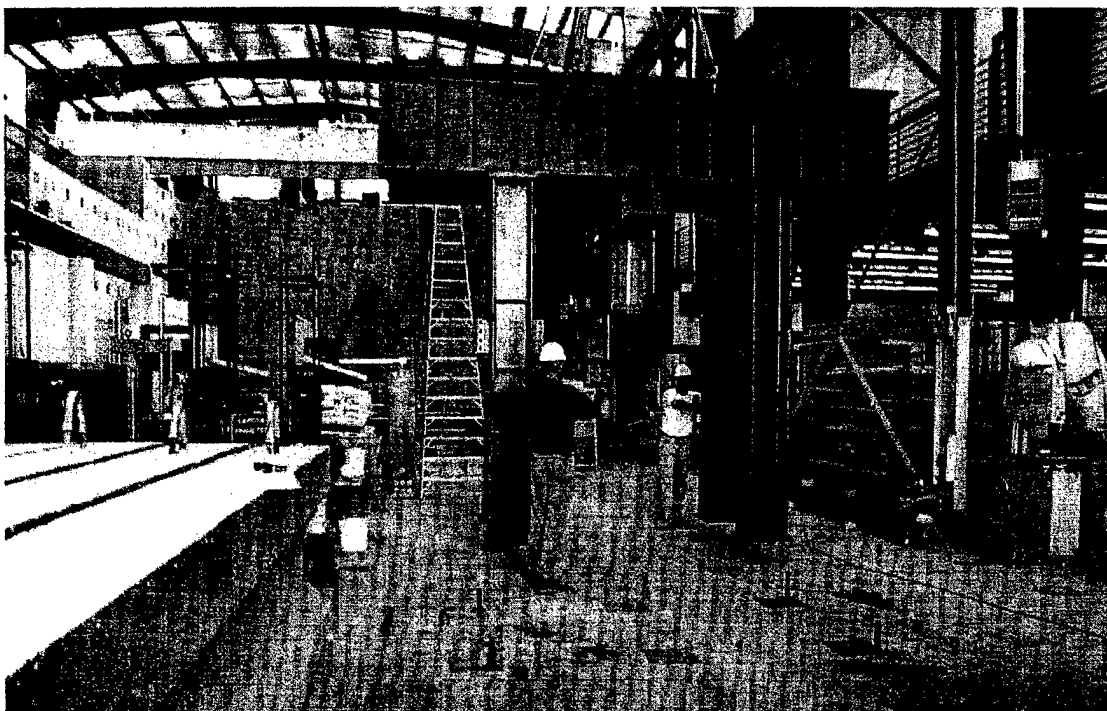
Figure 10.2 Load Frame

The linear variable displacement transducers (LVDT) were manufactured by the Lucas Schaevitz Company. The 3-inch LVDTs were model number HCD 1000. The 6-inch LVDTs were the HCD 2000. The LVDT measuring strain at the top of the girder was a 3-inch LVDT; the gage length was 24 inches. The LVDT measuring strain at the bottom of the girder was a 6-inch LVDT; the gage length was 24 inches. The 0 and 45 degree LVDTs in the rosette were 6-inch LVDTs. The 90 degree LVDT was a 3-inch LVDT. The 0 and 90 degree LVDTs had 10.5-inch gage lengths; the 45 degree LVDT had a 16.25 inch gage length. All LVDTs required a minimum of 12 volts ± up to a maximum of 15 volts ±. This voltage requirement is known as a "bi-polar" voltage. It was required to connect two power supplies in tandem to provide this voltage.
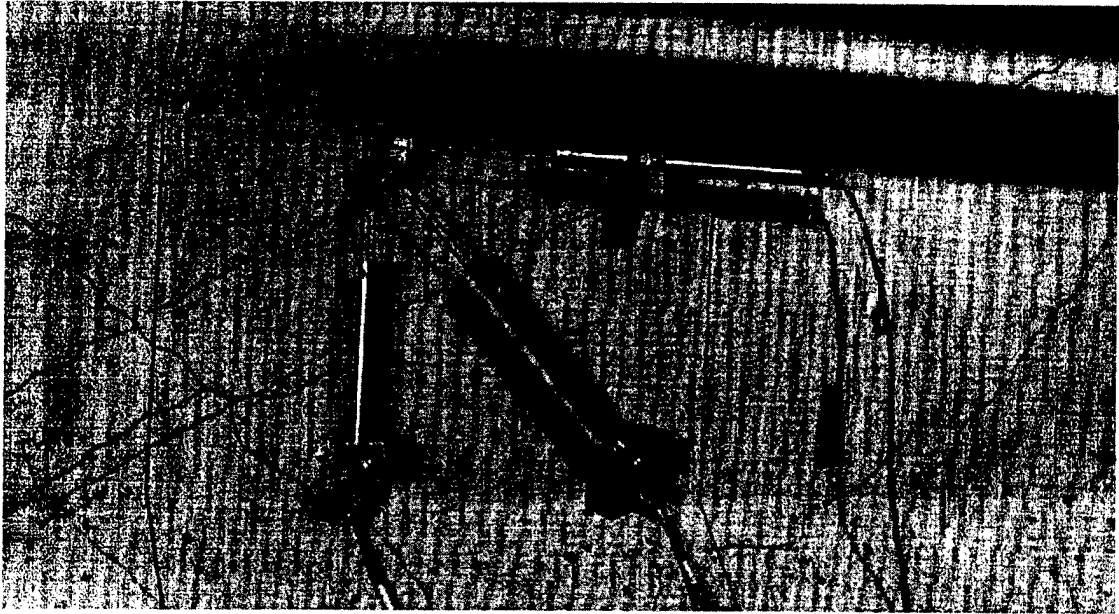
Figure 10.3 LVDTs Configured in Strain Rosette

The devices used to measure strand slip were linear potentiometers having a 2-inch maximum range. The devices had an excitation voltage requirement of 10 volts DC. The devices were calibrated prior to use to verify factory values. Figure 10.4 shows the strand slip indicators attached to the exposed strand segments.

To measure slip between the interface of the deck and the girder, a dial gage was installed halfway between the load point and a support. There was never any indication of slip seen in any of the tests. The only reading on the dial gage was related to the strain gradient between the gage connection points on the girder and the bottom surface of the deck. Figure 10.5 shows the dial gage positioned to record interface slip.
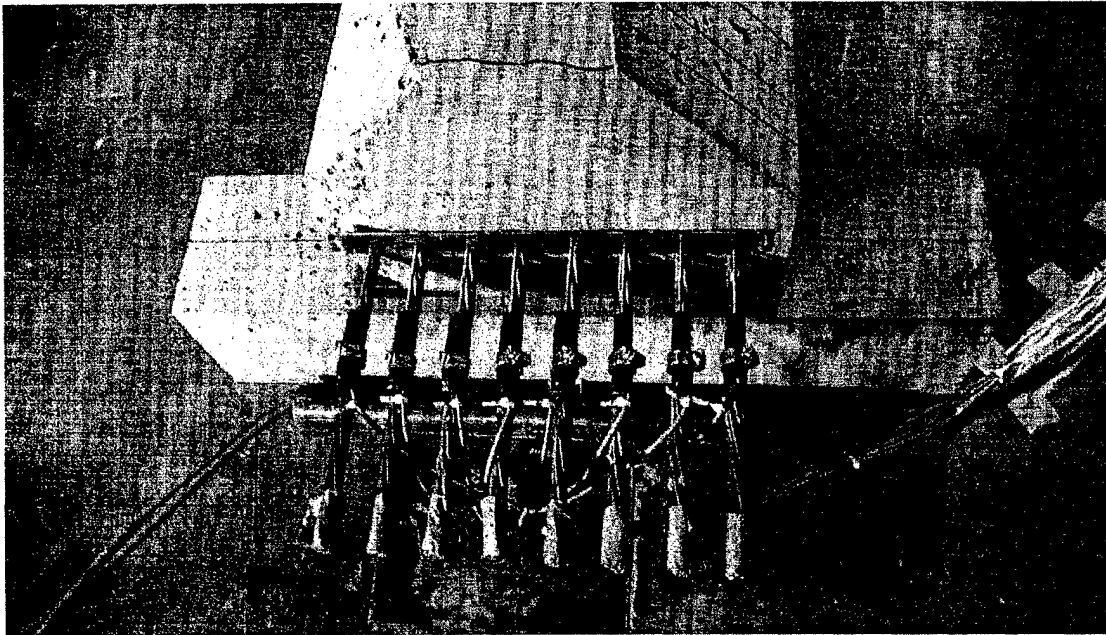
Figure 10.4 Strand Slip Indicators
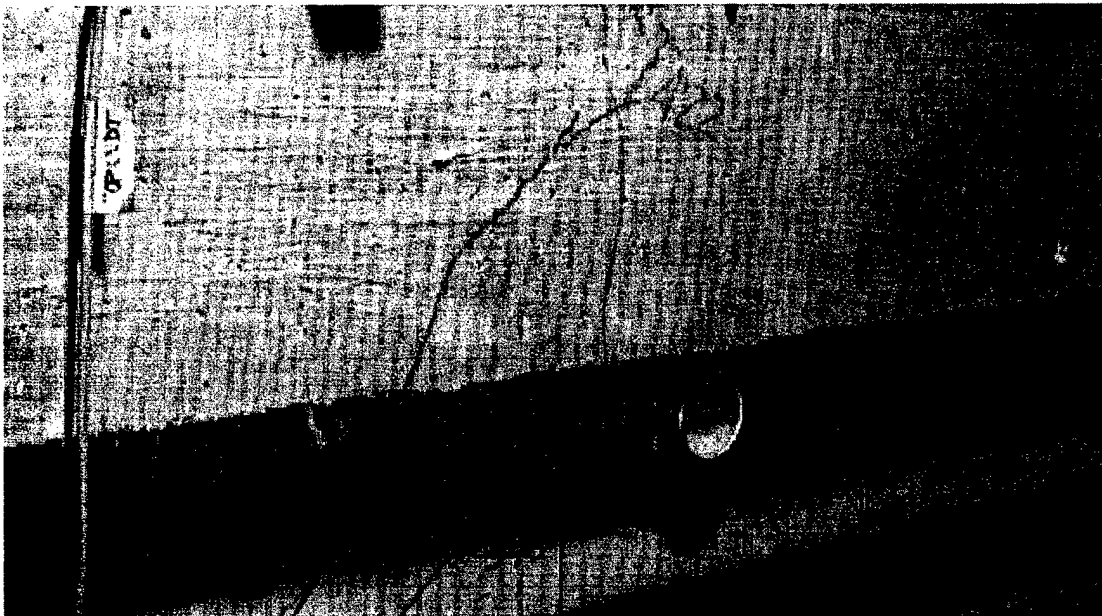
Figure 10.5 Dial Gage to Measure Interface Slip

243

10.4 Data Acquisition System

All instrumentation discussed in Section 10.3 was connected to a data acquisition

(DAQ) system. A National Instruments DAQ system was used for all tests. Table 10.1

identifies the DAQ system components and uses.

Table 10.1 DAQ System Components and Functions

DAQ Component	Component Description	Component Function(s)	DAQ Channel Assignments
SCXI-1000	4 Slot Chassis	Support DAQ Cards	NA
SCXI-1520	8 Channel Strain Card	Provided 8 Multi-Use Channels Which Supported all DAQ Requirements	0 – Load Cell 1 – Top LVDT 2 – Bottom LVDT 3 – Wire Pot 4 – 0 Deg LVDT 5 – 45 Deg LVDT 6 – 90 Deg LVDT
SCXI-1127	Multiplexer Capable of 64 ¼-Bridge Outputs 32 ½-Bridge Outputs 16 Full-Bridge Outputs	Multiplexed Output from 8 Strand Slip Indicators into Channel 7 of the SCXI-1520	7,0 – Strand 1 Slip 7,1 – Strand 2 Slip 7,2 – Strand 3 Slip 7,3 – Strand 4 Slip 7,4 – Strand 5 Slip 7,5 – Strand 6 Slip 7,6 – Strand 7 Slip 7,7 – Strand 8 Slip

Figure 10.6 shows a photo of the DAQ system connected to a laptop PC. The power

supplies providing the bipolar power for the LVDTs are also pictured. The DAQ system

was driven by LABVIEW, the proprietary software of National Instruments. A

LABVIEW program was written to support the girder testing.

244
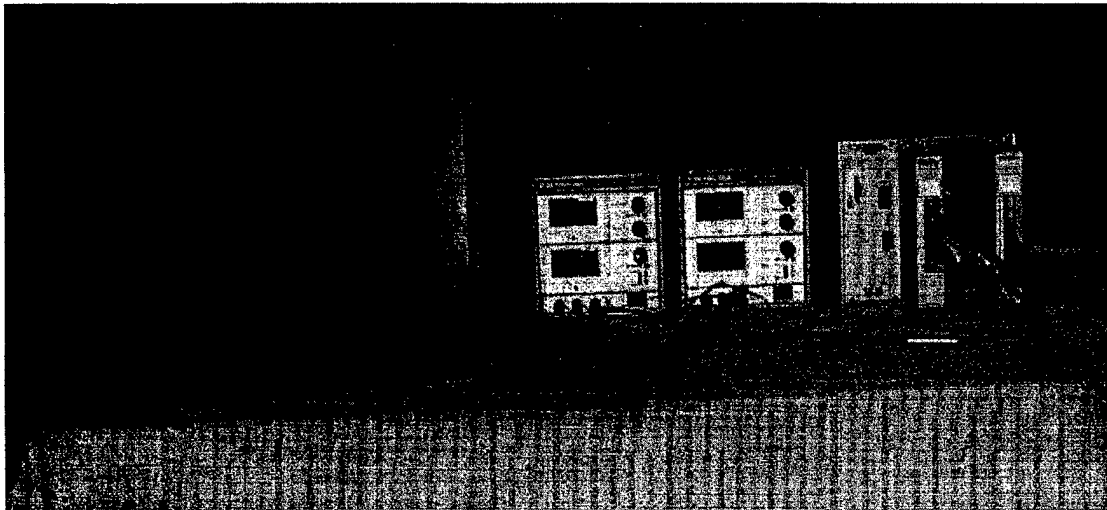
Figure 10.6 Data Acquisition System with Power Supplies and Laptop Computer

10.5 Conduct of Girder Test

Several steps were involved with the conduct of a girder test. A checklist was created as seen in Figure 10.7, which covered all aspects of test set-up and conduct. The checklist was followed for each test and prevented oversights during tests. Data recording sheets were also created and used to collect CSS readings, deflection measurements and other miscellaneous readings during the test.

Testing Checklist for Girder #	Test Configuration #	Date

TEST PREPARATION PERIOD

☐ Position beam on supports – confirm measurements with testing plan

☐ Identify all cylinders for breaking and modulus testing. Record numbers on this sheet

☐ Ensure beam is restrained laterally with chain for end tests. Not required for middle test

☐ Install all instrumentation to include slip gage between beam and deck

☐ Hook-up and test instrumentation

☐ Confirm volunteers to assist during test

ON DAY OF TESTING

☐ Test strength and modulus cylinders and record values on this sheet

☐ Install surge protector at wall for electronics power cord, Connect VWSG reader at midspan

☐ Set-up camera and check for operability. Check tape. Position lights.

☐ Label data sheets, place on clipboard and place on beam with crack marking pen of correct color

☐ Check for free travel of linear pots on prestressing strand

☐ Zero dial gage under point of load application and at beam / slab interface

☐ Check for free travel of wire potentiometer at point of load application

☐ Start EXCEL and bring up strength prediction sheet for test – check max predicted loading, M_{cr}

☐ Start MAX   (Never run MAX and LABVIEW concurrently)
- o   Check for operability of all instrumentation and zero all LVDTs close to below values
- o   LVDT Top (-0.2), LVDT Bot (+0.4), LVDT 0 (0), LVDT 45 (+0.2), LVDT 90 (+0.2)
- o   Close MAX

☐ Start LABVIEW and open Beam Testing VI dated 9 Oct 01. Check for proper operation then close.

☐ Brief assistants and visitors on safety and test procedure

☐ Take initial DEMEC and VWSG readings and record on data sheet

☐ Start LABVIEW and open Beam Testing VI dated 9 Oct 01
- o   Click on WHITE ARROW to START program
- o   At SET-UP tab do the following
  - ▪ Data acquisition rate = 1 reading every 5 seconds
  - ▪ Set Linear POT upper and lower levels (–0.1" – 0.2")
  - ▪ Set SAVE TO FILE to YES
  - ▪ Set LVDT Lengths (Top,Bot = 24", 0,90 = 12", 45 = 16.97")
- o   At NULL COMPENSATION tab do the following
  - ▪ Null all channels EXCEPT the WIRE POT.
  - ▪ Run null on Linear POTs 5 times.
- o   At SET-UP tab do the following
  - ▪ Click on START button – this will kick over to the display screens
  - ▪ Set deflection limits on Wire POT at first tab of display screens (~2.4", 1")
  - ▪ Set deflection limits on LOAD-DEFLECTION display (~2.4", 1")
  - ▪ Check all screens for initial readings and to ensure lines are plotting correctly
  - ▪ Record all initial values in table below.

Load Cell	Top LVDT	Bot LVDT	Wire POT	0 LVDT	45 LVDT	90 LVDT	
Strand 0	Strand 1	Strand 2	Strand 3	Strand 4	Strand 5	Strand 6	Strand 7

- o   Start applying load

☐ At conclusion of test, save data to hard-drive, back-up data on floppy disk and record any notes.

Figure 10.7 Girder Testing Checklist

10.5.1 Loading Sequence

Each girder was loaded monotonically until failure at a load of approximately 400 kips. Loading proceeded in increments of approximately 30 kips or in deflection increments of about 0.25 inches. After each load or deflection increment, CSS readings, deflection readings, crack spacings, and VWSG readings were recorded. Readings were also taken at special occurrences such as first flexural or shear crack observation or initial strand slip.

The decision to terminate loading was based on observed failure characteristics. If crushing in the deck was occurring and total strain in the bottom strands was over 2 percent, the failure was judged a flexural failure and loading was terminated. If shear cracking was extensive and indicative of impending failure, loading was sometimes terminated to prevent further extensive damage. If strand slip over 0.1 inches occurred, the girder was watched closely. Strand slip would allow shear cracks to open and sudden violent shear failures to occur. If the test became a potential safety issue, loading was terminated as well. In a few cases, sudden violent failures occurred.

10.5.2 Concrete Surface Strain Readings

Before loading commenced, CSS readings were taken from the DEMEC gage inserts on the girder-end being tested and at midspan. The girder end readings provided an initial value on which to base CSS readings during the test. The midspan readings were useful in verifying the level of effective prestress before load was applied.

After each load increment, CSS readings were taken on the 48-inch strips located on the bottom flange of the girder end being tested. No CSS readings were taken during center span tests because development length was not considered a problem.

10.5.3 Marking Cracks

After each load increment, any newly formed cracks were marked. At the end of the marked crack, the load at which the crack occurred was marked as well. Close examination of the girder surface was necessary to note all the cracks formed. Figure 10.8 shows the marking of cracks.

10.5.4 Visual and Audio Recording of Test

Each girder test was recorded on video in its entirety and photographed with a digital camera. The video footage allowed review of the test to determine the initiation point of failures. In several instances, violent failures were captured on video. Digital photos allowed easy review of important points of the test.

10.5.5 Conclusion of Test

After load was removed, the girder was repositioned for the next test. If all three tests had been conducted on the girder, it was removed from the frame, photographed and placed back in storage.

Figure 10.8 Marking of Cracks During Girder Test

CHAPTER XI

FLEXURAL BEHAVIOR RESULTS AND DISCUSSION

11.1 Introduction

This chapter discusses flexural behavior in HSLC pretensioned girders. Girder

material and section properties are provided. Based on experimentally measured values

during the 18 girder tests, current code provisions are evaluated.

11.2 Experimental Results

Table 11.1 provides an overview of experimental results listing failure types,

ultimate strain values and moments at cracking and ultimate conditions. The failure types

were classified using the definitions below:

FL - The girder failed by "BOTH" crushing of the deck and yielding of the strands.

SH - The girder failed purely in shear. It did not meet the criteria for a flexural failure.

SH/FL - The girder failed predominantly in shear, but still yielded the strands and

crushed the deck. The two failure states occurred almost simultaneously.

SH-SL - The girder underwent a shear failure initiated by the strands slipping.

FL/SH-SL or **SH-SL/FL** - The girder underwent both failure modes with one occurring

more predominantly than the other. Both failures would result in yielding of the strands

and crushing of the deck.

Table 11.1 Overview of Experimental Results

Test #	Failure Type	Crushing Status of Deck	Cracking Moment M_{cr} (ft-kips)	Ultimate Moment M_{ult} (ft-kips)	Max Deck Strain ε_{cu} (in/in)	Max Strand Strain ε_{ps} (in/in)
G1A-E	FL/SH-SL	Crushed	1224	1836	0.0038	0.0158
G1A-W	FL	Crushed	1109	1844	0.0042	0.0168
G1A-C	SH	Not Crushed	1064	1671	0.0029	0.0086
G1B-E	SH-SL	Not Crushed	1133	1578	0.0033	0.0078
G1B-W	FL	Crushed	1109	1840	0.0032	0.0190
G1B-C	SH/FL	Crushed	1188	1774	0.0039	0.0107
G1C-E	SH-SL/FL	Crushed	1155	1796	0.0032	0.0113
G1C-W	FL	Crushed	1145	1828	0.0036	0.0140
G1C-C	FL	Crushed	1142	1898	0.0049	0.0146
G2A-E	FL	Crushed	1220	1855	0.0036	0.0190
G2A-W	FL	Crushed	1176	1855	0.0072	0.0204
G2A-C	SH	Crushed	1124	1657	0.0086	0.0084
G2B-E	FL	Crushed	1110	1799	0.0082	0.0155
G2B-W	FL	Crushed	1124	1840	0.0064	0.0199
G2B-C	SH/FL	Crushed	1210	1869	0.0035	0.0122
G2C-E	FL	Crushed	1079	1870	0.0045	0.0228
G2C-W	FL	Crushed	1094	1793	0.0049	0.0198
G2C-C	FL	Crushed	1219	1885	0.0089	0.0215

G1 Avg			1141	1785	0.0037	0.0132
G2 Avg			1151	1824	0.0062	0.0177

Although there are five failure types listed in Table 11.1, the failures fell into two major categories; flexural failures and shear failures. Sections 11.2.1 and 11.2.2 provide photos of the failures, typical moment-curvature diagrams, and typical load-displacement diagrams for the two main failure categories.

251

11.2.1 Flexural Failures

Figure 11.1 shows a photo of girder test G1-B West, a typical flexural failure. The vertical lines indicate the location of shear reinforcement. Flexural failures were ductile in nature. A typical flexural failure showed flexural cracks extending from the bottom of the girder up into the deck and evenly spaced shear cracks less than 0.02 inches in width between the support and point of load application.

Spalling of concrete from the top surface was evidence of crushing in the deck. Figure 11.2 provides a picture of deck crushing from test G1B-West. In Figure 11.2, the loading hardware was removed and the crushed concrete chipped from the deck to show the extent of crushing.

Some flexural failures resulted in longitudinal cracking in the deck as shown in Figure 11.3. Since there was only temperature and shrinkage steel running longitudinally in the deck, the occurrence of this cracking was understandable.
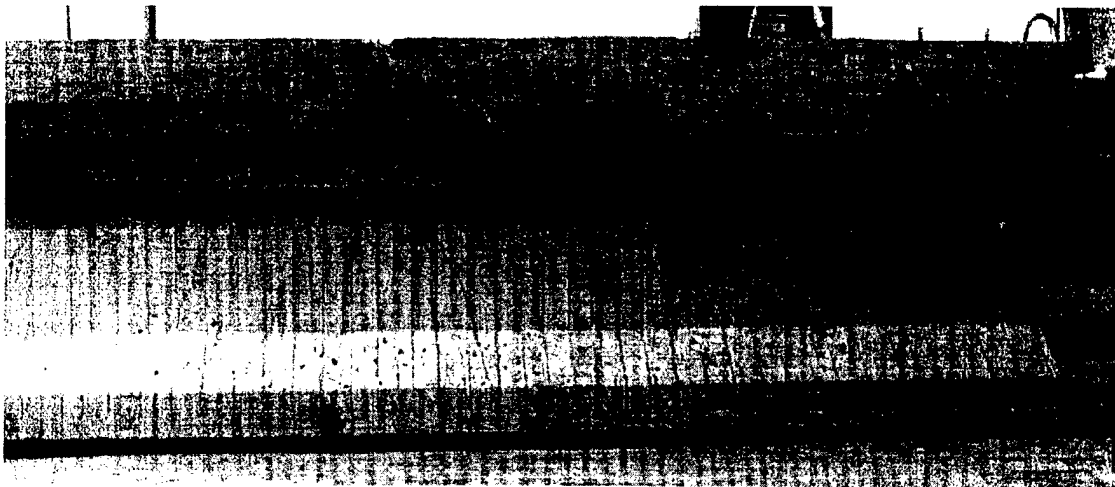
Figure 11.1 Typical Flexural Failure Shown in Girder Test G1B-West
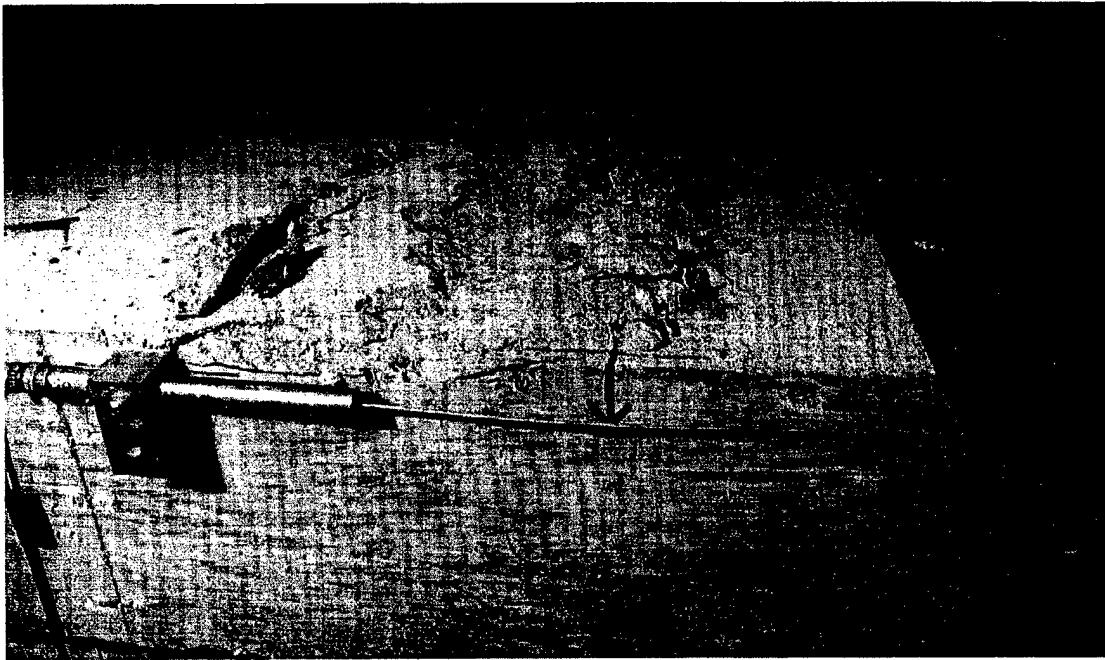
Figure 11.2 Details of Deck Crushing in Girder Test G1B-West
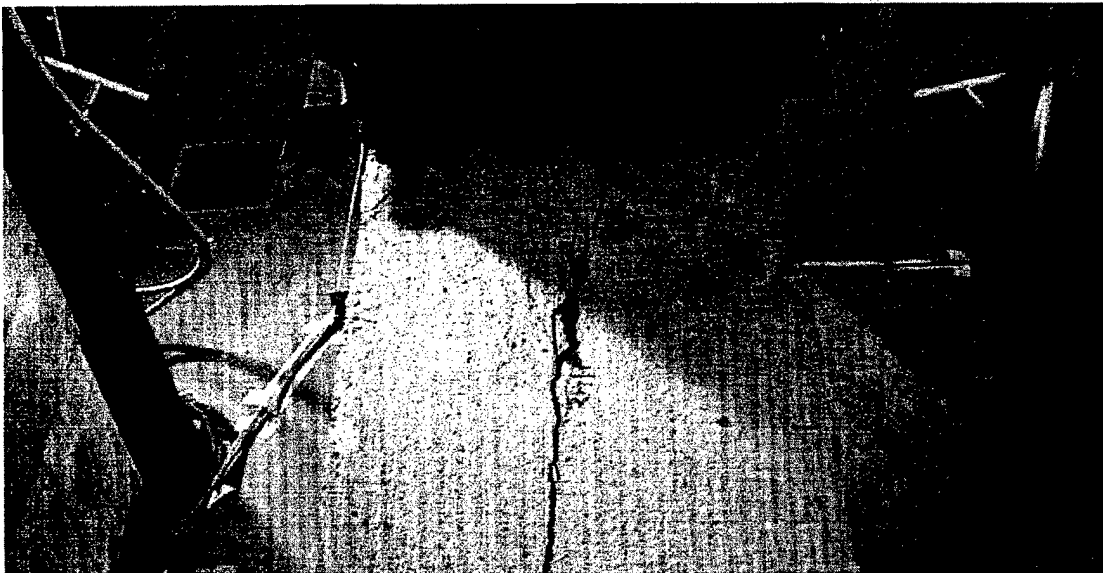
Figure 11.3 Example of Longitudinal Deck Cracking in Girder Test G1A-East

Figure 11.4 provides a typical moment-curvature plot from a flexural failure. This moment-curvature plot from girder test G1B-West shows the theoretical and experimental behavior. The theoretical behavior is slightly offset from the experimental behavior because the girder was assumed to have zero curvature at the initiation of testing. The theoretical curvature value accounted for initial negative curvature due to prestressing where the experimental value did not. Both the theoretical and experimental plots begin at a moment value greater than zero reflecting the initial dead load moment being carried by the girder. The theoretical curve was determined with values at zero applied load, decompression of concrete at the level of the bottom strands, flexural cracking, yielding of the strand, and deck surface strains of 0.001, 0.002 and 0.003. The Construction of the theoretical moment-curvature curve is described in Appendix L.
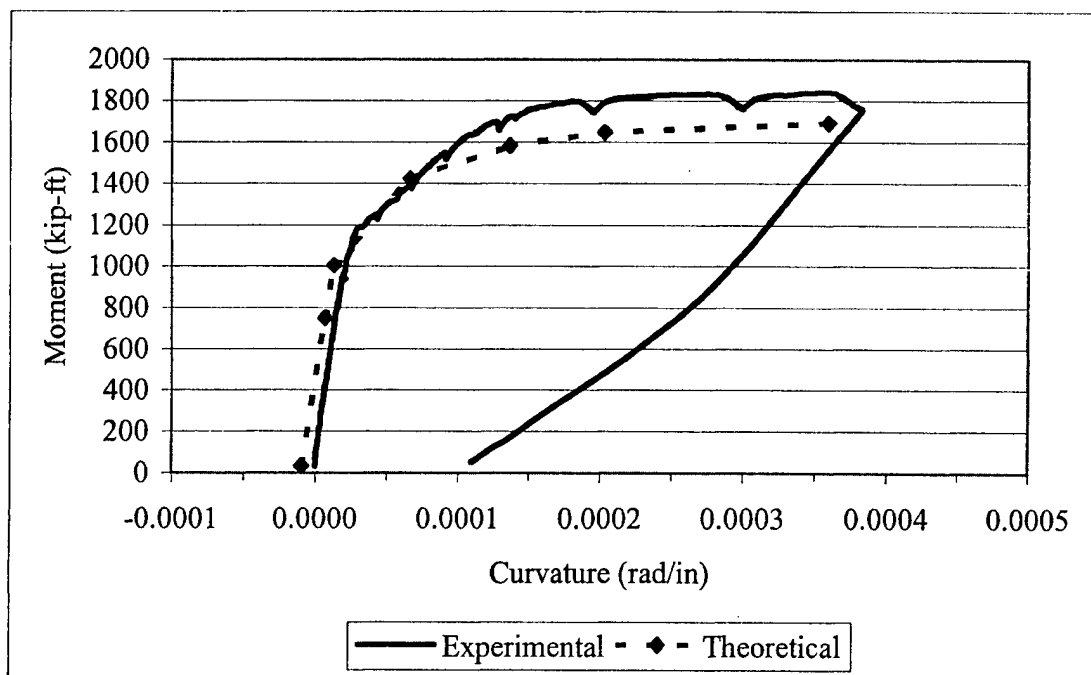
Figure 11.4 Moment-Curvature Plot from Girder Test G1B-West

Figure 11.5 shows the load-displacement curve from girder test G1B-W, a typical

flexural failure. The two points used to describe the predicted curve were based on

deflection at cracking and ultimate. A description of the calculation of predicted

deflection values is also included in Appendix L.
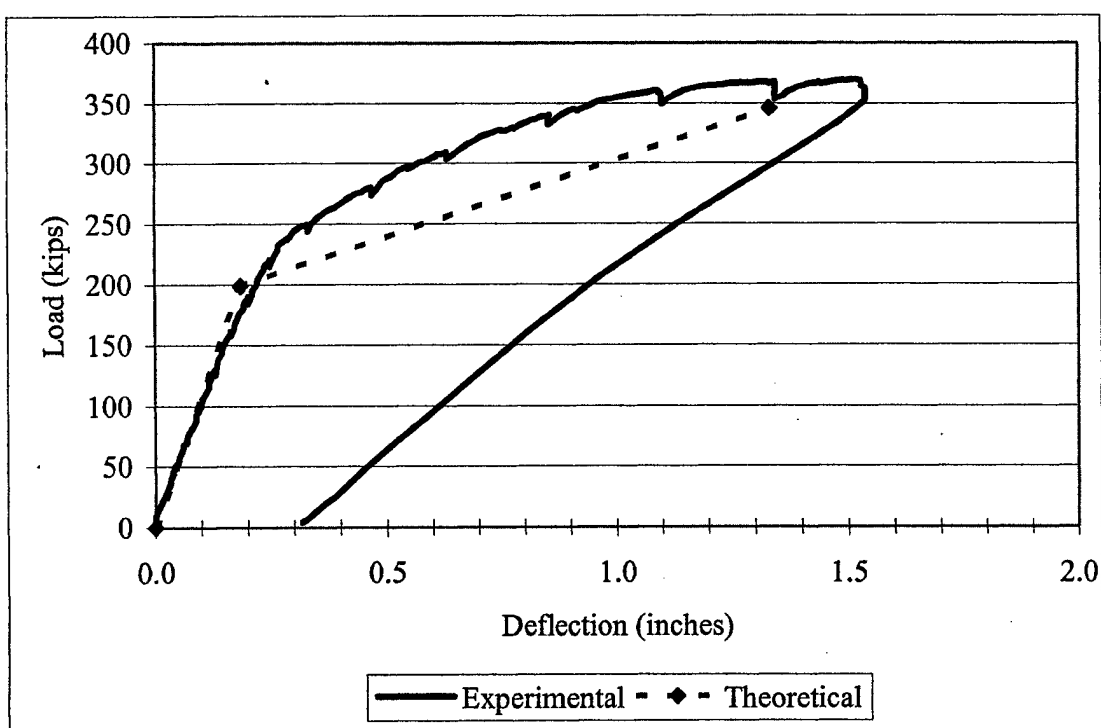
Figure 11.5 Load-Deflection Plot from Girder Test G1B-West

The load-displacement curves for flexural failures normally returned to within a

small deflection from zero reflecting any strand yielding or deck crushing that may have

occurred.

Figures 11.6 and 11.7 show a dramatic flexural failure where a large section of the

deck and top flange separated from the girder. Note the exposed prestressing strand.

Figure 11.6 Flexural Failure During Girder Test G2B-East.

Figure 11.7 Close-up of Girder-Deck Interface in Girder Test G2B-East Flexural Failure

11.2.2 Shear Failures

Within the category of shear failures were included girder tests that failed purely in shear and those that underwent a shear failure initiated by strand slip. In general, the resulting moment-curvature and load-displacement curves were similar. For explanation purposes, the categories were handled separately. A much more in-depth explanation of shear failures is provided in Chapter 12, Shear Behavior Results and Discussion; this section is provided for better understanding of Table 11.1.

11.2.2.1 Pure Shear Failures
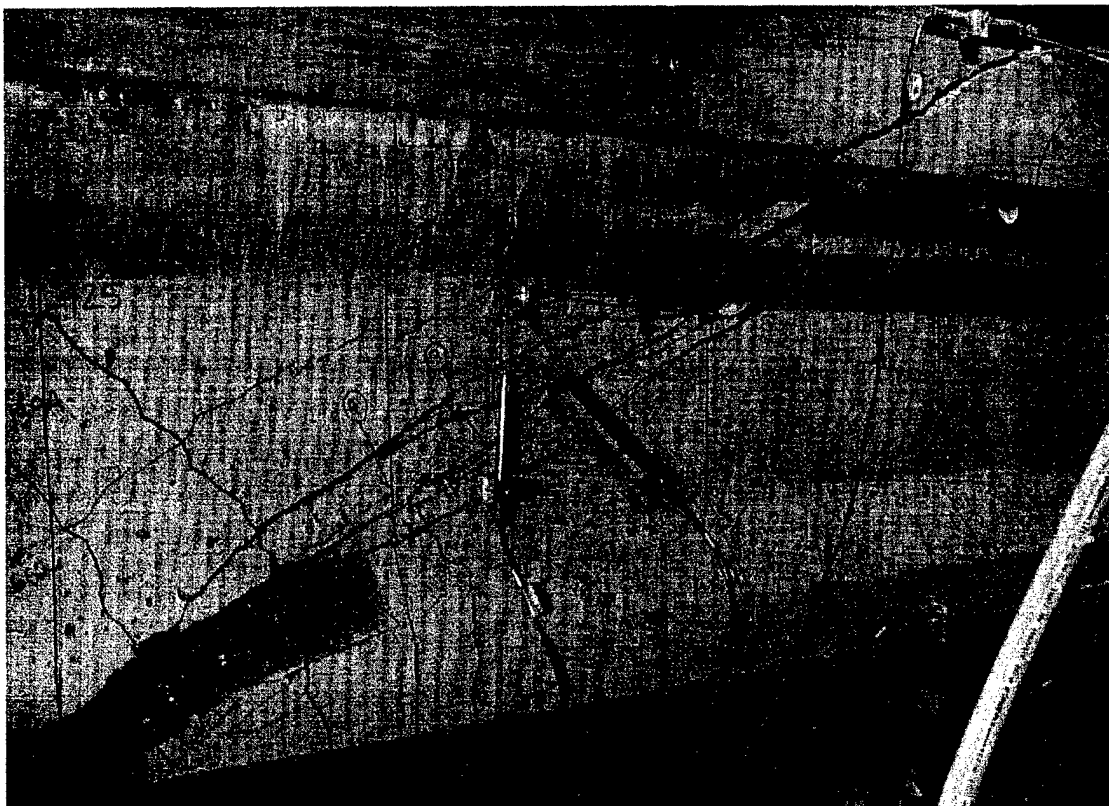
Figure 11.8 Girder Test G2A-Center Showing Pure Shear Failure

257

Girder test G2A-Center seen in Figure 11.6 involved a center span where the shear reinforcement was spaced at 24 inches. The objective of this test was to examine the shear strength of concrete. The shear crack running from bottom to top occurred very suddenly and violently and was indicative of a pure shear failure. Girders undergoing shear failures precipitated by strand slip showed different failure modes. Figure 11.9 shows a typical moment-curvature diagram for a pure shear failure.
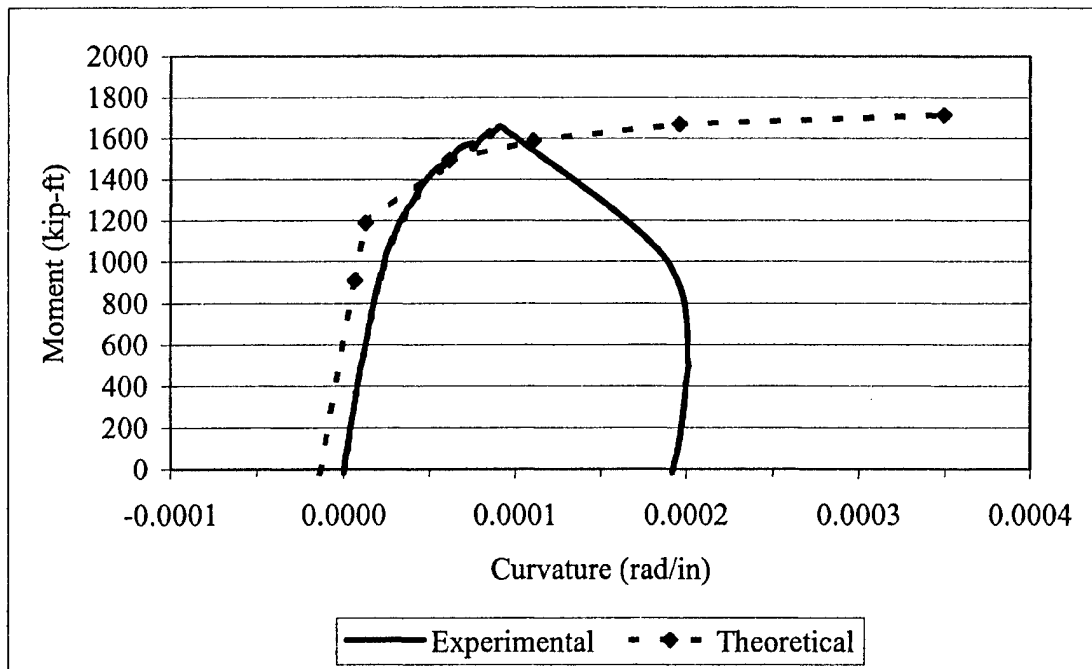
Figure 11.9 Moment-Curvature Plot for Girder Test G2A-Center, a Pure Shear Failure

The sudden shear failure is indicated in Figure 11.9 by the sudden drop on the moment-curvature diagram. Figure 11.10 shows the load-deflection plot for girder test G2A-Center. The same sudden drop in load and increase in deflection is seen.
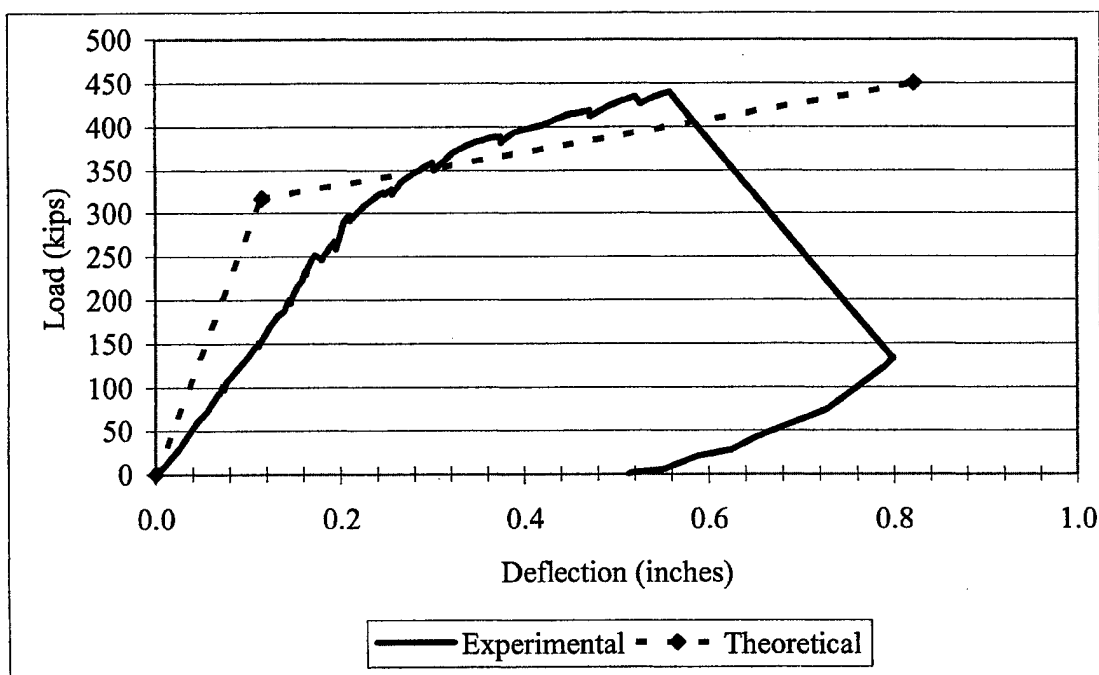
Figure 11.10 Load-Deflection Plot for Girder Test G2A-Center

11.2.2.2 Shear Failures Initiated by Strand Slip

Girders that underwent excessive strand slip experienced shear failures as well. However, the mode of failure appeared somewhat different. Figure 11.11 shows a photo of girder test G1C-East, a test where excessive strand slip resulted in a predominantly shear-based failure. Although the deck crushed and the strand yielded, the failure was dominated by shear. The shear cracking did not extend from bottom to top as in Figure 11.6, but ended prior to entering the deck. Figure 11.12 shows a photo of shear cracking at the bottom of the girder vicinity the support. The shear cracks were approximately 0.2 inches wide at the widest. Figures 11.13 and 11.14 show moment-curvature and load-deflection curves for girder test G1C-East.

259
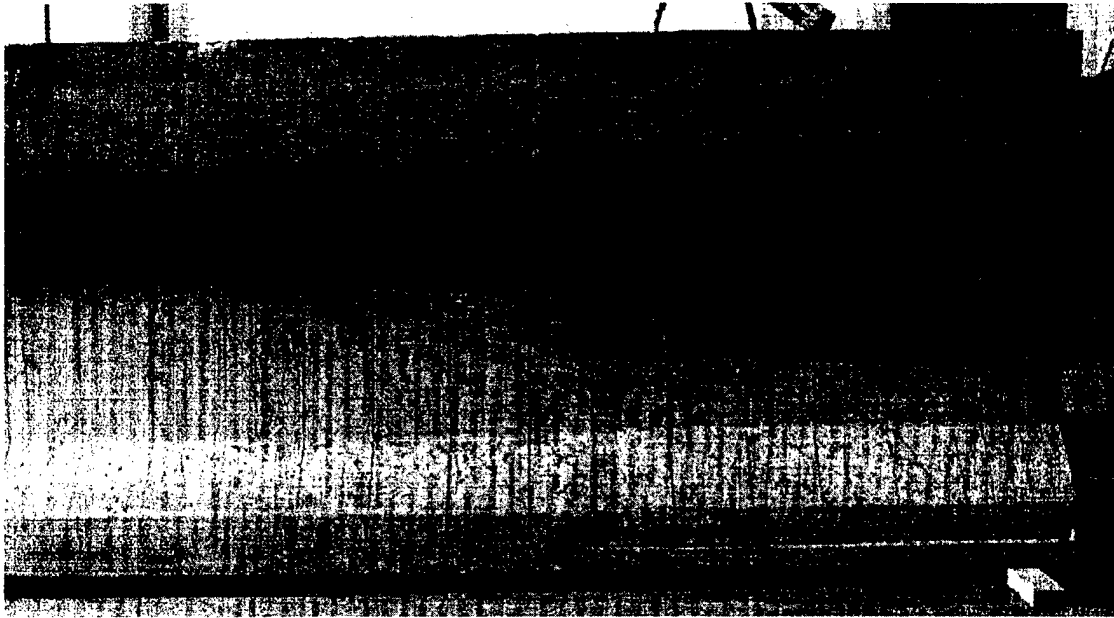
Figure 11.11 Girder Test G1C-East After Strand Slip Induced Shear Failure

Figure 11.12 Girder Test G1C-E Showing 0.2-inch Wide Shear Cracks
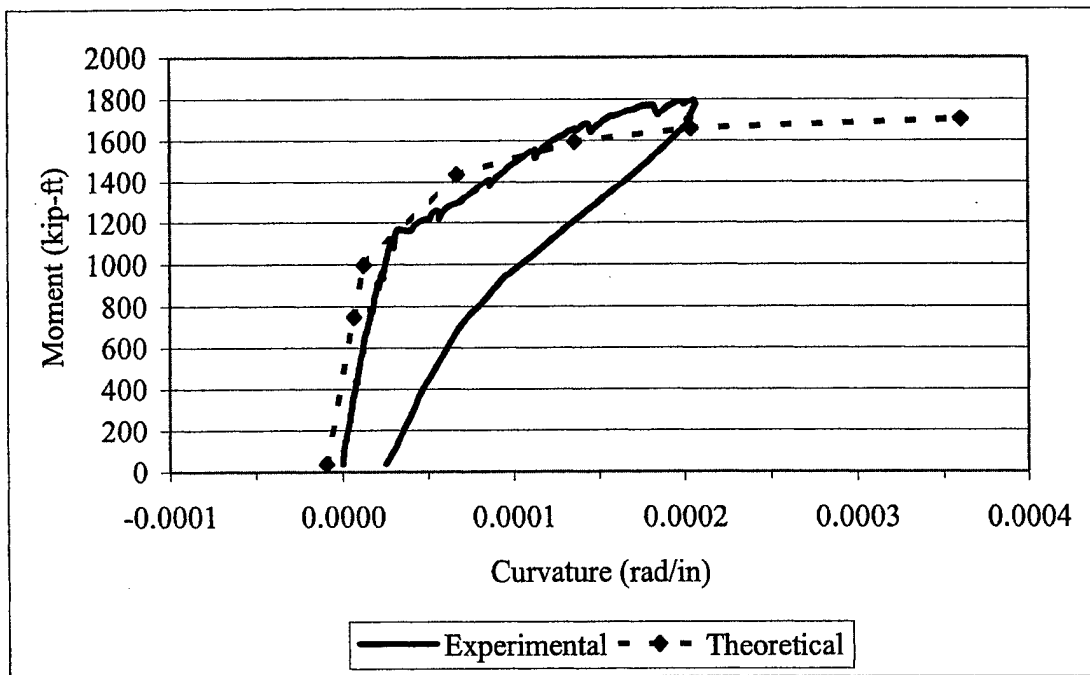
Figure 11.13 Moment-Curvature Plot for Girder Test G1C-East
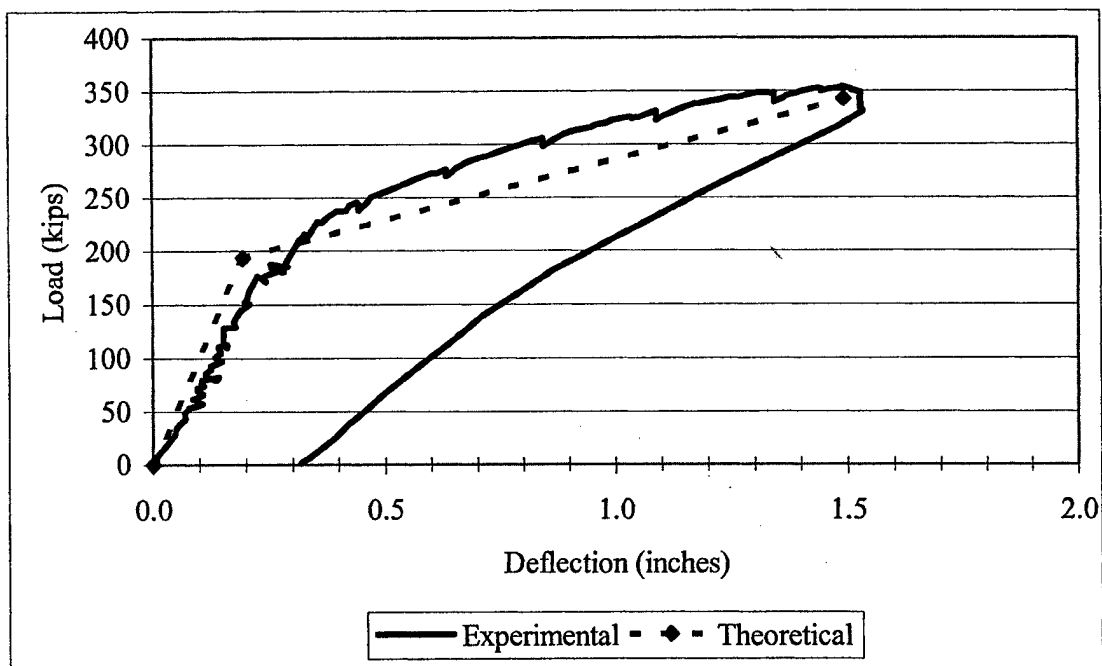
Figure 11.14 Load-Deflection Plot for Girder Test G1C-East

261

Examination of Figures 11.13 and 11.14 show the different behavior of this type

of shear failure compared to the pure shear failure. The shear failure precipitated by

strand slip was a gradual shear failure and not the sudden violent failure seen in pure

shear failures. Figure 11.13 indicates the girder was unable to reach its predicted

curvature value due to strand slip. Figure 11.14 shows that ultimate deflection was close

to predicted, however, it was more the result of shear deformation due to strand slip than

flexural deformation due to strand yielding as predicted. The girder's response to

unloading showed that it experienced some permanent deformation due to strand slip,

strand yielding and deck crushing. Its behavior on unloading more resembled a flexural

failure and did not resemble a pure shear failure.

11.2.3 Comments on Experimental Results

Specific discussion of experimental results was addressed at the cracking and

ultimate conditions in Sections 11.3 and 11.4 respectively. Appendix L provides a

complete listing of all moment-curvature and load-deflection diagrams for each test.

Photos of girder all end-span tests can be seen in Appendix Q. Photos of all center-span

tests can be seen in Appendix M. A spreadsheet encompassing the calculations to

evaluate the girders' flexural performance can be seen in Appendix K. All percent

difference calculations in the following sections are based on equation 11.1 below.

$$Percent\ Difference = \left(\frac{Value_{Exp} - Value_{Pred}}{Value_{Pred}} \right) 100 \qquad (11.1)$$

11.3 Results at Cracking

Table 11.2 provides an overview of the predicted and experimental cracking

moment for each girder test. Percent difference was calculated using equation 11.1.

Table 11.2 Cracking Moment Results

Test #	Predicted M_{cr} (ft-kips)	Experimental M_{cr} (ft-kips)	Percent Difference
G1A-East	1052	1224	16.4%
G1A-West	1005	1109	10.4%
G1A-Center	1065	1064	-0.2%
G1B-East	1019	1133	11.2%
G1B-West	1004	1109	10.4%
G1B-Center	1029	1188	15.5%
G1C-East	999	1155	15.6%
G1C-West	971	1145	17.9%
G1C-Center	1035	1142	10.4%
G2A-East	1165	1220	4.7%
G2A-West	1136	1176	3.5%
G2A-Center	1189	1124	-5.5%
G2B-East	1177	1110	-5.6%
G2B-West	1133	1124	-0.9%
G2B-Center	1200	1210	0.8%
G2C-East	1059	1079	1.9%
G2C-West	1025	1094	6.8%
G2C-Center	1082	1219	12.6%

G1 Average	1020	1141	12.0%
G2 Average	1130	1151	2.0%
G1 Std Dev			5.4%
G2 Std Dev			5.8%

The experimental cracking moment was determined by examining the

experimental load vs. deflection plot identifying the point at which a slope change

263

occurred. In every case, the cracking load indicated on the load vs. deflection plot matched the load recorded where visible flexural cracking first occurred.

Based on the use of equation 11.2, the predicted cracking moment for the G2 series girders was 10.8 percent greater than for G1 girders.

$$f_{cr-Pred} = 7.5\lambda\sqrt{f_c'}$$ (11.2)

Since G2 girders had a higher concrete compressive strength than G1 girders, this was logical. Experimentally, the G1 and G2 series average cracking moments were about identical. It is important to note that the predicted cracking moments appeared to become less conservative as compressive strength increased.

Table 11.3 provides an overview of the predicted cracking stress, $f_{cr-Pred}$, based on equation 11.2, the rupture stress, f_r, recorded during testing of beam specimens per ASTM C-78[82] at an age of 56 days, and the experimental cracking stress, f_{cr-Exp}.

The trend seen in Table 11.3 is the same seen in 11.2 for the cracking moment, except more dramatic. The experimental cracking stress, f_{cr-Exp}, was calculated using equation 11.3 below.

$$f_{cr-Exp} = \frac{M_{cr} - M_{DL}}{S_{bot-c}} + \frac{M_{DL}}{S_{bot-nc}} - \frac{F_{se}}{A_{nc}} + \frac{F_{se}e}{S_{bot-nc}}$$ (11.3)

Table 11.3 Cracking Stress Results

Test #	Predicted $f_{cr\text{-}Pred}$ (psi)	ASTM C-78 f_r (psi)	Experimental $f_{cr\text{-}Exp}$ (psi)	Percent Difference Exp. Vs. Pred.	Percent Difference Exp. vs. ASTM	Normalized Cracking Stress Factor, ξ_{cr}
G1A-East	624	1010	985	57.8%	-2.5%	11.83
G1A-West	624	1010	844	35.3%	-16.4%	10.14
G1A-Center	624	1010	621	-0.5%	-38.6%	7.46
G1B-East	624	1010	863	38.3%	-14.6%	10.37
G1B-West	624	1010	846	35.6%	-16.2%	10.17
G1B-Center	624	1010	964	54.5%	-4.5%	11.59
G1C-East	602	796	930	54.5%	16.8%	11.58
G1C-West	602	796	968	60.8%	21.6%	12.06
G1C-Center	602	796	825	37.1%	3.6%	10.28
G2A-East	668	1204	785	17.5%	-34.8%	8.81
G2A-West	668	1204	752	12.6%	-37.6%	8.44
G2A-Center	668	1204	999	49.6%	-17.0%	11.22
G2B-East	668	1204	528	-20.9%	-56.1%	5.93
G2B-West	668	1204	647	-3.1%	-46.3%	7.27
G2B-Center	668	1204	687	2.9%	-42.9%	7.72
G2C-East	654	905	697	6.6%	-22.9%	8.00
G2C-West	654	905	804	22.9%	-11.2%	9.22
G2C-Center	654	905	946	44.6%	4.5%	10.84

G1 Average	617	939	872	41.5%	-5.6%	10.61
G2 Average	663	1104	761	14.7%	-29.4%	8.61
G1 Std Dev						1.42
G2 Std Dev						1.67

Since all the girders were of approximately the same dimension, the only factors that affected the cracking stress were the experimental cracking moment and the effective prestressing force, F_{se}. In the G2 series girders, the modulus of elasticity was higher at release in comparison to the G1 series girders meaning less initial losses (ES). In addition, the denser matrix of the G2 mix design allowed less time dependent losses (CR and SH). Both factors meant a higher effective prestressing force at time of testing. A

265

higher prestressing force meant more of the cracking moment was required to overcome the effect of prestress thus the cracking stress was less. On average, the experimental cracking stress values for the G1 and G2 series tests were greater than the predicted values. The trend indicates that predicted cracking strengths become less conservative as the compressive strength increases.

The normalized rupture stress factor, ξ_{cr}, was calculated as below where λ was the lightweight concrete factor equal to 0.85 for SLWC:

$$\xi_{cr} = \frac{f_{cr-Exp}}{\lambda\sqrt{f'_c}} \tag{11.4}$$

As long as the factor ξ_{cr} was greater than 6, the predicted value was conservative. On average, both the G1 and G2 series were conservative. However, girder test G2B-East had a normalized value less than 6. There were no common trends between the girders that explained the lower cracking stress values. Figure 11.15 provides a plot of the normalized cracking stress factor, ξ_{cr}, vs. concrete compressive strength, f_c', showing the downward trend as compressive strength increased. Also plotted on Figure 11.15 for comparison were the normalized values based on modulus of rupture test results again showing the modulus of rupture, f_r, to be a poor predictor of cracking stress.

Comparison of the experimental cracking strengths with modulus of rupture strengths, f_r, determined with the ASTM[82] beam test showed it to be an unconservative

predictor of cracking strength. This finding also was reported by Dill for high-strength

normal weight concrete.[84]
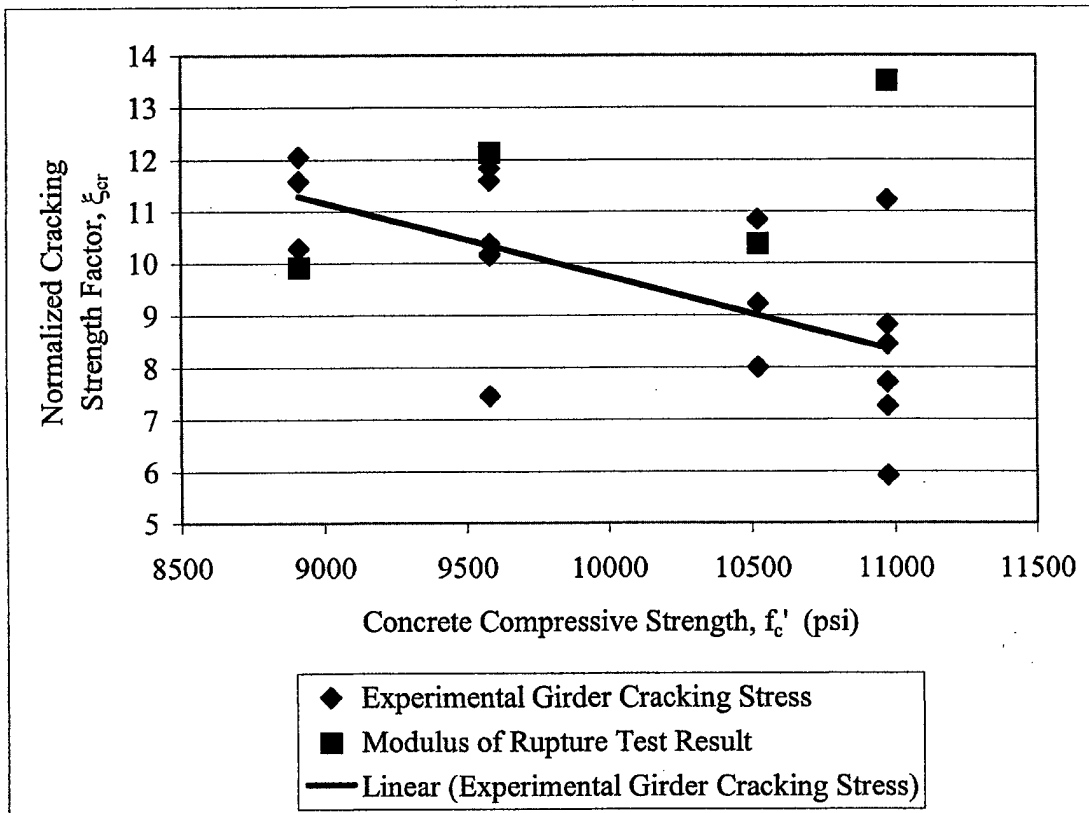
Figure 11.15 Normalized Rupture Strength Factor, ξ_{cr} vs. Compressive Strength, f_c'

Table 11.4 provides an overview of predicted and experimental deflections at

cracking. The experimental deflections at cracking were from 16 to 145 percent greater

for the G1 series girders and 17 to 96 percent greater for the G2 series girders. Some of

this error was due to material properties of the girders. Despite having made numerous

specimens, localized variations in the concrete could impact the cracking deflection. In

addition, minor errors in identifying the cracking deflection may have occurred. While

267

exact visual determination of initial flexural cracking was sometimes difficult, close

examination of data acquisition system output allowed its identification with good

accuracy. Since the gage length of the LVDTs measuring strain at the bottom of the

girder spanned 24 inches, initial flexural cracking almost always occurred somewhere in

that region. When flexural cracking was first visually noted, the load at which it occurred

was noted. In all cases but one, the visually noted cracking load matched the cracking

load identified from the test output.

Table 11.4 Deflection Results at Cracking

Test #	Predicted Deflection δ_{cr} (inches)	Experimental Deflection δ_{cr} (inches)	Percent Difference Predicted vs. Exp.
G1A-East	0.154	0.270	75.3%
G1A-West	0.267	0.330	23.6%
G1A-Center	0.106	0.260	145.3%
G1B-East	0.208	0.312	50.0%
G1B-West	0.185	0.250	35.1%
G1B-Center	0.123	0.230	87.0%
G1C-East	0.194	0.352	81.4%
G1C-West	0.273	0.441	61.5%
G1C-Center	0.149	0.173	16.1%
G2A-East	0.168	0.303	80.4%
G2A-West	0.294	0.344	17.0%
G2A-Center	0.115	0.220	91.3%
G2B-East	0.170	0.216	27.1%
G2B-West	0.265	0.312	17.7%
G2B-Center	0.134	0.210	56.7%
G2C-East	0.194	0.255	31.4%
G2C-West	0.279	0.357	28.0%
G2C-Center	0.148	0.290	95.9%

G1 Average		63.9%
G2 Average		49.5%
G1 Std Dev		39.6%
G2 Std Dev		32.1%

11.4 Results at Ultimate

Table 11.5 provides an overview of the ultimate moment predicted by the AASHTO[40] technique utilizing the rectangular stress block, the ultimate moment predicted by a cracked section analysis using a Todeschini[91] stress block, and the experimental ultimate moment.

Table 11.5 Moment Results at Ultimate

Test #	Predicted M_{ult} AASHTO[40] (ft-kips)	Predicted M_{ult} Todeschini[91] (ft-kips)	Exp. M_{ult} (ft-kips)	Percent Difference Exp. vs. AASHTO[40]	Percent Difference Exp. vs. Todeschini[91]
G1A-East	1719	1721	1836	6.8%	6.7%
G1A-West	1704	1707	1844	8.2%	8.0%
G1A-Center *	1711	1713	1671	-2.3%	-2.5%
G1B-East *	1716	1717	1578	-8.0%	-8.1%
G1B-West	1691	1692	1840	8.9%	8.8%
G1B-Center *	1687	1689	1774	5.2%	5.1%
G1C-East *	1705	1705	1796	5.3%	5.3%
G1C-West	1710	1710	1828	6.9%	6.9%
G1C-Center	1726	1726	1898	10.0%	10.0%
G2A-East	1693	1705	1855	9.6%	8.8%
G2A-West	1711	1717	1855	8.4%	8.0%
G2A-Center *	1707	1714	1657	-3.0%	-3.4%
G2B-East	1707	1718	1799	5.4%	4.7%
G2B-West	1699	1707	1840	8.3%	7.8%
G2B-Center *	1727	1733	1869	8.2%	7.8%
G2C-East	1708	1713	1870	9.5%	9.2%
G2C-West	1679	1688	1793	6.8%	6.2%
G2C-Center	1716	1720	1885	9.8%	9.6%

G1 Average	8.16	8.06
G2 Average	8.25	7.75
G1 Std Dev	1.35	1.37
G2 Std Dev	1.63	1.75

* Failed predominantly in shear. Not included in average or standard deviation.

As noted in Table 11.5, ultimate moment results for girders failing predominantly in shear were not included in the statistical values. On average, the two techniques produced very similar results. The Todeschini[91] stress block provided very slightly closer results. Both techniques produced conservative predictions of ultimate moment.

Table 11.6 provides an overview of deflection at ultimate.

Table 11.6 Deflections at Ultimate

Test #	Predicted Deflection δ_{ult} (inches)	Experimental Deflection δ_{ult} (inches)	Percent Difference Exp. vs. Predicted
G1A-East	1.394	1.245	-10.7%
G1A-West	2.067	2.416	16.9%
G1A-Center	0.900	0.625	-30.6%
G1B-East	1.508	1.350	-10.5%
G1B-West	1.331	1.539	15.6%
G1B-Center	1.067	1.122	5.2%
G1C-East	1.492	1.534	2.8%
G1C-West	2.332	2.270	-2.7%
G1C-Center	1.472	1.550	5.3%
G2A-East	1.262	1.428	13.2%
G2A-West	1.902	2.566	34.9%
G2A-Center	0.821	0.799	-2.7%
G2B-East	1.283	1.205	-6.1%
G2B-West	1.584	2.060	30.1%
G2B-Center	0.954	0.982	2.9%
G2C-East	1.330	1.891	42.2%
G2C-West	2.065	2.208	6.9%
G2C-Center	1.373	2.170	58.0%

G1 Average	-1.0%
G2 Average	19.9%
G1 Std Dev	14.7%
G2 Std Dev	22.3%

On average, the G1 series girders deflected 1 percent less than predicted. The G2 girders deflected 19.9 percent more than predicted on average. The reason for this variation was how far the girders were pushed during testing. The G1 girders were tested first and were not pushed to as high of strain levels as the G2 girders. As the test program proceeded, there was an increasing effort to push the girders such that the total strain in the prestressing strands approached or exceeded 2 percent. Overall, the ultimate deflection predictions matched experimental values well.

11.5 Conclusions

The current prediction for cracking strength when examined for HSLC showed indications of becoming unconservative as concrete compressive strengths approached 11,000 psi. In some cases, the predicted cracking strengths exceeded the experimental values. The use of a lambda factor of 0.85 for HSLC made with slate aggregate produced conservative results on average for compressive strengths below 11,000 psi. More research is required to examine a potential tension strength ceiling for HSLC and to examine the lambda factor for use with HSLC over 10,000 psi compressive strength.

The modulus of rupture test, ASTM C-78, did not accurately predict cracking strength of HSLC girders.

The current AASHTO procedure for ultimate moment calculation was conservative for HSLC girders with normal weight concrete decks having a compressive strength under 6,000 psi.

271

CHAPTER XII

SHEAR BEHAVIOR RESULTS AND DISCUSSION

12.1 Introduction

This chapter discusses shear behavior in the HSLC pretensioned girders. Based on experimentally measured values during testing, current code provisions were evaluated.

12.2 AASHTO 1996 Standard Shear Design Approach

The following sections outline the process for calculating the strength of the concrete, V_c, and strength of the steel reinforcement, V_s, based on the 1996 AASHTO Standard Specification for Highway Bridges.[40]

12.2.1 Concrete Strength, V_c

The concrete strength, V_c, is the lesser of the flexure shear strength, V_{ci}, and the web shear strength, V_{cw}. Based on the shear spans and characteristics of the girders in this research, the web shear strength, V_{cw}, was always the governing value. The calculation of both values is explained further in the following sections.

12.2.1.1 Flexure Shear Strength, V_{ci}

The flexure shear strength was calculated using AASHTO[40] equation (9-27):

$$V_{ci} = 0.6\lambda \frac{\sqrt{f_c'}}{1000} b'd + V_d + \frac{V_i M_{cr}}{M_{max}} \geq 1.7\lambda \frac{\sqrt{f_c'}}{1000} b'd \qquad (12.1)$$

The value b' was taken as the minimum web thickness of the girder which was 6 inches

for an AASHTO Type II. The code specifies that d, the distance from the topmost

compression fiber to the centroid of the prestressing strands need not be less than 0.8*h.

The value of d normally exceeded the minimum 0.8*h. V_i and M_{max} were the maximum

moment and shear at the section in question. The lightweight concrete factor, λ, having a

value of 0.85 was included in the equation based on the use of HSLC. The concrete

strength f_c' was listed in psi. Calculation of the cracking moment was accomplished with

AASHTO equation (9-28):

$$M_{cr} = \frac{I}{Y_t} (6\lambda \frac{\sqrt{f_c'}}{1000} + f_{pe} - f_d) \qquad (12.2)$$

The composite section properties were used in calculating M_{cr}. The concrete strength, f_c',

was based on cylinder tests at the time of girder testing.

12.2.1.2 Web Shear Strength, V_{cw}

The web shear strength was calculated using AASHTO[40] equation (9-29):

$$V_{cw} = (3.5\lambda \frac{\sqrt{f_c'}}{1000} + 0.3 f_{pc})b'd + V_p \qquad (12.3)$$

273

In the girders tested, there were no draped strands thus V_p was zero. The value f_{pc} accounted for the effect of prestress and the dead load of the girder alone at the centroid of the composite section. It was calculated as shown in equation 12.4 below:

$$f_{pc} = \frac{F_{se}}{A_{nc}} - \frac{F_{se}e(y_{bot-c} - y_{bot-nc})}{I_{nc}} - \frac{M_{DL}(y_{bot-c} - y_{bot-nc})}{I_{nc}} \tag{12.4}$$

The effective prestressing force was reduced when the section being examined was inside a distance equal to the transfer length from the end of the girder. The procedure also accounted for the reduced effective prestressing force in calculating f_{pc}. The λ factor equal to 0.85 was included to account for the use of HSLC.

12.2.2 Transverse Steel Shear Strength, V_s

The transverse steel shear strength was calculated using AASHTO[40] equation (9-30):

$$V_s = \frac{A_v f_y d}{s} \leq 8 \frac{\sqrt{f_c'}}{1000} b'd \tag{12.5}$$

For the girders tested, the shear area, A_v, was 0.4 in^2 for double # 4 bar stirrups. The value "s" was the spacing of the stirrups, which was 3.5 inches for the double density stirrups, 7" for single density stirrups and 24" for minimum stirrup spacing. The yield

strength of the stirrups was 62 ksi as determined experimentally. Refer to Appendix C

for more information on the material properties of the shear reinforcement.

12.2.3 Nominal Shear Strength, V_n

The nominal shear strength was calculated as:

$$V_n = V_c + V_s \tag{12.6}$$

12.3 ACI Alternate Approach for Calculating V_{cw}

ACI 11.4.2.2 provides an alternate technique for calculating V_{cw} that was

investigated in this evaluation.[2] The ACI Code states that V_{cw} shall be computed as the

shear force corresponding to dead load plus live load that results in a principal tension

stress of $4\lambda(f_c')^{1/2}$ at the centroidal axis of the member. In composite members, the

principal tensile stress is computed using the cross section that resists live load. Lin and

Burns[50] addressed this alternate technique and provided the following equations which

come directly from the application of Mohr's circle:

$$V_{cw-Pred} = f_{t-Pred}'' \sqrt{1 + \frac{f_{pc}}{f_{t-Pred}''}} \, bd_p \tag{12.7}$$

The predicted diagonal tensile strength, f_{t-Pred}'' was calculated using equation 12.8:

$$f_{t-Pred}^{"} = 4\lambda\sqrt{f_c'} \qquad (12.8)$$

The value of f_{pc} was calculated using equation 12.4 based on conditions at the midpoint of the shear span.

The experimental cracking load, V_{cw-Exp} was recorded when the first shear cracking occurred during the girder test. Based on V_{cw-Exp}, the experimental diagonal tensile strength, $f_t^{"}{}_{-Exp}$ was calculated using equation 12.9.

$$f_{t-Exp}^{"} = \sqrt{\left(\frac{V_{cw-Exp}}{bd_p}\right)^2 + \left(\frac{f_{pc}}{2}\right)^2} - \frac{f_{pc}}{2} \qquad (12.9)$$

The $f_t^{"}{}_{-EXP}$ value was then normalized using equation 12.10.

$$\xi_t = \frac{f_{t-Exp}^{"}}{\lambda\sqrt{f_c'}} \qquad (12.10)$$

A normalized value, ξ_t, less than 4 was an indication that equation 12.8 provided an unconservative prediction of the tensile stress at which initial web shear cracking occurred.

12.4 1998 AASHTO LRFD Shear Design Approach

The following sections outline the process for calculating the shear strength using

the 1998 AASHTO LRFD Specification for Highway Bridges.[92]

12.4.1 Concrete Strength, V_c

The LRFD approach for strength calculation is much different than the Standard

procedure. The first step was to calculate the effective shear depth, d_v, using equation

12.11.

$$d_v = d_p - \frac{a}{2}$$

(12.11)

The value "a" was the depth of the rectangular stress block required to balance the

prestress force at the particular section of interest.

The effective web width, b_v, was taken as the web width of the AASHTO Type II

girder, 6 inches.

The effective area of prestress, A_{pse}, was calculated by determining the effective

number of strands on the flexural tension side of the member. The flexural tension side

of the member indicated the bottom half of the composite member. If the distance "x"

from the free end of the member to the girder section being evaluated was less than the

experimental development length, the total number of bottom strands, 8, was multiplied

by x/l_d. If the section being evaluated was greater than l_d from the free end of the

member, the effective number of strands was the total number, 8. The effective number

of strands was then multiplied by the area of a prestressing strand, 0.2183 in^2, to

determine A_{psc}.

The shear stress on the concrete was calculated using AASHTO equation

(5.8.3.4.2-1):

$$v = \frac{V_u - \phi V_p}{\phi b_v d_v}$$ (12.12)

Since there were no draped strands in these girders, V_p was zero. The resistance factor

for shear, ϕ, was taken as 1.0 since the nominal stress was desired. The value v/f_c' was

then calculated.

In order to use the modified compression field theory from the AASHTO[92] LRFD

Specification, the angle of inclination of diagonal compressive stress, θ, was required.

To determine θ, crack angles were measured at the mid-point of the shear span as listed

in Table 12.1.

The strain in the tensile reinforcement on the flexural tension side, ε_x, was then

calculated using AASHTO equation (5.8.3.4.2-2):

$$\varepsilon_x = \frac{\dfrac{M_u}{d_v} + 0.5 N_u + 0.5 V_u \cot\theta - A_{ps} f_{po}}{E_s A_s + E_p A_{ps}} \leq 0.002$$ (12.13)

Table 12.1 Measured Crack Angles

Test #	Measured Crack Angle (degrees CCW from Horizontal)
G1A-East	31.0
G1A-West	25.0
G1A-Center	25.0
G1B-East	32.0
G1B-West	38.0
G1B-Center	25.0
G1C-East	30.0
G1C-West	30.0
G1C-Center	25.0
G2A-East	38.0
G2A-West	34.0
G2A-Center	33.0
G2B-East	35.0
G2B-West	33.0
G2B-Center	26.0
G2C-East	27.0
G2C-West	30.0
G2C-Center	33.0

Since there was no non-prestressed flexural reinforcement in the test girders and no axial load, equation 12.13 simplified to equation 12.14 as below:

$$\varepsilon_x = \frac{\dfrac{M_u}{d_v} + 0.5V_u \cot\theta - A_{ps}f_{po}}{E_p A_{ps}} \leq 0.002 \qquad (12.14)$$

The value f_{po}, the stress in the prestressing strand when the stress in the surrounding concrete is zero was conservatively taken as the effective prestress, f_{se}. A correction factor specified by AASHTO equation (5.8.3.4.2-3) was included in the event ε_x was

279

calculated as a negative number. Since the strain in the strand at effective prestress was 0.005 in/in at a minimum outside the transfer length region, the only point along the strand ε_x could ever approach a value less than 0.002 would be within approximately 12 inches from the free end of the girder.

Using the value v/f$_c$' and ε_x, a β value was determined from AASHTO Figure 5.8.3.4.2-1. The concrete shear strength, V$_c$ was calculated using AASHTO equation (5.8.3.3-3) below. The equation was modified to reflect the inclusion of the lightweight concrete factor, λ.

$$V_c = 0.0316\lambda\beta\sqrt{f_c'}b_v d_v \tag{12.15}$$

12.4.2 Transverse Steel Shear Strength, V$_s$

The strength of the shear reinforcing steel was calculated with AASHTO equation (C5.8.3.3-1):

$$V_s = \frac{A_v f_y d_v \cot\theta}{s} \tag{12.16}$$

The abbreviated version of the equation for V$_s$ was used because the shear stirrups were placed vertically.

12.4.3 Nominal Shear Strength, V_n

The nominal shear strength of the girder was then calculated using AASHTO

equations (5.8.3.3-1) and (5.8.3.3-2) combined below:

$$V_n = V_c + V_s \leq 0.25 f_c' b_v d_v \qquad (12.17)$$

12.5 Variable Angle Truss Model

The variable angle truss model (VATM) was used as an analysis tool for two

reasons. First, on the girder end tests where strand slip occurred, it was desired to

determine the force in the bottom strands near the girder end. Knowing the force in the

bottom strands, the bond stress could be estimated and compared to values calculated at

transfer, and to values calculated for girders not experiencing strand slip.

The VATM assumes that the girder experiences shear and flexural failure

simultaneously. The stirrups resist the entire shear force and are assumed to be at yield.

The concrete is assumed to resist zero shear force. The model is addressed in *Prestressed

Concrete Structures*, Michael P. Collins and Denis Mitchell.[48]

12.5.1 Shear Force

V_{ult} was equal to the support reaction at the support closest to the applied load.
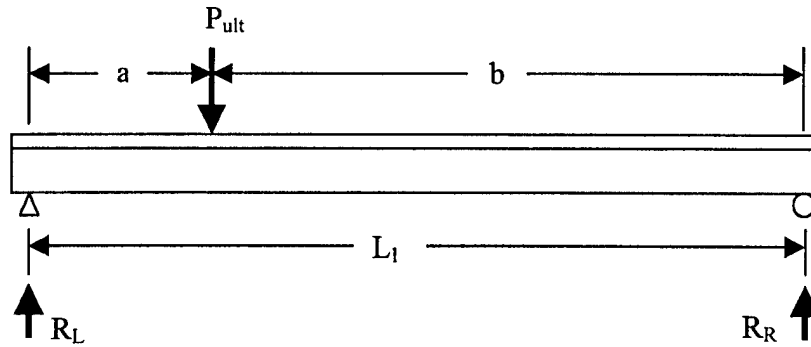
Figure 12.1 Figure for Calculation of V_{ult}

V_{ult} was calculated based on Figure 12.1 and equation 12.18.

$$V_{ult} = R_L = R_{L-self\,wt} + P_{ult} \frac{b}{L_1} \tag{12.18}$$

12.5.2 Stirrup Force

The force in the shear stirrups, $F_{stirrup}$, was calculated using equation 12.19.

$$F_{stirrup} = A_v f_y \tag{12.19}$$

12.5.3 Stirrups Required to Carry V_{ult}

The number of stirrups required, #$_{stirrups}$, to carry V_{ult} was calculated with equation 12.18.

$$\#_{Stirrups} = \frac{V_{ult}}{F_{stirrup}} \qquad (12.20)$$

The number of stirrups calculated determined the number of compression struts beginning at the applied load and carrying force to the intersection of stirrups with the centroid of the prestressing strands. In addition, the number of stirrups required indirectly determined the angle of the compression field. In general, the more stirrups required to carry V_{ult}, the shallower the compression field angle was to the horizontal. The same number of compression struts initiating at the applied load would also end at the support. The connecting pieces between the compression struts are the shear stirrups.

When configuring the VATM, the maximum angle a strut could make with the horizontal was 70 degrees and the minimum was 25 degrees. This limited the number of struts and stirrups that could carry shear force in the truss. It was possible that insufficient stirrups were available in the angle range from 25 to 70 degrees to carry V_{ult}. In this case, the predicted shear capacity of the girder could be limited by the VATM to a level well below that reached during testing. Girder test G1C-West was an example of this type of test. The VATM predicted a much lower shear capacity than the girder achieved. Figure 12.2 provides a diagram of the VATM for girder test G1C-West. The

critical point on the VATM was at a distance equal to the transfer length, l_t, from the

girder free end as labeled in Figure 12.2.

Stirrup Spacing = 7"
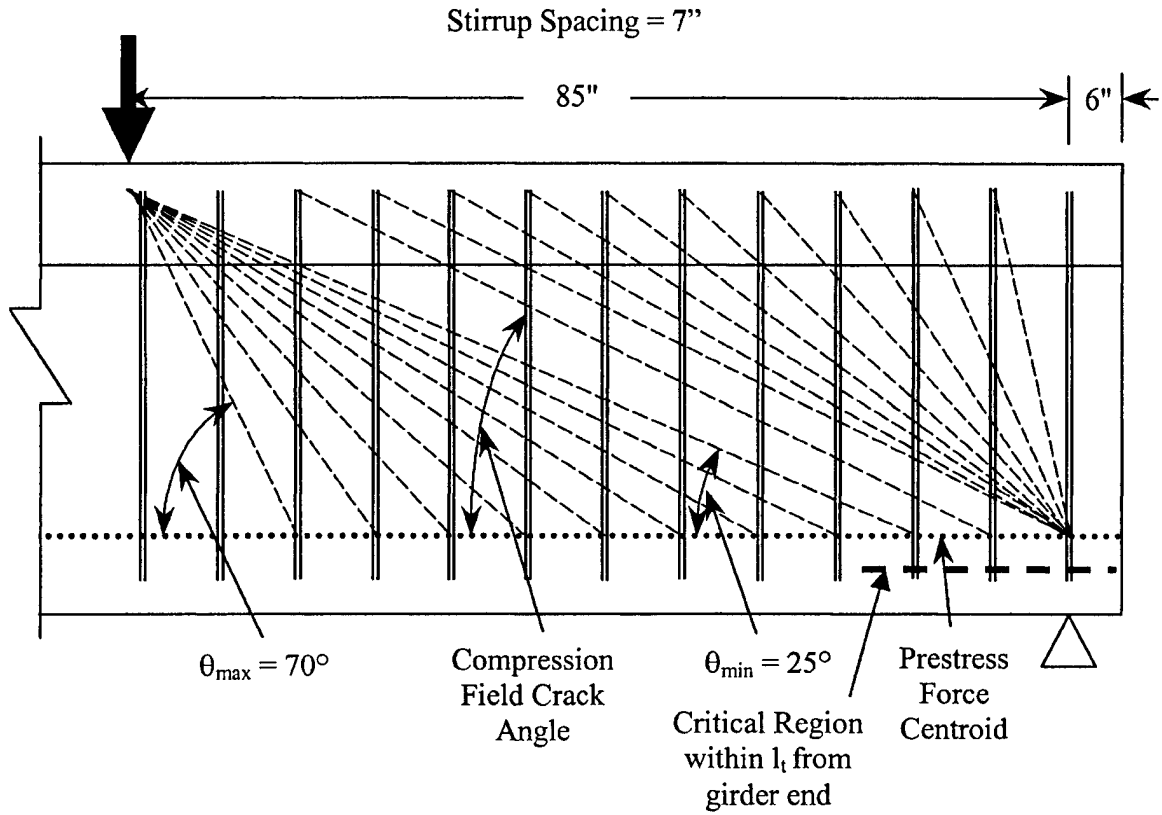
Figure 12.2 Variable Angle Truss Model for Girder Test G1C-West

12.5.4 Internal Moment Arm

The internal moment arm, jd, was calculated using equation 12.21.

$$jd = d_p - \frac{a}{2}$$

(12.21)

12.5.5 Force in Strands at Point of Loading

Since the VATM assumes the girder to be at flexural and shear failure simultaneously, the strands must be near failure. The values f_{su}^* and f_{se} were assumed as the stress in the bottom and top strands respectively. The total strand force at the point of loading was be $(f_{su}^* * 8$ strands $+ f_{se} * 2$ strands$) * 0.2183$ in^2. This strand force was assumed to act at the prestress force centroid labeled in Figure 12.2.

12.5.6 Strand Force Reduction

At each intersection of the strand force centroid with a stirrup, some of the strand force was removed and carried by truss action to the support. Equation 12.22 was used to determine the strand force reduction.

$$F_{Reduction} = \frac{x}{jd} F_{stirrup} \qquad (12.22)$$

The value x indicated the distance the stirrup was from the point of loading. As the distance x increases, the amount of reduction in the strands increases also. Figure 12.3 provides a typical plot of the strand force reduction from the point of loading to the support.
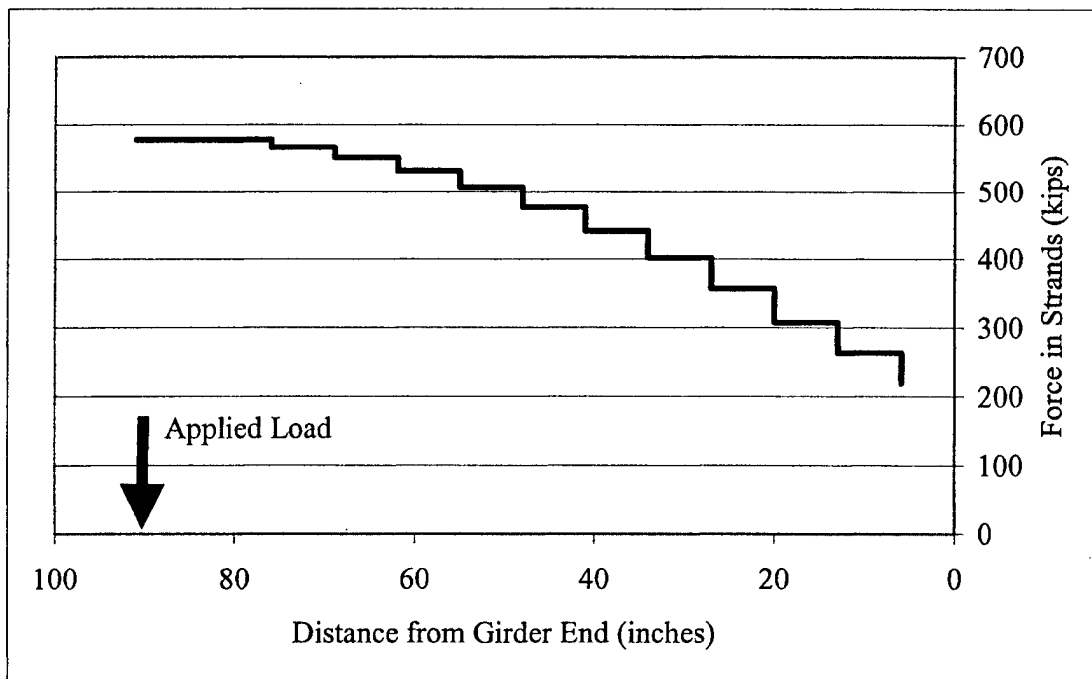
Figure 12.3 VATM Strand Force Reduction Plot for Girder Test G1C-West

12.5.7 Compression Field Crack Angle

The compression field crack angle is labeled in Figure 12.2. In the case of girder test G1C-West, the compression field crack angle was based on the angle of a "carryover strut." A carryover strut is one that neither begins at the point of loading nor ends at the support. If there is no carryover strut, the compression field crack angle will be the angle of the strut originating from the point of loading with smallest angle to the horizontal.

12.5.8 Strand Bond Stress

Strand bond stress was calculated based on the force remaining in the strand, F_{strand}, the length of embedment at the point, l_e, and the nominal circumference, πd_b, of the strand using equation 12.23 below.

286

$$f_{bond} = \frac{F_{strand}}{l_e \pi d_b}$$ (12.23)

A plot of bond stress from the point of loading to the support shows how the bond stress dramatically increases near the support. In the VATM, it was assumed that within one stirrup spacing of the support that only the bottom strands carried the strand force. A plot of bond stress can be seen in Figure 12.4. The bond stress over the transfer length due to the effective prestress was also plotted on the diagram for comparison purposes.

12.5.9 Stress in Compression Strut

Stress in the compression strut, f_{strut}, was calculated with equation 12.24 using V_{ult}.

$$f_{strut} = \frac{V_{ult}}{jd \cos\theta\, b_w \sin\theta} \leq 0.85 \beta_1 \lambda\, f_c'$$ (12.24)

The value β_1 was 0.6 based on the use of HSLC with a compressive strength over 6,000 psi. Compliance with this requirement as specified by ACI 318[91] (2002) ensured a level of stress in the strut below which shear crushing would not occur.

287
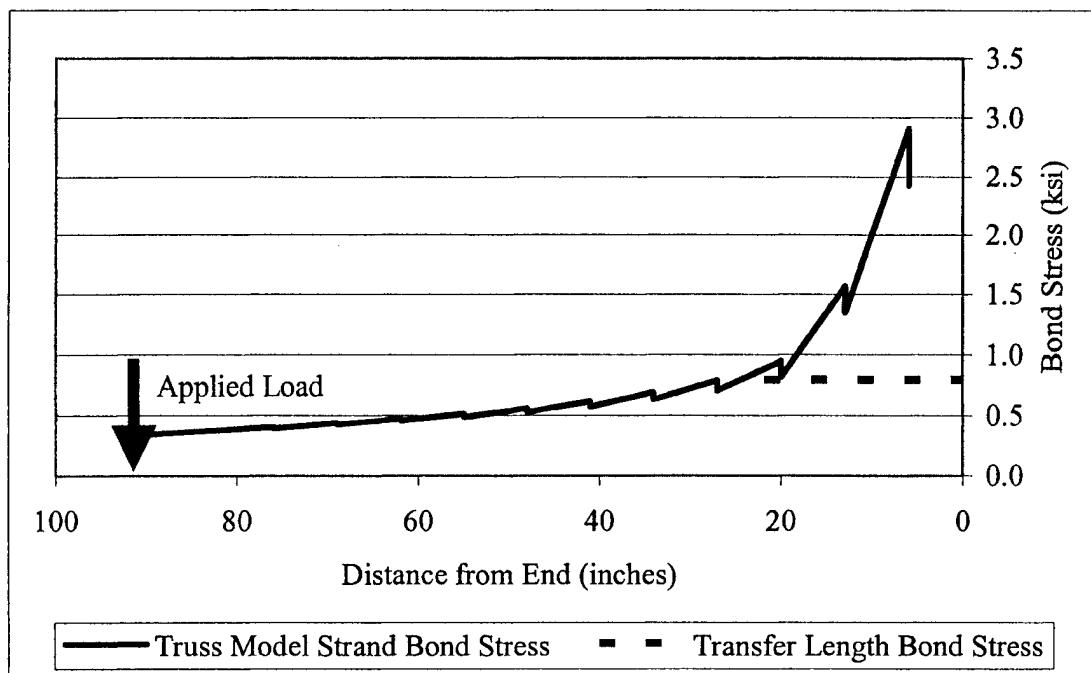
Figure 12.4 Bond Stress Plot for Girder Test G1C-West

12.6 Experimental Measurement of Shear Behavior

In order to monitor and measure girder shear behavior, a large strain rosette made with LVDTs was placed on the web of each girder at the mid point of the shear span as pictured in Figure 12.5.
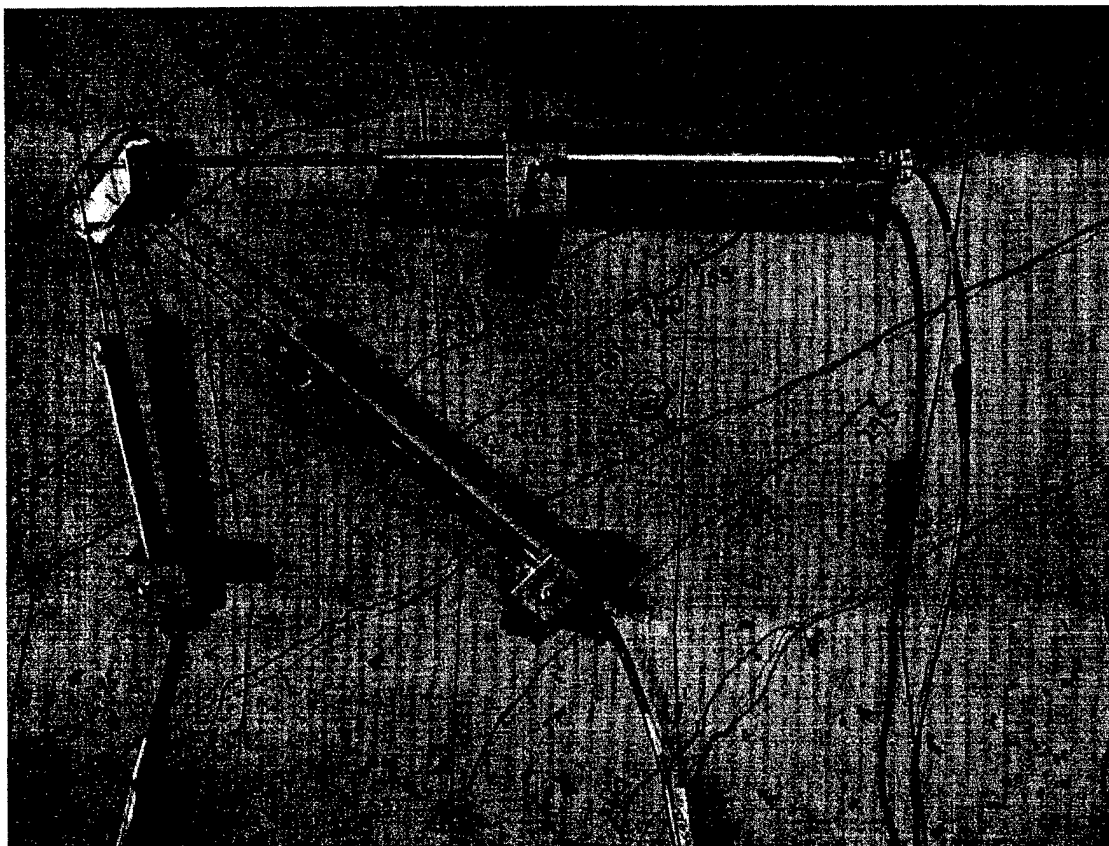
Figure 12.5 Strain Rosette Made with LVDTs on Girder Test G1C-West

The LVDTs oriented in the horizontal and vertical positions had gage lengths of approximately 10.5 inches. The LVDT at a 45-degree angle had a gage length of approximately 16.5 inches. To calculate strains in the three directions, the displacement of the LVDT was divided by its gage length. The gage lengths were carefully measured

for each girder test to ensure proper strain calculation. Having strain information for three distinct directions, and knowledge of the initial prestressing strain along the longitudinal axis of the girder, it was possible to calculate principal strains and directions using a simple strain transformation. Figure 12.6 below shows a typical plot of applied shear vs. principal strains.
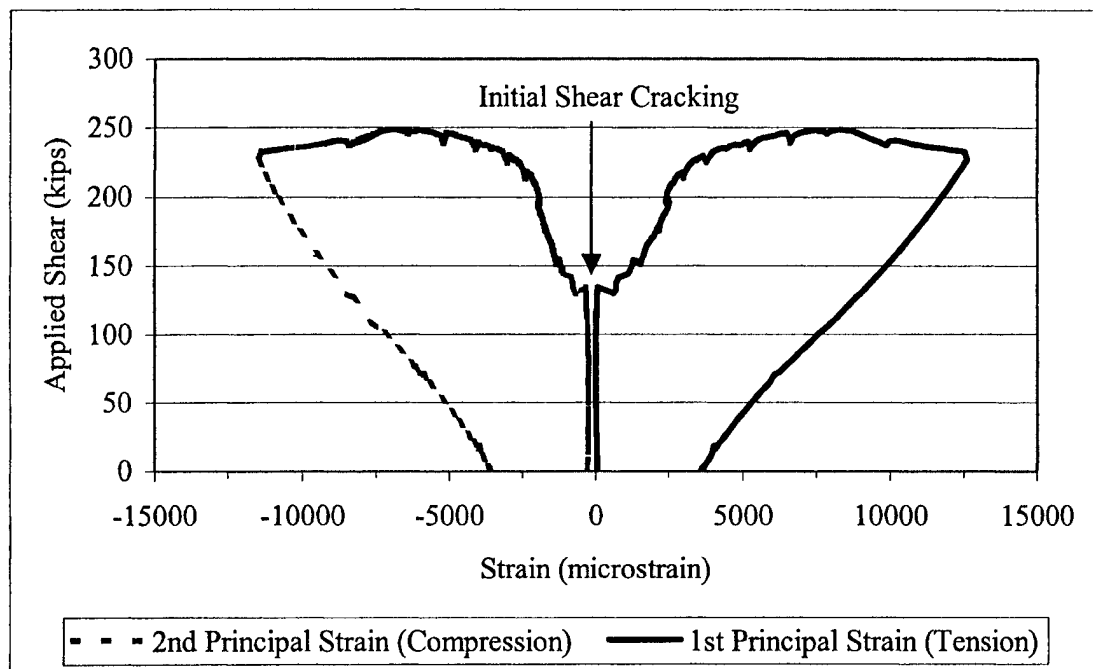
Figure 12.6 Plot of Applied Shear vs. Principal Strains for Girder Test G1C-West

The point at which initial shear cracking occurred was where the two principal strain plots separated. This value matched very closely the value at which initial shear cracking was visually and audibly detected during the test. The plot shows initial shear cracking at an applied shear of 134.2 kips. The latter agreed with the applied load of 155 kips at which a shear crack occurred. In order for the LVDTs to measure the onset of shear

cracking, the initial crack had to pass through the rosette. Initial cracking did not pass through the rosette on one girder test.

Another useful aspect of the principal strain information was a plot of how the principal angles varied during the test. Figure 12.7 below provides a typical plot of the second principal strain (compression strain) angle, which indicated the angle of shear cracking through the LVDT rosette.
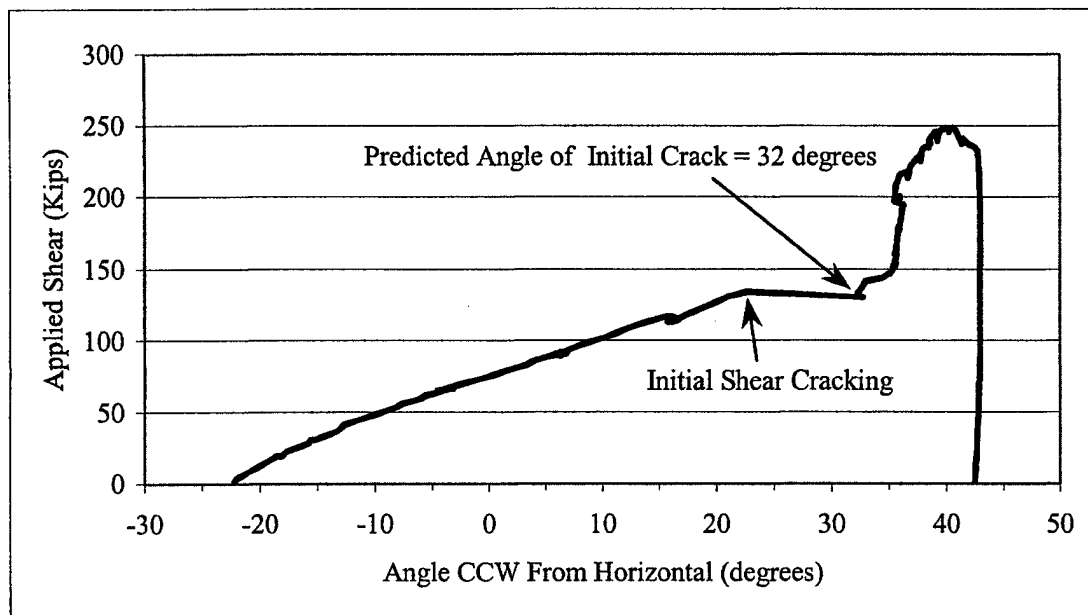
Figure 12.7 Second Principal Strain Direction (Cracking Angle) for Test G1C-West

The horizontal plateau from the point labeled "initial shear cracking" also was an indication of the applied shear at which cracking occurred. The angle indicated at the end of the plateau was most representative of the actual cracking angle on the girder; protractor measurements of the crack angle normally agreed within ± 5 degrees with this plateau angle.

Figure 12.7 shows an increase in crack angle with increased applied load. As applied shear increased, the stirrups were required to pick-up more shear increasing the vertical force component and causing the angle of cracking to become greater. This trend was observed during testing. As the applied shear increased, new shear cracks formed at greater angles than those seen at initial cracking. In Figure 12.7, the indicated crack angle appeared to increase from about 32 degrees to 40 degrees as the applied shear increased.

12.7 Experimental Results

Discussion of experimental results was divided into the discussion of the initial shear cracking, ultimate shear capacity, and the variable angle truss model (VATM). Percent difference was calculated using equation 11.1.

12.7.1 Initial Shear Cracking

Table 12.2 provides an overview of initial shear cracking. The predicted values were calculated at the midpoint of the shear span. The experimental value was the applied shear at which cracking was first recorded visually or electronically.

Examination of Table 12.2 showed that the AASHTO[40] Standard method of calculating concrete shear strength was conservative overall. In the case of girder tests G1C-Center and G2C-Center, the prediction was less than 3 percent unconservative. The AASHTO[92] LRFD technique provided predictions of concrete strength that far underestimated their capacity. The ACI[2] alternate approach provided the closest prediction for V_c where the cracking shear was equated to the shear strength provided by

the concrete. Overall, the predicted V_c values were within about 6 percent of experimental values for both the G1 and G2 girder tests. Girder tests G1C-Center and G2C-Center showed the greatest difference from the ACI alternate predicted values, about 18 percent unconservative overall. Both the tests involved the minimum stirrup spacing of 24 inches.

Table 12.2 Overview of Initial Cracking Shears

Test #	$V_{c\text{-EXP}}$ Exp. (kips)	V_{cw} AASHTO Standard (kips)	V_{cw} ACI Alternate (kips)	V_c AASHTO LRFD (kips)	Percent Diff. Exp. vs. Standard	Percent Diff. Exp. vs. ACI Alt	Percent Diff. Exp. vs. LRFD
G1A-E *	145.0	104.1	124.0	24.7	39.4%	16.9%	488%
G1A-W	120.0	107.1	127.5	26.3	12.1%	-5.9%	356%
G1A-C *	134.0	98.5	118.0	23.5	36.1%	13.6%	470%
G1B-E *	140.0	105.5	125.5	24.7	32.7%	11.6%	466%
G1B-W	141.2	103.9	123.6	24.3	35.9%	14.2%	482%
G1B-C *	136.1	98.9	118.4	25.0	37.6%	14.9%	445%
G1C-E *	123.5	101.5	120.7	23.6	21.7%	2.3%	423%
G1C-W	134.2	104.0	123.3	23.6	29.0%	8.8%	468%
G1C-C	94.0	96.7	115.8	24.6	-2.8%	-18.8%	282%
G2A-E	178.6	114.4	135.7	26.0	56.1%	31.6%	588%
G2A-W	157.3	118.1	139.5	28.8	33.2%	12.8%	447%
G2A-C *	140.0	109.4	130.6	25.0	27.9%	7.2%	460%
G2B-E	163.1	114.6	136.1	25.2	42.3%	19.8%	549%
G2B-W	148.0	117.4	138.7	25.8	26.1%	6.7%	473%
G2B-C *	120.4	110.5	131.9	25.2	9.0%	-8.7%	377%
G2C-E	143.4	112.0	133.0	25.6	28.1%	7.8%	461%
G2C-W	122.4	113.4	134.2	27.1	8.0%	-8.8%	352%
G2C-C	107.0	107.3	128.1	31.3	-0.2%	-16.5%	241%

G1 Avg	129.8	102.2	121.9	24.5	26.8%	6.4%	431%
G2 Avg	142.2	113.0	134.2	26.7	25.6%	5.8%	439%
G1 Std Dev					14.1%	11.9%	68.9%
G2 Std Dev					17.8%	15.2%	104.1%

* Girder failed in shear at ultimate as primary or secondary failure mode

12.7.2 Initial Shear Cracking Considering Stirrup Spacing

Figure 12.8, plots the concrete shear strength, V_{c-Exp}, vs. shear stirrup spacing. The trend lines indicated that V_{c-Exp} appeared to increase with smaller stirrup spacing. Since the stirrups carried some load prior to concrete cracking, it was understandable that the apparent V_{c-Exp} value would be higher with closer stirrup spacing. A very interesting aspect of Figure 12.8 was the convergence of the G1 and G2 trendlines at a stirrup spacing of 24 inches. The indication here was that little difference existed between V_c for the G1 and G2 girders. Based on the use of minimum stirrup spacing in these 6 center-span tests, it was likely that these data most truly reflected the V_c value of the girders.
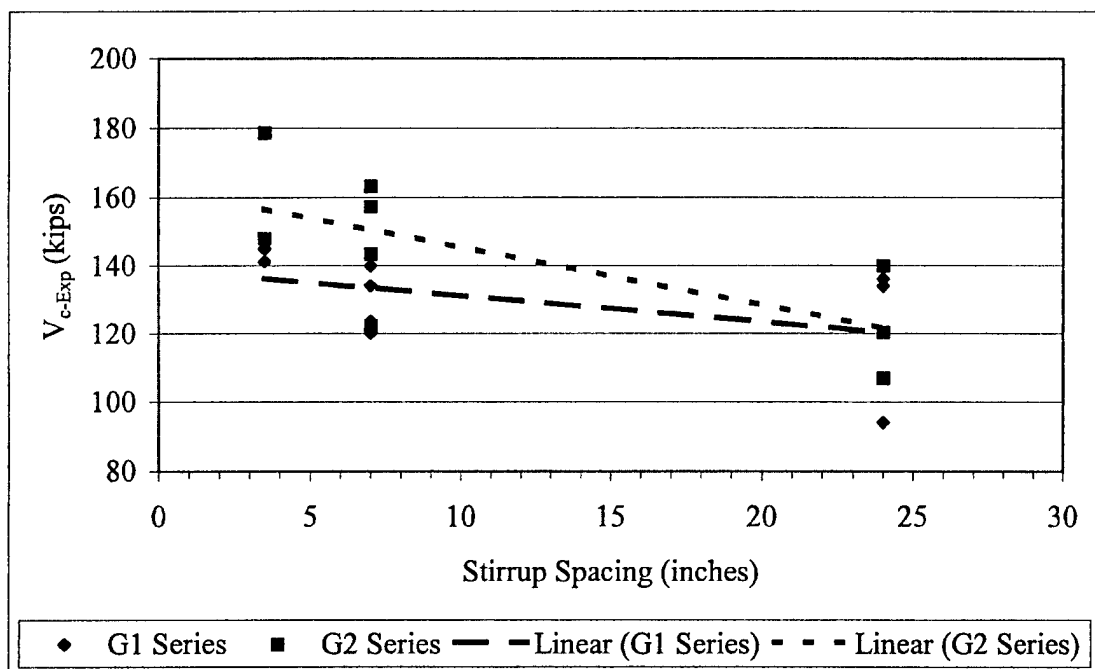
Figure 12.8 Concrete Shear Strength, V_c vs. Stirrup Spacing

The implication of this finding was that an apparent ceiling exists which limits the tension strength of concrete. In order to investigate this possibility, a similar normalization was conducted on the shear results as was done on the cracking strength results at flexural cracking.

12.7.3 Normalized Diagonal Tension Strength Factor, ξ_t

Table 12.3 provides an overview of predicted diagonal tension strengths using the ACI^2 alternate approach, experimental diagonal tension strengths and the normalized diagonal tension factor, ξ_t.

Table 12.3 shows that ξ_t becomes unconservative at 3.70 (less than 4) on average for the G2 series girders with 24-inch stirrup spacing. Figure 12.9 depicts graphically the data from Table 12.3 and shows how the ACI alternate prediction technique for diagonal tensile strength produced some unconservative predictions. Any data points below the 4.0 line were unconservative.

Table 12.3 Normalized Diagonal Tension Strength Factors, ξ_t

Test #	Stirrup Spacing (inches)	ACI Alternate Predicted Diagonal Tension Strength (Equation 12.8) $f_{t\text{-}Pred}$" (psi)	Experimental Diagonal Tension Strength $f_{t\text{-}Exp}$" (psi)	Normalized Diagonal Tension Strength Factor ξ_t
G1A-East	3.5	333	415	4.99
G1A-West	7	333	304	3.66
G1A-Center	24	333	396	4.76
G1B-East	7	333	389	4.67
G1B-West	3.5	333	402	4.83
G1B-Center	24	333	404	4.85
G1C-East	7	321	332	4.14
G1C-West	7	321	363	4.52
G1C-Center	24	321	238	2.96
G2A-East	3.5	356	525	5.89
G2A-West	7	356	424	4.77
G2A-Center	24	356	393	4.41
G2B-East	7	356	461	5.18
G2B-West	3.5	356	392	4.40
G2B-Center	24	356	312	3.51
G2C-East	7	349	389	4.46
G2C-West	7	349	304	3.49
G2C-Center	24	349	268	3.17

G1 Average	3.5		409	4.91
G2 Average	3.5		459	5.15
G1 Average	7		347	4.25
G2 Average	7		395	4.48
G1 Average	24		346	4.19
G2 Average	24		324	3.70
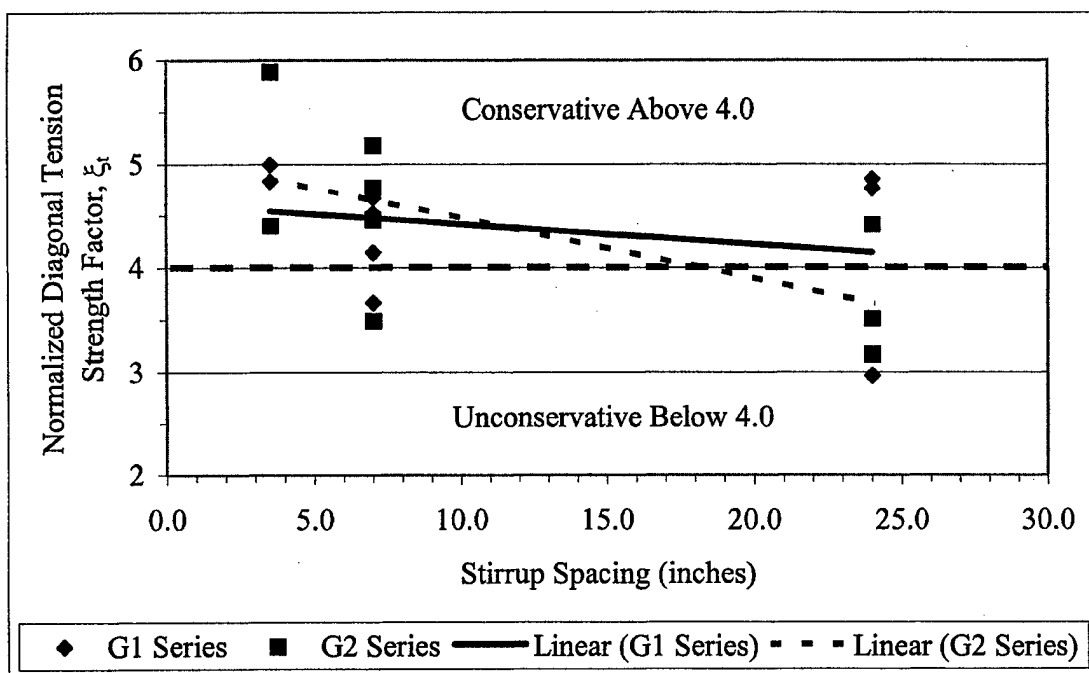
Figure 12.9 Normalized Diagonal Tension Strength Factor, ξ_t, vs. Stirrup Spacing

12.7.4 Ultimate Shear Capacity, V_u

Table 12.4 provides an overview of predicted ultimate shear capacity calculated by the AASHTO Standard method and the AASHTO LRFD method with the strength reduction factor, ϕ_s, of 1 and compares them to the experimental maximum shear values. Using the AASHTO Standard method, the stirrup yield strength was capped at 60 ksi as required by the code, and the results also recorded. Since the value of f_y was 62 ksi, there was an insignificant difference in predicted values.

Table 12.4 lists the results of all tests; Table 12.5 lists only the tests that exhibited a shear, shear-slip or shear-flexure failure. Both tables show the AASHTO[40] Standard technique produced conservative results overall. Limiting the yield strength to 60 ksi

297

caused the prediction to be slightly more conservative. The AASHTO[92] LRFD technique

produced more conservative results overall because the girders with 24-inch spacing were

predicted to carry much less shear. The AASHTO LRFD penalized those girders with a

very low concrete strength relative to the AASHTO Standard procedure.

Table 12.4 Predicted vs. Experimental V_u Values

Test #	AASHTO Standard $f_y = 62$ ksi V_u (kips)	AASHTO Standard $f_y = 60$ ksi V_u (kips)	AASHTO LRFD $f_y = 62$ ksi V_u (kips)	Exp. V_u (kips)	Percent Diff. Exp vs Std 62	Percent Diff. Exp vs Std 60	Percent Diff. Exp vs LRFD
G1A-East *	379.7	370.8	473.5	362.8	-4.5%	-2.2%	-23.4%
G1A-West *	244.9	240.4	312.8	248.9	1.6%	3.5%	-20.4%
G1A-Center	138.7	137.4	103.8	258.0	86.0%	87.8%	148.5%
G1B-East	243.3	238.9	241.1	312.2	28.3%	30.7%	29.5%
G1B-West *	376.0	367.2	363.5	296.3	-21.2%	-19.3%	-18.5%
G1B-Center	138.6	137.3	104.3	234.1	68.9%	70.5%	124.5%
G1C-East	238.4	234.0	255.5	289.2	21.3%	23.6%	13.2%
G1C-West *	241.4	237.0	255.6	260.3	7.8%	9.8%	1.8%
G1C-Center *	137.1	135.8	105.5	202.2	47.5%	48.9%	91.6%
G2A-East *	388.3	379.4	365.4	366.5	-5.6%	-3.4%	0.3%
G2A-West *	255.4	251.0	223.8	249.7	-2.3%	-0.5%	11.6%
G2A-Center	149.5	148.2	82.3	255.9	71.2%	72.7%	211.0%
G2B-East *	252.5	248.0	215.8	355.4	40.8%	43.3%	64.7%
G2B-West *	391.3	382.4	432.0	296.3	-24.3%	-22.5%	-31.4%
G2B-Center	150.9	149.6	102.7	246.3	63.2%	64.6%	139.9%
G2C-East *	249.8	245.3	268.9	301.0	20.5%	22.7%	11.9%
G2C-West *	249.9	245.5	254.2	255.2	2.1%	4.0%	0.4%
G2C-Center *	147.6	144.1	89.2	200.3	35.7%	39.0%	124.7%

G1 Average					26.2%	28.1%	38.5%
G2 Average					22.4%	24.4%	59.2%

* Tests which exhibited a flexural failure as the primary failure mode

Table 12.5 Predicted vs. Experimental V_u Values for Tests Failing in Shear

Test #	AASHTO Standard $f_y = 62$ ksi V_u (kips)	AASHTO Standard $f_y = 60$ ksi V_u (kips)	AASHTO LRFD $f_y = 62$ ksi V_u (kips)	Exp. V_u (kips)	Percent Diff. Exp vs Std 62	Percent Diff. Exp vs Std 60	Percent Diff. Exp vs LRFD
G1A-Center	138.7	137.4	103.8	258.0	86.0%	87.8%	148.5%
G1B-East	243.3	238.9	241.1	312.2	28.3%	30.7%	29.5%
G1B-Center	138.6	137.3	104.3	234.1	68.9%	70.5%	124.5%
G1C-East	238.4	234.0	255.5	289.2	21.3%	23.6%	13.2%
G2A-Center	149.5	148.2	82.3	255.9	71.2%	72.7%	211.0%
G2B-Center	150.9	149.6	102.7	246.3	63.2%	64.6%	139.9%

G1 Average	51.1%	53.2%	78.9%
G2 Average	67.2%	68.7%	175.5%
G1 Std Dev	31.3%	31.0%	67.5%
G2 Std Dev	5.7%	5.7%	50.3%

Figure 12.10 provides a plot of the data from Table 12.6 normalized by dividing the ultimate shear capacity, V_u, by the lightweight concrete factor, λ, and the square root of the compressive strength. Trendlines are depicted in Figure 12.9 for the AASHTO Standard[40] and LRFD[92] Specifications. The figure shows how the AASHTO[92] LRFD Specification becomes overly conservative at larger stirrup spacings where the contribution of V_s is low. At closer stirrup spacings, the figure shows how the results from the Standard and LRFD specifications provide very similar results.
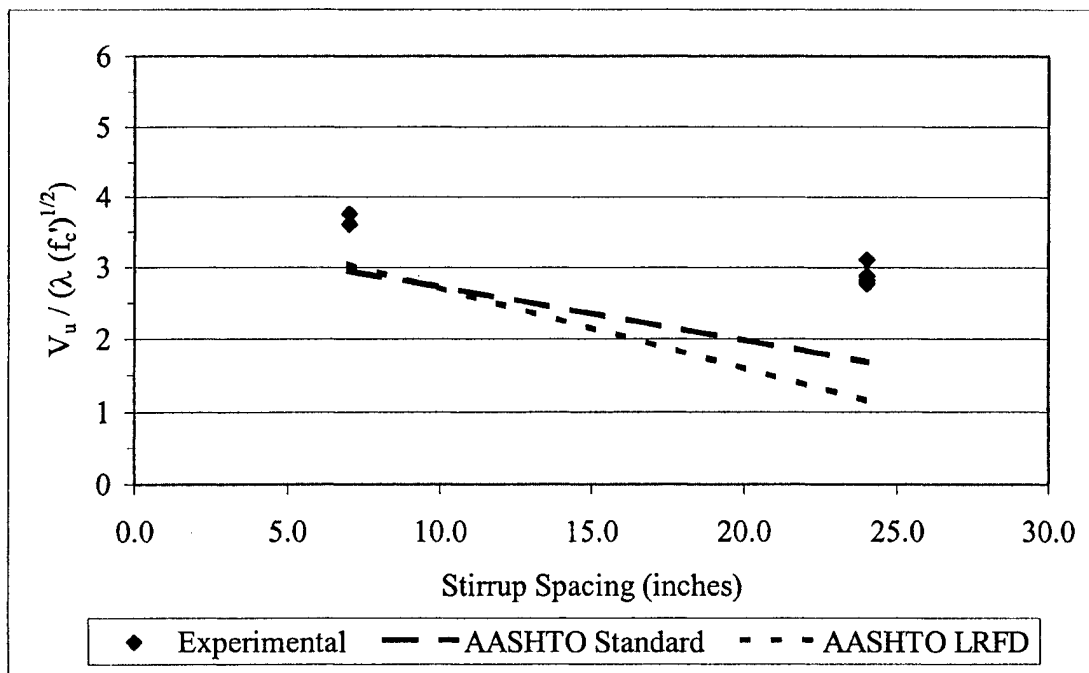
Figure 12.10 Normalized Ultimate Shear Capacity, V_u, vs. Stirrup Spacing

12.7.5 Variable Angle Truss Model

The variable angle truss model was considered as a technique for estimating the

shear capacity of HSLC girders. Table 12.6 provides an overview of the results for

girders failing in shear. On average for all G1 and G2 girders failing in shear, the VATM

under predicted shear capacity by a significant amount. Discounting the girders having

24-inch stirrup spacing, the predictions were about 35 percent conservative on average

for the G1 girders. The girders with 24-inch stirrup spacing were penalized because the

VATM does not consider concrete strength in determining shear capacity.

300

Table 12.6 Variable Angle Truss Model Results

Test #	VATM V_n (kips)	Experimental V_n (kips)	Percent Difference Experimental vs. VATM
G1A-Center	49.6	258.0	420.1%
G1B-East	223.2	312.2	39.9%
G1B-Center	49.6	234.1	372.0%
G1C-East	223.2	289.2	29.6%
G2A-Center	49.6	255.9	416.0%
G2B-Center	49.6	246.3	396.6%

G1 Average		215.4%
G2 Average		406.3%

12.7.6 Interface Shear

There was no recorded interface shear slip during any test.

12.8 Conclusions

The current AASHTO Standard specification provides a conservative prediction of concrete and ultimate shear capacity when shear steel capacity is capped at a yield strength of 60 ksi. The alternate design procedure listed in ACI-318 Section 11.4.2.2 for predicting shear strength produced some unconservative predictions for concrete compressive strengths over 10,000 psi. The method for predicting interface shear strength is conservative for HSLC.

The current AASHTO LRFD specification provides a conservative prediction of ultimate strength.

The VATM provides an overconservative prediction of shear capacity in HSLC girders.

301

CHAPTER XIII

DEVELOPMENT LENGTH RESULTS AND DISCUSSION

13.1 Introduction

This chapter presents the results of the development length tests, discusses the findings and compares the behavior to predicted values and that observed by others. Based on experimentally measured transfer length values from this experimental program and others, current code provisions and equations previously suggested for predicting development length are evaluated. New equations for predicting development length are suggested based on these findings.

13.2 Definition

The development length is the sum of the "transfer length" and the "flexural bond length." The flexural bond length is the additional length of pretensioning strand beyond the transfer length over which bond is developed to allow the strand to reach the stress level f_{ps} at the nominal flexural strength of the member. Development length can also be defined as the minimum distance from the end of the member beyond which the application of a point load will result in a flexural failure. The transfer of force from the strand to the concrete that occurs along the development length is represented in Figure 13.1.
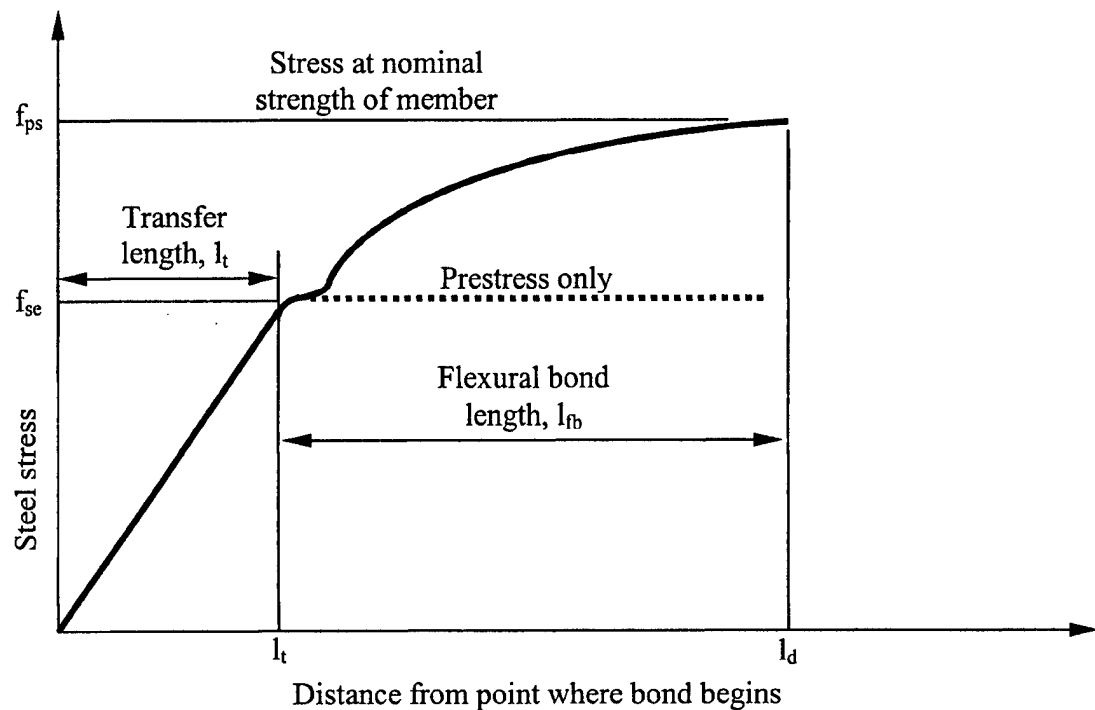
Figure 13.1 Diagram of Components of Development Length, l_d^2

The initial sloped portion of the diagram begins at a stress level of zero where

bond begins and is assumed to increase linearly over a distance equal to the transfer

length. The dashed line indicates the effective stress level due to prestressing only (f_{se}).

The sloped portion of the diagram beyond the transfer length where the stress level

increases gradually to the level f_{ps} is the flexural bond length. The shape of this diagram

is codified in the AASHTO[40] and ACI[2] design specifications. For the purpose of this

research, embedment length was defined as the distance from the girder end to the point

load.

13.3 Importance of Development Length

Similar to transfer length, development length will not likely be the governing design criteria on a pretensioned bridge girder. However, the development length extends three to four times farther than transfer length from the end of the member and thus impacts the girder design over a longer region. At a distance less than the development length from the end of the member, the required cracking moment is less than that at a distance greater than the development length. This change in cracking moment is important not only as a flexural design consideration, but for shear capacity as well. Shear design within the development length region must consider the variation of prestressing force.

13.4 Current Code Provisions

Current code provisions for determining development length are similar in form. AASHTO[40] Section 9.28.1 specifies the development length shall be determined using the Equation 13.1.

$$l_d = (f_{su}^* - \tfrac{2}{3} f_{se})D \tag{13.1}$$

where f_{su}^* is the average stress in the prestressing steel at ultimate load in ksi, f_{se} is the effective steel prestress after losses in ksi, and D is the nominal diameter of the prestressing steel in inches. Section 12.9.1 of the ACI 318 Code[2] specifies the development length shall be determined using the Equation 13.2.

$$l_d = (f_{ps} - \tfrac{2}{3} f_{se}) d_b \qquad\qquad (13.2)$$

where f_{ps} is the stress in the prestressed reinforcement at nominal strength in ksi, f_{se} is the effective stress in the prestressed reinforcement after allowance for all prestress losses in ksi, and d_b is the strand diameter in inches. Both equations produce the same prediction for development length.

13.5 Measurement of Development Length

Each girder end of the six Type II girders was tested for development length producing 12 sets of data. Girder end designations were the same as used in transfer length testing. In order to determine development length, the position of the point load must be varied from girder to girder. The precise development length would be where the point load resulted in concurrent flexural, shear and bond failure. If the failure mode is purely flexural, the tested embedment length is greater than the development length. If the failure mode is shear and bond failure, the tested embedment length is less than the development length. Load positioning in several locations is necessary to bracket the actual development length.

For this research, the girder ends were designed to allow the application of point loads at embedment lengths calculated as varying percentages of the current code-specified development length. The original girder design assumed f_{ps} and f_{su}^* to be 270 ksi. The values of f_{se} were calculated using the standard AASHTO[40] technique as 165.02 ksi and 165.65 ksi for the G1 and G2 girders, respectively. Using these values and a strand diameter of 0.6 inches, the predicted development lengths were 96 inches and 95.7

305

inches for the G1 and G2 girders respectively. Table 13.1 shows the embedment lengths

tested as a percentage of the estimated development length values and also shows the

embedment lengths tested as a percentage of the development length calculated based on

experimentally determined values of f_{ps}, f_{su}^*, and f_{se}, which are listed for each girder.

Table 13.1 Embedment Lengths Tested as Percentages of AASHTO[40] Predicted Values

Girder #	Stirrup Density 1X 2X	Embed. Length (in)	Percent of l_d based on estimated values of f_{ps}, f_{su}^*, and f_{se}	Experimental Values		l_d based on exp. values (in)	Percent of l_d based on experimental values of f_{ps}, f_{su}^* and f_{se}
				f_{ps}, f_{su}^* (ksi)	f_{se} (ksi)		
G1A-E	2X	67	70 %	265.1	153.7	97.6	69 %
G1A-W	1X	96	100 %	265.4	152.3	105.9	91 %
G1B-E	1X	67	70 %	227.6	151.2	106.3	63 %
G1B-W	2X	81	84 %	266.3	149.8	106.9	76 %
G1C-E	1X	81	84 %	263.0	149.0	107.2	76 %
G1C-W	1X	91	95 %	264.4	147.6	107.8	84 %
G2A-E	2X	67	70 %	266.3	175.8	96.5	70 %
G2A-W	1X	96	100 %	266.8	175.7	96.5	100 %
G2B-E	1X	67	70 %	265.0	176.2	96.3	70 %
G2B-W	2X	81	85 %	266.6	175.6	96.6	84 %
G2C-E	1X	81	85 %	267.7	159.3	103.1	79 %
G2C-W	1X	91	95 %	266.6	158.8	103.3	88 %

The value listed in the "Stirrups" column of Table 13.1 describes the amount of

shear stirrups used in the girder end. A "1X" indicates the AASHTO specified stirrup

spacing was used. A "2X" indicates that one half the AASHTO specified stirrup spacing

was used or stated otherwise, twice the amount of stirrups. The amount of stirrups is

referred to as the stirrup density. The AASHTO specified stirrup spacing is "Single

Density." One half the AASHTO specified spacing is "Double Density." As explained in Chapter 8, varying the stirrup density was designed to determine its effect on strand slip.

By determining the type of failure on each of the girder end tests, the actual development length can be bracketed into a tight range of values.

13.6 Development Length Test Results

One failure criteria for development length testing focused on end slip of the prestressing strands. Slip for each of the eight bottom strands was measured continually throughout girder loading as described in Chapter 10. For each data acquisition reading, an average of the eight values was calculated. If the average value exceeded 0.01 inches during the test, this was assumed to be a "bond" or "slip" type of failure. Russell[44] and Dill[82] also used this 0.01-inch slip to define a slip condition. This type of failure was often termed "shear-slip" because it was believed that the formation of a shear crack was the trigger for strand slip to begin. As discussed in Chapter 12, shear failure was always associated with slip at the girder ends. If the value did not exceed 0.01 inches, and girder end failed in flexure. For a failure to be considered a flexural failure, yielding of the prestressing strands and crushing of the deck had to occur.

CSS data were also collected after each load step. The CSS data were used to track the level of stress in the cross section and the location of cracks occurring in the first 48 inches of the girder. Perfect bond between the strand and concrete was assumed so that the concrete surface strains were equated to added strain in the strands. Table 13.2 provides the results of development length testing.

Table 13.2 Development Length Test Results

Test # E=East W=West	Stirrup Density 1X 2X	Strand Embedment (inches)	Average Strand Slip at P_{max} (inches)	Maximum Strand Strain ε_{ps} (in/in)	Maximum Deck Strain ε_{cu} (in/in)	Failure Mode FL-Flexure SH-Shear SL-Strand Slip
G1A-E	2X	67	0.0102	0.0158	0.0038	FL/SH-SL
G1A-W	1X	96	0.0000	0.0168	0.0042	FL
G1B-E	1X	67	0.7350	0.0078	0.0030	SH-SL
G1B-W	2X	81	0.0007	0.0190	0.0032	FL
G1C-E	1X	81	0.1988	0.0113	0.0032	SH-SL/FL
G1C-W	1X	91	0.0000	0.0140	0.0036	FL
G2A-E	2X	67	0.0033	0.0190	0.0036	FL
G2A-W	1X	96	0.0000	0.0204	0.0072	FL
G2B-E	1X	67	0.0065	0.0155	0.0045	FL
G2B-W	2X	81	0.0000	0.0199	0.0064	FL
G2C-E	1X	81	0.0041	0.0228	0.0045	FL
G2C-W	1X	91	0.0000	0.0198	0.0049	FL

13.6.1 Notes on Development Length Test Results

In girder tests G1A-East, G2A-East and G2B-East the flexural failure was accompanied by the deck splitting longitudinally down the middle as shown in Figure 13.2. The failure mode of Girder G1A-E is listed as FL/SH-SL. This indicates that the girder exhibited both flexural and shear-slip modes with the flexural mode occurring most predominantly. The failure mode of Girder G1C-E is listed as SH-SL/FL. This also indicates the girder exhibited both flexural and shear-slip modes, but the shear-slip mode was predominant. Girders listing just FL exhibited only flexural failure characteristics. Shear cracking occurred in all tests.

Figure 13.2 Longitudinal Cracking in Deck of Girder G1A-East

13.6.2 Development Length for G1 Girders

In order to evaluate the development length test results, strand end slip was

graphed against embedment length. Since only selected embedment lengths were tested,

it was not possible to exactly pinpoint the development length. It was possible, however,

to identify points at which the failure transitioned from flexure to shear-slip. Figure 13.3

shows a bar graph for all G1 girders. The G1 1X bar graphs for the 67 and 81-inch

embedment length strand slip results were limited to 0.02 inches to better show the 2X

bar graph results. The table below the bar graph shows the actual strand slip values.

	67	81	91	96
■ G1 1X Stirrups	0.7350	0.1988	0.0000	0.0000
▓ G1 2X Stirrups	0.0102	0.0007		

Strand Embedment Length (in)
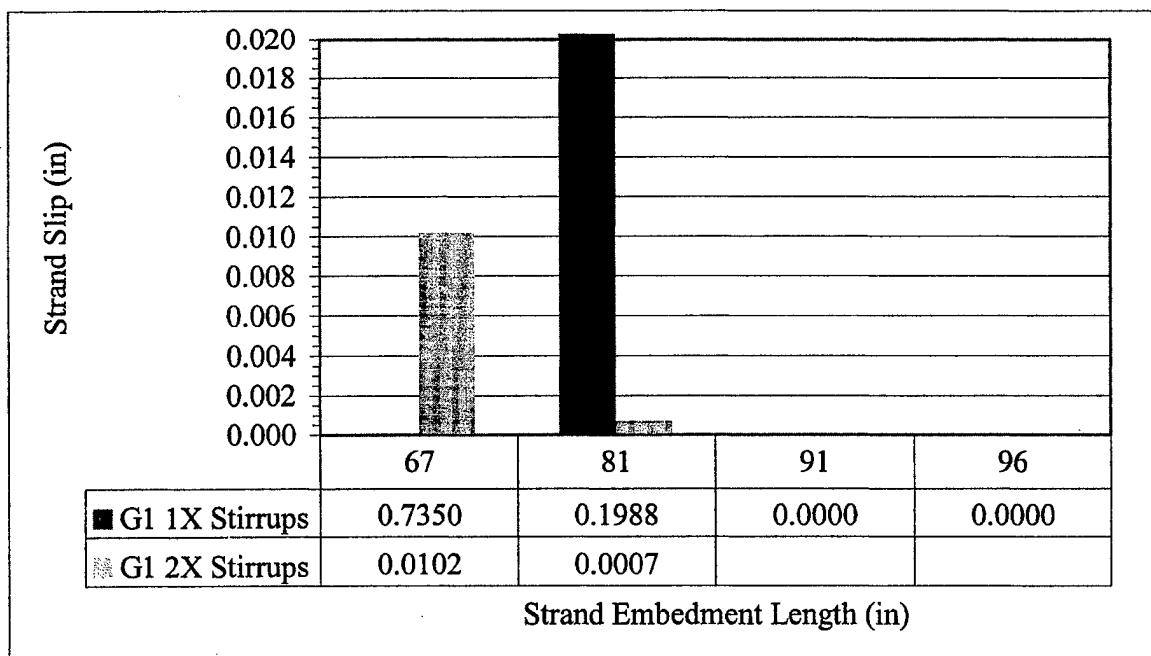
Figure 13.3 G1 Series Girder Average Strand End Slip vs Embedment Length Values

Figure 13.3 shows the development length for G1 series girders with single

density stirrups to be greater than 81 inches, but less than 91 inches. Since at an

embedment length of 81 inches, the level of average end slip exceeds the 0.01-inch limit,

the actual development length must be greater than 81 inches. At an embedment length

of 91 inches, the level of average slip is less than 0.01 inches; thus the actual

development length must be less than 91 inches. Without test data to fill the void

between 81 and 91 inches, the conservative conclusion is that the development length for

G1 series girders with single density stirrups was 91 inches.

310

A similar analysis for G1 series girders with double density stirrups indicates a development length greater than 67 inches but less than 81 inches. Again, without other data, a conservative conclusion is that the development length was 81 inches.

13.6.3 Development Length for G2 Girders

Figure 13.4 shows a bar graph for all G2 girder tests that compares average strand end slip with embedment length.

	67	81	91	96
■ G2 1X Stirrups	0.0065	0.0041	0.0000	0.0000
G2 2X Stirrups	0.0033	0.0000		

Strand Slip (in) vs Strand Embedment Length (in)
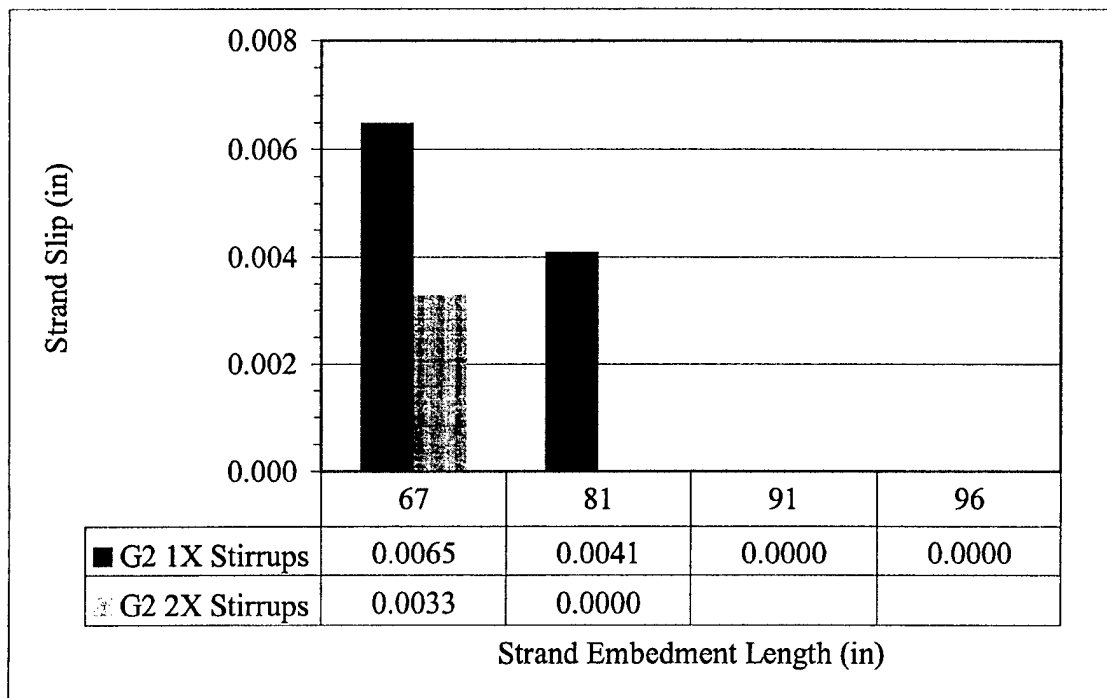
Figure 13.4 G2 Series Girder Average Strand End Slip vs Embedment Length Values

No G2 series girder test exceeded the end slip limit of 0.01 inches. Again, without additional test data to provide conclusive results for embedment lengths less than 67 inches, the conservative conclusion is that the development length for G2 series girders was 67 inches for both single and double density stirrups.

311

Table 13.3 provides a consolidated listing of development lengths.

Table 13.3 Experimentally Determined Development Lengths (inches)

Girder Series	Single Stirrup Density (1X)	Double Stirrup Density (2X)
G1	91	81
G2	67	67

13.7 Discussion of Results

13.7.1 Strand Stress Plots

This section addresses the level of strand stress determined based on CSS data. Each strand stress plot provides a depiction of the effective level of prestress over the entire embedment length, a plot of the strand stress over the first 48 inches of the girder when the strand was at its yield stress at the point of loading, and a plot of strand stress over the first 48 inches of the girder when the strand was at its maximum stress at the point of loading. A complete listing of photographs and strand stress graphs for each development length test is found in Appendix Q.

13.7.1.1 Strand Stress Plots When End Slip Occurred

If significant strand end slip over occurred during the test, it was impossible to accurately estimate what the level of stress was at a point along the strand based on CSS data. Strand end slip indicates there is a lack of adequate bond between the strand and concrete; near perfect bond is necessary for CSS to be a meaningful predictor of an increase in strand stress. A telling depiction of the effect of strand end slip can be seen in Figure 13.5 for test G1B-East, which shows the stress level in the strand to be 260 ksi

312

near the end of the girder and only 227 ksi at the point of load application. Extensive shear cracking in the transfer length region during test G1B-East initiated a strand slip failure resulting in strand end slip of 0.75 inches. The slip allowed the shear cracks to expand causing CSS values in that region to become extremely large. When used to predict strand strain, the values were found to be erroneous.
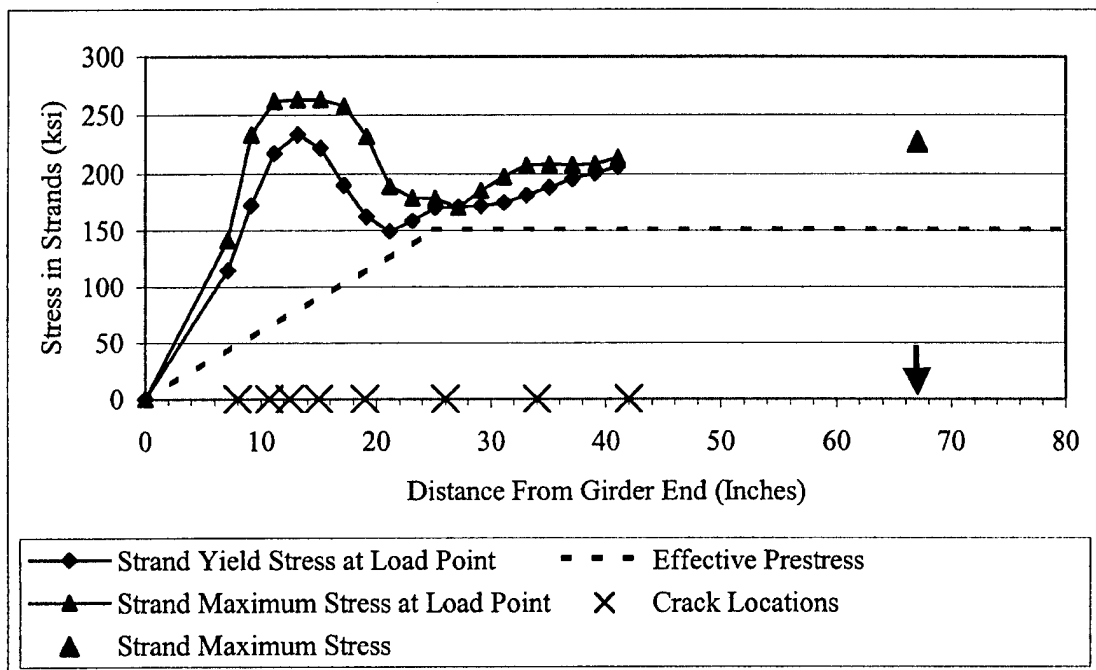
Figure 13.5 G1B-East Strand Stress vs. Distance from Girder end

13.7.1.2 Strand Stress Plots Where End Slip Was Less Than 0.01 Inches

In tests where strand slip was less than 0.01 inches, the CSS data appeared consistent and was used to determine the strain and the stress in the prestressing strand. Two trends became evident in examining these plots. First, in every case where strand slip was under 0.01 inches, there was an observed increase in strand stress in the transfer length region above the level of effective prestress. The effect was far more pronounced

313

with shorter embedment lengths. Second, in some cases, the length over which the largest amount of prestressing force was transferred appeared to be a distance somewhat less than the original transfer length discussed in Chapter 9. Figure 13.6 shows test G1A-East as an example of the strand stress increase in the transfer length region as well as the apparent reduction in transfer length. The embedment length on this test was only 67 inches. The "lone" triangle plots the maximum stress in the strand at the point of loading at the girder's ultimate load. This actual plot of strand stress differs significantly from the theoretical diagram shown in Figure 13.1.
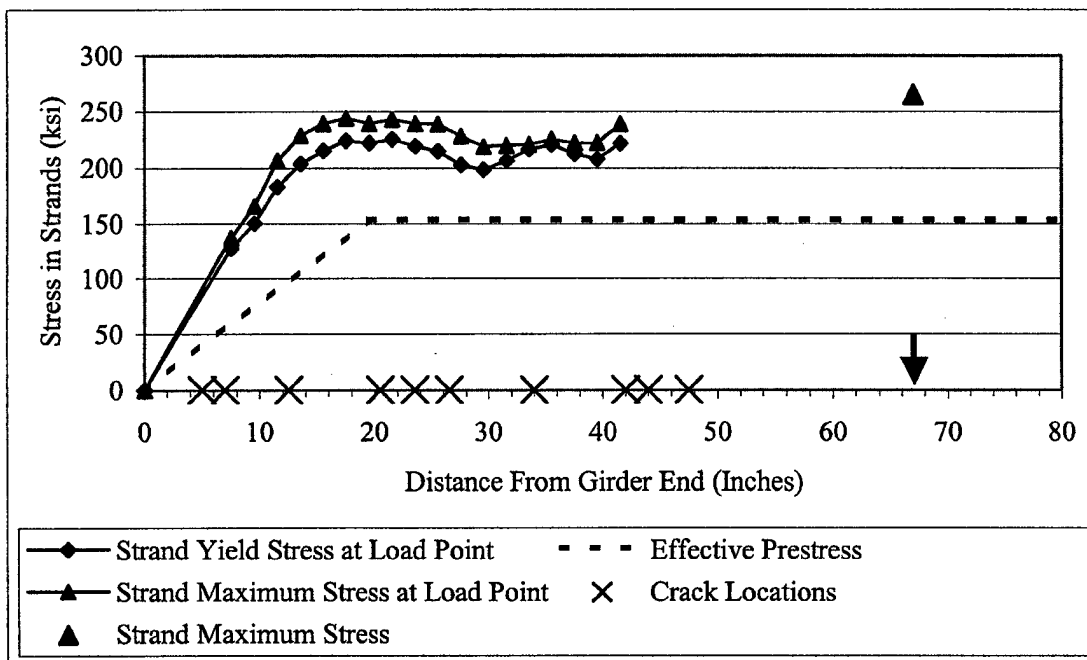
Figure 13.6 G1A-East Strand Stress vs. Distance from Girder End

The variable angle truss model concept discussed in Chapter 12, Shear Behavior Results and Discussion, required a high strand force at the end of the girders with low shear span-to-depth ratios or low values of embedment length. The high stress values

314

developed in the transfer length zone for the girders with embedment lengths of 67 and 81 inches correspond to the compression strut requirement.

Figure 13.7 shows test G2C-West, which resulted in a much less pronounced example of stress increase in the transfer length region. In this example, the embedment length was 91 inches. The strand stress increased above the level of effective prestress, but not to the extent seen in Figure 13.6. The apparent transfer length remained about the same. The dip in the stress plot in Figure 13.7 was based on a lack of cracking in the region of the girder between 12 and 40 inches from the girder end. Cracking across the DEMEC embedment line caused large increases in the CSS values read.
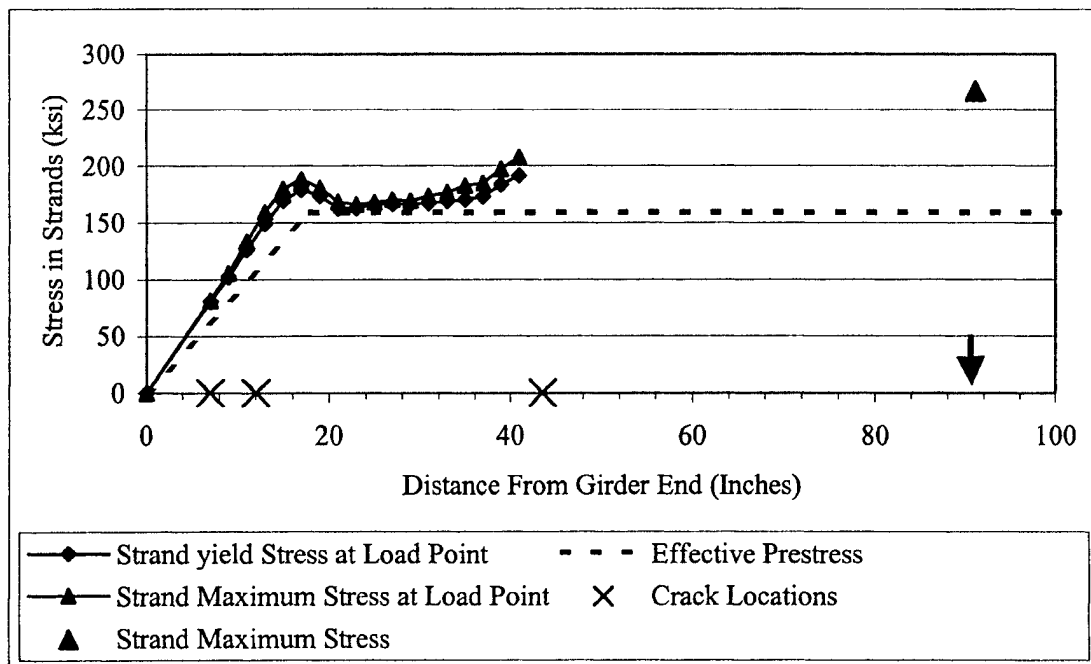
Figure 13.7 G2C-West Strand Stress vs. Distance from Girder End

13.7.2 Strand Slip vs. Shear Cracking

A comparison was made between the onset of shear cracking and strand slip. The comparison was accomplished by examining the plot of applied shear vs. average end slip to determine the applied shear at which slip initiated and comparing that shear value to cracks on the girder. This comparison was made for all tests where the initiation of end slip could be determined. Figure 13.8 shows an applied shear vs. average strand end slip for test G1A-East; diagram has a well-defined slip initiation point. Several tests produced slip diagrams as in Figure 13.9 where it was not possible to determine an end slip initiation point. Based on this level of scatter in the data, any average slip value less than 0.0006 inches was considered zero slip. Figure 13.8 also shows an increase in strand end slip as the girder was unloaded. This phenomenon was seen in several tests and appeared to relate to a clamping effect on the prestressing strand. With the ultimate load on the girder, the end reactions were at a maximum and tended to clamp the strand. As the girder was unloaded, this clamping action was reduced. As the reaction decreased, additional slip occurred. This phenomenon only occurred in tests where slip was greater than 0.0006 inches. This unloading end slip was not included in the average maximum slip values recorded. Appendix R presents all applied shear vs. average strand slip diagrams.
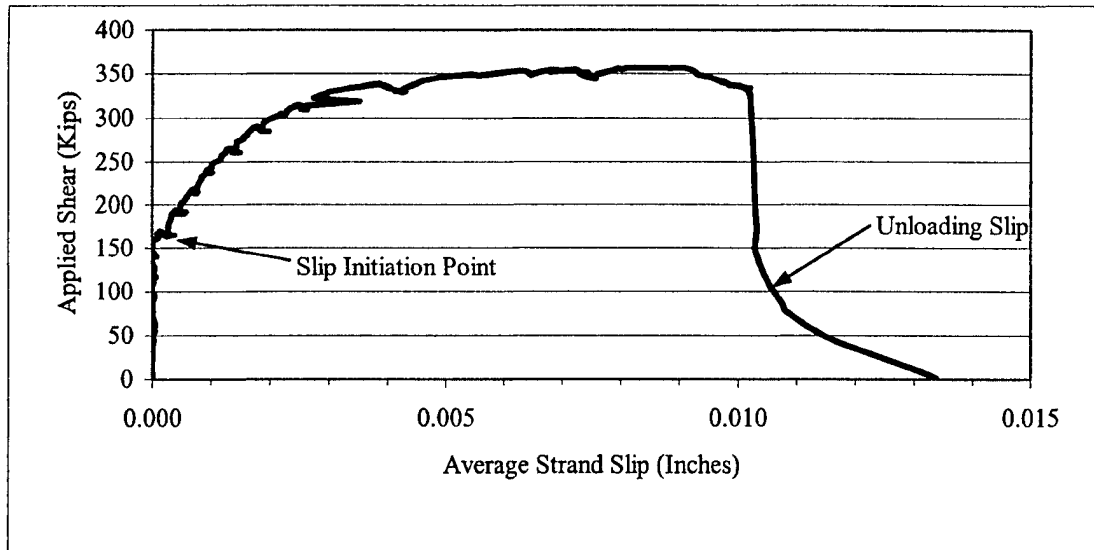
Figure 13.8 Applied Shear vs. Strand Slip (G1A-East) Showing Slip Initiation Point
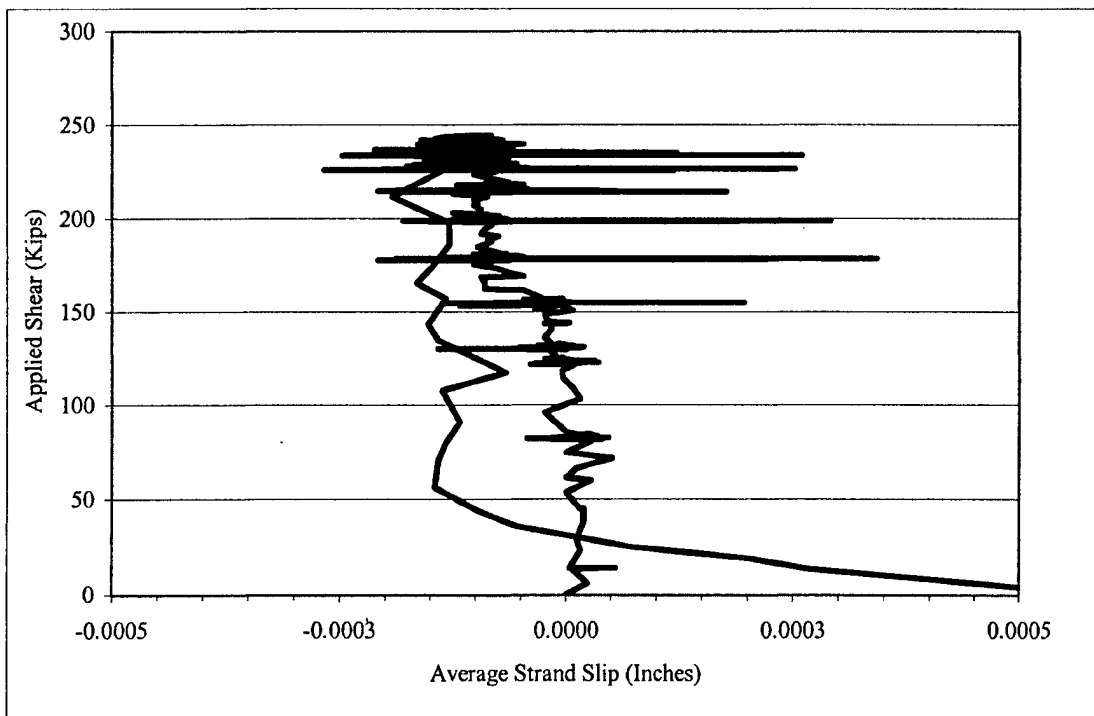
Figure 13.9 Applied Shear vs. Strand End Slip (G2C-West) Showing NO Slip Initiation

Figure 13.10 shows typical CSS data corresponding with applied shear levels, the location of shear cracks crossing the bottom strands, and the transfer length region. CSS data was plotted because it provided a measure of crack growth and allowed identification of the cracks that were increasing most significantly in size. Comparing crack locations with the resulting end slip allowed determination of the region where shear cracking most significantly impacted strand slip. Based on crack location, a comparison was made between strand slip in girders with single and double density shear reinforcement. Similar graphs for each girder test are listed in Appendix R.
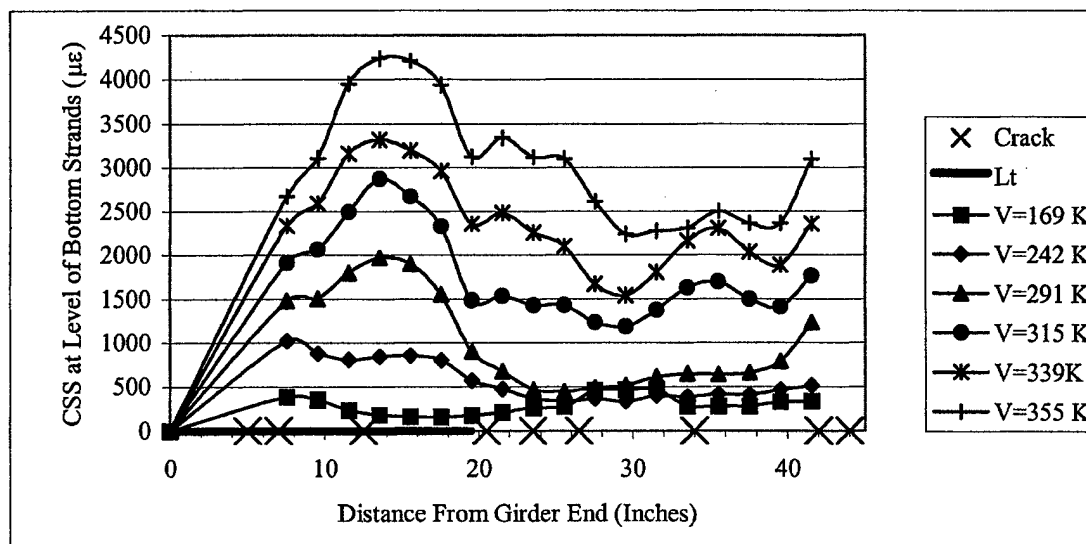
Shear Crack Data										
Distance From End (Inches)	5.0	7.0	12.5	20.5	23.5	26.5	34.0	42.0	44.0	47.5
Applied Shear at Cracking (Kips)	169	315	242	339	315	355	339	339	291	355

Figure 13.10 G1A-East CSS and Shear Cracking vs. Distance from Girder End

13.7.2.1 Results for Single Stirrup Density (1X)

Table 13.4 Applied Shear vs. Strand Slip Results for Single Stirrup Density

Test #	Strand Embedment l_e (l_t) (Inches)	Applied Shear At Crack Formation (Max Applied Shear) (Kips)	Shear Crack Distance From Girder End (Inches)	Average Strand Slip at Applied Shear (Maximum Average Slip Recorded) (Inches)
G1B-East	67 (25)	156 191 208 277 295 (302)	8 10.75 12.5 42 15, 19, 26, 34	No Slip 0.0006 0.0009 0.0138 0.0441 0.2133 (0.7350)
G1C-East	81 (28)	147 243 261 277 (282)	9 17 14, 20, 30 39	No Slip 0.0034 0.0126 0.0431 0.0944 (0.1988)
G2B-East	67 (13)	177 225 299 322 344 (349)	4 10 37, 43.5 13.5 30	No Slip 0.0008 0.0020 0.0034 0.0053 0.0060 (0.0065)
G2C-East	81 (19)	143 215 281 (294)	7 15 27.5, 34, 42	No Slip No Slip No Slip 0.0022 (0.0041)

Table 13.4 shows the results of examining the onset of strand slip in the development length tests with single stirrup density. The "Applied Shear at Crack Formation" column specifies the level of applied shear at which a specific crack formed across the bottom layer of strands. In the same column is also listed the maximum

319

applied shear reached during the test. The "Shear Crack Distance From Girder End" column specifies the distance the crack across the lower strands is from the end of the girder. The "Average Strand Slip at Applied Shear" column lists the strand end slip at the listed applied shear value. Also listed in the column is the value of the maximum average strand slip recorded.

Table 13.4 shows that in every case, a shear crack passing through the level of the bottom strands within the transfer length region initiated or dramatically increased strand end slip. When examining the result of a crack, one must look to the resulting end slip on the following line. For example, during test G1B-East, the recorded slip at an applied shear of 208 kips was 0.0009 inches. The next recorded slip value was 0.0138 inches at an applied shear of 277 kips. This was a fifteen-fold increase in end slip initiated by the formation of the crack at 12.5 inches from the girder end. Similar results were evident when cracks formed at 15, 19, 26, and 34 inches from the girder end at an applied shear of 295 kips. The resulting slip of 0.2133 measured at the maximum applied shear of 302 kips showed a five-fold increase in end slip. Test G1C-East showed a four-fold increase in end slip after the formation of a crack at 17 inches from the girder end, and a three-fold increase after the formation of cracks at 14, 20 and 30 inches from the girder end. Tests G2B-East and G2C-East also showed similar increases in end slip after cracking occurred in or near the transfer length region. Although neither test resulted in a shear-slip failure, the impact of transfer length region cracking is evident.

320

13.7.2.2 Results for Double Stirrup Density (2X)

Table 13.5 Applied Shear vs. Strand Slip Results for Double Stirrup Density

Test #	Strand Embedment l_e (l_t) (Inches)	Applied Shear At Crack Formation (Max Applied Shear) (Kips)	Shear Crack Distance From Girder End (Inches)	Average Strand Slip at Applied Shear (Maximum Average Slip Recorded) (Inches)
G1A-East	67 (19.5)	169 242 291 315 339 355 (357)	5 12.5 44 7, 23.5 20.5, 34, 42 26.5, 47.5	No Slip 0.0010 0.0018 0.0025 0.0039 0.0072 0.0082 (0.0102)
G1B-West	81 (18.75)	243 266 286 (289)	5 7.5, 12 29, 39.5, 42.5	No Slip No Slip No Slip No Slip (No Slip)
G2A-East	67 (17.5)	245 318 343 355 (361)	7.5 34, 39.5 14.5, 23 11, 46	No Slip No Slip 0.0007 0.0017 0.0030 (0.0033)
G2B-West	81 (13)	201 226 251 279 (286)	6 8 10, 14, 45 18.5, 32, 41.5	No Slip No Slip No Slip No Slip (No Slip)

Table 13.5 provides the results for girder ends having double stirrup density. The order of listing in Table 13.5 compares directly with the order in Table 13.4: the concrete grade and embedment lengths match. Direct comparison shows that the resulting slips were much less than the single density stirrups. The only double density stirrup test that

321

underwent a shear-slip greater than 0.01 inches was G1A-East with a slip of 0.0134 inches. For the G1 series girders, doubling the stirrup density dramatically reduced end slip values. For the G2 series girders, the effect was much less pronounced; however, the increased density did reduce end slip.

13.7.2.3 Results for Other Single Stirrup Density Tests

It was not possible to perform an analysis of shear cracking vs. strand slip for girder tests G1A-West, G1C-West, G2A-West and G2C-West since no strand slip occurred.

13.7.3 Shear Crack Location

Shear cracking across the bottom strands within the transfer length region initiated large increases in strand end slip. Other researchers have reported this phenomenon.[44] Despite several shear cracks in the transfer length region, tests G1B-West and G2B-West showed no slip because of the double stirrup density. Tests G1A-East and G2A-East showed slip, but at very small or almost acceptable levels. Russell[44] reported that additional bond stresses can be developed beyond initial strand slip and that small slips are not always followed by complete anchorage failure. Russell[44] also reported that closely spaced cracks were an indication of good bond and wide crack spacing indicated poor bond. Both of Russell's observations were confirmed in the present tests.

13.7.4 Effect of Concrete Grade

Concrete grade also played a significant role in determining development length. Table 13.3 clearly demonstrates a reduction in development length based on concrete grade alone. The G1 series girders had compressive strengths on average approximately 1500 psi less than the G2 series girders. The water cement ratios were approximately 0.29 for the G1 series girders and 0.23 for the G2 series girders. A significant difference between the two mix designs was the amount of silica fume. The G1 series girders had 2 percent silica fume by weight of the total cementitious materials, and the G2 series girders had 10 percent. Past researchers have stated that the addition of silica fume will significantly improve the tensile strength and bond of lightweight concrete to prestressing strand.[21,94,95] The results of the present research confirm this observation.

13.7.5 Bond Stress Examined with the Variable Angle Truss Model

The VATM was discussed in Chapter 12 as a technique for predicting girder shear capacity. Another use for the VATM was the evaluation of bond stress at the girder end, the calculation of which was addressed in Section 12.5.8. Figure 13.11 shows a typical plot of bond stress from girder test G1C-East, a shear failure. Table 13.6 provides an overview of bond stress predictions using the VATM for all girder end tests and compares them to strand slip that occurred during development length testing. The "Bond Stress at Ultimate-VATM" value was taken as the maximum bond stress value within the transfer length region as labeled in Figure 13.11. Appendix N provides strand force and bond stress plots for girder tests G1A-East, G1B-East, and G1C-East, those tests that resulted in development length failures due to excessive strand slip.
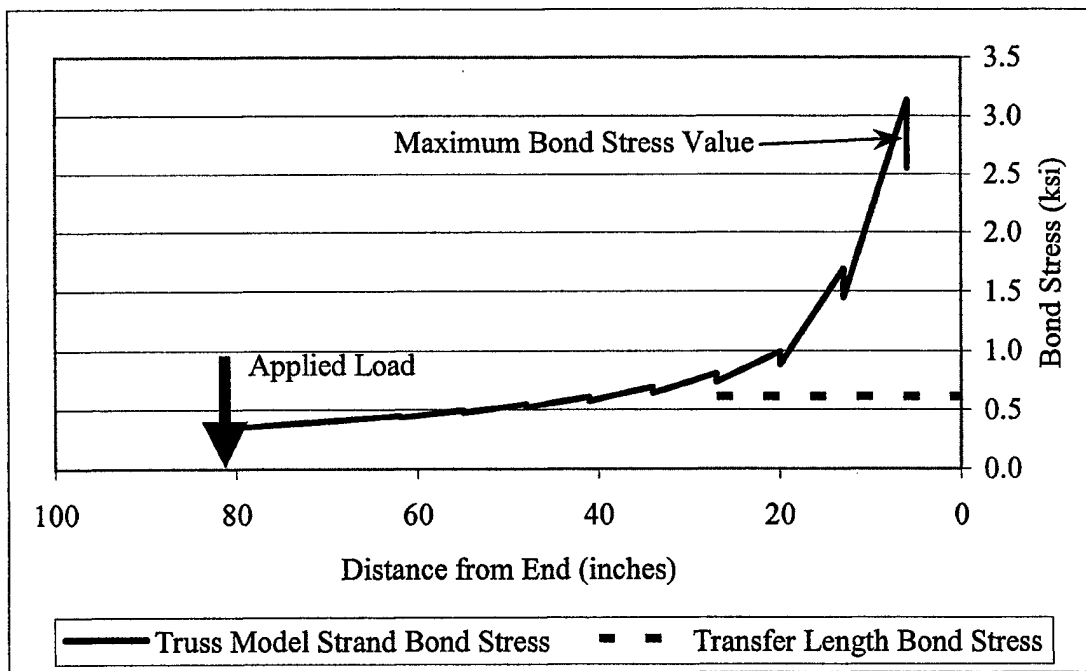
Figure 13.11 Bond Stress Plot Using VATM for Girder G1C-East

Only data from the girder-end tests was provided since strand slip and bond stress were not a problem in center-span tests. Table 13.6 shows that the VATM predicted higher bond stresses for those girder ends that underwent strand slip failures. Examining average VATM bond stress values, it was evident that the model was predicting higher bond stress values for the girder ends undergoing strand slip failures. For the G1 girders, the average bond stress from all tests was 2.55 ksi; the average bond stress for G1 girders not undergoing strand slip was 1.88 ksi. For the G2 girders, there was a wide scatter of bond stress predictions. Since no G2 girder failed due to strand slip, it was not possible to determine a bond stress above which slip would occur. It appeared the VATM was useful for verifying trends, but not for making predictions.

324

Table 13.6 VATM Bond Stress Prediction vs. Strand Slip Results

Test #	Bond Stress At Transfer (ksi)	Bond Stress At Ultimate VATM (ksi)	Average Maximum Strand Slip (inches)	Status of Development Length Test
G1A-East *	0.91	1.98	0.0102	FAIL
G1A-West	0.94	1.77	0.0000	PASS
G1B-East	0.70	3.92	0.7350	FAIL
G1B-West *	0.92	0.77	0.0007	PASS
G1C-East	0.62	2.84	0.1988	FAIL
G1C-West	0.80	2.10	0.0000	PASS
G2A-East *	1.16	2.02	0.0033	PASS
G2A-West	1.54	1.89	0.0000	PASS
G2B-East	1.57	4.02	0.0065	PASS
G2B-West *	1.56	0.92	0.0000	PASS
G2C-East	0.97	2.89	0.0041	PASS
G2C-West	1.02	2.28	0.0000	PASS

G1 Average All Tests	0.82	2.23
G2 Average All Tests	1.30	2.34
G1 Average Passing Tests		1.55
G2 Average Passing Tests		2.34

* Indicates Double Stirrup Density

13.8 Comparison of Results with Code Provisions and Proposed Equations

This section compares the development length results from this research with development lengths predicted by code specified provisions and with predictive equations proposed by other researchers. The goal of these comparisons was to determine if the code equations were adequate for design of slate HSLC girders and which variables provided the best prediction of development length. For comparison purposes, the twelve

development length values found from this HSLC research were evaluated along with eight values from a previous normal weight HPC study by Dill[84] to determine what differences, if any, existed between HSLC and HPC. All development length tests used 0.6-inch diameter prestressing strand.

13.8.1 Material Properties and Prestressing Strand Stresses

Table 13.7 lists material properties and prestressing strand stresses for the twenty development length tests. Included are concrete strengths at release, f_{ci}', and at time of testing, f_c'; strand stress values at time of prestressing, f_{pt}, just after strand release, f_{si}, just prior to girder testing, f_{se}, and at ultimate load, f_{ps}. Accelerated cure strengths were used for f_{ci}' (24-hour) and for f_c' (time of testing). Based on the evaluation of transfer length data, the accelerated cure strengths provided more consistent data. Strand load cells were used to measure strand stresses at the time of tensioning. Strand strain measurements after release and prior to testing were done with a VWSG. Strand strain at ultimate load was determined by measuring CSS with an LVDT, adding that strain to the strain due to effective prestress, and converting the total strand strain to a stress using the strand's stress-strain curve. Again, based on the evaluation of transfer length data, it was found that VWSG data provided a good estimate of strand stress values. Work by Reutlinger[37] used VWSG data for strand stress calculation; the use of VWSG data from this research helped maintain consistency for this evaluation.

326

Table 13.7 Concrete Strengths and Prestressing Levels

Girder #	Develop- ment Length (Inches)	f_{ci}' (psi)	f_c' Prior to Testing (psi)	f_{pt} Before Release (ksi)	f_{si} After Release VWSG (ksi)	f_{se} Prior To Testing VWSG (ksi)	f_{ps} at Ultimate Load CSS (ksi)
G1A-E	81	7465	9580	179	162	154	266
G1A-W	91	7465	9580	179	162	152	266
G1B-E	91	7465	9580	179	161	151	266
G1B-W	81	7465	9580	179	161	150	266
G1C-E	91	6315	8911	179	162	149	266
G1C-W	91	6315	8911	179	162	148	266
G2A-E	67	9640	10975	191	179	176	266
G2A-W	67	9640	10975	191	179	176	266
G2B-E	67	9640	10975	191	179	176	266
G2B-W	67	9640	10975	191	179	176	266
G2C-E	67	8261	10523	179	165	159	266
G2C-W	67	8261	10523	179	165	159	266
G2A-S*	80	14989	16770	191	178	170	275
G2A-N*	80	12379	13430	191	178	170	275
G2B-S*	80	12379	13430	191	177	169	275
G2B-N*	80	11721	12716	191	177	169	275
G4A-S*	80	14675	16418	191	179	171	275
G4A-N*	80	14395	16105	191	179	171	275
G4B-S*	80	14395	16105	191	179	170	275
G4B-N*	80	14610	16345	191	179	170	275

* Tests done by Reutlilnger[37]

13.8.2 Code and Suggested Development Length Equations

Development lengths were predicted using 12 different techniques. Table 13.8 provides an overview of the equations examined. The equation number listed refers to the discussion of the equation in Chapter 2, Background Review.

Table 13.8 Summary of Development Length Equations

Source / Author of Equation	Development Length, l_d	Equation Number
AASHTO[40] / ACI[2]	$(f_{ps} - \frac{2}{3} f_{se}) d_b$	2.16
Barnes, Burns and Kreger[55]	$1.25 \left(\frac{f_{pt}}{\sqrt{f'_{ci}}} + (f_{ps} - f_{pe}) \right) d_b$	2.27
Buckner[46]	$f_{si} \frac{d_b}{3} + \lambda \, (f_{su} - f_{se}) d_b$	2.23
Deatherage et al.[43]	$f_{si} \frac{d_b}{3} + 1.5 (f_{su} - f_{se}) d_b$	2.20
Lane 95% [47]	$\left(\frac{4 f_{pt} d_b}{f'_c} - 5 \right) + \left(\frac{6.4 (f_{su} - f_{se}) d_b}{f'_c} + 15 \right)$	2.26
Lane 95% [47] (10 ksi limit on f_c')	$\left(\frac{4 f_{pt} d_b}{f'_c} - 5 \right) + \left(\frac{6.4 (f_{su} - f_{se}) d_b}{f'_c} + 15 \right)$	2.26
Lane Mean[47]	$\left(\frac{4 f_{pt} d_b}{f'_c} - 21 \right) + \left(\frac{6.4 (f_{su} - f_{se}) d_b}{f'_c} + 26 \right)$	2.25
Lane Mean[47] (10 ksi limit on f_c')	$\left(\frac{4 f_{pt} d_b}{f'_c} - 21 \right) + \left(\frac{6.4 (f_{su} - f_{se}) d_b}{f'_c} + 26 \right)$	2.25
Martin and Scott[41]	$(f_{ps} - \frac{135}{d_b^{1/6}}) \frac{d_b}{0.39}$	2.18
Mitchell et al.[45]	$0.33 f_{si} d_b \sqrt{\frac{3}{f'_{ci}}} + (f_{su} - f_{se}) d_b \sqrt{\frac{4.5}{f'_c}}$	2.22
Zia and Mostafa[42]	$(1.5 \frac{f_{si}}{f'_{ci}} d_b - 4.6) + 1.25 (f_{su} - f_{se}) d_b$	2.19

d_b Prestressing strand diameter

f_{pt} Stress in prestressing strand prior to release

f_{si} Stress in prestressing strand immediately after release (f_{pt}-ES)

f_{se} Stress in prestressing strand after all losses (f_{pt}-ES-CR-SH)

f_{pe} Same as f_{se}

f_{ps} Stress in prestressing strand at member nominal strength

f_{su} Ultimate stress of prestressing strand

ES   Prestress losses due to elastic shortening

CR   Prestress losses due to creep

SH   Prestress losses due to shrinkage

f_{ci}' Concrete compressive strength at release

f_c' Concrete compressive strength at time of testing

M_n Nominal moment capacity of a member

M_{cr} Cracking moment capacity of a member

I_t Transformed moment of inertia of a member

λ $1.0 \le [\lambda = (0.6+40\varepsilon_{ps})] \le 2.0$

In order to compare the experimentally measured development length values with code and suggested equation results, the following relationship was used to determine the average difference between equation and experimental results:

$$Average\ Difference = \frac{l_{d(Equation)} - l_{d(Experimental)}}{l_{d(Equation)}}$$ (13.3)

By performing the difference comparison in this manner, the code or suggested equation served as the accepted value. If the experimental development length is less than that predicted, the ratio is positive, indicating a conservative prediction.

13.8.3 Results of Experimental and Predicted Results

Table 13.9 compares predicted and experimental development lengths.

329

Table 13.9 Overview of Development Length Prediction Results for HSLC

Equation Source	Equation	Overall Results		
		Avg Diff (%)	Max Over (%)	Max Under (%)
AASHTO[40] / ACI[2]	$(f_{ps} - \tfrac{2}{3}f_{se})d_b$	19%	30%	8%
Barnes, Burns, Kreger[55]	$1.25\left(\dfrac{f_{pt}}{\sqrt{f_{ci}'}} + (f_{ps}-f_{pe})\right)d_b$	37%	47%	31%
Buckner[46]	$f_{si}\dfrac{d_b}{3} + \lambda\,(f_{su}-f_{se})d_b$	42%	54%	18%
Deatherage et al.[43]	$f_{si}\dfrac{d_b}{3} + 1.5(f_{su}-f_{se})d_b$	44%	54%	39%
Lane 95%[47]	$\left(\dfrac{4f_{pt}d_b}{f_c'}-5\right)+\left(\dfrac{6.4(f_{su}-f_{se})d_b}{f_c'}+15\right)$	7%	30%	-28%
Lane 95%[47] (10 ksi limit on f_c')	$\left(\dfrac{4f_{pt}d_b}{f_c'}-5\right)+\left(\dfrac{6.4(f_{su}-f_{se})d_b}{f_c'}+15\right)$	17%	32%	1%
Lane Mean[47]	$\left(\dfrac{4f_{pt}d_b}{f_c'}-21\right)+\left(\dfrac{6.4(f_{su}-f_{se})d_b}{f_c'}+26\right)$	1%	27%	-39%
Lane Mean[47] (10 ksi limit on f_c')	$\left(\dfrac{4f_{pt}d_b}{f_c'}-21\right)+\left(\dfrac{6.4(f_{su}-f_{se})d_b}{f_c'}+26\right)$	12%	28%	-5%
Martin and Scott[41]	$(f_{ps}-\dfrac{135}{d_b^{1/6}})\dfrac{d_b}{0.39}$	58%	63%	50%
Mitchell et al.[45]	$0.33 f_{si} d_b\sqrt{\dfrac{3}{f_{ci}'}}+(f_{su}-f_{se})d_b\sqrt{\dfrac{4.5}{f_c'}}$	-27%	2%	-60%
Zia and Mostafa[42]	$(1.5\dfrac{f_{si}}{f_{ci}'}d_b - 4.6)+1.25(f_{su}-f_{se})d_b$	6%	24%	-3%

The average difference was calculated using equation 13.3 for the twelve lightweight girder tests and the eight normal weight HPC girder tests and is listed in the "Avg Diff" column. The "Max Over" column lists greatest positive percent difference between the

330

predicted and experimental value. The "Max Under" column lists the greatest negative percent difference between the predicted and experimental value.

13.8.3.1 Results of Analysis Based on Average Difference

Analysis of Table 13.9 showed that the equation by Zia and Mostafa produced the best overall prediction of development length. The Zia and Mostafa equation would be considered a "best-fit" equation where a "best-fit" equation was defined as the equation having the lowest average difference between experimental and predicted values as well as not having excessive overestimates or underestimates. Lane's Mean equation was within 1 percent on average, but had a maximum underestimate of −39 percent. Lane's 95 percent confidence equation was within 7 percent on average, but had a maximum underestimate of −28 percent. The AASHTO/ACI equation and equations by Lane (95 percent confidence with 10 ksi cap on f_c'), Barnes, Burns and Kreger, Buckner, Deatherage et al., and Martin and Scott did not provide as accurate a prediction, but always provided a conservative estimate of development length. Martin and Scott's equation as well as the equation by Deatherage et al. were overly conservative.

13.8.3.2 Results of Analysis Based on Maximum Underestimate

Analysis of Table 13.9 based on maximum underestimate showed that Lane's 95 percent confidence equation having a 10 ksi cap on f_c' to provide a good overall estimate of development length without being overconservative. This equation would be the best choice as a "design" equation. A "design" equation was defined as the equation having the lowest positive maximum underestimate value without being overly conservative.

The most favorable combination of these two values indicated the best "design" equation. Lane's 95 percent confidence equation having a 10 ksi cap on f_c' had a maximum underestimate value of 1 percent, which indicates the equation did not under predict any value, and had an average difference of 17 percent. The AASHTO/ACI equation produced a maximum underestimate of 8 percent again indicating the equation did not under predict any value, and had an average difference of 19 percent. The equation by Zia and Mostafa produced a maximum underestimate of -3 percent and had an average difference of 6 percent. Equations by Barnes, Burns and Kreger, Buckner, Martin and Scott, and Deatherage et al. never underestimated development lengths, but all had average differences in excess of 35 percent.

13.8.3.3 Evaluation of Top Five "Best-Fit" and "Design" Equations

Tables 13.10 and 13.11 show a listing of the top five equations in both the "best-fit" and "design" categories. From these tables it was possible to identify which variables used in the flexural bond portion of the equations were the best predictors. The variables d_b, f_{se}, f_{ps}, f_{su} and f_c' appeared to be the most important in predicting development length.

332

Table 13.10 Review of Top Five "Best-Fit" Equations

Best-Fit Equations						
Rank	Equation Source	Equation	Equation Variables			
			d_b	f_{se}	f_{su}	f_c'
1	Zia and Mostafa[42]	$(1.5\frac{f_{si}}{f_{ci}'}d_b - 4.6) + 1.25(f_{su}-f_{se})d_b$	X	X	X	
2	Lane Mean[47] (10 ksi limit on f_c')	$\left(\frac{4f_{pt}d_b}{f_c'}-21\right)+\left(\frac{6.4(f_{su}-f_{se})d_b}{f_c'}+26\right)$	X	X	X	X
3	Lane Mean[47]	$\left(\frac{4f_{pt}d_b}{f_c'}-21\right)+\left(\frac{6.4(f_{su}-f_{se})d_b}{f_c'}+26\right)$	X	X	X	X
4	Lane 95%[47]	$\left(\frac{4f_{pt}d_b}{f_c'}-5\right)+\left(\frac{6.4(f_{su}-f_{se})d_b}{f_c'}+15\right)$	X	X	X	X
5	Lane 95%[47] (10 ksi limit on f_c')	$\left(\frac{4f_{pt}d_b}{f_c'}-5\right)+\left(\frac{6.4(f_{su}-f_{se})d_b}{f_c'}+15\right)$	X	X	X	X

Table 13.11 Review of Top Five "Design" Equations

Design Equations							
Rank	Equation Source	Equation	Equation Variables				
			d_b	f_{se}	f_{ps}	f_{su}	f_c'
1	Lane 95%[47] (10 ksi limit on f_c')	$\left(\frac{4f_{pt}d_b}{f_c'}-5\right)+\left(\frac{6.4(f_{su}-f_{se})d_b}{f_c'}+15\right)$	X	X		X	X
2	Zia and Mostafa[42]	$(1.5\frac{f_{si}}{f_{ci}'}d_b - 4.6)+1.25(f_{su}-f_{se})d_b$	X	X		X	
3	Lane Mean[47] (10 ksi limit on f_c')	$\left(\frac{4f_{pt}d_b}{f_c'}-21\right)+\left(\frac{6.4(f_{su}-f_{se})d_b}{f_c'}+26\right)$	X	X		X	X
4	AASHTO[40] / ACI[2]	$(f_{ps}-\tfrac{2}{3}f_{se})d_b$	X	X	X		
5	Barnes, Burns, Kreger[55]	$1.25\left(\frac{f_{pt}}{\sqrt{f_{ci}'}}+(f_{ps}-f_{pe})\right)d_b$	X	X	X		

333

13.9 Development of an Improved Development Length Equation

13.9.1 Determination of Equation Forms

Two equations were presented in Chapter 9 for predicting transfer length. One

goal in determining a new development length equation was to incorporate the suggested

transfer length relations. The two transfer length equations suggested were:

Best Fit Equation:

$$l_t = 50 d_b \sqrt{\frac{4000}{f'_{ci}}} \qquad (9.6)$$

Design Equation:

$$l_t = 50 d_b \sqrt{\frac{6000}{f'_{ci}}} \qquad (9.7)$$

Based on equations suggested by other researchers in Tables 13.10 and 13.11, the

following equation characteristics were thought to show promise:

- Equations including d_b

- Equations incorporating $(f_{su} - f_{se})$

- Equations incorporating $(f_{ps} - f_{se})$

- Equations incorporating f'_c

- Equations based on current ACI or AASHTO forms

- Equations incorporating the transfer length equation suggested in this research

Using these guidelines, numerous equation forms were evaluated using data from the 20 development length tests from this research and that by Dill.[84] Percent difference was calculated using the following expression as articulated in Chapter 9.

$$Average\ Difference = \frac{l_{d(Equation)} - l_{d(Experimental)}}{l_{d(Experimental)}} \qquad (9.3)$$

13.9.2 Results of Equation Analysis

Sixteen equation forms were investigated which incorporated the basic form of the suggested transfer length equations. Current code equation forms were modified to provide more accurate results. Concrete compressive strengths were based on accelerated curing during the first 24 hours. All strand stress values were based on VWSG data. Two equation forms emerged from the process that met the "best fit" and "design" equation criteria. The most promising "best fit" equation was:

$$\left(50\sqrt{\frac{2500}{f'_{ci}}} + f_{ps} - f_{se} \right) d_b \qquad (13.3)$$

The most promising "design" equation was:

$$\left(50\sqrt{\frac{5000}{f'_{ci}}} + f_{ps} - f_{se} \right) d_b \qquad (13.4)$$

The "best-fit" equation has the smallest average difference and the most promising "design" equation has the smallest positive maximum under length prediction. The initial term of each equation is very similar to the equations for transfer length. Close comparison and evaluation indicates that the transfer length portion of the equation is apparently reduced in the development length equation. This further indicates the trends seen in the strand stress plots in Appendix Q and discussed in Section 13.7.1.2. As the girder was loaded, the strands tended to transfer more force in a region somewhat shorter than the specified transfer length. Tables 13.12 and 13.13 provide a comparison of the above equations with the top ranked "best fit" and "design" equations and current code equations. The comparison shows that the proposed equations provide better predictions of development, especially the design equation.

Table 13.12 Comparison of Proposed Best Fit Equation With Other Equations

Equation Source	Best Fit Equation	Overall Results		
		Avg Diff (%)	Max Over (%)	Max Under (%)
Proposed Equation	$\left(50\sqrt{\dfrac{2500}{f_{ci}'}} + f_{ps} - f_{se}\right)d_b$	1%	21%	-6%
Zia and Mostafa[42]	$(1.5\dfrac{f_{si}}{f_{ci}'}d_b - 4.6) + 1.25(f_{su} - f_{se})d_b$	6%	24%	-3%
AASHTO[40] / ACI[2]	$(f_{ps} - \tfrac{2}{3}f_{se})d_b$	19%	30%	8%

Table 13.13 Comparison of Proposed Design Equation With Other Equations

Equation Source	Design Equation	Overall Results		
		Avg Diff (%)	Max Over (%)	Max Under (%)
Proposed Equation	$\left(50\sqrt{\dfrac{5000}{f_{ci}'}}+f_{ps}-f_{se}\right)d_b$	9%	31%	0%
Lane 95% [47] (10 ksi limit on f_c')	$\left(\dfrac{4f_{pt}d_b}{f_c'}-5\right)+\left(\dfrac{6.4(f_{su}-f_{se})d_b}{f_c'}+15\right)$	17%	32%	1%
AASHTO[40] / ACI[2]	$(f_{ps}-\tfrac{2}{3}f_{se})d_b$	19%	30%	8%

13.9.3 Proposed Equation Evaluation for use on HSLC

Table 13.14 provides a comparison of results for the proposed equation for HSLC and high strength normal weight concrete.

Table 13.14 Proposed Equation Evaluation for use on HSLC

Basis of Comparison	AASHTO[40] ACI[2] Code $(f_{ps}-\tfrac{2}{3}f_{se})d_b$	Proposed Equation For Design $\left(50\sqrt{\dfrac{5000}{f_{ci}'}}+f_{ps}-f_{se}\right)d_b$	Proposed Equation For Best Fit $\left(50\sqrt{\dfrac{2500}{f_{ci}'}}+f_{ps}-f_{se}\right)d_b$
Avg Diff (HSLC)	19%	13%	4%
Max Over (HSLC)	30%	31%	21%
Max Under (HSLC)	8%	2%	-6%
Avg Diff (NWC)	18%	2%	-5%
Max Over (NWC)	18%	4%	-3%
Max Under (NWC)	17%	0%	-6%
Avg Diff (Overall)	19%	9%	1%
Max Over (Overall)	30%	31%	21%
Max Under (Overall)	8%	0%	-6%

Table 13.14 showed the AASHTO/ACI equation gave consistent and conservative values for both HSLC and NWC. There appears to be more scatter in the values for HSLC than for NWC. The proposed equation for design produced more conservative results for HSLC than for NWC. Since the proposed equation incorporates a term addressing initial concrete compressive strength, this could indicate the equation becomes less conservative as initial compressive strength increases. The initial compressive strengths for the NWC were about 5,000 psi higher than the HSLC strengths on average. Similar trends are seen for the proposed best-fit equation. Figure 13.12 provides a plot of the results in Table 13.14.
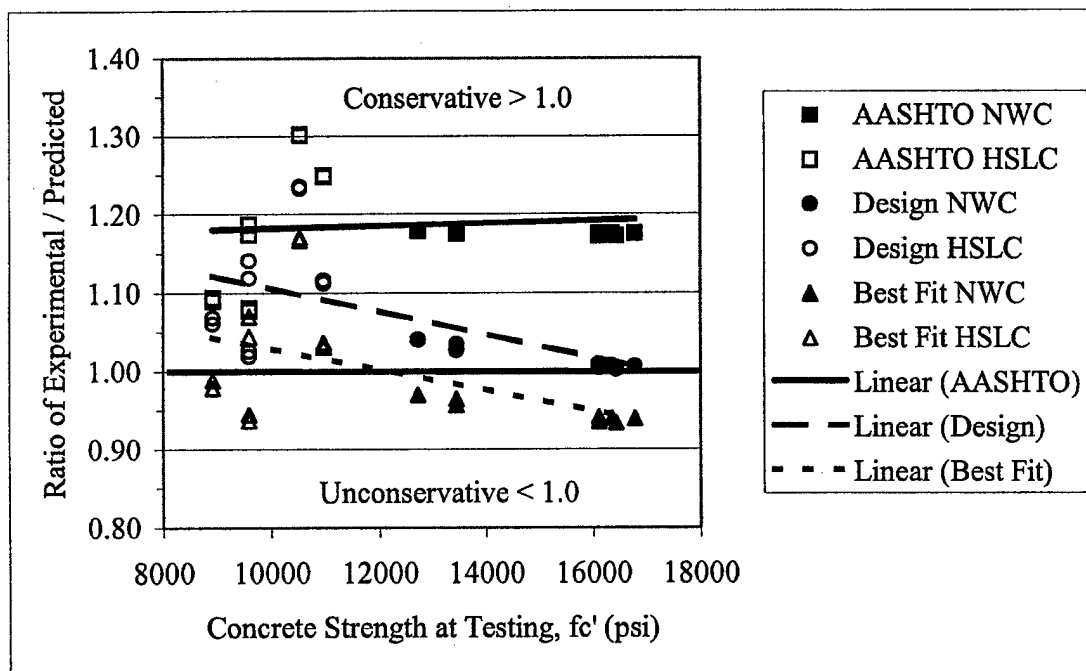
Figure 13.12 Comparison of Design and Best-Fit Equations to AASHTO Equation

To further verify the proposed equations, data from other researchers on HSLC would be useful. Yet no other development length data has been published for 0.6-inch prestressing strand used in lightweight concrete. Evaluation using data from other NWC and sand lightweight concrete tests would prove useful for comparison and further verification.

13.10   Conclusions

An evaluation of current code provisions using the twelve slate HSLC girder development length tests in this study and eight normal weight HPC girder tests from Dill[82] showed the current AASHTO[40] and ACI[2] provisions to be conservative. The code equations overestimated development lengths by 19 percent for both slate HSLC and normal weight HPC and never underestimated them. Use of the current code provisions for design of development length for slate HSLC and 0.6-inch diameter strand was conservative. Based on the concrete strength range addressed in this research project, modification of the current code specifications for development length was not necessary for HSLC or for 0.6-inch diameter strands.

An evaluation of other suggested equations for predicting development length showed an equation by Zia and Mostafa[42] to provide the best overall prediction of development length. Equations by Lane as identified in Table 13.10 also produced good overall predictions. The above equations were applicable to both slate HSLC and normal weight HPC with good results.

Based on an evaluation of 16 different equation forms, two new equations were suggested. The new equations for predicting development length based on "best-fit" and

339

"design" produced more accurate results than current code specifications and showed slight improvements over other suggested equation forms.

Test results showed conclusively that shear cracking in the transfer length region across the bottom strands did not induce significant strand slip if stirrup density was doubled over the current AASHTO[40] specified density in the region.

The addition of silica fume into the mix design at a 10% replacement rate by weight of cementitious materials substantially reduced development length. Although the silica fume increased compressive strength and early strength, the apparent major impact was the creation a much better bond between the prestressing strand and the concrete matrix.

There was no indication throughout this analysis that need existed to differentiate between slate HSLC and normal weight HPC. With regard to development length, for concrete compressive strengths over 8,000 psi, the prediction of development length was the same for both lightweight and normal weight concrete.

CHAPTER XIV

CONCLUSIONS AND RECOMMENDATIONS

14.1 Conclusions

Conclusions are presented in the following sections by topic.

14.1.1 Analytical Investigation

The use of HSLC has the potential to increase the length of simple span AASHTO

Type IV and V sections up to four percent and Bulb-Tee sections up to three percent.

However, AASHTO Type II and III sections do not benefit appreciably from the use of

HSLC. The Modified Bulb-Tee section extended the length of a Standard Bulb-Tee by

10 feet using 8, 10 and 12 ksi HSLC or high-strength NWC. Bulb-Tee (Standard or

Modified) sections provided longer spans at less weight for girders over 105 feet in

length when compared to AASHTO sections. For spans between 125 feet and 155 feet,

the use of HSLC can reduce the gross vehicle weight to less than 150 kips so that a super-

load permit is not required for transport of long span girders.

14.1.2 HSLC Mixes and Properties

HSLC mixes were developed in the laboratory for 8,000 psi and 10,000 psi using

slate lightweight ½-in coarse aggregate and normal weight, natural sand. The dry unit

weight of the concretes was approximately 117 and 119 pcf, respectively. A 12,000 psi

design strength mix could not be developed. The strengths of mixes using lightweight fine aggregate could not be controlled, therefore no recommended mix used lightweight fines.

The laboratory mixes were verified during field production. The field mixes yielded slightly higher strengths than found in the laboratory. Close monitoring of LWA moisture was required.

The HSLC, both 8,000 psi and 10,000 psi design strength continued to gain strength over the 100-day test period. Accelerated cured cylinders, which matched curing conditions of precast beams showed about 25 percent higher one-day strength than ASTM cured cylinders; at 56 days, the ASTM cured cylinders were about 4% stronger than the accelerated cured cylinders. Equation 7.4 was developed and provides a better estimate of the modulus of elasticity for slate HSLC than previous relations for normal strength concretes.

14.1.3 Transfer Length

An evaluation of current code provisions using the 12 HSLC transfer lengths in this research and 8 normal weight HPC transfer lengths from Reutlinger[84] showed the current AASHTO[40] and ACI[2] equations to be conservative. The AASHTO equation overestimated transfer lengths by 42% on average and never underestimated transfer lengths. The ACI equation using VWSG data to determine prestressing strand stress also overestimated transfer lengths by 46% and never underestimated transfer lengths. Use of either the AASHTO or ACI equations to predict transfer length for slate HSLC was conservative. Based on the concrete strength range addressed in this research project,

modification of the current code specifications for transfer lengths was not necessary for slate HSLC.

An evaluation of other suggested equations for predicting transfer length showed an equation by Mitchell et al.[45] to provide the best overall prediction of transfer length. Equations by Buckner[46] and Deatherage et al.[43] also produced good overall predictions. The above equations were applicable to both slate HSLC and normal weight HPC with good results.

An evaluation of the applicability of initial concrete compressive strength, f_{ci}', and initial modulus of elasticity, E_{ci}, and 32 possible equation forms showed that d_b and f_{ci}' were the best parameters for predicting transfer length.

There was no indication throughout this analysis that a need existed to differentiate between slate HSLC and normal weight HPC with regard to transfer length. For initial concrete strengths, f_{ci}', over 6,000 psi, the prediction of transfer length was the same for both slate lightweight and normal weight concrete.

14.1.4 Flexural Behavior

The current prediction of cracking stress and cracking moment, when examined for slate HSLC, showed indications of becoming unconservative as concrete compressive strengths approached 11,000 psi. In some cases, the predicted cracking moments exceeded the experimental values. The use of a lambda factor (λ) of 0.85 for HSLC made with slate LWA produced conservative results on average for compressive strengths below 11,000 psi. More research is required to examine a potential tension

strength ceiling for HSLC and adjustments to lambda for concrete compressive strengths over 10,000 psi.

The modulus of rupture test, ASTM C 78[82], did not accurately predict the cracking stress of HSLC girders.

The current AASHTO procedure for ultimate moment calculation was conservative for slate HSLC girders with normal weight concrete decks having a compressive strength under 6,000 psi.

14.1.5 Shear Behavior

The current AASHTO[40] Standard specification provided a conservative prediction of concrete and ultimate shear capacity when shear steel capacity was capped at a yield strength of 60 ksi. The alternate design procedure listed in ACI-318[2] Section 11.4.2.2 for predicting shear strength produced some unconservative predictions for concrete compression strengths over 10,000 psi. The method for predicting interface shear strength was conservative for slate HSLC.

The current AASHTO LRFD[92] specification provided a conservative prediction of ultimate shear strength for slate HSLC.

The variable angle truss model provided an overconservative prediction of shear capacity in HSLC girders.

14.1.6 Development Length

An evaluation of current code provisions using the twelve HSLC girder development length tests in this study and eight normal weight HPC girder tests from

344

Dill[84] showed the current AASHTO[40] and ACI[2] provisions to be conservative. The code equations overestimated development lengths by 19 percent for both HSLC and normal weight HPC and never underestimated them. Use of the current code provisions for design of development length for slate HSLC and 0.6-inch diameter strand was conservative. Based on the concrete strength range addressed in this research project, modification of the current code specifications for development length was not necessary for HSLC or for 0.6-inch diameter strands.

An evaluation of other suggested equations for predicting development length showed an equation by Zia and Mostafa[42] to provide the best overall prediction of development length. Equations by Lane[47] as identified in Table 13.10 also produced good overall predictions. The above equations were applicable to both slate HSLC and normal weight HPC with good results.

Test results showed conclusively that shear cracking in the transfer length region across the bottom strands did not induce significant strand slip if stirrup density was doubled over the current AASHTO[40] specified density in the region.

The addition of silica fume into the mix design at a 10% replacement rate by weight of cementitious materials gave indications of reducing development length.

There was no indication throughout this analysis that need existed to differentiate between slate HSLC and normal weight HPC. With regard to development length, for concrete compressive strengths over 8,000 psi, the prediction of development length was the same for both slate lightweight and normal weight concrete.

14.2 Recommendations

Recommendations are presented in the following sections by topic.

14.2.1 Analytical Investigation

When designing girders in excess of 105 feet, use Bulb-Tee sections (Standard or Modified). Use the Modified Bulb-Tee (one additional layer of strands in a 2-in deeper bottom flange) to gain an additional 10 feet in span length instead of designing for the next larger size Bulb-Tee section. Use slate HSLC to reduce both girder and gross vehicle weight.

14.2.2 HSLC Mixes and Properties

Accurately control the absorbed water in the LWA. Determine the percentage of absorbed moisture above which mix water will not be absorbed during concrete batching. Apply water by sprinkling or other method to the LWA stockpile for a sufficient length of time prior to batching such that the absorbed moisture is in excess of the minimum required amount. Test the LWA as often as is necessary during batching to insure that moisture contents are within the tolerance of the given mix design.

Use match curing of cylinders to predict initial strength of the concrete for precast prestressed concrete girder production. For later age testing (28-days and after) ASTM cured specimens are adequate. The 4 x 8 cylinders provide a reliable measure of compressive strength and may be used in place of 6 x 12 cylinders.

Use Equation 7.4 to predict the modulus of elasticity for slate HSLC.

346

$$E_c = 44,000\sqrt{f_c' \frac{w_c}{145}}$$ (7.4)

14.2.3 Transfer Length

Use the current AASHTO[40] and ACI[2] equations to conservatively predict transfer

length in pretensioned girders constructed with slate HSLC and 0.6-in pretensioning

strands. For a more accurate prediction that is still conservative, use equation 9.7.

$$50\, d_b \sqrt{\frac{6000}{f'_{ci}}}$$ (9.7)

14.2.4 Flexural Behavior

Do not use the modulus of rupture test, ASTM C 78,[82] for determining the

cracking stress and cracking moment for pretensioned slate HSLC girders.

More research is required to examine a potential tension strength ceiling for

HSLC, as related to flexural cracking, and adjustments to lambda for concrete

compressive strengths over 10,000 psi.

Use the current AASHTO procedure for ultimate moment calculation for slate

HSLC girders with normal weight concrete decks having a compressive strength under

6,000 psi.

14.2.5 Shear Behavior

Use the current AASHTO Standard specification to provide a conservative prediction of concrete and ultimate shear capacity in slate HSLC pretensioned girders when shear steel capacity is capped at a yield strength of 60 ksi.

More research is required to examine a potential tension strength ceiling for HSLC, as related to diagonal tension cracking, and adjustments to lambda for concrete compressive strengths over 10,000 psi. Examination of the alternate design procedure listed in ACI-318 Section 11.4.2.2 for predicting shear strength, V_c, is necessary for concrete compressive strengths over 10,000 psi.

The AASHTO Standard Specification can be used to conservatively predict interface shear strength between slate HSLC and normal weight concrete.

The AASHTO LRFD Specification can be used to conservatively predict ultimate shear strength in slate HSLC pretensioned girders.

14.2.6 Development Length

The current AASHTO[40] and ACI[2] provisions can be used to conservatively predict development length in pretensioned girders constructed with slate HSLC and 0.6-in diameter pretensioning strands. For a more accurate prediction that is still conservative, use equation 13.4.

$$\left(50\sqrt{\frac{5000}{f_{ci}'}} + f_{ps} - f_{se}\right)d_b \tag{13.4}$$

In the transfer length region, use two times the stirrup density currently specified by the AASHTO[40] Standard Specification to limit strand slip in the event of shear cracking.

Use silica fume at up to a 10% replacement rate by weight of cementitious materials to reduce development length.

14.2.7 Future Research

As a result of this research project, some areas requiring additional research became apparent.

First, the tension strength ceiling of HSLC and its effect on diagonal tension cracking strength and flexural cracking strength is unknown. The overall relation between concrete strength and the LWC reduction factor, λ, requires examination, especially for concrete compressive strengths over 10,000 psi.

Second, a spectrum of testing using the same concrete strengths with varying amounts of silica fume is required to determine its exact impact on development length.

Third, based on the tremendous property variation between different types of LWA, there is a need to thoroughly investigate the use of various light weight aggregates in like test configurations to determine material specific factors for each category of design.

REFERENCES

1. Murillo, J. A., Thoman S., Smith, D., "Lightweight Concrete for a Segmental Bridge," *Civil Engineering*, Vol. 64, No. 5, May 1994, pp. 68-70.

2. *Building Code Requirements for Reinforced Concrete*, ACI 318-99, *and Commentary*, ACI 318R-99, American Concrete Institute, Detroit, 1999.

3. Harmon, K., "Physical Characteristics of Rotary Kiln Expanded Slate Lightweight Aggregate," *Proceedings, Second International Symposium on Structural Lightweight Aggregate Concrete*, Kristiansand, Norway, June 2000, 11 pp.

4. Raithby, K. D., Lydon, F. D., "Lightweight Concrete in Highway Bridges," *The International Journal of Cement Composites and Lightweight Concrete*, Vol. 2, No. 3, May 1981, pp. 133-146.

5. Bender, B. F., "Economics and Use of Lightweight Concrete in Prestressed Structures," *PCI Journal*, Vol. 35, No. 6, November-December 1980, pp. 62-67.

6. Brown, W. R., Davis, C. R., *A Load Response Investigation of Long Term Performance of a Prestressed Lightweight Concrete Bridge at Fanning Springs, Florida*, Final Report, No. FL/DOT/SMO-93-401, Florida Department of Transportation, April 1993, 66 pp.

7. Hansen, H. H., "Shelby Creek Bridge," *Portland Cement Association Engineered Concrete Structures*, Vol. 5, No. 2, August 1992, p. 3.

8. Roberts, J. E., "Lightweight Concrete Bridges for California Highway System," *ACI SP 136*, American Concrete Institute, Detroit, 1992, pp. 254-271.

9. Expanded Shale, Clay and Slate Institute, "Back-up Statistics to Building Bridges," Information Sheet # 470.4, Salt Lake City, June 1994, 15 pp.

10. Melby, K., Jordet, E. A., Hansvold, C., "Long-span Bridges in Norway Constructed in High-Strength LWA Concrete," *Engineering Structures*, Vol. 18, No. 11, November 1996, pp. 845-849.

11. Holm, T. A., Bremner, T. W., *State-of-the-Art Report on High-Strength, High-Durability Structural Low-Density Concrete for Applications in Severe Marine Environments*, U. S. Army Corps of Engineers Engineer Research and Development Center No. ERDC/SL TR-00-3, August 2000, 103 pp.

12. Shideler, J. J., "Lightweight-Aggregate Concrete for Structural Use," *Journal of the American Concrete Institute*, Vol. 54, No. 10, October 1957, pp. 299-328.

13. Wang, P. T., Shah, S. P., Naaman A. E., "Stress-Strain Curves of Normal and Lightweight Concrete in Compression," *ACI Journal*, Vol. 75, No. 11, November 1978, pp. 603-611.

14. Hanson, J. A., "Tensile Strength and Diagonal Tension Resistance of Structural Lightweight Concrete," *Journal of the American Concrete Institute*, Vol. 58, No. 1, July 1961, pp. 1-37.

15. ASTM C 127, *Standard Test Method for Specific Gravity and Absorption of Coarse Aggregate*, American Society for Testing and Materials, West Conshohocken, PA, 1993, 5 pp.

16. ASTM C 128, *Standard Test Method for Specific Gravity and Absorption of Fine Aggregate*, American Society for Testing and Materials, West Conshohocken, PA, 1997, 5 pp.

17. Bremner, T. W., Newman, "Microstructure of Low Density Concrete Aggregate," *Proceedings of the Ninth Congress of the Federation Internationale de la Precontrainte*, Volume 3, Commission Reports, Stockholm, June 1982.

18. *ACI Manual of Concrete Practice*, "Standard Practice for Selecting Proportions for Structural Lightweight Concrete (ACI 211.2-91), American Concrete Institute, Detroit, 1996.

19. Pfeiffer, D. W., "Sand Replacement in Structural Lightweight Concrete," *ACI Journal*, Vol. 64, No. 7, July 1967, pp. 384-392.

20. Fujji, K., Kakizaki, M., Edahiro, H., Unisuga, Y., Yamamoto, Y., "Properties of High-Strength and High-Fluidity Lightweight Concrete," *ACI SP 179*, American Concrete Institute, Detroit, pp. 254-271.

21. Leming, M. L., *Properties of High Strength Concrete – An Investigation of High Strength Concrete Characteristics using Materials in North Carolina*, Final Report, No. 23241-86-3, North Carolina Department of Transportation, July 1988 186 pp.

351

22. Mor, A., "Steel-Concrete Bond in High Strength Lightweight Concrete," *ACI Materials Journal*, Vol. 89, No. 1, January-February 1992, pp. 76-82.

23. Smeplass, S., "Moisture in Light Weight Aggregates – Practical Consequences for the Production Properties of Light Weight Aggregate Concrete", *Proceedings, Second International Symposium on Structural Lightweight Aggregate Concrete*, Kristiansand, Norway, June, 2000.

24. Holm, T. A., Valsangkar, A. J., "Lightweight Aggregate Soil Mechanics: Properties and Applications," *Transportation Research Record 1422; Soils, Geology, and Foundations; Lightweight Artificial and Waste Materials for Embankments Over Soft Soils*, Transportation Research Board, January 1993, pp. 7-13.

25. Valum, R., Nilsskog, J. E., "Production and Quality Control of High Performance Lightweight Concrete for the Raftsundet Bridge," *Proceedings of the Fifth International Symposium on Utilization of High Strength / High Performance Concrete, Sandefjord, Norway*, June 2000, pp. 909-918.

26. Hoff, G. C., "High Strength Lightweight Aggregate Concrete for Arctic Applications," *ACI SP 136*, American Concrete Institute, Detroit, 1992, pp. 1-65.

27. Morales, J., *Short-Term Mechanical Properties of High Strength Lightweight Concrete*, Report 82-9 on NSF Grant No. ENG78-05124, Ithaca, August 1982.

28. Leming, M. L., *Creep and Shrinkage of Lightweight Concrete*, North Carolina State University Publication, 1990, 4 pp.

29. FIP Committee, "Chapter 7, Design of Prestressed Lightweight Concrete Structures," *Federation Internationale de la Precontrainte Manual of Lightweight Aggregate Concrete, 2nd Edition*, 1983, pp. 168-206.

30. Bilodeau, A., Chevrier, R., Malhotra, M., Hoff, G. C., "Mechanical Properties, Durability and Fire Resistance of High-Strength Lightweight Concrete," *Proceedings of the International Symposium on Structural Lightweight Aggregate Concrete*, Sandefjord, Norway, June 1995, pp. 432-443.

31. Holm, T. A., Bremner, T. W., "Chapter 10, High Strength Lightweight Aggregate Concrete," *High Performance Concretes and Applications*, S. P. Shah and S. H. Ahmad, ed., Edward Arnold, London, pp. 341-374.

32. Carolina Stalite, Information from Carolina Stalite Company, Salisbury, NC, 2000, 6 pp.

33. Holm, T. A., Bremner, T. W., "70 Year Performance record for High-Strength Structural Lightweight Concrete," *Proceedings of the First Materials Engineering Congress, Serviceability & Durability of Construction Materials*, Denver, August 2000, pp. 884-893.

34. Bremner, T. W., Holm, T. A., "Elastic Compatibility and the Behavior of Concrete," *ACI Journal*, Vol. 83, No. 2, March-April 1986, pp. 244-250.

35. Kohno, K., Okamoto, T., Isikawa, Y., Sibata, T., Mori, H., "Effects of Artificial Lightweight Aggregate on Autogenous Shrinkage of Concrete," *Cement and Concrete Research*, Vol. 29, 1999, pp. 611-614.

36. Bremner, T. W., Holm, T. A., Ries, J. P., "Enhanced Hydration and Properties of Specified Density Concrete," Expanded Shale, Clay and Slate Institute Information Sheet 4284.1, February 2001, 8 pp.

37. Reutlinger, C., "Direct Pull-Out Capacity and transfer Length of 0.6-inch Diameter Prestressing Strand in High-Performance Concrete," Masters Thesis, Georgia Institute of Technology, Atlanta, GA, May 1999, 352 pp.

38. Janney, J. R., "Nature of Bond in Pre-Tensioned Prestressed Concrete," *Journal of the American Concrete Institute*, Vol. 50, No. 9, May 1954, pp. 717-736.

39. Hanson, N. W., Karr, P. H., "Flexural Bond Tests of Pretensioned Prestressed Beams," *Journal of the American Concrete Institute*, Vol. 55, No. 7, January 1959, pp. 783-802.

40. *Standard Specifications for Highway Bridges*, 16th ed., American Association of State Highway and Transportation Officials, Washington, D. C., 1996.

41. Martin, L. D., Scott, N. L., "Development of Prestressing Strand in Pretensioned Members," *ACI Journal*, Vol. 73, No. 8, August 1976, pp. 453-456.

42. Zia, P., Mostafa, T., "Development Length of Prestressing Strands," *PCI Journal*, Vol. 22, No. 5, September/October 1977, pp. 54-65.

43. Deatherage, J. H., Burdette, E. G., and Chew, C. K., "Development Length and Lateral Spacing Requirements of Prestressing Strand for Prestressed Concrete Bridge Girders," *PCI Journal*, Vol. 39, No. 1, January/February 1994, pp. 70-83.

44. Russell, B. W., "Design Guidelines for Transfer, Development and Debonding of Large Diameter Seven Wire Strands in Pretensioned Concrete Girders," Doctoral Thesis, The University of Texas at Austin, 1992, 464 pp.

45. Mitchell, D., Cook, W. D., Khan, A. A., Tham, T., "Influence of High Strength Concrete on Transfer and Development Length of Pretensioning Strand," *PCI Journal*, Vol. 38, No. 3, May/June 1993, pp. 52-56.

46. Buckner, C. D., "A Review of Strand Development Length for Pretensioned Concrete Members," *PCI Journal*, Vol. 40, No. 2, March/April 1995, pp. 84-105.

47. Lane, S. N., *A New Development Length Equation for Pretensioned Strands in Bridge Beams and Piles, Final Report*, No. FHWA-RD-98-116, Federal Highway Administration, December 1998, 131 pp.

48. Collins, M. P., Mitchell, D., *Prestressed Concrete Structures*, Prentice Hall, Englewood Cliffs, New Jersey, 1991.

49. Nawy, E. G., *Prestressed Concrete A Fundamental Approach*, Third Edition, Prentice Hall, Upper Saddle River, New Jersey, 2000,

50. Lin, T. Y., Burns, N. H., *Design of Prestressed Concrete Structures*, Third Edition, John Wiley and Sons, New York, New York, 1981.

51. Holm, T. A., Personal telephone conversation on March 25, 2002 concerning the origination of the lightweight concrete factor, λ.

52. Johnson, M. K., Ramirez, J. A., "Minimum Shear Reinforcement in Beams with Higher Strength Concrete," *ACI Structural Journal*, Vol. 86, No. 4, July-August 1989, pp. 376-382.

53. *Building Code Requirements for Reinforced Concrete*, ACI 318-89, *and Commentary*, ACI 318R-89, American Concrete Institute, Detroit, 1989.

54. Shahawy, M. A., Batchelor, B., "Shear Behavior of Full-Scale Prestressed Concrete Girders: Comparison Between AASHTO Specifications and LRFD Code," *PCI Journal*, Vol. 41, No. 3, May-June 1996, pp. 48-62.

55. Barnes, R. W., Burns, N. H., Kreger, M. E., "Development Length of 0.6-inch Prestressing Strand in Standard I-Shaped Pretensioned Concrete Beams," Research Report 1388-1, Center for Transportation Research, Bureau of Engineering Research, The University of Texas at Austin, December 1999, 318 pp.

56. Ma, J., Tadros, M. H., Baishya, M, "Shear Behavior of Pretensioned High-Strength Concrete Bridge I-Girders," *ACI Structural Journal*, Vol. 97, No. 1, January-February 2000, pp. 185-192.

57. Ramirez, J., Olek, J., Rolle, E., Malone, B., "Performance of Bridge Decks and Girders with Lightweight Aggregate Concrete, Final Report," Report FHWA/IN/JTRP-98/17, Purdue University, October 2000, 616 pp.

58. *Guide for Structural Lightweight Aggregate Concrete*, ACI 213, (Draft Copy for Voting by Committee 213), American Concrete Institute, Detroit, 2002.

59. Peterman, R. J., Ramirez, J. A., Olek, J., "Design of Semi-lightweight Bridge girders, Development Length Considerations," Transportation Research Board Record 1696, Paper No. 5B0063, Transportation Research Board, 2000.

60. Peterman, R. J., Ramirez, J. A., Olek, J., "Evaluation of Strand Transfer and Development Lengths in Pretensioned Girders with Semi-Lightweight Concrete," Final Report," Report FHWA/IN/JTRP-99/3, Purdue University, July 1999, 89 pp.

61. Kolozs, R. T., "Transfer and Development Lengths of Fully Bonded 1/2-Inch Prestressing Strand in Standard AASHTO Type I Pretensioned High Performance Lightweight Concrete (HPLC) Beams," Masters Thesis, The University of Texas at Austin, May 2000, 155 pp.

62. *Bond of Reinforcement in Concrete*, International Federation for Structural Concrete (fib) State-of-Art Report, Bulletin 10, Lausanne, Switzerland, 2000, 427 pp.

63. den Uijl, J. A., "Bond Modeling of Prestressing Strand," *ACI SP 180*, ed. Roberto Leon, American Concrete Institute, Farmington Hills, pp. 145-169.

64. Kahn, L. F., Saber, A., "Analysis and Structural Benefits of High Performance Concrete for Pretensioned Bridge Girders," *PCI Journal*, Vol. 45, No. 4, July/August 2000, pp. 100-107.

65. Meyer, K. F., Kahn, L. F., "Annotated Bibliography for High-Strength, Lightweight Prestressed Concrete Bridge Girders," Task 1 Report, Georgia Department of Transportation Project No. 2004, Georgia Institute of Technology, January 2001, 14 pp.

66. Shams, M., "Time-Dependent Behavior of High-Performance Concrete," Doctoral Thesis, Georgia Institute of Technology, May 2000, 572 pp.

67. ASTM C 330, *Standard Specification for Lightweight Aggregates for Structural Concrete*, American Society for Testing and Materials, West Conshohocken, PA, 1999, 4 pp.

68. ASTM C 33, *Standard Specification for Concrete Aggregates*, American Society for Testing and Materials, West Conshohocken, PA, 1999, 8 pp.

69. Mehta, P. K., Monteiro, P. J. M., *Concrete Microstructure, Properties, and Materials*, Second Edition, McGraw Hill, New York, New York, 1993.

70. ASTM C 150, *Standard Specification for Portland Cement*, American Society for Testing and Materials, West Conshohocken, PA, 2000.

71. ASTM C 618, *Standard Specification for Coal Fly Ash and Raw or Calcined Natural Pozzolan for Use as a Mineral Admixture in Concrete*, American Society for Testing and Materials, West Conshohocken, PA, 1999, 4pp.

72. ASTM C 494, *Standard Specification for Chemical Admixtures for Concrete*, American Society for Testing and Materials, West Conshohocken, PA, 1999, 9 pp.

73. ASTM C 260, *Standard Specification for Air Entraining Admixtures for Concrete* American Society for Testing and Materials, West Conshohocken, PA, 2000, 3 pp.

74. ASTM C 143, *Standard Test Method for Slump of Hydraulic-Cement Concrete*, American Society for Testing and Materials, West Conshohocken, PA, 1998, 3 pp.

75. ASTM C 138, *Standard Test Method for Unit Weight, Yield, and air Content (Gravimetric) of Concrete*, American Society for Testing and Materials, West Conshohocken, PA, 2000, 3 pp.

76. ASTM C 1064, *Standard Test Method for Temperature of Freshly Mixed Portland Cement Concrete*, American Society for Testing and Materials, West Conshohocken, PA, 1999, 2 pp.

77. ASTM C 173, *Standard Test Method for Air Content of Freshly Mixed Concrete by the Volumetric Method*, American Society for Testing and Materials, West Conshohocken, PA, 1994, 3 pp.

78. ASTM C 231, *Standard Test Method for Air Content of Freshly Mixed Concrete by the Pressure Method*, American Society for Testing and Materials, West Conshohocken, PA, 1994, 3 pp.

79. ASTM C 31, *Standard Practice for Making and Curing Concrete Test Specimens in the Field*, American Society for Testing and Materials, West Conshohocken, PA, 1998, 5 pp.

80. ASTM C 39, *Standard Test Method for Compressive Strength of Cylindrical Concrete Specimens*, American Society for Testing and Materials, West Conshohocken, PA, 1999, 5 pp.

81. ASTM C 469, *Standard Test Method for Static Modulus of Elasticity and Poisson's Ratio of Concrete in Compression*, American Society for Testing and Materials, West Conshohocken, PA, 1994, 4 pp.

82. ASTM C 78, *Standard Test Method for Flexural Strength of Concrete (Using Simple Beam with Third-Point Loading)*, American Society for Testing and Materials, West Conshohocken, PA, 1994, 3 pp.

83. ASTM C 512, *Standard Test Method for Creep of Concrete in Compression*, American Society for Testing and Materials, West Conshohocken, PA, 1992, 4 pp.

84. Dill, J. C., "Development Length of 0.6-inch Diameter Prestressing Strand in High-Performance Concrete," Masters Thesis, Georgia Institute of Technology, May 2000, 322 pp.

85. ASTM C 1231, *Standard Practice for Use of Unbonded Caps in Determination of Compressive Strength of Hardened Concrete Cylinders*, American Society for Testing and Materials, West Conshohocken, PA, 2000, 4 pp.

86. Buchberg, B. S., "Investigation of Mix Design and Properties of High-Strength/High-Performance Lightweight Concrete," Masters Thesis, Georgia Institute of Technology, January 2002, 453 pp.

87. *Guide for High-Strength Concrete*, ACI 363, American Concrete Institute, Detroit, 2000.

88. ASTM C 496, *Standard Test Method for Splitting Tensile Strength of Cylindrical Concrete Specimens*, American Society for Testing and Materials, West Conshohocken, PA, 1996, 4 pp.

89. Sikes, G. H., Strougal, E. J., Meisner, J. L., "Computer Manual for Service Load Design of Concrete Bridge Slabs," Georgia Department of Transportation, January 1999, 18 pp.

90. Logan, D. R., "Acceptance Criteria for Bond Quality of Strand for Pretensioned Prestressed Concrete Applications," PCI Journal, Vol. 42, No. 2, March/April 1997. pp. 52-90.

91. MacGregor, J. G., *Reinforced Concrete*, Second Edition, Prentice Hall, Englewood Cliffs, New Jersey, 1992, 848 pp.

92. *LRFD Specifications for Highway Bridges*, American Association of State Highway and Transportation Officials, Washington, D. C., 1998.

93. Cagley, J. R., "Changing from ACI 318-99 to ACI 318-02, What's New?," *Concrete International*, Vol. 23, No. 6, June 2001, pp. 69-182.

94. Vaysburg, A., "Durability of Lightweight Concrete Bridges in Severe Environments," *Concrete International*, Vol. 18, No. 7, July 1996, pp. 33-38.

95. Yeginobali, A., Sobolev, K. G., Soboleva, S. V., Tokyay, M., "High Strength Natural Lightweight Aggregate Concrete with Silica Fume," *ACI SP 178*, American Concrete Institute, Detroit, May 1998, pp. 739-758.

Georgia Institute of Technology

School of Civil and Environmental Engineering

Structural Engineering, Mechanics and Materials
Research Report No. 02-5

Appendices for
Transfer and Development Length of High Strength Lightweight Concrete Precast Prestressed Bridge Girders

Task 5 Report

Prepared for

Office of Materials and Research
Georgia Department of Transportation

GDOT Research Project No. 2004

by

Karl F. Meyer, Lawrence F. Kahn
James S. Lai, and Kimberly E. Kurtis

June 2002

APPENDIX A

INPUT FILE CREATOR FOR GDOT COMPUTER PROGRAM

This Appendix contains an example of the spreadsheet used to create input files

for use with the Georgia Department of Transportation prestressed girder design program

The worksheet shown in Table A.1 shows the input variables. Most of the

variables were held constant; the shaded variables were changed for the parametric study.

The worksheet shown in Table A.2 lists values calculated based on the variables

entered in Table A.1. For determination of diaphragm locations, it was assumed that

diaphragm spacing would be at a maximum of 35 feet.

The worksheet shown in Table A.3 provides the values to be entered for rows 1

through 8 in the program input file. The shaded values were entered as listed except for

the decimal points that are shown for clarity. The initial row of the input file providing

information is not listed in Table A.3.

Table A.1 Input Values for Girder Design

INPUT VALUES FOR GDOT PRESTRESSED GIRDER PROGRAM IN DESIGN MODE

DECK VARIABLES

MINIMUM DECK THICKNESS	t_d	7.000	INCHES
AVERAGE COPING DEPTH		3.00	INCHES
FUTURE PAVING ALLOWANCE		0.015	KSF
LIGHTWEIGHT CONCRETE		NO	YES/NO
CONCRETE STRENGTH	f'_c	3500	PSI
CONCRETE WEIGHT	W_c	145	PCF
ALLOWANCE FOR GRINDING		0.00	INCHES
WEIGHT OF SIDEWALK		0.00	K/FT
DISTANCE FROM DECK TO GIRDER	DF	0.00	INCHES
DECK PANELS USED		NO	YES/NO

MISCELLANEOUS VARIABLES THAT ARE NORMALLY CONSTANT VALUES

WEIGHT OF BARRIERS		820	LB/FT
DISTRIBUTION FOR DEFLECTION	DFD	1.000	NO UNITS
WEIGHT OF FORMWORK		16	PSF
FACTOR INITIAL BM TOP STRESS	SIT	-3.0	NO UNITS
FACTOR FINAL BM BOTTOM STRESS	SFB	-6.0	NO UNITS
ALLOW FINAL BEAM END TOP STRESS	SFT	-200	PSF
AASHTO CODE VERSION		1996	
CONCRETE WEIGHT FOR DIAPHRAGMS		150	PCF
THICKNESS OF DIAPHRAGMS		10	INCHES
TOP OF BEAM TO TOP STRANDS	TCL	2.50	INCHES
BOTTOM OF BEAM TO BOTTOM STRANDS	BCL	3.00	INCHES
STRAND SPACING	SPAC	2.00	INCHES
NUMBER OF TOP STRANDS	NST	2	EACH
MAXIMUM DRAPED STRANDS PER ROW		2	NO UNITS

GIRDER VARIABLES

GIRDER TYPE (AASHTO,BT)		BT72	1-6,BT
NUMBER OF GIRDERS		13	EACH
GIRDER SPACING	s	84.00	INCHES
GIRDER LENGTH	L	146.00	FEET
LIGHTWEIGHT CONCRETE		YES	YES/NO
LIGHTWEIGHT CONCRETE REDUCTION FACTOR	λ	0.75	NO UNITS
CONCRETE STRENGTH	f'_c	10000	PSI
% CONCRETE STRENGTH AT RELEASE		90%	PERCENT
CONCRETE WEIGHT (WHOLE NUMBERS ONLY)	W_c	118	PCF
STRAND DIAMETER	D	0.6	INCHES
TOP STRAND C/S AREA	A_{st}	0.217	INCH^2
BOTTOM STRAND C/S AREA	A_{sb}	0.217	INCH^2
STRAND ULTIMATE STRENGTH	f_{pu}	270	KSI
STIRRUP SIZE		5	#
STIRRUP ULTIMATE STRENGTH	f_u	60	KSI
DISTANCE END TO SUPPORT	XDIST	8.00	INCHES
BOTTOM STRAND REDUCTION FACTOR	RBFPU	0.75	NO UNITS
TOP STRAND REDUCTION FACTOR	RTFPU	0.75	NO UNITS
LOLAX STRANDS USED	LL	YES	YES/NO
DRAPED STRANDS		YES	YES/NO
NUMBER OF DIAPHRAMS ON GIRDER	NPL	4	EACH

USER INPUT VALUES ————————> [OPEN]

USER INPUT VALUES ————————> [TMP LOCK]

USER INPUT VALUES (CONSTANTS) ————> [ ]

Table A.2 Calculated Values

NON-COMPOSITE DEAD LOAD			
WEIGHT OF SLAB		0.592	KIP/FT
WEIGHT OF COPINGS		0.127	KIP/FT
WEIGHT OF FORMWORK		0.056	KIP/FT
TOTAL NON-COMPOSITE DEAD LOAD	WDL$_{nc}$	0.775	KIP/FT
COMPOSITE DEAD LOAD			
FUTURE WEARING SURFACE		0.105	KIP/FT
BARRIERS		0.063	KIP/FT
TOTAL COMPOSITE DEAD LOAD	WDL$_c$	0.168	KIP/FT
MISCELLANEOUS CALCULATED VALUES			
WIDTH OF GIRDER TOP FLANGE		42	INCHES
GIRDER MODULUS OF ELASTICITY	E$_c$	3.82	1E6 PSI
GIRDER MODULUS AT RELEASE	E$_{ci}$	3.74	1E6 PSI
DISTRIBUTION FOR MOMENT	DFM	1.273	NO UNITS
DISTRIBUTION FOR SHEAR (INT)	DFV	1.571	NO UNITS
APPROXIMATE GIRDER WEIGHT		104.33	KIPS
DECK MODULUS OF ELASTICITY	E$_c$	3.41	1E6 PSI
DIAPHRAGM WEIGHT PER FOOT		0.667	KIPS
POINT LOADS ON GIRDER			
POINT LOAD # 1	->	4.001	KIPS
LOCATION # 1 FROM END		33.200	FEET
POINT LOAD # 2	->	4.001	KIPS
LOCATION # 2 FROM END		66.400	FEET
POINT LOAD # 3	->	4.001	KIPS
LOCATION # 3 FROM END		99.600	FEET
POINT LOAD # 4	->	4.001	KIPS
LOCATION # 4 FROM END		132.800	FEET
POINT LOAD # 5			KIPS
LOCATION # 5 FROM END			FEET
PROGRAM CALCULATED VALUES ———>			

Table A.3 Input File for GDOT Prestressed Girder Computer Program

ROW	DS/AN	LOADS	T.L.M	LENGTH	DFM	DFV	DFD	WDLnc	WDLc	Wsw	fc'	fci'	SKIP	NPL	SIT	SFB	SFT	CODE
1	D	HS20	XXX	166.000	1.273	1.571	1.000	0.775	0.168	0.000	10.000	09.000	XXXX	04	.285	2.000	.200	6

ROW	Wtc	Ht	Ft	Ws	Hb	Wb	Fb	Db	Wf	Tf	Df	EBM	fcs	SKIP	STIR	SKIP	IFL	FuST	R1	R3	RF
2	02.00	03.50	02.50	06.00	06.00	26.00	04.50	07.00	08.00	02.000	10.000	3.82	3.50	X	5	X	60	0	XX	XX	0.75

--------------------- MAXIMUM NUMBER OF STRANDS PER ROW ---------------------

ROW	TYPE	NST	XDIST																			
3	XX	12	0.667	12	08	04	02	02	02	02	02	02	02	02	02	02	02	01	02	02	02

ROW--------> 1 2 3 4 5 6 7 8 9 10 11 12 13 14 15 16 17 18 19

ROW (CONTINUED)

3																				20

ROW	RBFPU	BFPU	IBLOSS	FBLOSS	RTFPU	TFPU	ITLOSS	FTLOSS	LOLAX	ITLG	FTLG	DLG
4	0.75	270.00	XXXXX	XXXX	0.75	270.00	XXXX	XXXX	0.118	XXXX	XXXX	XXXX

ROW	DBOND
5	0

X = SPACE

	ASB	AST	DIAM	TCL	BCL	SPAC
02	.4170	.2770	0.600	2.50	3.00	1.00
20						

ROW
6

--------------------- MAXIMUM DRAPED STRANDS PER ROW ---------------------

ROW	DRAPE	RS HT	HOLD																			
7	XXXX	XX	XX	02	02	02	02	02	02	02	02	02	02	02	02	02	02	02	02	02	02

ROW--------> 1 2 3 4 5 6 7 8 9 10 11 12 13 14 15 16 17 18 19

ROW (CONTINUED)

7																			02	20

ROW	XP1	P1	XP2	P2	XP3	P3	XP4	P4	XP5	P5
8	033.200	04.001	066.400	04.001	099.600	04.001	132.800	04.001		

APPENDIX B

MIX DESIGN SPREADSHEET

This Appendix contains an example of the LWC Mix Design Spreadsheet. Table B.1 shows the spreadsheet with an example mix design.

The user does the following:

1. Enter values for SG (Specific Gravity) and Cost for each component to set the material parameters. Enter the desired air content and batch size.

2. Enters the weight of each particular component per cubic yard at SSD, except chemical admixtures, in the "Theoretical Mix Design at SSD" Section.

3. Enter the dose of chemical admixtures in fl oz / 100 weight of cementitious materials.

4. Adjust the components until the W/CM ratio is as desired. The percent cement paste and ratio of coarse to fine aggregate are listed at the bottom of the page.

5. While batching, if additional chemical admixtures or water are added, enter the values in the spreadsheet in ml for chemical admixtures and pounds for water.

6. The final mix design reflecting added amounts during batching, if any, is reflected in the "Final Mix Design at SSD" section. If nothing additional was added, this will be the same as the "Theoretical Mix Design at SSD."

363

Table B.1 Mix Design Spreadsheet

LIGHTWEIGHT CONCRETE MIX DESIGN			ID #	XXXX		f'c	X	ksi	Date	

Material Data / Moisture Data / Theoretical Mix Design at SSD / H₂O Adjusted Batch / Final Mix Design at SSD

Description	SG	Cost Per		% SSD	SGF	% As Is	% Free	Per Cubic Yard		Per Batch		EDV(cf)	Amount		Per Cubic Yard	
3/4" - NWA	2.649	$ 0.0046	lb	0.60	2.665	0.60	0.00	0	0.00	0.00		0.00	0.00		0	$ -
1/2" - NWA	2.665	$ 0.0048		0.60	2.681	0.60	0.00	0	lb	0.00	lb	0.00	0.00	lb	0	$ -
3/8" - NWA	2.665	$ 0.0050		0.60	2.681	0.60	0.00	0		0.00		0.00	0.00		0	$ -
NW Sand	2.608	$ 0.0054		0.50	2.621	0.00	-0.50	1215	7.43	45.00		0.27			1205	$ 6.48
3/4" - LWA	1.415	$ 0.0276	lb	6.00	1.500	6.00	0.00	0	0.00	0.00		0.00	0.00		0	$ -
1/2" - LWA	1.440	$ 0.0276		7.67	1.550	9.27	1.60	945	lb 9.77	35.00	lb	0.37	35.5		937	$ 25.86
3/8" - LWA	1.570	$ 0.0300		6.00	1.664	6.00	0.00	0	0.00	0.00		0.00	0.00		0	$ -
LW Fines	1.710	$ 0.0275		5.00	1.796	5.00	0.00	0	0.00	0.00		0.00	0.00		0	$ -
Tot Aggregate >								2160 lb	17.20 cf	80.00 lb		0.64	80.30	lb	2141.7 lb	$ 32.34

	SG	Cost Per		% by Wt				Per CY		Per Batch		EDV	Amount		Final	
FA - Class C	2.250	$ 0.0300		0.0				0	0.00	0.00		0.00	0.00		0	$ -
FA - Class F	2.250	$ 0.0300		19.4				150	1.07	5.56		0.04	5.56		149	$ 4.46
GGBFS	2.900	$ 0.0300	lb	0.0				0	lb 0.00	0.00	lb	0.00	0.00	lb	0	$ -
Metakaolin	2.500	$ 0.0500		0.0				0	0.00	0.00		0.00	0.00		0	$ -
SF - (F 10,000)	2.200	$ 0.0500		7.1				55	0.40	2.04		0.01	2.04		55	$ 2.73
Type III Cement	3.150	$ 0.0440	lb	73.5				570 lb	2.90 cf	21.11 lb		0.11	21.11	lb	565 lb	$ 24.87
Tot Cementitious >								775 lb	4.37 cf	28.70 lb		0.16	28.70	lb	768.4 lb	$ 32.06

W/CM	0.358
$/CY	75.48
LB/FT³	118.3

	SG	Cost Per		fl oz / 100 wt		ml	Per CY		Per Batch		EDV	Amount		Final	
WRDA 35	1.199	$ 0.0500	fl	2 - 8	7.00	10	54.3	0.057 cf	2.01		0.002		ml	8.18 fluid oz	$ 3.14
Daracem 65	1.139	$ 0.0500		3 - 9	0.00	added	0.0	0.000 cf	0.00		0.000	0.00		0.00 per 100	$ -
ADVA Flow	1.043	$ 0.1197	oz	3 - 10	8.00	during	62.0 fl	0.065 cf	2.30	fl	0.002			8.59 wt	$ 7.90
Daravair 1000	1.000	$ 0.0500		1/4 - 3	0.00	mixing	0.0 oz	0.000 cf	0.00	oz	0.000	0.00		0.00	$ -
Total additional volume added >	0.0085	cf					Tot Admixtures >	116.3 lb	0.121 cf	4.31 lb		0.004	0.31	lb	9.40 lb	$ 11.04
Water	1.000	$ 0.0013	gal	Pounds water added =>		0.50	264.2 lb	4.23 cf	9.78 lb		0.152	9.49	gal/lb	275.3 lb	$ 0.04
Design Air =>	4.00	%					Percent Cement Paste >	36	1.08 cf			0.04	cf		3.97 %	Air
Design Slump =>	3-5	Inches		Batch Size =>	1.00	cf			Coarse / Fine Aggregate Ratio				1.31			

Direct any questions about this spreadsheet to LTC Fred Meyer, Georgia Institute of Technology, Atlanta, GA (404) 385-1429 -- Version 4, 7 Feb 2001

The following calculations verify the values listed in Table B.1.

Assumed Values

Brown Brothers Sand (NW Sand) : Theoretical Mix Design at SSD = 1215 pcy
Specific gravity (SG) = 2.608
SSD moisture = 0.5%
As-Is moisture = 0%

1/2" Stalite LWA (1/2" - LWA) : Theoretical Mix Design = 945 pcy,
SG = 1.44
SSD moisture = 7.67%
As-is moisture = 9.27%

Class "F" flyash (FA - Class F) : Theoretical Mix Design = 150 pcy
SG = 2.25

Silica Fume (SF - F 10,000) : Theoretical Mix Design = 55 pcy
SG = 2.2

Type III Cmt (Type III Cement) : Theoretical Mix Design = 570 pcy
SG = 3.15

Water Reducer (WRDA 35) : Theoretical Mix Design = 7 oz/100 weight
of cementitious material
SG = 1.199

Superplasticizer (ADVA Flow) : Theoretical Mix Design = 8 oz/100 weight
of cementitious material
SG = 1.043

AEA (Daravair 1000) : Theoretical Mix Design = 1 oz/100 weight
of cementitious material
SG = 1.0

Air - 4%

During batching the following were added: WRDA 35 = 10 ml = .00003531 cf
ADVA Flow = 5 ml = .00001766 cf
water = 0.5 lbs = .008013 cf

Batch Size = 1 cubic foot

Calculated Values

NW Sand :

Specific gravity factor (SGF) = (2.608) x (1+0.005) = <u>2.621</u>

percent free moisture = 0 % - 0.05 % = <u>-0.5</u> %

volume of material per cy = (1215 pcy) x (1 / ((62.4pcf) x (2.621)) = <u>7.428</u> cf

weight of material per cf of batch = (1215 pcy) / (27 cf/cy) = <u>45</u> lbs

Water adjusted weight of material per cf of batch =
 (45 lbs) x (1/(1+(.5 / 100))) x (1+0.0 / 100) = <u>44.776</u> lbs

Water adjusted volume of material per cf of batch =
 ((45 lb) / ((2.621) x (62.4 pcf)))+((44.776 lbs) - (45 lbs)) / 62.4 pcf = <u>0.2716</u> cf

1/2" - LWA:

Specific gravity factor (SGF) = (1.44) x (1+0.0767) = <u>1.550</u>

percent free moisture = 9.27 % - 7.67 % = <u>1.60</u> %

volume of material per cy = (945 pcy) x (1 / ((62.4pcf) x (1.55)) = <u>9.77</u> cf

weight of material per cf of batch = (945 pcy) / (27 cf/cy) = <u>35</u> lbs

Water adjusted weight of material per cf of batch =
 (35 lbs) x (1 / (1+(7.67 / 100))) x (1+9.27 / 100) = <u>35.52</u> lbs

Water adjusted volume of material per cf of batch =
 ((35 lb) / ((1.55) x (62.4 pcf)))+((35.52 lbs) - (35 lbs)) / 62.4 pcf = <u>0.3702</u> cf

Total Aggregate:

weight = 1215 lbs (NW Sand) + 945 lbs (1/2" - LWA) = <u>2,160</u> lbs

volume = 7.43 cf (NW Sand) + 9.77 (1/2" - LWA) = <u>17.20</u> cf

Calculated Values (cont'd)

FA - Class F:

volume per cy = (150 lbs) / ((2.25) x (62.4 pcf)) = <u>1.0683</u> cf

weight = (150 pcy)) / (27cuf/cuy) x (1 cf/batch) = <u>5.555</u> lbs/batch

volume = (5.555 lbs/batch) / ((2.25) x (62.4 pcf)) = <u>0.0395</u> cf/batch

SF - F 10,000:

volume per cy = (55 lbs) / ((2.2) x (62.4 pcf)) = <u>0.4006</u> cf

weight = (55 pcy)) / (27cf/cy) x (1 cf/batch) = <u>2.037</u> lbs/batch

volume = (2.037 lbs/batch) / ((2.5) x (62.4 pcf)) = <u>0.01484</u> cf/batch

Type III Cement:

volume = (570 lbs/cy) / ((3.15) x (62.4 pcf)) = <u>2.8998</u> cf/cy

weight = (570 pcy)) / (27cuf/cuy) x (1 cf/batch) = <u>21.11</u> lbs/batch

volume = (21.11 lbs/batch) / ((3.15) x (62.4 pcf)) = <u>0.1074</u> cf/batch

Total Cementitious:

weight = 150 lbs (FA -Class F) + 55 lbs (SF - F 10,000) + 570 lbs (Type III Cement) = <u>775</u> lbs

volume = 1.0683 cf (FA - Class F) + 0.4006 cf (SF - F 10,000) + 2.8998 cf (Type III Cement) = <u>4.37</u> cf

Calculated Values (cont'd)

WRDA 35:

volume = (7 fl oz/100 wt) x ((775 / 100) 100 wt/cy) = <u>54.25</u> fl oz/cy

volume = (54.25 fl oz/cy) x (1 cf/batch) / (27 cf/cy) = <u>2.009</u> fl oz/batch

volume = (54.25 fl oz/cy) / (957.5065 fl oz/cf) = <u>0.05666</u> cf/cy

volume = (.05666 cf/cy) x (1 cf/batch) / (27 cf/cy) = <u>0.00210</u> cf/batch

volume = (.00210 cf/batch) x (28316.8466 ml/cf) = <u>59.42</u> ml/batch

ADVA Flow:

volume = (8 fl oz/100 wt) x ((775 / 100) 100 wt/cy) = <u>62</u> fl oz/cy

volume = (62 fl oz/cy) x (1 cf/batch) / (27 cf/cy) = <u>2.296</u> fl oz/batch

volume = (62 fl oz/cy) / (957.5065 fl oz/cf) = <u>0.06475</u> cf/cy

volume = (.06475 cf/cy) x (1 cf/batch) / (27 cf/cy) = <u>0.00239</u> cf/batch

volume = (.00239 cf/batch) x (28316.8466 ml/cf) = <u>67.909</u> ml/batch

Total Admixtures: By using the milliliters of admixtures and the specific gravities, a weight of equivalent water can be found.

equivalent water mass = 59.42 ml (WRDA 35) x (1.199) = <u>71.2446</u> g

equivalent water mass = 67.909 ml (ADVA Flow) x (1.043) = <u>70.8291</u> g

total equivalent water mass = 71.2466 g (WRDA 35) + 70.8291 g (ADVA
Flow) = <u>142.0757</u> g

weight = (142.0757 g) x (1 oz / 28.3498 g) x (1 lb / 16 oz) =
= <u>0.3132</u> lb

volume = .05666 cf (WRDA 35) + .06475 cf (ADVA Flow) = <u>0.121</u> cf

Calculated Values (cont'd)

Water:

volume of water per cy = 27 cf - $\text{vol}_{aggregate}$ - vol_{cement} - $\text{vol}_{admixture}$ - vol_{air}

volume of air (4 %) = (.04) x (27 cf/cy) = 1.08 cf/cy

volume of water = 27 cf - 17.20 cf - 4.37 cf - 0.121 cf - 1.08 cf = 4.233 cf/cy

volume of water = 1.0 cf - 0.64 cf - 0.16 cf - 0.004 cf - 0.04 = 0.152 cf/batch

weight = (4.233 cf/cy) x (62.4 pcf) = 264.1392 pcy

weight = (264.1392 pcy) x (1 cf/batch) x (1 cy / 27 cf) = 9.783 lbs/batch

Final Mix Design: The additions of WRDA 35, ADVA Flow and water need to be accounted for when reporting the final mix design

volume added = .00003531 cf (WRDA 35) + .00001766 cf (ADVA FLOW) +
.008013 cf = .008066 cf

new volume of mix = (1 cy) + (.008066 cf) = 1.008066 cf

Final NW Sand weight = (1215 lbs) / (1.008066) = 1205.28 lbs

Final 1/2" - LWA weight = (945 lbs) / (1.008066) = 937.44 lbs

Final FA - Class F weight = (150 lbs) / (1.008066) = 148.80 lbs

Final SF - F 10,000 weight = (55 lbs) / (1.008066) = 54.55 lbs

Final Type III Cement weight = (570 lbs) / (1.008066) = 565.44 lbs

Final WRDA 35 volume = (7 fl oz/100 wt) + (10 ml/cf) x (27 cf/cy) x (1 fl oz /
29.5735 ml) x (1 cy / 775 lb) x (100 lb / per 100 wt) =
= 8.178 fl oz/100 wt

Final WRDA 35 volume = (8 fl oz/100 wt) + (5 ml/cf) x (27 cf/cy) x (1 fl oz /
29.5735 ml) x (1 cy / 775 lb) x (100 lb / per 100 wt) =
= 8.589 fl oz/100 wt

Final admixture water equivalent weight = (8.178 fl oz) x (1.199) + (8.589 fl oz) x
(1.043) = 18.76719 fl oz of water

369

Calculated Values (cont'd)

Final admixture weight = (18.76719 fl oz) x (768 lbs / 100 lbs) x (29.5735 ml/fl oz) x (.002205 lb/ml) = 9.397 lbs

Final Water weight = ((267.1 lbs) + (.5 lb) x (1 / 1cf) x (27 cf/cy)) x (1 / (1 + .0085) = 275.3 lbs

Final Air Content = 4 % x (1 / (1+.0085)) = 3.97 %

Cost:

NW Sand	= (1205.28 lbs) x ($0.0054/lbs)	= $ 6.48
1/2" - LWA	= (937.44 lbs) x ($0.0276/lbs)	= $ 25.86
FA - Class F	= (148.80lbs) x ($0.03/lbs)	= $ 4.46
SF - F 10,000	= (54.55 lbs) x ($0.05/lbs)	= $ 2.73
Type III Cement	= (565.44 lbs) x ($0.044/lbs)	= $ 24.87
WRDA 35	= (8.18 fl oz/100 wt) x (7.6879**) x ($0.05)	= $ 3.14
ADVA Flow	= (8.59 fl oz/100 wt) x (7.6879**) x ($0.1197/fl oz)	= $ 7.90
Water	= (275.3 lb) x ($0.0013/gal) / (8.34 lbs/gal)	= $ 0.04
Total		$ 75.48

Water/Cementitious Ratio = (275.3 lbs) / (768.79) = 0.358

Unit Weight = (aggregate wt + cement wt + admixture wt + water wt)/ 27
= ((2142.7 lbs) + (768.4 lbs) + (9.40 lbs) + (275.3 lbs)) / 27 = 3195.8
= 118.3 lbs/cf

** The number of 100 weight of cement in the cubic yard

APPENDIX C

MATERIAL PROPERTIES

This Appendix contains material property data in the sections listed below.

C.1 HSLC material properties used in evaluating modulus of elasticity equations in

Chapter 7.

C.2 Tension test results of #4 bar reinforcing steel used for all shear stirrups.

C.3 Tension test results of #3 bar reinforcing steel used for "doghouse" bars in the

transfer region.

C.1 Material Properties for Modulus of Elasticity Specimens

Table C.1 16-Hour Curebox Cured Specimens

Specimen Identification	Wet Unit Weight (pcf)	As-Tested Unit Weight (pcf)	Compression Strength (4 x 8) (psi)	Modulus of Elasticity (psi)
8F-1	118.6	117.9	7,920	3,407,479
8F-2	118.6	117.9	7,920	3,530,161
8F-3	118.6	117.9	7,920	3,515,616
10F-1	121.0	120.3	7,710	3,427,358
10F-2	121.0	120.3	7,710	3,430,741
10F-3	121.0	120.3	7,710	3,572,510
12F-1	124.0	123.3	10,990	3,998,394
12F-2	124.0	123.3	10,990	3,592,513
12F-3	124.0	123.3	10,990	4,161,776
8L-1	122.0	121.3	7,320	3,458,627
8L-2	122.0	121.3	7,320	3,658,242
8L-3	122.0	121.3	7,320	3,467,933
12L-1	122.8	122.1	9,840	4,058,913
12L-2	122.8	122.1	9,840	4,019,955
12L-3	122.8	122.1	9,840	4,167,468

Table C.2 24-Hour Curebox Cured Specimens

Specimen Identification	Wet Unit Weight (pcf)	As-Tested Unit Weight (pcf)	Compression Strength (4 x 8) (psi)	Modulus of Elasticity (psi)
G1A-1-24	118.7	117.7	7,093	3,386,729
G1A-2-24	118.7	117.7	7,093	3,524,518
G1A-3-24	118.7	117.7	7,093	3,508,675
G1B-1-24	119.8	118.8	5,915	2,975,988
G1B-2-24	119.8	118.8	5,915	3,005,111
G1B-3-24	119.8	118.8	5,915	3,032,753
G2A-1-24	120.0	119.0	9,807	3,789,901
G2A-2-24	120.0	119.0	9,807	3,745,692
G2A-3-24	120.0	119.0	9,807	3,109,247
G2B-1-24	114.0	113.0	8,313	3,963,880
G2B-2-24	114.0	113.0	8,313	3,865,080
G2B-3-24	114.0	113.0	8,313	3,888,308
8F-4	118.6	117.6	8,870	3,577,737
8F-5	118.6	117.6	8,870	3,673,648
8F-6	118.6	117.6	8,870	3,747,778
10F-4	121.0	120.0	9,750	3,744,977
10F-5	121.0	120.0	9,750	3,686,261
10F-6	121.0	120.0	9,750	3,801,950
12F-4	124.0	123.0	11,490	4,139,841
12F-5	124.0	123.0	11,490	4,188,613
12F-6	124.0	123.0	11,490	4,031,863
8L-4	122.0	121.0	7,730	3,748,723
8L-5	122.0	121.0	7,730	3,688,108
8L-6	122.0	121.0	7,730	3,558,556
12L-4	122.8	121.8	11,101	4,224,670
12L-5	122.8	121.8	11,101	4,262,995
12L-6	122.8	121.8	11,101	4,262,688

Table C.3 28-Day Curebox Cured Specimens

Specimen Identification	Wet Unit Weight (pcf)	As-Tested Unit Weight (pcf)	Compression Strength (4 x 8) (psi)	Modulus of Elasticity (psi)
8F-7	118.6	116.6	9,830	3,890,477
8F-8	118.6	116.6	9,830	3,849,350
8F-9	118.6	116.6	9,830	3,806,191
10F-7	121.0	119.0	10,430	4,016,648
10F-8	121.0	119.0	10,430	4,684,482
10F-9	121.0	119.0	10,430	4,043,618
10F-10	121.0	119.0	10,430	4,120,260
12F-7	124.0	122.0	11,460	4,361,462
12F-8	124.0	122.0	11,460	4,331,051
12F-9	124.0	122.0	11,460	4,207,477

Table C.4 56-Day Curebox Cured Specimens

Specimen Identification	Wet Unit Weight (pcf)	As-Tested Unit Weight (pcf)	Compression Strength (4 x 8) (psi)	Modulus of Elasticity (psi)
G1A-1-56	118.7	116.2	9,084	3,814,994
G1A-2-56	118.7	116.2	9,084	3,901,364
G1A-3-56	118.7	116.2	9,084	3,877,308
G1B-1-56	119.8	117.3	7,750	3,302,301
G1B-2-56	119.8	117.3	7,750	3,247,403
G1B-3-56	119.8	117.3	7,750	3,295,650
G2A-1-56	120.0	117.5	10,418	4,036,274
G2A-2-56	120.0	117.5	10,418	3,874,421
G2A-3-56	120.0	117.5	10,418	3,891,948
G2B-1-56	114.0	111.5	10,249	4,076,345
G2B-2-56	114.0	111.5	10,249	4,184,515
G2B-3-56	114.0	111.5	10,249	4,029,685
8F-10	118.6	116.1	10,600	3,875,411
8F-11	118.6	116.1	10,600	3,671,790
8F-12	118.6	116.1	10,600	4,016,215
10F-11	121.0	118.5	11,170	4,195,290
10F-12	121.0	118.5	11,170	4,176,745
10F-13	121.0	118.5	11,170	3,861,762
12F-10	124.0	121.5	11,550	4,209,773
12F-11	124.0	121.5	11,550	4,276,240
12F-12	124.0	121.5	11,550	4,295,494
8L-7	119.4	116.9	10,430	4,034,355
8L-8	119.4	116.9	10,430	4,040,931
8L-9	119.4	116.9	10,430	3,990,007
10L-1	122.4	119.9	9,920	4,104,663
10L-2	122.4	119.9	9,920	4,067,865
10L-3	122.4	119.9	9,920	4,075,294
12L-7	121.7	119.2	10,860	4,207,700
12L-8	121.7	119.2	10,860	4,207,945
12L-9	121.7	119.2	10,860	4,304,298

Table C.5 56-Day ASTM Cured Specimens

Specimen Identification	Wet Unit Weight (pcf)	As-Tested Unit Weight (pcf)	Compression Strength (4 x 8) (psi)	Modulus of Elasticity (psi)
G1A-1-ASTM-56	118.7	116.2	9,352	3,875,746
G1A-2-ASTM-56	118.7	116.2	9,575	3,774,216
G1A-3-ASTM-56	118.7	116.2	9,834	4,096,713
G1A-4-ASTM-56	118.7	116.2	8,715	3,593,701
G1A-5-ASTM-56	118.7	116.2	9,252	3,816,347
G1B-1-ASTM-56	119.8	117.3	8,063	3,623,900
G1B-2-ASTM-56	119.8	117.3	8,252	3,328,719
G1B-3-ASTM-56	119.8	117.3	9,056	3,740,114
G2A-1-ASTM-56	120.0	117.5	10,377	3,984,773
G2A-2-ASTM-56	120.0	117.5	11,377	3,927,559
G2A-3-ASTM-56	120.0	117.5	11,369	4,297,258
G2A-4-ASTM-56	120.0	117.5	10,555	4,131,074
G2A-5-ASTM-56	120.0	117.5	10,405	3,979,495
G2B-1-ASTM-56	114.0	111.5	10,244	4,283,444
G2B-2-ASTM-56	114.0	111.5	10,826	3,912,993
G2B-3-ASTM-56	114.0	111.5	10,523	3,964,648
8F-13	118.6	116.1	11,090	4,059,005
8F-14	118.6	116.1	11,090	4,272,725
8F-15	118.6	116.1	11,090	4,051,198
10F-14	121.0	118.5	11,300	4,273,372
10F-15	121.0	118.5	11,300	4,353,486
10F-16	121.0	118.5	11,300	4,163,007
12F-13	124.0	121.5	11,620	4,344,719
12F-14	124.0	121.5	11,620	4,535,964
12F-15	124.0	121.5	11,620	4,313,065
8L-10	119.4	116.9	10,520	4,382,289
8L-11	119.4	116.9	10,520	4,461,557
8L-12	119.4	116.9	10,520	4,318,485
10L-4	122.4	119.9	11,040	4,406,935
10L-5	122.4	119.9	11,040	4,285,072
10L-6	122.4	119.9	11,040	4,283,424
12L-10	121.7	119.2	11,480	4,429,366
12L-11	121.7	119.2	11,480	4,304,119
12L-12	121.7	119.2	11,480	4,262,217

C.2 Tension Test Results of Steel Used for Shear Stirrups
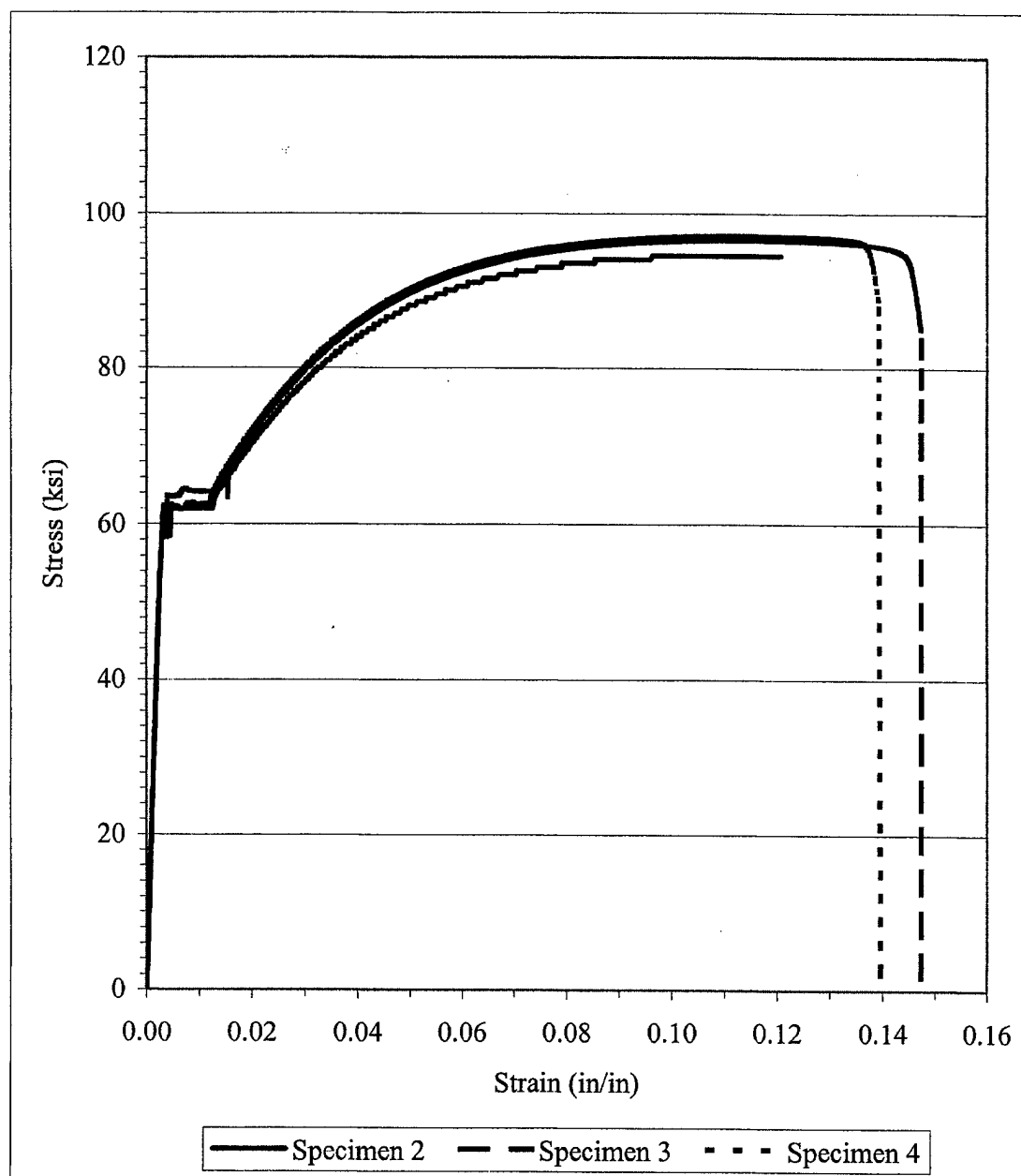
Figure C.1 Stress vs. Strain Plot for Shear Reinforcement Steel

377

C.3 Tension Test Results of Steel Used for "Doghouse Bars"
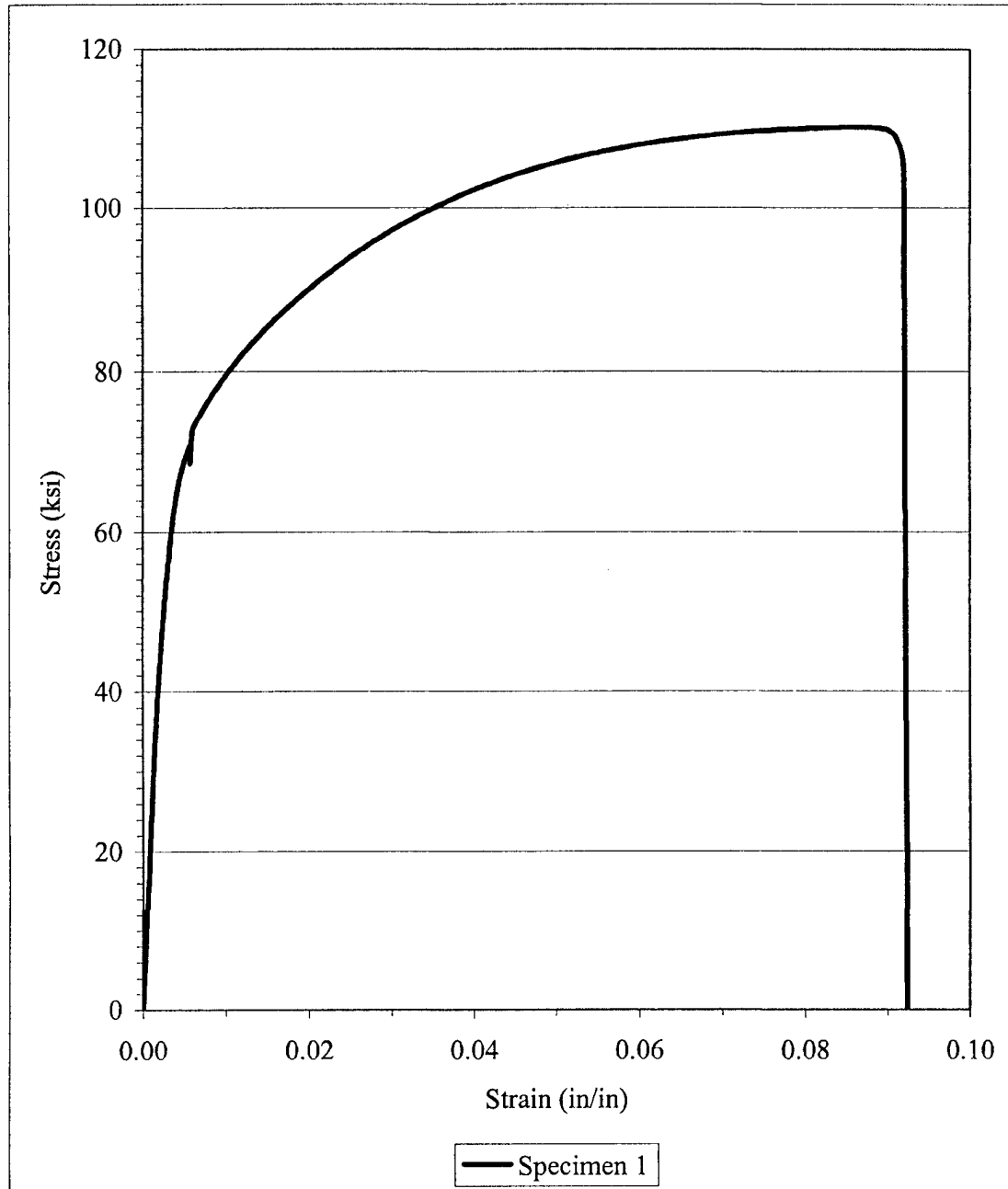
Figure C.2 Stress vs. Strain Plot for "Doghouse Bar" Reinforcement Steel

APPENDIX D

GIRDER DESIGN SPREADSHEET

Appendix D contains the individual pages from the Girder Design Spreadsheet.
The entire set of worksheet pages is provided from the design of girder test G1C-West.
The pages are listed in the order the calculations occur. All calculations are based on the
1996 AASHTO[40] Standard Specification for Highway Bridges. A similar series of
worksheets was prepared for each girder test to determine girder test design
characteristics. Listed below are the individual worksheets within the overall spreadsheet
and a brief description of the worksheet's function. The Tables are all placed at the end
of this Appendix.

Table D.1 – Section and Material Properties for Girder Design

Table D.2 – Support Conditions, Calculation of M_f and P_u – Worksheet used to
specify support conditions and determine predicted ultimate load.

Table D.3 – Predicted Loss

Table D.4 – Non-Composite Girder Stress Calculations

Table D.5 – Composite Girder Stress Calculations

Tables D.6 and D.7 – Shear Design Calculations

Table D.8 – Deck / Girder Interface Shear Calculations

Below is a description of each page of the spreadsheet. The general concept of the spreadsheet was to determine the flexural capacity based on the selected girder and strand pattern, then design the shear reinforcement to allow reaching the flexural capacity. Interface shear was checked as a precaution to insure no problems would occur during testing.

D.1 Assumptions for Using Spreadsheet

This spreadsheet assumed the prestressed girder had straight prestressing strand. The strand could be set at any height, but was assumed to be straight. It was not possible to drape the strands within this spreadsheet. A possible modification to provide better flexibility in the spreadsheet would be to include this option.

D.2 Worksheet 1 - Section and Material Properties for Girder Design

Worksheet 1 seen in Table D.1 allowed the user to enter variable data describing the girder's section and material properties. Following user-entered variables, the spreadsheet calculated values as follows.

The modulus of elasticity was based on the entered unit weight value. A unit weight greater than 135 pcf triggered the use of equation 3.1. A unit weight less than or equal to 135 pcf triggered the use of equation 3.3.

The modular ratio, η, was calculated using equation D.1.

$$\eta = \frac{E_{c-Deck}}{E_{c-Girder}} \qquad (D.1)$$

The non-composite girder properties (girder only) were hard-wired into the spreadsheet and triggered by user entry of the AASHTO or PCI Bulb Tee Type. The weight per foot of the girder was calculated based on the girder cross sectional area times the estimated equilibrium weight of the concrete. An allowance was incorporated into the worksheet where the user could enter a value for the added weight of steel (prestressed and non-prestressed) per cubic foot of concrete. This value was assumed to be 3 pcf for each girder design.

Composite girder properties were calculated as follows assuming full composite action between the girder and deck. The composite moment of inertia, I_c, was calculated using equations D.2 and D.3.

$$I_c = I_{nc} + A_{nc}(y_{bot-c} - y_{bot-nc})^2 + \frac{1}{12}\eta W_f t_d^3 + (\eta W_f t_d)(\frac{t_d}{2} + h_{g-nc} - y_{bot-c})^2 \qquad (D.2)$$

$$y_{bot-c} = \frac{A_{g-nc} y_{bot-nc} + \eta W_f t_d (h_{g-nc} + \frac{t_d}{2})}{A_{g-nc} + \eta W_f t_d} \qquad (D.3)$$

The remaining composite girder properties were calculated using equations D.4 through D.8.

$$y_{top-c} = h_{g-nc} - y_{bot-c} \qquad (D.4)$$

381

$$S_{bot-c} = \frac{I_c}{y_{bot-c}}$$

(D.5)

$$A_{g-c} = A_{g-nc} + \eta W_f t_d$$

(D.6)

$$Q_d = (\eta W_f t_d)(\frac{t_d}{2} + y_{top-c})$$

(D.7)

$$h_{g-c} = h_{g-nc} + t_d$$

(D.8)

The composite girder weight per foot was the combined weight of the non-composite girder, the deck and the specified steel allowance.

The depth to prestressing steel, d_p, was calculated using equations D.9 and D.10.

$$d_p = MAX\left(h_{g-nc} + t_d - (y_{bot-nc} + e), 0.8h_{g-c}\right)$$

(D.9)

$$e = \frac{\sum F_{ps} d}{\sum F_{ps}} - y_{bot-nc}$$

(D.10)

The variable "e" described the location of the centroid of the prestressing force in reference to the non-composite girder centroid. A negative value of "e" indicated the prestressing force centroid was below the non-composite centroid.

The predicted strand development length, l_d, was calculated using AASHTO[40] equation (9-32) shown in equation D.11 below.

$$l_d = (f_{ps} - \frac{2}{3}f_{se})d_b \qquad (D.11)$$

The predicted strand transfer length, l_t, was calculated using the AASHTO[40] specified $50*d_b$.

D.3 Worksheet 2 – Supports, Applied Load and Moment Furnished

Worksheet 2 shown in Table D.2 provided the user a visual image of the girder with support locations and location of point load application. This page allowed the user to input values describing the location of the left and right support and the location at which the point load was applied. Based on this input, the spreadsheet adjusted the support locations, determined the moment furnished at all points along the girder based on the number of prestressing strands developed, then determined the maximum point load, based on flexural capacity, that could be applied at the location specified. The spreadsheet accounted for the self-weight of the girder and deck in determining the maximum point load and also calculated the support reactions.

At the lower right portion of the page were values required to calculate the maximum furnished moment. This section of Worksheet 2 determined, based on user input on the girder and deck characteristics, whether the girder was "under" or "over" reinforced and whether "a" was within the deck. The spreadsheet provided calculations

383

for all combinations except "over" reinforced and "a" being greater than the deck thickness. The desired condition for this research was to be under-reinforced and to have "a" within the deck. Equations D.12 through D.18 were used to determine the moment furnished.

$$f_{ps} = f_{pu}\left(1 - \frac{\gamma_p \rho_p f_{pu}}{\beta_1 f_c'}\right) \qquad (D.12)$$

$$\gamma_p = 0.55 \ for \frac{f_{py}}{f_{pu}} \geq 0.80, \ 0.40 \ for \frac{f_{py}}{f_{pu}} \geq 0.85, \ 0.28 \ for \frac{f_{py}}{f_{pu}} \geq 0.90 \qquad (D.13)$$

$$\rho_p = \frac{A_{ps}}{bd_p} \qquad (D.14)$$

$$\beta_1 = 0.85 - (f_c' - 4{,}000)0.05 \geq 0.65 \qquad (D.15)$$

$$\varpi_p = \frac{\rho_p f_{ps}}{f_{c-Deck}'} \qquad (D.16)$$

If ω_p was less than $0.36\beta_1$, the girder was considered under-reinforced. The rectangular stress block depth, "a" was determined based on the composite girder characteristics. If "a" was less than the deck thickness, the girder was considered a rectangular section and the moment furnished (nominal moment) was calculated using equation D.17.

384

$$M_n = A_{ps} f_{ps} (d_p - \frac{a}{2})$$ (D.17)

If "a" was greater than the deck thickness, the moment furnished (nominal moment) was calculated using equation D.18.

$$M_n = 0.85 f'_{c-Dk} t_d W_f (d_p - \frac{a}{2}) + 0.85 f'_{c-Girder} \left(W_{f-Girder} (a - t_d) \left(d_p - t_d - \frac{(a - t_d)}{2} \right) \right)$$ (D.18)

D.4 Worksheet 3 – Loss Calculations

Worksheet 3 as shown in Table D.3 provided loss calculations based on procedures specified in the 1996 AASHTO[40] Specification. The losses were divided into three groups. The first group included elastic shortening (ES) and initial steel relaxation (R) losses experienced at the time prestressing strands were released. The second group included creep (CR), shrinkage (S) and additional steel relaxation (R) experienced from the time of strand release until the time of deck placement. The third and final group included additional steel relaxation (R) and creep (CR) that occurred in the time between deck placement and testing. The user had only limited input on this page. It was necessary for the user to input an assumption for the percent of losses due to elastic shortening (ES) which occurred at the time the prestressing strand was cut. It was necessary for the user to iterate this guess until the assumed amount and the actual amount were within 0.1 percent of each other. A good initial assumption was around six

385

percent. It was also necessary for the user to input percentages of steel relaxation that occurred during the different stages. If the user-entered percentages did not total 100, the spreadsheet automatically indicated an error was made. At the bottom of the sheet, a consolidated listing was provided showing the effective levels of prestress at the different stages of the girder's construction sequence. Losses were calculated using equations D.19 through D.22.

$$ES = \frac{E_{ps}}{E_{ci-g}} \left(\frac{P_i}{A_{g-nc}} \left(1 + \frac{e^2}{r_{nc}^2}\right) - \frac{M_D e}{I_{nc}} \right) \qquad (D.19)$$

$$CR = 12 \left(\frac{P_i}{A_{g-nc}} \left(1 + \frac{e^2}{r_{nc}^2}\right) - \frac{M_D e}{I_{nc}} \right) + 7 f_{cds} \qquad (D.20)$$

In the case of the test girders, f_{cds}, the stress at the centroid of the prestressing strand was zero at the time of deck placement. At testing, f_{cds} was no longer zero based on the addition of the deck. An additional creep component, although small, was added at that stage.

$$SH = (17,000 - 150 RH) \qquad (D.21)$$

$$R = 5000 - 0.10 ES - 0.05(SH + CR) \qquad (D.22)$$

Steel relaxation losses were broken into three pieces including "initial", "at deck placement" and "at testing." Percentages were assigned to each particular component as deemed appropriate.

D.5 Worksheet 4 - Non-Composite Stress Calculations (Stages 1 and 2)

Worksheet 4 as shown in Table D.4 provided stresses at the TOP and BOTTOM of the girder at the 20th points at stages 1 (Strand Release) and 2 (Deck Placement). Shown on the girder were the values of girder self-weight and deck self-weight. Included in the self-weight values was a small component due to the weight of the reinforcing and prestressing steel. This value was entered on Worksheet 1 as the Steel Weight Allowance per Cubic Foot. The stresses were broken down by axial component, strand eccentricity (F*e) component, and dead load (DL) component. The stress level used at stage 1 was the effective prestress after elastic shortening (ES) and initial strand relaxation (R) losses occurred. The stress level used at stage 2 was the effective prestress after all losses occurred except final strand relaxation and final creep losses. The stress levels at the various stages can be seen on Worksheet 3, Table D.3 at the bottom left corner. In order to calculate the stress level at a given 20th point, the spreadsheet calculated the transfer length on Worksheet 1 then determined the number of strands developed. Throughout the sheet, negative (-) values indicate compression stress and positive (+) values indicate tension stress. Equations D.23 and D.24 were used to calculate stresses at the top and bottom of the non-composite girder at stages 1 and 2.

$$f_{top} = -\frac{F_{se}}{A_{g-nc}} - \frac{F_{se}e}{S_{top-nc}} - \frac{M_{DL}}{S_{top-nc}} \qquad (D.23)$$

$$f_{bot} = -\frac{F_{se}}{A_{g-nc}} + \frac{F_{se}e}{S_{bot-nc}} + \frac{M_{DL}}{S_{bot-nc}} \qquad (D.24)$$

The values of F_{se} and M_{DL} were different between the two stages. Fse became less over time. M_{DL} was the weight of the girder only for stage 1. For stage 2, it was the weight of the girder and the deck.

D.6 Worksheet 5 - Composite Stress Calculations (Stage 3)

Worksheet 5 shown in Table D.5 provided calculations of composite stresses at the top and bottom of the girder and slab at time of testing. The stresses were broken down by axial component, strand eccentricity (F*e) component, dead load (DL) component, and live load (LL) component. The stress level used at stage 3 was the effective prestress after all losses occurred. The live load component reflected stresses resulting from the point load application. Determination of the number of strands developed was based on the strand development length specified in Worksheet 1. Moment values shown were listed in ft-kips. The support condition number indicated the position of the supports. A support condition number "1" indicated the supports were located at the ends of the girder offset by the X-DIST. A support condition "2" indicated the right-side support was moved in from the end forming a cantilever. A support condition "3" indicated both the left and right side supports were moved in from their

respective ends forming a double-cantilevered girder. The spreadsheet referred to these support condition numbers when determining the dead load moment values. As a note, these support condition numbers were not shown on the non-composite stress calculations page since at stages 1 and 2 the girder was supported at its centers of bearing (COB). Only during testing would the supports be moved to other than the end center of bearing locations. Equations D.25 and D.26 were used to calculate stresses at top and bottom of the girder at stage 3.

$$f_{top} = -\frac{F_{se}}{A_{g-nc}} - \frac{F_{se}e}{S_{top-nc}} - \frac{M_{DL}}{S_{top-nc}} - \frac{M_{LL}}{S_{top-c}} \qquad (D.25)$$

$$f_{bot} = -\frac{F_{se}}{A_{g-nc}} + \frac{F_{se}e}{S_{bot-nc}} + \frac{M_{DL}}{S_{bot-nc}} + \frac{M_{LL}}{S_{bot-c}} \qquad (D.26)$$

The stresses at the top and bottom of the deck were calculated based on the live load moment only using equations D.27 and D.28.

$$f_{top} = -\frac{M_{LL}(y_{top-c} + t_d)}{I_c} \qquad (D.27)$$

$$f_{bot-Deck} = -\frac{M_{LL}y_{top-c}}{I_c} \qquad (D.28)$$

D.7 Worksheet 6 – Girder Shear Design (Left of Load)

Worksheet 6 shown in Table D.6 performed shear design calculations for the section of the girder at 10th points from the left support to the point load based on the 1996 AASHTO[40] Specification. The distance from the left support to the point load was "a." Values of M_u and V_u were calculated at each point based on all dead and live loads. The value of M_u at the point load location was the same as the maximum furnished moment if all strands were developed at that point. V_{ci} (flexure shear strength) and V_{cw} (web shear strength) were calculated to determine the concrete strength component V_c using equations D.29 through D.32. V_c was the minimum of the V_{ci} and V_{cw} values.

$$V_{ci} = 0.6\lambda \frac{\sqrt{f_c'}}{1000} bd_p + V_d + \frac{V_i M_{cr}}{M_{max}} \geq 1.7\lambda \frac{\sqrt{f_c'}}{1000} bd_p \qquad (D.29)$$

$$M_{cr} = \frac{I}{Y_t}(6\lambda \frac{\sqrt{f_c'}}{1000} + f_{pe} - f_d) \qquad (D.30)$$

$$V_{cw} = (3.5\lambda \frac{\sqrt{f_c'}}{1000} + 0.3 f_{pc})bd_p + V_p \qquad (D.31)$$

$$f_{pc} = \frac{F_{se}}{A_{nc}} - \frac{F_{se} e(y_{bot-c} - y_{bot-nc})}{I_{nc}} - \frac{M_{DL}(y_{bot-c} - y_{bot-nc})}{I_{nc}} \qquad (D.32)$$

Based on the required shear, V_u, the spreadsheet determined the shear to be

carried by shear stirrups, V_s, using equation D.33.

$$V_s = \frac{V_u - V_c}{\phi_s}$$ (D.33)

The required minimum stirrup spacing, s, was calculated based on several criteria

as specified in equations D.34 through D.35. If $V_s > 8 \, (f_c')^{1/2} \, bd_p$, web crushing was

considered a potential a problem. The girder section was not adequate to handle the shear

force. If $V_s > 4 \, (f_c')^{1/2} \, bd_p$, the value from D.34 was divided by 2. The resulting

minimum stirrup spacing was the minimum of equations D.34 and D.35.

$$s_{max} = MAX(0.75h_{g-c}, 24 \; inches)$$ (D.34)

$$s = \frac{A_v f_y d_p}{V_s}$$ (D.35)

D.8 Worksheet 7 - Girder Shear Design (Right of Load)

Worksheet 7 shown in Table D.7 performed the same calculations as Worksheet 6

at 10th points from the load to the right support. The distance from the load to the right

support was "b."

D.9 Worksheet 8 – Interface Shear Check

Worksheet 8 shown in Table D.8 performed calculations to insure adequate capacity existed at the interface between the girder and deck. The basic interface shear capacity, V_{nh}, was determined based on the condition of the surface of the girder and the contact area using equation D.36.

$$V_{nh} = v_{nh} A_c \qquad (D.36)$$

$$A_{v-min} = \frac{50bs}{f_y} \frac{1}{s} \qquad (D.37)$$

Based on the cleanliness and roughness of the contact surface and the inclusion of minimum shear reinforcement steel per linear inch of girder according to equation D.37, the spreadsheet listed the basic interface shear stress, v_{nh}, the maximum value being 350 psi. The contact area, A_c, was determined as the interface shear contact width (width of the top of girder in this case) multiplied by the contact length, d, which was the distance from the point load to the closest support or one tenth of the span length, L_1, whichever was less. For this research, the length "d" was typically taken as one tenth of the span. The basic interface shear capacity was compared with the shear at the left support (worst case based on the configuration of this spreadsheet). If the basic capacity exceeded the worst-case shear, no further steel was required. If the basic capacity was inadequate, the added capacity of the shear steel was calculated.

The added capacity was calculated based on the amount of steel beyond the code-specified minimum in equation D.37. For every one percent of steel provided beyond the minimum, the interface shear capacity increased by an amount calculated in equation D.38.

$$Additional\ V_{nh}\ per\ one\ \%\ steel = \left(\frac{160 f_y}{40,000}\right) bd \qquad (D.38)$$

In most cases, as was true in this research, the steel provided by minimum shear reinforcement more than satisfied the requirement. No additional steel was required to meet interface shear requirements.

On the right-hand side of worksheet 8 are calculations for tensile stress at the shear interface. These calculations were provided to check the resulting tensile stress under maximum live load for comparison with acceptable levels. Acceptable levels were defined as $7.5 * \lambda * (f_c')^{1/2}$. For slab concrete which was assumed to be normal weight concrete, $\lambda = 1$. For the girder which was constructed with HSLC, $\lambda = 0.85$. Using a Mohr's circle calculation to determine tensile stress at the interface, the result was compared with the acceptable levels for both the slab and girder. If the tensile stress was less than both levels, the indicator window indicated, "Tensile Stress at Interface is OK."

393

Table D.1 Section and Material Properties for Girder Design

Section and Material Properties for Pretensioned Girder Design

Glc-West

Deck Variables

Deck Variables			
Deck Thickness	t_d	7.5	IN
Deck Width	W_f	40	IN
Concrete Strength	f'_c	3500	PSI
Concrete Weight	W_c	145	PCF

Girder Cross Section Variables

Girder Type		2	1-5,BT
Girder Top Flange Width		12	IN
Concrete Design Strength	f'_c	8000	PSI
Concrete Equilibrium Weight	W_c	116	PCF
% Concrete Strength at Release		75%	%
LWC Reduction Factor	λ	0.85	None
Strand Diameter	d_b	0.6	IN
Strand C/S Area	A_st	0.217	IN²
Strand Ultimate Strength	f_pu	270	KSI
Strand Yield as % of Ultimate		0.9	None
Strand Modulus of Elasticity	E_ps	28500	KSI
Stirrup Size		4	#
Stirrup Yield Strength	f_y	75	KSI
Distance from End to COB	XDIST	6.00	IN
Percent Strand Ultimate at Jacking		75%	%
Top of Beam to Top Strands	TCL	2.50	IN
Bottom of Beam to Bottom Strands	BCL	3.00	IN
Strand Spacing	SPAC	2.00	IN

Miscellaneous Variables Normally Constant

Steel Weight Allowance / Cubic Ft		3.0	PCF
Prestress stress for l_d calculation	f_ps	270	KSI
Ratio of Prestressed Reinforcement	ρ_p	0.0030	None
Shear Strength Reduction Factor	φ_s	1.00	None
Flexural Strength Reduction Factor	φ_f	1.00	None

Elasticity Modulus Values

Deck Modulus	E_cd	3.41E+06	PSI
Girder Modulus	E_cg	3.59E+06	PSI
Modular Ratio (E_cd/E_cb)	η	0.950	None

Non-Composite Girder Properties

Moment of Inertia	I_nc	50979	IN⁴
Distance from Centroid to Top of Beam	Y_top-nc	20.17	IN
Distance from Centroid to Bot. of Beam	Y_bot-nc	15.83	IN
Section Modulus (Top)	S_top-nc	2527.47	IN³
Section Modulus (Bot)	S_bot-nc	3220.40	IN³
Cross Sectional Area	A_g-nc	369	IN²
Weight per Foot (Concrete & Steel)	W_g-nc	0.305	K/FT
Web Thickness	b	6	IN
Height of Girder	h_g-nc	36	IN

Composite Girder Properties

Moment of Inertia	I_c	142547.25	IN⁴
Distance from Centroid to Top of Beam	Y_top-c	10.84	IN
Distance from Centroid to Bot. of Beam	Y_bot-c	25.16	IN
Section Modulus (Bot)	S_bot-c	5664.62	IN³
Cross Sectional Area	A_g-c	576.68	IN²
Weight per Foot (Concrete & Steel)	W_g-c	0.5295	K/FT
First Moment of Deck About Centroid	Q_d	3444.42	IN³
Overall Depth of Composite Girder	h_g-c	47.5	IN

Miscellaneous Properties

Stirrup Area	A_v	0.4	IN²
Depth to Prestressing Steel	d_p	38.4	IN
Ratio of Prestressed Reinforcement	ρ_p	0.0030	None
Strand Yield to Ultimate Factor	γ_p	0.28	None
Ratio of a/c (Based on Deck Concrete)	β_1	0.85	None

Strand Data (No Drape)

Ref. #	Dist. IN	Nbr #	% f_ps %	F_ps KIP	F_ps·d KIP-IN
18	TOP 33.5	2	0.75	87.89	2944.1
17		0	0.00	0.00	0.0
16		0	0.00	0.00	0.0
15	31.0	0	0.00	0.00	0.0
14	29.0	0	0.00	0.00	0.0
13	27.0	0	0.00	0.00	0.0
12	25.0	0	0.00	0.00	0.0
11	23.0	0	0.00	0.00	0.0
10	21.0	0	0.00	0.00	0.0
9	19.0	0	0.00	0.00	0.0
8	17.0	0	0.00	0.00	0.0
7	15.0	0	0.00	0.00	0.0
6	13.0	0	0.00	0.00	0.0
5	11.0	0	0.00	0.00	0.0
4	9.0	0	0.00	0.00	0.0
3	7.0	0	0.00	0.00	0.0
2	5.0	0	0.00	0.00	0.0
1	3.0	8	0.75	351.54	1054.6

Eccentricity from NC Centroid

Distance	-6.73	IN

Strand Development Length

AASHTO-STD (96)	96.14	IN
Dist. from Bearing	90.14	IN

Strand Transfer Length

AASHTO-STD (96)	38.04	IN

Table D.2 Support Conditions, Calculation of Moment Furnished and Predicted Ultimate Load

G1C-West — Support Conditions, Applied Load (KIP) and Moment Furnished (FT-KIP)

REF	BRNG	0.05L	0.10L	0.15L	0.20L	0.25L	0.30L	0.35L	0.40L	0.45L	0.50L	0.55L	0.60L	0.65L	0.70L	0.75L	0.80L	0.85L	0.90L	0.95L	BRNG
FT	0.00	2.10	4.20	6.30	8.40	10.50	12.60	14.70	16.80	18.90	21.00	23.10	25.20	27.30	29.40	31.50	33.60	35.70	37.80	39.90	42.00
IN	0.00	25.20	50.40	75.60	100.80	126.00	151.20	176.40	201.60	226.80	252.00	277.20	302.40	327.60	352.80	378.00	403.20	428.40	453.60	478.80	504.00

Number of Strands Developed Assuming l_d

REF	BRNG	0.05L	0.10L	0.15L	0.20L	0.25L	0.30L	0.35L	0.40L	0.45L	0.50L	0.55L	0.60L	0.65L	0.70L	0.75L	0.80L	0.85L	0.90L	0.95L	BRNG
# Top	0.12	0.65	1.17	1.70	2.00	2.00	2.00	2.00	2.00	2.00	2.00	2.00	2.00	2.00	2.00	2.00	2.00	1.70	1.17	0.65	0.12
# Bot	0.50	2.60	4.69	6.79	8.00	8.00	8.00	8.00	8.00	8.00	8.00	8.00	8.00	8.00	8.00	8.00	8.00	6.79	4.69	2.60	0.50
M_f	94.7	492.3	889.9	1287.5	1516.9	1516.9	1516.9	1516.9	1516.9	1516.9	1516.9	1516.9	1516.9	1516.9	1516.9	1516.9	1516.9	1287.5	889.9	492.3	94.7

Max Load (KIPS): 233

SUPT: 1

Type of Load	L Support Reaction (KIPS)	R Support Reaction (KIPS)
Dead	11.38	11.38
Point	193.46	39.25
Total	204.85	50.63

UNBRACED CONSTRUCTION

a	Distance from left support to point load	85.0	IN	7.08	FT
L_1	Distance from left support to right support	504.0	IN	42.00	FT
L_2	Distance from left COB to left support	0.00	IN	0.00	FT
L	Overall Length of Beam (COB-COB)	504.0	IN	42.00	FT
b	Distance from point load to right support	419.0	IN	34.92	FT
L_3	Distance from right support to right COB	0.0	IN	0.00	FT
a/d	Ratio of shear distance to depth	2.36		NA	

M_f (Max) Calculations

d_p	38.40	IN	
ρ_p	0.00297	None	
f_{ps}	249.6	KSI	
ω_p	0.2121	$.36\beta_1$	0.306
Beam is Under-reinforced			
$a <$ Deck Thickness			
a	9.58	IN	
M_f	1516.9	FT-KIP	

DECK

BEAM

Table D.3 Loss Calculations

Prestressed Girder Loss Calculations

G1C-West

Beam Values

Description	Symbol	Value	Units
Girder Length (COB-COB)	L	42.00	FT
Girder Cross Sectional Area	A_{g-nc}	369	IN²
NC Moment of Inertia	I_{nc}	50979	IN⁴
NC Section Modulus (Top)	S_{top-nc}	2527.47	IN³
NC Section Modulus (Bot)	S_{bot-nc}	3220.40	IN³
Strand Eccentricity from NC Centroid	e	-6.73	IN
NC Girder Weight / Foot (Concrete & Steel)	W_D	0.305	K/FT
Deck Weight / Foot (Concrete & Steel)	W_{SD}	0.225	K/FT

Steel Values

Description	Symbol	Value	Units
Area of Prestressing Steel	A_{ps}	2.17	IN²
Strand Ultimate Strength	f_{pu}	270	KSI
Strand Yield Strength	f_{py}	243	KSI
Strand Modulus of Elasticity	E_{ps}	28500	KSI
Percent Strand Ultimate at Jacking	%	0.75	None
Strand Jacking Stress	f_{si}	202.5	KSI

Concrete Values

Description	Symbol	Value	Units
Girder Concrete Design Strength	f_c'	8000	PSI
Girder Design Modulus	E_{cg}	3.59E+06	PSI
% Girder Concrete Strength at Release	%	75%	%
Girder Concrete Strength at Release	f_{ci}'	6000	PSI
Girder Modulus at Release	E_{cig}	3.43E+06	PSI

ES-Elastic Shortening (Release)

Description	Symbol	Value	Units
Radius of Gyration	r_{nc}^2	138.2	IN²
Initial Jacking Force	P_i	439.4	KIPS
Est. Jacking Force Loss	OK	-5.7%	%
Final Jacking Force	P_i	414.4	KIPS
MAX Dead Load Moment	M_D	806.9	IN-KIPS
Stress at Steel Centroid	f_{cir}	-1.385	KSI
Modular Ratio (E_{ps}/E_{cig})	η	8.30	None
ES Losses (KSI - %)	Δ_{pES}	-11.49	-5.7%

R-Steel Stress Relax (Release)

Description	Symbol	Value	Units
% Relax at Release			%
Time (Jack to Release)	t_{rel}		HRS
R Losses (KSI - %)	Δ_{pR}	-0.81	-0.4%

R-Steel Stress Relax (Deck Placement)

Description	Symbol	Value	Units
% Relax at Release			%
Time (Release to Slab)	t_{slab}		DAYS
R Losses (KSI - %)	Δ_{pR}	-1.62	-0.8%

R-Steel Stress Relax (Testing)

Description	Symbol	Value	Units
% Relax at Release			%
Time (Release to Test)	t_{test}		DAYS
R Losses (KSI - %)	Δ_{pR}	-0.27	-0.1%

Steel Stress Relaxation Percentages-OK

CR-Creep (Deck Placement)

Description	Symbol	Value	Units
Modular Ratio (E_{ps}/E_{cb})	η	7.95	None
Stress at Steel Centroid	f_{cir}	-1.385	KSI
Addl. DL Since Release	W_{SD}	0.000	K/FT
Moment due to W_{SD}	M_{SD}	0.0	IN-KIP
Stress at Steel Centroid	f_{csd}	0.000	KSI
LWC Factor		1.0	None
Creep Factor	K_{CR}	1.0	None
CR Losses (KSI - %)	Δ_{pCR}	-16.62	-8.2%

CR-Creep (Testing)

Description	Symbol	Value	Units
Modular Ratio (E_{ps}/E_{cb})	η	7.95	None
Stress at Steel Centroid	f_{cir}	-1.385	KSI
Addl. DL Since Release	W_{SD}	0.225	K/FT
Moment due to W_{SD}	M_{SD}	594.2	IN-KIP
Stress at Steel Centroid	f_{csd}	0.078	KSI
LWC Factor		1.0	None
Creep Factor	K_{CR}	1.0	None
CR Losses (KSI - %)	Δ_{pCR}	-0.55	-0.3%

SH-Shrinkage (Deck Placement)

Description	Symbol	Value	Units
Shrinkage Factor	K_{SH}	1.0	None
Relative Humidity	RH	70	%
SH Losses (KSI - %)	Δ_{pSH}	-6.50	-3.2%

Consolidated Loss Calculations

Stage	Total KSI Loss	% Loss	Remaining Prestress (KSI)		Losses
1. At Release	-12.30	-6%	190.20	f_{ps}	ES & R
2. At Deck Placement	-37.03	-18%	165.47	f_{se}	CR, SH & R
3. At Testing	-37.85	-19%	164.65	f_{se}	CR & R

Table D.4 Non-Composite Stress Calculations

G1C-West — Non-Composite Girder Stresses at Stages 1 and 2 of Construction

REF	BRNG	0.05L	0.10L	0.15L	0.20L	0.25L	0.30L	0.35L	0.40L	0.45L	0.50L	0.55L	0.60L	0.65L	0.70L	0.75L	0.80L	0.85L	0.90L	0.95L	BRNG
FT	0.00	2.10	4.20	6.30	8.40	10.50	12.60	14.70	16.80	18.90	21.00	23.10	25.20	27.30	29.40	31.50	33.60	35.70	37.80	39.90	42.00
IN	0.00	25.20	50.40	75.60	100.80	126.00	151.20	176.40	201.60	226.80	252.00	277.20	302.40	327.60	352.80	378.00	403.20	428.40	453.60	478.80	504.00

Number of Strands Developed Assuming l_t

	BRNG	0.05L	0.10L	0.15L	0.20L	0.25L	0.30L	0.35L	0.40L	0.45L	0.50L	0.55L	0.60L	0.65L	0.70L	0.75L	0.80L	0.85L	0.90L	0.95L	BRNG
# Top	0.32	1.64	2.00	2.00	2.00	2.00	2.00	2.00	2.00	2.00	2.00	2.00	2.00	2.00	2.00	2.00	2.00	2.00	2.00	1.64	0.32
# Bot	1.26	6.56	8.00	8.00	8.00	8.00	8.00	8.00	8.00	8.00	8.00	8.00	8.00	8.00	8.00	8.00	8.00	8.00	8.00	6.56	1.26

DECK 0.2246 K/FT

BEAM 0.3049 K/FT

1 — Stresses in Non-Composite Beam due to Effective Prestress & Beam DL (At Release) After Initial Losses Have Occurred (ES & R) Assuming l_t (KSI)

	BRNG	0.05L	0.10L	0.15L	0.20L	0.25L	0.30L	0.35L	0.40L	0.45L	0.50L	0.55L	0.60L	0.65L	0.70L	0.75L	0.80L	0.85L	0.90L	0.95L	BRNG
Axial	-0.176	-0.917	-1.119	-1.119	-1.119	-1.119	-1.119	-1.119	-1.119	-1.119	-1.119	-1.119	-1.119	-1.119	-1.119	-1.119	-1.119	-1.119	-1.119	-0.917	-0.176
Fe (T)	0.173	0.901	1.099	1.099	1.099	1.099	1.099	1.099	1.099	1.099	1.099	1.099	1.099	1.099	1.099	1.099	1.099	1.099	1.099	0.901	0.173
Fe (B)	-0.136	-0.707	-0.863	-0.863	-0.863	-0.863	-0.863	-0.863	-0.863	-0.863	-0.863	-0.863	-0.863	-0.863	-0.863	-0.863	-0.863	-0.863	-0.863	-0.707	-0.136
DL (T)	0.000	-0.061	-0.115	-0.163	-0.204	-0.239	-0.268	-0.291	-0.306	-0.316	-0.319	-0.316	-0.306	-0.291	-0.268	-0.239	-0.204	-0.163	-0.115	-0.061	0.000
DL (B)	0.000	0.048	0.090	0.128	0.160	0.188	0.210	0.228	0.241	0.248	0.251	0.248	0.241	0.228	0.210	0.188	0.160	0.128	0.090	0.048	0.000
Tot (T)	-0.003	-0.077	-0.134	-0.182	-0.224	-0.259	-0.288	-0.310	-0.326	-0.336	-0.339	-0.336	-0.326	-0.310	-0.288	-0.259	-0.224	-0.182	-0.134	-0.077	-0.003
Tot (B)	-0.312	-1.577	-1.891	-1.853	-1.821	-1.793	-1.771	-1.753	-1.741	-1.733	-1.731	-1.733	-1.741	-1.753	-1.771	-1.793	-1.821	-1.853	-1.891	-1.577	-0.312

2 — Stresses in Non-Composite Beam due to Effective Prestress & All Permanent DL after Slab Placement (ES, R, CR & SH) Assuming l_t (KSI)

	BRNG	0.05L	0.10L	0.15L	0.20L	0.25L	0.30L	0.35L	0.40L	0.45L	0.50L	0.55L	0.60L	0.65L	0.70L	0.75L	0.80L	0.85L	0.90L	0.95L	BRNG
Axial	-0.153	-0.798	-0.973	-0.973	-0.973	-0.973	-0.973	-0.973	-0.973	-0.973	-0.973	-0.973	-0.973	-0.973	-0.973	-0.973	-0.973	-0.973	-0.973	-0.798	-0.153
Fe (T)	0.151	0.784	0.956	0.956	0.956	0.956	0.956	0.956	0.956	0.956	0.956	0.956	0.956	0.956	0.956	0.956	0.956	0.956	0.956	0.784	0.151
Fe (B)	-0.118	-0.615	-0.750	-0.750	-0.750	-0.750	-0.750	-0.750	-0.750	-0.750	-0.750	-0.750	-0.750	-0.750	-0.750	-0.750	-0.750	-0.750	-0.750	-0.615	-0.118
DL (T)	0.000	-0.105	-0.200	-0.283	-0.355	-0.416	-0.466	-0.504	-0.532	-0.549	-0.554	-0.549	-0.532	-0.504	-0.466	-0.416	-0.355	-0.283	-0.200	-0.105	0.000
DL (B)	0.000	0.083	0.157	0.222	0.278	0.326	0.365	0.396	0.418	0.431	0.435	0.431	0.418	0.396	0.365	0.326	0.278	0.222	0.157	0.083	0.000
Tot (T)	-0.003	-0.119	-0.217	-0.300	-0.372	-0.433	-0.483	-0.521	-0.549	-0.566	-0.571	-0.566	-0.549	-0.521	-0.483	-0.433	-0.372	-0.300	-0.217	-0.119	-0.003
Tot (B)	-0.272	-1.331	-1.567	-1.502	-1.445	-1.397	-1.358	-1.328	-1.306	-1.293	-1.288	-1.293	-1.306	-1.328	-1.358	-1.397	-1.445	-1.502	-1.567	-1.331	-0.272

Table D.5 Composite Stress Calculations

G1C-West — Composite Beam Stresses at Stage 3 of Construction (Testing)

REF	BRNG	0.05L	0.10L	0.15L	0.20L	0.25L	0.30L	0.35L	0.40L	0.45L	0.50L	0.55L	0.60L	0.65L	0.70L	0.75L	0.80L	0.85L	0.90L	0.95L	BRNG
FT	0.00	2.10	4.20	6.30	8.40	10.50	12.60	14.70	16.80	18.90	21.00	23.10	25.20	27.30	29.40	31.50	33.60	35.70	37.80	39.90	42.00
# Top	0.12	0.65	1.17	1.70	2.00	2.00	2.00	2.00	2.00	2.00	2.00	2.00	2.00	2.00	2.00	2.00	2.00	1.70	1.17	0.65	0.12
# Bot	0.50	2.60	4.69	6.79	8.00	8.00	8.00	8.00	8.00	8.00	8.00	8.00	8.00	8.00	8.00	8.00	8.00	6.79	4.69	2.60	0.50

Number of Strands Developed Assuming l_d

Max Load (KIPS): 233

SUPT: 1

DECK 0.2246 K/FT
BEAM 0.3049 K/FT

Stresses in Composite Beam due to Prestressing, Permanent DL and Point Load with Above Support Conditions (All Losses) Assuming l_d (KSI)

REF	BRNG	0.05L	0.10L	0.15L	0.20L	0.25L	0.30L	0.35L	0.40L	0.45L	0.50L	0.55L	0.60L	0.65L	0.70L	0.75L	0.80L	0.85L	0.90L	0.95L	BRNG
M_{DL}	0.0	22.2	42.0	59.5	74.7	87.6	98.1	106.2	112.1	115.6	116.8	115.6	112.1	106.2	98.1	87.6	74.7	59.5	42.0	22.2	0.0
M_{LL}	0.0	406.3	812.5	1218.8	1318.7	1236.3	1153.9	1071.4	989.0	906.6	824.2	741.8	659.3	576.9	494.5	412.1	329.7	247.3	164.8	82.4	0.0
Axial	-0.060	-0.314	-0.568	-0.822	-0.968	-0.968	-0.968	-0.968	-0.968	-0.968	-0.968	-0.968	-0.968	-0.968	-0.968	-0.968	-0.968	-0.822	-0.568	-0.314	-0.060
Fe (T)	0.059	0.309	0.558	0.808	0.951	0.951	0.951	0.951	0.951	0.951	0.951	0.951	0.951	0.951	0.951	0.951	0.951	0.808	0.558	0.309	0.059
Fe (B)	-0.047	-0.242	-0.438	-0.634	-0.747	-0.747	-0.747	-0.747	-0.747	-0.747	-0.747	-0.747	-0.747	-0.747	-0.747	-0.747	-0.747	-0.634	-0.438	-0.242	-0.047
DL-T	0.000	-0.105	-0.200	-0.283	-0.355	-0.416	-0.466	-0.504	-0.532	-0.549	-0.554	-0.549	-0.532	-0.504	-0.466	-0.416	-0.355	-0.283	-0.200	-0.105	0.000
DL-B	0.000	0.083	0.157	0.222	0.278	0.326	0.365	0.396	0.418	0.431	0.435	0.431	0.418	0.396	0.365	0.326	0.278	0.222	0.157	0.083	0.000
LL-T	0.000	-0.371	-0.741	-1.112	-1.203	-1.128	-1.053	-0.977	-0.902	-0.827	-0.752	-0.677	-0.601	-0.526	-0.451	-0.376	-0.301	-0.226	-0.150	-0.075	0.000
LL-B	0.000	0.861	1.721	2.582	2.794	2.619	2.444	2.270	2.095	1.921	1.746	1.571	1.397	1.222	1.048	0.873	0.698	0.524	0.349	0.175	0.000
Grd-T	-0.001	-0.481	-0.951	-1.409	-1.575	-1.560	-1.535	-1.499	-1.451	-1.393	-1.323	-1.242	-1.150	-1.048	-0.934	-0.809	-0.672	-0.523	-0.360	-0.186	-0.001
Grd-B	-0.107	0.387	0.872	1.348	1.357	1.230	1.095	0.951	0.798	0.636	0.466	0.287	0.099	-0.097	-0.302	-0.516	-0.738	-0.710	-0.500	-0.299	-0.107
Deck-T	0.000	-0.764	-1.528	-2.292	-2.479	-2.325	-2.170	-2.015	-1.860	-1.705	-1.550	-1.395	-1.240	-1.085	-0.930	-0.775	-0.620	-0.465	-0.310	-0.155	0.000
Deck-B	0.000	-0.371	-0.741	-1.112	-1.203	-1.128	-1.053	-0.977	-0.902	-0.827	-0.752	-0.677	-0.601	-0.526	-0.451	-0.376	-0.301	-0.226	-0.150	-0.075	0.000

Table D.6 Girder Shear Design Calculations (Left of Load)

G1C-West		Girder Shear Design (Left of Load)										
	IN	L-SUPT	0.1 a	0.2 a	0.3 a	0.4 a	0.5 a	0.6 a	0.7 a	0.8 a	0.9 a	P-LOAD
Distance from Left Support (Inches)	IN	0.00	8.50	17.00	25.50	34.00	42.50	51.00	59.50	68.00	76.50	85.00
Ultimate Moment Furnished	FT-KIP	94.67	228.79	362.91	497.02	631.14	765.26	899.38	1033.49	1167.61	1301.73	1435.85
Transferred Strands Factor		0.16	0.38	0.60	0.83	1.00	1.00	1.00	1.00	1.00	1.00	1.00
Transferred # Top Strands	#	0.32	0.76	1.21	1.66	2.00	2.00	2.00	2.00	2.00	2.00	2.00
Transferred # Bottom Strands	#	1.26	3.05	4.84	6.62	8.00	8.00	8.00	8.00	8.00	8.00	8.00
Developed Strands Factor		0.06	0.15	0.24	0.33	0.42	0.50	0.59	0.68	0.77	0.86	0.95
Developed # Top Strands	#	0.12	0.30	0.48	0.66	0.83	1.01	1.19	1.36	1.54	1.72	1.89
Developed # Bottom Strands	#	0.50	1.21	1.91	2.62	3.33	4.04	4.74	5.45	6.16	6.87	7.57
Non-composite DL Moment (BM+SL)	FT-KIP	0.00	7.74	15.22	22.43	29.38	36.06	42.48	48.63	54.51	60.13	65.48
Total DL Shear (BM+SL)	KIP	11.38	11.01	10.63	10.26	9.88	9.51	9.13	8.76	8.38	8.01	7.63
Available Moment Capacity	FT-KIP	94.67	221.04	347.68	474.59	601.76	729.20	856.90	984.87	1113.10	1241.60	1370.36
Ultimate Moment, M_u	FT-KIP	0.00	144.78	289.29	433.54	577.53	721.24	864.70	1007.88	1150.80	1293.46	1435.85
Ultimate Shear, Vu	KIP	204.85	204.47	204.10	203.72	203.35	202.97	202.60	202.22	201.85	201.47	201.10
f_d	KSI	0.000	0.029	0.057	0.084	0.109	0.134	0.158	0.181	0.203	0.224	0.244
SFPF (Based on l_d)	KIPS	22.30	53.89	85.48	117.07	148.66	180.25	211.84	243.43	275.01	306.60	338.19
f_{pe}	KSI	-0.107	-0.259	-0.410	-0.562	-0.714	-0.865	-1.017	-1.168	-1.320	-1.472	-1.623
M_{CR}	FT-KIP	265.85	323.81	382.23	441.12	500.47	560.30	620.59	681.34	742.57	804.26	866.42
V_{ci} (Flexure Shear)	KIPS	29.78	478.83	290.81	228.05	196.61	177.70	165.05	155.97	149.14	143.79	139.49
FPF (Based on l_t)	KIPS	56.35	136.19	216.03	295.86	357.29	357.29	357.29	357.29	357.29	357.29	357.29
f_{pc}	KSI	-0.083	-0.218	-0.353	-0.486	-0.593	-0.607	-0.621	-0.635	-0.648	-0.660	-0.672
V_{cw} (Web Shear)	KIPS	67.06	76.39	85.68	94.93	102.26	103.28	104.25	105.19	106.08	106.93	107.75
V_c	KIPS	29.78	76.39	85.68	94.93	102.26	103.28	104.25	105.19	106.08	106.93	107.75
$V_u \phi$	KIPS	204.85	204.47	204.10	203.72	203.35	202.97	202.60	202.22	201.85	201.47	201.10
Shear Steel Beyond Minimum Required	Y/N	YES	YES	YES	YES	YES	YES	YES	YES	YES	YES	YES
Web Crushing		CRUSH	OK	OK	OK	OK	OK	OK	OK	OK	OK	OK
Required Strength of Steel, Vs	KIPS	175.07	128.08	118.41	108.79	101.08	99.69	98.34	97.04	95.77	94.54	93.35
Required Stirrup Spacing, s	IN	6.58	8.99	9.73	10.59	11.40	11.56	11.71	11.87	12.00	12.00	12.00

399

Table D.7 Girder Shear Design Calculations (Right of Load)

G1C-West		Girder Shear Design (Right of Load)										
Distance from Left Support (Inches)	IN	P-LOAD	0.1 b	0.2 b	0.3 b	0.4 b	0.5 b	0.6 b	0.7 b	0.8 b	0.9 b	R-SUPT
		85.00	126.90	168.80	210.70	252.60	294.50	336.40	378.30	420.20	462.10	504.00
Ultimate Moment Furnished	FT-KIP	1435.85	1516.94	1516.94	1516.94	1516.94	1516.94	1516.94	1516.94	1416.91	755.79	94.67
Transferred Strands Factor		1.00	1.00	1.00	1.00	1.00	1.00	1.00	1.00	1.00	1.00	0.16
Transferred # Top Strands	#	2.00	2.00	2.00	2.00	2.00	2.00	2.00	2.00	2.00	2.00	0.32
Transferred # Bottom Strands	#	8.00	8.00	8.00	8.00	8.00	8.00	8.00	8.00	8.00	8.00	1.26
Developed Strands Factor		0.95	1.00	1.00	1.00	1.00	1.00	1.00	1.00	0.93	0.50	0.06
Developed # Top Strands	#	1.89	2.00	2.00	2.00	2.00	2.00	2.00	2.00	1.87	1.00	0.12
Developed # Bottom Strands	#	7.57	8.00	8.00	8.00	8.00	8.00	8.00	8.00	7.47	3.99	0.50
Non-composite DL Moment (BM+SL)	FT-KIP	65.48	87.98	104.03	113.62	116.76	113.44	103.66	87.43	64.74	35.60	0.00
Total DL Shear (BM+SL)	KIP	7.63	5.78	3.94	2.09	0.24	-1.61	-3.46	-5.31	-7.16	-9.01	-10.85
Available Moment Capacity	FT-KIP	1370.36	1428.95	1412.91	1403.32	1400.18	1403.50	1413.28	1429.51	1352.17	720.19	94.67
Ultimate Moment, M_u	FT-KIP	1435.85	1321.31	1200.32	1072.88	938.97	798.62	651.81	498.54	338.81	172.63	0.00
Ultimate Shear, V_u	KIP	31.61	33.46	35.31	37.16	39.01	40.86	42.71	44.56	46.40	48.25	50.10
f_d	KSI	0.244	0.328	0.388	0.423	0.435	0.423	0.386	0.326	0.241	0.133	0.000
SFPF (Based on l_d)	KIPS	338.19	357.29	357.29	357.29	357.29	357.29	357.29	357.29	333.73	178.02	22.30
f_{pe}	KSI	-1.623	-1.715	-1.715	-1.715	-1.715	-1.715	-1.715	-1.715	-1.602	-0.854	-0.107
M_{CR}	FT-KIP	866.42	870.12	841.89	825.02	819.50	825.34	842.54	871.09	857.62	556.06	265.85
V_{ci} (Flexure Shear)	KIPS	37.22	38.33	39.21	41.17	44.79	51.12	62.25	83.05	120.81	156.93	########
FPF (Based on l_t)	KIPS	357.29	357.29	357.29	357.29	357.29	357.29	357.29	357.29	357.29	357.29	56.35
f_{pc}	KSI	-0.672	-0.721	-0.757	-0.778	-0.785	-0.777	-0.756	-0.720	-0.670	-0.606	-0.083
V_{cw} (Web Shear)	KIPS	107.75	111.16	113.60	115.06	115.53	115.03	113.55	111.08	107.63	103.21	67.06
V_c	KIPS	37.22	38.33	39.21	41.17	44.79	51.12	62.25	83.05	107.63	103.21	67.06
V_u/ϕ	KIPS	31.61	33.46	35.31	37.16	39.01	40.86	42.71	44.56	46.40	48.25	50.10
Shear Steel Beyond Minimum Required	Y/N	NO	NO	NO	NO	NO	NO	NO	NO	NO	NO	NO
Web Crushing		OK	OK	OK	OK	OK	OK	OK	OK	OK	OK	OK
Required Strength of Steel, V_s	KIPS	0.00	0.00	0.00	0.00	0.00	0.00	0.00	0.00	0.00	0.00	0.00
Required Stirrup Spacing, s	IN	24.00	24.00	24.00	24.00	24.00	24.00	24.00	24.00	24.00	24.00	24.00

400

Table D.8 Deck / Girder Interface Shear Calculations

G1C-West		Deck / Girder Interface Shear Calculations			
Interface Shear Calculation Values				**Tensile Stress at Interface**	
Lightweight Concrete Reduction Factor	λ	0.85	None	Deck Concrete Design Strength	f'_c	3500	PSI
Shear Strength Reduction Factor	ϕ_s	1.00	None	Maximum Allowable Deck Tensile Stress		443.71	PSI
Maximum Unfactored Shear	V_u	204.85	KIPS	Girder Concrete Design Strength	f'_c	8000	PSI
First Moment of Deck About Centroid	QS	3444.42	IN^3	Maximum Allowable Beam Tensile Stress		570.20	PSI
Composite Moment of Inertia	I_c	142547	IN^4	Maximum Interface Shear Stress (VQ/Ib)	v_h	412.48	PSI
Interface Shear Contact Width	b_v	12	IN	Effective Prestress Force	F_{pe}	338.19	KIPS
Contact Length, d (a+XDIST<=SPAN/10)	Span/10	50.40	IN	Girder Cross Sectional Area	A_{nc}	369	IN^2
Contact Area (b_v*Contact Length)	A_c	604.8	IN^2	Strand Eccentricity from NC Centroid	e	-6.73	IN
Yield Strength of Tie Reinforcement	f_y	75	KSI	Distance from NC Centroid to Beam Top	y_{top-nc}	20.17	IN
Stirrup Area	A_v	0.4	IN^2	Distance from C Centroid to Beam Top	y_{top-c}	10.84	IN
				Non-Composite Moment of Inertia	I_{nc}	50979	IN^4
				Composite Moment of Inertia	I_c	142547	IN^4
Interface Condition				Dead Load Moment	M_{DL}	65.48	FT-KIP
Contact Surface Clean		YES	YES/NO	Live Load Moment	M_{LL}	1370.36	FT-KIP
Contact Surface Roughened 1/4"		YES	YES/NO	Maximum Compressive Stress at Interface	f_{ca}	-1576.88	PSI
Minimum Ties Provided		YES	YES/NO	Maximum Tensile Stress at Interface	f_t	101.381	PSI
Maximum Basic Interface Stress		350	PSI	**Tensile Stress at Interface is OK**			
Maximum Basic Interface Force	V_{nh}	211.68	KIPS				
Basic Interface Shear Capacity Adequate							

Additional Interface Capacity Provided by Shear Reinforcement			
Additional Interface Capacity Required		0.00	KIPS
Worst Case Stirrup Spacing over "a"	s	12.00	IN
Minimum Tie Area per Inch of Beam		0.0080	IN^2/IN
Additional V_{nh} Capacity per Percent		181.4	KIPS
Additional Percent Required		0.00	%
Additional Required Tie Area		0.000000	IN^2/IN
Total Tie Area Required		0.008000	IN^2/IN
Min. Tie Area Provided by V Reinforcement		0.033333	IN^2/IN
Resulting Contact Area Stress		338.70	PSI
Interface Shear Capacity Adequate			

APPENDIX E

LOAD CELL CALIBRATION

This Appendix contains the calibration curves for strand load cells used to monitor the force in the prestressing strands from initial tensioning through the time of strand release. Figures E.1 through E.10 show the calibration curves determined for each strand load cell. The following procedure was used in determining the calibration curves.

1. All load cells were connected to the BLH 1225 Portable 10 Channel Switch and Balance Unit, which was connected to a BLH 1200B Portable Digital Strain Indicator. The load cells were a "full-bridge" configuration. The same units used for this calibration were used during girder construction.

2. The load cells were placed individually in an 800 kip SATEK compression testing machine. After being properly positioned, load was applied to the cells slowly through a load of 45 kips, the maximum anticipated load during strand tensioning. At the 10, 20, 30, 40, and 45 kip readings indicated on the SATEK machine, corresponding strain readings were taken from the digital strain indicator.

3. After testing, all load and strain data was entered into an EXCEL spreadsheet and plotted. The slope of each stress vs. strain plot was determined using the linear trendline option in EXCEL. The slope values are listed in the bottom right of each calibration plot.
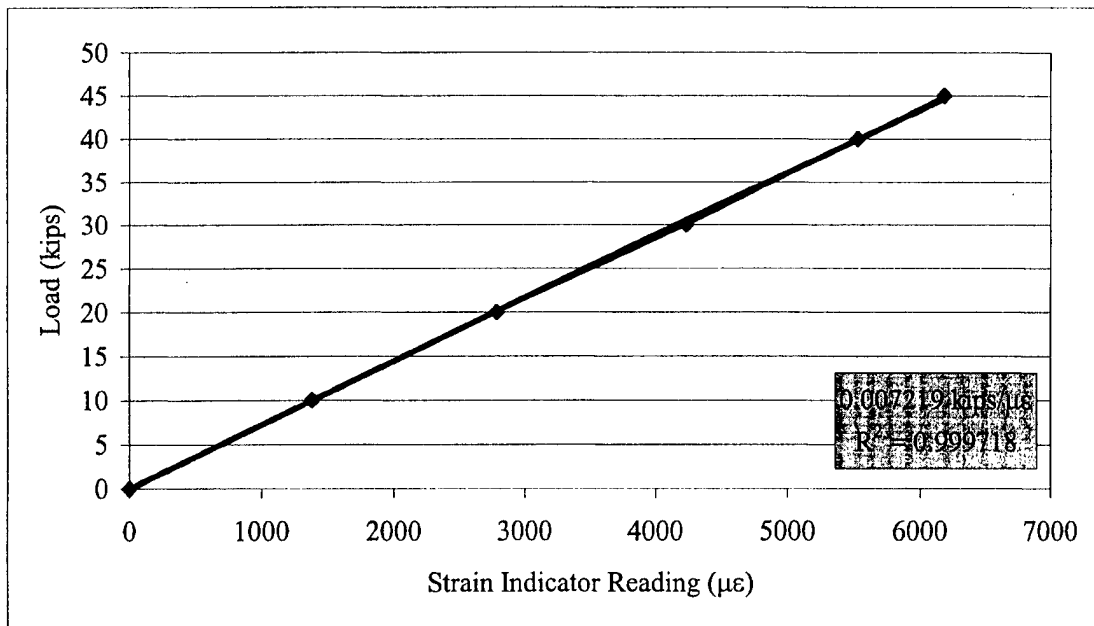
Figure E.1 Calibration Curve for Strand Load Cell # 1
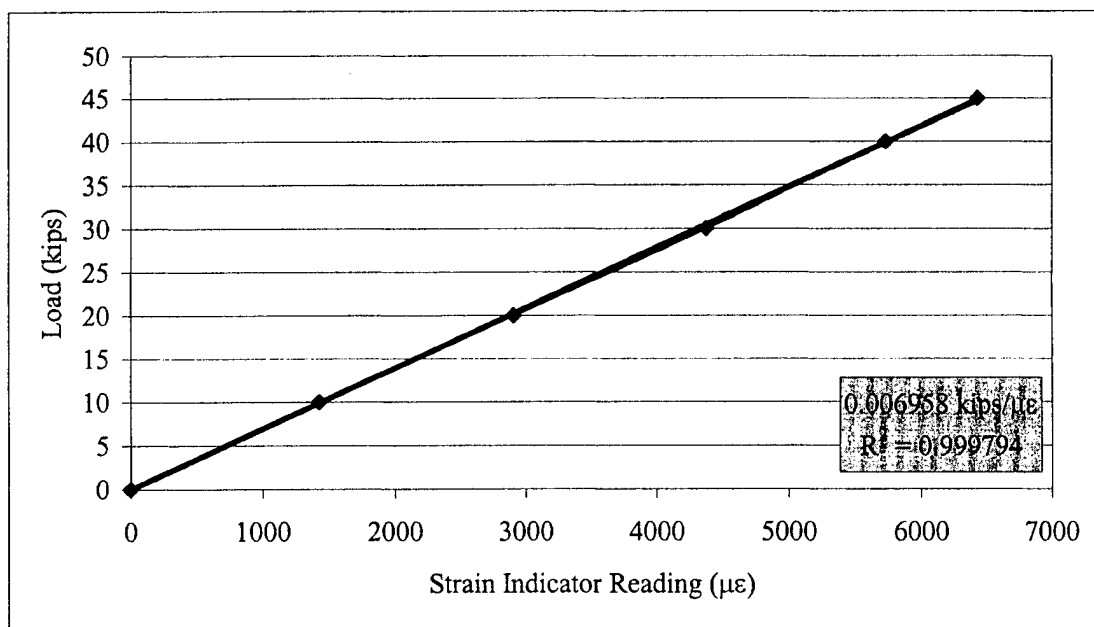
Figure E.2 Calibration Curve for Strand Load Cell # 2
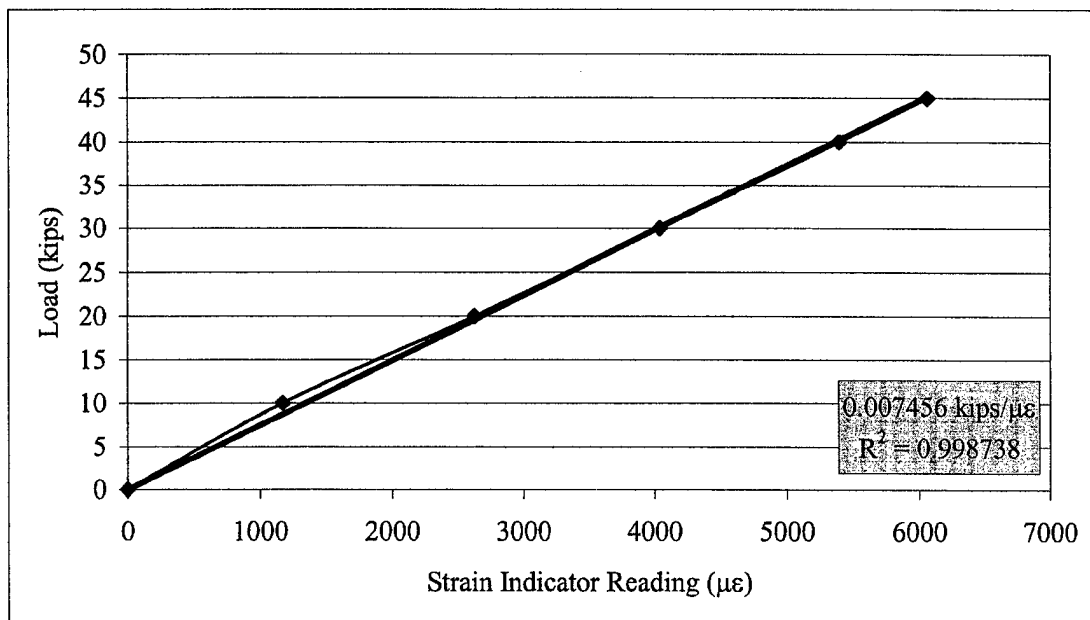
Figure E.3 Calibration Curve for Strand Load Cell # 3
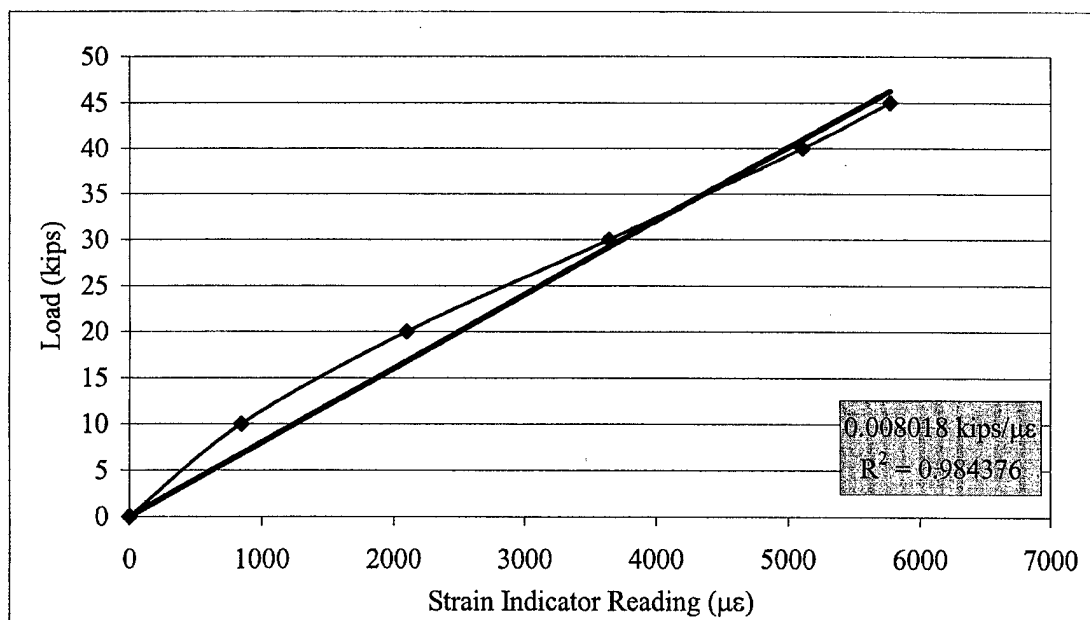
Figure E.4 Calibration Curve for Strand Load Cell # 4
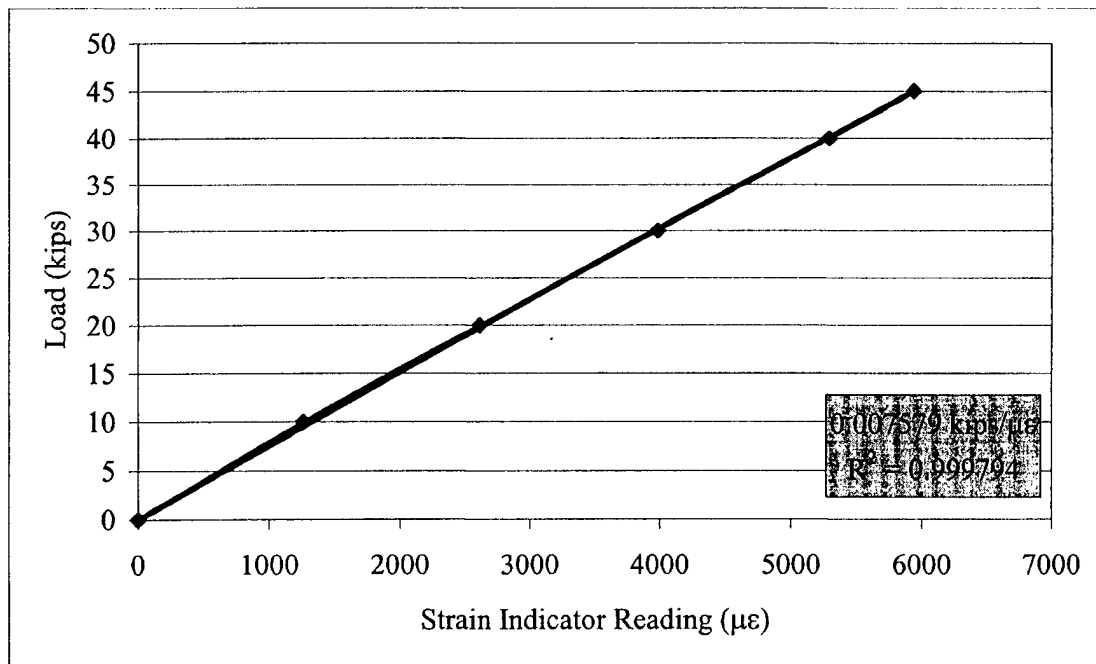
Figure E.5 Calibration Curve for Strand Load Cell # 5
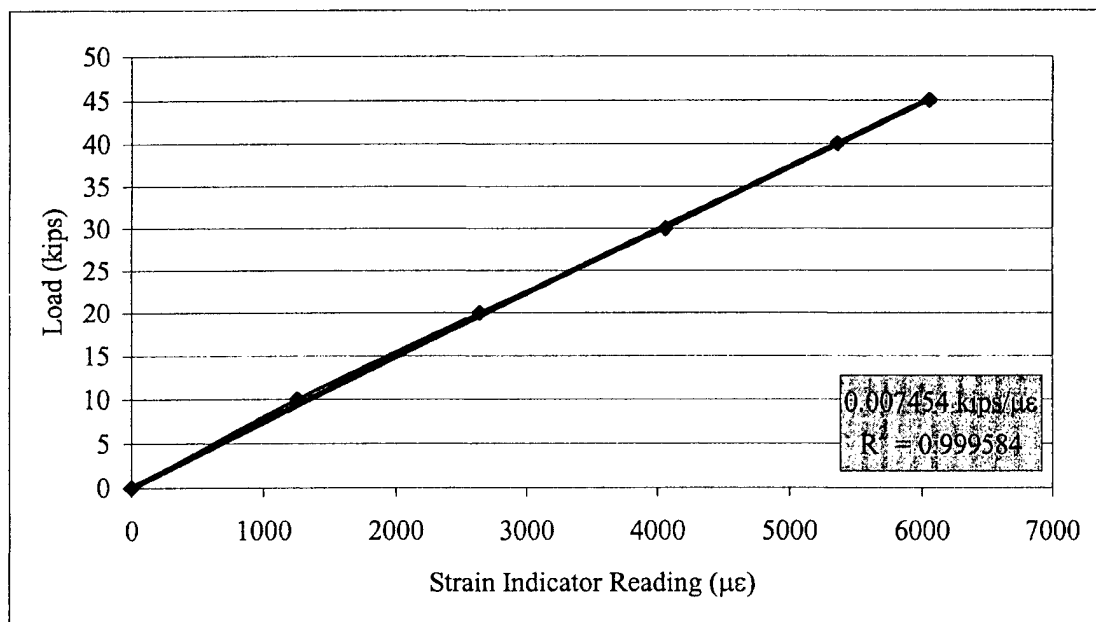
Figure E.6 Calibration Curve for Strand Load Cell # 6
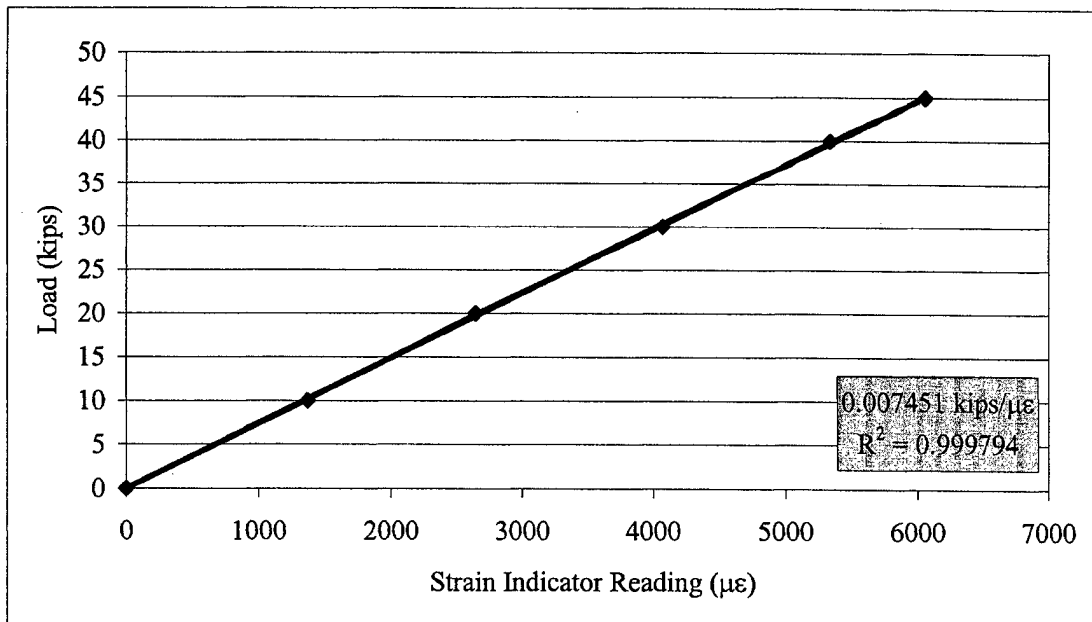
Figure E.7 Calibration Curve for Strand Load Cell # 7
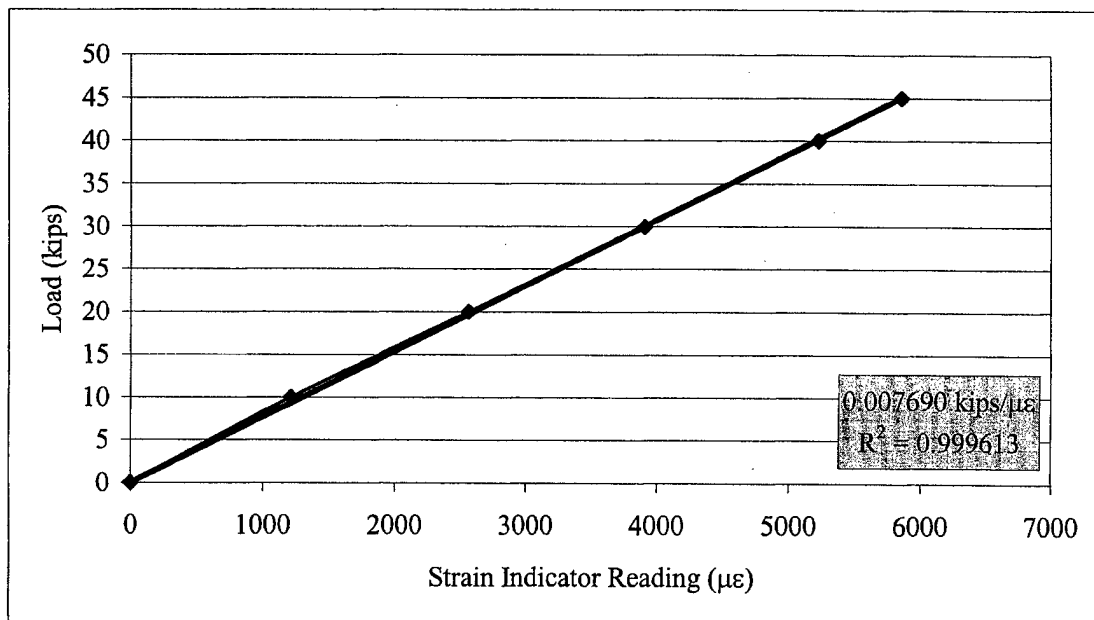
Figure E.8 Calibration Curve for Strand Load Cell # 8
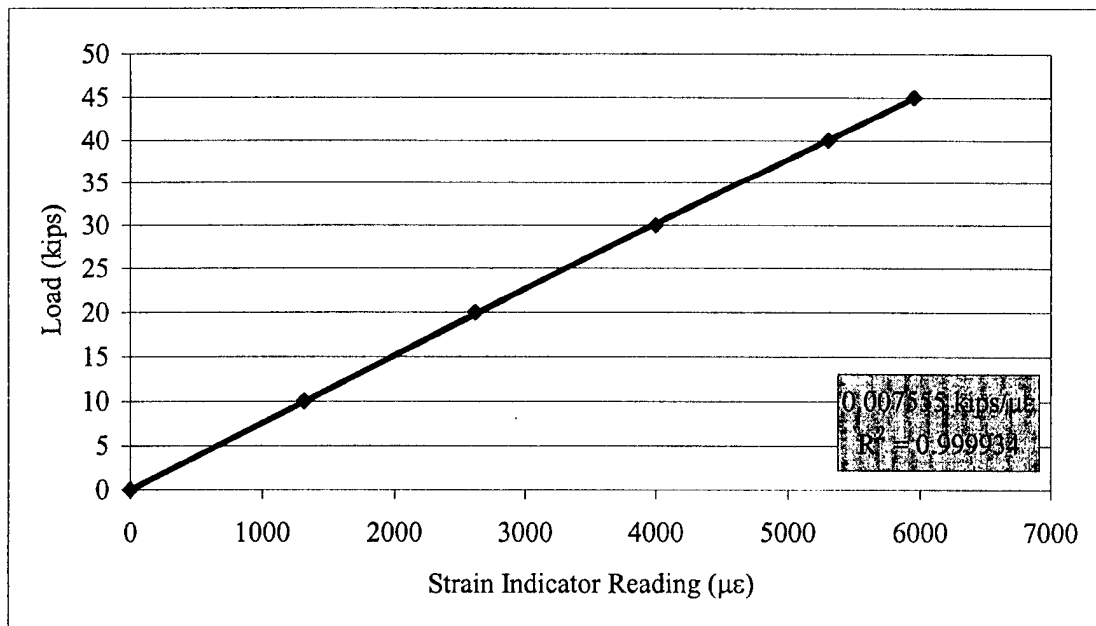
Figure E.9 Calibration Curve for Strand Load Cell # 9
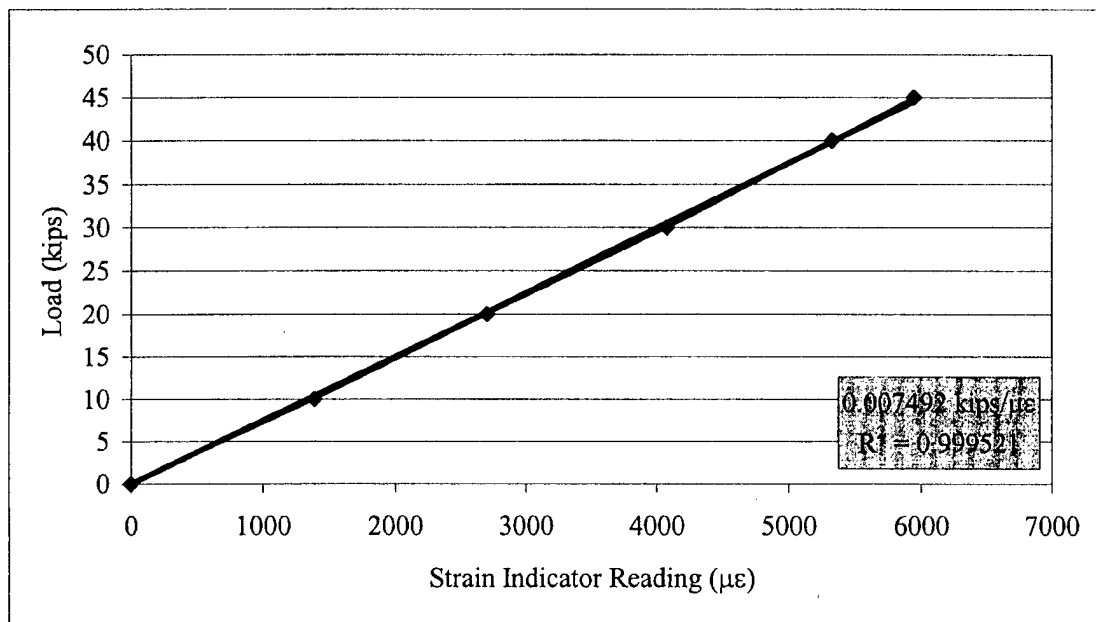
Figure E.10 Calibration Curve for Strand Load Cell # 10

407

APPENDIX F

PRESTRESSING STRESS CALCULATION

This Appendix contains the procedures used to determine the stress in the prestressing strands at initial tensioning of strands, just prior to release of strands, and as necessary at other times during testing.

At the time of strand tensioning and just prior to strand release, strand load cell values were used. Table F.1 shows a spreadsheet listing the calibration constants reported in Appendix E and the load cell strain readings for each series of girders. The resulting stress just prior to release, f_{pt}, is listed for each series of girders. The f_{pt} values were used in the transfer length analysis and are reported in Table 9.5.

After release of the strands, the level of prestress was determined with vibrating wire strain gages (VWSG) cast into the girders at midspan at the level of the bottom strands (Figure 8.21). Output from the gages was measured using the device pictured in Figure F.1. The device sent a small excitation voltage to the VWSG causing the wire within to vibrate. The frequency at which the wire in the gage vibrated was based on the amount of tension or compression the gage was experiencing. The values recorded at each measurement were an internal gage resistance used to determine a temperature correction factor and the frequency at which the wire was vibrating. A spreadsheet was created as shown in Table F.2 to determine the strain values.

Table F.1 Prestressing Strand Stress Values at Time of Tensioning and Just Prior to Release

Strand Load Cell Strain Conversion Factors From Graph Trendlines and PT Forces

		Load Cell 1	Load Cell 2	Load Cell 3	Load Cell 4	Load Cell 5	Load Cell 6	Load Cell 7	Load Cell 8	Load Cell 9	Load Cell 10
Kips / μ-strain		0.007219	0.006958	0.007456	0.008018	0.007579	0.007454	0.007451	0.007690	0.007555	0.007492
Strand Area (in²)	0.2183	Strand 1	Strand 2	Strand 3	Strand 4	Strand 5	Strand 6	Strand 7	Strand 8	Strand 9	Strand 10
		Bottom L							Bottom R	Top L	Top R
Girders G1A / G1B											
At Stressing	μ-strains	4533	5275	5430	4975	5352	5286	5206	5340	5430	5532
392.09	Kips	32.72	36.70	40.49	39.89	40.56	39.40	38.79	41.06	41.02	41.45
Before Release	μ-strains	4513	5270	5438	4960	5313	5270	5150	5357	5448	5479
390.89	Kips	32.58	36.67	40.55	39.77	40.27	39.28	38.37	41.20	41.16	41.05
Bottom / Top Totals						308.68				82.21	
f_pt (ksi)	179.06										
Girders G2A / G2B											
At Stressing	μ-strains	6013	5107	5193	4742	5516	5432	5296	5452	5587	5824
405.21	Kips	43.41	35.53	38.72	38.02	41.81	40.49	39.46	41.93	42.21	43.63
Before Release	μ-strains	6140	5310	5351	4891	5727	5572	5426	5612	5781	6011
417.62	Kips	44.32	36.95	39.90	39.22	43.40	41.53	40.43	43.16	43.68	45.03
Bottom / Top Totals						328.91				88.71	
f_pt (ksi)	191.30										
Girders G1C / G2C											
At Stressing	μ-strains	5163	5218	5640	5549	5484	5456	5126	5115	5489	5601
403.31	Kips	37.27	36.31	42.05	44.49	41.56	40.67	38.19	39.33	41.47	41.96
Before Release	μ-strains	4989	5023	5387	5406	5279	5309	5000	4970	5387	5443
391.01	Kips	36.02	34.95	40.17	43.35	40.01	39.57	37.26	38.22	40.70	40.78
Bottom / Top Totals						309.53				81.48	
f_pt (ksi)	179.12										

409
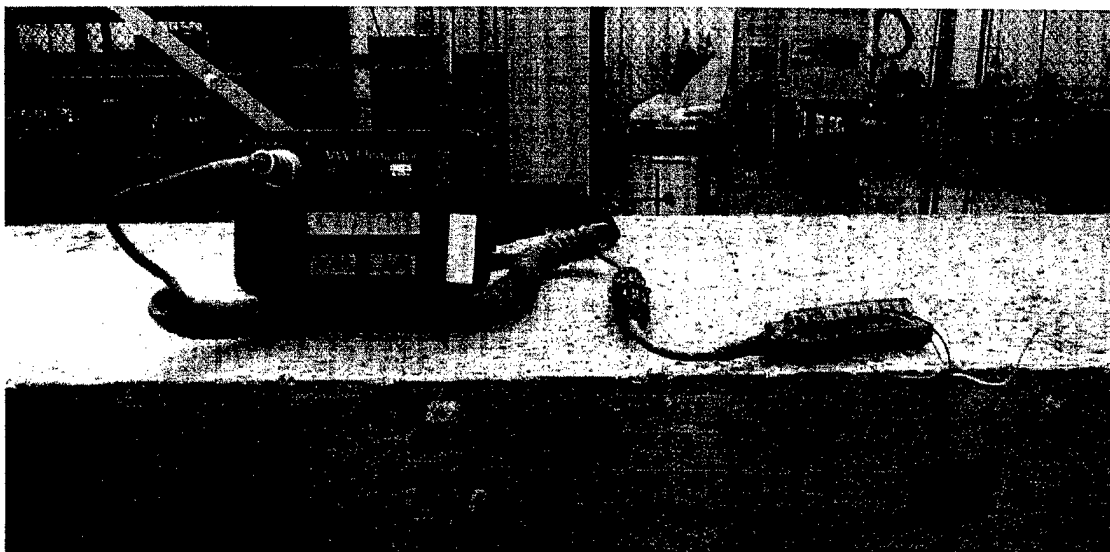
Figure F.1 Vibrating Wire Strain Gage Reader

To convert the frequency readings (Hz) to strains, Equation F.1 was used where

$\varepsilon_{Apparent}$ was the uncorrected strain value, GF was the gage factor provided by the

manufacturer (0.9996), and HZ was the wire vibration frequency read by the gage reader.

$$\varepsilon_{Apparent} = 0.003304\,GF\,(Hz)^2 \qquad\qquad (F.1)$$

To calculate temperature from the gage resistance reading (ΩWG), Equation F.2

was used where T_t was the temperature and ΩWG was the gage resistance in ohms.

$$T_t = \frac{1}{(0.0014051 + 0.0002369\ln(\Omega WG) + 0.0000001019\ln(\Omega WG)^3)} - 273.2 \qquad (F.2)$$

To correct the strain reading for temperature effects, Equation F.3 was used where $\varepsilon_{Initial}$ was the strain reading taken just prior to strand release, $T_{Initial}$ was the temperature of the gage when the first strain reading was taken, and the CTE values are the coefficients of thermal expansion for steel and concrete, 12.2 and 10.2 $\mu\varepsilon/^{o}C$, respectively.

$$\varepsilon_{Corrected} = (\varepsilon_{Apparent} - \varepsilon_{Initial})GF + (T_t - T_{Initial})(CTE_{Steel} - CTE_{Concrete}) \qquad (F.3)$$

The temperature correction was based on changes from the temperature at which the first VWSG reading was taken. In general, a drop in temperature meant a lower strain value; an increase in temperature meant a higher strain.

The force in the prestressing strand at any time after strand release was determined using the three equations shown in Figure F.2. The appropriate equation was determined depending on whether $\varepsilon_{Corrected}$ was in the elastic (0 - 0.7135 percent strain), transition (0.7135 – 1.25 percent strain), or plastic (> 1.25 percent strain) portion of the force vs. strain curve. Once the force was determined, the stress was calculated by dividing the strand force by the area of the strand, 0.2183 in^2. The shape of the curve in Figure F.2 was determined using the actual force vs. strain curve from the strand manufacturer.

Table F.2 Calcultion of Prestressing Strand Stress Values for Girder Test G1C-West

Determination of Initial Strand Strain Due to Prestressing

Strand #	1	2	3	4	5	6	7	8	9	10	TOTAL
											Prestressing Values Reported by Tindall QC
Elongation (In)	10.625	9.875	9.75	9.875	9.875	10.125	9.875	10.25	10.125	10.25	(Kips)
Tensioning Load (Kip)	45	45	45	45	45	45	45	45	45	45	450.00
											Prestressing Values Read From Strain Boxes Using Load Cells
kips/μ-strain	0.007219	0.006958	0.007456	0.008018	0.007579	0.007454	0.007451	0.007690	0.007555	0.007492	TOTAL
μ-strains at Tensioning	5163	5218	5640	5549	5484	5456	5126	5115	5489	5601	(Kips)
Tensioning Load (Kip)	37.27	36.31	42.05	44.49	41.56	40.67	38.19	39.33	41.47	41.96	403.31
μ-strains at Release	4989	5023	5387	5406	5279	5309	5000	4970	5387	5443	(Kips)
Release Load (Kip)	36.02	34.95	40.17	43.35	40.01	39.57	37.26	38.22	40.70	40.78	391.01

Values Used to Calculate Strain in Strand at Prestressing and Just Before Release (Enter Tindall or Load Cell) — Load Cell

Initial Strand Strain Values

	1	2	3	4	5	6	7	8	9	10	Average
% Strain at Release	0.56	0.55	0.63	0.68	0.63	0.62	0.58	0.60	0.64	0.64	0.61
f_{pu} Strand Ult Stress	283.20	KSI	Strand Area, A_s		0.2183	IN^2	Level of Prestressing as % of f_{pu}			63.25%	

Vibrating Wire Strain Gage Readings and Strand Strain/Force Values

Vibrating Wire Strain Gage Factor - Enter Value from Strain Gage Certification Sheet — 0.9996 | CTE Steel 12.2 | CTE Conc 10.2

Time of Reading							Prestressing Strand Strain / Force / Stress				
	Vibrating Wire Strain Gage Values						f_{pt} = Before Release, f_{si} = f_{pt} - ES, f_{se} = f_{pt} - ES - CR - SH				
	Hz	WWG (Ohms)	Temp (deg C)	Apparent ε (μ-strains)	Temp Corr (μ-strains)	Corrected ε (μ-strains)	μ-strains	% Strain	Force (K)	Stress (ksi)	Value
Before Release (0)	902.66	1308	44.99	2691	NA	2691	6131	0.61	39.10	179.11	f_{pt}
Just After Release	799.65	1387	43.49	2112	-3	2109	5550	0.55	35.39	162.11	f_{si}
1 Day	791.59	2407	30.04	2070	-30	2040	5480	0.55	34.95	160.09	
7 Days	762.00	2868	25.97	1918	-38	1880	5320	0.53	33.93	155.42	
14 Days	749.82	2863	26.01	1857	-38	1819	5260	0.53	33.54	153.65	f_{se}
Just Before Testing	708.37	3360	22.38	1657	-45	1612	5053	0.51	32.22	147.61	f_{test}
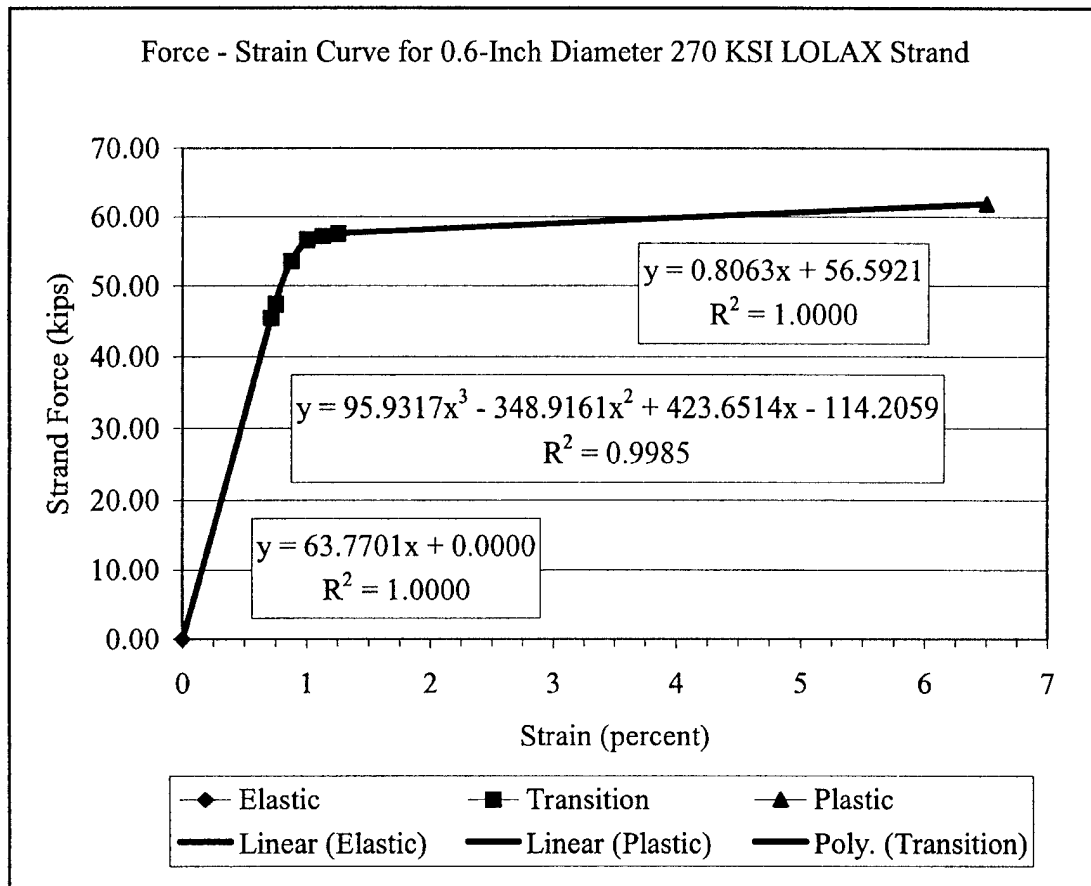
Figure F.2 Strand Force vs. Strain Curve for Prestressing Strand

APPENDIX G

TRANSFER LENGTH CALCULATION SPREADSHEET

Appendix G contains the individual pages from the Transfer Length Calculation Spreadsheet. The entire set of worksheet pages is provided for Girder G1C. The pages are listed in the order the calculations occur. A similar series of worksheets was prepared for each girder to determine transfer lengths. Listed below are the individual worksheets within the overall spreadsheet and a brief description of the worksheet's function.

Table G.1 - Data Taking Sheet – Used to record CSS readings taken with DEMEC gages.

Table G.2 – Data Worksheet – Worksheet used to enter background data information on girder readings to include times, temperatures, strain readings and jacking forces.

Tables G.3-G.4 – Gage Locations, North & South – Worksheets used to enter distances to ends of embedment strips. Initial gage lengths calculated.

Tables G.5-G.16 - CSS Reading Sheets – Data entry worksheets for each embedment strip (12 total). Readings entered from **Data Taking Sheets**.

Tables G.17-G.18 - Raw CSS Data Sheets, North & South – Worksheets listing raw strain data calculated from CSS readings and initial gage lengths.

414

Tables G.19-G.20 – Smoothed CSS Data Sheets, North & South – Worksheets listing smoothed strain data determined by a three-point floating average.

Table G.21 - Average Raw Transfer Length Plot Data – Worksheets averaging North and South raw data.

Figures G.1-G.2 - Raw Plots East and West – Raw CSS plots for East and West ends.

Table G.22 - Average Smoothed Plot Data – Worksheets averaging North and South smoothed data.

Figures G.3-G.4 - Smoothed Plots East and West – Smoothed CSS plots for East and West ends.

Figures G.5-G.6 - Transfer Length Plots East and West – 14-day transfer length calculation plots based on the 95% AMS Method.

NOTE ON DATA COLLECTION: Prior to girder construction, it was decided that CSS data collection and recording would be made more consistent and "foolproof" by establishing a basic rule. The rule was that all CSS readings would be taken from LEFT to RIGHT as the data taker looked at the embedment strip. The CSS data form (Table G.1) was configured such that the table provided areas for data entry that matched the location of the embedment strips on the girder. The LEFT to RIGHT rule applied to both sides of the girder. This was done to help alleviate errors from occurring in the field.

Table G.1 Transfer Length Data Taking Sheet

Beam Number		Beam Side				Take Readings From Left to Right on Each Plate			

Dates, Times and Notes for Readings - Gage Length is 8" on DEMEC Gage Reader – Zero Gage on Bar Before Taking Readings

Reading #	Date	Time	Deflection	TCA	TCI	Hz	103Hz2	WWG	Notes
1									
2									
3									
4									
5									

Reading 1	Reading 2	Reading 3	Reading 4	Reading 5	Reading 1	Reading 2	Reading 3	Reading 4	Reading 5
30 Inch Top Left					26 Inch Top Center				30 Inch Top Right

48 Inch Bottom Left					26 Inch Bottom Center				48 Inch Bottom Right

Table G.2 Data Worksheet for Girder G1C

| Beam # | G1C | | Raw Data for Transfer and Development Length | | | | | | |

Reading #	Date (DD/MM/YY)	Time	Midspan Deflection (Inches)	Ambient Temperature (Degrees F)	Internal Temperature (Degrees F)	Vibrating Wire Strain Gage Data			Notes
						HZ	10^3HZ^2	W WG	
Initial 1	07/18/2001	12:10	2.031	85.0	117.4	902.66	814.85	1308	Initial Reading 1, Sunny
Initial 2	07/18/2001	12:10	2.031	85.0	117.4	902.66	814.85	1308	Initial Reading 2, Sunny
Release	07/18/2001	15:15	2.453	87.8	108.5	799.65	639.55	1387	After Cutting Strand, Cloudy
1-Day	07/19/2001	7:08	2.469	74.2	84.6	791.59	626.65	2407	1-Day, At Sunrise, Dry and Clear
2-Day	07/20/2001	6:53	2.484	73.6	83.5	784.09	614.80	2514	2-Day, At Sunrise, Dry and Clear
3-Day	07/21/2001	6:50	2.500	72.5	79.0	780.30	608.70	2829	3-Day, At Sunrise, Overcast
7-Day	07/25/2001	7:10	2.531	73.8	78.7	762.00	580.60	2868	7-Day, At Sunrise, Overcast
14-Day	08/01/2001	6:30	2.555	72.0	78.1	749.82	563.00	2863	14-Day, At Sunrise, Mostly Clear
95%									
Slope									

Load Cell and Jacking Data

Strand #	Strand Jacking Force (Pounds)	Strand Elongation (Inches)	Date/Time	Temp (Deg F)	Notes
1	45000	9.875			
2	45500	9.750			
3	46000	9.750			
4	46000	9.875			
5	46000	9.875	17 Jul 01	75	
6	46000	9.875			
7	45000	10.000			
8	45000	10.000			
9	46000	9.750			
10	46000	9.750			

Load Cell (Strand) #	Time of Stressing (me)	Prior to Release (me)
1	5163	4989
2	5218	5023
3	5640	5387
4	5549	5406
5	5484	5279
6	5456	5309
7	5126	5000
8	5115	4970
9	5489	5387
10	5601	5443

Table G.3 North Side Gage Locations

Gages - North

Distance from Beam End to 1st Gage (IN)

		1.25
33.63	←— Elevation of End Gage (IN) —→	33.63

← Elevation of End Gage (IN) → 33.75

1 Top - L 11	33.75	1 Top - C 9	1 Top - R 11

Position ———————→   ←——————— Position

1 Bot - L 20	G1C - N	1 Bot - R 20

1 Bot - C 9	1

3	←— Elevation (IN) —→	3	3.063	←— Elevation (IN) —→	3
0.625					1.5

Distance from Beam End to 1st Gage (IN)

30" Top - L

Elev	Posn	Init	Lgth
33.64	5.07	1420	8.14
33.65	7.10	1212	8.12
33.66	9.13	1221	8.12
33.67	11.16	1208	8.12
33.68	13.18	843	8.08
33.69	15.20	874	8.09
33.70	17.23	809	8.08
33.71	19.25	959	8.10
33.71	21.27	989	8.10
33.72	23.30	1072	8.11
33.73	25.33	1144	8.11
Length =>	28.40		IN

48" Bot - L

Elev	Posn	Init	Lgth
3.00	4.63	110	8.01
3.00	6.63	-45	8.00
3.00	8.63	-160	7.98
3.00	10.62	-207	7.98
3.00	12.62	3	8.00
3.00	14.63	526	8.05
3.00	16.65	665	8.07
3.00	18.66	489	8.05
3.00	20.67	338	8.03
3.00	22.67	53	8.01
3.00	24.67	-28	8.00
3.00	26.68	241	8.02
3.00	28.68	-50	8.00
3.00	30.68	-92	8.01
3.00	32.68	-91	7.99
3.00	34.67	-302	7.97
3.00	36.67	25	8.00
3.00	38.67	179	8.02
3.00	40.68	358	8.04
3.00	42.69	386	8.04
Length =>	46.07		IN

26" Top - C

Elev	Posn	Init	Lgth
33.75	250.0	-574	7.94
33.75	252.0	-597	7.94
33.75	254.0	-339	7.97
33.75	256.0	-180	7.98
33.75	258.0	-146	7.99
33.75	260.0	-299	7.97
33.75	262.0	-302	7.97
33.75	264.0	-283	7.97
33.75	266.0	-537	7.95
Length =>	23.88		IN

26" Bot - C

#	Elev	Posn	Init	Lgth
1	3.01	249.9	1258	8.13
2	3.02	251.9	1166	8.12
3	3.02	253.9	909	8.09
4	3.03	256.0	1022	8.10
5	3.03	258.0	987	8.10
6	3.04	260.0	1019	8.10
7	3.04	262.1	1620	8.16
8	3.05	264.1	1310	8.13
9	3.05	266.1	1117	8.11
10	Length =>	24.35		IN
11				
12				
13				
14				
15				
16				
17				
18				
19				
20				

30" Top - R

Elev	Posn	Init	Lgth
33.63	25.46	762	8.08
33.63	23.44	743	8.07
33.63	21.42	865	8.09
33.63	19.40	922	8.09
33.63	17.38	753	8.08
33.63	15.36	696	8.07
33.63	13.35	606	8.06
33.63	11.33	740	8.07
33.63	9.31	549	8.05
33.63	7.30	639	8.06
33.63	5.29	409	8.04
Length =>	28.25		IN

48" Bot - R

Elev	Posn	Init	Lgth
2.99	43.53	104	8.01
2.99	41.53	148	8.01
2.99	39.52	190	8.02
2.99	37.52	96	8.01
2.98	35.52	146	8.01
2.98	33.51	109	8.01
2.98	31.52	-219	7.98
2.98	29.52	-255	7.97
2.97	27.54	-530	7.95
2.97	25.55	-420	7.96
2.97	23.55	69	8.01
2.96	21.54	127	8.01
2.96	19.53	361	8.04
2.96	17.53	257	8.03
2.96	15.53	12	8.00
2.95	13.53	56	8.01
2.95	11.52	142	8.01
2.95	9.52	208	8.02
2.95	7.51	283	8.03
2.94	5.51	216	8.02
Length =>	46.04		IN

Beam Length	43.00	FT
DEMEC Gage Length	8.00	IN

Table G.4 South Side Gage Locations

Beam Gage Locations - South

Distance from Beam End to 1st Gage (IN)

Elevation of End Gage (IN)

	0.875	0.813
	33.88	33.75

Position	Top - L	11	Top - C	9	Top - R	11
		33.63	33.88		33.75	
	Bot - L	20	Bot - C	9	Bot - R	20

G1C - S

	3.125	3.125	3.125
	3.063	3.375	1.313
	0.75		

30" Top - L

Elev	Posn	Init	Lgth
33.86	4.90	576	8.06
33.85	6.92	614	8.06
33.84	8.94	758	8.08
33.83	10.95	501	8.05
33.82	12.96	566	8.06
33.81	14.98	669	8.07
33.80	17.00	619	8.06
33.79	19.02	925	8.09
33.79	21.04	847	8.08
33.78	23.06	786	8.08
33.77	25.08	761	8.08
Length =>	28.23		IN

48" Bot - L

Elev	Posn	Init	Lgth
3.12	4.73	-500	7.95
3.12	6.72	-192	7.98
3.11	8.72	-192	7.98
3.11	10.72	48	8.00
3.11	12.72	170	8.02
3.11	14.72	-18	8.00
3.10	16.72	-23	8.00
3.10	18.72	-56	7.99
3.10	20.71	-313	7.97
3.10	22.71	-75	7.99
3.09	24.71	-95	7.99
3.09	26.70	-252	7.97
3.09	28.71	253	8.03
3.08	30.71	-37	8.00
3.08	32.70	-155	7.98
3.08	34.70	-101	7.99
3.08	36.68	-580	7.94
3.07	38.67	-469	7.95
3.07	40.67	-178	7.98
3.07	42.67	-107	7.99
Length =>	45.89		IN

26" Top - C

#	Elev	Posn	Init	Lgth
1	33.67	249.9	1162	8.12
2	33.69	251.9	686	8.07
3	33.71	254.0	854	8.09
4	33.73	256.0	736	8.07
5	33.75	258.0	641	8.06
6	33.77	260.0	770	8.08
7	33.79	262.0	721	8.07
8	33.81	264.1	694	8.07
9	33.83	266.1	879	8.09
10	Length =>	24.27		IN
11				
12				
13				
14				
15				
16				
17				
18				
19				
20				

26" Bot - C

Elev	Posn	Init	Lgth
3.13	249.9	911	8.09
3.13	252.0	827	8.08
3.13	254.0	692	8.07
3.13	256.0	626	8.06
3.13	258.0	755	8.08
3.13	260.0	574	8.06
3.13	262.0	715	8.07
3.13	264.1	703	8.07
3.13	266.1	757	8.08
Length =>	24.23		IN

30" Top - R

Elev	Posn	Init	Lgth
33.75	25.03	686	8.07
33.75	23.01	677	8.07
33.75	20.99	802	8.08
33.75	18.97	786	8.08
33.75	16.95	798	8.08
33.75	14.93	779	8.08
33.75	12.91	776	8.08
33.75	10.90	678	8.07
33.75	8.88	623	8.06
33.75	6.86	670	8.07
33.75	4.85	691	8.07
Length =>	28.25		IN

48" Bot - R

Elev	Posn	Init	Lgth
3.35	43.25	1065	8.11
3.34	41.24	463	8.05
3.33	39.23	338	8.03
3.32	37.22	228	8.02
3.31	35.21	267	8.03
3.30	33.21	88	8.01
3.29	31.21	-18	8.00
3.28	29.22	-177	7.98
3.27	27.22	-289	7.97
3.26	25.23	-376	7.96
3.24	23.24	-370	7.96
3.23	21.26	-505	7.95
3.22	19.28	-774	7.92
3.21	17.29	-709	7.93
3.20	15.31	-703	7.93
3.19	13.33	-703	7.93
3.18	11.34	-423	7.96
3.17	9.35	-511	7.95
3.16	7.36	-324	7.97
3.15	5.37	-247	7.98
Length =>	45.99		IN

Beam Length	43.00	FT
DEMEC Gage Length	8.00	IN

419

Table G.5 CSS Reading Sheet for 30-inch Top Left Embedment Strip on North Side

Beam Number		G1C	Beam Side		North		30 Inch Top Left		
Initial 1	Initial 2	Release	1-Day	2-Day	3-Day	7-Day	14-Day	95%	Slope
1418	1422	1422	1409	1398	1402	1398	1402		
1209	1215	1211	1198	1191	1191	1186	1191		
1221	1220	1217	1205	1192	1198	1190	1191		
1204	1211	1206	1194	1187	1189	1181	1192		
0844	0842	0836	0824	0816	0817	0805	0819		
0875	0873	0866	0849	0843	0845	0836	0844		
0807	0810	0800	0784	0782	0784	0774	0779		
0963	0954	0929	0940	0932	0933	0914	0932		
0990	0987	0986	0971	0964	0963	0962	0965		
1071	1072	1066	1049	1042	1046	1038	1042		
1143	1145	1138	1119	1119	1119	1111	1117		

420

Table G.6 CSS Reading Sheet for 48-inch Bottom Left Embedment Strip on North Side

Beam Number		G1C	Beam Side		North		48 Inch Bottom Left		
Initial 1	Initial 2	Release	1-Day	2-Day	3-Day	7-Day	14-Day	95%	Slope
0110	0109	0101	0086	0081	0081	0072	0081		
-0046	-0044	-0057	-0070	-0074	-0070	-0083	-0077		
-0160	-0160	-0172	-0185	-0203	-0205	-0209	-0196		
-0196	-0218	-0234	-0258	-0256	-0252	-0256	-0243		
0003	0003	-0021	-0032	-0035	-0038	-0044	-0040		
0523	0529	0503	0492	0481	0481	0475	0482		
0665	0664	0630	0615	0610	0608	0603	0607		
0483	0494	0463	0439	0446	0429	0428	0438		
0338	0338	0297	0281	0275	0273	0264	0266		
0049	0056	0014	-0013	-0019	-0013	-0028	-0017		
-0031	-0024	-0070	-0085	-0089	-0086	-0096	-0095		
0244	0237	0194	0166	0163	0161	0152	0154		
-0049	-0051	-0098	-0115	-0127	-0124	-0135	-0136		
0089	0094	0033	-0005	0002	-0017	-0015	0012		
-0091	-0091	-0143	-0164	-0179	-0184	-0192	-0194		
-0303	-0300	-0345	-0365	-0375	-0375	-0383	-0380		
0023	0026	-0017	-0039	-0045	-0051	-0058	-0057		
0178	0179	0132	0113	0109	0102	0095	0101		
0358	0357	0321	0289	0277	0283	0273	0268		
0389	0382	0339	0316	0314	0303	0292	0303		

Table G.7 CSS Reading Sheet for 26-inch Top Center Embedment Strip on North Side

Beam Number		G1C		Beam Side		North		26 Inch Top Center		
Initial 1	Initial 2	Release	1-Day	2-Day	3-Day	7-Day	14-Day	95%	Slope	
-0570	-0577	-0587	-0609	-0610	-0619	-0628	-0624			
-0596	-0598	-0614	-0641	-0652	-0647	-0658	-0653			
-0336	-0341	-0353	-0372	-0383	-0380	-0392	-0386			
-0179	-0181	-0200	-0215	-0223	-0221	-0229	-0228			
-0145	-0147	-0170	-0199	-0196	-0179	-0209	-0186			
-0297	-0301	-0315	-0340	-0341	-0335	-0352	-0341			
-0302	-0301	-0313	-0342	-0345	-0339	-0353	-0339			
-0281	-0285	-0305	-0326	-0326	-0325	-0334	-0321			
-0533	-0540	-0557	-0589	-0587	-0586	-0609	-0595			

Table G.8 CSS Reading Sheet for 26-inch Bottom Center Embedment Strip on North Side

| Beam Number | | G1C | Beam Side | | North | | 26 Inch Bottom Center | | |
Initial 1	Initial 2	Release	1-Day	2-Day	3-Day	7-Day	14-Day	95%	Slope
1254	1262	1272	1192	1181	1180	1165	1158		
1167	1164	1110	1087	1078	1081	1073	1072		
0911	0907	0842	0839	0832	0824	0813	0822		
1023	1021	0971	0948	0935	0919	0909	0915		
0986	0988	0943	0924	0922	0921	0917	0920		
1020	1017	0976	0964	0959	0954	0942	0957		
1623	1617	1567	1549	1547	1546	1534	1541		
1312	1307	1253	1235	1243	1230	1225	1228		
1117	1117	1060	1044	1037	1031	1013	1032		

Table G.9 CSS Reading Sheet for 30-inch Top Right Embedment Strip on North Side

| Beam Number | | G1C | Beam Side | | North | | 30 Inch Top Right | | |
Initial 1	Initial 2	Release	1-Day	2-Day	3-Day	7-Day	14-Day	95%	Slope
0763	0760	0570	0730	0730	0727	0721	0729		
0742	0744	0732	0712	0709	0710	0702	0709		
0865	0865	0852	0833	0830	0829	0820	0832		
0926	0918	0902	0893	0887	0891	0882	0895		
0752	0753	0738	0722	0719	0723	0714	0720		
0697	0695	0685	0667	0661	0663	0658	0662		
0605	0607	0596	0579	0575	0580	0573	0578		
0740	0740	0714	0693	0689	0689	0686	0693		
0548	0550	0538	0522	0516	0521	0514	0520		
0639	0639	0628	0614	0611	0611	0604	0616		
0409	0409	0405	0388	0384	0387	0379	0387		

Table G.10 CSS Reading Sheet for 48-inch Bottom Right Embedment Strip on North Side

| Beam Number | G1C | Beam Side | North | 48 Inch Bottom Right | | | | | |
Initial 1	Initial 2	Release	1-Day	2-Day	3-Day	7-Day	14-Day	95%	Slope
0103	0105	0041	0026	0016	0016	0005	0010		
0147	0149	0090	0057	0059	0062	0052	0054		
0188	0191	0137	0123	0115	0109	0103	0114		
0098	0093	0042	0021	0014	0016	0007	0010		
0144	0148	0091	0068	0063	0059	0055	0066		
0107	0110	0057	0049	0040	0038	0028	0053		
-0219	-0219	-0278	-0297	-0301	-0306	-0315	-0304		
-0254	-0256	-0308	-0327	-0336	-0339	-0351	-0341		
-0524	-0536	-0588	-0610	-0617	-0635	-0643	-0631		
-0416	-0423	-0507	-0513	-0502	-0504	-0518	-0501		
0068	0070	0025	0003	0000	-0002	-0011	0006		
0128	0126	0078	0059	0055	0053	0047	0051		
0357	0365	0316	0302	0296	0298	0283	0290		
0258	0256	0218	0204	0201	0197	0189	0198		
0014	0009	-0015	-0017	-0033	-0052	-0052	-0028		
0064	0048	0031	0022	0000	-0003	0007	0022		
0143	0141	0111	0094	0092	0093	0082	0095		
0203	0213	0189	0168	0168	0161	0149	0159		
0289	0276	0258	0225	0243	0224	0211	0230		
0209	0223	0208	0190	0191	0187	0181	0204		

Table G.11 CSS Reading Sheet for 30-inch Top Left Embedment Strip on South Side

Beam Number		G1C		Beam Side		South		30 Inch Top Left	
Initial 1	Initial 2	Release	1-Day	2-Day	3-Day	7-Day	14-Day	95%	Slope
0574	0578	0567	0553	0554	0565	0552	0554		
0615	0613	0605	0594	0592	0596	0587	0593		
0753	0762	0749	0733	0733	0741	0733	0735		
0499	0503	0478	0473	0472	0476	0471	0467		
0568	0563	0563	0550	0567	0576	0568	0571		
0673	0665	0661	0647	0617	0652	0640	0647		
0626	0611	0605	0591	0590	0596	0587	0590		
0922	0928	0903	0894	0888	0904	0899	0904		
0855	0838	0806	0783	0790	0802	0813	0814		
0785	0787	0775	0763	0759	0759	0754	0757		
0760	0761	0752	0735	0730	0739	0729	0728		

Table G.12 CSS Reading Sheet for 48-inch Bottom Left Embedment Strip on South Side

| Beam Number | G1C | Beam Side | South | | 48 Inch Bottom Left | | | | |
Initial 1	Initial 2	Release	1-Day	2-Day	3-Day	7-Day	14-Day	95%	Slope
-0500	-0500	-0533	-0546	-0545	-0542	-0551	-0545		
-0192	-0192	-0234	-0244	-0250	-0250	-0252	-0248		
-0192	-0192	-0222	-0233	-0233	-0233	-0243	-0228		
0040	0056	0007	-0005	-0009	-0011	-0010	-0014		
0170	0170	0140	0135	0129	0126	0115	0124		
-0010	-0025	-0068	-0085	-0076	-0086	-0078	-0094		
-0026	-0019	-0068	-0086	-0089	-0082	-0087	-0089		
-0055	-0056	-0107	-0123	-0128	-0123	-0138	-0132		
-0313	-0313	-0353	-0367	-0374	-0370	-0373	-0369		
-0077	-0073	-0134	-0150	-0157	-0154	-0165	-0160		
-0095	-0095	-0150	-0171	-0176	-0168	-0182	-0171		
-0266	-0237	-0329	-0343	-0353	-0348	-0353	-0352		
0253	0253	0192	0175	0167	0182	0165	0166		
-0038	-0035	-0130	-0141	-0146	-0145	-0154	-0155		
-0154	-0155	-0203	-0194	-0211	-0210	-0216	-0210		
-0101	-0100	-0167	-0175	-0184	-0179	-0191	-0188		
-0580	-0580	-0620	-0636	-0638	-0637	-0647	-0644		
-0467	-0470	-0500	-0505	-0516	-0512	-0528	-0522		
-0178	-0178	-0263	-0270	-0276	-0278	-0294	-0283		
-0108	-0106	-0151	-0159	-0163	-0160	-0174	-0170		

Table G.13 CSS Reading Sheet for 26-inch Top Center Embedment Strip on South Side

| Beam Number | | G1C | Beam Side | | South | | 26 Inch Top Center | | |
Initial 1	Initial 2	Release	1-Day	2-Day	3-Day	7-Day	14-Day	95%	Slope
1161	1163	1147	1122	1124	1124	1115	1118		
0686	0686	0633	0617	0614	0621	0609	0613		
0861	0847	0838	0815	0824	0828	0817	0821		
0739	0732	0726	0710	0709	0720	0713	0720		
0642	0639	0637	0638	0621	0617	0606	0613		
0770	0770	0748	0754	0739	0741	0729	0734		
0721	0721	0705	0690	0685	0688	0677	0682		
0695	0693	0647	0659	0660	0661	0652	0654		
0881	0877	0866	0845	0864	0862	0852	0859		

428

Table G.14 CSS Reading Sheet for 26-inch Bottom Center Embedment Strip on South Side

Beam Number		G1C		Beam Side		South		26 Inch Bottom Center		
Initial 1	Initial 2	Release	1-Day	2-Day	3-Day	7-Day	14-Day	95%	Slope	
0913	0908	0851	0840	0834	0834	0824	0819			
0829	0824	0769	0756	0753	0755	0737	0736			
0692	0692	0646	0631	0630	0625	0616	0619			
0635	0616	0546	0565	0563	0559	0549	0547			
0758	0752	0702	0697	0688	0680	0677	0673			
0575	0572	0512	0509	0498	0565	0496	0508			
0716	0713	0643	0644	0624	0633	0619	0636			
0707	0699	0667	0646	0646	0640	0633	0642			
0760	0753	0703	0692	0687	0681	0679	0681			

429

Table G.15 CSS Reading Sheet for 30-inch Top Right Embedment Strip on North Side

Beam Number	G1C	Beam Side	South	30 Inch Top Right						
Initial 1	Initial 2	Release	1-Day	2-Day	3-Day	7-Day	14-Day	95%	Slope	
0694	0678	0670	0649	0654	0653	0642	0647			
0673	0680	0660	0639	0636	0645	0636	0638			
0797	0806	0779	0771	0769	0776	0768	0771			
0786	0785	0761	0746	0747	0746	0741	0742			
0799	0797	0780	0763	0762	0759	0764	0760			
0781	0777	0758	0743	0742	0748	0740	0742			
0772	0779	0761	0742	0740	0745	0738	0741			
0678	0678	0666	0647	0646	0648	0643	0649			
0625	0621	0610	0591	0593	0594	0590	0592			
0670	0670	0662	0648	0645	0652	0647	0650			
0696	0686	0684	0670	0667	0669	0664	0671			

430

Table G.16 CSS Reading Sheet for 48-inch Bottom Right Embedment Strip on South Side

Beam Number		G1C	Beam Side		South	48 Inch Bottom Right			
Initial 1	Initial 2	Release	1-Day	2-Day	3-Day	7-Day	14-Day	95%	Slope
1065	1065	1005	0952	0949	0943	0935	0935		
0469	0457	0402	0381	0377	0381	0371	0370		
0337	0338	0281	0261	0253	0255	0245	0246		
0225	0230	0149	0131	0133	0127	0115	0120		
0270	0263	0208	0188	0182	0185	0174	0174		
0085	0091	0034	0017	0013	0010	0000	-0008		
-0019	-0016	-0073	-0090	-0096	-0095	-0106	-0107		
-0178	-0175	-0237	-0249	-0260	-0259	-0273	-0271		
-0289	-0288	-0366	-0378	-0388	-0387	-0388	-0373		
-0378	-0373	-0411	-0426	-0450	-0439	-0455	-0449		
-0369	-0370	-0419	-0436	-0445	-0443	-0454	-0454		
-0505	-0504	-0550	-0568	-0575	-0572	-0582	-0580		
-0773	-0775	-0792	-0816	-0831	-0837	-0851	-0837		
-0712	-0706	-0734	-0759	-0758	-0758	-0765	-0758		
-0714	-0691	-0721	-0746	-0749	-0746	-0752	-0746		
-0706	-0699	-0724	-0740	-0746	-0740	-0755	-0742		
-0426	-0419	-0449	-0459	-0460	-0466	-0484	-0476		
-0511	-0511	-0514	-0529	-0522	-0532	-0540	-0527		
-0325	-0322	-0330	-0347	-0347	-0351	-0355	-0348		
-0244	-0249	-0187	-0215	-0212	-0220	-0222	-0217		

Table G.17 Raw Concrete Surface Strains for North Side of Girder G1C

Raw Transfer Length Data - North Side of Girder G1C

Bot-L

Gage #	Release	1-Day	2-Day	3-Day	7-Day	14-Day	95%	Slope
1	106	293	356	356	468	356		
2	150	313	363	313	475	400		
3	150	313	539	564	614	451		
4	338	639	614	564	614	451		
5	300	437	475	512	587	537		
6	286	422	559	559	633	546		
7	428	614	676	700	762	713		
8	317	615	528	739	752	627		
9	510	710	784	809	921	896		
10	481	818	893	818	1006	868		
11	531	719	769	732	857	844		
12	580	928	966	991	1103	1078		
13	600	813	963	926	1063	1076		
14	730	1205	1117	1355	1330	993		
15	651	914	1101	1164	1264	1289		
16	546	797	922	922	1023	985		
17	519	794	868	943	1031	1018		
18	580	817	867	954	1041	967		
19	454	852	1002	927	1052	1114		
20	578	865	889	1026	1163	1026		

CSS - Microstrains

Bot-R

Gage #	Release	1-Day	2-Day	3-Day	7-Day	14-Day	95%	Slope
1	786	974	1099	1099	1236	1173		
2	724	1135	1110	1073	1198	1173		
3	655	829	929	1004	1079	942		
4	668	930	1018	993	1105	1067		
5	686	973	1036	1086	1135	998		
6	643	743	855	880	1005	693		
7	740	978	1028	1090	1203	1065		
8	665	903	1016	1053	1204	1078		
9	730	1007	1095	1321	1422	1271		
10	1100	1175	1037	1062	1238	1024		
11	550	824	862	887	999	787		
12	612	849	899	924	998	948		
13	560	734	809	784	971	884		
14	486	660	698	748	847	735		
15	331	356	556	794	794	494		
16	312	425	700	737	612	425		
17	387	599	624	611	749	586		
18	237	499	499	586	736	611		
19	305	716	492	729	891	654		
20	100	324	312	362	436	150		

CSS - Microstrains

432

Table G.18 Raw Concrete Surface Strains for South Side of Girder G1C

Raw Transfer Length Data - South Side of Girder G1C

Bot-L		CSS - Microstrains						
Gage #	Release	1-Day	2-Day	3-Day	7-Day	14-Day	95%	Slope
1	415	579	566	528	642	566		
2	526	652	727	727	752	702		
3	376	514	514	514	639	451		
4	512	662	712	737	725	775		
5	374	437	511	549	686	574		
6	631	844	731	856	756	956		
7	569	794	831	744	806	831		
8	644	844	907	844	1032	957		
9	502	678	765	715	753	703		
10	738	938	1026	988	1126	1063		
11	688	951	1014	914	1089	951		
12	972	1147	1273	1210	1273	1260		
13	760	972	1072	885	1097	1084		
14	1169	1307	1369	1357	1469	1482		
15	607	495	708	695	770	695		
16	832	932	1045	982	1133	1095		
17	504	705	730	718	844	806		
18	396	459	597	547	748	673		
19	1065	1153	1228	1253	1453	1315		
20	551	651	701	663	839	789		

Bot-R		CSS - Microstrains						
Gage #	Release	1-Day	2-Day	3-Day	7-Day	14-Day	95%	Slope
1	740	1394	1431	1505	1604	1604		
2	758	1019	1069	1019	1143	1156		
3	703	952	1052	1027	1151	1139		
4	978	1203	1178	1253	1402	1340		
5	729	978	1053	1015	1152	1152		
6	674	887	936	974	1099	1199		
7	694	906	981	969	1106	1119		
8	758	908	1046	1034	1209	1184		
9	972	1123	1248	1236	1248	1060		
10	446	634	936	797	998	923		
11	622	835	948	923	1061	1061		
12	572	799	887	849	975	950		
13	227	530	719	795	972	795		
14	315	631	618	618	706	618		
15	233	549	586	549	624	549		
16	271	473	549	473	662	498		
17	333	459	471	547	773	672		
18	38	226	138	264	365	201		
19	82	295	295	345	395	307		
20	746	395	433	332	307	370		

433

Table G.19 Smoothed Concrete Surface Strains for North Side of Girder G1C

Smoothed Transfer Length Data - North Side of Girder G1C

Bot-L Gage #	CSS - Microstrains							
	Release	1-Day	2-Day	3-Day	7-Day	14-Day	95%	Slope
1								
2	135	306	419	411	519	402		
3	213	422	505	480	568	434		
4	263	463	543	547	605	480		
5	308	500	549	545	612	512		
6	338	491	570	591	661	599		
7	343	550	587	666	716	629		
8	418	646	663	750	812	745		
9	436	714	735	789	893	797		
10	508	749	815	786	928	869		
11	531	822	876	847	988	930		
12	570	820	899	883	1008	999		
13	637	982	1015	1090	1165	1049		
14	661	977	1061	1148	1219	1119		
15	642	972	1047	1147	1205	1089		
16	572	835	964	1010	1106	1097		
17	548	802	886	940	1032	990		
18	518	821	912	942	1041	1033		
19	538	845	919	969	1085	1036		
20								

Bot-R Gage #	CSS - Microstrains							
	Release	1-Day	2-Day	3-Day	7-Day	14-Day	95%	Slope
1								
2	722	979	1046	1058	1171	1096		
3	682	965	1019	1023	1127	1061		
4	670	911	994	1027	1106	1002		
5	666	882	969	986	1082	919		
6	690	898	973	1019	1115	919		
7	682	874	966	1008	1137	946		
8	711	962	1046	1155	1276	1138		
9	831	1028	1049	1145	1288	1124		
10	793	1002	998	1090	1220	1027		
11	754	949	932	957	1078	920		
12	574	802	856	865	989	873		
13	552	748	802	818	939	856		
14	459	584	688	775	871	704		
15	376	480	651	759	751	551		
16	343	460	627	714	718	502		
17	312	507	607	645	699	541		
18	310	605	538	642	792	617		
19	214	513	434	559	688	471		
20								

434

Table G.20 Smoothed Concrete Surface Strains for South Side of Girder G1C

Smoothed Transfer Length Data - South Side of Girder G1C

Bot-L		CSS - Microstrains							Bot-R		CSS - Microstrains						
Gage #	Release	1-Day	2-Day	3-Day	7-Day	14-Day	95%	Slope	Gage #	Release	1-Day	2-Day	3-Day	7-Day	14-Day	95%	Slope
1									1								
2	439	581	602	590	677	573			2	734	1122	1184	1184	1299	1299		
3	471	609	651	659	705	642			3	813	1058	1100	1100	1232	1212		
4	421	537	579	600	683	600			4	804	1044	1094	1098	1235	1210		
5	506	648	652	714	722	768			5	794	1022	1056	1081	1218	1230		
6	525	691	691	716	750	787			6	699	924	990	986	1119	1157		
7	615	827	823	815	865	915			7	709	900	988	992	1138	1167		
8	572	772	835	768	864	830			8	808	979	1092	1079	1188	1121		
9	628	820	899	849	970	908			9	725	888	1077	1022	1152	1056		
10	643	856	935	872	989	906			10	680	864	1044	985	1103	1015		
11	799	1012	1104	1037	1163	1092			11	547	756	924	857	1011	978		
12	807	1023	1119	1003	1153	1098			12	474	721	851	856	1003	935		
13	967	1142	1238	1151	1280	1275			13	372	653	741	754	884	788		
14	846	924	1050	979	1112	1087			14	259	570	641	654	767	654		
15	870	911	1041	1011	1124	1091			15	273	551	584	546	664	555		
16	648	711	828	798	916	865			16	279	493	535	523	686	573		
17	577	699	791	749	908	858			17	214	386	386	428	600	457		
18	655	772	852	839	1015	931			18	151	327	302	385	511	394		
19	671	754	842	821	1013	926			19	288	305	289	314	356	293		
20									20								

435

Table G.21 Averaged Raw Concrete Surface Strains for Girder G1C (North Reference)

Averaged Raw Transfer Length Plot Data for Girder G1C - (North Reference)

Bot-L

Posn	Release	1-Day	2-Day	3-Day	7-Day	14-Day	95%	Slope
0	0	0	0	0	0	0		
5.00	426	344	394	344	388	363		
6.99	116	304	329	329	435	354		
8.99	94	270	338	414	489	326		
10.98	336	549	543	555	693	562		
12.97	286	455	512	493	625	518		
14.97	259	485	573	554	629	547		
16.97	371	622	647	659	734	665		
18.97	272	573	624	767	862	711		
20.96	541	754	836	829	948	923		
22.96	551	827	921	871	1033	965		
24.95	489	677	852	764	927	884		
26.95	776	1026	1107	1113	1176	1069		
28.95	679	861	1005	980	1136	1130		
30.95	712	1056	1049	1162	1218	1056		
32.94	662	900	1019	1069	1181	1244		
34.94	637	887	987	969	1088	1069		
36.95	749	998	1023	1098	1217	1179		
38.95	642	885	959	991	1096	1053		
40.96	606	936	1035	973	1097	1135		
42.97	659	1129	1160	1266	1383	1315		

CSS - microstrains (Normal Order)

Bot-R

Posn	Release	1-Day	2-Day	3-Day	7-Day	14-Day	95%	Slope
0	0	0	0	0	0	0		
5.12	257	451	439	445	539	358		
7.12	416	684	609	728	821	678		
9.12	306	506	506	550	687	531		
11.12	450	631	668	674	737	680		
13.12	343	431	605	643	649	499		
15.12	481	600	644	825	775	725		
17.12	527	727	765	746	827	783		
19.13	602	789	858	814	1001	920		
21.13	557	763	832	819	876	826		
23.13	644	881	944	938	1063	925		
25.13	894	1063	1025	988	1163	988		
27.12	851	1077	1184	1266	1347	1266		
29.12	712	937	1044	969	1150	1081		
31.11	954	1142	1199	1224	1336	1274		
33.11	625	619	781	788	888	694		
35.11	759	953	1040	1034	1134	1047		
37.10	586	818	874	855	974	937		
39.10	525	644	763	775	913	807		
41.10	894	1144	1169	1163	1326	1244		
43.10	669	812	900	881	1037	981		

CSS - microstrains (Reverse Order)

436
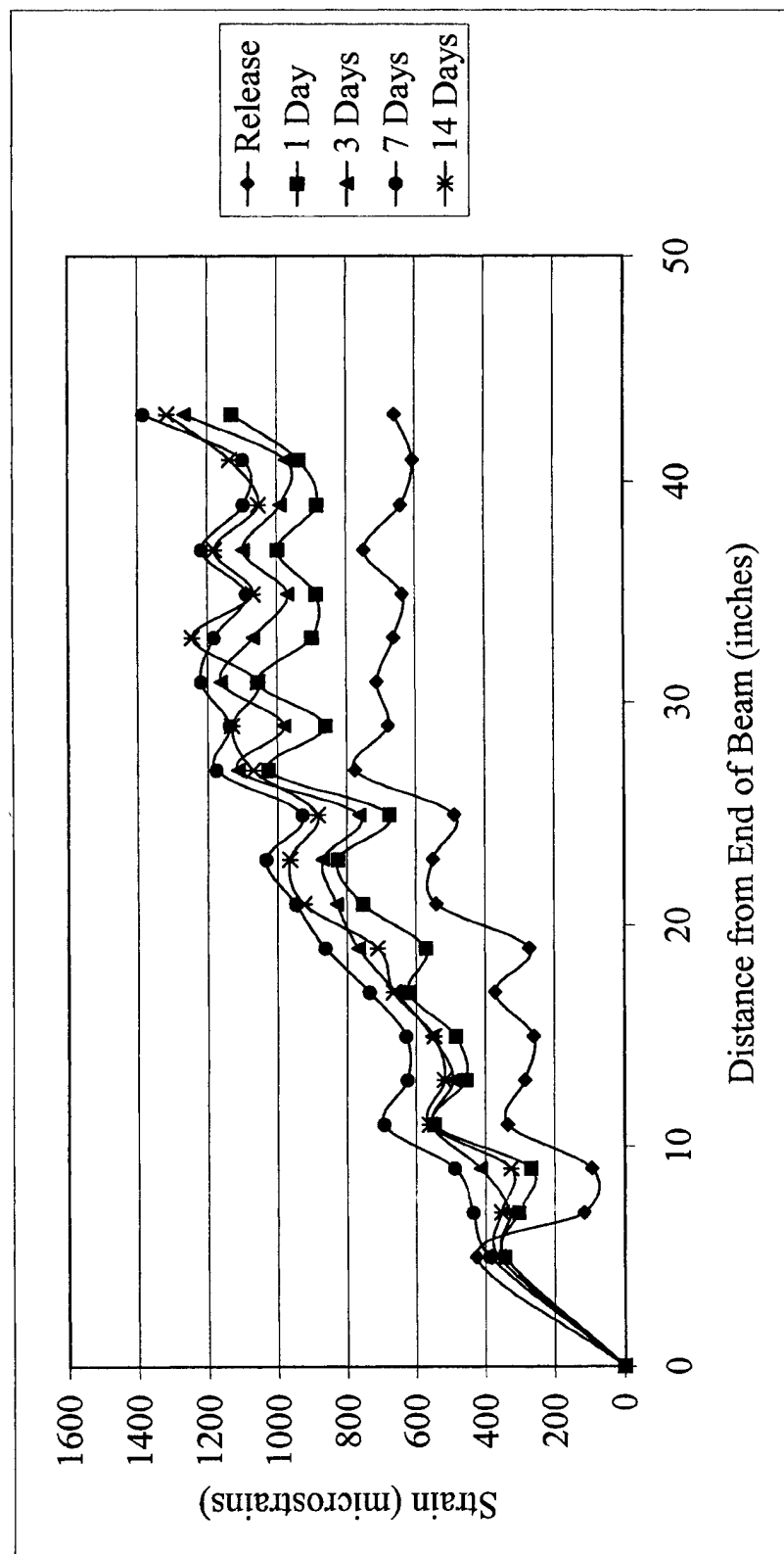
Figure G.1 Raw CSS Data for East End of Girder G1C
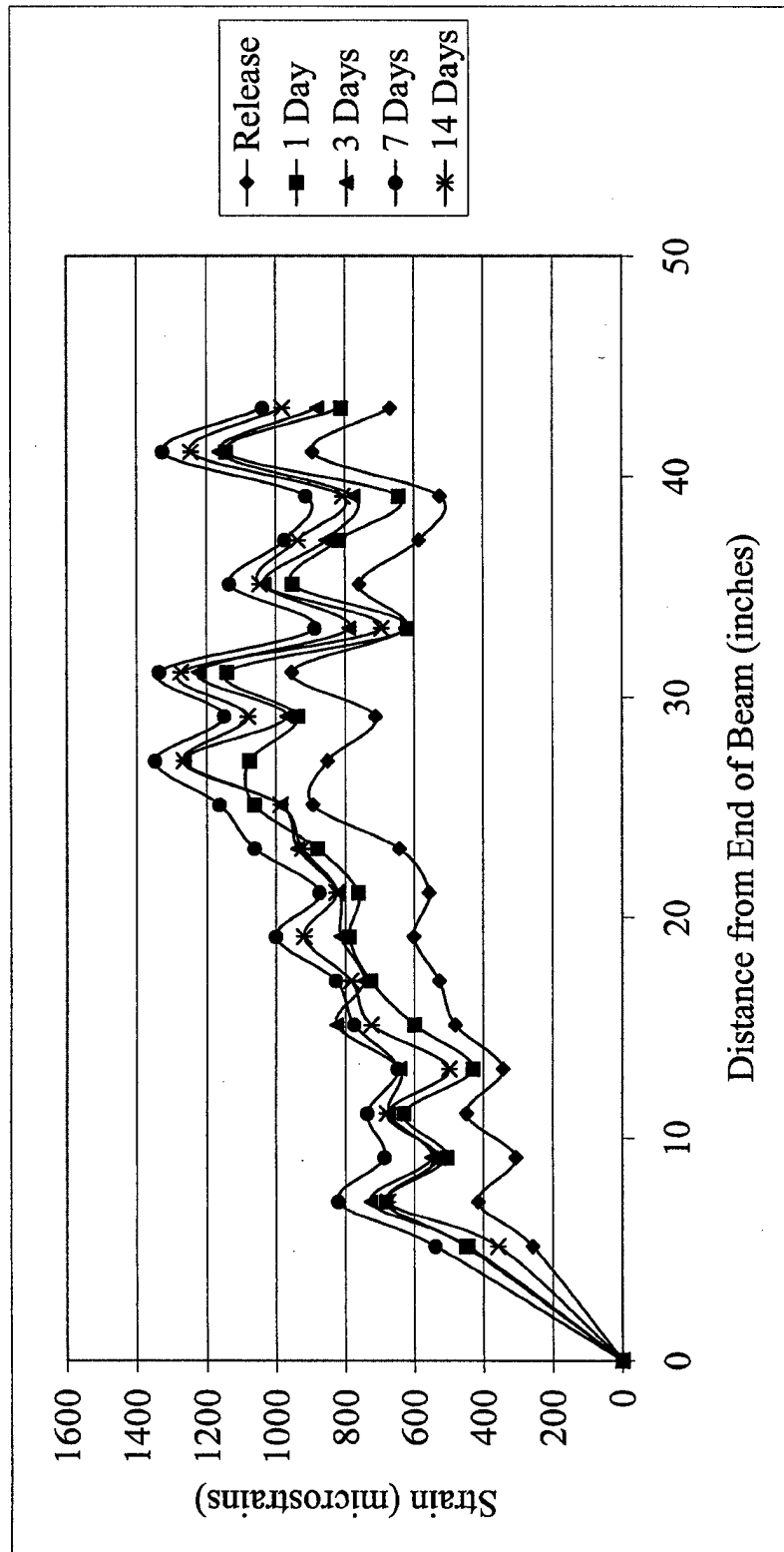
Figure G.2 Raw CSS Data for West End of Girder G1C

Table G.22 Averaged Smoothed Concrete Surface Strains for Girder G1C (North Reference)

Averaged Smoothed Transfer Length Plot Data for Girder G1C - (North Reference)

Bot-L	CSS - microstrains (Normal Order)							
Posn	Release	1-Day	2-Day	3-Day	7-Day	14-Day	95%	Slope
0	0	0	0	0	0	0	1137	0
6.99	212	306	354	362	437	348	1137	348
8.99	182	374	403	433	539	414	1137	414
10.98	238	425	464	487	603	469	1137	469
12.97	294	497	542	534	649	542	1137	542
14.97	306	521	577	569	663	577	1137	577
16.97	301	560	614	660	742	641	1137	641
18.97	395	650	702	752	848	767	1137	767
20.96	455	718	793	822	948	866	1137	866
22.96	527	752	869	821	970	924	1137	924
24.95	605	843	960	916	1045	972	1137	972
26.95	648	854	988	952	1080	1027	1137	
28.95	722	981	1054	1085	1177	1085	1137	
30.95	685	939	1024	1070	1179	1143	1137	
32.94	671	948	1019	1067	1162	1123	1137	
34.94	683	929	1010	1045	1162	1164	1137	
36.95	676	923	990	1019	1134	1100	1137	
38.95	665	940	1006	1021	1137	1122	1137	
40.96	636	983	1052	1076	1192	1168	1137	
42.97								

Bot-R	CSS - microstrains (Reverse Order)							
Gage #	Release	1-Day	2-Day	3-Day	7-Day	14-Day	95%	Slope
0	0	0	0	0	0	0	975	0
7.12	327	547	518	574	682	522	975	522
9.12	391	607	595	651	748	630	975	630
11.12	366	522	593	622	691	570	975	570
13.12	425	554	639	714	720	635	975	635
15.12	451	586	671	738	750	669	975	669
17.12	537	706	755	795	868	810	975	810
19.13	562	760	818	793	901	843	975	843
21.13	601	811	878	857	980	890	975	890
23.13	698	903	934	915	1034	913	975	913
25.13	796	1007	1051	1064	1191	1059	975	1059
27.12	819	1026	1084	1074	1220	1111	975	
29.12	839	1052	1142	1153	1278	1207	975	
31.11	764	899	1008	993	1125	1016	975	
33.11	780	905	1007	1015	1119	1005	975	
35.11	657	796	899	892	999	892	975	
37.10	623	805	892	888	1007	930	975	
39.10	668	869	935	931	1071	996	975	
41.10	696	867	944	940	1092	1011	975	
43.10								
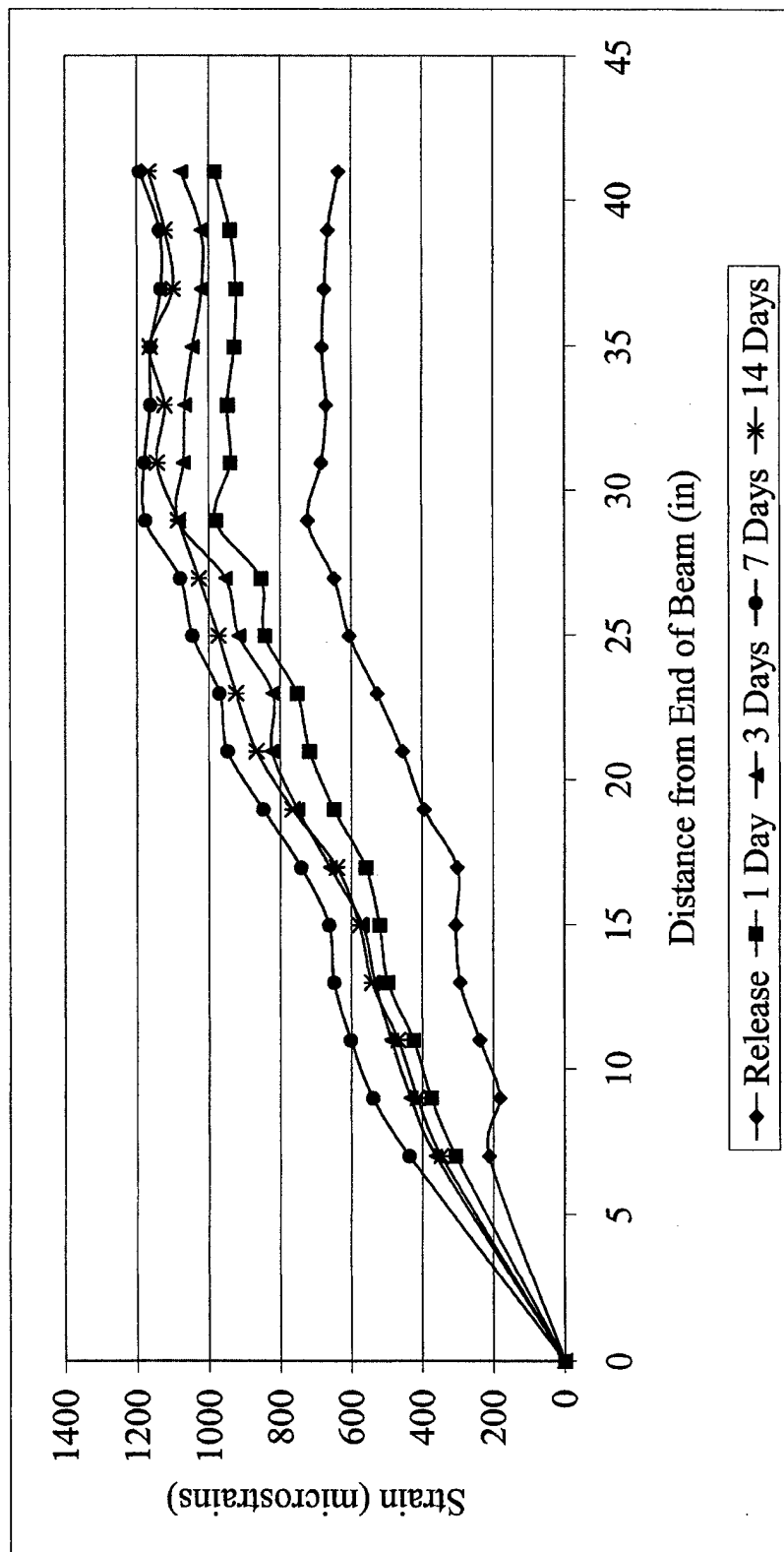
Figure G.3 Smoothed CSS Data for East End of Girder G1C
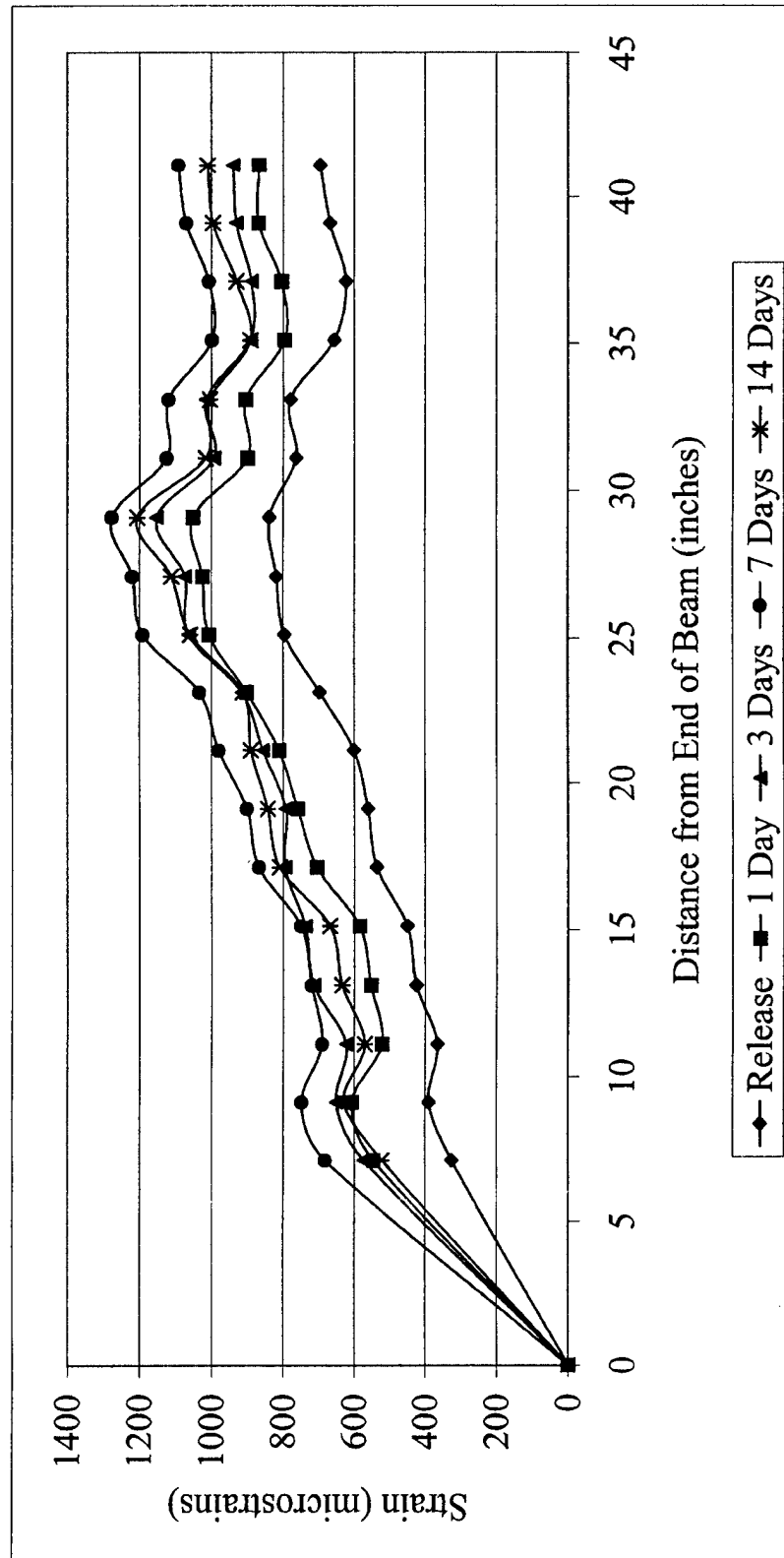
Figure G.4 Smoothed CSS Data for West End of Girder G1C
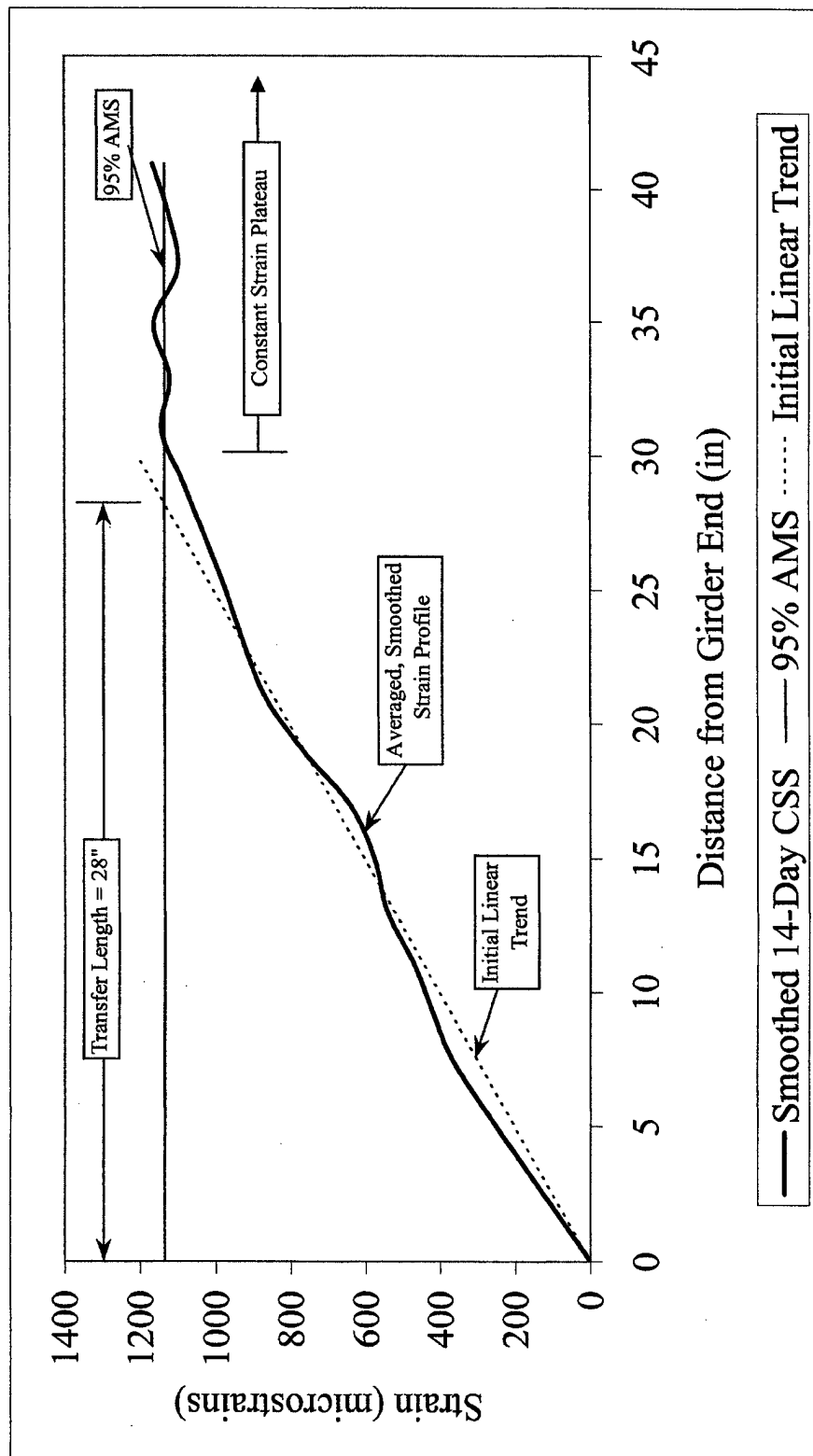
Figure G.5 Transfer Length Determined Using 95% AMS Method for East End of Girder G1C
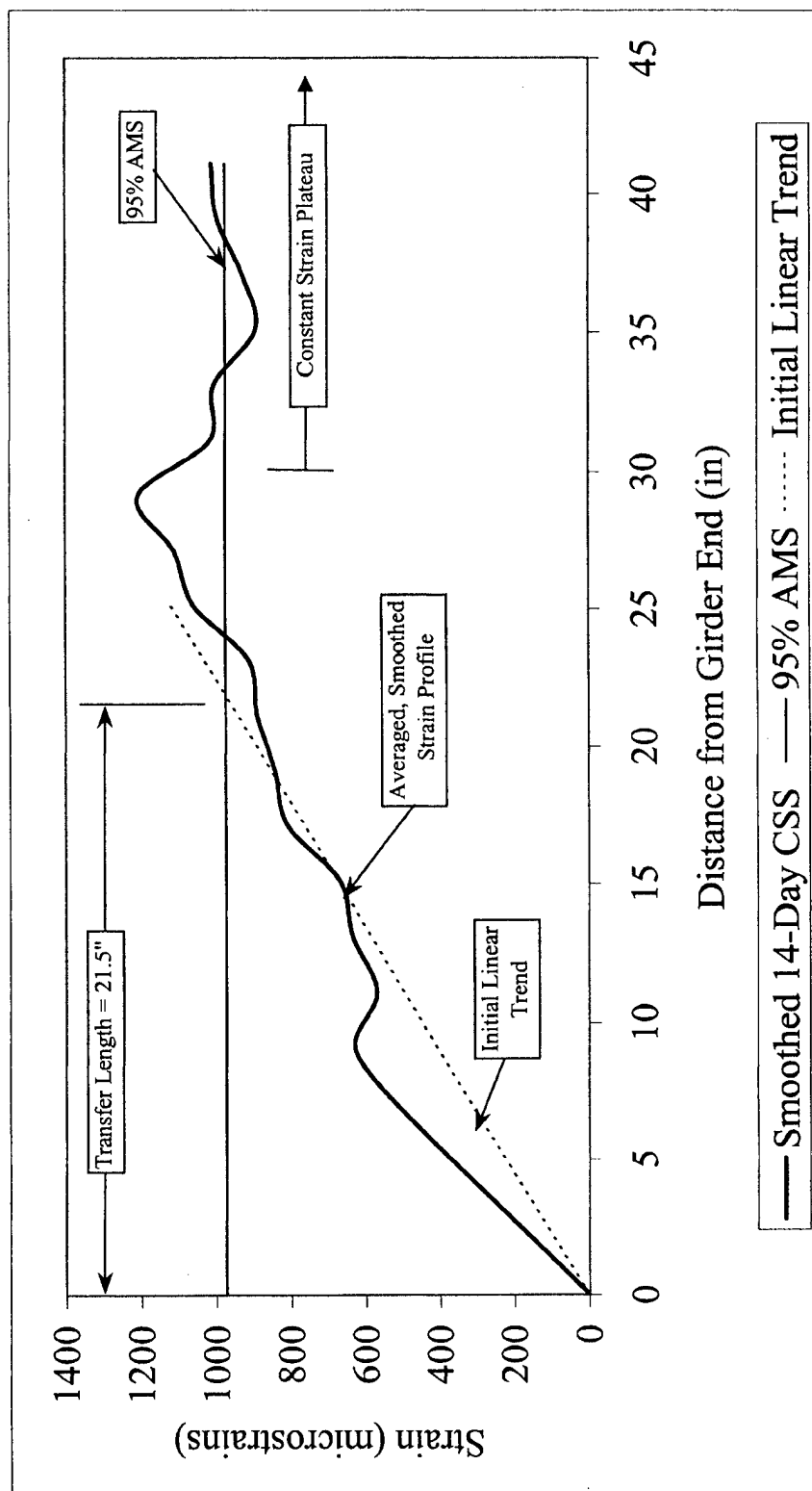
Figure G.6 Transfer Length Determined Using 95% AMS Method for West End of Girder G1C

APPENDIX H

CONCRETE SURFACE STRAIN AND OTHER DATA

This Appendix contains raw data for each girder. The following data items were recorded before strand release (initial), just after release, and 1, 2, 3, 7 and 14-days after strand release. The data taken through 14 days were used to determine transfer length.

Date and time

Midspan deflection

Ambient temperature

Internal girder temperature

Reading in hertz from the vibrating wire strain gage at midspan

Resistance reading from the thermistor in the vibrating wire strain gage

CSS readings from each embedment strip

The following values were also recorded for each girder at the time of strand tensioning.

Strain reading from strand load cell

Strand jacking force

Strand elongation

Date and time

Ambient temperature

Strand load cell readings were also recorded immediately prior to strand release for comparison with initial load cell readings. The sections correspond with the individual girders as follows:

Section H.1 – Girder G1A

Section H.2 – Girder G1B

Section H.3 – Girder G1C

Section H.4 – Girder G2A

Section H.5 – Girder G2B

Section H.6 – Girder G2C

The directions North and South refer to girder sides based on orientation at time of construction. East and West refer to girder ends. The gage positions on embedment strips are always referenced from left to right as shown in Figures G.3 and G.4. Gage locations are numbered from 1 to 20 meaning there are 20 CSS readings taken on each bottom embedment strip. The embedment strips are located at the ends of the girders on both sides at the level of the bottom row of prestressing strands. Positive CSS values indicate a compressive strain.

H.1 Girder G1A

Table H.1 G1A Girder Data

Girder #		G1A	Raw Data for Transfer and Development Length				
Reading #	Date (m/dd/yy)	Time (24 hr)	Midspan Deflection (inches)	Ambient Temp (Deg F)	Internal Temp (Deg F)	VWSG Data	
						Hz	ΩWG
Initial 1	7/10/01	11:30	1.703	80.0		924.84	2128
Initial 2	7/10/01	12:10	1.703	80.0		924.84	2128
Release	7/10/01	15:07	2.063	90.0		822.05	2128
1-Day	7/11/01	7:40	2.078	75.0			
2-Day	7/12/01	7:45	2.094	75.0	73.8	809.31	2470
3-Day	7/13/01	7:05	2.094	74.7	72.2	802.80	2515
7-Day	7/17/01	6:30	2.109	72.4	67.0	790.57	2884
14-Day	7/24/01	6:55	2.125	74.5	68.4	778.42	2568

Strand Jacking Data from Load Cells and Tensioning Machine						
	Load Cell Readings		Tension Machine Readings		Date and Time Of	Ambient Temp
Load Cell (Strand) #	At Time of Stressing (με)	Prior To Release (με)	Strand Jacking Force (lbs)	Strand Elongation (inches)	Tensioning (m/dd/yy) (24 hr)	(Deg F)
1	4533	4513	45000	10.250		
2	5275	5270	45000	9.875		
3	5430	5438	45000	10.125		
4	4975	4960	45000	9.875		
5	5352	5313	45000	9.875	9 Jul 01	90
6	5286	5270	45000	9.750	11:30	
7	5206	5150	45500	9.875		
8	5340	5357	45000	10.625		
9	5430	5448	45000	10.250		
10	5532	5479	45000	10.125		

Table H.2 Raw Concrete Surface Strain Data for Girder G1A-North

East Gage #	Raw CSS - microstrains					
	Release	1-Day	2-Day	3-Day	7-Day	14-Day
1	157	244	307	269	420	457
2	250	350	463	375	550	600
3	237	350	412	375	525	637
4	243	380	405	380	480	517
5	450	512	587	525	774	837
6	344	432	407	382	545	632
7	419	557	632	594	695	720
8	344	444	557	507	895	682
9	456	780	905	818	955	1030
10	482	657	757	707	932	1007
11	499	674	699	737	861	886
12	468	643	693	705	942	980
13	356	494	544	556	744	606
14	531	681	644	631	794	869
15	451	488	576	589	902	764
16	513	738	851	876	964	1101
17	457	569	632	644	845	1082
18	449	674	736	736	936	1010
19	475	674	737	724	1086	1149
20	431	281	807	757	857	957

West Gage #	Raw CSS - microstrains					
	Release	1-Day	2-Day	3-Day	7-Day	14-Day
1	401	526	514	526	764	777
2	450	801	901	813	1063	1088
3	632	944	1019	957	1182	1294
4	588	639	751	676	964	1014
5	514	564	740	765	1003	1053
6	358	421	484	409	861	987
7	88	615	615	615	640	678
8	407	707	745	795	907	982
9	501	739	939	814	1052	1127
10	592	879	941	792	555	1203
11	639	551	639	701	1139	1152
12	263	313	489	489	890	1065
13	382	495	557	570	795	708
14	413	125	276	363	651	614
15	318	517	580	580	704	754
16	589	288	175	63	100	251
17	407	307	319	357	369	457
18	281	432	444	469	557	544
19	19	144	19	6	169	257
20	162	37	287	249	336	448

Table H.3 Raw Concrete Surface Strain Data for Girder G1A-South

East Gage #	Raw CSS - microstrains					
	Release	1-Day	2-Day	3-Day	7-Day	14-Day
1	411	722	760	772	872	897
2	618	693	843	830	930	955
3	468	805	855	855	967	992
4	588	763	825	800	900	925
5	474	699	736	724	611	649
6	530	629	729	754	854	854
7	455	679	804	791	854	916
8	610	722	834	809	909	984
9	978	916	1190	1265	1277	1240
10	529	754	754	816	754	828
11	473	771	821	809	846	833
12	416	714	702	640	665	677
13	497	634	721	671	696	671
14	542	879	941	904	1003	1041
15	306	892	917	892	980	830
16	256	693	768	756	831	843
17	256	493	430	493	468	443
18	330	542	492	504	529	156
19	100	338	563	438	701	688
20	94	357	408	395	508	508

West Gage #	Raw CSS - microstrains					
	Release	1-Day	2-Day	3-Day	7-Day	14-Day
1	75	300	325	275	613	526
2	232	545	557	307	820	770
3	224	511	499	499	499	524
4	312	561	598	524	661	686
5	319	731	706	406	643	818
6	437	762	787	824	837	824
7	507	745	845	883	1033	1083
8	530	830	880	892	980	992
9	527	765	1003	1078	1191	1179
10	502	765	803	803	891	916
11	784	1034	934	1047	884	884
12	510	863	876	914	939	989
13	532	757	770	845	882	607
14	532	832	857	895	983	970
15	381	731	744	756	719	669
16	548	810	847	872	959	959
17	486	910	997	1096	1184	1258
18	491	802	827	1286	988	827
19	690	1150	1200	1225	1324	1312
20	584	870	895	920	1045	1007

H.2 Girder G1B

Table H.4 G1B Girder Data

Girder #		G1B	Raw Data for Transfer and Development Length				
Reading #	Date (m/dd/yy)	Time (24 hr)	Midspan Deflection (inches)	Ambient Temp (Deg F)	Internal Temp (Deg F)	VWSG Data	
						Hz	WG
Initial 1	7/10/01	11:30	1.938	80.0		929.61	2009
Initial 2	7/10/01	12:10	1.938	80.0		929.61	2009
Release	7/10/01	15:25	2.250	90.0		822.64	2009
1-Day	7/11/01	7:55	2.266	75.0			
2-Day	7/12/01	7:50	2.297	75.0	85.3	808.81	2448
3-Day	7/13/01	7:45	2.297	77.2	82.6	802.40	2534
7-Day	7/17/01	7:30	2.320	70.0	78.5	788.66	2905
14-Day	7/24/01	7:00	2.328	75.6	83.0	775.01	2499

Strand Jacking Data from Load Cells and Tensioning Machine						
	Load Cell Readings		Tension Machine Readings		Date and Time Of	Ambient Temp
Load Cell (Strand) #	At Time of Stressing ($\mu\varepsilon$)	Prior To Release ($\mu\varepsilon$)	Strand Jacking Force (lbs)	Strand Elongation (inches)	Tensioning (m/dd/yy) (24 hr)	(Deg F)
1	4533	4513	45000	10.250		
2	5275	5270	45000	9.875		
3	5430	5438	45000	10.125		
4	4975	4960	45000	9.875		
5	5352	5313	45000	9.875	9 Jul 01	90
6	5286	5270	45000	9.750	11:30	
7	5206	5150	45500	9.875		
8	5340	5357	45000	10.625		
9	5430	5448	45000	10.250		
10	5532	5479	45000	10.125		

449

Table H.5 Raw Concrete Surface Strain Data for Girder G1B-North

East Gage #	Raw CSS - microstrains					
	Release	1-Day	2-Day	3-Day	7-Day	14-Day
1	37	174	224	199	422	497
2	6	156	193	193	380	430
3	337	175	912	212	237	62
4	256	169	219	169	156	219
5	75	38	126	113	414	477
6	87	500	512	500	612	700
7	424	649	711	836	998	973
8	238	450	500	488	663	801
9	243	593	456	418	655	805
10	350	350	413	388	588	725
11	419	618	743	743	806	906
12	535	573	797	834	759	909
13	478	763	813	850	999	1073
14	224	385	509	559	832	584
15	453	552	639	614	925	1011
16	494	569	656	669	844	881
17	539	627	727	702	928	966
18	533	445	771	720	1121	1422
19	444	657	732	720	895	932
20	537	599	724	674	1011	1024

West Gage #	Raw CSS - microstrains					
	Release	1-Day	2-Day	3-Day	7-Day	14-Day
1	381	618	705	705	930	955
2	312	599	661	661	811	874
3	343	580	580	605	855	892
4	462	487	549	574	874	824
5	357	532	607	644	832	882
6	368	630	667	692	867	904
7	383	458	558	608	822	834
8	301	690	652	527	928	941
9	478	578	692	754	918	993
10	126	604	579	717	805	918
11	343	618	705	705	1005	1217
12	381	644	744	656	982	1032
13	392	702	802	1001	963	1001
14	137	337	411	349	623	773
15	300	512	612	587	849	887
16	50	237	200	225	437	575
17	150	287	400	412	562	612
18	181	355	418	430	530	630
19	62	312	374	361	374	399
20	106	44	181	156	243	243

Table H.6 Raw Concrete Surface Strain Data for Girder G1B-South

East Gage #	Raw CSS - microstrains					
	Release	1-Day	2-Day	3-Day	7-Day	14-Day
1	553	452	515	917	666	766
2	723	911	999	987	1163	1213
3	545	859	946	972	1072	1034
4	490	842	968	930	1069	1081
5	661	837	1039	1089	1177	1328
6	763	1078	1216	1166	1191	1254
7	391	858	1022	1073	1148	1249
8	581	961	1024	1011	1138	1188
9	541	906	1007	981	1095	1120
10	490	653	741	402	502	578
11	509	760	860	747	835	873
12	383	483	508	445	571	596
13	408	633	872	784	922	959
14	519	795	895	857	995	958
15	507	569	682	607	594	532
16	274	449	6043	473	473	473
17	193	442	492	417	542	529
18	361	274	460	361	448	410
19	56	43	155	192	354	329
20	346	136	333	197	148	309

West Gage #	Raw CSS - microstrains					
	Release	1-Day	2-Day	3-Day	7-Day	14-Day
1	38	163	250	225	463	338
2	13	138	413	188	263	238
3	131	344	319	294	406	344
4	287	449	424	499	687	612
5	281	582	544	544	582	544
6	263	501	538	538	714	601
7	457	820	832	870	958	882
8	532	857	882	920	970	970
9	476	839	889	1001	1026	1014
10	394	732	757	732	844	807
11	470	846	871	883	984	1009
12	389	703	741	766	879	879
13	439	777	827	802	927	902
14	726	801	852	826	952	889
15	451	889	977	1002	1140	1140
16	450	775	813	813	938	888
17	558	846	947	909	1085	1147
18	666	1005	1419	1608	1633	1620
19	438	676	714	726	827	827
20	495	746	821	821	1272	1147

H.3 Girder G1C

Table H.7 G1C Girder Data

Girder #		G1C	Raw Data for Transfer and Development Length				
Reading #	Date (m/dd/yy)	Time (24 hr)	Midspan Deflection (inches)	Ambient Temp (Deg F)	Internal Temp (Deg F)	VWSG Data	
						Hz	WG
Initial 1	7/18/01	12:10	2.031	85.0	117.4	902.66	1308
Initial 2	7/18/01	12:10	2.031	85.0	117.4	902.66	1308
Release	7/18/01	15:15	2.453	87.8	108.5	799.65	1387
1-Day	7/19/01	7:08	2.469	74.2	84.6	791.59	2407
2-Day	7/20/01	6:53	2.484	73.6	83.5	784.09	2514
3-Day	7/21/01	6:50	2.500	72.5	79.0	780.30	2829
7-Day	7/25/01	7:10	2.531	73.8	78.7	762.00	2868
14-Day	8/1/01	6:30	2.555	72.0	78.1	749.82	2863

Strand Jacking Data from Load Cells and Tensioning Machine						
	Load Cell Readings		Tension Machine Readings		Date and Time Of	Ambient Temp
Load Cell (Strand) #	At Time of Stressing (με)	Prior To Release (με)	Strand Jacking Force (lbs)	Strand Elongation (inches)	Tensioning (m/dd/yy) (24 hr)	(Deg F)
1	5163	4989	45000	9.875		
2	5218	5023	45500	9.750		
3	5640	5387	46000	9.750		
4	5549	5406	46000	9.875		
5	5484	5279	46000	9.875	17 Jul 01 9:40	75
6	5456	5309	46000	9.875		
7	5126	5000	45000	10.000		
8	5115	4970	45000	10.000		
9	5489	5387	46000	9.750		
10	5601	5443	46000	9.750		

452

Table H.8 Raw Concrete Surface Strain Data for Girder G1C-North

East Gage #	Raw CSS - microstrains					
	Release	1-Day	2-Day	3-Day	7-Day	14-Day
1	106	293	356	356	468	356
2	150	313	363	313	475	400
3	150	313	539	564	614	451
4	338	639	614	564	614	451
5	300	437	475	512	587	537
6	286	422	559	559	633	546
7	428	614	676	700	762	713
8	317	615	528	739	752	627
9	510	710	784	809	921	896
10	481	818	893	818	1006	868
11	531	719	769	732	857	844
12	580	928	966	991	1103	1078
13	600	813	963	926	1063	1076
14	730	1205	1117	1355	1330	993
15	651	914	1101	1164	1264	1289
16	546	797	922	922	1023	985
17	519	794	868	943	1031	1018
18	580	817	867	954	1041	967
19	454	852	1002	927	1052	1114
20	578	865	889	1026	1163	1026

West Gage #	Raw CSS - microstrains					
	Release	1-Day	2-Day	3-Day	7-Day	14-Day
1	786	974	1099	1099	1236	1173
2	724	1135	1110	1073	1198	1173
3	655	829	929	1004	1079	942
4	668	930	1018	993	1105	1067
5	686	973	1036	1086	1135	998
6	643	743	855	880	1005	693
7	740	978	1028	1090	1203	1065
8	665	903	1016	1053	1204	1078
9	730	1007	1095	1321	1422	1271
10	1100	1175	1037	1062	1238	1024
11	550	824	862	887	999	787
12	612	849	899	924	998	948
13	560	734	809	784	971	884
14	486	660	698	748	847	735
15	331	356	556	794	794	494
16	312	425	700	737	612	425
17	387	599	624	611	749	586
18	237	499	499	586	736	611
19	305	716	492	729	891	654
20	100	324	312	362	436	150

Table H.9 Raw Concrete Surface Strain Data for Girder G1C-South

East Gage #	Raw CSS - microstrains					
	Release	1-Day	2-Day	3-Day	7-Day	14-Day
1	740	1394	1431	1505	1604	1604
2	758	1019	1069	1019	1143	1156
3	703	952	1052	1027	1151	1139
4	978	1203	1178	1253	1402	1340
5	729	978	1053	1015	1152	1152
6	674	887	936	974	1099	1199
7	694	906	981	969	1106	1119
8	758	908	1046	1034	1209	1184
9	972	1123	1248	1236	1248	1060
10	446	634	936	797	998	923
11	622	835	948	923	1061	1061
12	572	799	887	849	975	950
13	227	530	719	795	972	795
14	315	631	618	618	706	618
15	233	549	586	549	624	549
16	271	473	549	473	662	498
17	333	459	471	547	773	672
18	38	226	138	264	365	201
19	82	295	295	345	395	307
20	746	395	433	332	307	370

West Gage #	Raw CSS - microstrains					
	Release	1-Day	2-Day	3-Day	7-Day	14-Day
1	415	579	566	528	642	566
2	526	652	727	727	752	702
3	376	514	514	514	639	451
4	512	662	712	737	725	775
5	374	437	511	549	686	574
6	631	844	731	856	756	956
7	569	794	831	744	806	831
8	644	844	907	844	1032	957
9	502	678	765	715	753	703
10	738	938	1026	988	1126	1063
11	688	951	1014	914	1089	951
12	972	1147	1273	1210	1273	1260
13	760	972	1072	885	1097	1084
14	1169	1307	1369	1357	1469	1482
15	607	495	708	695	770	695
16	832	932	1045	982	1133	1095
17	504	705	730	718	844	806
18	396	459	597	547	748	673
19	1065	1153	1228	1253	1453	1315
20	551	651	701	663	839	789

H.4 Girder G2A

Table H.10 G2A Girder Data

Girder #	G2A	Raw Data for Transfer and Development Length				
					VWSG Data	
Reading #	Date (m/dd/yy)	Time (24 hr)	Midspan Deflection (inches)	Ambient Temp (Deg F)	Internal Temp (Deg F)	Hz	WG
Initial 1	7/13/01	10:15	2.047	82.8	112.0	920.40	1377
Initial 2	7/13/01	10:15	2.047	82.8	112.0	920.40	1377
Release	7/13/01	15:30	2.359	98.8	106.4	846.40	1410
1-Day	7/14/01	7:25	2.313	73.6	81.0	844.75	2771
2-Day							
3-Day	7/16/01	6:40	2.320	75.3	80.5	843.64	2813
7-Day	7/20/01	7:55	2.344	74.2	82.3	838.23	2556
14-Day	7/27/01	6:55	2.344	73.1	78.7	839.09	2759

Strand Jacking Data from Load Cells and Tensioning Machine						
	Load Cell Readings		Tension Machine Readings		Date and Time Of	Ambient Temp
Load Cell (Strand) #	At Time of Stressing ($\mu\varepsilon$)	Prior To Release ($\mu\varepsilon$)	Strand Jacking Force (lbs)	Strand Elongation (inches)	Tensioning (m/dd/yy) (24 hr)	(Deg F)
1	6013	6140	45000	10.500		
2	5107	5310	45500	9.875		
3	5193	5351	45500	10.000		
4	4742	4891	45000	10.000		
5	5516	5727	45000	9.750	12 Jul 01 11:30	95
6	5432	5572	45000	9.750		
7	5296	5426	45000	9.875		
8	5452	5612	45000	10.000		
9	5587	5781	45500	10.500		
10	5824	6011	45500	10.375		

455

Table H.11 Raw Concrete Surface Strain Data for Girder G2A-North

East Gage #	Raw CSS - microstrains					
	Release	1-Day	2-Day	3-Day	7-Day	14-Day
1	205	441		541	553	665
2	479	653		727	653	715
3	318	518		555	568	555
4	375	525		338	350	300
5	351	627		715	690	777
6	437	687		825	837	862
7	200	474		723	624	723
8	718	1343		1318	1381	1531
9	281	505		455	318	405
10	582	819		894	894	1044
11	800	963		1038	1026	1213
12	454	728		778	703	790
13	584	733		819	844	1018
14	452	614		564	490	614
15	459	645		632	620	694
16	487	761		936	923	1023
17	795	1095		1158	1158	1233
18	494	782		857	845	945
19	375	663		726	726	763
20	399	624		611	636	711

West Gage #	Raw CSS - microstrains					
	Release	1-Day	2-Day	3-Day	7-Day	14-Day
1	474	924		1048	1036	1136
2	443	855		855	818	905
3	462	774		761	774	848
4	543	668		705	705	880
5	606	831		918	931	981
6	537	800		837	812	887
7	332	759		759	796	846
8	407	658		720	670	733
9	521	823		923	898	973
10	308	659		709	684	785
11	1456	1244		1156	1206	1131
12	719	906		969	981	1069
13	467	790		828	815	877
14	518	767		817	829	904
15	431	843		905	918	1005
16	319	644		706	656	706
17	331	543		543	531	581
18	268	455		480	443	493
19	318	567		505	517	630
20	380	355		430	380	442

Table H.12 Raw Concrete Surface Strain Data for Girder G2A-South

East	Raw CSS - microstrains					
Gage #	Release	1-Day	2-Day	3-Day	7-Day	14-Day
1	339	740		916	991	891
2	232	508		1022	1060	822
3	207	570		695	833	620
4	577	1080		1230	716	1193
5	283	674		674	1177	699
6	359	801		901	990	788
7	411	790		853	878	828
8	398	727		968	1081	1006
9	283	586		674	774	724
10	246	497		573	636	548
11	333	696		797	885	809
12	376	714		840	1015	902
13	332	1210		1310	1285	1298
14	262	600		762	825	787
15	188	551		576	639	651
16	230	479		529	542	616
17	118	629		753	716	790
18	56	292		367	379	317
19	6	217		254	378	353
20	49	234		296	308	247

West	Raw CSS - microstrains					
Gage #	Release	1-Day	2-Day	3-Day	7-Day	14-Day
1	100	150		363	163	138
2	213	413		575	638	651
3	0	13		225	213	325
4	237	449		537	424	337
5	200	475		650	700	587
6	382	733		858	870	1008
7	288	738		926	1026	1013
8	351	438		576	739	613
9	395	758		1022	1084	1034
10	332	607		882	920	807
11	201	590		728	803	728
12	263	564		715	727	589
13	282	582		595	708	595
14	300	526		663	638	538
15	219	443		606	618	518
16	225	514		651	702	601
17	207	470		582	595	507
18	232	496		672	722	621
19	188	464		539	539	501
20	257	495		633	633	558

H.5 Girder G2B

Table H.13 G2B Girder Data

Girder #		G2B	Raw Data for Transfer and Development Length				
Reading #	Date (m/dd/yy)	Time (24 hr)	Midspan Deflection (inches)	Ambient Temp (Deg F)	Internal Temp (Deg F)	VWSG Data	
						Hz	WG
Initial 1	7/13/01	10:50	1.875	82.8	112.0	900.40	1363
Initial 2	7/13/01	10:50	1.875	82.8	112.0	900.40	1363
Release	7/13/01	15:50	2.172	98.8	107.1	826.40	1396
1-Day	7/14/01	7:46	2.094	73.6	82.6	823.30	2653
2-Day							
3-Day	7/16/01	6:40	2.117	75.8	80.6	822.40	2789
7-Day	7/20/01	7:57	2.148	75.4	81.5	818.38	2614
14-Day	7/27/01	7:02	2.164	73.1	78.5	817.30	2797

Strand Jacking Data from Load Cells and Tensioning Machine						
	Load Cell Readings		Tension Machine Readings		Date and Time Of	Ambient Temp
Load Cell (Strand) #	At Time of Stressing ($\mu\varepsilon$)	Prior To Release ($\mu\varepsilon$)	Strand Jacking Force (lbs)	Strand Elongation (inches)	Tensioning (m/dd/yy) (24 hr)	(Deg F)
1	6013	6140	45000	10.500		
2	5107	5310	45500	9.875		
3	5193	5351	45500	10.000		
4	4742	4891	45000	10.000		
5	5516	5727	45000	9.750	12 Jul 01	95
6	5432	5572	45000	9.750	11:30	
7	5296	5426	45000	9.875		
8	5452	5612	45000	10.000		
9	5587	5781	45500	10.500		
10	5824	6011	45500	10.375		

458

Table H.14 Raw Concrete Surface Strain Data for Girder G2B-North

East	Raw CSS - microstrains					
Gage #	Release	1-Day	2-Day	3-Day	7-Day	14-Day
1	269	282		394	232	407
2	218	368		456	418	493
3	188	538		613	575	588
4	362	562		487	512	562
5	306	643		718	718	755
6	307	846		896	896	921
7	357	745		833	858	870
8	482	670		745	732	845
9	426	764		751	802	802
10	387	562		624	761	699
11	443	643		717	680	705
12	412	750		775	800	787
13	425	575		675	712	725
14	526	751		776	801	801
15	495	608		758	821	808
16	387	600		637	687	675
17	431	731		831	881	881
18	443	693		768	793	793
19	411	648		686	711	711
20	469	770		895	907	995

West	Raw CSS - microstrains					
Gage #	Release	1-Day	2-Day	3-Day	7-Day	14-Day
1	577	903		916	903	966
2	469	932		770	745	982
3	294	620		632	620	645
4	269	694		756	794	781
5	432	807		969	982	1007
6	345	697		860	848	948
7	470	808		871	908	996
8	414	927		815	1053	1028
9	426	751		751	751	776
10	156	730		630	755	780
11	457	909		909	1021	1084
12	457	733		771	821	796
13	464	639		765	790	740
14	370	683		770	846	921
15	337	511		499	598	548
16	31	570		570	608	608
17	131	407		457	469	544
18	150	250		462	575	837
19	125	501		551	614	614
20	137	436		535	510	660

Table H.15 Raw Concrete Surface Strain Data for Girder G2B-South

East Gage #	Raw CSS - microstrains					
	Release	1-Day	2-Day	3-Day	7-Day	14-Day
1	486	786		698	748	673
2	274	474		548	524	548
3	306	656		793	780	705
4	262	637		749	861	811
5	212	623		511	561	387
6	262	674		712	762	737
7	424	523		573	561	573
8	299	585		623	685	623
9	243	841		865	828	940
10	317	678		703	753	753
11	311	646		658	671	646
12	298	634		621	845	659
13	261	573		623	747	685
14	224	623		623	760	660
15	244	582		569	607	569
16	300	550		625	737	687
17	641	928		803	878	803
18	44	342		330	280	243
19	25	375		450	537	462
20	38	388		401	489	401

West Gage #	Raw CSS - microstrains					
	Release	1-Day	2-Day	3-Day	7-Day	14-Day
1	38	263		389	363	38
2	131	281		269	306	31
3	19	393		455	417	368
4	243	1028		1028	1003	941
5	187	674		724	612	749
6	294	606		606	556	444
7	163	539		639	601	639
8	256	656		631	618	568
9	376	689		777	752	765
10	351	740		715	690	652
11	219	621		596	771	583
12	321	736		736	799	723
13	256	569		557	607	507
14	545	1108		1146	1196	1171
15	237	587		550	562	537
16	293	681		730	743	730
17	305	417		455	505	480
18	329	652		615	665	652
19	292	728		790	865	740
20	242	640		677	776	665

H.6 Girder G2C

Table H.16 G2C Girder Data

Girder #		G2C	Raw Data for Transfer and Development Length				
Reading #	Date (m/dd/yy)	Time (24 hr)	Midspan Deflection (inches)	Ambient Temp (Deg F)	Internal Temp (Deg F)	VWSG Data	
						Hz	WG
Initial 1	7/18/01	12:40	2.047	85.0	125.5	913.36	1427
Initial 2	7/18/01	12:40	2.047	85.0	125.5	913.36	1427
Release	7/18/01	15:00	2.469	87.8	108.9	827.12	1428
1-Day	7/19/01	6:55	2.438	74.2	86.0	817.71	2353
2-Day	7/20/01	6:55	2.469	73.6	84.6	814.71	2469
3-Day	7/21/01	6:50	2.453	72.5	78.8	813.58	2807
7-Day	7/25/01	7:10	2.469	73.8	78.0	806.60	2886
14-Day	8/1/01	6:30	2.477	72.0	78.5	802.68	2850

Strand Jacking Data from Load Cells and Tensioning Machine						
	Load Cell Readings		Tension Machine Readings		Date and Time Of	Ambient Temp
Load Cell (Strand) #	At Time of Stressing (με)	Prior To Release (με)	Strand Jacking Force (lbs)	Strand Elongation (inches)	Tensioning (m/dd/yy) (24 hr)	(Deg F)
1	5163	4989	45000	9.875		
2	5218	5023	45500	9.750		
3	5640	5387	46000	9.750		
4	5549	5406	46000	9.875		
5	5484	5279	46000	9.875	17 Jul 01	75
6	5456	5309	46000	9.875	9:40	
7	5126	5000	45000	10.000		
8	5115	4970	45000	10.000		
9	5489	5387	46000	9.750		
10	5601	5443	46000	9.750		

461

Table H.17 Raw Concrete Surface Strain Data for Girder G2C-North

East Gage #	Raw CSS - microstrains					
	Release	1-Day	2-Day	3-Day	7-Day	14-Day
1	100	251	276	238	226	138
2	200	437	499	537	562	387
3	44	469	582	506	619	256
4	281	505	443	568	555	418
5	431	668	743	781	756	643
6	445	632	632	658	670	582
7	494	1220	782	807	794	569
8	513	789	852	952	952	801
9	519	706	831	819	844	719
10	543	756	818	831	856	731
11	649	899	899	924	936	861
12	512	662	699	737	749	587
13	506	706	718	743	731	643
14	532	669	794	845	870	719
15	457	682	670	670	720	545
16	444	619	694	719	694	656
17	500	700	800	825	825	738
18	468	668	693	755	780	693
19	369	693	731	781	818	668
20	494	757	769	769	832	669

West Gage #	Raw CSS - microstrains					
	Release	1-Day	2-Day	3-Day	7-Day	14-Day
1	370	633	684	633	734	408
2	395	595	620	570	570	369
3	307	632	657	670	695	532
4	444	607	732	657	657	444
5	445	670	746	758	758	696
6	433	659	671	671	696	533
7	419	620	532	532	557	394
8	463	776	739	638	689	488
9	469	681	669	656	694	569
10	604	779	779	804	804	629
11	539	765	802	840	903	752
12	771	846	771	796	921	407
13	558	758	796	896	846	683
14	388	551	589	639	664	501
15	386	586	536	549	573	474
16	113	138	476	513	476	13
17	338	489	439	489	464	188
18	344	494	469	507	507	382
19	169	332	419	382	394	194
20	93	429	728	641	740	292

462

Table H.18 Raw Concrete Surface Strain Data for Girder G2C-South

East Gage #	Raw CSS - microstrains					
	Release	1-Day	2-Day	3-Day	7-Day	14-Day
1	673	798	760	873	873	661
2	573	773	835	860	823	723
3	687	850	887	925	962	875
4	506	681	730	743	768	693
5	531	731	881	918	1055	818
6	593	780	767	917	867	730
7	574	686	711	736	748	711
8	747	846	846	871	871	859
9	591	740	1014	765	765	728
10	629	803	828	853	903	928
11	547	671	759	846	821	746
12	640	776	751	963	925	813
13	560	734	784	871	883	833
14	137	200	462	499	524	424
15	512	624	787	799	961	861
16	269	331	469	569	669	506
17	112	224	312	474	424	436
18	137	261	485	386	435	249
19	0	163	250	288	275	288
20	44	169	282	357	407	294

West Gage #	Raw CSS - microstrains					
	Release	1-Day	2-Day	3-Day	7-Day	14-Day
1	6	220	270	270	408	245
2	62	262	337	337	425	375
3	81	106	5254	243	280	168
4	144	406	431	369	494	469
5	368	455	543	555	618	580
6	357	482	545	545	632	482
7	350	475	538	551	638	576
8	462	612	649	674	749	699
9	376	476	527	564	664	501
10	514	577	665	614	677	702
11	508	571	709	684	709	696
12	887	510	787	1001	711	1001
13	719	669	706	706	844	832
14	550	676	738	776	813	713
15	550	512	662	675	762	675
16	462	75	562	662	699	412
17	405	467	604	617	692	480
18	447	423	534	559	646	534
19	559	622	584	647	709	572
20	379	553	553	602	714	577

APPENDIX I

SMOOTHED CONCRETE SURFACE STRAIN PROFILES AND DETERMINATION OF TRANSFER LENGTH

This Appendix contains smoothed CSS profiles for each girder end as well as

plots showing the determination of transfer length based on 14-day CSS data.

I.1 Girder G1A-East
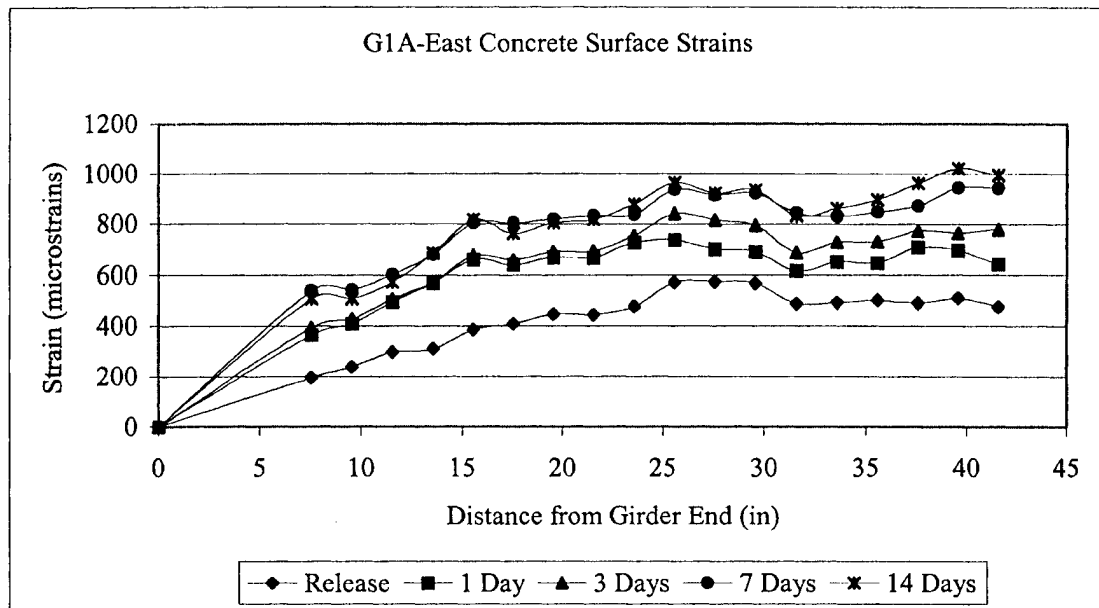
Figure I.1 Concrete Surface Strains for G1A-East
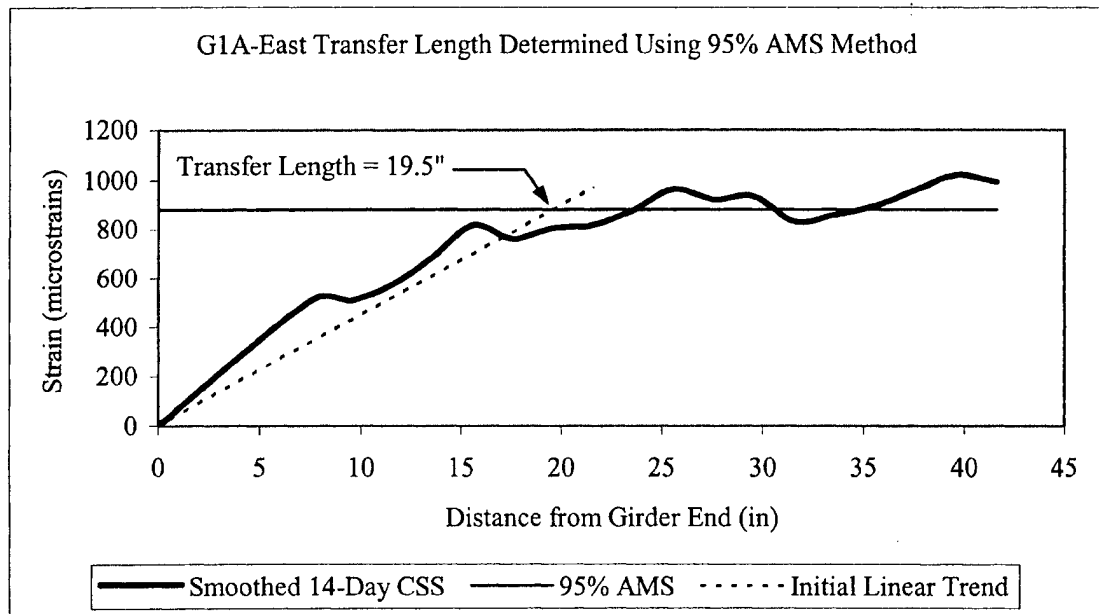
Figure I.2 14-Day Transfer Length Determined for G1A-East

465
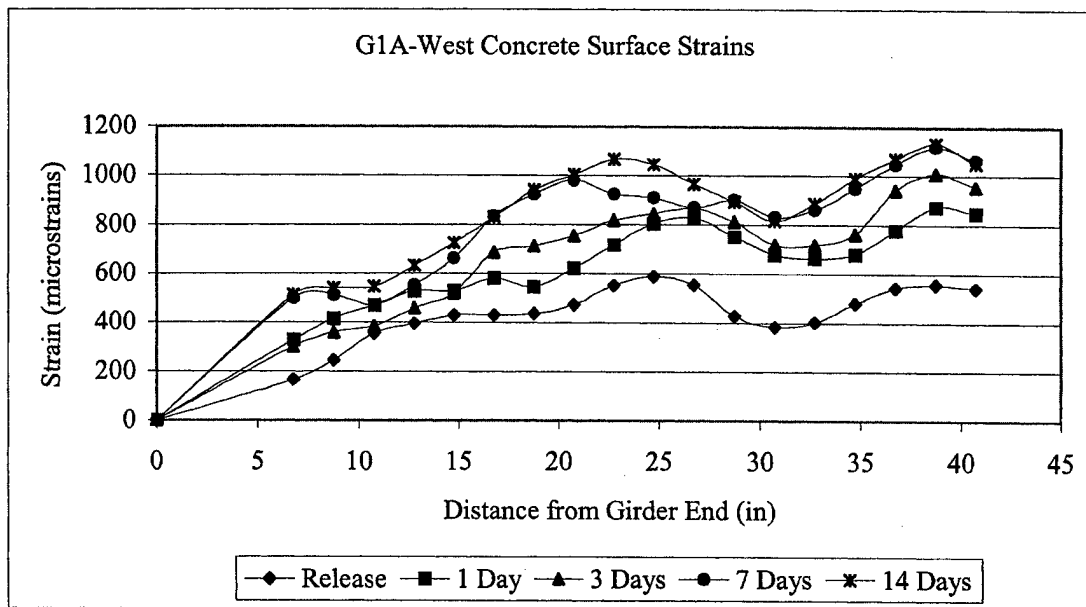
I.2 Girder G1A-West

Figure I.3 Concrete Surface Strains for G1A-West
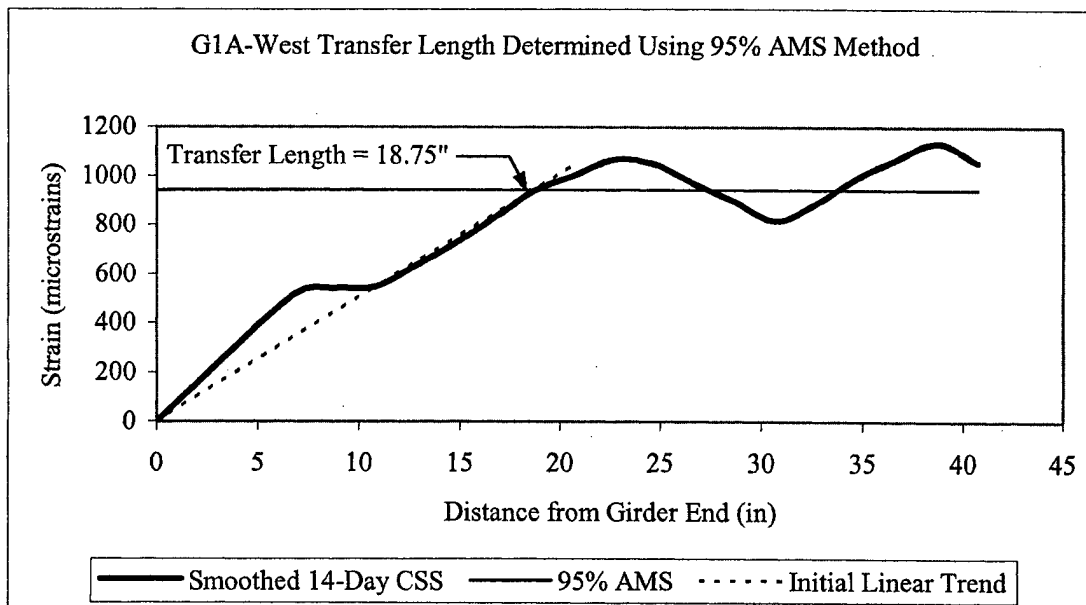
Figure I.4 14-Day Transfer Length Determined for G1A-West

I.3 Girder G1B-East
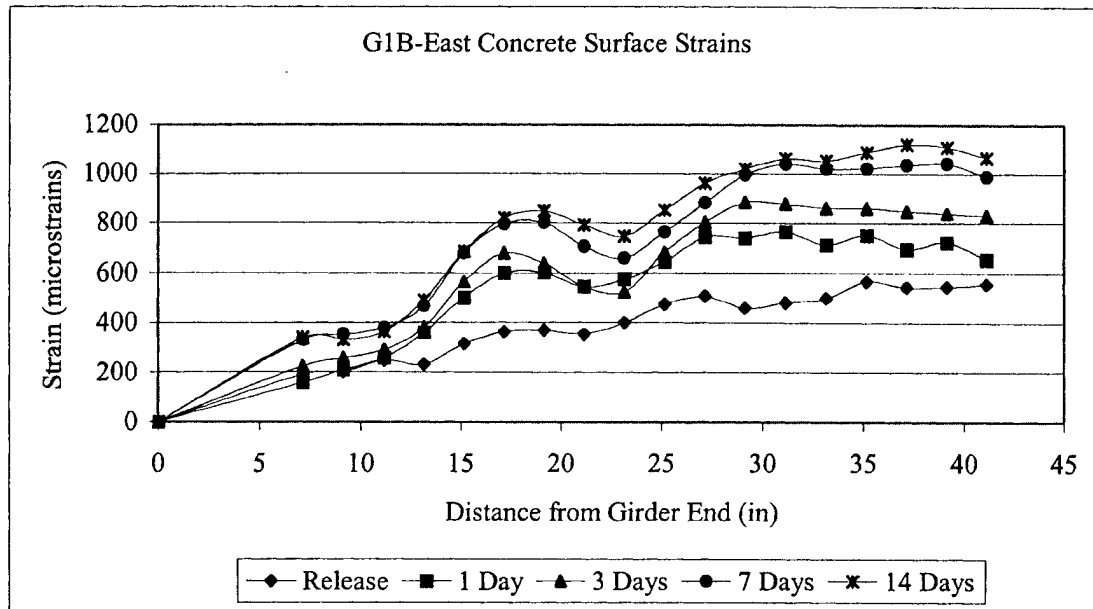
Figure I.5 Concrete Surface Strains for G1B-East
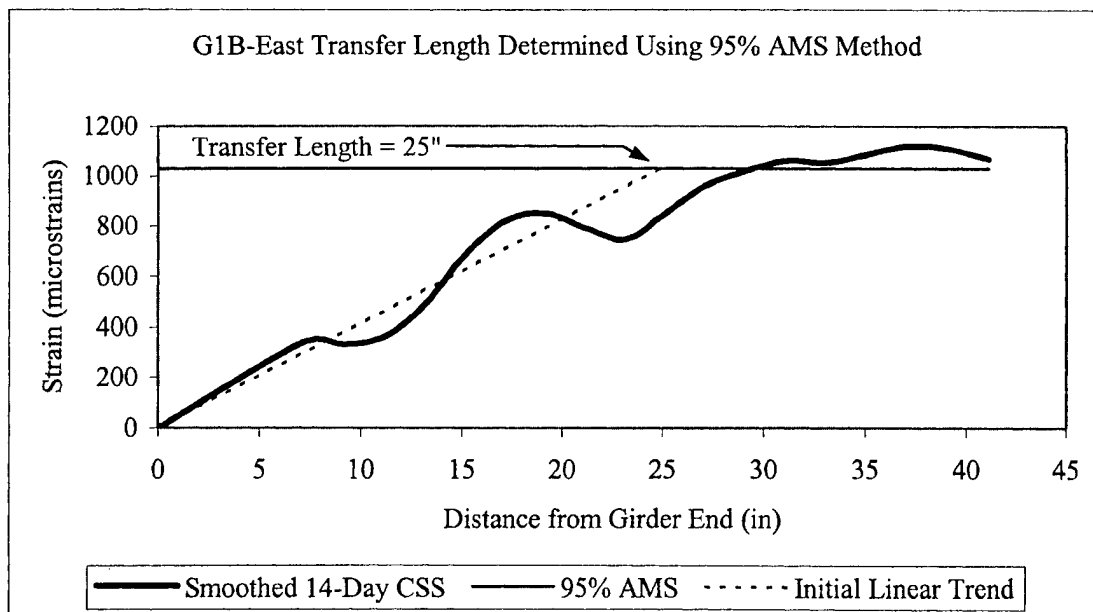
Figure I.6 14-Day Transfer Length Determined for G1B-East

467
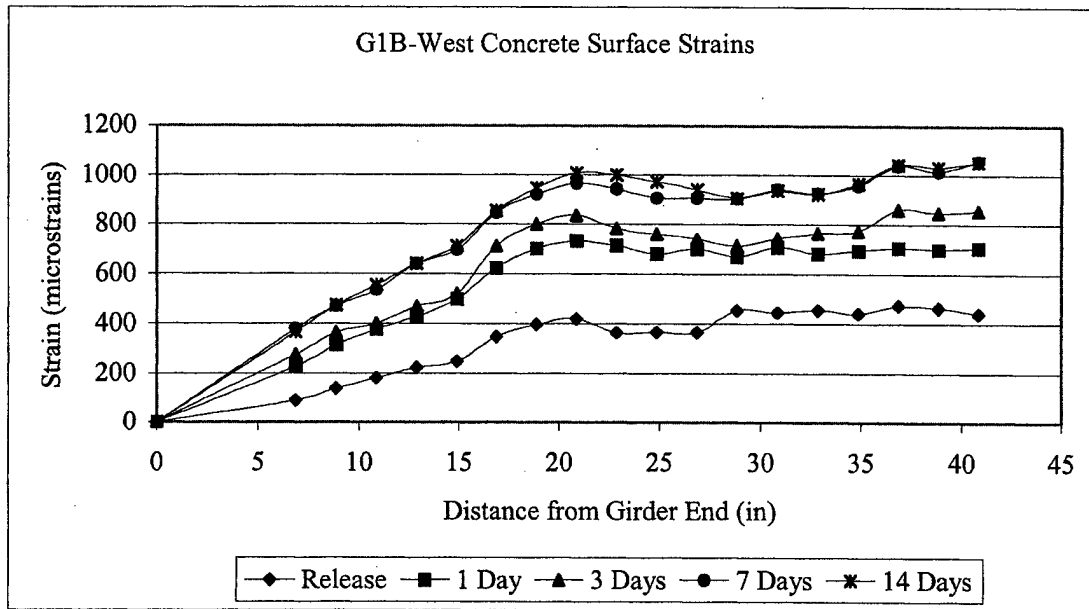
I.4 Girder G1B-West

Figure I.7 Concrete Surface Strains for G1B-West
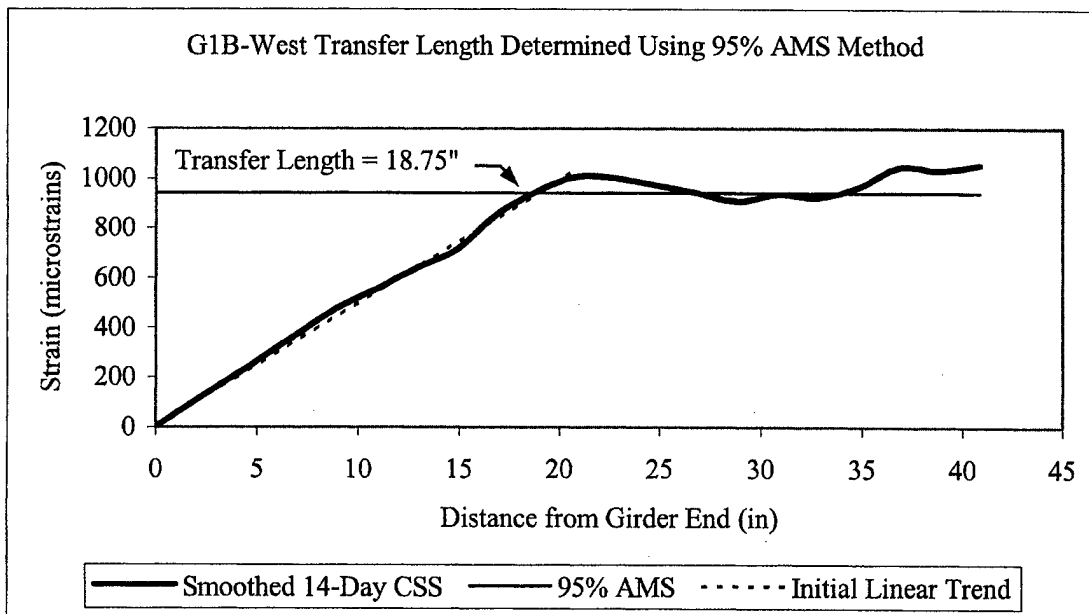
Figure I.8 14-Day Transfer Length Determined for G1B-West

I.5 Girder G1C-East
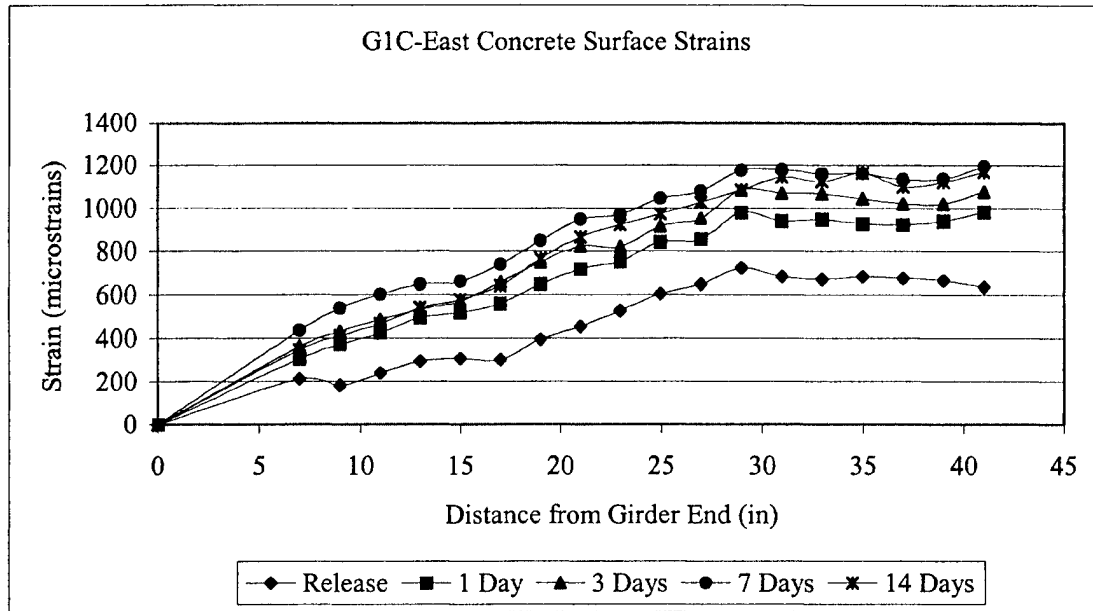
Figure I.9 Concrete Surface Strains for G1C-East
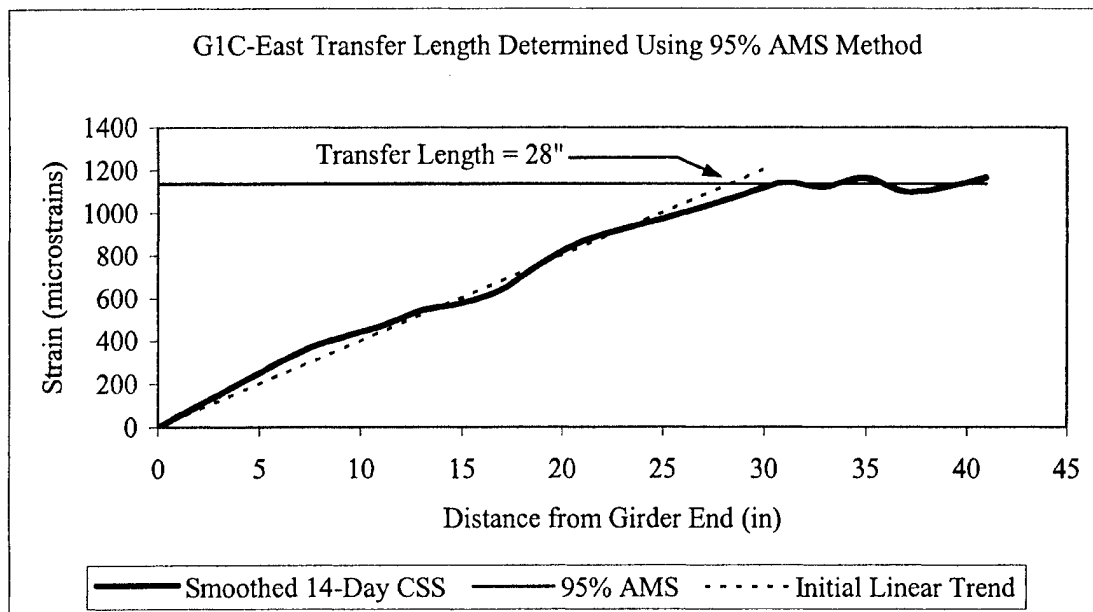
Figure I.10 14-Day Transfer Length Determined for G1C-East

469
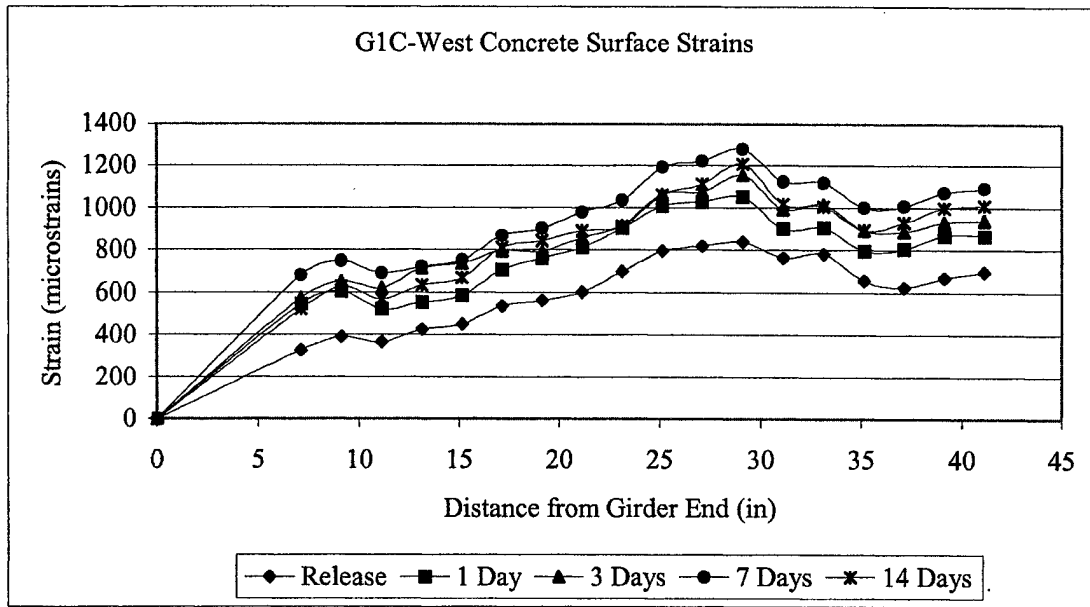
I.6 Girder G1C-West

Figure I.11 Concrete Surface Strains for G1C-West
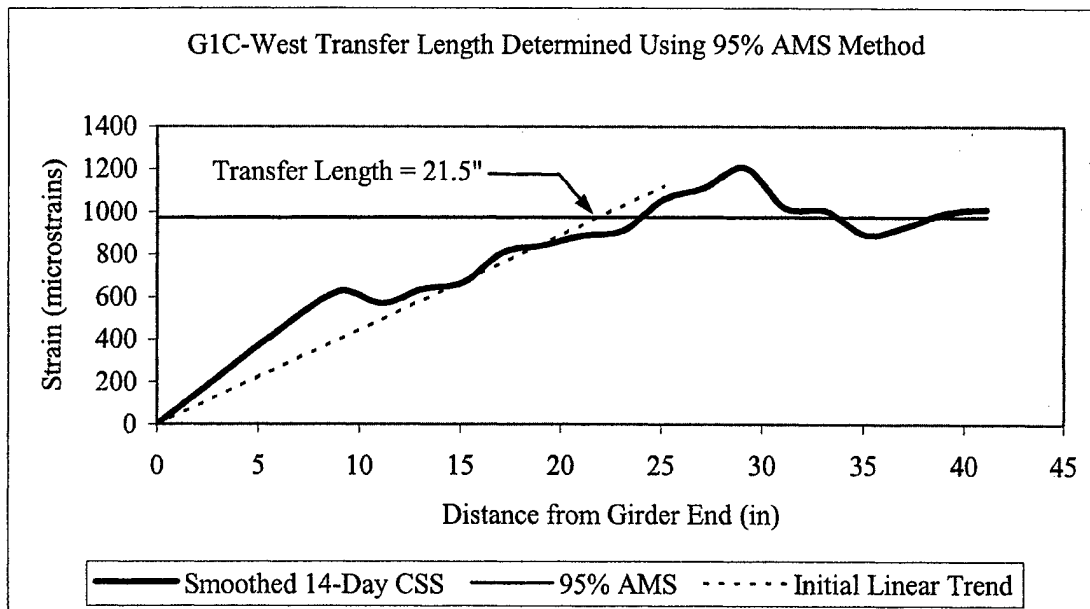
Figure I.12 14-Day Transfer Length Determined for G1C-West

I.7 Girder G2A-East
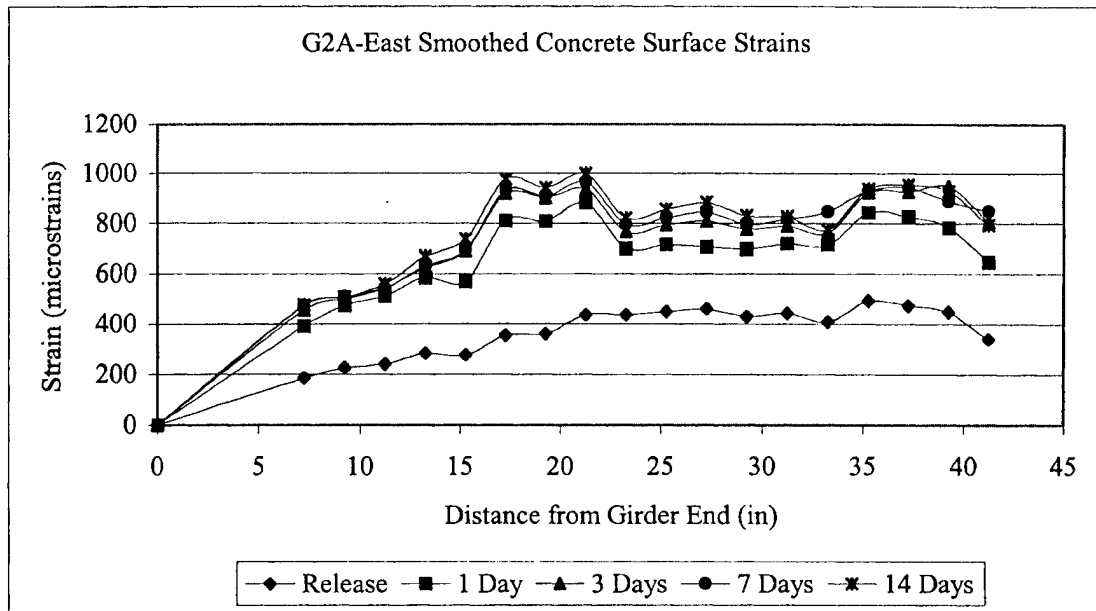
Figure I.13 Concrete Surface Strains for G2A-East
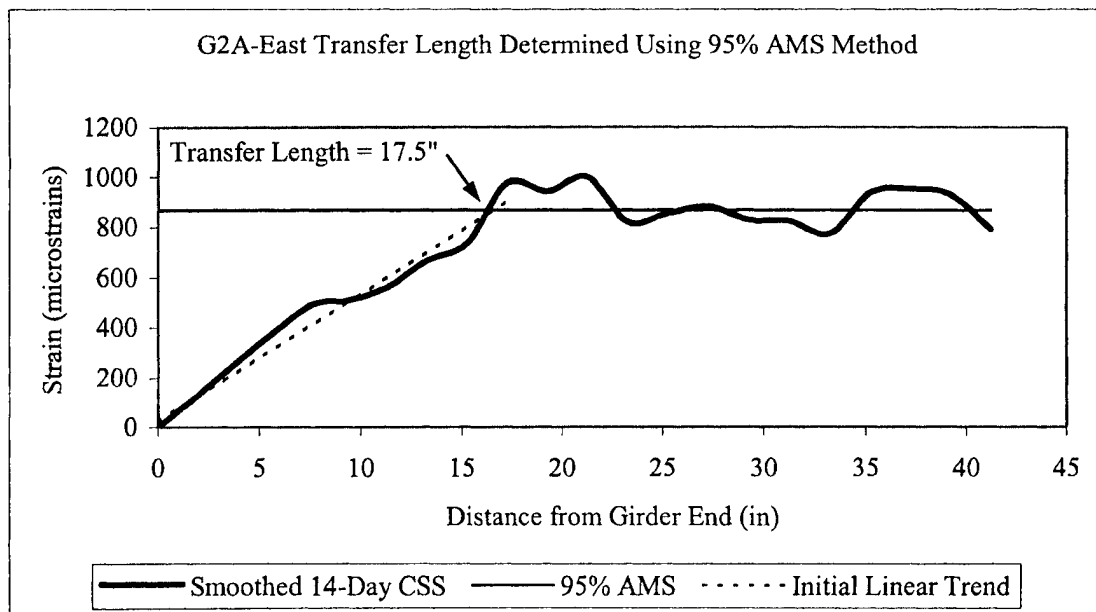
Figure I.14 14-Day Transfer Length Determined for G2A-East

471
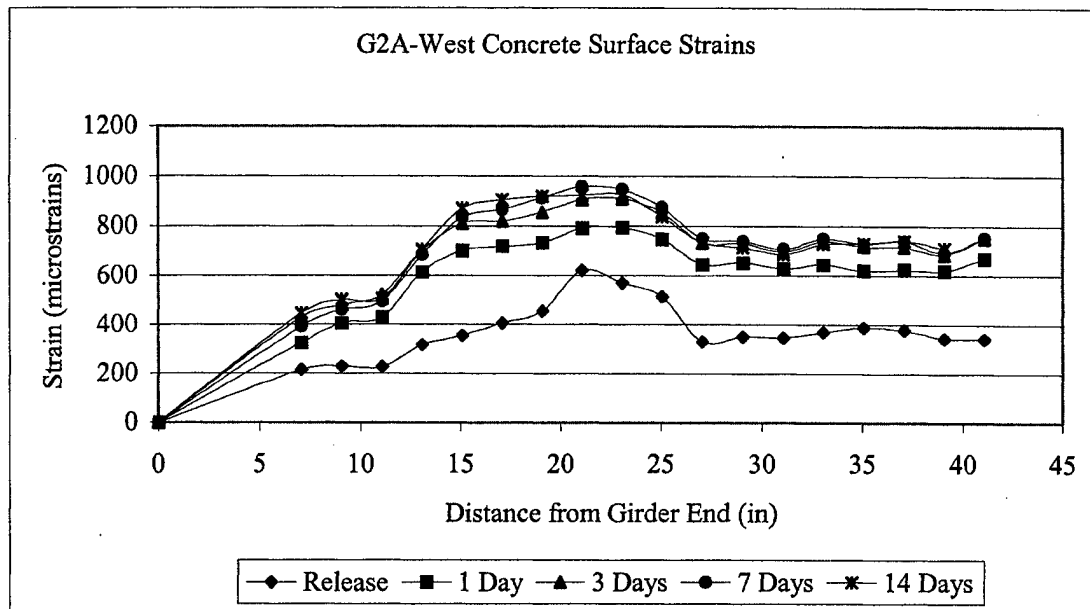
I.8 Girder G2A-West

Figure I.15 Concrete Surface Strains for G2A-West
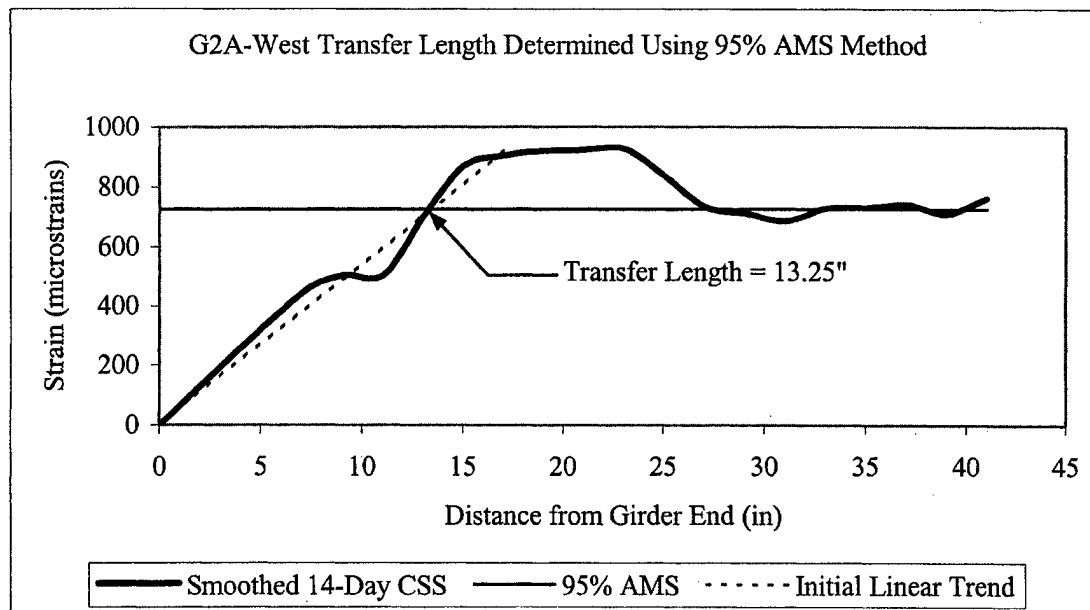
Figure I.16 14-Day Transfer Length Determined for G2A-West

472
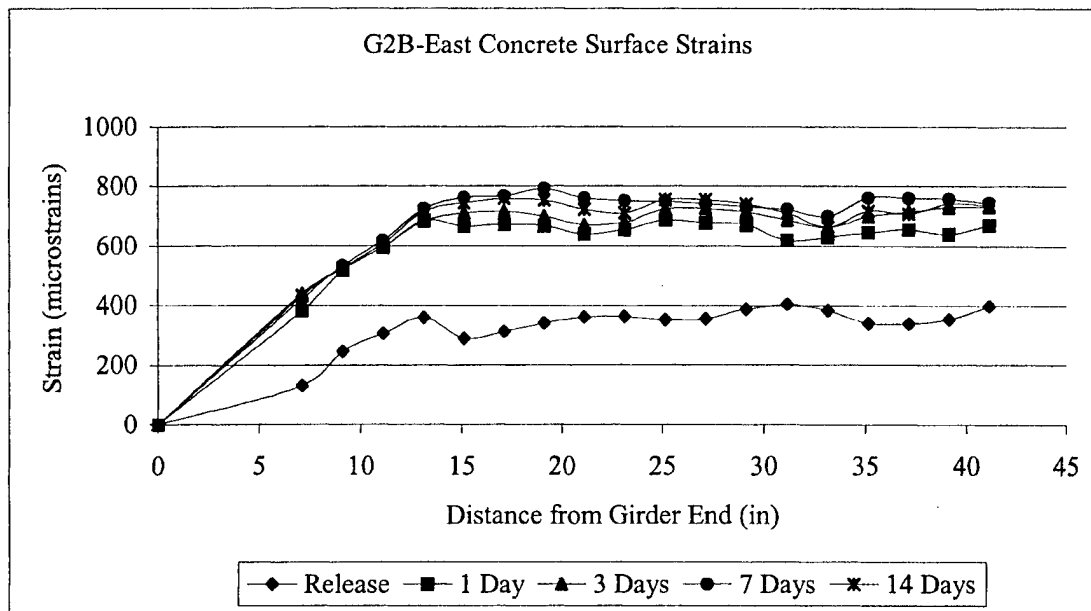
I.9 Girder G2B-East

Figure I.17 Concrete Surface Strains for G2B-East
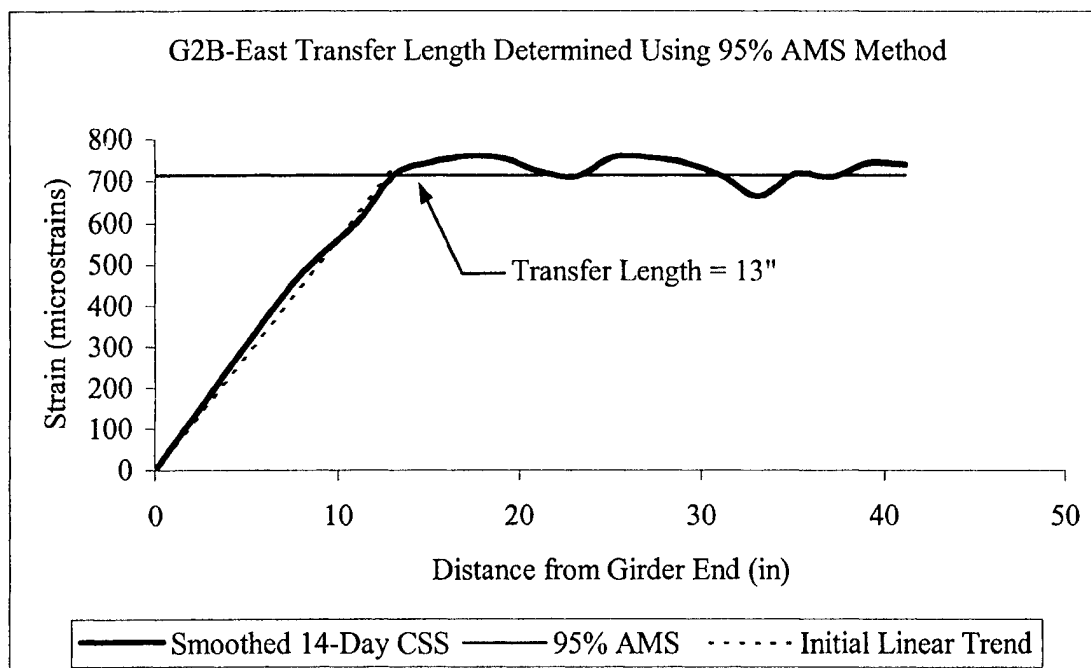
Figure I.18 14-Day Transfer Length Determined for G2B-East

473

I.10 Girder G2B-West
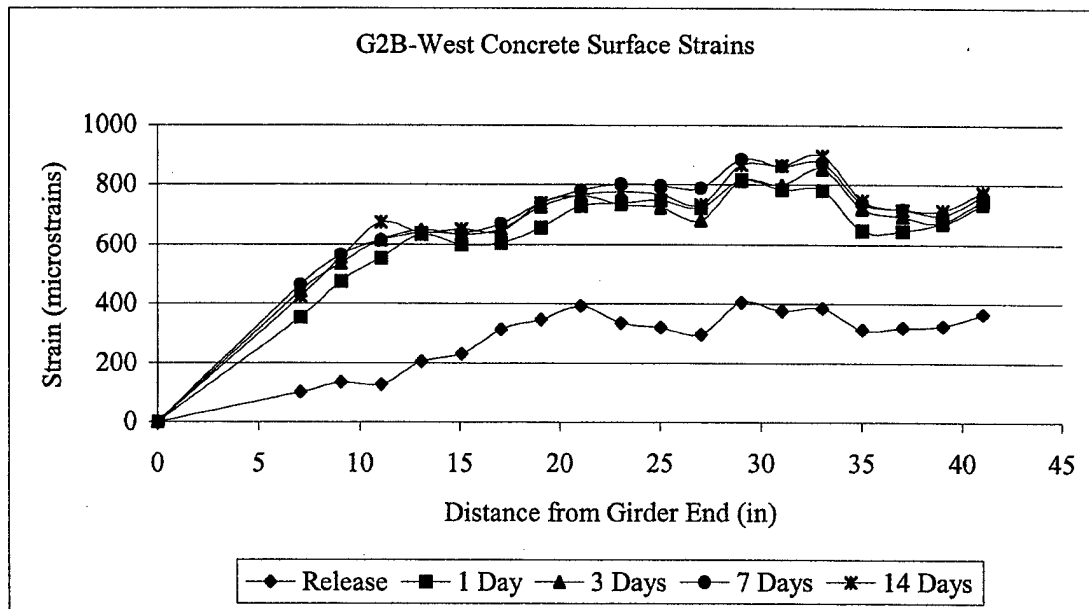
Figure I.19 Concrete Surface Strains for G2B-West
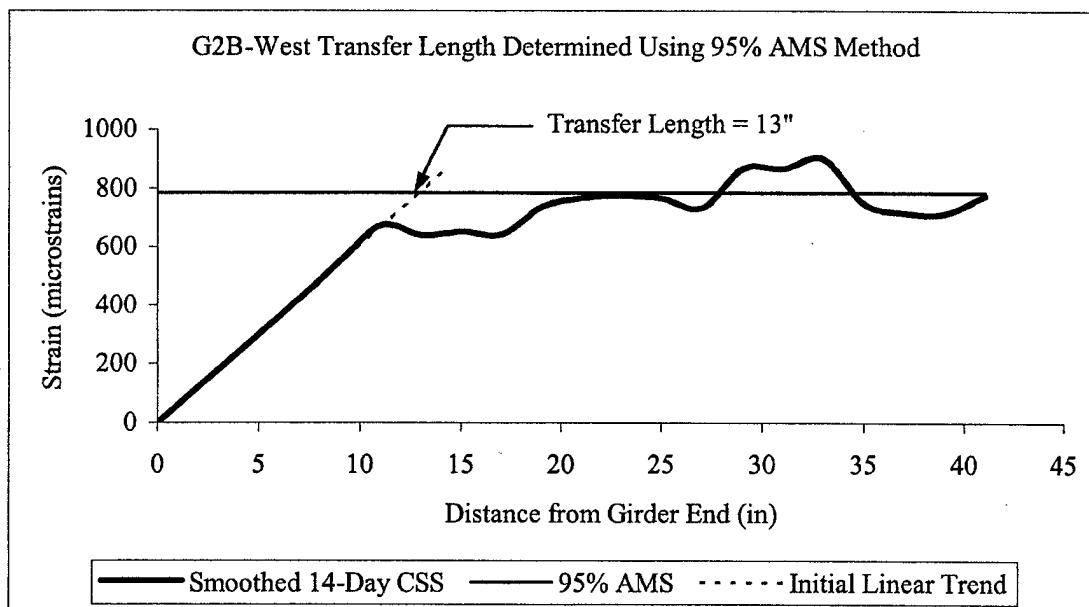
Figure I.20 14-Day Transfer Length Determined for G2B-West

474

I.11 Girder G2C-East
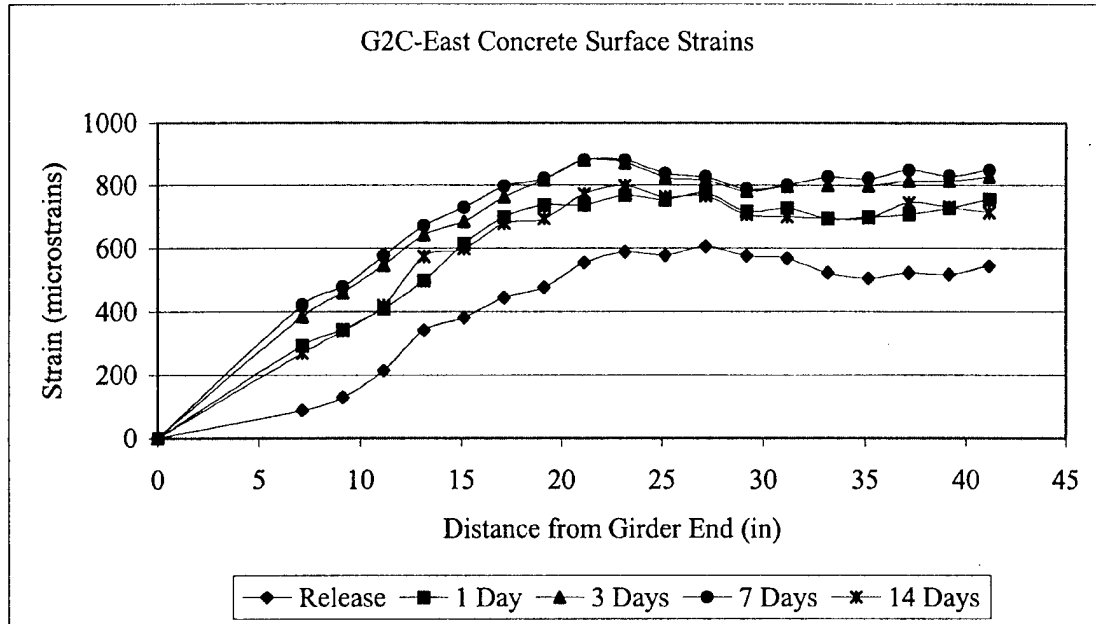
Figure I.21 Concrete Surface Strains for G2C-East
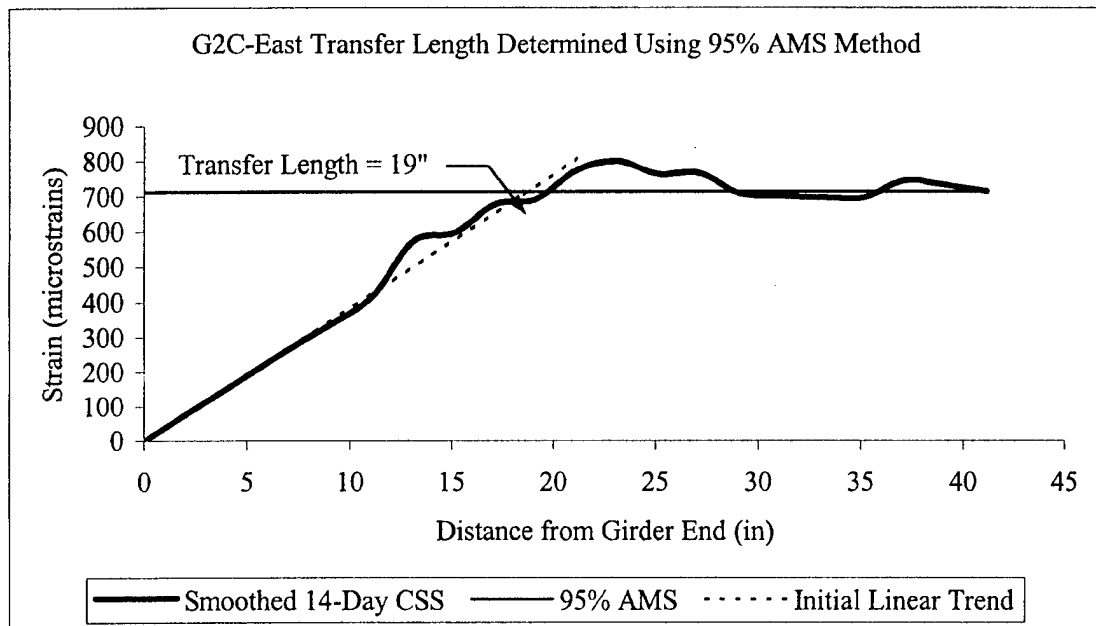
Figure I.22 14-Day Transfer Length Determined for G2C-East

I.12 Girder G2C-West
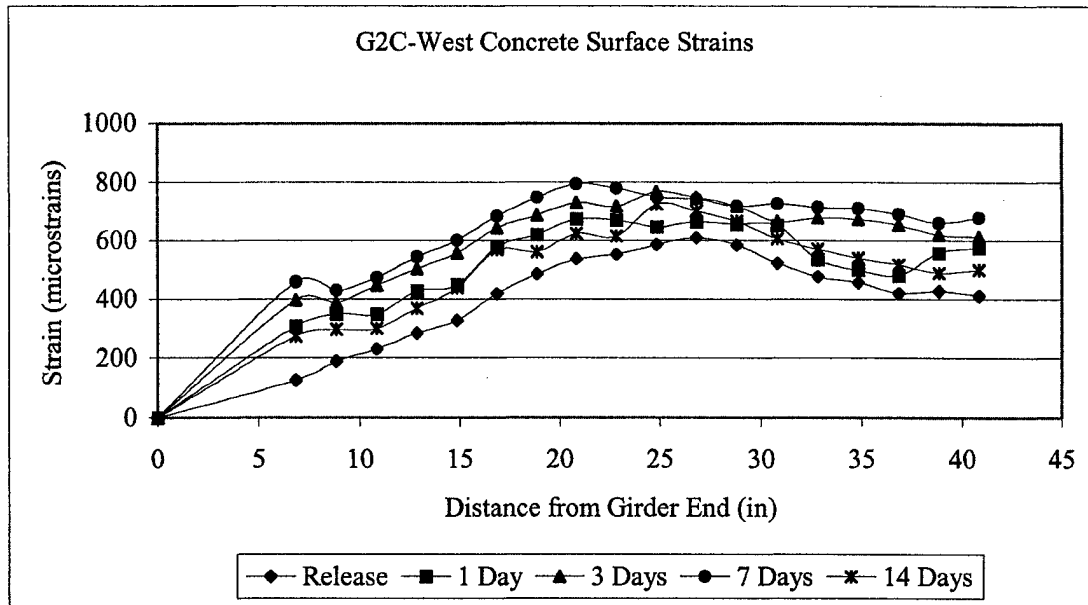
Figure I.23 Concrete Surface Strains for G2C-West
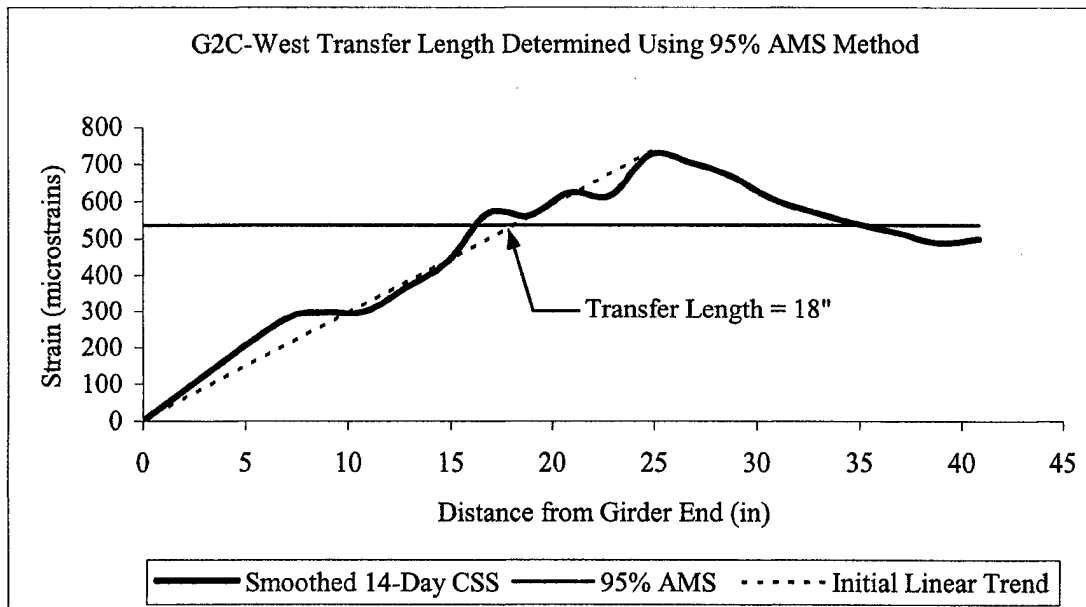
Figure I.24 14-Day Transfer Length Determined for G2C-West

476

APPENDIX J

TRANSFER LENGTH DATA FROM OTHER RESEARCHERS

This Appendix contains transfer length data from this project and other researchers. All transfer length data is based on the use of 0.6-inch prestressing strand. The data were used to evaluate the usefulness of the transfer length equations based on initial concrete compressive strength developed in Section 9.9.

Table J.1 Transfer Length Data from Researchers Using 0.6" Strand

Specimen #	Name of Researcher	Concrete (LWC or NWC)	Specimen Cross Section	# Strands	Transfer Length (in)	f_{ci}' (psi)
G1A-E	Meyer	LWC	AASHTO Type II	8	19.50	7465
G1A-W	Meyer	LWC	AASHTO Type II	8	18.75	7465
G1B-E	Meyer	LWC	AASHTO Type II	8	25.00	7465
G1B-W	Meyer	LWC	AASHTO Type II	8	18.75	7465
G1C-E	Meyer	LWC	AASHTO Type II	8	28.00	6315
G1C-W	Meyer	LWC	AASHTO Type II	8	21.50	6315
G2A-E	Meyer	LWC	AASHTO Type II	8	17.50	9640
G2A-W	Meyer	LWC	AASHTO Type II	8	13.25	9640
G2B-E	Meyer	LWC	AASHTO Type II	8	13.00	9640
G2B-W	Meyer	LWC	AASHTO Type II	8	13.00	9640
G2C-E	Meyer	LWC	AASHTO Type II	8	19.00	8261
G2C-W	Meyer	LWC	AASHTO Type II	8	18.00	8261
FA4601N	Russell	NWC	AASHTO Type	4	24.00	4900
FA4601S	Russell	NWC	AASHTO Type	4	44.00	4900
FA4602N	Russell	NWC	AASHTO Type	4	33.00	4450
FA4602S	Russell	NWC	AASHTO Type	4	34.00	4450
FA4603N	Russell	NWC	AASHTO Type	4	32.00	4450
FA4603S	Russell	NWC	AASHTO Type	4	33.00	4450
FA4604N	Russell	NWC	AASHTO Type	4	25.00	4900
FA4604S	Russell	NWC	AASHTO Type	4	30.00	4900
FA4605N	Russell	NWC	AASHTO Type	4	33.00	4700
FA4605S	Russell	NWC	AASHTO Type	4	37.00	4700
FA4606N	Russell	NWC	AASHTO Type	4	33.00	4700
FA4606S	Russell	NWC	AASHTO Type	4	30.00	4700
6-1-EXT	Deatherage	NWC	AASHTO Type I	7	25.00	4100
6-1-INT	Deatherage	NWC	AASHTO Type I	7	27.00	4100
6-2-EXT	Deatherage	NWC	AASHTO Type I	7	30.00	4280
6-2-INT	Deatherage	NWC	AASHTO Type I	7	24.00	4280
6-3-EXT	Deatherage	NWC	AASHTO Type I	7	23.00	5230
6-3-INT	Deatherage	NWC	AASHTO Type I	7	21.00	5230
6-4-EXT	Deatherage	NWC	AASHTO Type I	7	22.00	5450
6-4-INT	Deatherage	NWC	AASHTO Type I	7	23.00	5450
LOB-A	Barnes	NWC	AASHTO Type I	6	26.00	4240
LOB-B	Barnes	NWC	AASHTO Type I	6	25.00	4240
LOB-C	Barnes	NWC	AASHTO Type I	6	30.00	4240
LOB-D	Barnes	NWC	AASHTO Type I	6	36.00	4240
MOB-A	Barnes	NWC	AASHTO Type I	8	22.00	6610
MOB-B	Barnes	NWC	AASHTO Type I	8	19.00	6610
MOB-C	Barnes	NWC	AASHTO Type I	8	18.00	6610
MOB-D	Barnes	NWC	AASHTO Type I	8	16.00	6610
HOB-A	Barnes	NWC	AASHTO Type I	8	15.00	11030
HOB-B	Barnes	NWC	AASHTO Type I	8	16.00	11030
HOB-C	Barnes	NWC	AASHTO Type I	8	16.00	11030
HOB-D	Barnes	NWC	AASHTO Type I	8	17.00	11030

Table J.1 Transfer Length Data from Researchers Using 0.6" Strand (Cont.)

Specimen #	Name of Researcher	Concrete (LWC or NWC)	Specimen Cross Section	# Strands	Transfer Length (in)	f_{ci}' (psi)
G2A-S	Reutlinger	NWC	AASHTO Type II	8	15.40	14989
G2A-N	Reutlinger	NWC	AASHTO Type II	8	17.00	12379
G2B-S	Reutlinger	NWC	AASHTO Type II	8	17.90	12379
G2B-N	Reutlinger	NWC	AASHTO Type II	8	17.80	11721
G4A-S	Reutlinger	NWC	AASHTO Type II	8	16.70	14675
G4A-N	Reutlinger	NWC	AASHTO Type II	8	13.80	14395
G4B-S	Reutlinger	NWC	AASHTO Type II	8	13.50	14395
G4B-N	Reutlinger	NWC	AASHTO Type II	8	13.40	14610
KLM1-C	Kaar	NWC			51.50	2220
KLM1-D	Kaar	NWC			33.50	2220
KLM2-C	Kaar	NWC			52.00	2410
KLM2-D	Kaar	NWC			41.50	2410
KLM3-C	Kaar	NWC			49.00	3180
KLM3-D	Kaar	NWC			42.50	3180
KLM4-C	Kaar	NWC			36.00	4070
KLM4-D	Kaar	NWC			29.00	4070
KLM5-C	Kaar	NWC			39.50	5465
KLM5-D	Kaar	NWC			27.50	5465
Mayfield - A1	Mayfield	NWC			16.73	7120
Mayfield - A2	Mayfield	NWC			16.73	7120
Mayfield - A3	Mayfield	NWC			16.73	7120
Mayfield - A4	Mayfield	NWC			16.73	7120
Mayfield - A5	Mayfield	NWC			16.73	7120
Mayfield - A6	Mayfield	NWC			16.73	7120
Mayfield - A7	Mayfield	NWC			16.73	7120
Mayfield - B1	Mayfield	NWC			26.07	7120
Mayfield - B2	Mayfield	NWC			26.07	7120
Mayfield - B3	Mayfield	NWC			26.07	7120
Mayfield - B4	Mayfield	NWC			26.07	7120
Mayfield - B5	Mayfield	NWC			26.07	7120
Mayfield - B6	Mayfield	NWC			26.07	7120
Mayfield - B7	Mayfield	NWC			26.07	7120
Mayfield - B8	Mayfield	NWC			26.07	7120
Mayfield - C1	Mayfield	NWC			29.53	6120
Mayfield - C2	Mayfield	NWC			29.53	6120
Mayfield - C3	Mayfield	NWC			29.53	6120
Mayfield - C4	Mayfield	NWC			29.53	6120
Mayfield - C5	Mayfield	NWC			29.53	6120
Mayfield - C6	Mayfield	NWC			29.53	6120
Mayfield - C7	Mayfield	NWC			29.53	6120
Mayfield - C8	Mayfield	NWC			29.53	6120
Mayfield - C9	Mayfield	NWC			29.53	6120

Table J.1 Transfer Length Data from Researchers Using 0.6" Strand (Cont.)

Specimen #	Name of Researcher	Concrete (LWC or NWC)	Specimen Cross Section	# Strands	Transfer Length (in)	f_{ci}' (psi)
16/31-1865 A	Mitchell	NWC	Rectangular	1	32.90	3000
16/31-1500 A	Mitchell	NWC	Rectangular	1	35.90	3000
16/31-1500 B	Mitchell	NWC	Rectangular	1	38.20	3000
16/65-1150 A	Mitchell	NWC	Rectangular	1	20.80	6950
16/65-1150 B	Mitchell	NWC	Rectangular	1	16.80	6950
16/65-725-A	Mitchell	NWC	Rectangular	1	21.10	6950
16/65-725-B	Mitchell	NWC	Rectangular	1	17.10	6950
16/89-675B	Mitchell	NWC	Rectangular	1	16.10	7310
16/89-975B	Mitchell	NWC	Rectangular	1	13.60	7310
FC160-12 N	Russell	NWC	Rectangular	1	48.00	3853
FC160-12 S	Russell	NWC	Rectangular	1	46.00	3853
FC360-1 N	Russell	NWC	Rectangular	3	42.00	4201
FC360-1 S	Russell	NWC	Rectangular	3	41.00	4201
FC360-2 N	Russell	NWC	Rectangular	3	37.00	4201
FC360-2 N	Russell	NWC	Rectangular	3	48.00	4201
FCT360-3 N	Russell	NWC	Rectangular	3	40.00	4201
FCT360-3 S	Russell	NWC	Rectangular	3	46.00	4201
FCT360-4 N	Russell	NWC	Rectangular	3	51.00	4792
FCT360-4 S	Russell	NWC	Rectangular	3	42.00	4792
FCT362-11 N	Russell	NWC	Rectangular	3	46.00	4759
FCT362-11 S	Russell	NWC	Rectangular	3	44.00	4759
FCT362-12 N	Russell	NWC	Rectangular	3	44.00	4759
FCT362-12 S	Russell	NWC	Rectangular	3	42.00	4759
FCT362-13 N	Russell	NWC	Rectangular	3	42.00	4759
FCT362-13 S	Russell	NWC	Rectangular	3	40.00	4759
FC560-1 S	Russell	NWC	Rectangular	5	46.00	4481
FC560-1 N	Russell	NWC	Rectangular	5	37.00	4481
FCT560-2 S	Russell	NWC	Rectangular	5	48.00	4481
FCT560-2 N	Russell	NWC	Rectangular	5	47.00	4481
FC560-3 S	Russell	NWC	Rectangular	5	48.00	4481
FC560-3 N	Russell	NWC	Rectangular	5	52.00	4481

APPENDIX K

GIRDER "AS-BUILT" ANALYSIS SPREADSHEET

Appendix K contains the individual pages from the Girder "AS-BUILT" Analysis

Spreadsheet. This sheet was used to process the DAQ output from the 18 girder tests

based on "as-built" girder characteristics. The entire set of worksheet pages is provided

from girder test G1C-W. A similar series of worksheets was prepared for each of the 18

girder tests. Listed below are the individual worksheets within the overall spreadsheet

and a brief description of the worksheet's function.

Table K.1 – DAQ Output – A sample of the raw data output from the data acquisition

system. Only a small percentage of the total number of DAQ lines is shown.

Table K.2 – Load, Shear, Moment, Deflection, Strain and Curvature Values – The

values are calculated based on DAQ and other user input values regarding the test. Only

a small percentage of the total number of lines in this worksheet is shown.

Table K.3 – Calculated Principal Strains, Angles and Maximum Shear Strain – The

values are calculated based on DAQ and other user input values regarding the test. Only

a small percentage of the total number of lines in this worksheet is shown.

Table K.4 – Input Values for Girder Test – The user enters values in the shaded cells

for LVDT gage length, test configuration and prestressing values.

Table K.5 – Section Properties for Girder "AS-BUILT" – The user enters all values in the table. The shaded values are the ones that change between tests.

Table K.6 – Support Conditions, Reactions, Max Load and Moment Furnished – The user enters values in the shaded areas. All other values are calculated automatically based on input and values from other worksheets. This worksheet provides a visual depiction of the support conditions to verify their location.

Table K.7 – AASHTO Loss Calculations – This worksheet calculates losses using the AASHTO[152] 1996 Standard Specifications. The user enters values in the shaded cells. Iteration may be required to determine the elastic shortening loss.

Table K.8 – Girder Shear Capacity by 1996 AASHTO[40] Standard Procedure – This worksheet calculates girder shear capacity at the tenth points of the shear span based on the 1996 AASHTO Standard Specification. The user enters the stirrup spacing in the shaded box.

Table K.9 – Deflection Calculations – This worksheet calculates predicted deflections at cracking and at ultimate condition.

Table K.10 – Variable Angle Truss Model – This worksheet determines the shear capacity of the girder, the angle of the compression strut, forces in the prestressing strand and bond stress using the variable angle truss model.

Figure K.1 – Force in Prestressing Strand vs. Distance from Girder End

Figure K.2 – Bond Stress of Prestressing Strand vs. Distance from Girder End

Table K.11 – Theoretical Moment-Curvature Stages 1-3 – This worksheet calculates moment and curvature for the elastic stages.

Table K.12 - Theoretical Moment-Curvature Stages 4-6 – This worksheet calculates moment and curvature for the stages after cracking; top of deck strain equal to 0.001, 0.002, 0.003 in/in. The user must enter values in the shaded boxes until the compression force and tension force are equal. ($F_{se} = F_c$)

Figure K.3 – Moment-Curvature Plot

Table K.13 – Girder Shear Capacity by 1998 AASHTO[92] LRFD Procedure – This worksheet calculates girder shear capacity at the tenth points of the shear span based on the 1998 AASHTO LRFD Specification. The user enters the values in the shaded boxes for crack angle, then the β value from the chart in the specification.

Table K.14 – Girder-Deck Interface Shear Calculations – This worksheet determines the interface shear adequacy between the girder and deck. The user enters values in the shaded boxes.

Table K.15 – Prestressing Strand Tension Curve – This worksheet provides a mathematical depiction of the stress strain curve for the prestressing strand. It is based on the actual curve received from the manufacturer.

Table K.16 – Principal Strain and Maximum Shear Strain Plots – Provides a visual depiction of the progression of principal strain angles and values as well as maximum shear strain. The user enters values for V_{crack} and the low and high values of crack angles.

Figure K.4 – Load vs. Displacement Plot

Table K.17 – Overview of Girder Test Results – This worksheet provides an overview of the most important values from the girder test. It is meant to provide a snapshot of the test output.

483

Table K.1 DAQ Output

11/02/2001 Load Cell	12:07 PM LVDT Top	LVDT Bottom	Wire Pot	LVDT 0	LVDT 45	LVDT 90
11.442372	-0.00048	-0.001137	2.465919	-0.00249	-0.002784	-0.001542
13.463793	-0.00056	-0.001176	2.461571	-0.002496	-0.00279	-0.001566
16.630684	-0.000659	-0.00129	2.455239	-0.002484	-0.002856	-0.001548
27.815872	-0.000462	-0.001888	2.433496	-0.002496	-0.0031	-0.001554
35.0256	0.000148	-0.00232	2.415492	-0.002477	-0.003245	-0.001554
34.789768	0.000173	-0.00232	2.415569	-0.002484	-0.00327	-0.00156
39.236893	0.000457	-0.002524	2.410762	-0.002471	-0.003343	-0.001548
45.536983	0.001055	-0.002905	2.396878	-0.002477	-0.003495	-0.001566
48.872326	0.001227	-0.003109	2.392224	-0.002465	-0.003543	-0.001548
48.653339	0.00127	-0.003121	2.392148	-0.002496	-0.003562	-0.001554
55.509319	0.001424	-0.003541	2.377653	-0.002459	-0.00372	-0.001573
61.371441	0.002059	-0.003808	2.368269	-0.002453	-0.003841	-0.001517
71.697525	0.002632	-0.004393	2.349273	-0.002399	-0.004096	-0.001542
75.369766	0.003138	-0.004635	2.340576	-0.002405	-0.004175	-0.001554
78.907257	0.003428	-0.0048	2.332566	-0.002393	-0.004248	-0.001535
83.1017	0.003797	-0.005105	2.326692	-0.002375	-0.004364	-0.001542
82.832176	0.003841	-0.005105	2.326615	-0.002381	-0.004364	-0.001548
82.663727	0.003834	-0.005131	2.326615	-0.002363	-0.004364	-0.001535
86.20121	0.004118	-0.005334	2.321809	-0.002357	-0.004431	-0.001529
89.233345	0.004291	-0.005474	2.313188	-0.002357	-0.004491	-0.00156
92.753983	0.004475	-0.005652	2.308458	-0.00232	-0.004577	-0.001548
92.551834	0.004728	-0.00569	2.308382	-0.002332	-0.004583	-0.001542
92.383385	0.004549	-0.005652	2.308382	-0.002314	-0.004577	-0.001554
92.248627	0.004697	-0.005716	2.308458	-0.002332	-0.004589	-0.001554
92.181244	0.004636	-0.005678	2.308535	-0.00235	-0.004589	-0.001542
92.063324	0.004697	-0.005703	2.308306	-0.002338	-0.004577	-0.001542
91.945412	0.004586	-0.005716	2.308229	-0.002332	-0.004589	-0.001554
91.878029	0.00463	-0.00569	2.308382	-0.002326	-0.004577	-0.00156

Table K.2 Calculated Load, Shear, Moment, Strain and Curvature Values

Data Point #	Applied Load (Kips)	Applied Shear (Kips)	Total Moment (ft-kips)	Top LVDT (Inches) Compression ε = (−)	Top Strain (m-strain) Compression ε = (−)	Bot LVDT (Inches) Tension ε = (+)	Bot Strain (m-strain) Tension ε = (+)	Vertical Deflection (Inches)	Neutral Axis Location (In from Bot)	Top of Slab (+) = Comp (in/in)	At Level of Bot Strands (in/in)	Total Strand Strain (in/in)	Phi (rad/in)
0	0.0	0.0	67.2	0.000000	0.00	0.000000	0.00	0.000000	NA	0.00	0.00	0.00505	0.000000
1	2.0	1.7	79.1	-0.000080	3.33	-0.000039	1.63	0.004348	17.38	0.00000	0.00000	0.00505	0.000000
2	5.2	4.3	97.8	-0.000179	7.46	-0.000153	6.38	0.010680	23.22	-0.00001	0.00001	0.00506	0.000000
3	16.4	13.6	163.6	0.000018	-0.75	-0.000751	31.29	0.032423	45.85	0.00000	0.00003	0.00508	0.000001
4	23.6	19.6	206.1	0.000628	-26.17	-0.001183	49.29	0.050427	31.66	0.00003	0.00005	0.00510	0.000002
5	23.3	19.4	204.7	0.000653	-27.21	-0.001183	49.29	0.050350	31.27	0.00003	0.00005	0.00510	0.000002
6	27.8	23.1	230.9	0.000937	-39.04	-0.001387	57.79	0.055157	29.19	0.00004	0.00006	0.00511	0.000002
7	34.1	28.3	268.0	0.001535	-63.96	-0.001768	73.67	0.069041	26.49	0.00007	0.00007	0.00513	0.000003
8	37.4	31.1	287.6	0.001707	-71.13	-0.001972	82.17	0.073695	26.52	0.00007	0.00008	0.00514	0.000003
9	37.2	30.9	286.3	0.001750	-72.92	-0.001984	82.67	0.073771	26.31	0.00008	0.00008	0.00514	0.000004
10	44.1	36.6	326.7	0.001904	-79.33	-0.002404	100.17	0.088266	27.48	0.00008	0.00010	0.00515	0.000004
11	49.9	41.5	361.2	0.002539	-105.79	-0.002671	111.29	0.097650	25.49	0.00011	0.00011	0.00516	0.000005
12	60.3	50.1	422.0	0.003112	-129.67	-0.003256	135.67	0.116646	25.43	0.00014	0.00014	0.00519	0.000006
13	63.9	53.1	443.7	0.003618	-150.75	-0.003498	145.75	0.125343	24.57	0.00016	0.00015	0.00520	0.000007
14	67.5	56.1	464.5	0.003908	-162.83	-0.003663	152.63	0.133353	24.23	0.00017	0.00015	0.00521	0.000007
15	71.7	59.6	489.2	0.004277	-178.21	-0.003968	165.33	0.139227	24.12	0.00019	0.00017	0.00522	0.000008
16	71.4	59.3	487.6	0.004321	-180.04	-0.003968	165.33	0.139304	24.00	0.00019	0.00017	0.00522	0.000008
17	71.2	59.2	486.6	0.004314	-179.75	-0.003994	166.42	0.139304	24.09	0.00019	0.00017	0.00522	0.000008
18	74.8	62.2	507.4	0.004598	-191.58	-0.004197	174.88	0.144110	23.94	0.00020	0.00017	0.00523	0.000008
19	77.8	64.7	525.3	0.004771	-198.79	-0.004337	180.71	0.152731	23.89	0.00021	0.00018	0.00523	0.000009
20	81.3	67.6	546.0	0.004955	-206.46	-0.004515	188.13	0.157461	23.92	0.00022	0.00019	0.00524	0.000009
21	81.1	67.4	544.8	0.005208	-217.00	-0.004553	189.71	0.157537	23.47	0.00023	0.00019	0.00524	0.000009
22	80.9	67.3	543.8	0.005029	-209.54	-0.004515	188.13	0.157537	23.76	0.00022	0.00019	0.00524	0.000009
23	80.8	67.2	543.1	0.005177	-215.71	-0.004579	190.79	0.157461	23.59	0.00022	0.00019	0.00524	0.000009
24	80.7	67.1	542.7	0.005116	-213.17	-0.004541	189.21	0.157384	23.63	0.00022	0.00019	0.00524	0.000009
25	80.6	67.0	542.0	0.005177	-215.71	-0.004566	190.25	0.157613	23.56	0.00022	0.00019	0.00524	0.000009
26	80.5	66.9	541.3	0.005066	-211.08	-0.004579	190.79	0.157690	23.83	0.00022	0.00019	0.00524	0.000009
27	80.4	66.9	540.9	0.005110	-212.92	-0.004553	189.71	0.157537	23.67	0.00022	0.00019	0.00524	0.000009
28	80.4	66.8	540.4	0.005060	-210.83	-0.004528	188.67	0.157384	23.72	0.00022	0.00019	0.00524	0.000009
29	80.3	66.7	540.0	0.005110	-212.92	-0.004528	188.67	0.157461	23.61	0.00022	0.00019	0.00524	0.000009
30	80.1	66.6	539.2	0.005079	-211.63	-0.004528	188.67	0.157613	23.68	0.00022	0.00019	0.00524	0.000009
31	80.1	66.6	538.9	0.005227	-217.79	-0.004503	187.63	0.157613	23.31	0.00023	0.00019	0.00524	0.000009
32	80.1	66.6	538.7	0.005171	-215.46	-0.004528	188.67	0.157461	23.48	0.00022	0.00019	0.00524	0.000009
33	80.0	66.5	538.3	0.005060	-210.83	-0.004528	188.67	0.157537	23.72	0.00022	0.00019	0.00524	0.000009
34	79.9	66.4	537.9	0.005060	-210.83	-0.004464	186.00	0.157537	23.56	0.00022	0.00019	0.00524	0.000009

Table K.3 Calculated Principal Strains, Angles and Maximum Shear Strain

Data Point	Load	Shear	LVDT 0	LVDT 45	LVDT 90	Shear Zone Strain 45 Compression ε=(-)	Strain XX Compression ε=(-)	Strain YY Tension ε=(+)	Strain XY ε=(+)	θp	Principal Strains Tension ε=(+) ε₁	θp1	Comp ε=(-) ε₂	θp2	γmax
#	(Kips)	(Kips)	(Inches)	(Inches)	(Inches)	(m-strain)	(m-strain)	(m-strain)	(m-rads)	(degrees)	(m-strain)	(deg)	(m-strain)	(deg)	(m-rads)
0	0.0	0.0	0.000000	0.000000	0.000000	0.00	-236.42	0.00	236.42	NA	48.96	NA	-285.39	NA	334.35
1	2.0	1.7	-0.000006	-0.000006	-0.000024	0.37	-235.86	2.26	232.86	-22.18	49.73	67.82	-283.33	-22.18	333.05
2	5.2	4.3	0.000006	-0.000072	-0.000006	4.43	-236.99	0.56	227.56	-21.88	46.27	68.12	-282.69	-21.88	328.96
3	16.4	13.6	-0.000006	-0.000316	-0.000012	19.45	-235.86	1.13	195.84	-19.78	36.35	70.22	-271.08	-19.78	307.43
4	23.6	19.6	0.000013	-0.000461	-0.000012	28.37	-237.65	1.13	179.78	-18.49	31.19	71.51	-267.70	-18.49	298.89
5	23.3	19.4	0.000006	-0.000486	-0.000018	29.91	-236.99	1.69	175.48	-18.16	30.48	71.84	-265.77	-18.16	296.25
6	27.8	23.1	0.000019	-0.000559	-0.000006	34.40	-238.21	0.56	168.85	-17.63	27.40	72.37	-265.05	-17.63	292.44
7	34.1	28.3	0.000013	-0.000711	-0.000024	43.75	-237.65	2.26	147.88	-15.83	23.22	74.17	-258.61	-15.83	281.82
8	37.4	31.1	0.000025	-0.000759	-0.000006	46.71	-238.78	0.56	144.80	-15.59	20.76	74.41	-258.97	-15.59	279.73
9	37.2	30.9	-0.000006	-0.000778	-0.000012	47.88	-235.86	1.13	138.98	-15.19	20.00	74.81	-254.73	-15.19	274.73
10	44.1	36.6	0.000031	-0.000936	-0.000031	57.60	-239.34	2.92	121.22	-13.29	17.24	76.71	-253.66	-13.29	270.90
11	49.9	41.5	0.000037	-0.001057	0.000025	65.05	-239.91	-2.35	112.17	-12.64	10.22	77.36	-252.48	-12.64	262.70
12	60.3	50.1	0.000091	-0.001312	0.000000	80.74	-244.99	0.00	83.51	-9.41	6.92	80.59	-251.91	-9.41	258.83
13	63.9	53.1	0.000085	-0.001391	-0.000012	85.60	-244.42	1.13	72.09	-8.18	6.31	81.82	-249.61	-8.18	255.92
14	67.5	56.1	0.000097	-0.001464	0.000007	90.09	-245.55	-0.66	66.03	-7.54	3.71	82.46	-249.93	-7.54	253.64
15	71.7	59.6	0.000115	-0.001580	0.000000	97.23	-247.25	0.00	52.79	-6.03	2.79	83.97	-250.03	-6.03	252.82
16	71.4	59.3	0.000109	-0.001580	-0.000006	97.23	-246.68	0.56	51.66	-5.90	3.23	84.10	-249.35	-5.90	252.59
17	71.2	59.2	0.000127	-0.001580	0.000007	97.23	-248.38	-0.66	54.57	-6.21	2.31	83.79	-251.35	-6.21	253.66
18	74.8	62.2	0.000133	-0.001647	0.000013	101.35	-248.94	-1.22	47.46	-5.42	1.03	84.58	-251.19	-5.42	252.22
19	77.8	64.7	0.000133	-0.001707	-0.000018	105.05	-248.94	1.69	37.16	-4.22	3.06	85.78	-250.31	-4.22	253.37
20	81.3	67.6	0.000170	-0.001793	-0.000006	110.34	-252.42	0.56	31.18	-3.51	1.52	86.49	-253.38	-3.51	254.90
21	81.1	67.4	0.000158	-0.001799	0.000000	110.71	-251.29	0.00	29.88	-3.39	0.89	86.61	-252.18	-3.39	253.06
22	80.9	67.3	0.000176	-0.001793	-0.000012	110.34	-252.99	1.13	31.18	-3.50	2.08	86.50	-253.94	-3.50	256.02
23	80.8	67.2	0.000158	-0.001805	-0.000012	111.08	-251.29	1.13	28.01	-3.17	1.90	86.83	-252.07	-3.17	253.97
24	80.7	67.1	0.000140	-0.001805	0.000000	111.08	-249.60	0.00	27.45	-3.14	0.75	86.86	-250.35	-3.14	251.10
25	80.6	67.0	0.000152	-0.001793	0.000000	110.34	-250.73	0.00	30.05	-3.42	0.90	86.58	-251.63	-3.42	252.52
26	80.5	66.9	0.000158	-0.001805	-0.000012	111.08	-251.29	1.13	28.01	-3.17	1.90	86.83	-252.07	-3.17	253.97
27	80.4	66.9	0.000164	-0.001793	-0.000018	110.34	-251.86	1.69	29.49	-3.32	2.55	86.68	-252.71	-3.32	255.26
28	80.4	66.8	0.000170	-0.001786	-0.000012	109.91	-252.42	1.13	31.48	-3.54	2.10	86.46	-253.40	-3.54	255.50
29	80.3	66.7	0.000158	-0.001793	0.000025	110.34	-251.29	-2.35	32.97	-3.77	-1.27	86.23	-252.38	-3.77	251.12
30	80.1	66.6	0.000164	-0.001786	-0.000006	109.91	-251.86	0.56	31.48	-3.55	1.54	86.45	-252.84	-3.55	254.38
31	80.1	66.6	0.000158	-0.001805	-0.000006	111.08	-251.29	0.56	28.58	-3.24	1.37	86.76	-252.10	-3.24	253.48
32	80.1	66.6	0.000164	-0.001768	0.000000	108.80	-251.86	0.00	34.26	-3.87	1.16	86.13	-253.02	-3.87	254.18
33	80.0	66.5	0.000146	-0.001786	0.000000	109.91	-250.17	0.00	30.35	-3.46	0.92	86.54	-251.08	-3.46	252.00
34	79.9	66.4	0.000146	-0.001786	-0.000012	109.91	-250.17	1.13	29.22	-3.32	1.98	86.68	-251.01	-3.32	252.99

Table K.4 Input Values for Girder Test

G1C-W	Girder Test Information		
Test Configuration #	4	Date	02-Nov-01
Stirrup Density	Single		

Enter values in shaded fields and adjust limits of functions to include all data points in DAQ file.

LVDT 0 Length	10762.5	Inches
LVDT 45 Length	15250	Inches
LVDT 90 Length	10762.5	Inches

Top LVDT

Top LVDT Length	21000	Inches
Top Edge Distance	1500	Inches

Actual Strand Prestressing Values (ksi)		
Jacking Stress	f_{pt}	170.01
Stress After Release	f_{si}	162.16
Stress at 14 Days	f_{se}	153.65
Strain at Test ($\mu\varepsilon$)	ε_{se}	5053
Stress At Testing	f_{se}	147.61
Actual Girder Prestressing Values		
Initial X-X Stress (ksi)	$f_{pc\,INIT}$	0.87
Initial X-X Strain (me)	ε_{cipx}	2.36E-04

Initial Cracking Load	P_{cr}	1833.00	Kips
Cracking Moment	M_{cr}	1144.85	Ft-Kips
Cracking Deflection	δ_{cr}	0.41	Inches
Max Applied Load	P_{max}	299.04	Kips
Nominal Moment	M_n	1828.17	Ft-Kips
Max Deflection	δ_{max}	2.27	Inches
Max Deck Strain	ε_{cu}	0.0036	in/in
Max Bot Strand Stm	ε_{ps}	1.3960	Percent
Max Bot Strand Force	F_{ps}	57.72	Kips

Bot LVDT

Bottom LVDT Length	21000	Inches
Bot Edge Distance	1500	Inches

Measured Transfer Length	27.5	Inches
Actual Development Length	90	Inches

The M_{cr} and M_n values include the M_{DL} value.

0

45

90

Table K.5 Section Properties for "AS BUILT" Prestressed Girder Analysis

G1C-W — Section Properties for "AS BUILT" Prestressed Girder Analysis

Deck Variables

Description	Symbol	Value	Units
Deck Thickness	t_d	[illegible]	IN
Deck Width	W_f	[illegible]	IN
Concrete Actual Strength	f'_c	[illegible]	PSI
Concrete Weight	W_c	[illegible]	PCF

Beam Cross Section Variables

Description	Symbol	Value	Units
Girder Type		2	1-5,BT
Girder Top Flange Width		12	IN
Concrete Strength at Release	f'_{ci}	[illegible]	PSI
Concrete Actual Strength	f'_c	[illegible]	PSI
Concrete Equilibrium Weight	W_c	[illegible]	PCF
LWC Reduction Factor	λ	0.85	None
Strand Diameter	d_b	0.6	IN
Strand C/S Area	A_{st}	0.2183	IN^2
Strand Ultimate Strength	f_{pu}	283.25	KSI
Strand Yield as % of Ultimate		0.9	None
Strand Modulus of Elasticity	E_{ps}	29000	KSI
Stirrup Size		4	#
Stirrup Yield Strength	f_y	62	KSI
Distance from End to COB	XDIST	6.00	IN
Tension Strength Factor	a	7.50	
Top of Beam to Top Strands	TCL	2.50	IN
Bottom of Beam to Bottom Strands	BCL	3.00	IN
Strand Spacing	SPAC	2.00	IN

Miscellaneous Variables Normally Constant

Description	Symbol	Value	Units
Steel Weight Allowance / Cubic Ft		3.0	PCF
Prestress stress for l_d calculation	f_{ps}	266	KSI
Shear Strength Reduction Factor	Φ_s	1.00	None
Flexural Strength Reduction Factor	Φ_f	1.00	None

Elasticity Modulus Values

Description	Symbol	Value	Units
Deck Mod. of Elast. at Testing (Actual)	E_{cd}	3.35E+06	PSI
Beam Mod. Of Elast. At Testing (Est)	E_{cg}	3.69E+06	PSI
Modular Ratio (E_{cd}/E_{cb})	η	0.907	None

Non-Composite Beam Properties

Description	Symbol	Value	Units
Moment of Inertia	I_{nc}	50979	IN^4
Distance from Centroid to Top of Beam	Y_{top}	20.17	IN
Distance from Centroid to Bot. of Beam	Y_{bot}	15.83	IN
Section Modulus (Top)	S_{top}	2527.47	IN^3
Section Modulus (Bot)	S_{bot}	3220.40	IN^3
Cross Sectional Area	A_{bm}	369	IN^2
Weight per Foot (Concrete & Steel)	W_D	0.307	K/FT
Web Thickness	WS	6	IN
Height of Beam	DB	36	IN

Composite Beam Properties

Description	Symbol	Value	Units
Moment of Inertia	I_c	144285.39	IN^4
Distance from Centroid to Top of Beam	Y_{top}	10.74	IN
Distance from Centroid to Bot. of Beam	Y_{bot}	25.26	IN
Section Modulus (Bot)	S_{bot}	5711.81	IN^3
Cross Sectional Area	A_{bm}	577.68	IN^2
Weight per Foot (Concrete & Steel)	W_D	0.5435	K/FT
First Moment of Deck About Centroid	QS	3480.00	IN^3
Overall Depth of Composite Beam	H	47.875	IN

Miscellaneous Properties

Description	Symbol	Value	Units
Stirrup Area	A_v	0.4	IN^2
Depth to Prestressing Steel	d_p	38.78	IN
Ratio of Prestressed Reinforcement	p*	0.0029	None
Strand Yield to Ultimate Factor	γ_p	0.28	None
Ratio of a/c (Based on Beam Concrete)	β_1	0.65	None

Strand Data (No Drape)

Ref. (#)	Dist. (IN)	Nbr (#)	% f_{pu} (%)	F_{ps} (KIP)	F_{ps}d (KIP-IN)
18	TOP 33.5	2	0.63	78.20	2619.7
17		0	0.00	0.00	0.0
16		0	0.00	0.00	0.0
15	31.0	0	0.00	0.00	0.0
14	29.0	0	0.00	0.00	0.0
13	27.0	0	0.00	0.00	0.0
12	25.0	0	0.00	0.00	0.0
11	23.0	0	0.00	0.00	0.0
10	21.0	0	0.00	0.00	0.0
9	19.0	0	0.00	0.00	0.0
8	17.0	0	0.00	0.00	0.0
7	15.0	0	0.00	0.00	0.0
6	13.0	0	0.00	0.00	0.0
5	11.0	0	0.00	0.00	0.0
4	9.0	0	0.00	0.00	0.0
3	7.0	0	0.00	0.00	0.0
2	5.0	0	0.00	0.00	0.0
1	3.0	8	0.63	312.80	938.4

Eccentricity from NC Centroid

Distance	-6.73	IN

Development Length (Inches)

AASHTO	100.56	Actual	91.00
COB Dist.	94.56	COB	85.00

Transfer Length (Inches)

AASHTO	30.73	Actual	21.50

Table K.6 Support Conditions, Reactions, Max Load and Moment Furnished

G1C-W		Support Conditions, Applied Load (KIP) and Moment Furnished (FT-KIP)																			
REF	BRNG	0.05L	0.10L	0.15L	0.20L	0.25L	0.30L	0.35L	0.40L	0.45L	0.50L	0.55L	0.60L	0.65L	0.70L	0.75L	0.80L	0.85L	0.90L	0.95L	BRNG
FT	0.00	2.10	4.20	6.30	8.40	10.50	12.60	14.70	16.80	18.90	21.00	23.10	25.20	27.30	29.40	31.50	33.60	35.70	37.80	39.90	42.00
IN	0.00	25.20	50.40	75.60	100.80	126.00	151.20	176.40	201.60	226.80	252.00	277.20	302.40	327.60	352.80	378.00	403.20	428.40	453.60	478.80	504.00

Number of Strands Developed Assuming l_d

	BRNG	0.05L	0.10L	0.15L	0.20L	0.25L	0.30L	0.35L	0.40L	0.45L	0.50L	0.55L	0.60L	0.65L	0.70L	0.75L	0.80L	0.85L	0.90L	0.95L	BRNG
# Top	0.13	0.69	1.24	1.79	2.00	2.00	2.00	2.00	2.00	2.00	2.00	2.00	2.00	2.00	2.00	2.00	2.00	1.79	1.24	0.69	0.13
# Bot	0.53	2.74	4.96	7.17	8.00	8.00	8.00	8.00	8.00	8.00	8.00	8.00	8.00	8.00	8.00	8.00	8.00	7.17	4.96	2.74	0.53
M_r	112.7	586.2	1059.6	1533.0	1709.6	1709.6	1709.6	1709.6	1709.6	1709.6	1709.6	1709.6	1709.6	1709.6	1709.6	1709.6	1709.6	1533.0	1059.6	586.2	112.7

Max Load (KIPS): 279

SUPT: 1

DECK

BEAM

Type of Load	L Support Reaction (KIPS)	R Support Reaction (KIPS)
Dead	11.68	11.68
Point	231.87	47.04
Total	243.55	58.72

Strength Reduction for Shear Cap.	
STD,LRFD	STD
0.930	

a	Distance from left support to point load	85.0	IN	7.08	FT
L_1	Distance from left support to right support	504.0	IN	42.00	FT
L_2	Distance from left COB to left support	0.00	IN	0.00	FT
L	Overall Length of Beam (COB-COB)	504.0	IN	42.00	FT
b	Distance from point load to right support	419.0	IN	34.92	FT
L_3	Distance from right support to right COB	0.0	IN	0.00	FT
a/d	Ratio of shear distance to depth	2.36		NA	

MAX LOAD	259	KIPS	SHEAR CTRLS

M_r (Max) Calculations		
d_p	38.78	IN
p^*	0.00291	None
f^*_{su}	264.60	KSI
w_p	0.1428 $.36b_1$	0.234
Beam is Under-reinforced		
a < Deck Thickness		
a	6.51	IN
M_f	1709.6	FT-KIP

Table K.7 Prestressed Beam Loss Calculations (AASHTO-STD '96)

G1C-W — Prestressed Beam Loss Calculations (AASHTO-STD '96)

Beam Values

Description	Symbol	Value	Unit
Beam Length (COB-COB)	L	42.00	FT
Beam Cross Sectional Area	A_{bm}	369	IN²
NC Moment of Inertia	I_{nc}	50979	IN⁴
NC Section Modulus (Top)	S_{top}	2527.47	IN³
NC Section Modulus (Bot)	S_{bot}	3220.40	IN³
Strand Eccentricity from NC Centroid	e	-6.73	IN
Beam Weight / Foot (Concrete & Steel)	W_D	0.307	K/FT
Deck Weight / Foot (Concrete & Steel)	W_{SD}	0.236	K/FT

ES-Elastic Shortening (Release)

Description	Symbol	Value	Unit
Radius of Gyration	r^2	138.2	IN²
Initial Jacking Force	P_j	391.0	KIPS
Est. Jacking Force Loss	OK	▩	%
Final Jacking Force	P_i	368.7	KIPS
MAX Dead Load Moment	M_D	812.3	IN-KIPS
Stress at Steel Centroid	f_{cir}	-1.220	KSI
Modular Ratio (E_{ps}/E_{cb})	h	9.67	None
ES Losses (KSI - %)	Δ_{pES}	-11.79	-6.6%

CR-Creep (Slab Placement)

Description	Symbol	Value	Unit
Modular Ratio (E_{ps}/E_{cb})	η	7.85	None
Stress at Steel Centroid	f_{cir}	-1.220	KSI
Addl. DL Since Release	W_{SD}	0.000	K/FT
Moment due to W_{SD}	M_{SD}	0.0	IN-KIP
Stress at Steel Centroid	f_{csd}	0.000	KSI
LWC Factor		1.0	None
Creep Factor	K_{CR}	1.0	None
CR Losses (KSI - %)	Δ_{pCR}	-14.63	-8.2%

Steel Values

Description	Symbol	Value	Unit
Area of Prestressing Steel	Aps	2.183	IN²
Strand Ultimate Strength	f_{pu}	283.25	KSI
Strand Yield Strength	f_{py}	254.925	KSI
Strand Modulus of Elasticity	E_{ps}	29000	KSI
Percent Strand Ultimate at Jacking	%	0.63	None
Strand Jacking Stress	f_{pt}	179.11	KSI

R-Steel Stress Relax (Release)

Description	Symbol	Value	Unit
% Relax at Release		30%	%
Time (Jack to Release)	t_{rel}	24	HRS
R Losses (KSI - %)	Δ_{pR}	-0.83	-0.5%

R-Steel Stress Relax (Slab Placement)

Description	Symbol	Value	Unit
% Relax at Release		60%	%
Time (Release to Slab)	t_{slab}	30	DAYS
R Losses (KSI - %)	Δ_{pR}	-1.66	-0.9%

SH-Shrinkage (Slab Placement)

Description	Symbol	Value	Unit
Shrinkage Factor	K_{SH}	1.0	None
Relative Humidity	RH	70	%
SH Losses (KSI - %)	Δ_{pSH}	-6.50	-3.6%

R-Steel Stress Relax (Testing)

Description	Symbol	Value	Unit
% Relax at Release		10%	%
Time (Release to Test)	t_{test}	120	DAYS
R Losses (KSI - %)	Δ_{pR}	-0.28	-0.2%

Concrete Values

Description	Symbol	Value	Unit
Beam Concrete Design Strength	f_c'	8911	PSI
Beam Design Modulus	E_{cb}	3.69E+06	PSI
% Beam Concrete Strength at Release		71%	%
Beam Concrete Strength at Release	f_{ci}'	6315	PSI
Beam Mod. Of Elast. at Release (Act)	E_{cb}	▩	PSI

Steel Stress Relaxation Percentages-OK — AASHTO Loss Calculations and PT (KSI)

Stage	%	Loss	PT
At Release, f_{si}	-7%	-12.62	166.49
At Slab Placement, f_{se}	-20%	-35.41	143.70
At Testing, f_{se}	-20%	-35.69	143.42

Shrinkage Factors-OK — Actual Losses and PT (KSI)

Stage	%	Loss	PT
At Release, f_{si}	-9%	-17.00	162.1
At 14 Days, f_{se}	-14%	-25.46	153.7
At Testing, f_{se}	-18%	-31.50	147.6

Table K.8 Girder Shear Capacity by 1996 AASHTO[40] Standard Procedure

G1C-W		Girder Shear Capacity AASHTO STD-96 (Left of Point Load)										
	IN	L-SUPT	0.1 a	0.2 a	0.3 a	0.4 a	0.5 a	0.6 a	0.7 a	0.8 a	0.9 a	P-LOAD
Distance from Left Support (Inches)	IN	0.00	8.50	17.00	25.50	34.00	42.50	51.00	59.50	68.00	76.50	85.00
Ultimate Moment Furnished	FT-KIP	112.72	272.42	432.11	591.80	751.50	911.19	1070.88	1230.58	1390.27	1549.96	1709.64
Transferred Strands Factor		0.28	0.67	1.00	1.00	1.00	1.00	1.00	1.00	1.00	1.00	1.00
Transferred # Top Strands	#	0.56	1.35	2.00	2.00	2.00	2.00	2.00	2.00	2.00	2.00	2.00
Transferred # Bottom Strands	#	2.23	5.40	8.00	8.00	8.00	8.00	8.00	8.00	8.00	8.00	8.00
Developed Strands Factor		0.07	0.16	0.25	0.35	0.44	0.53	0.63	0.72	0.81	0.91	1.00
Developed # Top Strands	#	0.13	0.32	0.51	0.69	0.88	1.07	1.25	1.44	1.63	1.81	2.00
Developed # Bottom Strands	#	0.53	1.27	2.02	2.77	3.52	4.26	5.01	5.76	6.51	7.25	8.00
Non-composite DL Moment (BM+SL)	FT-KIP	0.00	7.95	15.62	23.02	30.15	37.01	43.60	49.91	55.95	61.71	67.21
Total DL Shear (BM+SL)	KIP	11.68	11.30	10.91	10.53	10.14	9.76	9.37	8.99	8.60	8.22	7.83
Available Moment Capacity	FT-KIP	112.72	264.47	416.49	568.78	721.34	874.18	1027.29	1180.67	1334.32	1488.25	1642.43
Ultimate Moment, M_u	FT-KIP	0.00	172.19	344.11	515.75	687.13	858.23	1029.05	1199.61	1369.89	1539.90	1709.64
Ultimate Shear, V_u	KIP	243.55	243.17	242.78	242.40	242.01	241.63	241.24	240.86	240.47	240.09	239.70
f_d	KSI	0.000	0.030	0.058	0.086	0.112	0.138	0.162	0.186	0.208	0.230	0.250
SFPF (Based on l_d)	KIPS	21.25	51.34	81.44	111.54	141.64	171.74	201.84	231.94	262.04	292.13	322.23
f_{pe}	KSI	-0.102	-0.246	-0.391	-0.535	-0.680	-0.824	-0.969	-1.113	-1.258	-1.402	-1.547
M_{CR}	FT-KIP	277.69	332.36	387.51	443.15	499.27	555.87	612.96	670.53	728.58	787.12	846.13
V_d (Flexure Shear)	KIPS	31.73	491.86	295.52	230.01	197.19	177.46	164.27	154.82	147.70	142.14	137.67
FPF (Based on l_t)	KIPS	89.92	217.32	322.23	322.23	322.23	322.23	322.23	322.23	322.23	322.23	322.23
f_{pc}	KSI	-0.132	-0.336	-0.507	-0.523	-0.539	-0.554	-0.569	-0.583	-0.596	-0.609	-0.621
V_{cw} (Web Shear)	KIPS	74.53	88.79	100.70	101.85	102.96	104.02	105.04	106.02	106.95	107.85	108.70
V_c	KIPS	31.73	88.79	100.70	101.85	102.96	104.02	105.04	106.02	106.95	107.85	108.70
V_u/ϕ	KIPS	243.55	243.17	242.78	242.40	242.01	241.63	241.24	240.86	240.47	240.09	239.70
Shear Steel Beyond Minimum Required	Y/N	YES	YES	YES	YES	YES	YES	YES	YES	YES	YES	YES
Web Crushing		CRUSH	CRUSH	OK	OK	OK	OK	OK	OK	OK	OK	OK
Required Strength of Steel, Vs	KIPS	211.82	154.38	142.08	140.55	139.06	137.61	136.21	134.84	133.52	132.24	131.01
Required Stirrup Spacing, s	IN	4.54	6.23	6.77	6.84	6.92	6.99	7.06	7.13	7.20	7.27	7.34
Actual Stirrup Spacing, s	IN	2.00										
Strength of Steel, Vs	KIPS	480.81	137.37	137.37	137.37	137.37	137.37	137.37	137.37	137.37	137.37	137.37
Total Beam Shear Strength, Vc + Vs	KIPS	512.54	226.16	238.08	239.23	240.33	241.39	242.41	243.39	244.33	245.22	246.07
Beam "AS BUILT" Shear Capacity	P/F	PASS	FAIL	FAIL	FAIL	FAIL	FAIL	PASS	PASS	PASS	PASS	PASS
Ratio of (Vc + Vs) / (Vu / φ)	NONE	2.10	0.93	0.98	0.99	0.99	1.00	1.00	1.01	1.02	1.02	1.03

491

Table K.9 Deflection Calculations

G1C-W

Member and Section Dimensions

Description	Symbol	Value	Units
Distance from Left Support to Load	a	85.001	IN
Distance from Load to Right Support	b	418.999	IN
Distance Between Supports	L_1	504	IN
Height of Beam	DB	36	IN
Deck Thickness	t_d	11.875	IN
Bottom of Beam to Bottom Strands	BCL	3.00	IN
Moment of Inertia	I_c	144285	IN^4
Beam Mod. Of Elast. At Testing (Est)	E_{cb}	3.69E+06	PSI
Web Thickness	WS	6	IN
Depth to Prestressing Steel	d_p	38.78	IN
Shear Modulus Factor (Cracking)	G Factor	▓▓▓	None
Shear Modulus Factor (Ultimate)	G Factor	▓▓▓	None
Shape Factor for Shear (I Section)	k	1	None
Length of Plastic Hinge at Point of Loading	L_{dpc}	44.88	IN

Girder Predicted Values

Description	Symbol	Value	Units
Predicted Cracking Moment	M_{cr}	970.63	FT-KIP
Dead Load Moment	M_{DL}	67.21	FT-KIP
Predicted Applied Cracking Load	P_{cr}	153.41	KIP
Predicted L Support Reaction at Cracking	R_{lcr}	127.54	KIP
Predicted R Support Reaction at Cracking	R_{rcr}	25.87	KIP
Predicted Curvature at Cracking	ϕ_{cr}	0.000013	RAD/IN

Girder Predicted Ultimate Values Using a Cracked Section Analysis

Description	Symbol	Value	Units
Maximum Experimentally Applied Load	P_{ult}	290.31	KIP
Maximum Left Support Reaction	R_l	241.35	KIP
Maximum Right Support Reaction	R_r	48.96	KIP
Predicted Curvature at Ultimate	ϕ_{ult}	0.000358	RAD/IN

Predicted Approximate Deflection Calculations

First Moment WRT Right Support

Dist From L Supt (IN)		Area of Section (RAD)		Dist Cent to R Supt (IN)		A*C (IN)
X_1	44.92	A_1	0.0002944	C_1	474.05	0.1396
X_2	62.56	A_2	0.0002313	C_2	450.26	0.1041
X_3	85.00	A_3	0.0030466	C_3	447.32	1.3628
X_4	107.44	A_4	0.0080421	C_4	430.22	3.4599
X_5	282.58	A_5	0.0080421	C_5	407.78	3.2794
X_6	504.00	A_6	0.0022959	C_6	308.99	0.7094
		A_7	0.0302401	C_7	338.18	10.2266
		A_8	0.0014512	C_8	147.61	0.2142

θ_L*L (IN)		19.4960
θ_L (RAD)		0.0387
θ_L*a (IN)		3.2881

First Moment WRT Point of Loading

Area of Section (RAD)		Dist Cent to Load (IN)		A*C (IN)
A_1	0.0002944	CP_1	55.06	0.0162
A_2	0.0002313	CP_2	31.26	0.0072
A_3	0.0030466	CP_3	28.32	0.0863
A_4	0.0080421	CP_4	11.22	0.0902
		ΔP_6		0.1999

Deflections Due to Predicted Loads at Cracking and Ultimate

Stage of Loading	Flexure	Shear	Flexure + Shear	Units
Cracking	0.241	0.03154	0.273	IN
Ultimate	3.088	0.05968	3.148	IN

492

Table K.10 Variable Angle Truss Model

G1C-W — Variable Angle Truss Model

Variables and Values

Variable	Value	Units
$V_{ult} = V_{DL}+V_{applied}$	260.29	KIPS
Shear Area, A_v	0.4	IN^2
Yield Strength of Stirrups, f_y	62	KSI
Top of Deck to Centroid of PT, d_p	38.78	IN
Maximum Depth of RSB, a	6.51	IN
f^*_{su}	264.60	KSI
Stirrup Spacing	7.00	IN
Shear Span	85.00	IN
XDIST	6.00	IN
Maximum Crack Angle	70	Deg
Minimum Crack Angle (A2.5)	25	Deg
$F_{stirrup}$	24.8	KIPS
Min 1st Stirrup Distance from Load	12.93	IN
Max Nth Stirrup Distance from Load	76.17	IN
Maximum Stirrups in Fan	9	EACH
# Stirrups Reqd for V_{ult}	11	EACH
Total Stirrups Available	11	EACH
Internal Moment Arm, jd	35.52	IN
Total Strand Force Based on f_{su}^*, f_{se}	526.54	KIPS
Nominal Strand Circumference	1.885	IN
Maximum VATM Predicted Shear	223.2	KIPS
Maximum VATM Predicted Moment	1581.0	FT-KIP
Compression Field Crack Angle θ	29.41	DEG
Compression Strut (Based on V_{ult})		
Width of Strut (jd cos θ)	30.94	IN
Compressive Force D	530.01	KIPS
Compressive Stress in Strut, f_{cd}	2.86	KSI
Lightweight Concrete Factor, l	0.85	None
Allowable Stress in Strut, A3.2	3.86	KSI
VATM IS CONSERVATIVE		

Stirrup Data

Stirrup #	Distance From Load (IN)	Stirrup Force (KIPS)	X/jd	F_{Strand} Reduction (KIPS)	F_{Strand} Remaining (KIPS)
1	15.00	24.80	0.422	10.47	516.06
2	22.00	24.80	0.619	15.36	500.70
3	29.00	24.80	0.817	20.25	480.45
4	36.00	24.80	1.014	25.14	455.32
5	43.00	24.80	1.211	30.03	425.29
6	50.00	24.80	1.408	34.91	390.38
7	57.00	24.80	1.605	39.80	350.58
8	64.00	24.80	1.802	44.69	305.89
9	71.00	24.80	1.999	49.58	256.31
10	78.00	24.80	1.774	43.99	212.32
11	85.00	24.80	1.774	43.99	168.33

Plot Data

Distance (IN)	F_{strand} (KIPS)	l_e (IN)	σ_{bond} (KSI)
85.00	526.54	91.00	0.3070
70.00	526.54	76.00	0.3675
70.00	516.06	76.00	0.3602
63.00	516.06	69.00	0.3968
63.00	500.70	69.00	0.3850
56.00	500.70	62.00	0.4284
56.00	480.45	62.00	0.4111
49.00	480.45	55.00	0.4634
49.00	455.32	55.00	0.4392
42.00	455.32	48.00	0.5032
42.00	425.29	48.00	0.4700
35.00	425.29	41.00	0.5503
35.00	390.38	41.00	0.5051
28.00	390.38	34.00	0.6091
28.00	350.58	34.00	0.5470
21.00	350.58	27.00	0.6888
21.00	305.89	27.00	0.6010
14.00	305.89	20.00	0.8114
14.00	256.31	20.00	0.6799
7.00	256.31	13.00	1.3075
7.00	212.32	13.00	1.0831
0.00	212.32	6.00	2.3467
0.00	168.33	6.00	1.8605
	168.33		

Angle minimum and maximum values and the allowable stress in the compressive strut are based on ACI318-02. Changes are in CI, June 2001, pp. 125-132. Bond stress inside 1 stirrup space from the support is based on only the bottom 8 strands. Stirrup spacing initiates at the support and moves to the load. All plot data is based on the ultimate (experimental) shear value.

493
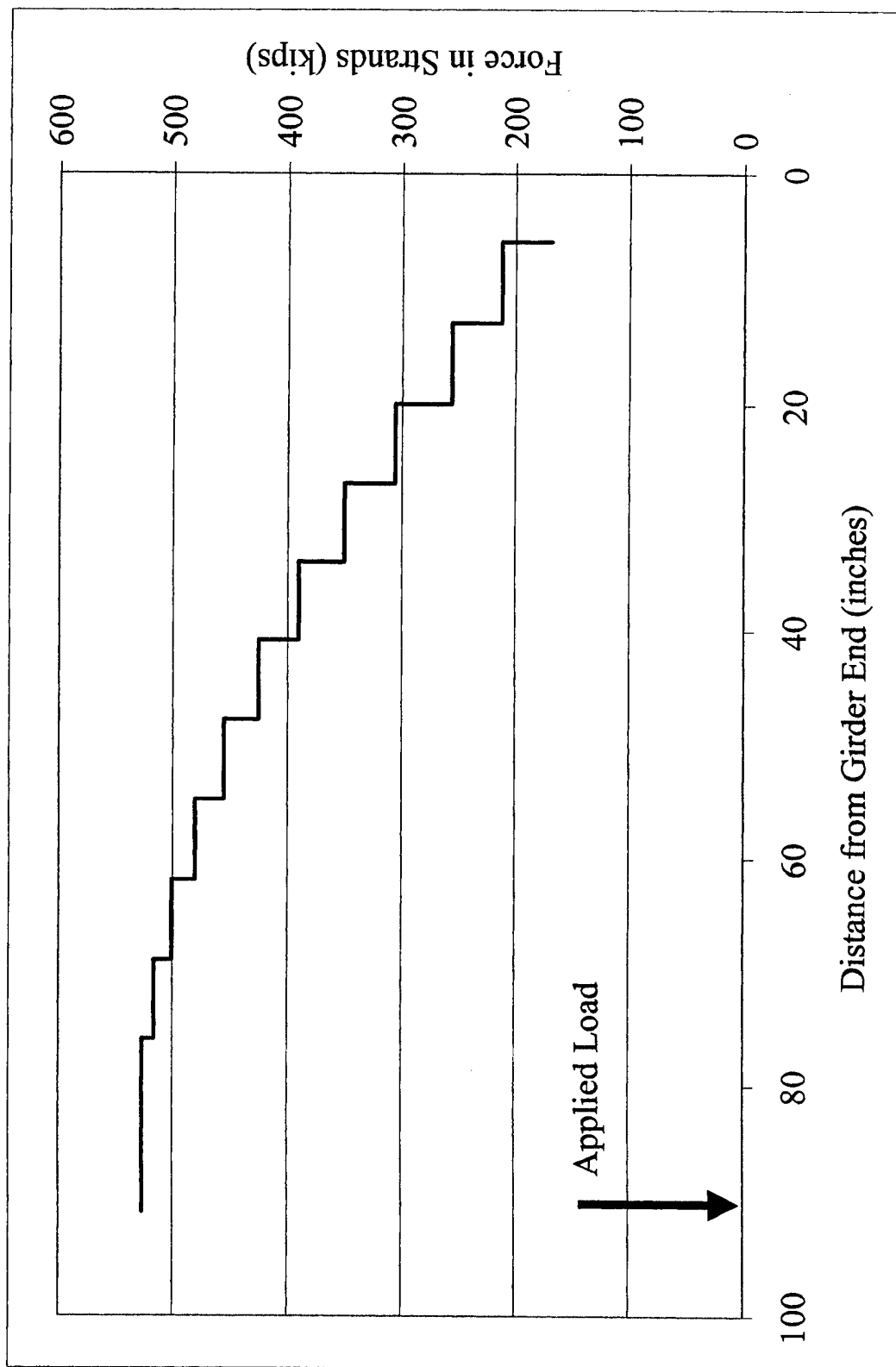
Figure K.1 Force in Prestressing Strands vs. Distance From Girder End
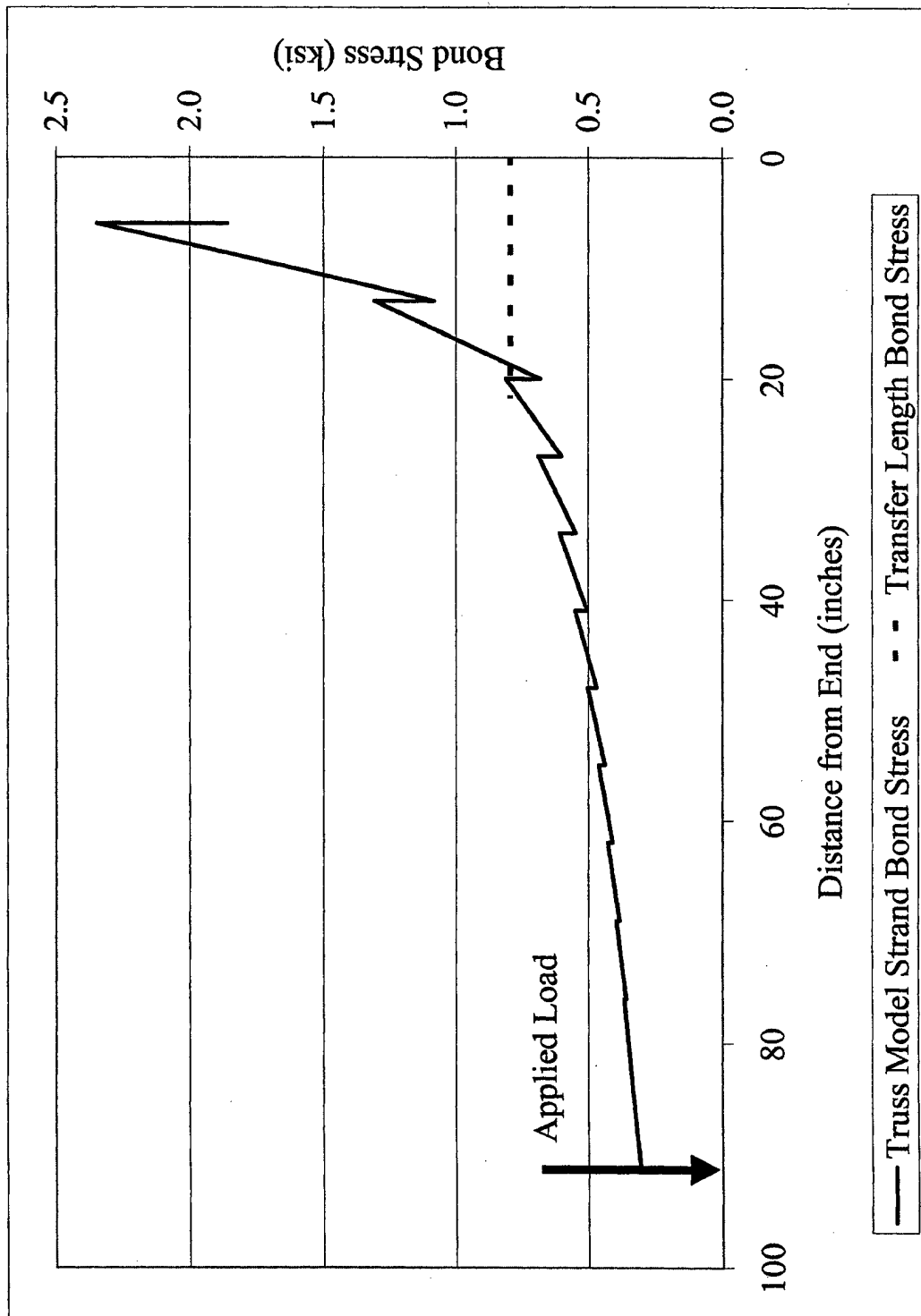
Figure K.2 Prestressing Strand Bond Stress vs. Distance From Girder End

Legend: —— Truss Model Strand Bond Stress   - - Transfer Length Bond Stress

Table K.11 Theoretical Moment-Curvature Stages 1 - 3 (Elastic Portion)

Theoretical Moment-Curvature (Elastic Portion)

G1C-W

Stage 1 - No Load

NC Moment of Inertia	I_{nc}	50979	IN^4
NC Section Modulus (Top)	S_{top-nc}	2527.47	IN^3
NC Section Modulus (Bot)	S_{bot-nc}	3220.40	IN^3
NC Girder Area	A_{nc}	369	IN^2
NC Girder Height	DB	36	IN
Ecc from NC Centroid	e	-6.73	IN
Girder E_c (Est)	E_{cg}	3.69E+06	PSI
Effective PT Force	F_{se}	322.23	KIPS
M_{DL}	M_{DL}	67.21	FT-KIP

NC Girder Stress	TOP	BOTTOM	
Axial Prestress	-0.873	-0.873	KSI
Eccentricity Prestress	0.858	-0.673	KSI
Dead Load Moment	-0.319	0.250	KSI
Total Concrete Stress	-0.334	-1.296	KSI
Total Concrete Strain	-90.5	-350.9	µε
Conc Strain at Bot Strands	ε_{ce}	-329.2	µε
Conc Stress at Bot Strands	σ_{ce}	-1.2161	KSI
Steel Strain in Bot Strands	ε_{se}	5053.0	µε
Curvature of Girder	-7.23E-06		rad/in

Stage 2 - Zero Strain in Conc at Bot Strand Level

C Moment of Inertia	I_c	144285	IN^4
C Section Modulus (Girder)	S_{top-c}	13436	IN^3
C Section Modulus (Girder)	S_{bot-c}	5712	IN^3
C Girder Area	A_c	577.68	IN^2
Deck Thickness	t_d	11.875	IN
C Centroid to NC Girder Bot	Y_{bot-c}	25.26	IN
NC Girder Top to Top Strds	TCL	2.50	IN
NC Girder Bot to Bot Strds	BCL	3.00	IN
Required Additional Moment	M_2	656.83	FT-KIP
Total Moment ($M_{DL}+M_2$)		724.04	FT-KIP

NC Girder Stress	TOP	BOTTOM	
Axial Prestress	-0.873	-0.873	KSI
Eccentricity Prestress	0.858	-0.673	KSI
Dead Load Moment	-0.319	0.250	KSI
Additional Moment M_2	-0.587	1.380	KSI
Total Concrete Stress	-0.921	0.084	KSI
Total Concrete Strain	-249	23	µε
Steel Strain in Bot Strands	ε_{s2}	5382.2	µε
Curvature of Girder	7.56E-06		rad/in

Stage 3 - Cracking on Bottom Fiber

Tension Strength Factor	a	7.5	None
LWC Reduction Factor	1	0.85	None
Concrete Actual Strength	f'_c	8911	PSI
Rupture Stress	f_r	0.602	KSI
Required Addl Stress	f_3	0.518	KSI
Required Addl Moment	M_3	246.59	FT-KIP
Total Moment ($M_{DL}+M_2+M_3$)=M_{CR}		970.63	FT-KIP

NC Girder Stress	TOP	BOTTOM	
Axial Prestress	-0.873	-0.873	KSI
Eccentricity Prestress	0.858	-0.673	KSI
Dead Load Moment	-0.319	0.250	KSI
Additional Moment M_2	-0.587	1.380	KSI
Additional Moment M_3	-0.22	0.518	KSI
Total Concrete Stress	-1.141	0.602	KSI
Total Concrete Strain	-309.0	162.9	µε
Conc Strain at Bot Strands	ε_{ce}	123.6	µε
Conc Strain on Top of Deck	ε_{cd}	-460.0	µε
Steel Strain in Bot Strands	ε_{s3}	5505.8	µε
Curvature of Girder	1.31E-05		rad/in

Table K.12 Theoretical Moment-Curvature Stages 4-6 (Cracked Portion)

| G1C-W	Theoretical Moment-Curvature (Cracked Portion)										
Stage 4 - Deck Strain =	ε_{cd}	1000.0	με	**Stage 5 - Deck Strain =**	ε_{cd}	2000.0	με	**Stage 6 - Deck Strain =**	ε_{cd}	3000	με
Conc Strain on Top of Deck	ε_{cd}	1000.0	με	Conc Strain on Top of Deck	ε_{cd}	2000.0	με	Conc Strain on Top of Deck	ε_{cd}	3000.0	με
Guess for NA Depth "c"	c		IN	Guess for NA Depth "c"	c	0.80	IN	Guess for NA Depth "c"	c		IN
Resulting Top Strand Strain	ε_{set}	5011.3	με	Resulting Top Strand Strain	ε_{set}	6216.4	με	Resulting Top Strand Strain	ε_{set}	7698.8	με
Resulting Top Strand Stress	σ_{set}	146.39	KSI	Resulting Top Strand Stress	σ_{set}	181.59	KSI	Resulting Top Strand Stress	σ_{set}	224.10	KSI
Resulting Top Strand Force	F_{set}	63.91	KIPS	Resulting Top Strand Force	F_{set}	79.28	KIPS	Resulting Top Strand Force	F_{set}	97.84	KIPS
Bot Strand Strain Increase	ε_{sebi}	2991.7	με	Bot Strand Strain Increase	ε_{sebi}	9074.8	με	Bot Strand Strain Increase	ε_{sebi}	16084.2	με
Resulting Bot Strand Strain	ε_{seb}	8373.9	με	Resulting Bot Strand Strain	ε_{seb}	14457.1	με	Resulting Bot Strand Strain	ε_{seb}	21466.5	με
Resulting Bot Strand Stress	σ_{seb}	239.20	KSI	Resulting Bot Strand Stress	σ_{seb}	264.58	KSI	Resulting Bot Strand Stress	σ_{seb}	267.17	KSI
Resulting Bot Strand Force	F_{seb}	417.73	KIPS	Resulting Bot Strand Force	F_{seb}	462.06	KIPS	Resulting Bot Strand Force	F_{seb}	466.58	KIPS
Resulting Strand Force	F_{se}	481.65	KIPS	Resulting Strand Force	F_{se}	541.34	KIPS	Resulting Strand Force	F_{se}	564.42	KIPS
Resulting Concrete Force	F_c	481.22	KIPS	Resulting Concrete Force	F_c	542.26	KIPS	Resulting Concrete Force	F_c	564.83	KIPS
Within Tolerance		YES	Y/N	Within Tolerance		YES	Y/N	Within Tolerance		YES	Y/N
Resulting Moment	M_4	1433.0012	FT-KIP	Resulting Moment	M_5	1661.3037	FT-KIP	Resulting Moment	M_6	1709.5994	FT-KIP
Curvature of Girder		6.67E-05	rad/in	Curvature of Girder		2.02E-04	rad/in	Curvature of Girder		3.58E-04	rad/in
Todeschini Variable	$f"_c$	4845.6	PSI	Todeschini Variable	$f"_c$	4845.6	PSI	Todeschini Variable	$f"_c$	4845.6	PSI
Todeschini Variable	ε_0	2748.3	με	Todeschini Variable	ε_0	2748.3	με	Todeschini Variable	ε_0	2748.3	με
Todeschini Variable	x	0.364	None	Todeschini Variable	x	0.728	None	Todeschini Variable	x	1.092	None
Todeschini Variable	β_1	0.342	None	Todeschini Variable	β_1	0.584	None	Todeschini Variable	β_1	0.719	None
Todeschini Variable	k_2	0.342	None	Todeschini Variable	k_2	0.362	None	Todeschini Variable	k_2	0.387	None
Average Stress	σ_{avg}	1656	PSI	Average Stress	σ_{avg}	2830	PSI	Average Stress	σ_{avg}	3483	PSI

497

Figure K.3 Moment-Curvature Plot

Table K.13 Girder Shear Capacity by 1998 AASHTO[92] LRFD Procedure

G1C-W	IN	Beam Shear Capacity AASHTO LRFD-98 (Left of Point Load)										
		L-SUPT	0.1 a	0.2 a	0.3 a	0.4 a	0.5 a	0.6 a	0.7 a	0.8 a	0.9 a	P-LOAD
Distance from Left Support (Inches)	IN	0.00	8.50	17.00	25.50	34.00	42.50	51.00	59.50	68.00	76.50	85.00
Ultimate Moment Furnished	FT-KIP	112.72	272.42	432.11	591.80	751.50	911.19	1070.88	1230.58	1390.27	1549.96	1709.64
Developed # Top Strands	#	0.13	0.32	0.51	0.69	0.88	1.07	1.25	1.44	1.63	1.81	2.00
Developed # Bottom Strands	#	0.53	1.27	2.02	2.77	3.52	4.26	5.01	5.76	6.51	7.25	8.00
Non-composite DL Moment (BM+SL)	FT-KIP	0.00	7.95	15.62	23.02	30.15	37.01	43.60	49.91	55.95	61.71	67.21
Total DL Shear (BM+SL)	KIP	11.68	11.30	10.91	10.53	10.14	9.76	9.37	8.99	8.60	8.22	7.83
Available Moment Capacity	FT-KIP	112.72	264.47	416.49	568.78	721.34	874.18	1027.29	1180.67	1334.32	1488.25	1642.43
Ultimate Moment, M_u	FT-KIP	0.00	172.19	344.11	515.75	687.13	858.23	1029.05	1199.61	1369.89	1539.90	1709.64
Ultimate Shear, Vu	KIP	243.55	243.17	242.78	242.40	242.01	241.63	241.24	240.86	240.47	240.09	239.70
Stress in Prestressing Strands at M_u, f_{ps}	KSI	9.73	23.52	37.31	51.10	64.88	78.67	92.46	106.25	120.03	133.82	264.60
Depth of Compression Block, a	IN	0.24	0.58	0.92	1.26	1.60	1.94	2.28	2.62	2.96	3.29	6.51
Effective Shear Depth, d_v	IN	38.66	38.49	38.32	38.15	37.98	37.81	37.64	37.47	37.30	37.13	35.52
Effective Area of Prestress, A_{pse}	IN^2	0.12	0.28	0.44	0.60	0.77	0.93	1.09	1.26	1.42	1.58	1.75
Shear Stress on Concrete, v / f'c	None	0.118	0.118	0.119	0.119	0.119	0.120	0.120	0.120	0.121	0.121	0.126
Measured θ From Beam	DEG	30	30	30	30	30	30	30	30	30	30	30
Strain in Reinforcement, $\varepsilon_{x, Actual}$	IN/IN	0.0581	0.0277	0.0198	0.0161	0.0141	0.0128	0.0118	0.0112	0.0107	0.0103	0.0104
Strain in Reinforcement, $\varepsilon_{x, Allowed}$	IN/IN	0.0020	0.0020	0.0020	0.0020	0.0020	0.0020	0.0020	0.0020	0.0020	0.0020	0.0020
Adjustment Factor for "-" Value, F_e	None	NA	NA	NA	NA	NA	NA	NA	NA	NA	NA	NA
Strain in Reinforcement, $\varepsilon_{x, Allowed}$	IN/IN	0.0020	0.0020	0.0020	0.0020	0.0020	0.0020	0.0020	0.0020	0.0020	0.0020	0.0020
Value of β From Figure	None											
Shear Strength of Concrete, V_c	KIPS	24.18	24.07	23.96	23.86	23.75	23.64	23.54	23.43	23.33	23.22	22.21
Stirrup Spacing, s	IN	2.00	7.00	7.00	7.00	7.00	7.00	7.00	7.00	7.00	7.00	7.00
Strength of Steel, V_s	KIPS	830.21	236.16	235.12	234.08	233.04	232.00	230.95	229.91	228.87	227.83	217.95
Total Beam Shear Strength, $V_c + V_s$	KIPS	854.39	260.23	259.08	257.94	256.79	255.64	254.49	253.35	252.20	251.05	240.16
Beam "AS BUILT" Shear Capacity	P/F	PASS	PASS	PASS	PASS	PASS	PASS	PASS	PASS	PASS	PASS	PASS
Ratio of (Vc + Vs) / (Vu / φ)	NONE	3.51	1.07	1.07	1.06	1.06	1.06	1.05	1.05	1.05	1.05	1.00
Longitudinal Reinforcement Satisfied	Y/N	YES	NO	NO	NO	NO	NO	NO	NO	NO	NO	NO
Addl Non-Prestressed Steel Required	IN^2	NA	3.17	3.35	3.54	3.73	3.93	4.14	4.35	4.57	4.80	5.52

Table K.14 Girder-Deck Interface Shear Calculations

G1C-W	Deck / Beam Interface Shear Calculations (AASHTO-STD '96)		

Interface Shear Calculation Values

Lightweight Concrete Reduction Factor	1	1	None
Shear Strength Reduction Factor	ϕ_s	0.85	None
Maximum Unfactored Shear	V_u	243.55	KIPS
First Moment of Deck About Centroid	QS	3480.00	IN^3
Composite Moment of Inertia	I_c	144285	IN^4
Interface Shear Contact Width	b_v	12	IN
Contact Length, d (a+XDIST<=SPAN/10)	Span/10	50.40	IN
Contact Area (b_v*Contact Length)	A_c	604.8	IN^2
Yield Strength of Tie Reinforcement	f_y	62	KSI
Stirrup Area	A_v	0.4	IN^2

Interface Condition

Contact Surface Clean		(shaded)	YES/NO
Contact Surface Roughened 1/4"		(shaded)	YES/NO
Minimum Ties Provided		(shaded)	YES/NO
Maximum Basic Interface Stress		350	PSI
Maximum Basic Interface Force	V_{nh}	211.68	KIPS

Basic Interface Shear Capacity Inadequate

Additional Interface Capacity Provided by Shear Reinforcement

Additional Interface Capacity Required		31.87	KIPS
Worst Case Stirrup Spacing over "a"	s	7.00	IN
Minimum Tie Area per Inch of Beam		0.0097	IN^2/IN
Additional V_{nh} Capacity per Percent		150.0	KIPS
Additional Percent Required		0.21	%
Additional Required Tie Area		0.000021	IN^2/IN
Total Tie Area Required		0.009698	IN^2/IN
Min. Tie Area Provided by V Reinforcement		0.057143	IN^2/IN
Resulting Contact Area Stress		402.70	PSI

Interface Shear Capacity Adequate

Tensile Stress at Interface

Deck Concrete Actual Strength	f'_c	5384	PSI
Maximum Allowable Deck Tensile Stress		550.32	PSI
Beam Concrete Actual Strength	f'_c	8911	PSI
Maximum Allowable Beam Tensile Stress		601.79	PSI
Maximum Interface Shear Stress (VQ/Ib)	v_h	489.52	PSI
Effective Prestress Force	F_{se}	322.23	KIPS
Beam Cross Sectional Area	A_{bm}	369	IN^2
Strand Eccentricity from NC Centroid	e	-6.73	IN
Distance from NC Centroid to Beam Top	y_{top}	20.17	IN
Distance from C Centroid to Beam Top	y_{top}	10.74	IN
Non-Composite Moment of Inertia	I_{nc}	50979	IN^4
Composite Moment of Inertia	I_c	144285	IN^4
Dead Load Moment	M_{DL}	67.21	FT-KIP
Live Load Moment	M_{LL}	1642.43	FT-KIP
Maximum Compressive Stress at Interface	f_{ca}	-1801.27	PSI
Maximum Tensile Stress at Interface	f_t	124.438	PSI

Tensile Stress at Interface is OK

Table K.15 Prestressing Strand Tension Test Curve

Prestressing Strand Tension Test Curve and Zone Limit Data

Strain -Stress Curve for 0.6-Inch Diameter 270 KSI LOLAX Strand

$y = 0.8063x + 56.5921$
$R^2 = 1.0000$

$y = 95.9317x^3 - 348.9161x^2 + 423.6514x - 114.2059$
$R^2 = 0.9985$

$y = 63.7701x + 0.0000$
$R^2 = 1.0000$

Strand Force (kips)

Strain (percent)

♦ Elastic　■ Transition　▲ Plastic　—— Linear (Elastic)　—— Linear (Plastic)　—— Poly. (Transition)

Prestressing Strand Loading Data		
Point of Loading	Strain (%)	Load (Kips)
Start of Elastic	0	0.00
End of Elastic	0.7135	45.50
Transition 1	0.7500	47.45
Transition 2	0.8750	53.63
Transition 3	1.0000	56.67
Transition 4	1.1250	57.20
Start of Plastic	1.2500	57.60
End of Plastic	6.5000	61.83

Zone	Percent Strain		
Elastic	0	< e <	0.7135
Transition	0.7135	< e <	1.2500
Plastic	1.2500	> e	

| Zone	Load		
Elastic	0	< Kips <	45.50
Transition	45.50	< Kips <	57.60
Plastic	57.60	> Kips	

Table K.16 Principal Strain and Maximum Shear Strain Plots

Figure K.4 Load Displacement Plot

Table K.17 Overview of Girder Test Results

G1C-W	4	Single	02-Nov-01
Support and Load Dimensions			
Shear Span	a	85.001	IN
Distance Between Supports	L1	504	IN
Deck Variables			
Deck Thickness	t_d	11.875	IN
Deck Width	W_f	19.375	IN
Concrete Strength at Testing	f'_c	5384	PSI
Elasticity Modulus at Testing	E_{cd}	3.35E+06	PSI
Girder Variables			
Concrete Strength at Release	f'_{ci}	6315	PSI
Concrete Strength at Testing	f'_c	8911	PSI
Concrete Equilibrium Weight	W_c	116.8	PCF
Lightweight Concrete Factor	1	0.85	None
Elasticity Modulus at Release	E_{ci}	3.00E+06	PSI
Elasticity Modulus at Test (Est)	E_{cb}	3.69E+06	PSI
Prestressing Strand Variables			
Strand C/S Area	A_{st}	0.2183	IN^2
Strand Ultimate Strength	f_{pu}	283.25	KSI
Strand Modulus of Elasticity	E_{ps}	29000	KSI
Strand Percent f_{pu} at Jacking		63%	%
Stress at Jacking	f_{pt}	179.11	KSI
Stress after Release	f_{si}	162.11	KSI
Stress after 14 Days	f_{se}	153.65	KSI
Stress at Testing	f_{se}	147.61	KSI
Stirrup Variables			
Strain at Testing	ε_{se}	5053	µε
Strain at Ultimate Load	ε_{ps}	13960	µε
Stirrup Size		4	#
Stirrup Yield Strength	f_y	62	KSI

Girder Test Overview

Value		Predicted	Experimental	Units
Transfer Length	l_t	30.73	21.50	IN
Development Length	l_d	100.56	91.00	IN
Cracking Load	P_{cr}	153.41	183.00	KIPS
Cracking Moment	M_{cr}	970.63	1144.85	FT-KIPS
Rupture Stress	f_r	601.79	967.82	PSI
Ultimate Load (AASHTO-Flexure)	P_{ult}	278.91	299.04	KIPS
Ultimate Moment (AASHTO-Flexure)	M_{ult}	1709.64	1828.17	FT-KIPS
Ultimate Load (Cracked Section)	P_{ult}	290.31	299.04	KIPS
Ultimate Moment (Cracked Section)	M_{ult}	1709.60	1828.17	FT-KIPS
Deflection at Cracking (Flex & Shear)	δ_{cr}	0.273	0.441	IN
Ultimate Deflection (Flex & Shear)	δ_{ult}	3.148	2.270	IN
Ultimate Concrete Deck Surface Strain	ε_{cu}	0.0030	0.0036	IN/IN
Initial Losses on Release	ES	-12.62	-17.00	KSI
Time Dependant Losses (14-Day)	CR,SH	-35.41	-25.46	KSI
Time Dependant Losses (Test)	CR,SH	-35.69	-31.50	KSI
Web Shear Strength ($V_{cw\text{-}ALT} / V_{crack}$)	V_{cw}	123.3	134.2	KIPS
Tensile Strength for Shear Cracking	f_t''	0.321	0.363	KSI
Tensile Strength Factor (Includes λ)	ξ_v	**4.00**	4.52	None
Strand Stress at Ultimate Load	f_{ps}	264.60	264.40	KSI
Ultimate Shear Capacity (VATM/V_{exp})	$V_{U\text{-}VATM}$	223.20	260.29	KIPS
Ultimate Shear Capacity (STD/V_{exp})	$V_{U\text{-}STD}$	241.39	260.29	KIPS
Comp Field Angle (VATM/Girder) θ		29.4	30.0	DEG
LVDT Rosette Tension Crack Angles (Low/High)		22.7	40.9	DEG

The predicted f_t'' is based on the ACI alternate technique specified in 11.4.2.2 using a of 4. The regular approach in 11.4.2.2 uses 3.5 as the multiplier as is seen in equation 11-12. a can be changed in the "predicted a" cell. The experimental V_{cw} value is shear at which shear cracking occurred. The predicted f_t'' is based on the equation from Burns' book, page 254. The f_{pc} value comes from the STD Shear Page at the 0.5a location.

APPENDIX L

MOMENT vs. CURVATURE PLOTS
AND
LOAD vs. DEFLECTION PLOTS

Appendix L contains moment vs. curvature plots and load vs. displacement plots

for each girder test. The predicted and experimental values are listed on both plots. The

following sections describe the calculations required for both plots.

L.1 Moment-Curvature

Predicted moment and curvature values were determined at several stages

progressing from zero applied load to the ultimate applied load. The predicted moment

and curvature values were then used to predict deflections at the point of loading and for

comparison with experimental values. The process for calculating moment and curvature

values can be found in *Design of Prestressed Concrete Structures*, T.Y. Lin and Ned H.

Burns.[126] The process for determining stresses in a composite section can be found in

Prestressed Concrete Structures, Michael P. Collins and Denis Mitchell.[145] Several

assumptions were made to determine the values.

1. The concrete and prestressing strands were considered perfectly bonded.

Strains in the concrete and steel were considered to be the same.

2. The stress-strain relationship was known for the concrete and steel.

3. Strains were distributed linearly over the height of the girder.

4. The girder was in static equilibrium.

A Todeschini[151] stress distribution was assumed for the deck during the cracked section analysis. Moment and curvature values were determined at six specific points as described in the following sections. Tables K.11 and K.12 show calculation of moment and curvature values. Variables are defined in Appendix T.

L.1.1 Stage 1 - Zero Applied Load

The following procedure was used to determine curvature with zero applied load.

$$ f_{top} = -\frac{F_{se}}{A_{nc}} - \frac{F_{se}\,e}{S_{top-nc}} - \frac{M_{DL}}{S_{top-nc}} \tag{L.1} $$

$$ f_{bot} = -\frac{F_{se}}{A_{nc}} + \frac{F_{se}\,e}{S_{bot-nc}} + \frac{M_{DL}}{S_{bot-nc}} \tag{L.2} $$

Strains at the top and bottom of the girder were calculated with the following equations:

$$ \varepsilon_{top} = \frac{f_{top}}{E_{cg}} \tag{L.3} $$

$$ \varepsilon_{bot} = \frac{f_{bot}}{E_{cg}} \tag{L.4} $$

The predicted curvature at Stage 1 was calculated with the following equation:

$$\phi = \frac{-(\varepsilon_{top} - \varepsilon_{bot})}{h_{g-nc}} \qquad (L.5)$$

The resulting stress in the concrete at the level of the bottom strands was calculated as:

$$\sigma_{ce} = \frac{(\varepsilon_{top} + (\varepsilon_{bot} - \varepsilon_{top})) * (h_{g-nc} - BCL)}{h_{g-nc}} * E_{cg} \qquad (L.6)$$

L.1.2 Stage 2 – Zero Concrete Strain at the Level of Bottom Strands

The following procedure was used to determine the curvature at the point where the applied load produced zero concrete strain at the level of the bottom strands. This point is known as the "decompression load." The effect of the applied load was determined using the composite section properties. The effects of prestressing and any dead load moment were the same as in Stage 1. The effect of the applied load was added to the Stage 1 values to determine the total affect. To determine the applied moment required, M_2, to produce zero strain and thus zero stress in the concrete at the level of the bottom strands, the following equation was used. Refer to Table K.11.

$$M_2 = \frac{-\sigma_{ce} I_c}{(y_{bot-c} + BCL)} \qquad (L.7)$$

507

The resulting stresses at the top and bottom of the girder were calculated with the following equations:

$$f_{top} = -\frac{F_{se}}{A_{nc}} - \frac{F_{se}\,e}{S_{top-nc}} - \frac{M_{DL}}{S_{top-nc}} - \frac{M_2}{S_{top-c}} \qquad (L.8)$$

$$f_{bot} = -\frac{F_{se}}{A_{nc}} + \frac{F_{se}\,e}{S_{bot-nc}} + \frac{M_{DL}}{S_{bot-nc}} + \frac{M_2}{S_{bot-c}} \qquad (L.9)$$

The resulting strains at the top and bottom of the girder were calculated using equations L.3 and L.4. The resulting strain in the bottom strands was calculated using the following equation where the effective strain prior to applying load, ε_{se}, was determined from VWSG readings prior to girder testing.

$$\varepsilon_{s2} = \varepsilon_{se} - \frac{\sigma_{ce}}{E_{cg}} \qquad (L.10)$$

Curvature was calculated using equation L.5.

L.1.3 Stage 3 – Cracking Stress on Bottom Fiber

The following procedure was used to determine the curvature at the point where the additional applied load produced a stress at the bottom fiber equal to the predicted

508

cracking stress, f_{cr}. The moment that produces the cracking stress on the bottom fiber is the cracking moment, M_{cr}. The predicted cracking stress was calculated using the following equation:

$$f_{cr} = 7.5\lambda\sqrt{f_c'}$$ (L.11)

The effect of the applied load was determined using the composite section properties. The effects of prestressing and any dead load moment were the same as in Stage 1. The effect of the applied load was added to the Stage 1 values to determine the total effect. To determine the additional applied moment required, M_3, to produce M_{cr} and the cracking stress, f_{cr}, at the bottom fiber, the following equation was used. The subscript "-2" indicates the bottom stress from Stage 2.

$$M_3 = (f_{cr} - f_{bot-2})S_{bot-c}$$ (L.12)

The cracking moment, M_{cr}, was determined with the following equation:

$$M_{cr} = M_{DL} + M_2 + M_3$$ (L.13)

The total concrete stress at the top and bottom of the girder were calculated with the following equations:

$$f_{top} = -\frac{F_{se}}{A_{nc}} - \frac{F_{se}e}{S_{top-nc}} - \frac{M_{DL}}{S_{top-nc}} - \frac{M_2}{S_{top-c}} - \frac{M_3}{S_{top-c}} \qquad (L.14)$$

$$f_{bot} = -\frac{F_{se}}{A_{nc}} + \frac{F_{se}e}{S_{bot-nc}} + \frac{M_{DL}}{S_{bot-nc}} + \frac{M_2}{S_{bot-c}} + \frac{M_3}{S_{bot-c}} \qquad (L.15)$$

The resulting strains at the top and bottom of the girder were calculated with equations L.3 and L.4. The resulting strain in the bottom strands, ε_{s3}, was calculated with the following equation:

$$\varepsilon_{s3} = \varepsilon_{s2} + \frac{(f_{cr} - f_{bot-2})}{E_{cg}} * \left(\frac{y_{bot-c} - BCL}{y_{bot-c}} \right) \qquad (L.16)$$

Curvature was calculated using equation L.5.

L.1.4 Cracked Section Analysis

Force equilibrium was used to calculate the moment and curvature values after cracking occurred. Once a strain on the surface of the deck or in the prestressing strand was assumed, the depth to the neutral axis was determined which balanced the tension and compression forces. The procedure was identical for the assumed deck strains, ε_{cd}, of 0.001 in/in (Stage 4), 0.002 in/in (Stage 6) and 0.003 in/in (Stage 7). Stage 5 was the point at which the strand was at a strain of 0.01 in/in and began to yield. To approximate the stress distribution for the deck, a Todeschini[151] distribution was used since the deck

concrete was a normal weight concrete with less than 6,000 psi compressive strength.

Details of the Todeschini distribution are shown in Figure L.1
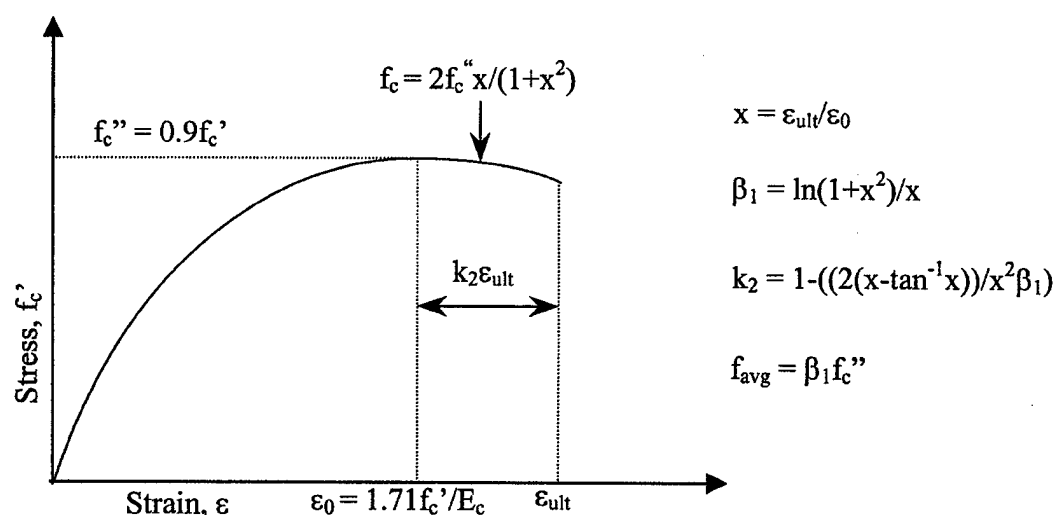
Figure L.1 Todeschini Stress Distribution

Once a deck surface strain or prestressing strand strain was selected and an

estimate entered for the depth to the neutral axis, c, it was necessary to determine the

force in the prestressing strands. After Stage 3, the strain in the bottom strands, ε_{s3}, was

known. Since there was very little rotation in the girder up to the cracking load, it was

assumed that the strain in the top strands at M_{cr} was the effective prestress strain, ε_{se}. An

"if" statement was used in the spreadsheet to calculate resulting strand forces in the top

strands based on the location of the assumed neutral axis relative to the top strands. If the

neutral axis fell below the top strands, there would be a reduction in strand strain as

calculated below:

$$\varepsilon_{set} = \varepsilon_{se} - \frac{(c - (t_d + TCL))}{c}\varepsilon_{cd} \qquad (L.17)$$

If the neutral axis fell above the top strands, there would be an increase in strand strain as calculated below:

$$\varepsilon_{set} = \varepsilon_{se} + \frac{(t_d + TCL - c)}{(t_d + h_{g-nc} - c - BCL)}\varepsilon_{sebi} \qquad (L.18)$$

The force in the top strands was then calculated using the prestressing strand stress-strain plot described in Chapter 8. The strain in the bottom strands was calculated using the following equations:

$$\varepsilon_{seb} = \frac{(t_d + h_{g-nc} - BCL)}{c}\varepsilon_{cd} + \varepsilon_{se2} \qquad (L.19)$$

$$\varepsilon_{sebi} = \varepsilon_{seb} - \varepsilon_{se2} \qquad (L.20)$$

The force in the bottom strands was then calculated using the prestressing strand tension curve plot seen in Table K.15. The total tension force, F_s, was the sum of the force in the top strands and the force in the bottom strands.

The concrete compression force, F_c, was calculated using the Todeschini technique. Referring to Figure L.1, the compressive force was calculated as below:

512

$$F_c = f_{avg}W_f c \qquad\qquad (L.21)$$

Values of "c" were varied until F_c was within 1 kip of F_s.

The resulting moment was calculated using the equation below based on the force in the top and bottom strands.

$$M_{4,5,6} = F_{top}(t_d + TCL - k_2 c) + F_{bot}(t_d + h_{g-nc} - BCL - k_2 c) \qquad\qquad (L.22)$$

The curvature was calculated using the equation:

$$\phi_{4,5,6,7} = \frac{\varepsilon_{cd}}{c} \qquad\qquad (L.23)$$

This procedure was used for each of the selected deck strain values. The girder's ultimate moment and curvature values were determined at a deck surface strain of 0.003 in/in.

L.1.5 Experimental Moment-Curvature

The experimental moment and curvature were calculated using the equations below:

$$M_{exp} = M_{DL} + P\frac{(L_1 - a)}{L_1}a \qquad\qquad (L.24)$$

$$\phi = \frac{\varepsilon_{bot} - \varepsilon_{top}}{h_g} \qquad\qquad (L.25)$$

M_{DL} is the dead load moment caused by the girder and deck. P is the applied

load. L_1 and "a" are the distance between supports and shear span respectively. ε_{bot} and

ε_{top} are the strains at the bottom and top of the composite girder that were calculated from

strain readings recorded using LVDTs placed close to the bottom and top of the

composite girder assuming a linear strain distribution. Table L.1 lists the L_1 and "a"

distances for each girder test.

The predicted plot begins with a negative curvature reflecting the initial upward

camber due to prestressing. The moment value also starts above zero in most cases

reflecting the initial dead load moment.

Table L.1 Dimensions "a" and L_1 for Girder Tests

Girder Test #	Configuration #	Shear Span "a" (inches)	Support to Support Distance L_1 (inches)
G1A-East, G2A-East	2	61	316
G1A-West, G2A-West	1	90	456
G1A-Center, G2A-Center	7	82	185
G1B-East, G2B-East	5	61	456, 321
G1B-West, G2B-West	3	75	345, 456
G1B-Center, G2B-Center	8	96	210
G1C-East, G2C-East	6	75	369
G1C-West, G2C-West	4	85	504
G1C-Center, G2C-Center	9	120	244

L.2 Deflection

Calculations for deflection at cracking and at ultimate were compared to experimental results. An elastic technique was used to calculate the deflection at cracking and a moment area technique was used for the ultimate deflection. The moment area technique used provided a good estimate but was not an exact solution. Table K.9 provides details on deflection calculations. Table K.2 shows experimental deflections.

L.2.1 Calculations for Deflection at Flexural Cracking

An elastic technique was used to predict the deflection at initial flexural cracking as specified in *Mechanics of Materials*, Gere and Timoshenko.[124] Table K.9 provides details on elastic deflection calculations. Included in the elastic deflection calculations were components due to both flexure and shear. Figure L.2 provides a diagram of variables used in calculating elastic deflections.
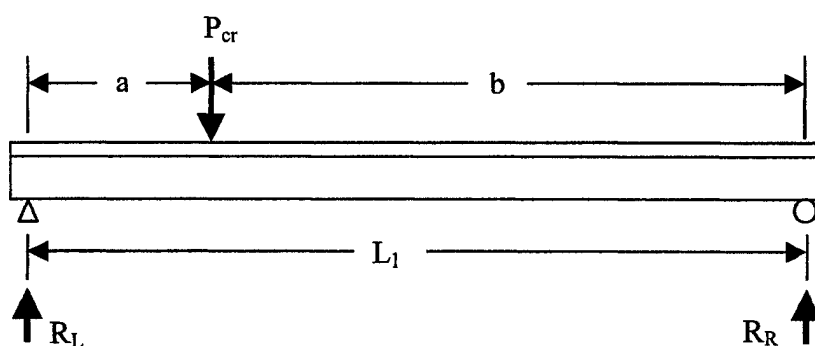
Figure L.2 Diagram Showing Variables for Elastic Deflection Calculations

P_{cr} was the predicted cracking load. The value of $0.4\,E_{cg}$ was used for the shear

modulus, G. The cracking deflection at the point of load application was calculated with

the following equations for flexural deflection and shear deflection:

$$\delta_{cr-flex} = \frac{P_{cr}ba}{6E_{cg}I_cL_1}(L_1^2 - b^2 - a^2)$$ (L.26)

$$\delta_{cr-shear} = R_L \frac{a}{0.4E_{cg}\,b\,d_p}$$ (L.27)

The total elastic cracking deflection was the sum of the flexural and shear deflections.

L.2.2 Calculations for Ultimate Deflection

A moment area technique was used to calculate deflection at the ultimate

condition as described in *Mechanics of Materials*, Gere and Timoshenko.[124] At the

ultimate condition, a plastic hinge forms at the point of load application. The length of

the plastic hinge was assumed to equal the distance from the surface of the deck to the

bottom strands. Over the plastic hinge, the curvature was assumed to be at ϕ_{ult} as

described in Section L.1.4. The variables shown in Figure L.2 also apply during the

ultimate deflection calculations.

Two different curvature diagrams were required for ultimate deflection

calculations. The diagram shown in Figure L.3, the "modified" curvature diagram,

applied when distances from the point of loading to a support were small. The hinge

region effectively encompassed the region where a yielding curvature point, ϕ_y, would be considered. Figure L.4, the "normal" curvature diagram, applied when the distances from the point of loading to a support would allow consideration of a yielding curvature point, ϕ_y. The yielding curvature, ϕ_y, was the point at which the prestressing strand first yielded. The curvature value, ϕ_{cr}, was the curvature at initial flexural cracking. The curvature value, ϕ_{ult} was the curvature at ultimate. The calculations in Table K.9 automatically determined the characteristics of the curvature diagram based on the dimensions of the girder test and curvature values. In most cases, the diagram to the left of the load was the modified diagram and to the right of the load was the normal diagram
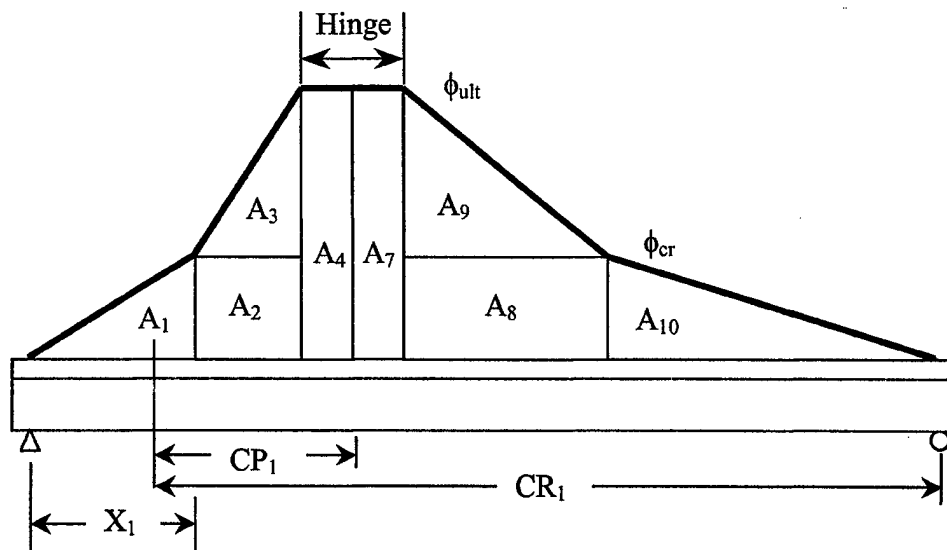
Figure L.3 "Modified" Curvature Diagram for Ultimate Deflection Calculations
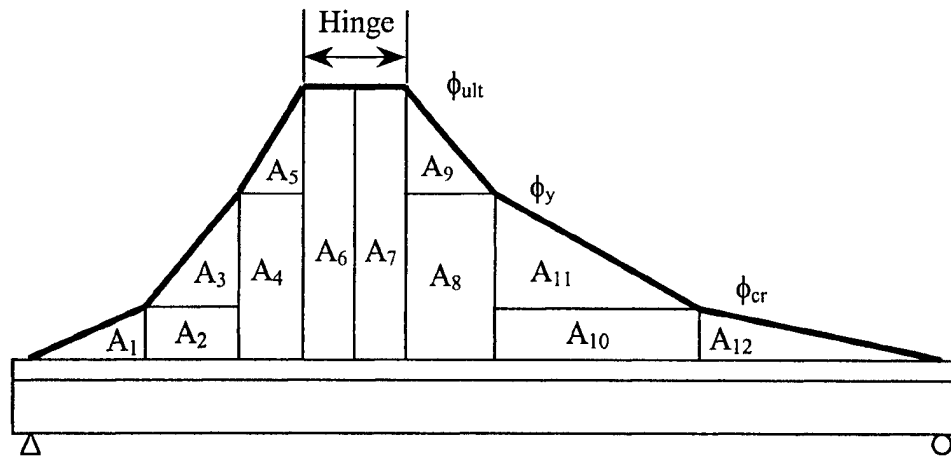
Figure L.4 "Normal" Curvature Diagram for Ultimate Deflection Calculations

The values X_x, CR_x and CP_x, and A_x are referenced in Table K.9 and shown in Figure L.3. The same definitions apply to Figure L.4. The X distances are distances from the left support to the far side of a particular area. The CR values measure the distance from the centroid of an area to the right support. The CP values measure the distance from the centroid of an area to the point of load application.

Figure L.5 shows a diagram describing the calculation of deflections. It is important to emphasize again that the resulting ultimate deflection calculation was a good estimate, but not an exact value.
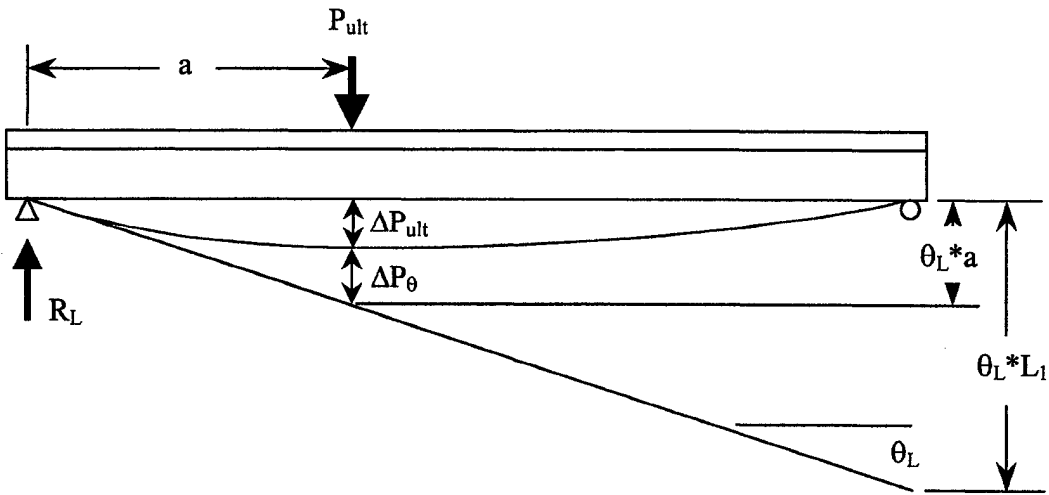
Figure L.5 Diagram Showing Ultimate Deflection Calculation

The following equations were used to calculate the ultimate deflection, ΔP_{ult}:

$$\theta_L a = \sum A_x CR_x \frac{a}{L_1} \qquad (L.28)$$

$$\Delta_{p\theta} = \sum A_x CP_x \qquad (L.29)$$

$$\Delta P_{ult} = \theta_L a - \Delta P_\theta + R_L \frac{a}{0.4 E_{cg}\, b\, d_p} \qquad (L.30)$$

519

Equation L.30 reflects the deflection component due to shear deformation. The percentage of total deflection due to shear is much less in the ultimate deflection; however, it must be included for accuracy. The value $0.4E_{cg}$ used in the denominator represents the shear modulus, G. If cracking was extreme during a test, this value was reduced to $0.2E_{cg}$ to reflect a reduced shear modulus.

L.2.3 Experimental Deflections

Measurement of experimental deflections was accomplished with a wire potentiometer placed under girder at the point of load application.

L.3 Girder Test G1A-East
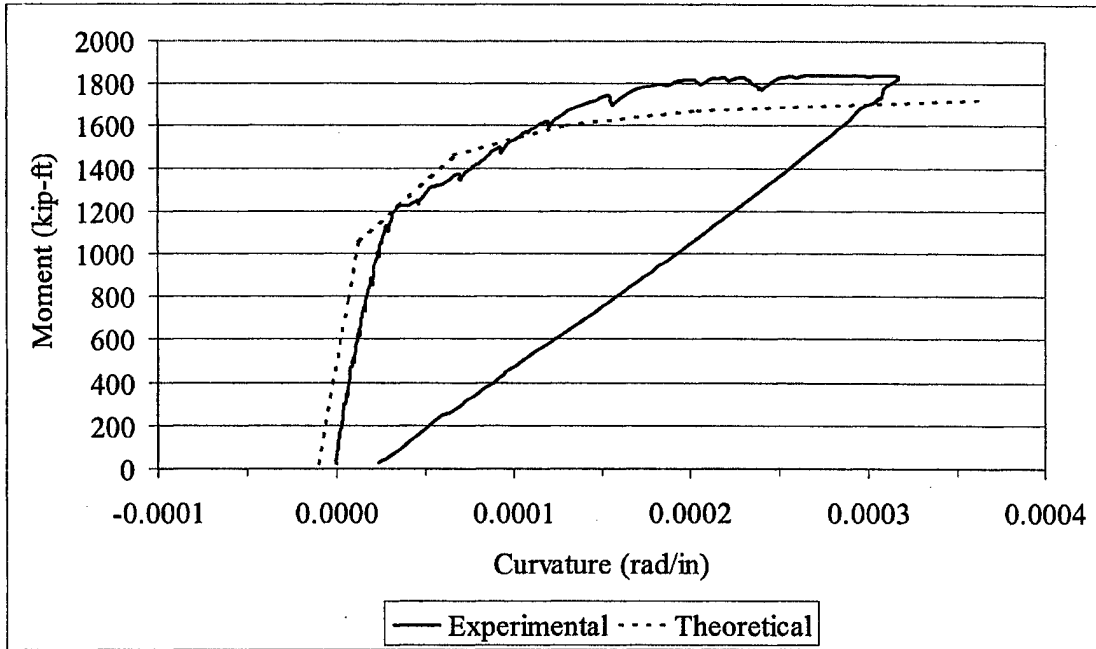

Figure L.6 G1A-East Moment vs. Curvature Plot
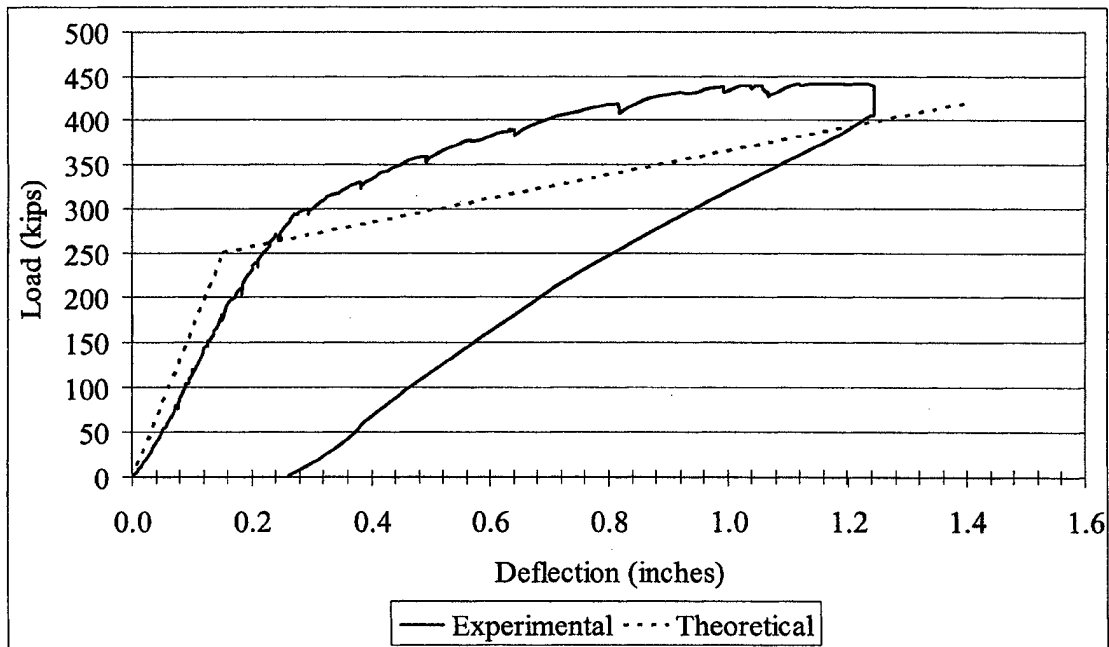
Figure L.7 G1A-East Load vs. Deflection Plot

521

## L.4 Girder Test G1A-West
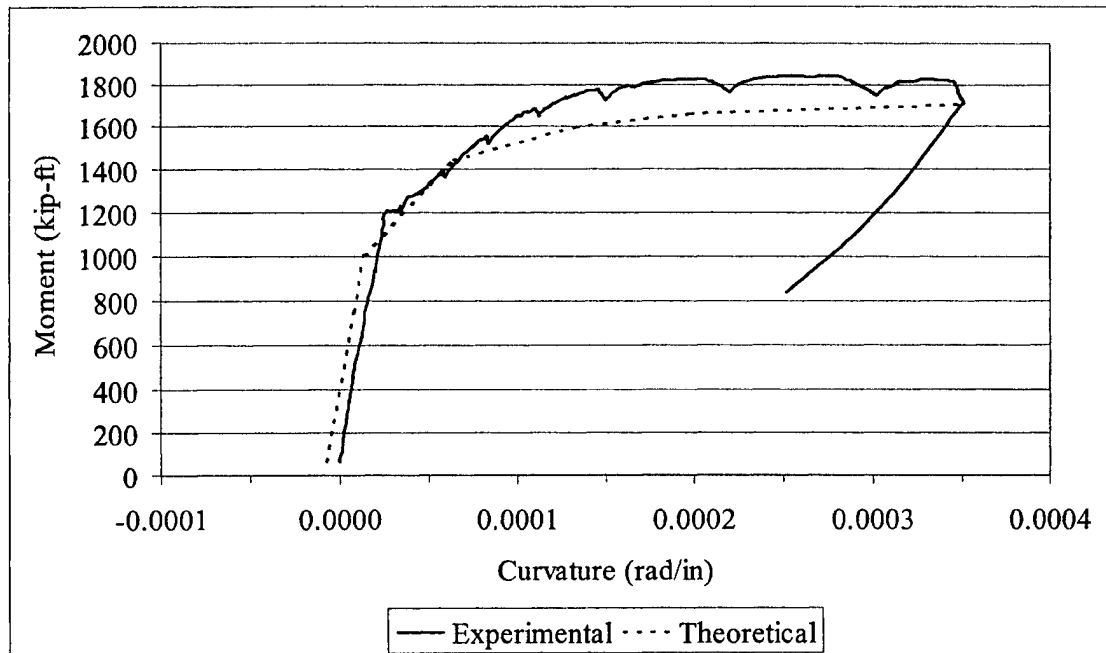
Figure L.8 G1A-West Moment vs. Curvature Plot
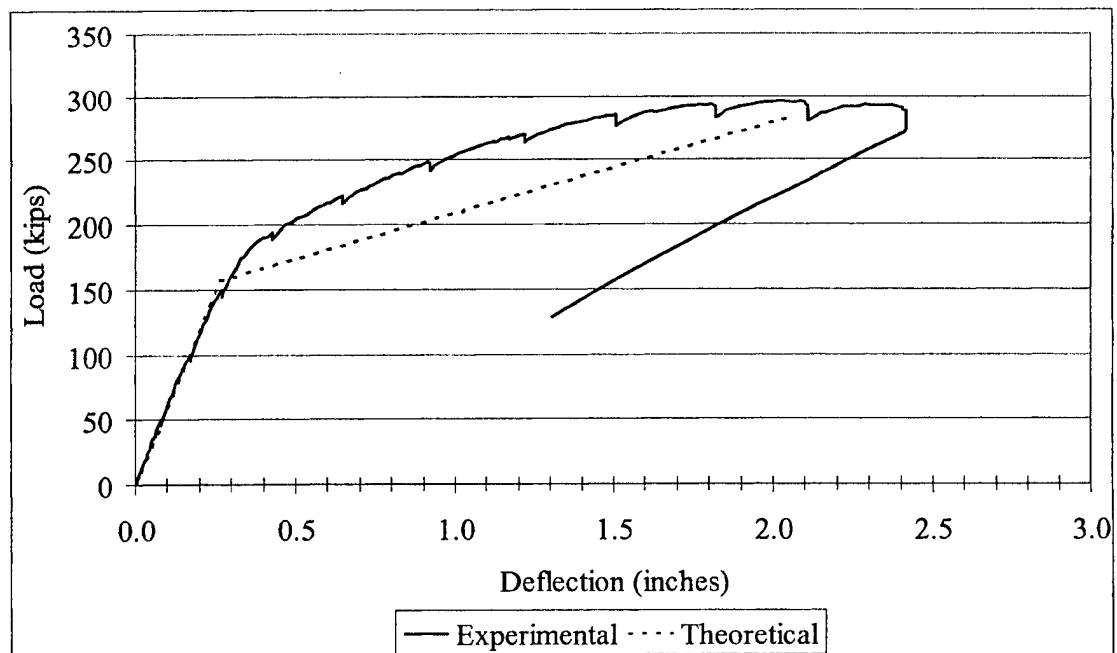
Figure L.9 G1A-West Load vs. Deflection Plot

522

L.5 Girder Test G1A-Center
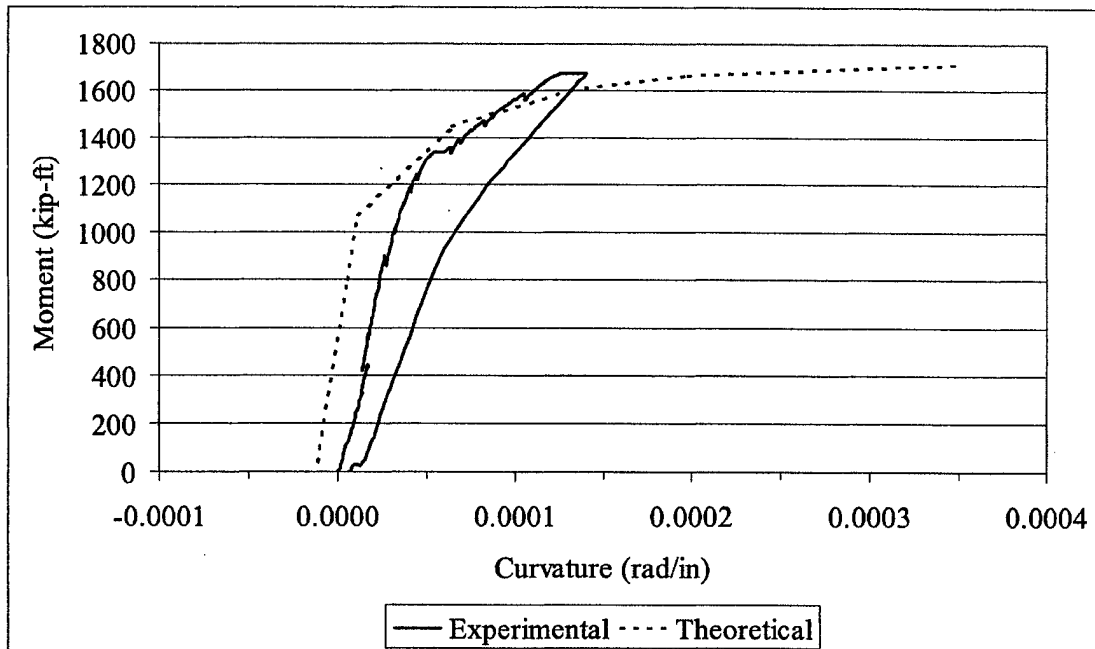
Figure L.10 G1A-Center Moment vs. Curvature Plot
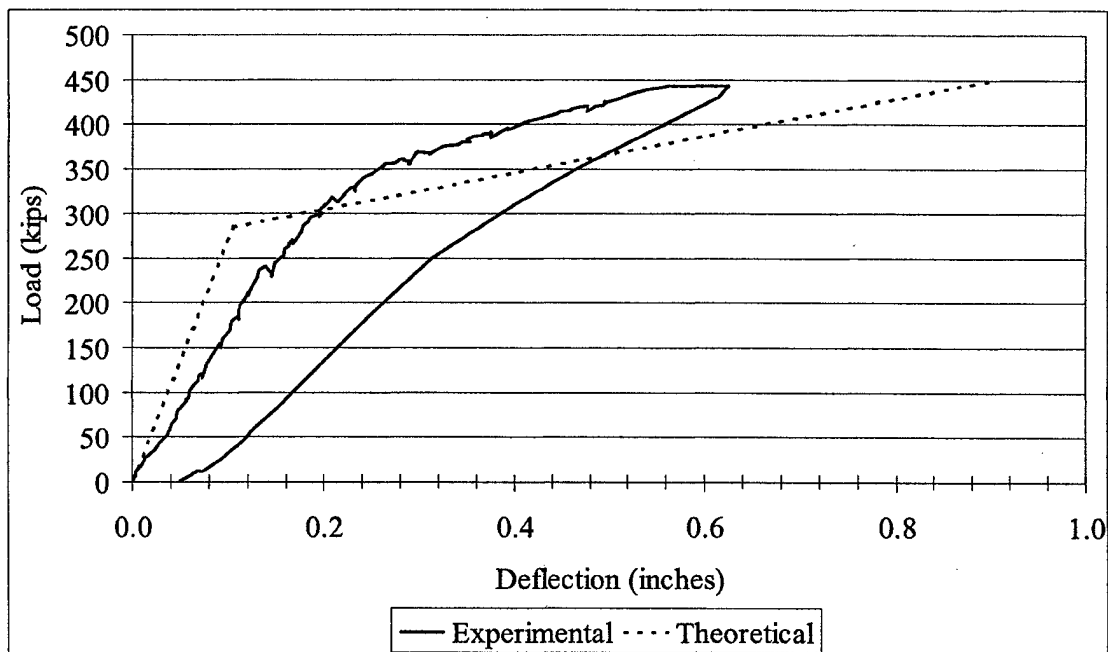
Figure L.11 G1A-Center Load vs. Deflection Plot

L.6 Girder Test G1B-East
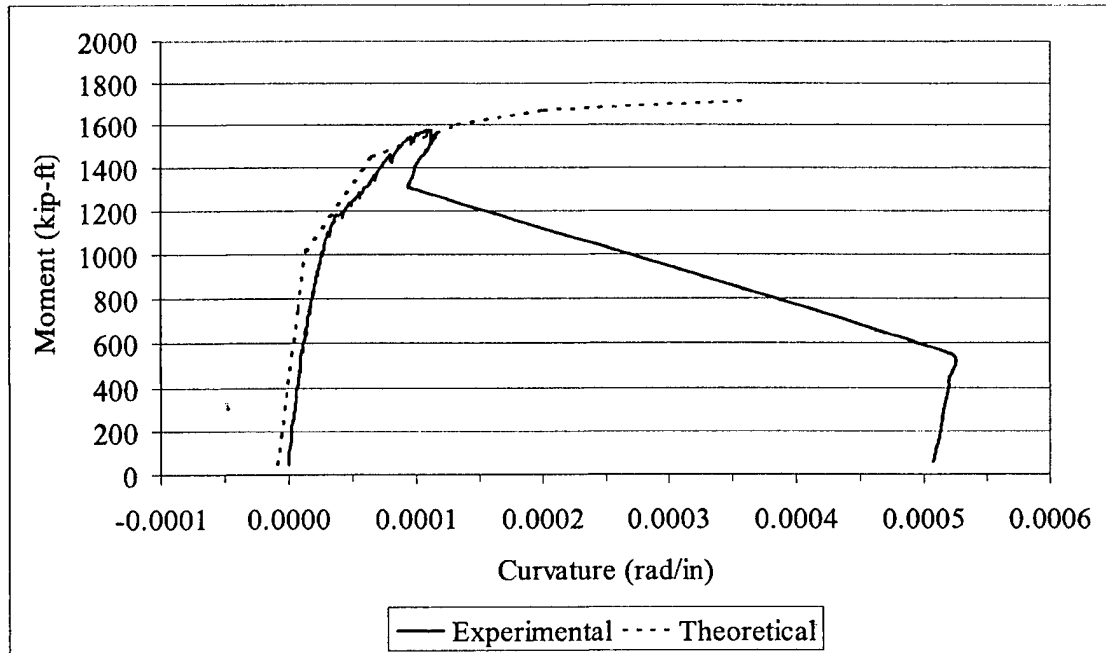
Figure L.12 G1B-East Moment vs. Curvature Plot
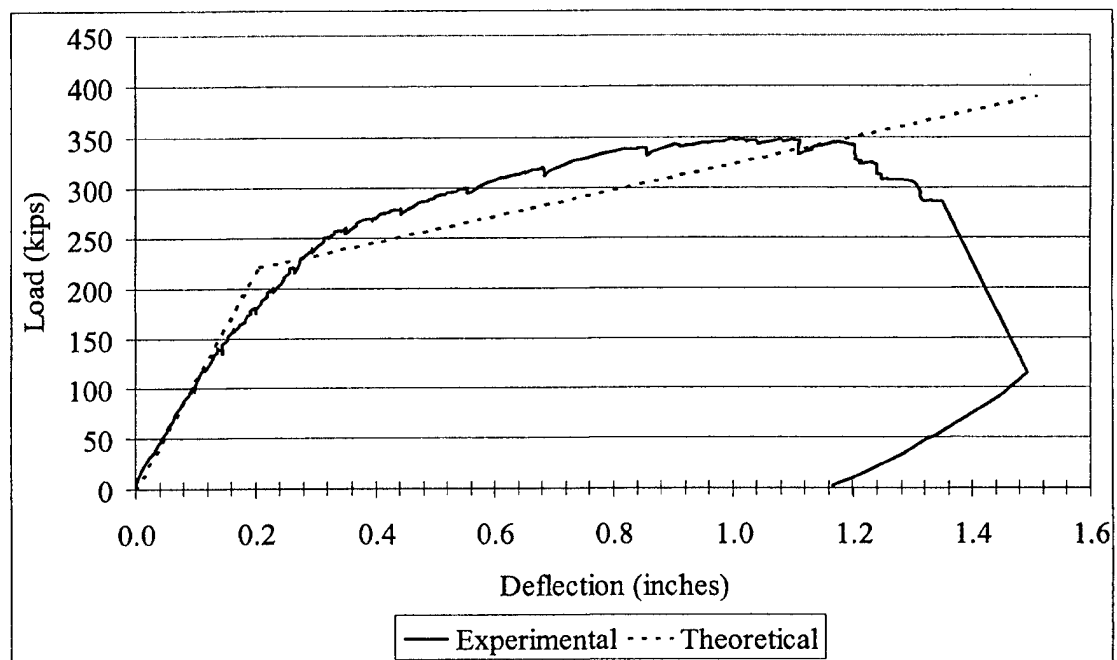
Figure L.13 G1B-East Load vs. Deflection Plot

L.7 Girder Test G1B-West
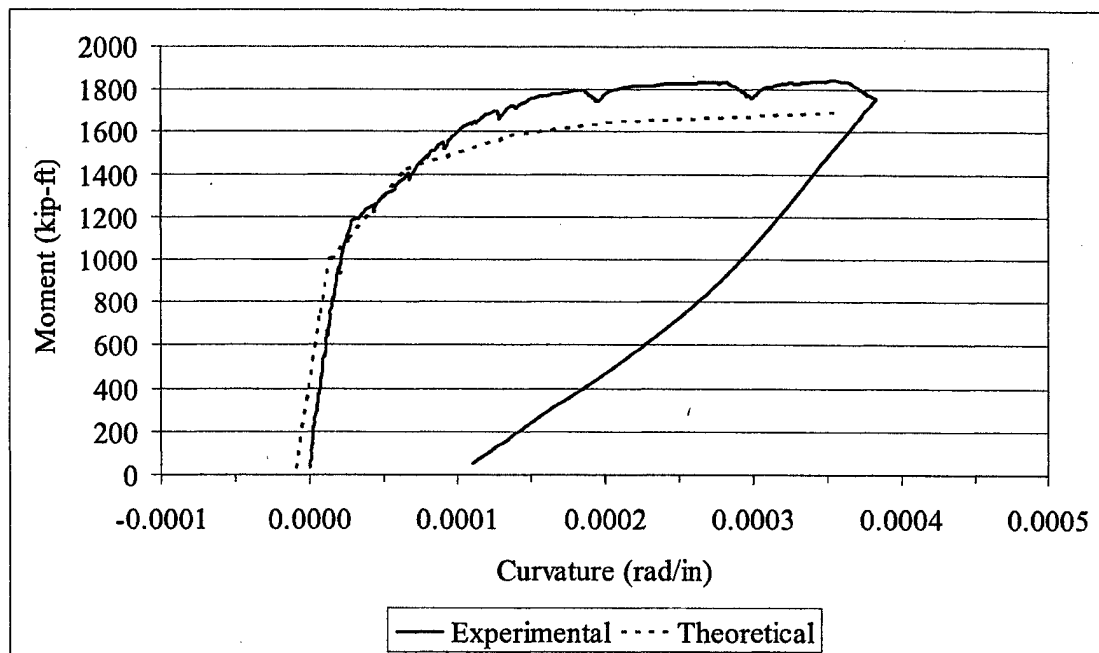
Figure L.14 G1B-West Moment vs. Curvature Plot
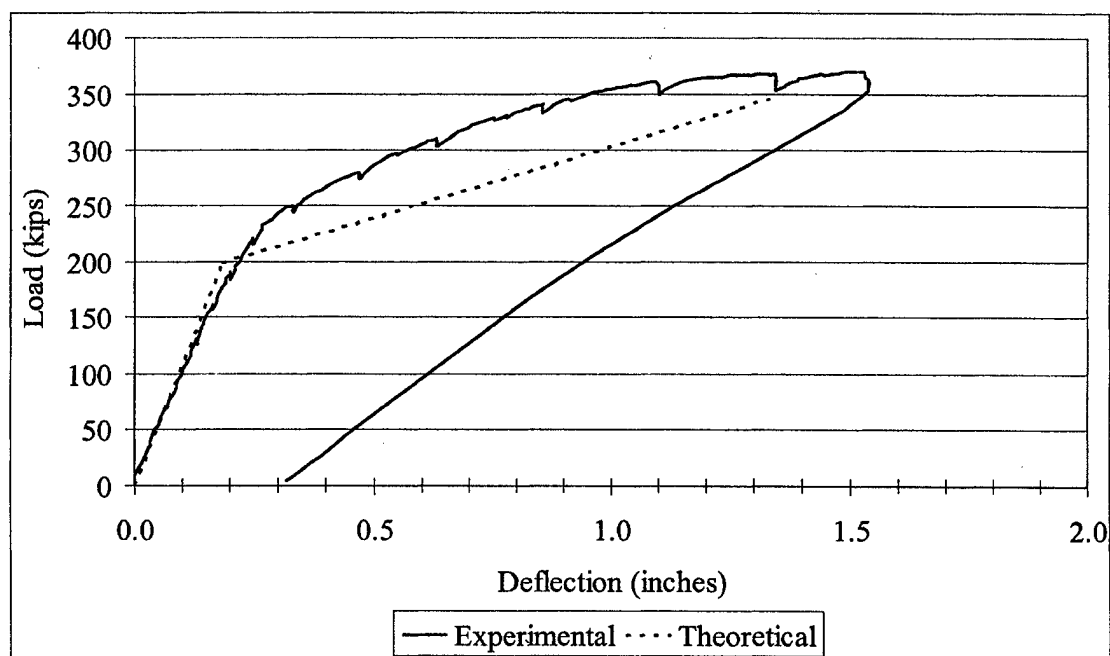
Figure L.15 G1B-West Load vs. Deflection Plot

L.8 Girder Test G1B-Center
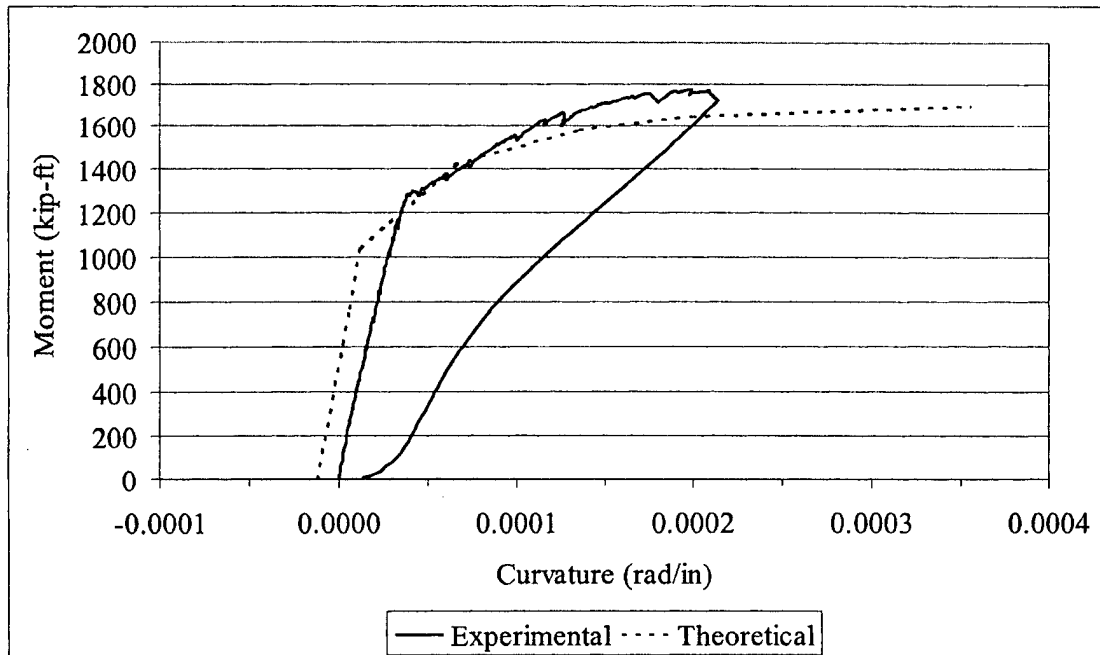
Figure L.16 G1B-Center Moment vs. Curvature Plot
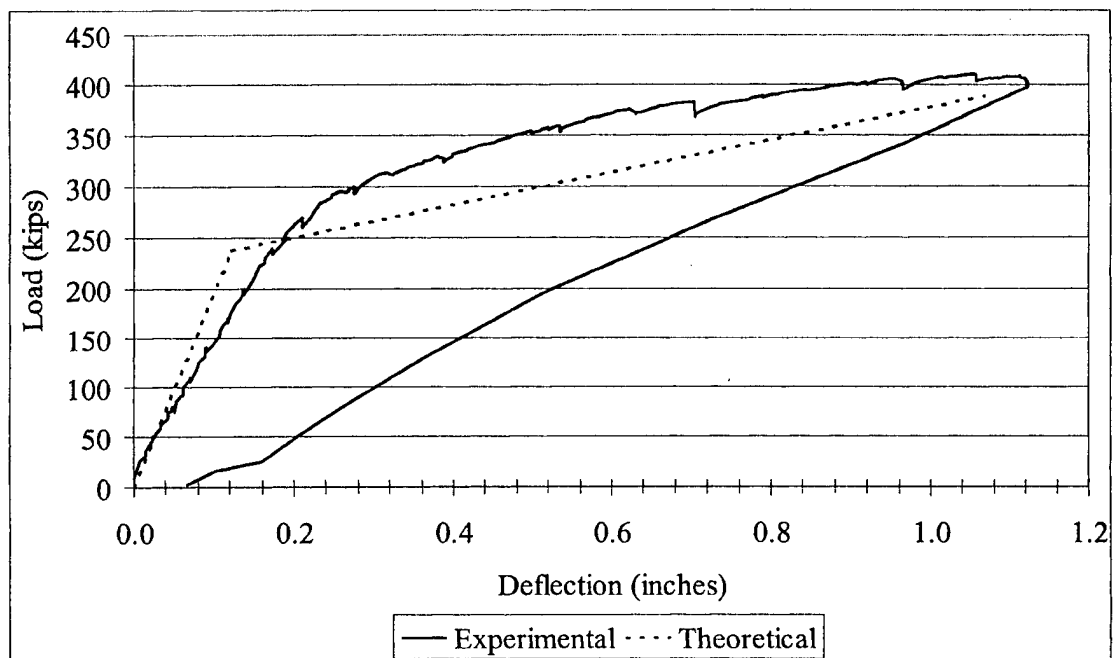
Figure L.17 G1B-Center Load vs. Deflection Plot

L.9 Girder Test G1C-East
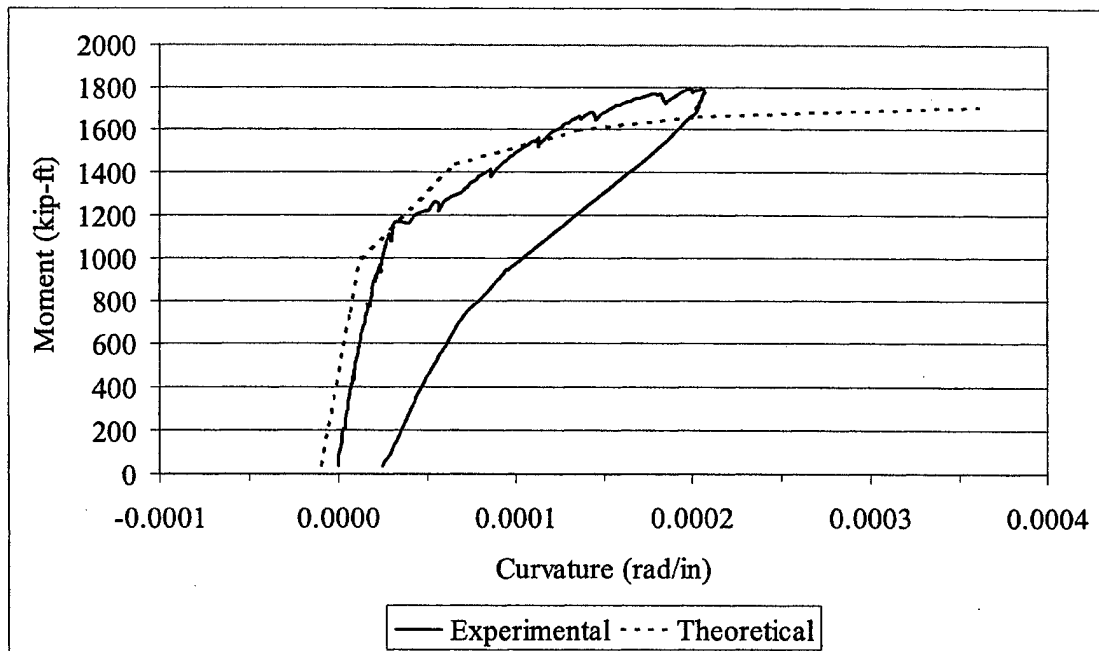
Figure L.18 G1C-East Moment vs. Curvature Plot
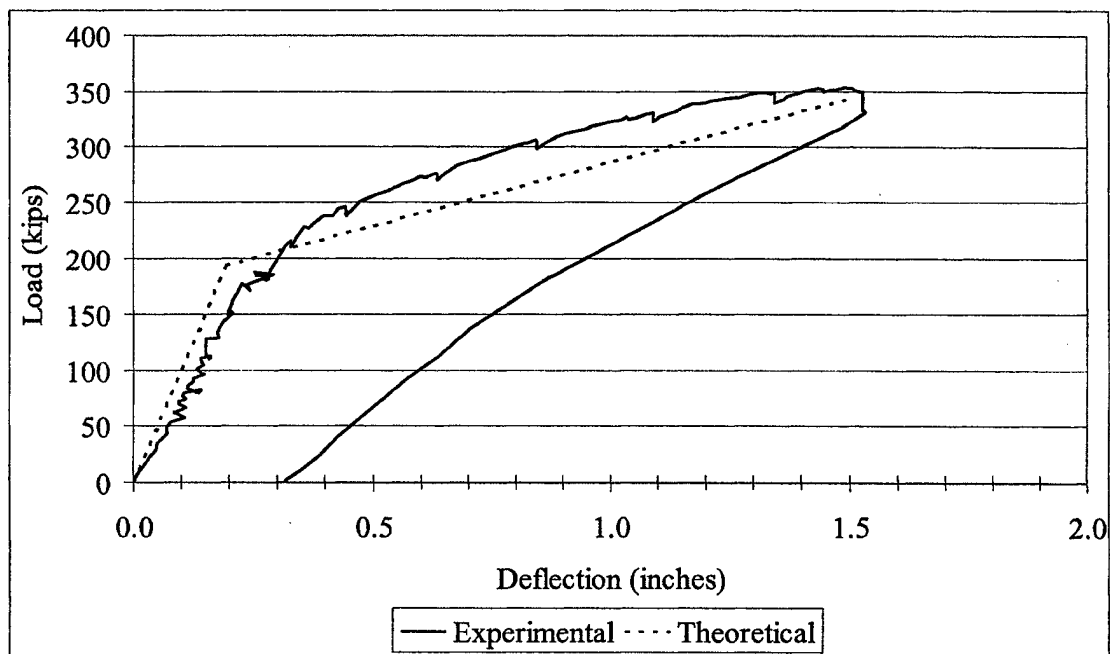
Figure L.19 G1C-East Load vs. Deflection Plot

527

L.10 Girder Test G1C-West
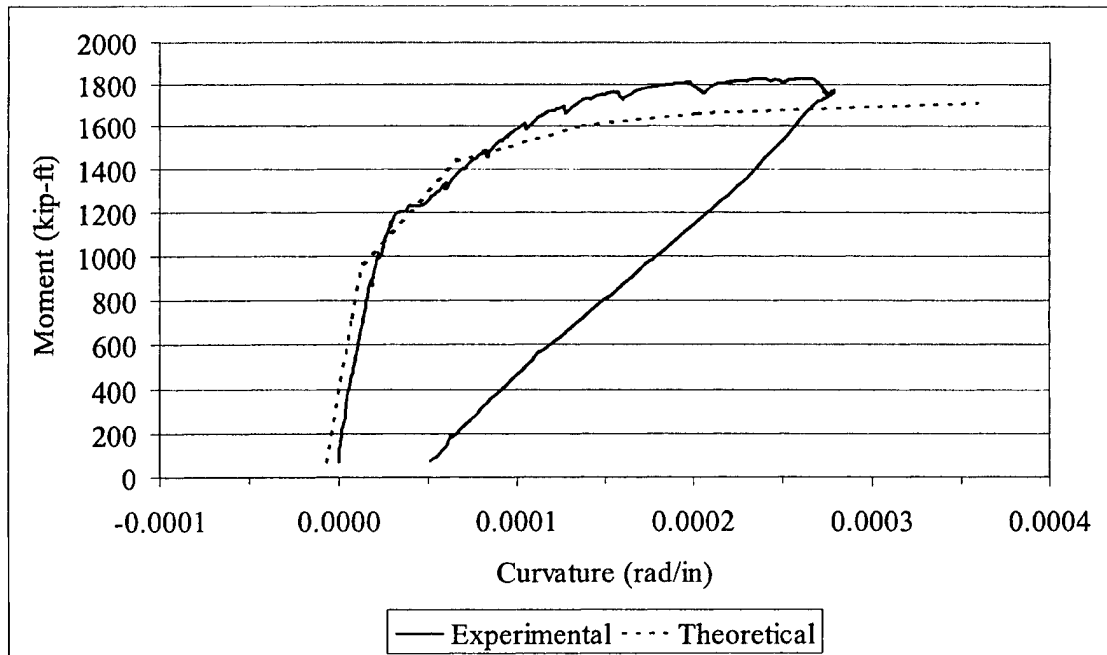
Figure L.20 G1C-West Moment vs. Curvature Plot
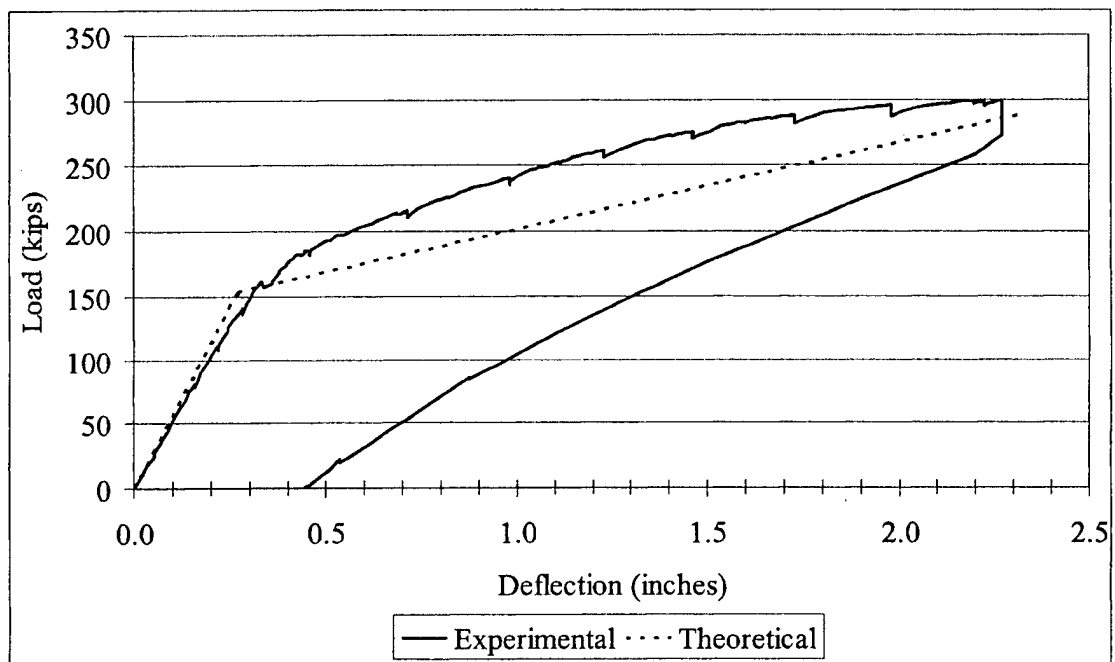
Figure L.21 G1C-West Load vs. Deflection Plot

528

L.11 Girder Test G1C-Center
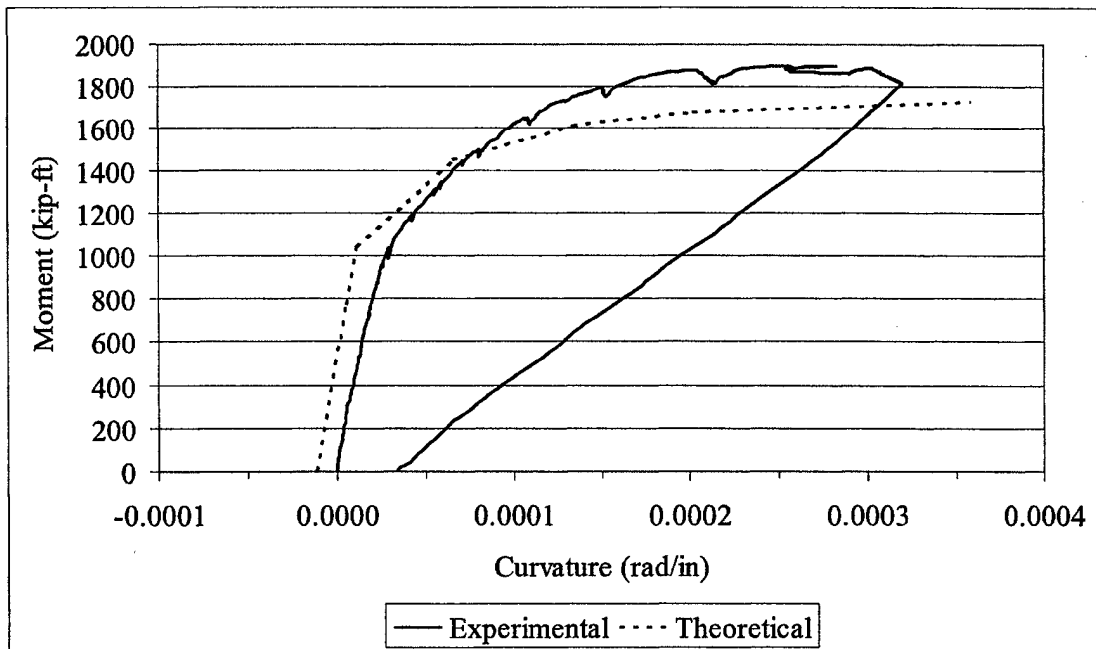
Figure L.22 G1C-Center Moment vs. Curvature Plot
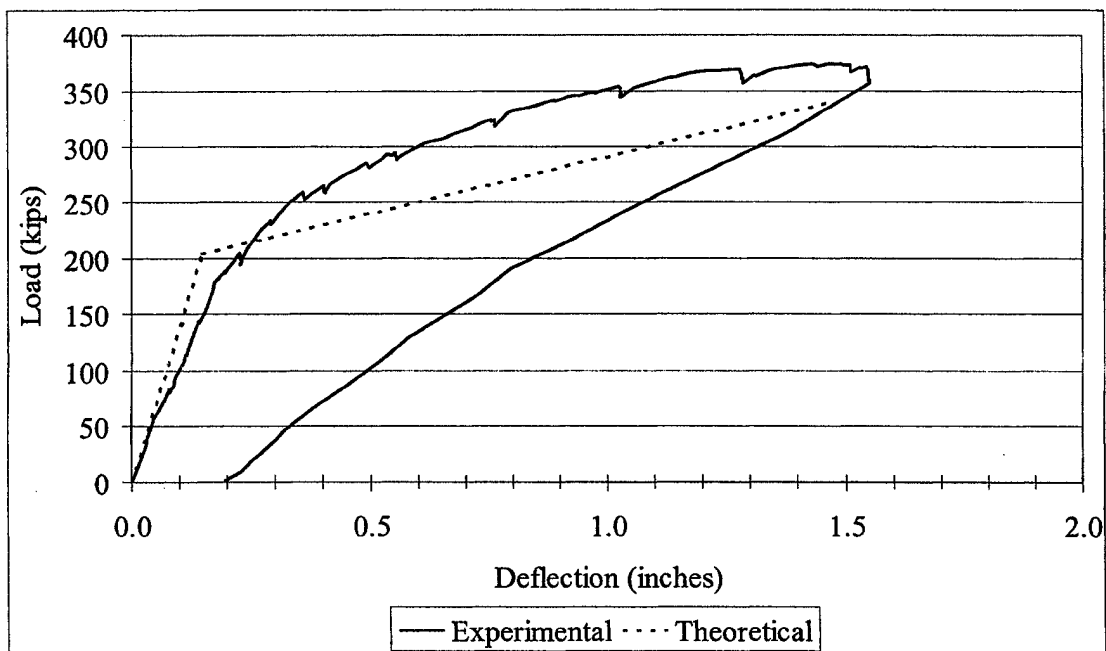
Figure L.23 G1C-Center Load vs. Deflection Plot

529

L.12 Girder Test G2A-East
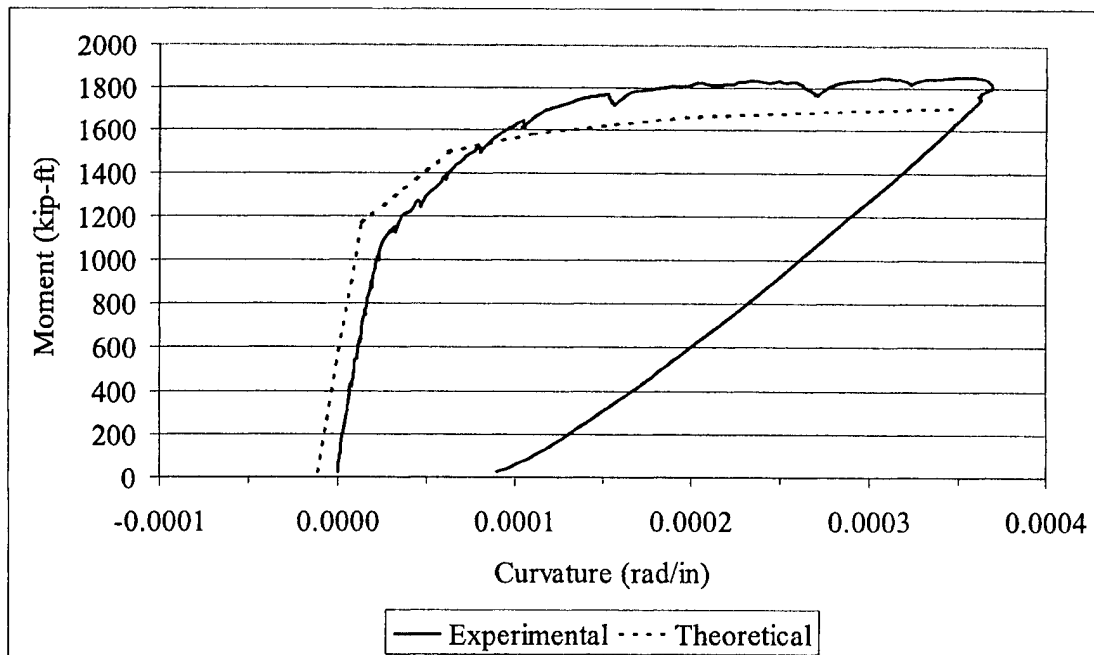

Figure L.24 G2A-East Moment vs. Curvature Plot
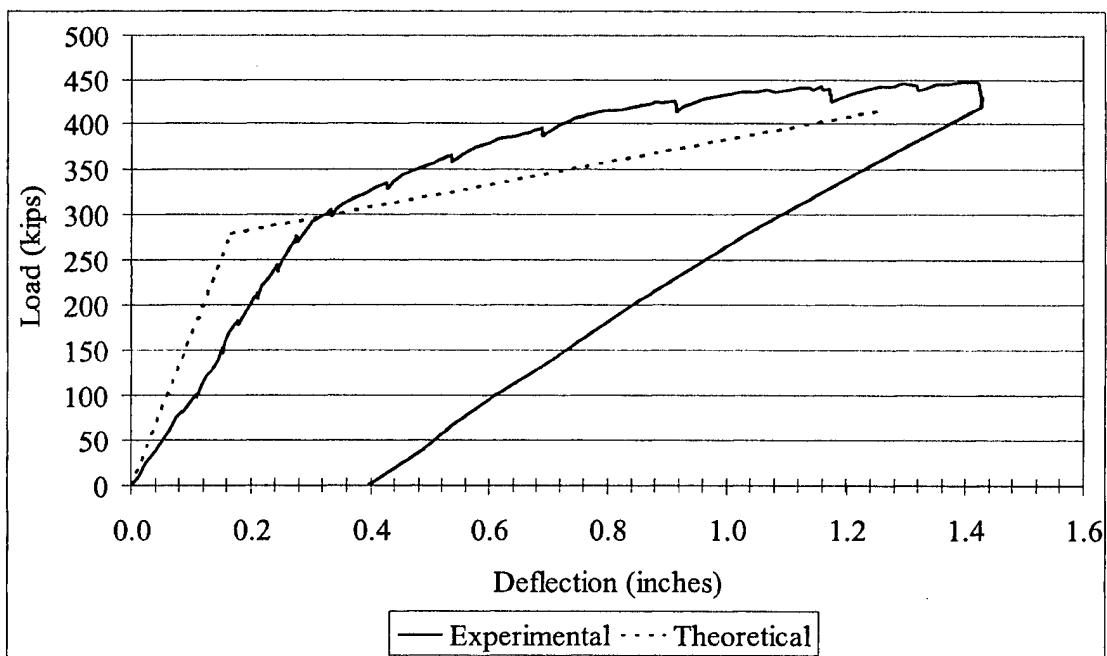
Figure L.25 G2A-East Load vs. Deflection Plot

530

L.13 Girder Test G2A-West
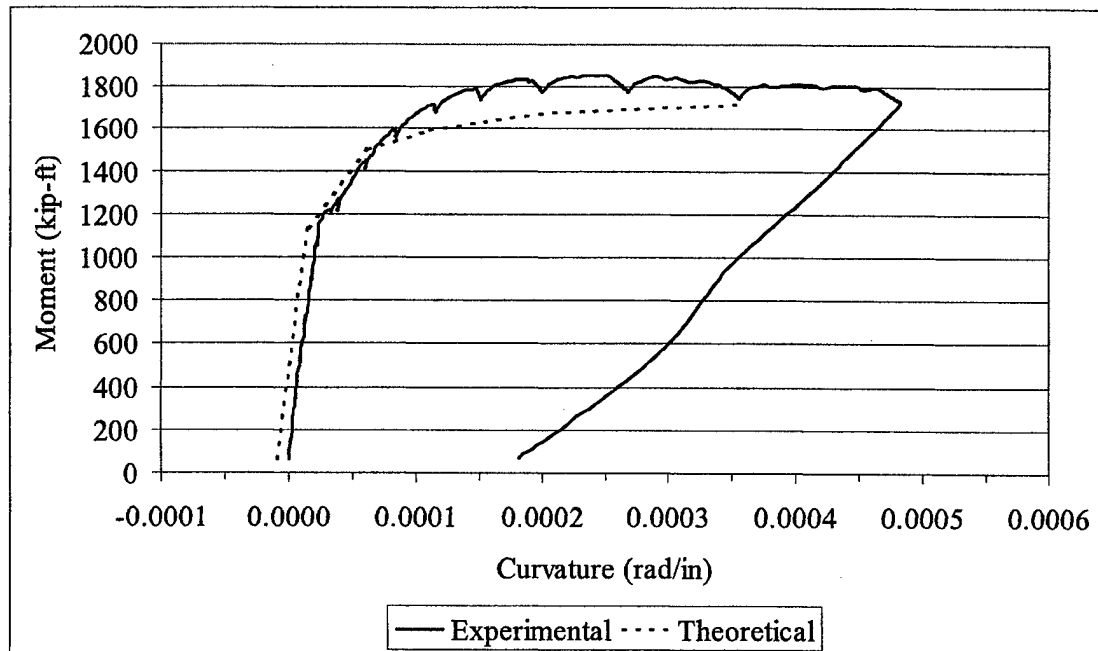
Figure L.26 G2A-West Moment vs. Curvature Plot
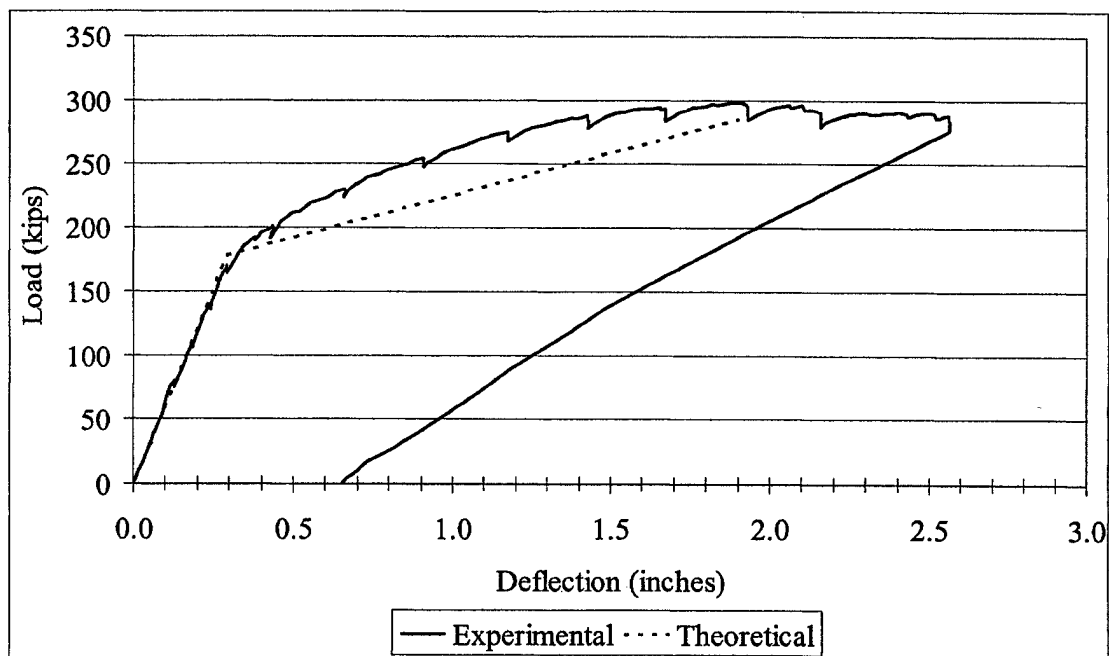
Figure L.27 G2A-West Load vs. Deflection Plot

531

L.14 Girder Test G2A-Center
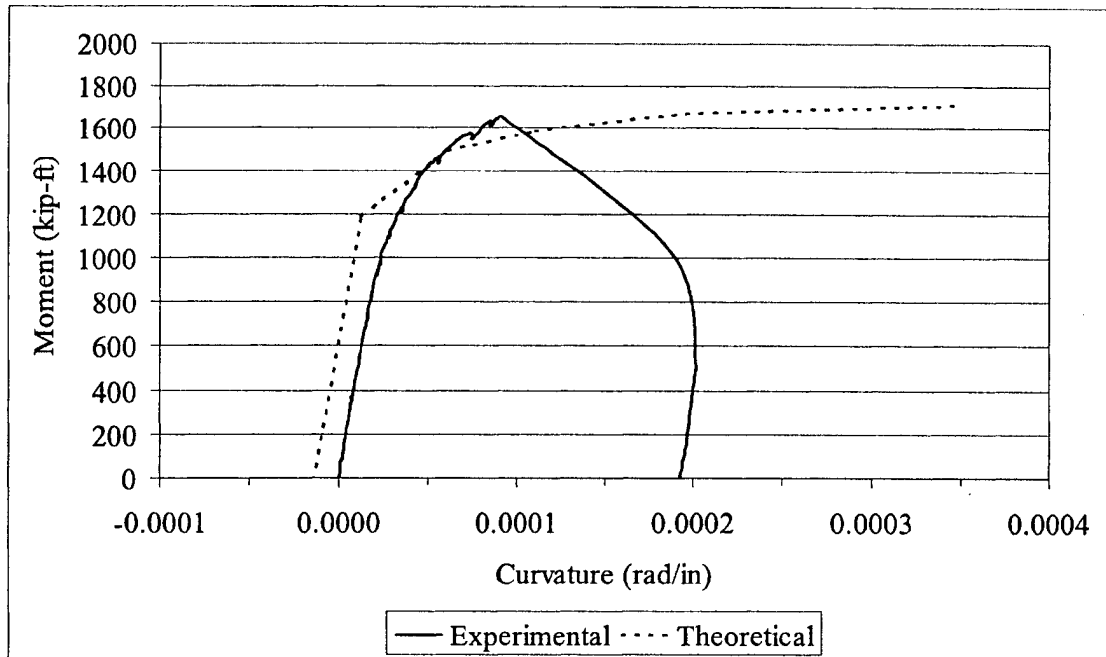
Figure L.28 G2A-Center Moment vs. Curvature Plot
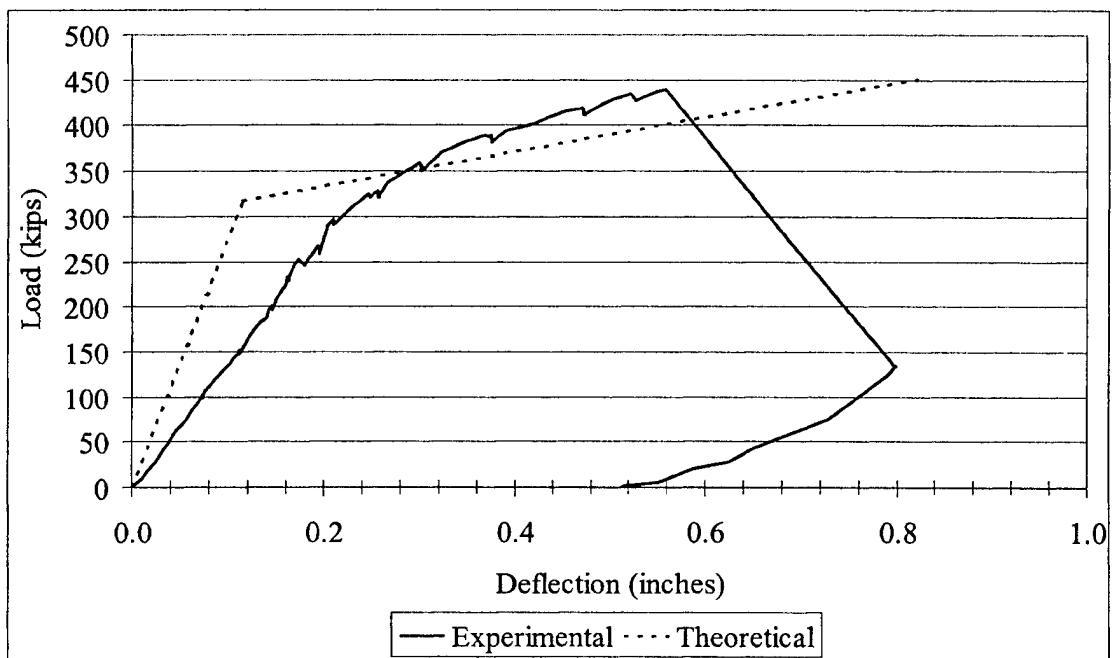
Figure L.29 G2A-Center Load vs. Deflection Plot

L.15 Girder Test G2B-East
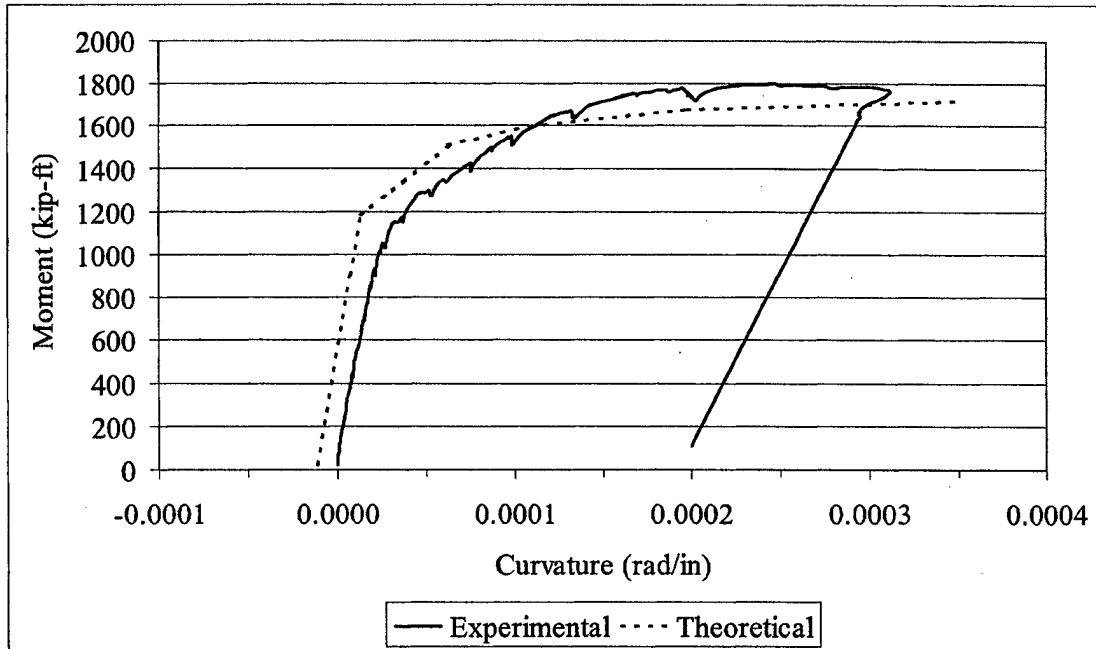
Figure L.30 G2B-East Moment vs. Curvature Plot
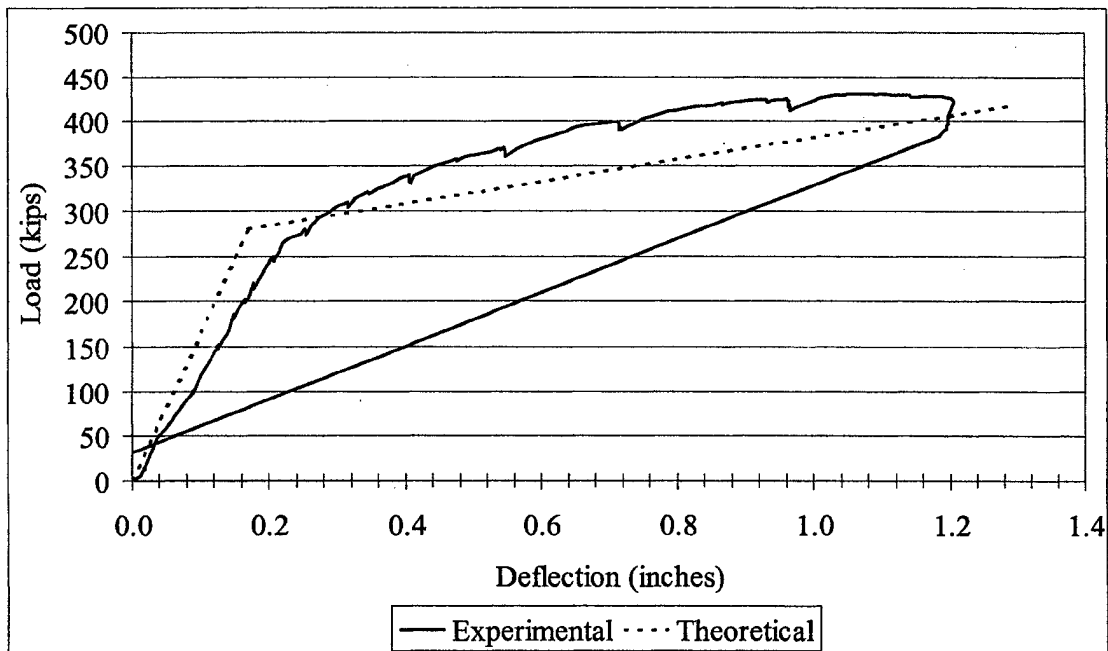
Figure L.31 G2B-East Load vs. Deflection Plot

L.16 Girder Test G2B-West
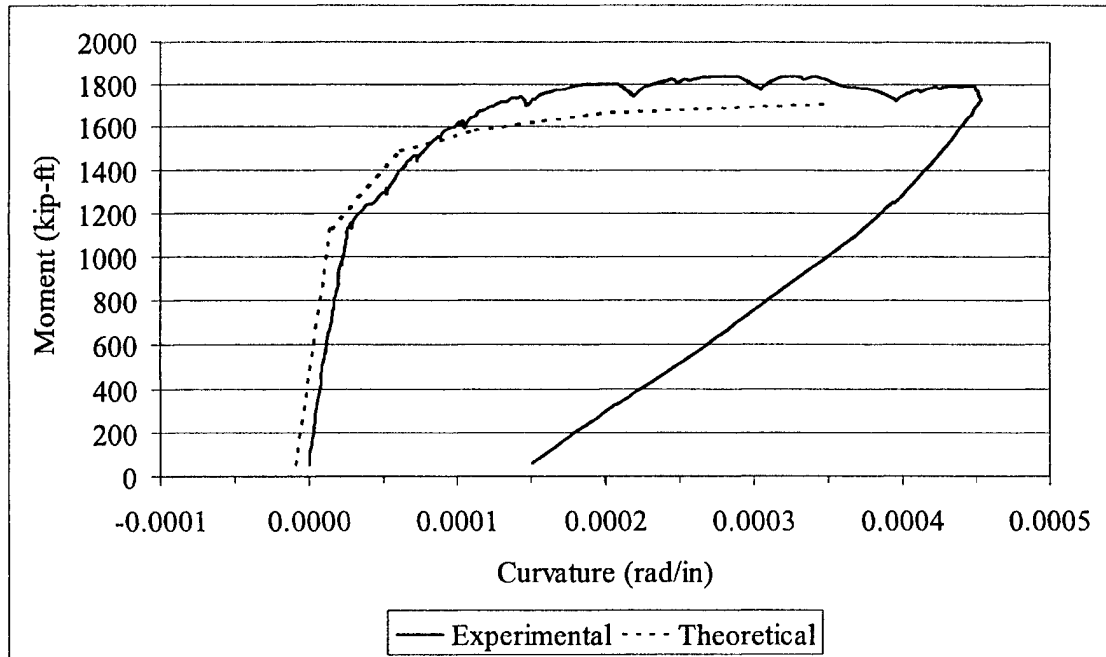

Figure L.32 G2B-West Moment vs. Curvature Plot
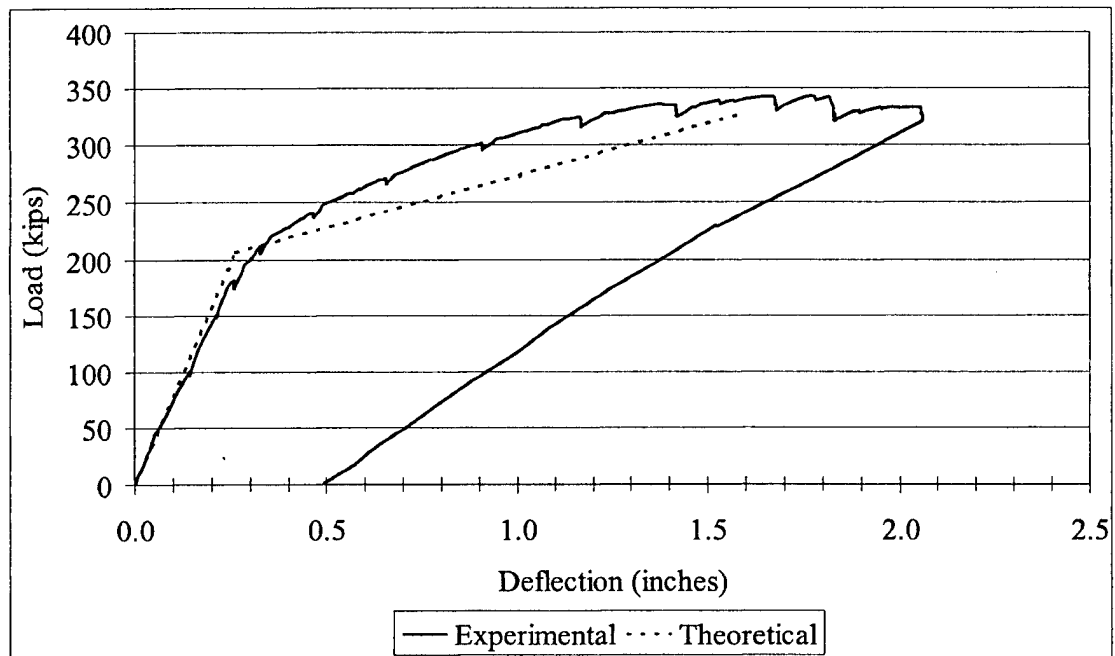
Figure L.33 G2B-West Load vs. Deflection Plot

534

L.17 Girder Test G2B-Center
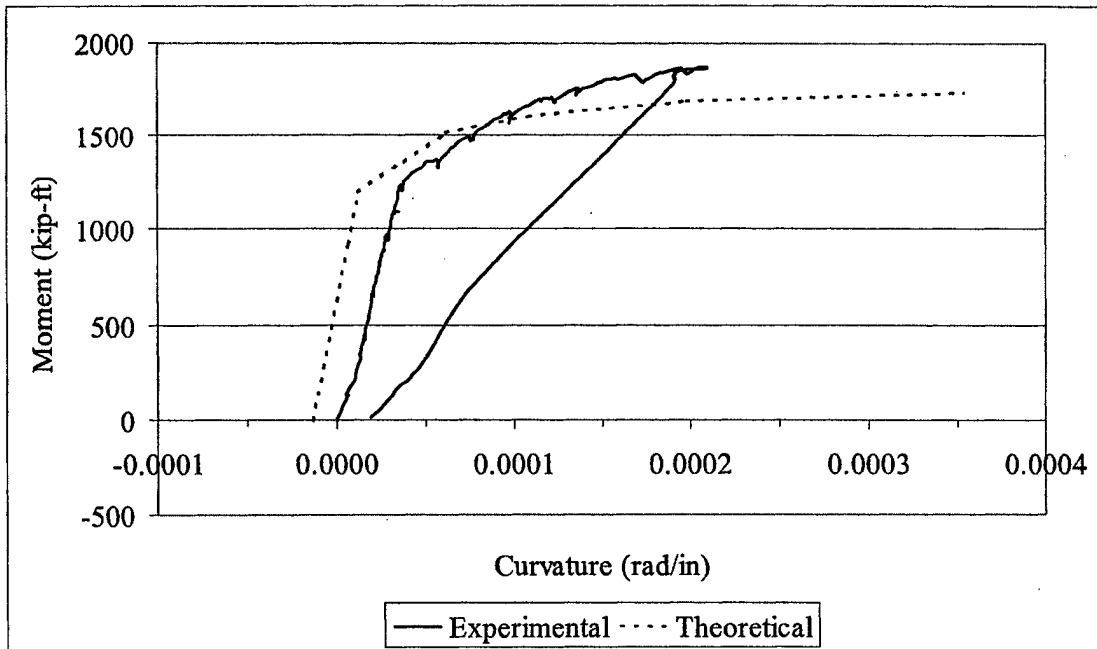
Figure L.34 G2B-Center Moment vs. Curvature Plot
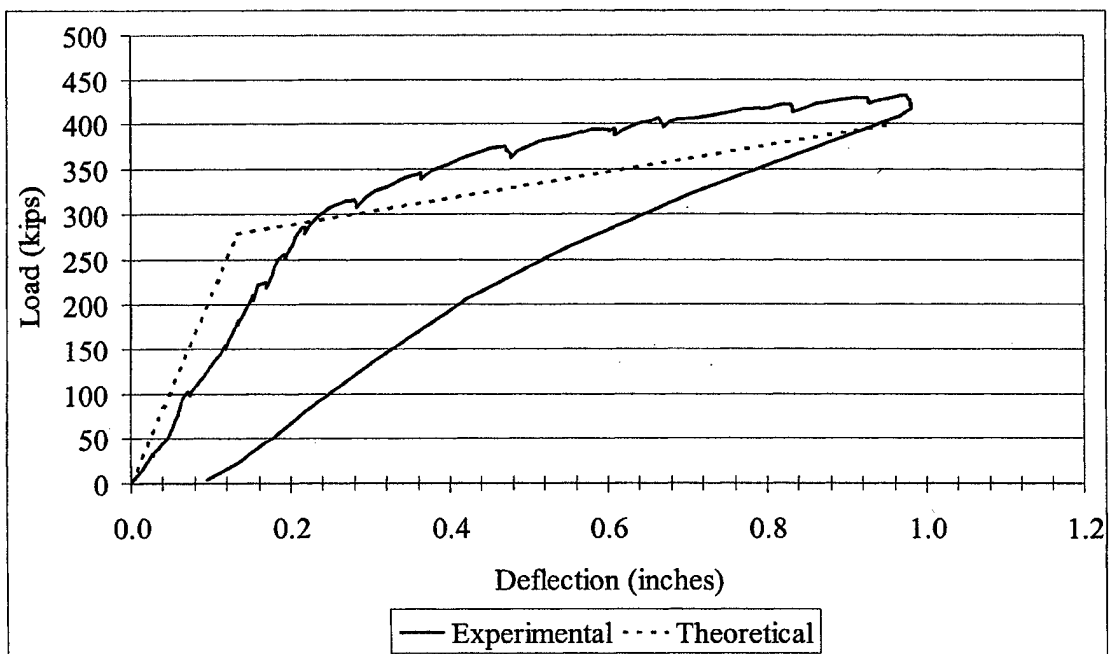
Figure L.35 G2B-Center Load vs. Deflection Plot

535

## L.18 Girder Test G2C-East
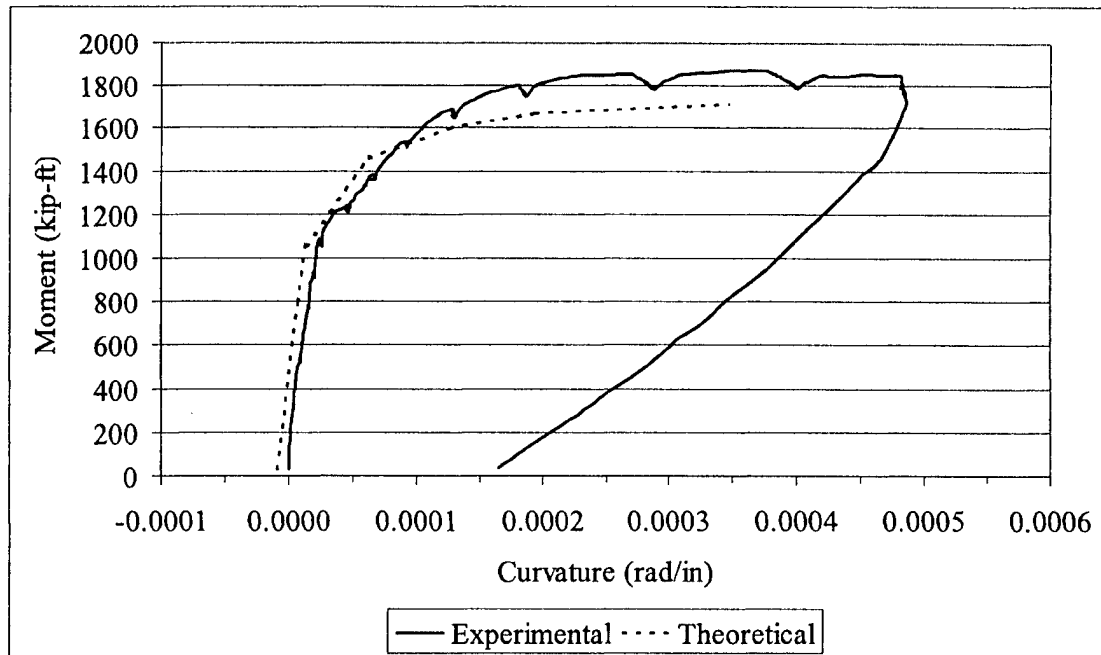
Figure L.36 G2C-East Moment vs. Curvature Plot
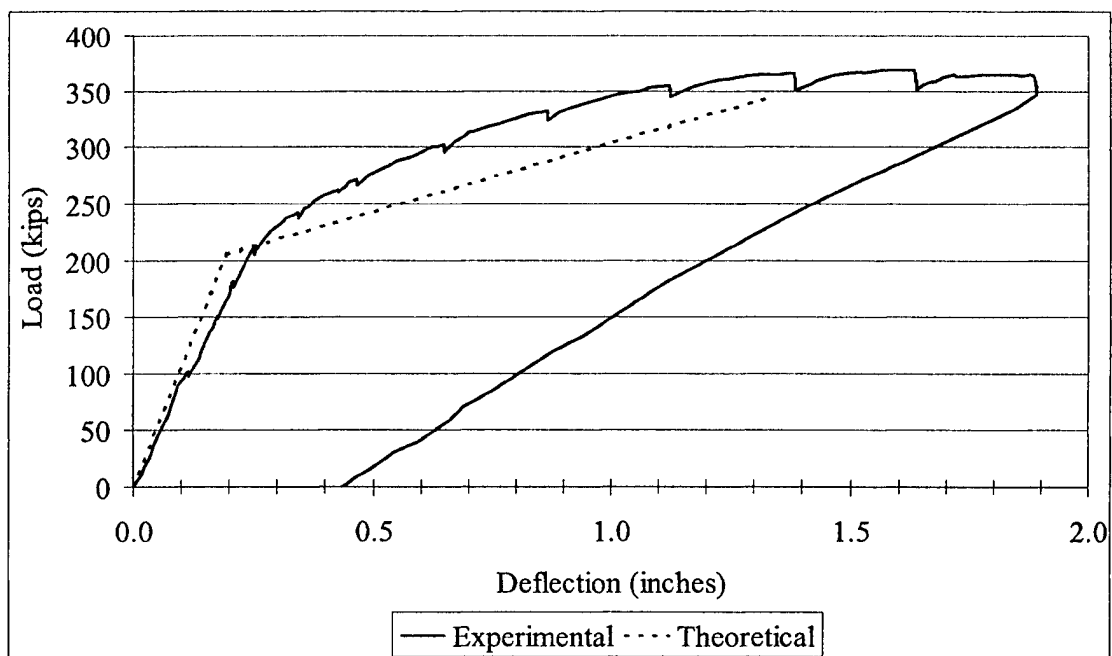
Figure L.37 G2C-East Load vs. Deflection Plot

536

L.19 Girder Test G2C-West
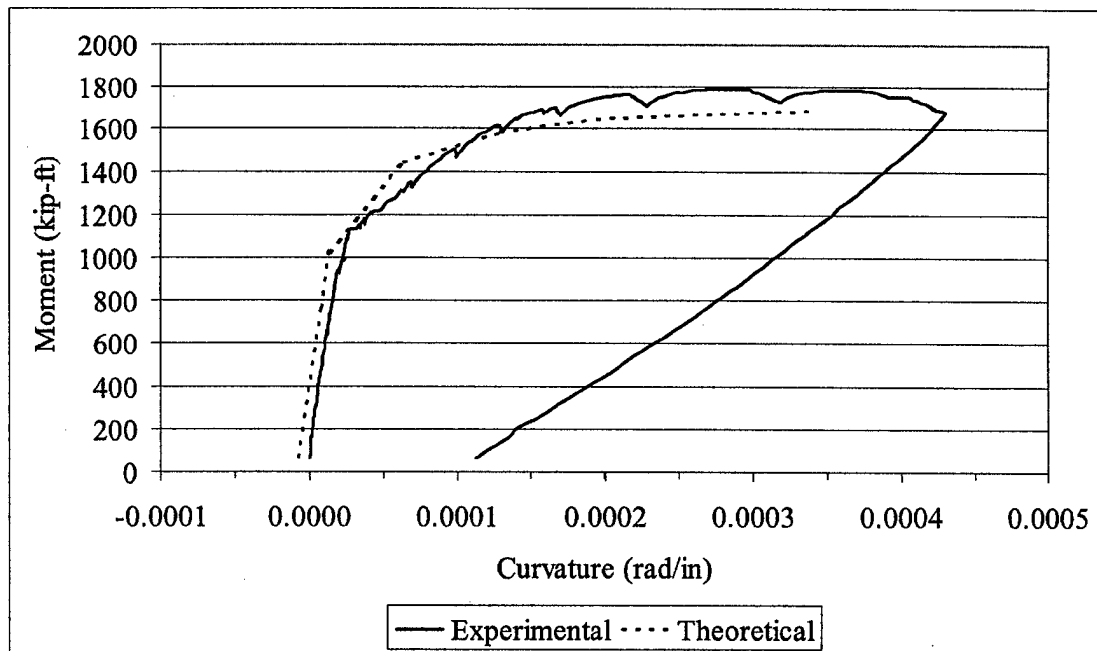
Figure L.38 G2C-West Moment vs. Curvature Plot
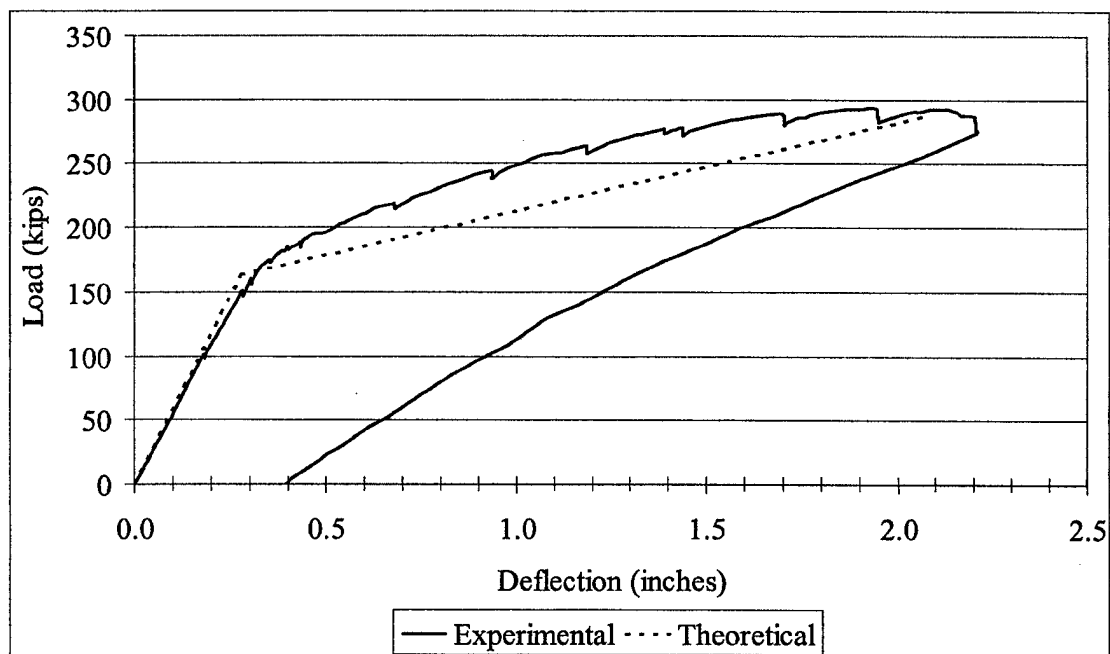
Figure L.39 G2C-West Load vs. Deflection Plot

537

L.20 Girder Test G2C-Center
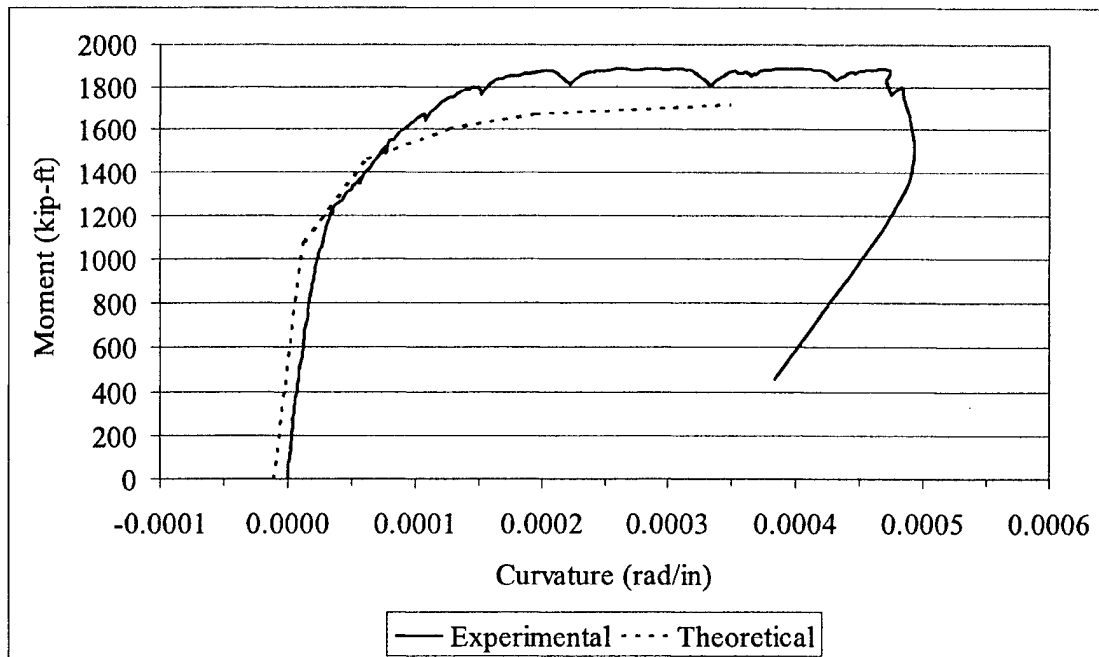
Figure L.40 G2C-Center Moment vs. Curvature Plot
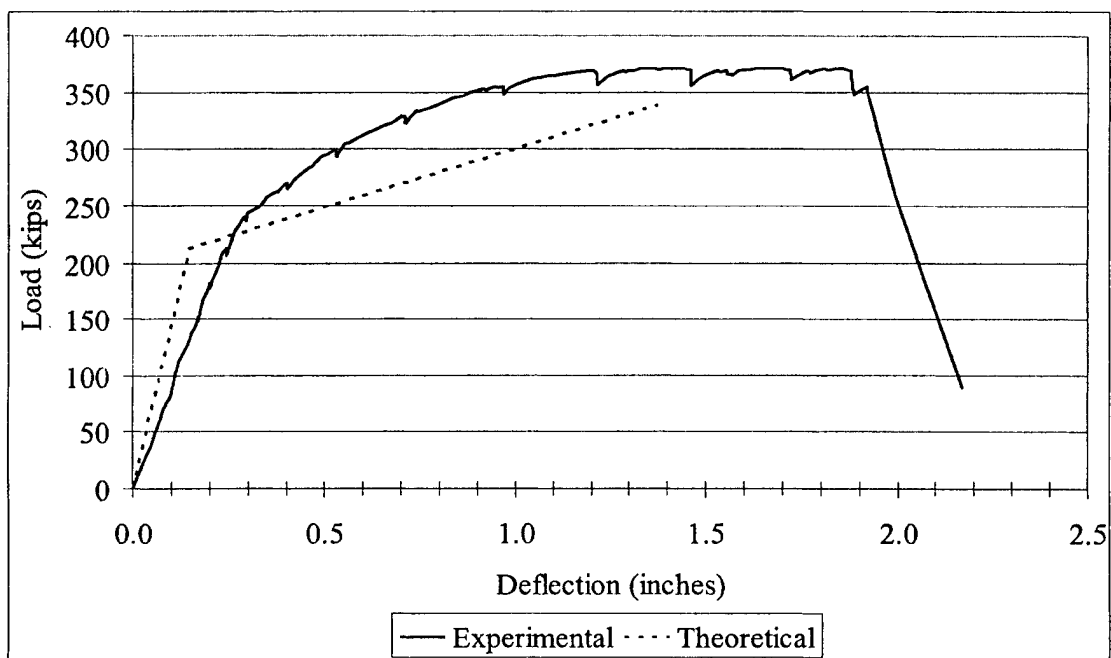
Figure L.41 G2C-Center Load vs. Deflection Plot

APPENDIX M

PHOTOS OF GIRDER CENTER SPAN TESTS

Appendix M contains photos from each center span girder test. Photos of the girder end spans are located in Appendix Q. The photos in this appendix are matched by test configuration. For example, Girder tests G1A-Center and G2A-Center are shown on the same page to allow comparison of test results between the two grades of HSLC.

M.1 Girder Test G1A-Center
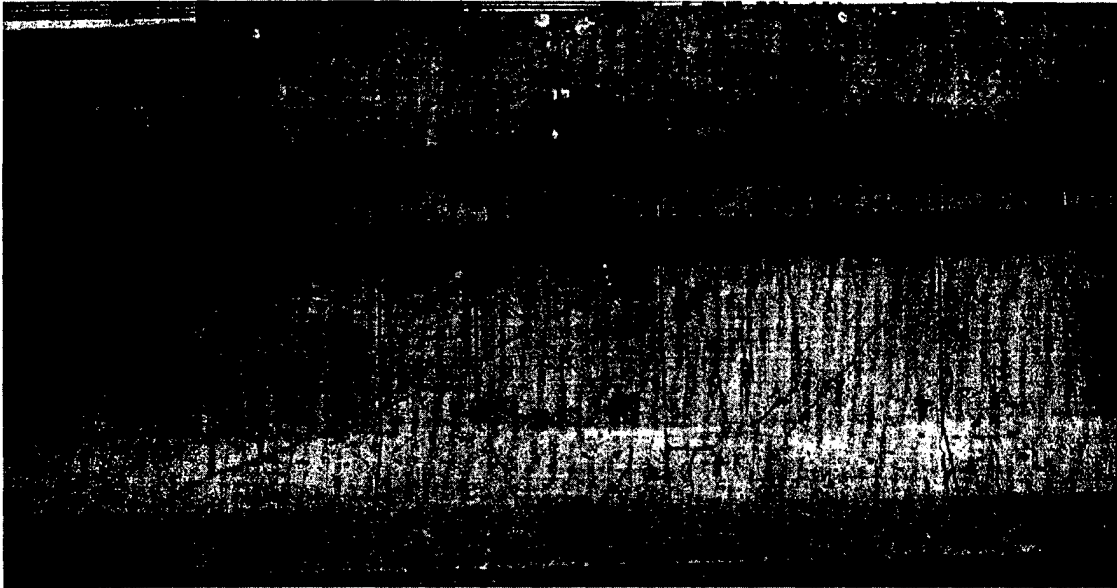
Figure M.1 G1A-Center Crack Patterns

M.2 Girder Test G2A-Center
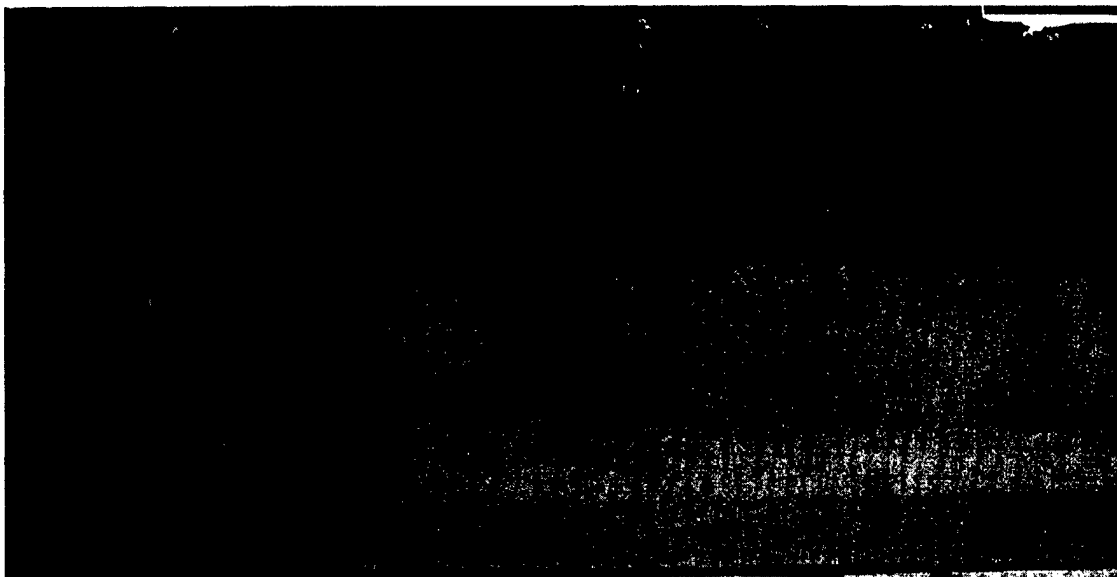
Figure M.2 G2A-Center Crack Patterns

M.3 Girder Test G1B-Center
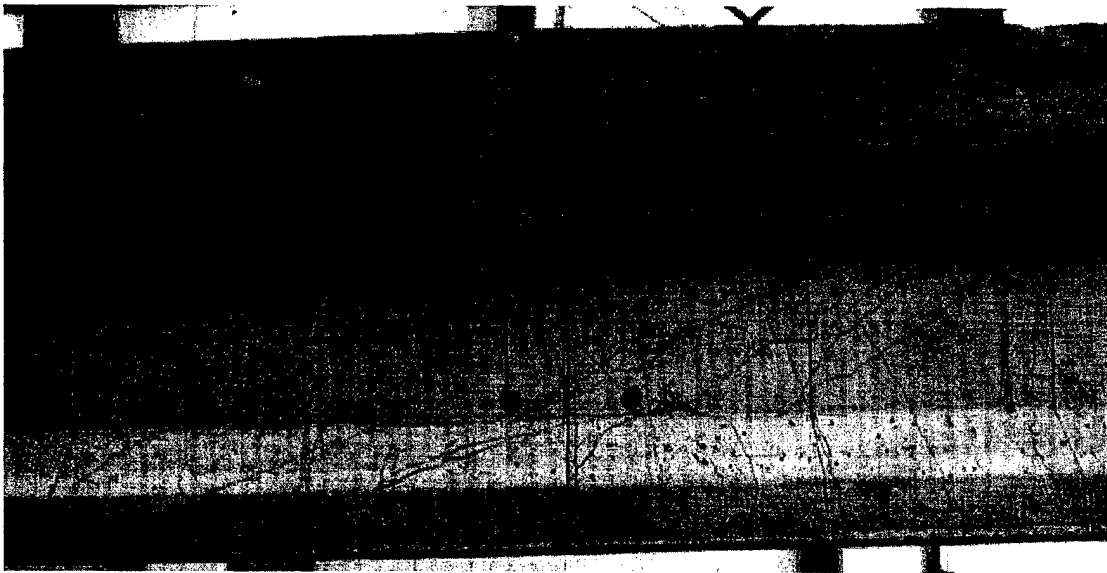
Figure M.3 G1B-Center Crack Patterns

M.4 Girder Test G2B-Center
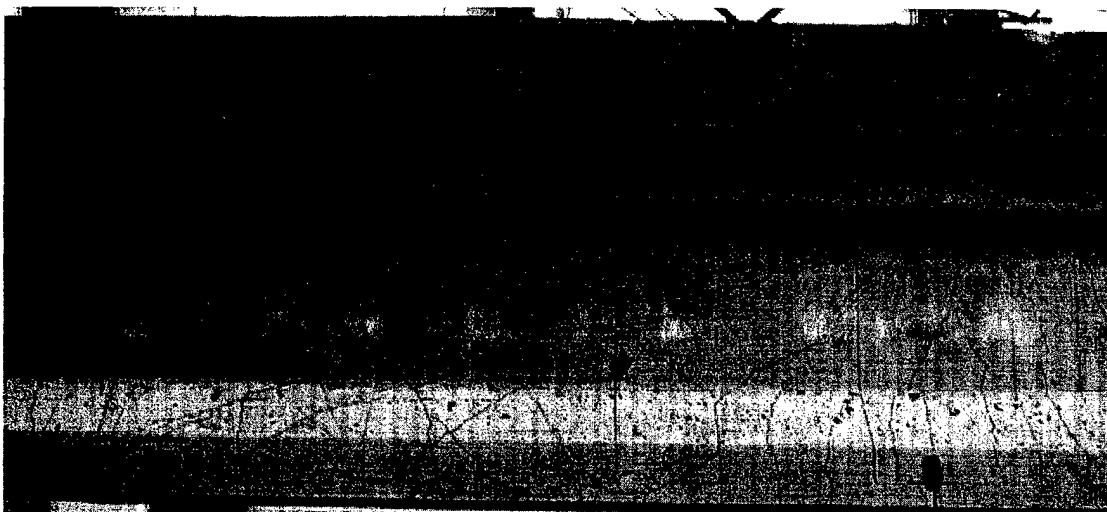
Figure M.4 G2B-Center Crack Patterns

M.5 Girder Test G1C-Center
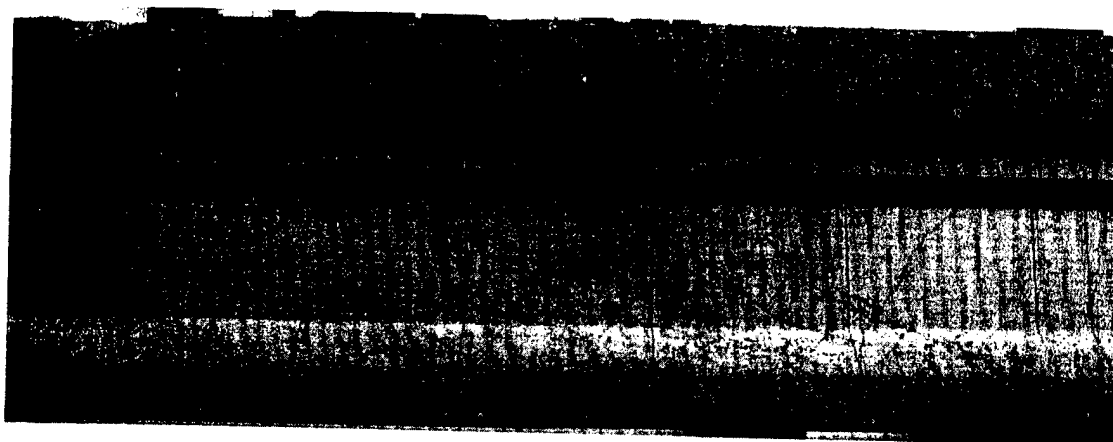
Figure M.5 G1C-Center Crack Patterns

M.6 Girder Test G2C-Center
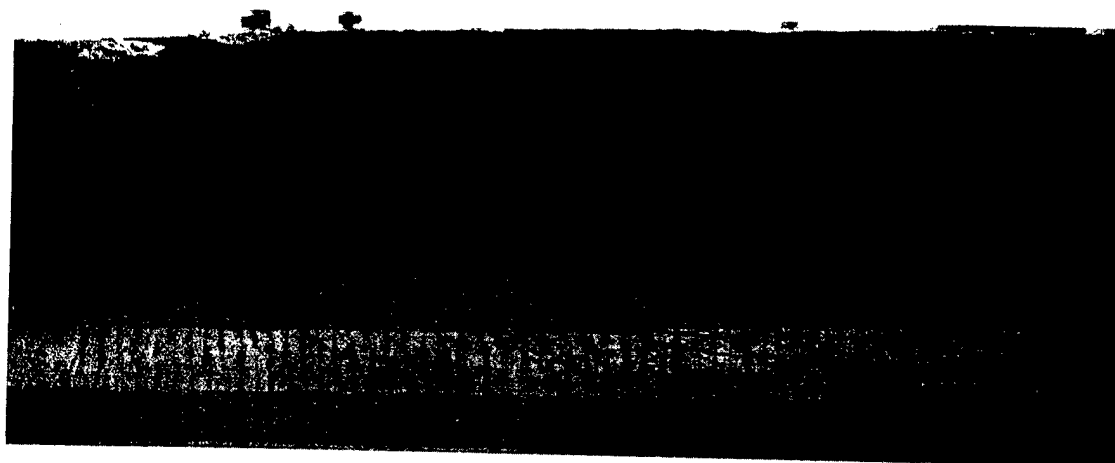
Figure M.6 G2C-Center Crack Patterns

APPENDIX N

VARIABLE ANGLE TRUSS MODEL PLOTS
OF
STRAND FORCE AND BOND STRESS

Appendix N contains plots of strand force and bond stress as predicted using the

variable angle truss model for girder tests that failed due to shear induced by strand slip.

For the girder tests, it was assumed that once the strands were within a distance equal to

one stirrup space from the support that only the bottom eight strands carried the strand

force.

N.1 Girder Test G1A-East
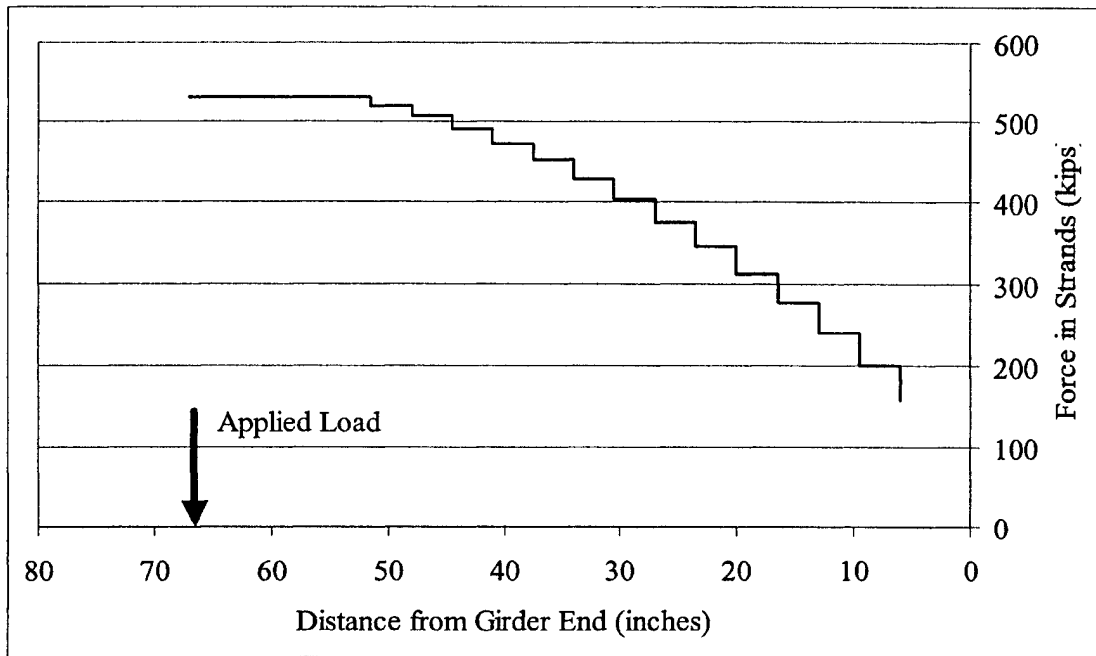
Figure N.1 G1A-East Strand Force Plot
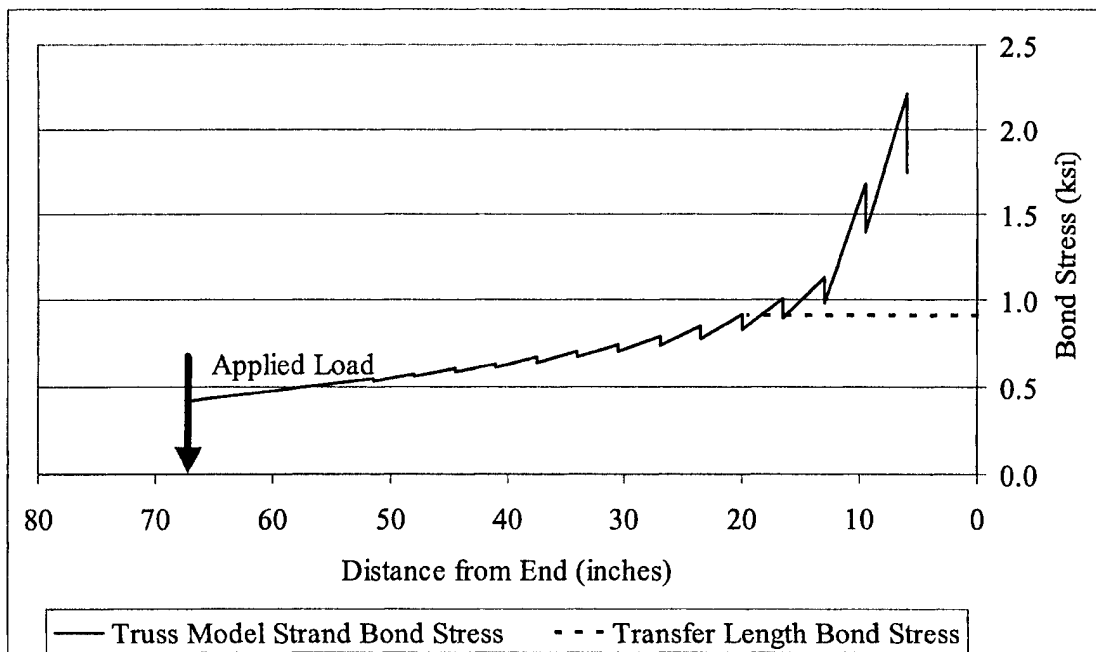
Figure N.2 G1A-East Bond Stress Plot

N.2 Girder Test G1B-East
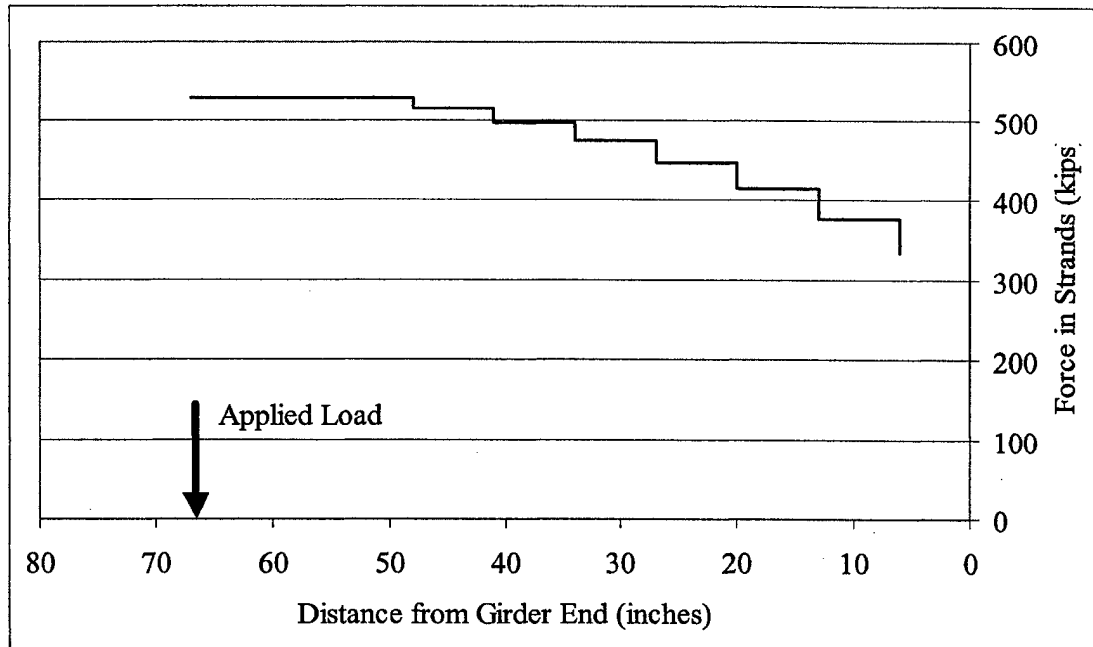
Figure N.3 G1B-East Strand Force Plot
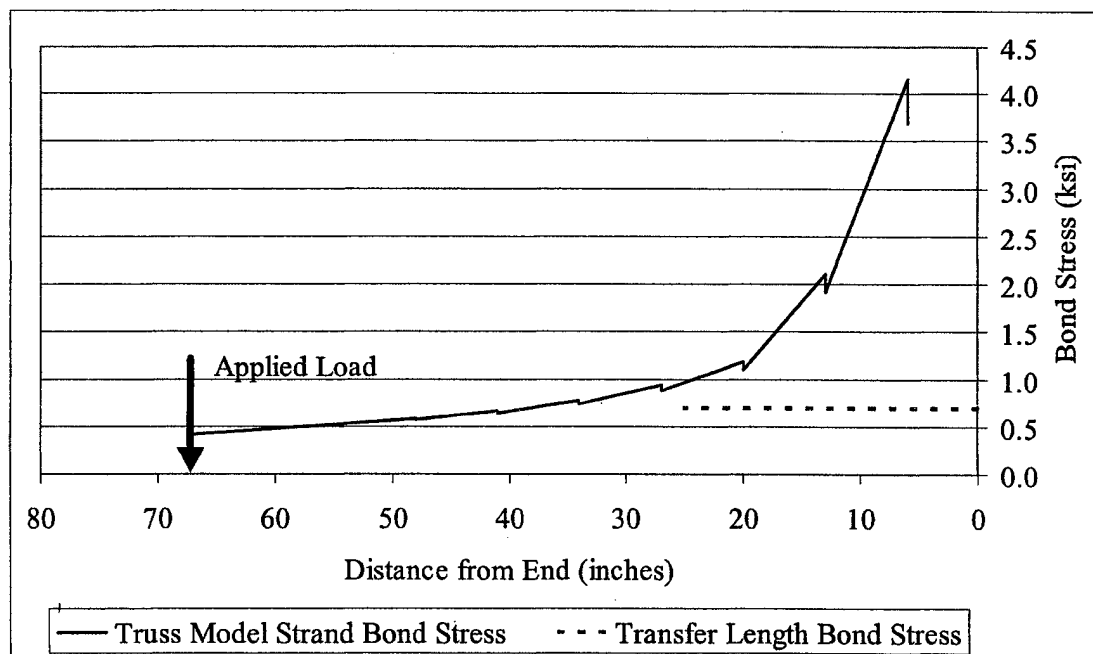
Figure N.4 G1B-East Bond Stress Plot

545

N.3 Girder Test G1C-East
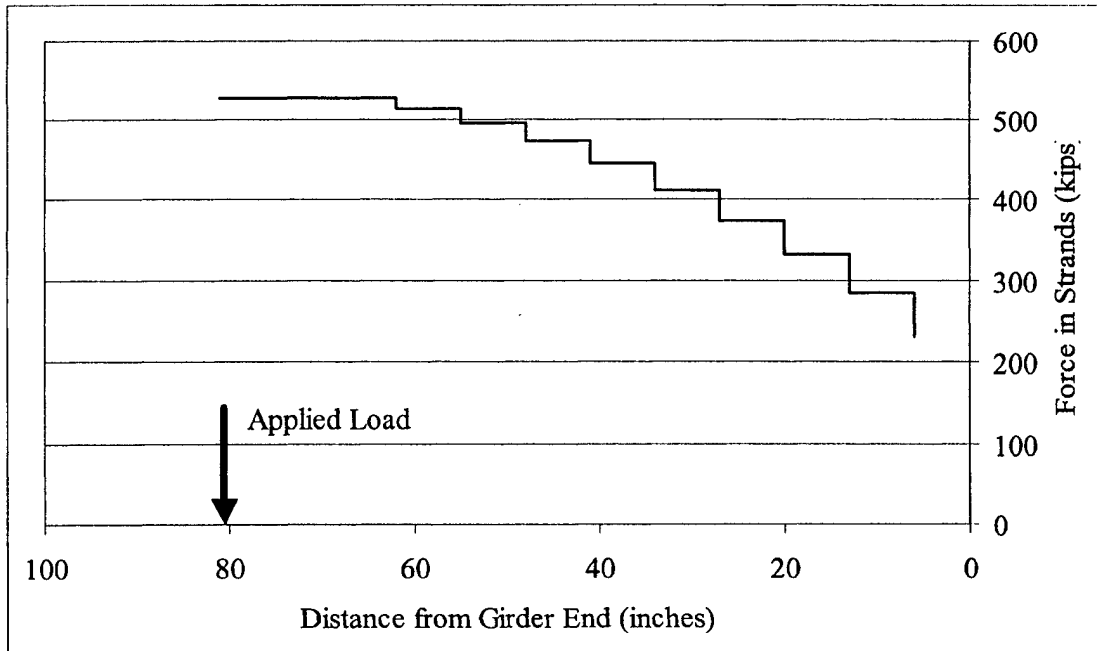
Figure N.5 G1C-East Strand Force Plot
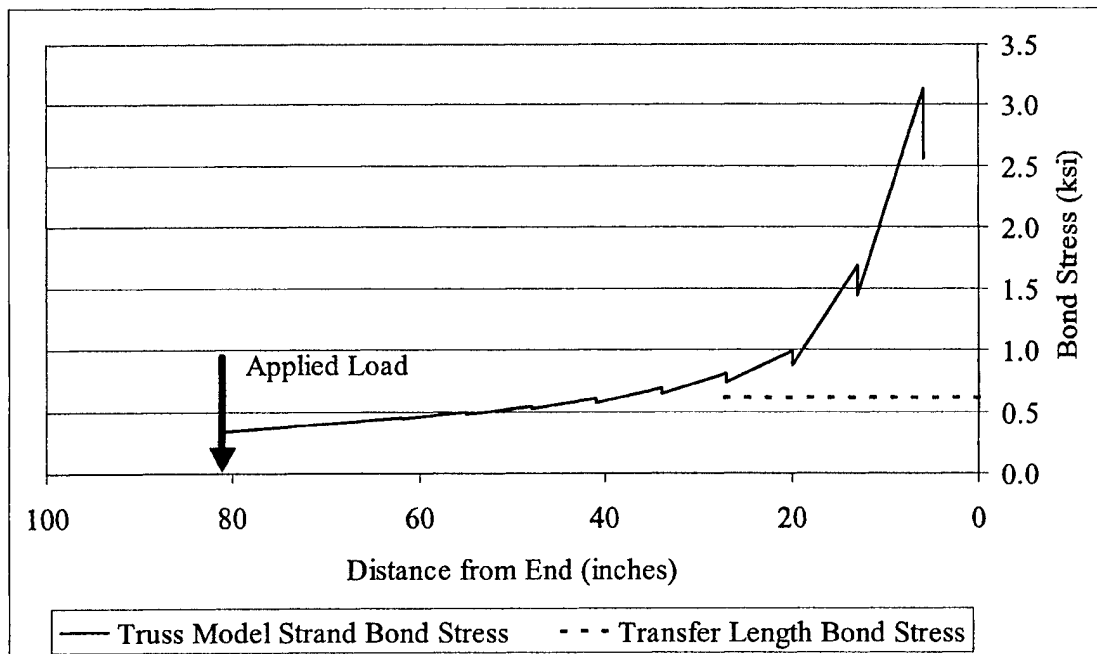
Figure N.6 G1C-East Bond Stress Plot

APPENDIX O

DEVELOPMENT LENGTH DAQ OUTPUT PROCESSING SPREADSHEET

Appendix O contains the individual pages from the Development Length DAQ Output Processing Spreadsheet. This sheet was used to process the DAQ output from the 12 development length tests. The entire set of worksheet pages is provided from development length test G1C-W. The pages are listed in the order the calculations occur. A similar series of worksheets was prepared for each development length test. Listed below are the individual worksheets within the overall spreadsheet and a brief description of the worksheet's function.

Table O.1 – Input Variables – Used to enter information about the development length test. The user enters values in the shaded fields. All other fields are automatic and provide key information about the test. The value for P_{crack} must be determined and entered by the user from the load-displacement curve.

Table O.2 – DAQ Output – A sample of the raw data output from the data acquisition system. Only a small percentage of the total number of DAQ lines is shown.

Table O.3 – Prestressing Strand Tension Test Curve – Used to determine forces and stresses in prestressing strand based on strand strain data.

Table O.4 – Load, Strain, Deflection and Strain Values – Calculates applied load and

shear, vertical deflection, and strain values on the top surface of the deck and at bottom

strand level. Calculates the position of the neutral axis based on a linear strain

distribution assumption.

Table O.5 – Strand Slip – Calculates strand slip values for each strand and the average

slip.

Figure O.1 – Load vs. Vertical Displacement Plot

Figure O.2 – Applied Shear vs. Average Strand Slip

Figure O.3 – Load vs. Top of Deck Strain

Figure O.4 – Load vs. Strand Strain – Calculates total strain in strand by adding the

strain due to effective prestressing and flexural strain due to load application.

Table O.1 Input Variables

Input Variables

Beam #	GHC-W	Test Configuration #	H-4	Date	02-Nov-01

Enter values in blue fields and adjust limits of functions to include all data points in DAQ file.

Support Span	L	50.00 ft	Inches
Shear Distance	a	85.00	Inches
Beam Height	H	36.00	Inches
Composite Bm Ht		47.00	Inches
Deck Width	W_D	103.375	Inches

Top Strand Height	33.50	Inches

Gage Length	24.00 ft	Inches
Top Edge Distance	1.00	Inches

Top LVDT

Stirrup Design	Single	Inches

Girder Test Values			
Initial Cracking Load	P_{crack}	188.00	Kips
Cracking Moment	M_{cr}	1077.64	Ft-Kips
Max Applied Load	P_{max}	299.04	Kips
Nominal Moment	M_n	1760.95	Ft-Kips
Max Deflection	d_{max}	2.27	Inches
Max Deck Strain	e_{cu}	0.0036	in/in
Max Strand Strain	e_{ps}	1.3960	Percent
Max Strand Force	F_{ps}	57.72	Kips

Maximum Strand Slip	
Strand 0	0.0011
Strand 1	0.0018
Strand 2	0.0003
Strand 3	0.0001
Strand 4	0.0002
Strand 5	0.0001
Strand 6	0.0001
Strand 7	0.0002

Inches

Max Avg Strand Slip	0.0001	Inches

Gage Length	24.00 ft	Inches
Bot Edge Distance	3.00	Inches

Bot LVDT

Bot Strand Height	3.00	Inches
Effective Strand Strain	5053	me

0

45

90

Table O.2 DAQ Output

11/02/2001 Load Cell	12:07 PM LVDT Top	LVDT Bot	Wire Pot	LVDT 0	LVDT 45	LVDT 90	LIN 0	LIN 1	LIN 2	LIN 3	LIN 4	LIN 5	LIN 6	LIN 7
11.442372	-0.00048	-0.001137	2.465919	-0.00249	-0.002784	-0.001542	0.002204	0.001449	0.000915	0.000915	0.000883	0.000946	0.000915	0.000946
13.463793	-0.00056	-0.001176	2.461571	-0.002496	-0.00279	-0.001566	0.002267	0.001386	0.000883	0.000915	0.000883	0.000978	0.000946	0.001041
16.630684	-0.000659	-0.00129	2.455239	-0.002484	-0.002856	-0.001548	0.002046	0.001418	0.001009	0.000883	0.000852	0.000978	0.000978	0.001009
27.815872	-0.000462	-0.001888	2.433496	-0.002496	-0.0031	-0.001554	0.002172	0.001512	0.000978	0.000978	0.000915	0.001072	0.000978	0.000946
35.0256	0.000148	-0.00232	2.415492	-0.002477	-0.003245	-0.001554	0.002172	0.001449	0.000946	0.000883	0.000852	0.001009	0.001009	0.000946
34.789768	0.000173	-0.00232	2.415569	-0.002484	-0.00327	-0.00156	0.002172	0.001355	0.000915	0.000883	0.000915	0.000978	0.000852	0.000915
39.236893	0.000457	-0.002524	2.410762	-0.002471	-0.003343	-0.001548	0.002204	0.001386	0.001009	0.000852	0.000852	0.000946	0.000915	0.000978
45.536983	0.001055	-0.002905	2.396878	-0.002477	-0.003495	-0.001566	0.002046	0.001481	0.001009	0.000852	0.000789	0.001009	0.000915	0.000978
48.872326	0.001227	-0.003109	2.392224	-0.002465	-0.003543	-0.001548	0.002078	0.001386	0.000946	0.000978	0.000821	0.001072	0.000883	0.000915
48.653339	0.00127	-0.003121	2.392148	-0.002459	-0.003562	-0.001554	0.002109	0.001386	0.000883	0.000978	0.000821	0.000946	0.000915	0.000978
55.509319	0.001424	-0.003541	2.377653	-0.002453	-0.00372	-0.001573	0.002015	0.001386	0.001009	0.000883	0.000821	0.001072	0.000883	0.000946
61.371441	0.002059	-0.003808	2.368269	-0.002399	-0.003841	-0.001542	0.002204	0.001386	0.000946	0.000978	0.000695	0.000978	0.000915	0.000978
71.697525	0.002632	-0.004393	2.349273	-0.002405	-0.004096	-0.001554	0.002141	0.001449	0.001009	0.000946	0.000883	0.000946	0.000946	0.000946
75.369766	0.003138	-0.004635	2.340576	-0.002393	-0.004175	-0.001535	0.002046	0.001386	0.000946	0.000915	0.000883	0.001009	0.000915	0.000946
78.907257	0.003428	-0.0048	2.332566	-0.002375	-0.004248	-0.001542	0.002046	0.001418	0.001009	0.000852	0.000852	0.000978	0.000915	0.000915
83.1017	0.003797	-0.005105	2.326692	-0.002381	-0.004364	-0.001548	0.002204	0.001418	0.000978	0.000915	0.000821	0.001009	0.000883	0.000978
82.832176	0.003841	-0.005105	2.326615	-0.002363	-0.004364	-0.001535	0.002046	0.001386	0.000883	0.000915	0.000821	0.000978	0.000915	0.001009
82.663727	0.003834	-0.005131	2.326615	-0.002357	-0.004431	-0.001529	0.002046	0.001449	0.000946	0.000852	0.000821	0.000946	0.000852	0.000946
86.20121	0.004118	-0.005334	2.321809	-0.00232	-0.004491	-0.00156	0.002015	0.001481	0.000946	0.000883	0.000789	0.001041	0.000946	0.000946
89.233345	0.004291	-0.005474	2.313188	-0.002357	-0.004577	-0.001548	0.002046	0.001355	0.000915	0.000883	0.000821	0.000946	0.000883	0.000883
92.753983	0.004475	-0.005652	2.308458	-0.00232	-0.004583	-0.001542	0.002109	0.001386	0.001009	0.000883	0.000821	0.000978	0.000852	0.001009
92.551834	0.004728	-0.00569	2.308382	-0.002332	-0.004577	-0.001554	0.002046	0.001323	0.000946	0.000946	0.000883	0.001009	0.000883	0.000883
92.383385	0.004549	-0.005652	2.308382	-0.002314	-0.004589	-0.001554	0.002046	0.001386	0.001041	0.000946	0.000821	0.000946	0.000978	0.000946
92.248627	0.004697	-0.005716	2.308458	-0.002332	-0.004589	-0.001554	0.002078	0.001418	0.001072	0.000978	0.000852	0.000946	0.000852	0.000978
92.181244	0.004636	-0.005678	2.308535	-0.00235	-0.004589	-0.001542	0.002015	0.001355	0.000946	0.000946	0.000852	0.000978	0.000946	0.000946
92.063324	0.004697	-0.005703	2.308306	-0.002338	-0.004577	-0.001554	0.002015	0.001386	0.000915	0.000852	0.000852	0.000978	0.000852	0.000946
91.945412	0.004586	-0.005716	2.308229	-0.002332	-0.004589	-0.001554	0.002078	0.001386	0.001009	0.000915	0.000821	0.000883	0.000915	0.000978
91.878029	0.00463	-0.00569	2.308382	-0.002326	-0.004577	-0.00156	0.002015	0.001386	0.000946	0.000915	0.000946	0.000946	0.000946	0.000978
91.7938	0.00458	-0.005665	2.308535	-0.00232	-0.00457	-0.001554	0.002046	0.001323	0.001009	0.000883	0.000883	0.001041	0.000978	0.000978
91.726425	0.00463	-0.005665	2.308458	-0.002332	-0.004577	-0.001517	0.001984	0.001292	0.001009	0.000883	0.000821	0.000946	0.000883	0.000946
91.591667	0.004599	-0.005665	2.308306	-0.002326	-0.00457	-0.001548	0.002015	0.001449	0.000946	0.000978	0.000852	0.000915	0.000915	0.001009
91.541122	0.004747	-0.00564	2.308306	-0.002332	-0.004589	-0.001548	0.001952	0.001449	0.000915	0.000883	0.000852	0.000978	0.000946	0.000978
91.507439	0.004691	-0.005665	2.308458	-0.002326	-0.004552	-0.001542	0.002015	0.001386	0.000883	0.000946	0.000852	0.000978	0.000915	0.000978
91.440056	0.00458	-0.005665	2.308382	-0.002344	-0.00457	-0.001542	0.001984	0.001355	0.000978	0.000946	0.000852	0.000883	0.000915	0.000915
91.372681	0.00458	-0.005601	2.308382	-0.002344	-0.00457	-0.001554	0.001984	0.001418	0.001009	0.000946	0.000789	0.001009	0.000852	0.001009
91.30529	0.004389	-0.005678	2.308535	-0.00235	-0.00457	-0.00156	0.001984	0.001481	0.000978	0.000883	0.000852	0.001041	0.000915	0.000915
91.288452	0.004482	-0.005652	2.308382	-0.002344	-0.004564	-0.001554	0.002078	0.001418	0.000978	0.000978	0.000821	0.001009	0.000946	0.000946
91.187378	0.004531	-0.005665	2.308382	-0.002332	-0.004546	-0.001548	0.002046	0.001418	0.000915	0.000915	0.000789	0.000978	0.000852	0.000915
91.120003	0.004475	-0.005652	2.308535	-0.002296	-0.004552	-0.001554	0.001984	0.001386	0.000946	0.000978	0.000883	0.000946	0.000915	0.000883

Table O.3 Prestressing Strand Tension Curve

Prestressing Strand Tension Test Curve and Zone Limit Data

Strain -Stress Curve for 0.6" 270 KSI LOLAX Strand

$$y = 0.8063x + 56.5921$$
$$R^2 = 1.0000$$

$$y = 95.9317x^3 - 348.9161x^2 + 423.6514x - 114.2059$$
$$R^2 = 0.9985$$

$$y = 63.7701x + 0.0000$$
$$R^2 = 1.0000$$

Load (Kips) — Strain (Percent)

♦ Elastic   ■ Transition   ▲ Plastic   —Linear (Elastic)   —Linear (Plastic)   —Poly. (Transition)

Prestressing Strand Loading Data		
Point of Loading	Strain (%)	Load (Kips)
Start of Elastic	0	0.00
End of Elastic	0.7135	45.50
Transition 1	0.7500	47.45
Transition 2	0.8750	53.63
Transition 3	1.0000	56.67
Transition 4	1.1250	57.20
Start of Plastic	1.2500	57.60
End of Plastic	6.5000	61.83

Zone	Percent Strain		
Elastic	0	< e <	0.7135
Transition	0.7135	< e <	1.2500
Plastic	1.2500	> e	

Zone	Load		
Elastic	0	< Kips <	45.50
Transition	45.50	< Kips <	57.60
Plastic	57.60	> Kips	

Table O.4 Load, Shear, Deflection and Strain Values

Load, Shear, Deflection and Strain Values

Data Point #	Load (Kips)	Shear (Kips)	At Point of Loading					Neutral Axis Location (Inches from Bot)	Adjusted Values (Linear Assumption)		
			Top LVDT (Inches) Compression e=(-)	Top Strain (m-strain) Compression e=(-)	Bot LVDT (Inches) Tension e=(+)	Bot Strain (m-strain) Tension e=(+)	Vertical Deflection (Inches)		Top of Slab (in/in)	At Level of Bottom Strands (m-strain)	Total Strand Strain (percent strain)
0	0.0	0.0	0.000000	0.00	0.000000	0.00	0.000000	NA	0.00	0.00	0.505
1	2.0	1.7	-0.000080	3.33	-0.000039	1.63	0.004348	17.38	0.00000	1.63	0.505
2	5.2	4.3	-0.000179	7.46	-0.000153	6.38	0.010680	23.22	-0.00001	6.38	0.506
3	16.4	13.6	0.000018	-0.75	-0.000751	31.29	0.032423	45.85	0.00000	31.29	0.508
4	23.6	19.6	0.000628	-26.17	-0.001183	49.29	0.050427	31.66	0.00003	49.29	0.510
5	23.3	19.4	0.000653	-27.21	-0.001183	49.29	0.050350	31.27	0.00003	49.29	0.510
6	27.8	23.1	0.000937	-39.04	-0.001387	57.79	0.055157	29.19	0.00004	57.79	0.511
7	34.1	28.3	0.001535	-63.96	-0.001768	73.67	0.069041	26.49	0.00007	73.67	0.513
8	37.4	31.1	0.001707	-71.13	-0.001972	82.17	0.073695	26.52	0.00007	82.17	0.514
9	37.2	30.9	0.001750	-72.92	-0.001984	82.67	0.073771	26.31	0.00008	82.67	0.514
10	44.1	36.6	0.001904	-79.33	-0.002404	100.17	0.088266	27.48	0.00008	100.17	0.515
11	49.9	41.5	0.002539	-105.79	-0.002671	111.29	0.097650	25.49	0.00011	111.29	0.516
12	60.3	50.1	0.003112	-129.67	-0.003256	135.67	0.116646	25.43	0.00014	135.67	0.519
13	63.9	53.1	0.003618	-150.75	-0.003498	145.75	0.125343	24.57	0.00016	145.75	0.520
14	67.5	56.1	0.003908	-162.83	-0.003663	152.63	0.133353	24.23	0.00017	152.63	0.521
15	71.7	59.6	0.004277	-178.21	-0.003968	165.33	0.139227	24.12	0.00019	165.33	0.522
16	71.4	59.3	0.004321	-180.04	-0.003968	165.33	0.139304	24.00	0.00019	165.33	0.522
17	71.2	59.2	0.004314	-179.75	-0.003994	166.42	0.139304	24.09	0.00019	166.42	0.522
18	74.8	62.2	0.004598	-191.58	-0.004197	174.88	0.144110	23.94	0.00020	174.88	0.523
19	77.8	64.7	0.004771	-198.79	-0.004337	180.71	0.152731	23.89	0.00021	180.71	0.523
20	81.3	67.6	0.004955	-206.46	-0.004515	188.13	0.157461	23.92	0.00022	188.13	0.524
21	81.1	67.4	0.005208	-217.00	-0.004553	189.71	0.157537	23.47	0.00023	189.71	0.524
22	80.9	67.3	0.005029	-209.54	-0.004515	188.13	0.157537	23.76	0.00022	188.13	0.524
23	80.8	67.2	0.005177	-215.71	-0.004579	190.79	0.157461	23.59	0.00022	190.79	0.524
24	80.7	67.1	0.005116	-213.17	-0.004541	189.21	0.157384	23.63	0.00022	189.21	0.524
25	80.6	67.0	0.005177	-215.71	-0.004566	190.25	0.157613	23.56	0.00022	190.25	0.524
26	80.5	66.9	0.005066	-211.08	-0.004579	190.79	0.157690	23.83	0.00022	190.79	0.524
27	80.4	66.9	0.005110	-212.92	-0.004553	189.71	0.157537	23.67	0.00022	189.71	0.524
28	80.4	66.8	0.005060	-210.83	-0.004528	188.67	0.157384	23.72	0.00022	188.67	0.524
29	80.3	66.7	0.005110	-212.92	-0.004528	188.67	0.157461	23.61	0.00022	188.67	0.524
30	80.1	66.6	0.005079	-211.63	-0.004528	188.67	0.157613	23.68	0.00022	188.67	0.524
31	80.1	66.6	0.005227	-217.79	-0.004503	187.63	0.157613	23.31	0.00023	187.63	0.524
32	80.1	66.6	0.005171	-215.46	-0.004528	188.67	0.157461	23.48	0.00022	188.67	0.524
33	80.0	66.5	0.005060	-210.83	-0.004528	188.67	0.157537	23.72	0.00022	188.67	0.524
34	79.9	66.4	0.005060	-210.83	-0.004464	186.00	0.157537	23.56	0.00022	186.00	0.524

Table O.5 Strand Slip

Strand Slip

Data Point #	Applied Shear (kips)	Strand Slip Indicators								Avg Slip (Inches)
		LIN 0 (Inches)	LIN 1 (Inches)	LIN 2 (Inches)	LIN 3 (Inches)	LIN 4 (Inches)	LIN 5 (Inches)	LIN 6 (Inches)	LIN 7 (Inches)	
0	0.0	0.000000	0.000000	0.000000	0.000000	0.000000	0.000000	0.000000	0.000000	0.000000
1	1.7	0.000063	-0.000063	-0.000032	0.000000	0.000000	0.000032	0.000031	0.000095	0.000016
2	4.3	-0.000158	-0.000031	0.000094	-0.000032	-0.000031	0.000032	0.000063	0.000063	0.000000
3	13.6	-0.000032	0.000063	0.000063	0.000063	0.000032	0.000126	0.000063	0.000000	0.000047
4	19.6	-0.000032	0.000000	0.000031	-0.000032	-0.000031	0.000063	0.000094	0.000031	0.000012
5	19.4	-0.000032	-0.000094	0.000000	-0.000032	0.000032	0.000032	-0.000063	-0.000031	-0.000024
6	23.1	0.000000	-0.000063	0.000094	-0.000063	-0.000031	0.000000	0.000000	0.000032	-0.000004
7	28.3	-0.000158	0.000032	0.000094	-0.000063	-0.000094	0.000063	0.000000	0.000032	-0.000012
8	31.1	-0.000126	-0.000063	0.000031	0.000063	-0.000062	0.000126	0.000032	-0.000031	-0.000012
9	30.9	-0.000095	-0.000063	-0.000032	0.000063	-0.000062	0.000000	0.000000	0.000032	-0.000020
10	36.6	-0.000189	-0.000063	0.000063	-0.000032	-0.000062	0.000126	-0.000032	0.000000	-0.000024
11	41.5	0.000000	-0.000063	0.000094	-0.000032	-0.000188	0.000032	-0.000032	0.000032	-0.000020
12	50.1	-0.000063	-0.000063	0.000031	0.000063	0.000000	0.000000	0.000000	0.000000	-0.000004
13	53.1	-0.000158	0.000000	0.000031	0.000031	0.000000	0.000063	0.000031	0.000000	0.000000
14	56.1	-0.000158	-0.000063	0.000094	0.000000	0.000000	0.000032	0.000000	-0.000031	-0.000015
15	59.6	0.000000	-0.000031	0.000063	-0.000063	-0.000031	0.000063	-0.000032	0.000032	0.000000
16	59.3	-0.000158	-0.000031	-0.000032	0.000000	-0.000062	0.000032	0.000000	0.000063	-0.000024
17	59.2	-0.000158	-0.000063	0.000031	-0.000063	-0.000062	0.000000	-0.000063	0.000000	-0.000039
18	62.2	-0.000189	0.000000	0.000031	-0.000063	-0.000062	0.000095	0.000031	0.000000	-0.000020
19	64.7	-0.000158	0.000032	0.000000	-0.000032	-0.000094	0.000000	-0.000032	-0.000063	-0.000043
20	67.6	-0.000095	-0.000094	0.000031	-0.000032	-0.000062	0.000032	-0.000063	0.000063	-0.000028
21	67.4	-0.000158	-0.000063	0.000094	-0.000032	0.000062	0.000063	-0.000032	-0.000063	-0.000024
22	67.3	-0.000158	-0.000126	0.000031	-0.000031	-0.000062	0.000000	0.000063	0.000000	-0.000028
23	67.2	-0.000126	-0.000031	0.000126	0.000031	-0.000031	0.000000	-0.000063	0.000032	-0.000008
24	67.1	-0.000189	-0.000094	0.000157	0.000063	-0.000031	0.000032	0.000031	0.000000	-0.000004
25	67.0	-0.000189	-0.000063	0.000031	0.000031	-0.000031	0.000032	-0.000063	0.000000	-0.000032
26	66.9	-0.000126	-0.000063	0.000000	-0.000063	-0.000062	-0.000063	0.000000	0.000032	-0.000043
27	66.9	-0.000189	-0.000063	0.000031	0.000000	0.000063	0.000000	0.000031	0.000032	-0.000012
28	66.8	-0.000158	-0.000126	0.000094	0.000031	0.000000	0.000095	0.000031	0.000032	0.000000
29	66.7	-0.000220	-0.000157	0.000094	-0.000032	-0.000062	0.000000	0.000063	0.000000	-0.000039
30	66.6	-0.000189	0.000000	0.000031	0.000063	-0.000031	-0.000031	0.000032	-0.000063	-0.000032
31	66.6	-0.000252	0.000000	0.000000	0.000032	-0.000031	0.000032	0.000031	0.000032	-0.000028
32	66.6	-0.000189	-0.000063	-0.000032	0.000031	-0.000031	0.000032	0.000000	0.000032	-0.000028
33	66.5	-0.000220	-0.000094	0.000063	0.000031	-0.000031	-0.000063	0.000000	-0.000031	-0.000043
34	66.4	-0.000220	-0.000031	0.000094	0.000031	-0.000094	0.000063	-0.000063	0.000063	-0.000020
35	66.4	-0.000220	0.000032	0.000063	-0.000032	-0.000031	0.000095	0.000000	-0.000031	-0.000016
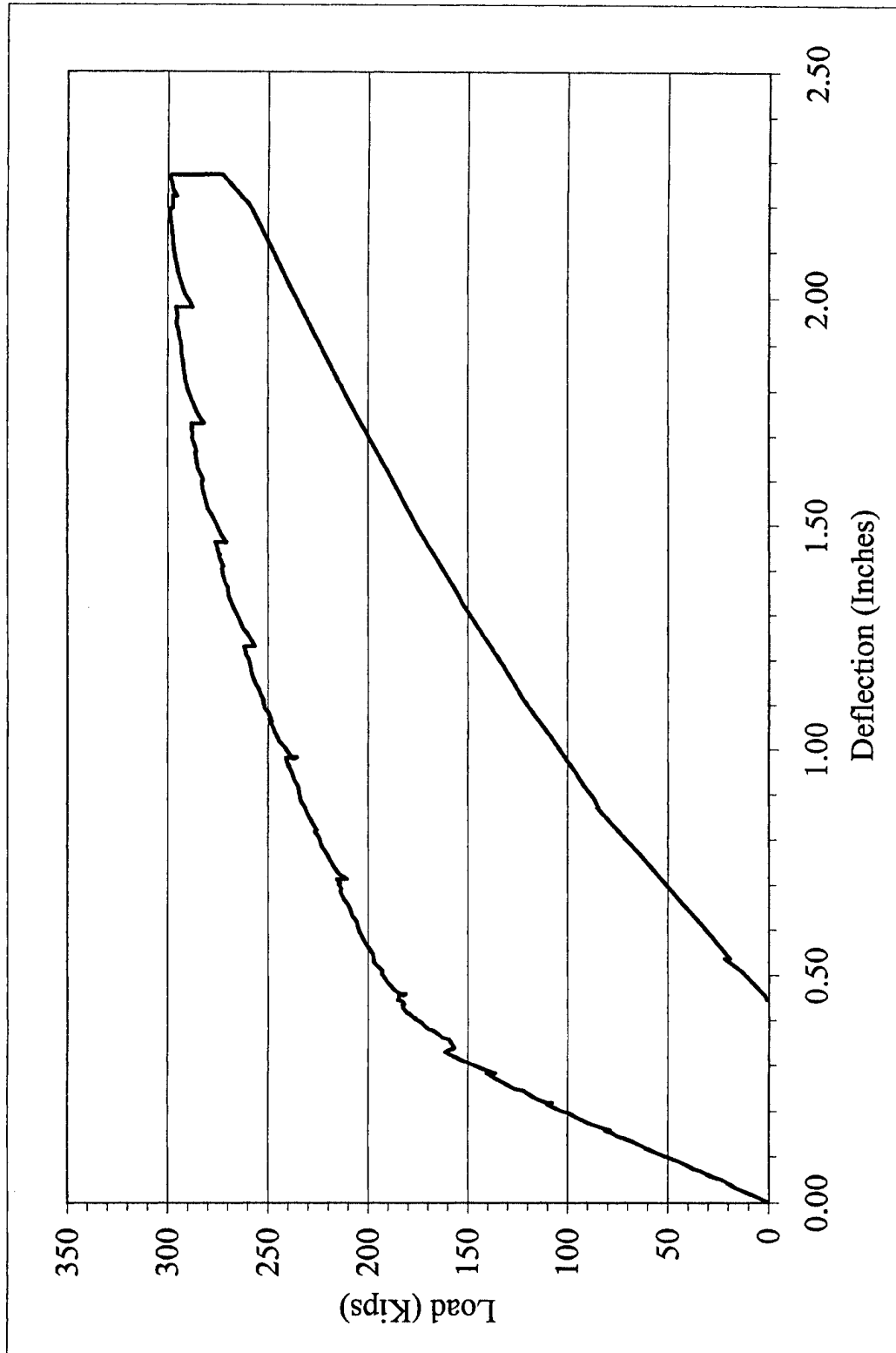
Figure O.1 Load vs. Vertical Deflection Plot for Girder Test G1C-West
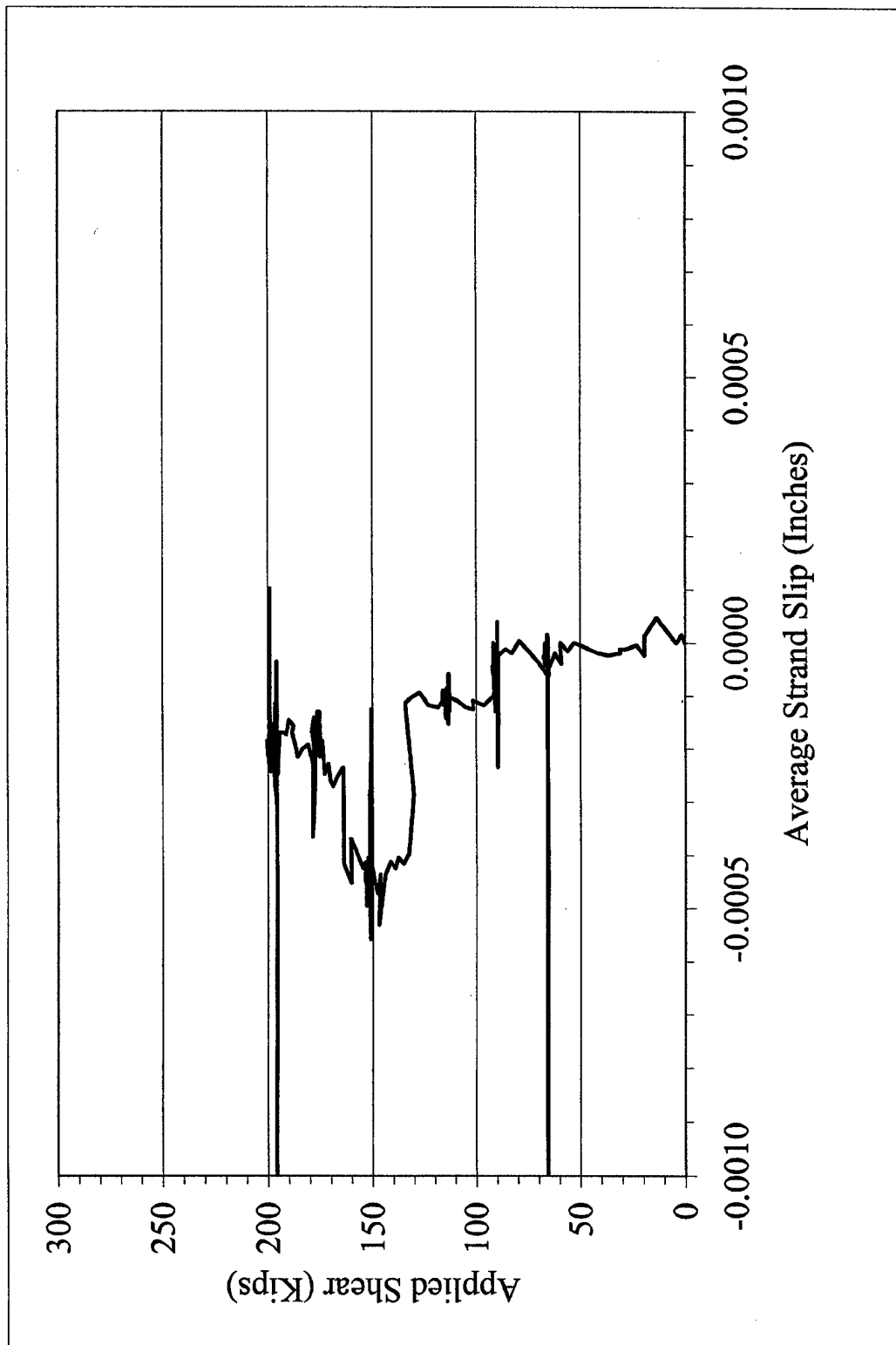
Figure O.2 Applied Shear vs. Average Strand Slip for Girder Test G1C-West
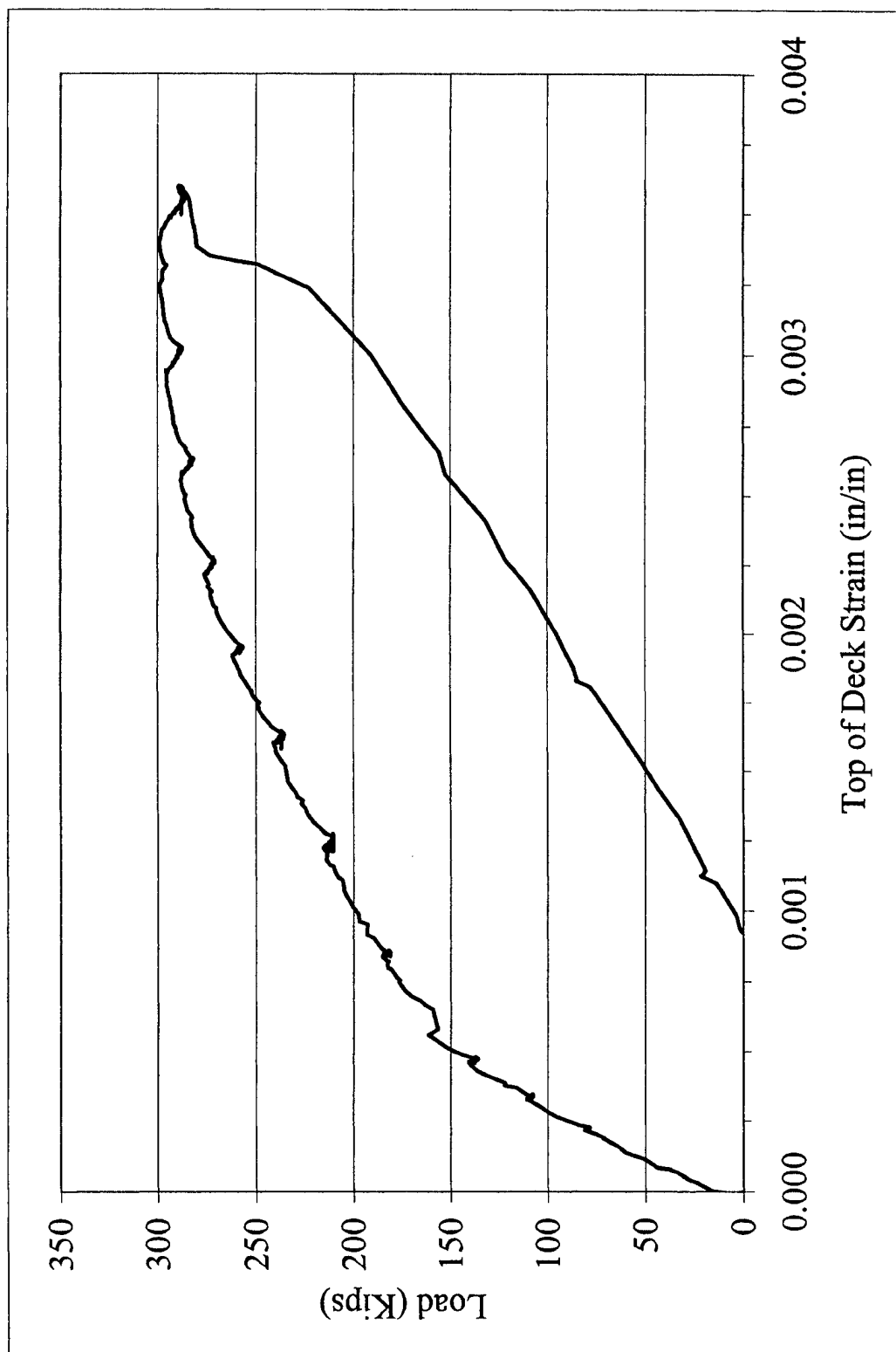
Figure O.3 Load vs. Top of Deck Strain for Girder Test G1C-West
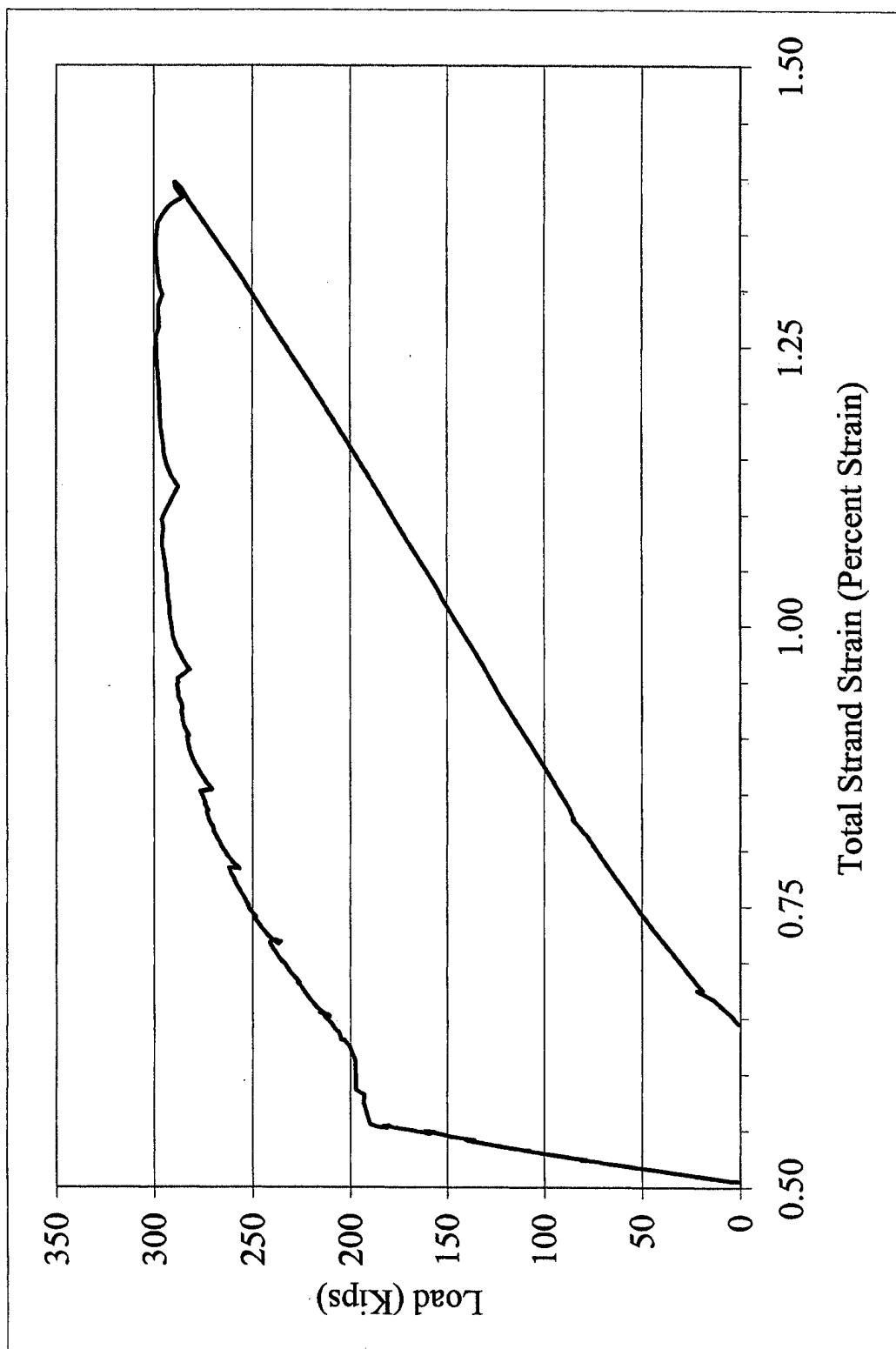
Figure O.4 Load vs. Total Strand Strain for Girder Test G1C-West

APPENDIX P

DEVELOPMENT LENGTH CSS DATA PROCESSING SPREADSHEET

Appendix P contains the individual pages from the Development Length CSS Data Processing Spreadsheet. This sheet was used to process the CSS data collected before and during the 12 development length tests. The entire set of worksheet pages is provided from development length test G1C-West. The pages are listed in the order the calculations occur. A similar series of worksheets was prepared for each development length test. Listed below are the individual worksheets within the overall spreadsheet and a brief description of the worksheet's function.

Table P.1 – Girder Information Sheet – Used to enter information about the girder end being tested. The diagram depicts both sides of the girder end being tested. The user enters values in the shaded boxes. The program automatically calculates the values that are displayed in unshaded boxes.

Table P.2, Table P.3 – Initial Readings (Release and Testing) and 14-Day Readings – Used to enter CSS readings just before strand release, 14 days after strand release, and just prior to testing. Table P.2 is for the North side of the girder; Table P.3 is for the South side.

Table P.4, Table P.5 – CSS Data Taken During Development Length Test – Used to record CSS data during the development length test. Table P.4 is for the North side of the girder; Table P.5 is for the South side of the girder.

Table P.6, Table P.7 – Calculated Raw Strains - Table P.6 is for the North side of the girder; Table P.7 is for the South side of the girder.

Table P.8 – Average Raw Strains – Averages raw strains from Tables P.6 and P.7.

Table P.9 – Smoothed Strains – Calculates a three point floating average of the average raw strain values from Table P.8.

Table P.10 – Strand Stress Values Based on Smoothed CSS Values – Calculates the total strand strain based on the smoothed CSS values from Table P.9 and the initial strand strain due to the effective prestress.

Figure P.1 – Plot of Strand Stress vs. Distance from Girder End – Plots stress in the strand at the following stress levels:

- When the strand stress is at effective prestress.

- When the strand stress at the point of loading is approximately at yield stress.

- When the strand stress at the point of loading is at ultimate stress.

- The ultimate stress the strand reaches at the point of loading

The plot also indicates locations where shear cracking passed through bottom layer of strands.

Table P.11 – Smoothed CSS Data for Tracking Effect of Surface Cracking – Lists pure CSS data for tracking the effect of shear cracking.

Table P.12 – Plot of CSS with Information About Crack Formation – The user enters data into the shaded fields reference the location of shear cracks in or near the transfer length region at the level of the bottom strands. The plot indicates CSS data at key applied shear levels that coincide with the formation of shear cracks. Also depicted in the plot is the transfer length, and the location of cracks.

Table P.13 – Prestressing Strand Tension Curve – Used to determine forces and stresses in prestressing strand based on strand strain data.

Table P.1 Girder Information Sheet

Girder Information for Development Length Plots

G1C-W

Position

| 1 | Top - L | 11 | 1 | SW | 1 | Top - C | 9 | 1 | Top - C | 9 | 1 | Top - C | 1 | NW | 1 | Top - C | 9 | 1 | Top - R | 11 |

Position

| 1 | Bot - L | 20 | 1 | Bot - C | 9 | 1 | Bot - C | 1 | 1 | Bot - R | 9 | 1 | Bot - R | 20 |

<----- Elevation (IN) ----->

<----- Elevation (IN) ----->

<----- Distance from Beam End to 1st Gage (IN) ----->

48" Bot - L

Elev	Posn	Init	Lgth
3.12	4.76	154	8.02
3.12	6.75	-263	7.97
3.11	8.74	-248	7.98
3.11	10.74	-42	8.00
3.11	12.75	100	8.01
3.11	14.74	-111	7.99
3.10	16.74	-112	7.99
3.10	18.74	-156	7.98
3.10	20.73	-401	7.96
3.10	22.72	-188	7.98
3.09	24.72	-206	7.98
3.09	26.71	-380	7.96
3.09	28.71	151	8.02
3.08	30.71	-180	7.98
3.08	32.70	-241	7.98
3.08	34.70	-213	7.98
3.08	36.68	-673	7.93
3.07	38.67	-548	7.95
3.07	40.66	-307	7.97
3.07	42.65	-192	7.98
Length =>		45.91	IN

48" Bot - R

Elev	Posn	Init	Lgth
2.99	43.48	-17	8.00
2.99	41.48	32	8.00
2.99	39.48	86	8.01
2.99	37.48	-19	8.00
2.98	35.48	44	8.00
2.98	33.48	13	8.00
2.98	31.48	-331	7.97
2.98	29.49	-367	7.96
2.97	27.51	-659	7.93
2.97	25.52	-527	7.95
2.97	23.52	-30	8.00
2.96	21.52	36	8.00
2.96	19.52	276	8.03
2.96	17.51	188	8.02
2.96	15.51	-48	8.00
2.95	13.51	-11	8.00
2.95	11.51	70	8.01
2.95	9.51	136	8.01
2.95	7.50	205	8.02
2.94	5.50	154	8.02
Length =>		45.98	IN

Initial Gage Lengths are Based on Readings Taken Just Prior to Girder Testing

Date of Strand Release	
Date of Girder End Test	02-Nov-01
Age at Testing (Days)	107

| 14-Day Transfer Lgth (in) | |

| Strand Initial Strain (me) | ~50? |
| From Prestress Force Calc Spreadsheet | |

Load at ~1% Strain (kips)	
Ultimate Load (kips)	209
Ultimate CSS (me)	8907
From DAQ Spreadsheet	

Embedment Length (in)	
Shear Span "a" (in)	385
Supt to Supt Dist. (in)	504
Strand Area (in²)	0.2183

| f_{se} | 147.6 | ksi |
| f_{ps} | 264.4 | ksi |

| F_{se} | 32.2 | kips |
| F_{ps} | 57.7 | kips |

| Gage Lgth | | IN |

NW

| Beam Lgth | | FT |

SW

Table P.2 Initial Readings Prior to Testing, Initial Readings Prior to Release and 14 Day Readings (North Side)

Beam #	GIC-W	Beam Side	North	Test #	4	Read LEFT to RIGHT

Initial Readings Just Prior to Testing, Initial Readings Prior to Release and 14-Day Readings

Notes for Readings - Gage Length is 8" on DEMEC Gage Reader - Zero Gage on Bar Before Taking Readings

30 Inch Top Left

26 Inch Top Center — Test # 1, Test # 2

30 Inch Top Right — Test # 1, Test # 2

48 Inch Bottom Left

26 Inch Bottom Center — Test # 1, Test # 2

48 Inch Bottom Right — Test # 1, Test # 2, Rel # 1, Rel # 2, 14-Day

Table P.3 Initial Readings Prior to Testing, Initial Readings Prior to Release and 14 Day Readings (South Side)

Beam #	G1C-W	Beam Side	South	Test #	4	Read LEFT to RIGHT

Initial Readings Just Prior to Testing, Initial Readings Prior to Release and 14-Day Readings

Notes for Readings - Gage Length is 8" on DEMEC Gage Reader - Zero Gage on Bar Before Taking Readings

30 Inch Top Left

Test # 1	Test # 2
.0593	.0514
.0556	.0584
.0530	.0721
.0464	.0452
.0655	.0561
.0624	.0621
.0503	.0555
.0833	.0884
.0780	.0680
.0515	.0754
.0709	.0709

26 Inch Top Center

Test # 1	Test # 2
.0584	.0686
.0631	.0578
.0735	.0786
.0685	.0689
.0695	.0586
.0649	.0590
.0671	.0644
.0682	.0619
	.0817

48 Inch Bottom Left

Test # 1	Test # 2	Rel # 1	Rel # 2	14-Day

26 Inch Bottom Center

Test # 1	Test # 2
.0817	.0800
.0710	.0709
.0595	.0596
.0538	.0548
.0699	.0648
.0473	.0472
.0598	.0596
.0616	.0606
.0649	.0647

30 Inch Top Right

48 Inch Bottom Right

Table P.4 CSS Data Taken During Development Length Testing (North Side)

Beam #		G1C-W			Side			North			Test #		4		Read LEFT to RIGHT			
		Notes for Readings - Gage Length is 8" on DEMEC Gage Reader - Zero Gage on Bar Before Taking Readings																
Reading	1	2	3	4	5	6	7	8	9	10	11	12	13	14	15	16	17
Load (K)																	
Gage #																	
1																	
2																	
3																	
4																	
5																	
6																	
7																	
8																	
9																	
10																	
11																	
12																	
13																	
14																	
15																	
16																	
17																	
18																	
19																	
20																	

Table P.5 CSS Data Taken During Development Length Testing (South Side)

Beam #	G1C-W		Side		South			Test #			4	Read LEFT to RIGHT				
Reading	1	2	3	4	5	6	7	8	9	10	11	12	13	14	15	16	17
Load (K)	80	110	140	155	184	215	240	261	276	287	295	296					

Notes for Readings - Gage Length is 8" on DEMEC Gage Reader - Zero Gage on Bar Before Taking Readings

Gage #																	
1																	
2																	
3																	
4																	
5																	
6																	
7																	
8																	
9																	
10																	
11																	
12																	
13																	
14																	
15																	
16																	
17																	
18																	
19																	
20																	

Table P.6 Calculated Raw Strains (North Side)

G1C-W

48"

Raw Strains - North Side

| Gage Point | Transfer Length | | | CSS Reading (microstrains) — Development Length | | | | | | | | | | | | | | | | |
Load	Rel	14-Day	Test	1	2	3	4	5	6	7	8	9	10	11	12	13	14	15	16	17
	0	0	0	80	110	140	155	184	215	240	261	276	287	295	296	0	0	0	0	0
1	0	1175	1507	194	194	231	369	381	469	556	944	1769	2469	2694	3057					
2	0	1175	1456	219	231	294	381	469	569	668	1056	1881	2693	2830	3043					
3	0	943	1299	219	243	268	368	418	518	581	1130	2042	2966	3153	3515					
4	0	1069	1432	175	188	213	313	388	488	550	713	1013	1500	1600	1688					
5	0	999	1274	187	175	237	275	362	425	487	700	800	1049	1049	775					
6	0	694	1194	200	250	275	337	425	500	562	700	875	1450	1662	1700					
7	0	1067	1400	207	207	220	320	383	408	483	533	496	973	1462	1789					
8	0	1080	1400	182	107	220	295	333	358	446	496	496	1036	1965	10894					
9	0	1273	1620	158	208	208	296	372	359	410	485	460	1002	1909	11211					
10	0	1026	1353	138	164	189	277	352	340	440	466	528	617	1208	10532					
11	0	788	1232	156	194	194	281	394	381	456	506	556	594	844	10110					
12	0	950	1143	169	169	181	244	356	369	394	444	519	444	431	668					
13	0	884	1059	149	187	224	336	461	436	498	573	698	2952	5568	6054					
14	0	736	867	143	143	118	218	330	368	405	443	555	3087	5967	6553					
15	0	494	738	119	106	6	106	231	344	1132	1832	2583	5247	8586	9024					
16	0	425	838	138	213	138	175	200	388	1088	1750	2513	5288	8589	9089					
17	0	587	899	112	125	100	162	200	412	1062	1711	2410	2897	3547	3622					
18	0	611	898	62	50	12	237	537	1048	1809	2533	3369	3594	4218	3968					
19	0	655	973	131	268	118	305	605	1004	916	1054	1166	1315	1390	1365					
20	0	150	774	175	137	162	362	661	948	1023	1060	1198	1223	1260	1310					

Compression +   Tension +

Table P.7 Calculated Raw Strains (South Side)

G1C-W, 48" — Raw Strains - South Side

CSS Reading (microstrains)

Gage Point Load	Transfer Length Rel	14-Day	Test	1	2	3	4	5	6	7	8	9	10	11	12	13	14	15	16	17
	0	0	0	80	110	140	155	184	215	240	261	276	287	295	296	0	0	0	0	0
1	0	-561	-674	175	137	162	362	661	948	1023	1060	1198	1223	1260	1310					
2	0	702	890	113	163	201	451	564	564	640	702	790	890	916	966					
3	0	451	696	-6	132	94	445	520	533	596	646	746	871	934	947					
4	0	775	1126	88	63	75	100	213	963	1463	1976	2601	4940	5403	5390					
5	0	574	874	75	62	25	100	674	1411	2047	2697	3296	5730	5630	5543					
6	0	958	1170	-13	50	75	150	751	1477	2115	2866	3918	6647	8837	9013					
7	0	832	1120	63	75	50	125	764	1540	2191	2904	3918	6672	9200	9363					
8	0	958	1252	106	106	144	169	570	695	820	1046	1346	1860	3901	4064					
9	0	704	1106	75	88	88	151	138	151	201	276	528	678	3467	3731					
10	0	1065	1410	94	94	94	182	106	119	157	182	194	157	232	219					
11	0	952	1385	157	132	132	207	169	207	320	232	269	583	2137	7726					
12	0	1262	1608	69	107	144	182	82	82	157	157	182	546	2531	8647					
13	0	1085	1273	162	150	162	237	125	299	287	299	274	711	2645	12514					
14	0	1485	1798	113	150	163	238	213	238	238	326	376	802	2869	12704					
15	0	696	1078	107	94	119	169	157	132	244	169	445	809	1147	5598					
16	0	1097	1410	88	100	138	288	238	263	363	514	752	965	990	4725					
17	0	807	1166	95	120	158	233	208	221	271	460	662	952	1103	977					
18	0	673	994	94	107	132	220	208	208	308	447	673	875	1064	1466					
19	0	1318	1619	176	176	188	251	238	314	402	979	1443	1907	2133	2409					
20	0	789	1065	138	175	213	301	313	338	464	890	1328	1854	2118	2531					

Compression +   Tension +

Table P.8 Average Raw Strains

G1C-W

48"

Average of North and South Data (From North Perspective)

CSS Reading (microstrains)

Gage Point	Transfer Length			Development Length																
	Rel	14-Day	Test	1	2	3	4	5	6	7	8	9	10	11	12	13	14	15	16	17
Load	0	0	0	80	110	140	155	184	215	240	261	276	287	295	296	0	0	0	0	0
1	0	982	1286	166	185	222	335	347	404	510	917	1549	2162	2406	2794					
2	0	1246	1537	197	203	241	316	353	441	535	1017	1662	2300	2482	2726					
3	0	808	1146	156	175	200	294	313	363	444	788	1357	1920	2108	2491					
4	0	938	1299	135	154	185	273	298	354	411	586	837	1226	1352	1332					
5	0	1048	1342	138	138	188	282	300	344	425	607	776	1007	1020	2750					
6	0	695	1136	153	172	197	253	291	316	403	435	660	1129	1405	3649					
7	0	1276	1599	160	179	191	279	298	323	361	430	436	887	2166	7246					
8	0	1083	1336	172	128	191	266	229	329	366	398	385	874	2305	11704					
9	0	1268	1614	113	157	176	239	227	220	283	321	321	774	2220	9929					
10	0	989	1369	148	148	160	242	261	273	380	349	399	600	1672	9129					
11	0	926	1321	125	144	144	232	250	250	307	344	375	375	538	5165					
12	0	827	1124	122	128	135	197	247	260	297	360	523	561	1949	2200					
13	0	921	1156	128	147	184	253	515	566	659	809	1022	2406	4735	5059					
14	0	784	994	103	109	84	172	547	954	1298	1673	2236	4879	7584	7958					
15	0	726	954	53	78	41	128	491	911	1624	2349	3250	5947	8712	9018					
16	0	500	856	106	137	81	137	437	899	1568	2223	2904	5509	7110	7316					
17	0	681	1012	100	94	87	131	206	688	1262	1844	2506	3919	4475	4506					
18	0	531	797	28	91	53	341	528	791	1203	1589	2058	2233	2576	2457					
19	0	678	931	122	216	160	378	585	784	778	878	978	1103	1153	1165					
20	0	-206	50	175	137	162	362	661	948	1023	1060	1198	1223	1260	1310					

Compression +   Tension +

568

Table P.9 Smoothed Strains

G1C-W — Smoothed Average Plot Data From the SOUTH Perspective

48"

Strain Readings (microstrains)

Development Length Test CSS + Initial Strand Strain Due to Pretensioning

Gage Point	Distance From End (inches)	Rel	14-Day	Test	Strand Initial	1	2	3	4	5	6	7	8	9	10	11	12	13	14	15	16	17
Load		0	0	0	0	80	110	140	155	184	215	240	261	276	287	295	296	0	0	0	0	0
0	0	0	0	0	0	0	0	0	0	0	0	0	0	0	0	0	0	0	0	0	0	0
2	7.13	0	335	593	1675	1783	1823	1800	2035	2266	2516	2676	2851	3086	3194	3338	3319					
3	9.13	0	630	914	2145	2228	2278	2245	2429	2585	2899	3226	3582	3992	4563	4880	4855					
4	11.13	0	571	888	2615	2693	2723	2689	2819	3006	3408	3959	4501	5105	6502	7335	7375					
5	13.13	0	636	941	3086	3172	3189	3156	3218	3464	3918	4570	5225	5973	8211	9851	10033					
6	15.13	0	670	934	3556	3643	3664	3624	3701	4047	4477	5052	5638	6353	9001	11357	11653					
7	17.13	0	810	1034	4025	4120	4136	4128	4209	4543	4835	5219	5636	6195	8436	11035	11370					
8	19.13	0	844	1091	4495	4613	4623	4630	4702	4932	5088	5247	5443	5756	7111	9251	9568					
9	21.13	0	891	1200	4965	5090	5105	5119	5192	5302	5323	5386	5469	5605	6079	7372	9106					
10	23.12	0	914	1271	5053	5185	5193	5199	5277	5306	5314	5381	5404	5485	5565	6439	10551					
11	25.12	0	1061	1434	5053	5182	5203	5213	5290	5299	5301	5376	5391	5418	5636	6530	13127					
12	27.11	0	1113	1440	5053	5197	5197	5229	5302	5292	5327	5396	5409	5421	5802	7119	15307					
13	29.10	0	1209	1516	5053	5201	5208	5239	5314	5304	5344	5390	5436	5434	5898	7283	14679					
14	31.10	0	1018	1357	5053	5215	5213	5246	5319	5326	5375	5430	5474	5547	6016	7011	12586					
15	33.09	0	1006	1359	5053	5203	5216	5245	5324	5349	5381	5449	5543	5677	6061	6583	9601					
16	35.09	0	894	1259	5053	5195	5207	5243	5322	5349	5391	5466	5596	5811	6174	6312	7630					
17	37.08	0	931	1262	5053	5196	5208	5244	5336	5357	5407	5480	5714	6043	6437	6546	7244					
18	39.07	0	997	1327	5053	5216	5230	5262	5347	5374	5439	5516	5850	6339	6868	7034	7236					
19	41.07	0	1012	1323	5053	5226	5241	5274	5368	5391	5456	5549	5961	6576	7180	7385	7723					
20	43.07	0																					

Transfer Lgth CSS

Compression +   Tension +

569

Table P.10 Strand Stress Values Based on Smoothed CSS Values

G1C-W — Smoothed Average Plot Data From SOUTH Perspective

48" Gage Point	Distance From End (inches)	Stress in Strand due to Effective Prestress and Load Applied to Girder																
		1	2	3	4	5	6	7	8	9	10	11	12	13	14	15	16	17
Load		80	110	140	155	184	215	240	261	276	287	295	296	0	0	0	0	0
0	0	0	0	0	0	0	0	0	0	0	0	0	0	0	0	0	0	0
2	7.13	52.09	53.25	52.58	59.46	66.21	73.50	78.18	83.28	90.15	93.32	97.51	96.96					
3	9.13	65.09	66.55	65.58	70.94	75.50	84.69	94.24	104.64	116.62	133.30	142.54	141.81					
4	11.13	78.68	79.53	78.56	82.34	87.81	99.55	115.66	131.48	149.12	189.94	213.82	215.02					
5	13.13	92.67	93.16	92.18	94.01	101.19	114.46	133.51	152.62	174.47	235.99	257.63	258.83					
6	15.13	106.42	107.03	105.87	108.12	118.23	130.77	147.58	164.69	185.57	249.16	263.03	263.26					
7	17.13	120.35	120.83	120.59	122.96	132.71	141.24	152.45	164.63	180.96	240.34	262.57	263.04					
8	19.13	134.75	135.06	135.24	137.37	144.07	148.64	153.27	159.00	168.14	207.72	252.20	255.37					
9	21.13	148.69	149.11	149.54	151.67	154.90	155.51	157.33	159.77	163.73	177.58	214.94	250.50					
10	23.12	151.45	151.70	151.88	154.14	154.99	155.23	157.19	157.86	160.24	162.56	188.11	261.28					
11	25.12	151.37	151.98	152.29	154.55	154.79	154.85	157.05	157.48	158.27	164.64	190.75	264.09					
12	27.11	151.82	151.83	152.74	154.88	154.58	155.62	157.63	158.00	158.37	169.49	207.96	264.89					
13	29.10	151.95	152.13	153.05	155.25	154.94	156.10	157.45	158.79	158.73	172.29	212.21	264.66					
14	31.10	152.33	152.27	153.25	155.38	155.57	157.03	158.62	159.90	162.03	175.75	204.82	263.89					
15	33.09	152.00	152.36	153.22	155.53	156.26	157.18	159.19	161.93	165.83	177.05	192.30	255.67					
16	35.09	151.75	152.12	153.16	155.47	156.26	157.48	159.68	163.46	169.74	180.35	184.38	222.28					
17	37.08	151.78	152.15	153.19	155.87	156.48	157.94	160.08	166.90	176.53	188.05	191.23	210.98					
18	39.07	152.36	152.79	153.71	156.21	157.00	158.89	161.14	170.90	185.16	200.64	205.46	210.72					
19	41.07	152.67	153.09	154.07	156.81	157.48	159.37	162.11	174.12	192.09	208.94	215.32	224.73					
20	43.07																	

G1C-W — Plot Data for Strand Stress vs Distance from Girder End

	Distance From Girder End (in)	Strain in Strand (me)	Stress in Strand (ksi)
Girder End	0	0	0
Transfer Lgth	21.5	5053	147.61
End of Plot	109.2	5053	147.61
e_{ps-ULT}	91	13960	264.40

Load at ~1% Strand Strain	291	Kips
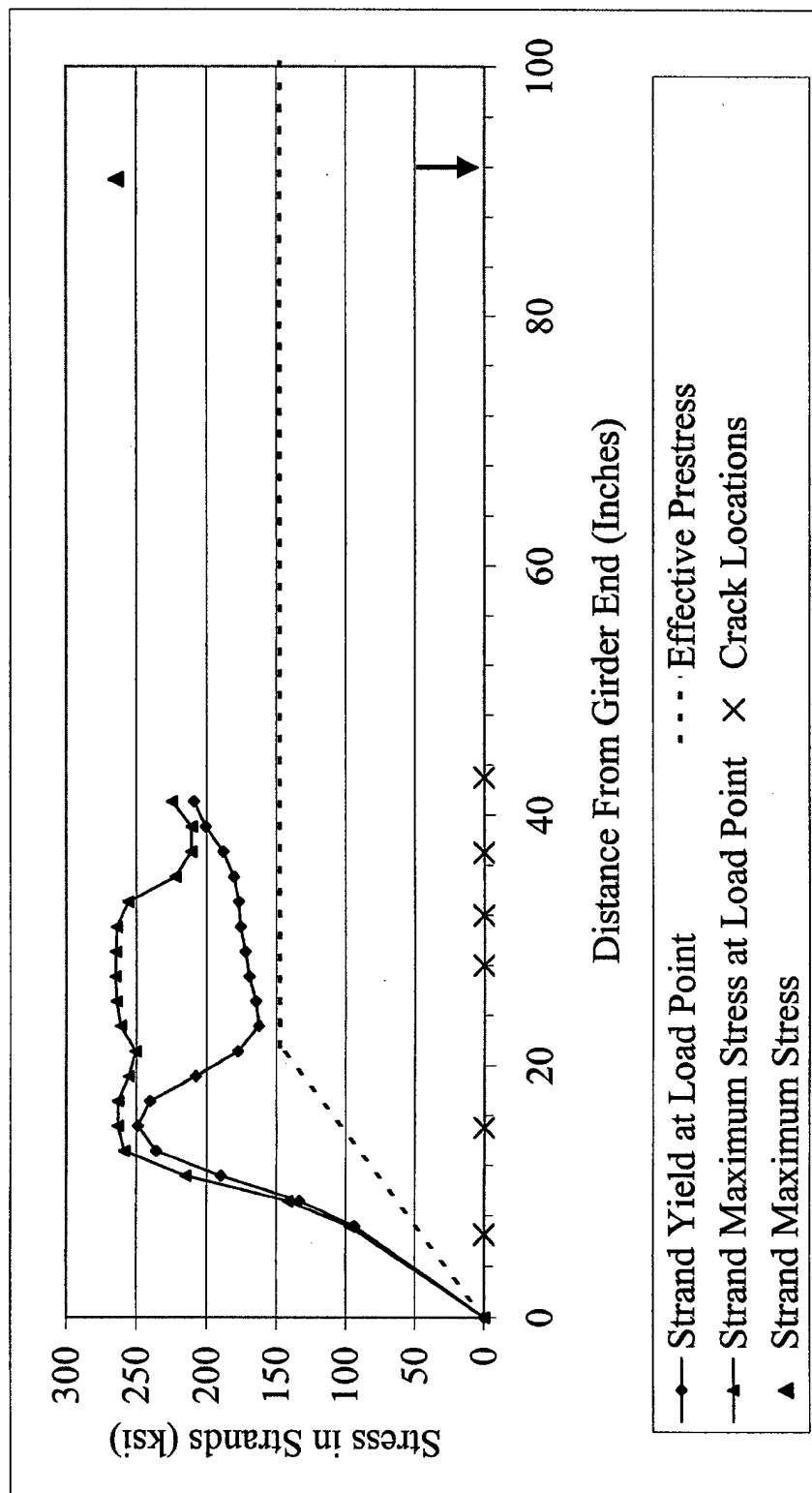
Figure P.1 Plot of Strand Stress vs. Distance From Girder End

Table P.11 Smoothed CSS Data for Tracking Effect of Surface Cracking

G1C-W 48"   Smoothed Average Plot Data From the SOUTH Perspective   (CSS Only)

Strain Readings (microstrains) — Development Length Test CSS

48" Gage Point	Distance From End (inches)	Strand	1	2	3	4	5	6	7	8	9	10	11	12	13	14	15	16	17
Load		Initial	80	110	140	155	184	215	240	261	276	287	295	296	0	0	0	0	0
0	0	0	0	0	0	0	0	0	0	0	0	0	0	1	0	0	0	0	0
2	7.13	0	108	148	125	360	591	841	1001	1176	1411	1519	1663	1644					
3	9.13	0	83	133	100	284	440	754	1081	1437	1847	2418	2735	2710					
4	11.13	0	78	107	74	203	391	792	1344	1885	2489	3887	4720	4760					
5	13.13	0	86	103	70	132	378	832	1485	2139	2887	5125	6765	6947					
6	15.13	0	87	108	69	146	492	921	1496	2082	2797	5445	7802	8097					
7	17.13	0	95	111	103	184	518	810	1194	1611	2170	4411	7010	7345					
8	19.13	0	118	128	134	207	437	593	752	948	1261	2615	4756	5072					
9	21.13	0	125	140	154	227	338	358	421	504	640	1114	2407	4141					
10	23.12	0	132	140	146	224	253	261	328	351	432	512	1386	5498					
11	25.12	0	129	150	160	237	246	248	323	338	365	583	1477	8074					
12	27.11	0	144	144	176	249	239	274	343	356	368	749	2066	10254					
13	29.10	0	148	155	186	261	251	291	337	383	381	845	2230	9626					
14	31.10	0	162	160	193	266	273	322	377	421	494	963	1958	7533					
15	33.09	0	150	163	192	271	296	328	396	490	624	1008	1530	4548					
16	35.09	0	142	154	190	269	296	338	413	543	758	1121	1259	2577					
17	37.08	0	143	155	191	283	304	354	427	661	990	1384	1493	2191					
18	39.07	0	163	177	209	294	321	386	463	797	1286	1815	1981	2183					
19	41.07	0	173	188	221	315	338	403	496	908	1523	2127	2332	2670					
20	43.07																		

Tension +

G1C-W   Plotting Data for Transfer Length on Crack ID Plot

	Distance From Girder End (In)	Plot Data
Girder End	0	0
Transfer Lgth	21.5	0

572

Table P.12 Plot of CSS with Information About Crack Formation

G1C-W	Crack Data - Enter Location of Cracks Crossing DEMEC Gage Strips									
Crack Number	1	2	3	4	5	6	7	8	9	10
Distance from Girder End (in)	0.5	13	28	32	37	43				
Load at Which Crack Crosses Strand	184	184	296	295	240	296				
Shear at Which Crack Crosses Strand	153	153	246	246	200	246	0	0	0	0
Plotting Data for Y-Axis	0	0	0	0	0	0	0	0	0	0

Load Step vs Shear	
Step	Shear (kips)
1	67
2	91
3	116
4	129
5	153
6	179
7	200
8	217
9	229
10	239
11	245
12	246
13	0
14	0
15	0

CSS vs Distance From Girder End

CSS at Level of Bottom Strands (µε) vs Distance From Girder End (Inches)

Legend: ✕ Crack, — Lt, V=153 K, V=200 K, V=246 K

573

Table P.13 Prestressing Strand Tension Curve

Prestressing Strand Tension Test Curve and Zone Limit Data

Strain -Stress Curve for 0.6" 270 KSI LOLAX Strand

$y = 0.8063x + 56.5921$
$R^2 = 1.0000$

$y = 95.9317x^3 - 348.9161x^2 + 423.6514x - 114.2059$
$R^2 = 0.9985$

$y = 63.7701x + 0.0000$
$R^2 = 1.0000$

Load (Kips) — axis: 70.00, 60.00, 50.00, 40.00, 30.00, 20.00, 10.00, 0.00

Strain (Percent) — axis: 0 1 2 3 4 5 6 7

Legend: ◆ Elastic ■ Transition ▲ Plastic ── Linear (Elastic) ── Linear (Plastic) ── Poly. (Transition) ── Linear (Plastic)

Prestressing Strand Loading Data		
Point of Loading	Strain (%)	Load (Kips)
Start of Elastic	0	0.00
End of Elastic	0.7135	45.50
Transition 1	0.7500	47.45
Transition 2	0.8750	53.63
Transition 3	1.0000	56.67
Transition 4	1.1250	57.20
Start of Plastic	1.2500	57.60
End of Plastic	6.5000	61.83

Zone	Percent Strain		
Elastic	0	< e <	0.7135
Transition	0.7135	< e <	1.2500
Plastic	1.2500	> e	

Zone	Load		
Elastic	0	< Kips <	45.50
Transition	45.50	< Kips <	57.60
Plastic	57.60	> Kips	

574

APPENDIX Q

PHOTOS AND STRAND STRESS PLOTS FROM DEVELOPMENT LENGTH TESTS

Appendix Q contains a photo and a plot of stress in the prestressing strand from each of the 12 development length tests. The stress increase in the prestressing strand during loading was determined with concrete surface strain (CSS) data taken at the level of the bottom strands over the initial 48 inches of the girder. The CSS data was measured using DEMEC points with an 8-inch gage length; a three gage moving average was used to determine each value. This additional stress due to loading was added to the effective prestress to plot the resulting strand stress. The following items are shown on each plot.

- Effective stress due to prestressing over entire embedment length (dashed line)

- Stress in the strand over the initial 48 inches of the girder when the strand begins to yield at the point of load application (line with diamonds)

- Stress in the strand over the initial 48 inches of the girder when the strand is at ultimate stress at the point of load application (line with triangles)

- Stress in the strand at ultimate load at the point of load application (triangle). The CSS data at the load point was found using an LVDT with a gage length of 24 inches.

- Point of load application indicator (downward arrow along x-axis)

575

- Cracks passing through the level of the bottom strands along the initial 48 inches of the girder (marked with X along x-axis)

In the tests where the average strand end slip is over 0.01" (G1A-East, G1B-East and G1C-East), the level of stress indicated in the strand indicated is not considered accurate. With slip between the strand and concrete, it is impossible to know with any certainty the level of stress in the strand using CSS data. If the level of average strand end slip is less than 0.01 inches, it is assumed the resulting strand stress plots are reasonable because the affect on strand stress calculations would be less than 0.015 percent. On the plots, cracking in the girder causes the peaks and valleys. The sections correspond with the individual development length tests as follows:

Section Q.1 – Test G1A-East

Section Q.2 – Test G1A-West

Section Q.3 – Test G1B-East

Section Q.4 – Test G1B-West

Section Q.5 – Test G1C-East

Section Q.6 – Test G1C-West

Section Q.7 – Test G2A-East

Section Q.8 – Test G2A-West

Section Q.9 – Test G2B-East

Section Q.10 – Test G2B-West

Section Q.11 – Test G2C-East

Section Q.12 – Test G2C-West

Q.1 Development Length Test G1A-East
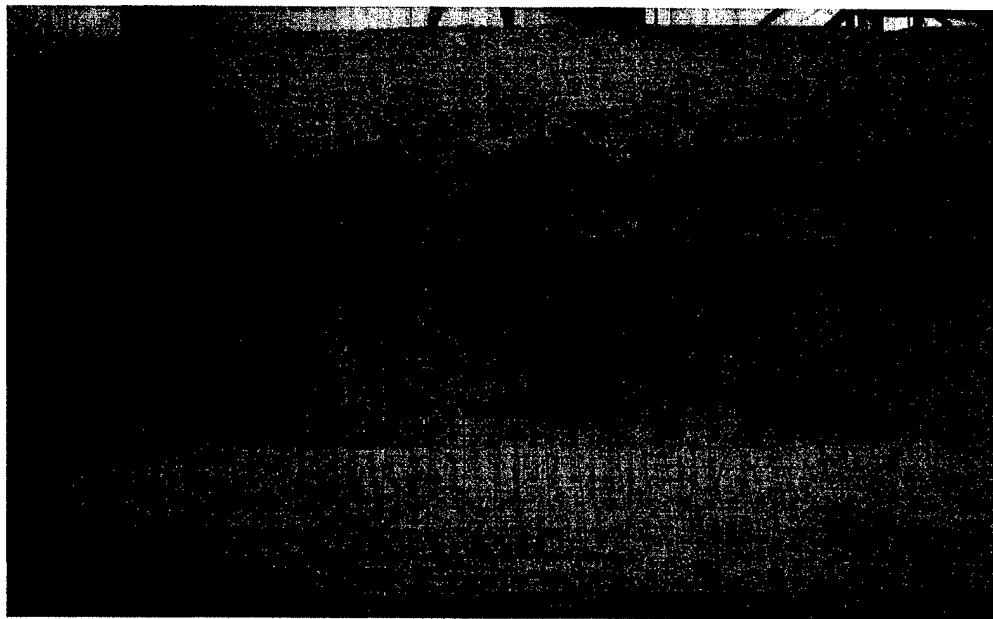
Figure Q.1 G1A-East Crack Patterns from Development Length Test
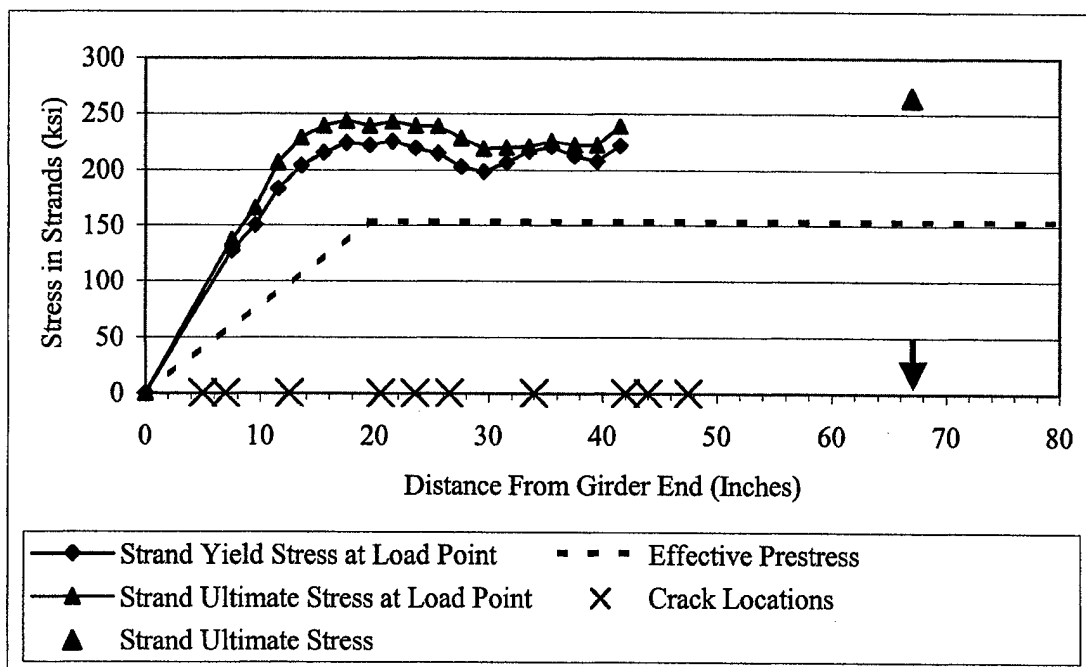
Figure Q.2 G1A-East Strand Stress vs Distance from Girder End

Q.2 Development Length Test G1A-West
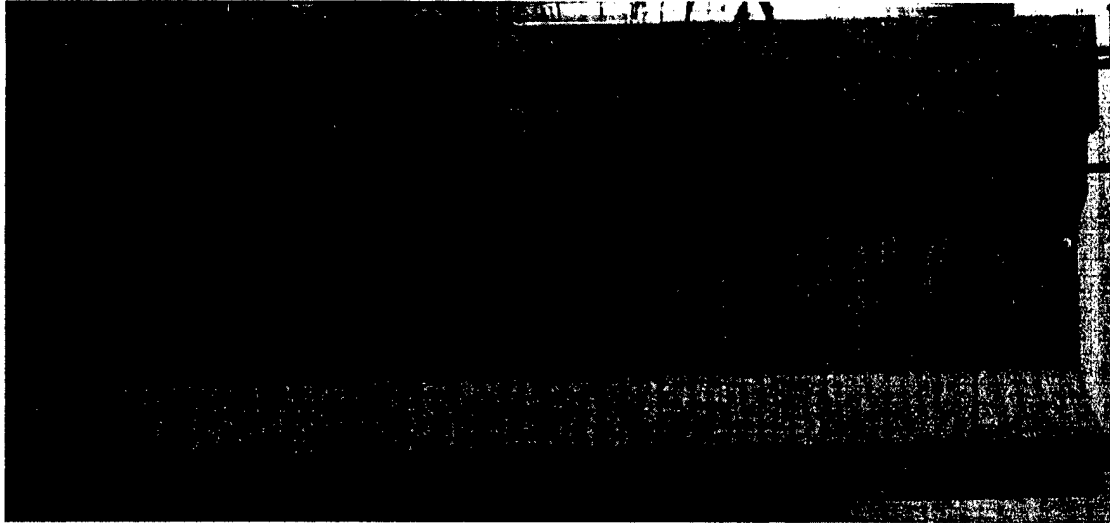
Figure Q.3 G1A-West Crack Patterns from Development Length Test
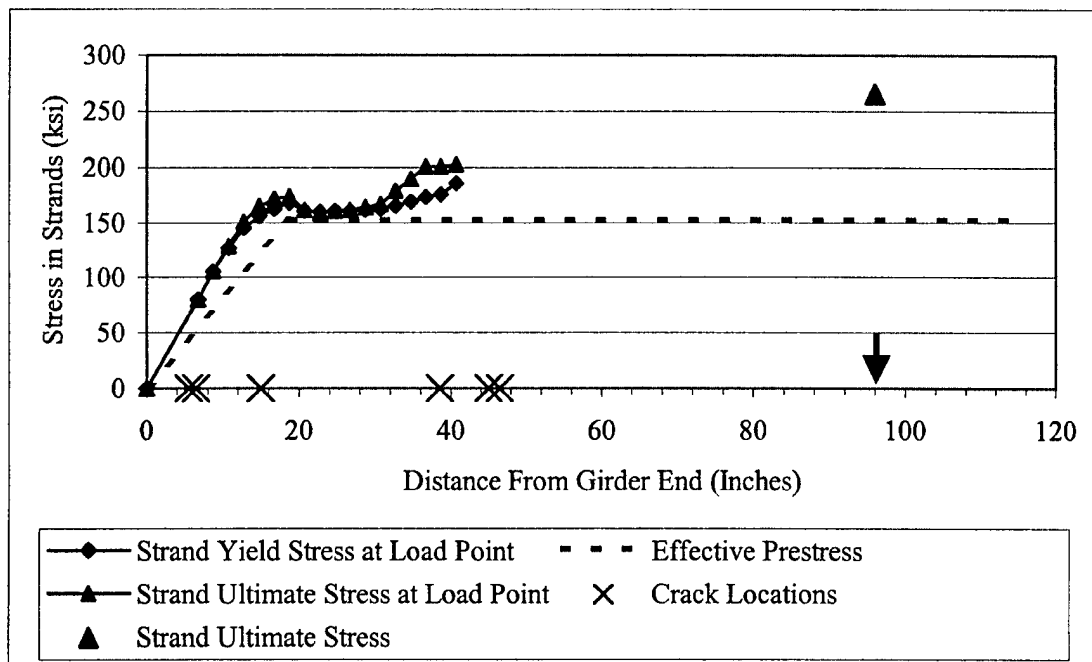
Figure Q.4 G1A-West Strand Stress vs Distance from Girder End

578

Q.3 Development Length Test G1B-East
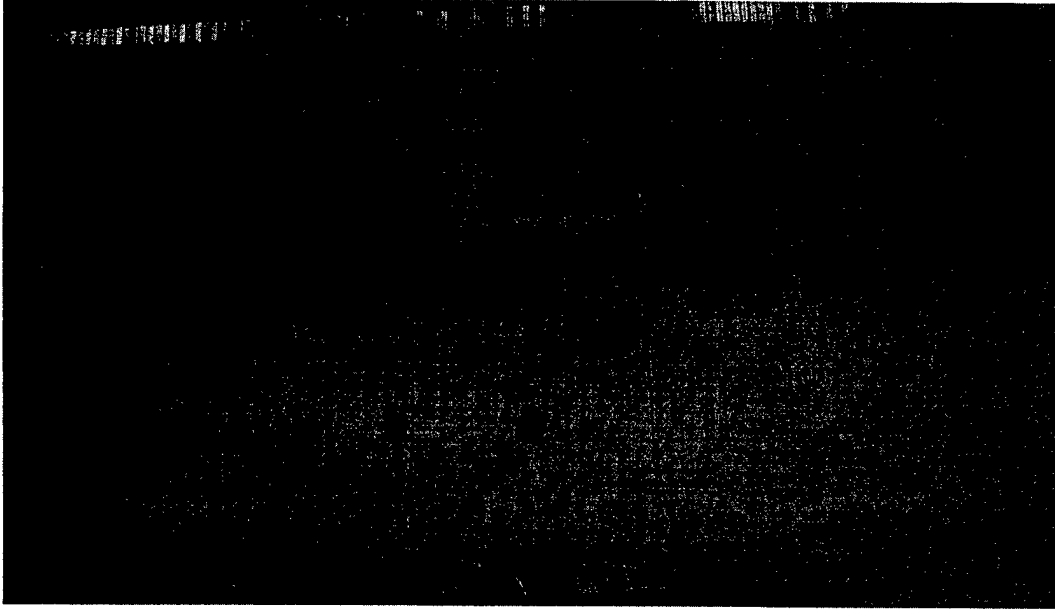
Figure Q.5 G1B-East Crack Patterns from Development Length Test
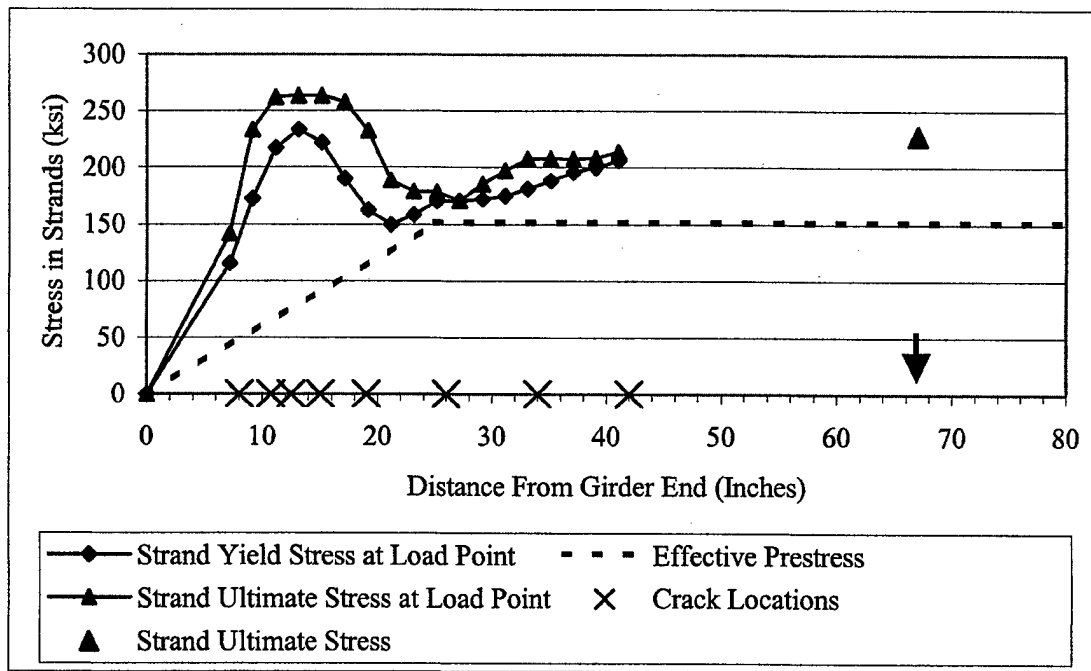
Figure Q.6 G1B-East Strand Stress vs Distance from Girder End

Q.4 Development Length Test G1B-West
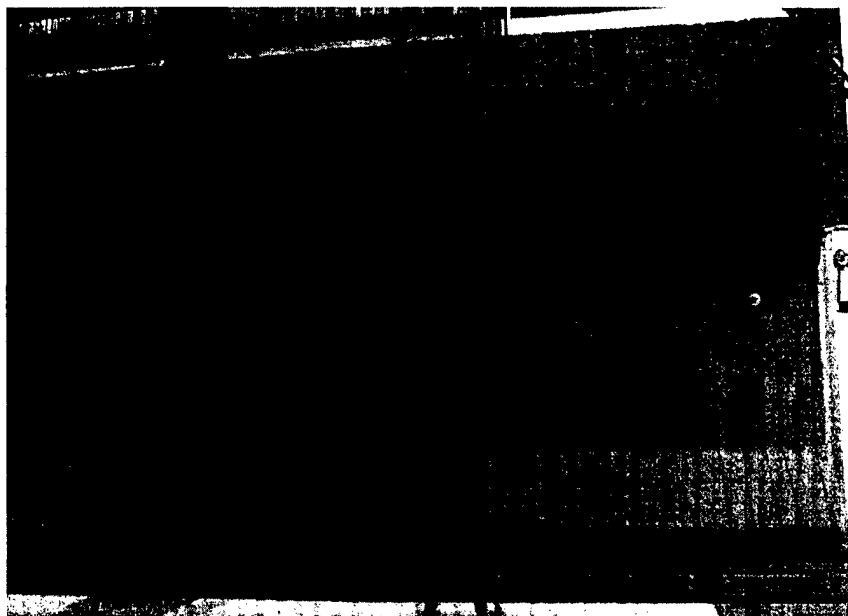
Figure Q.7 G1B-West Crack Patterns from Development Length Test
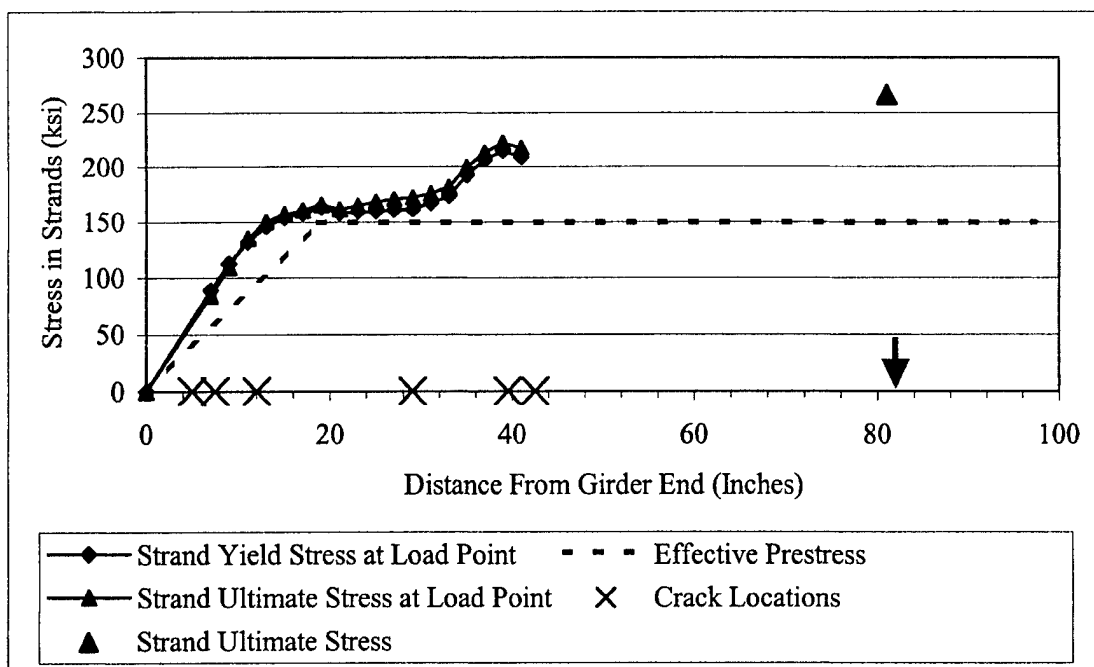
Figure Q.8 G1B-West Strand Stress vs Distance from Girder End

Q.5 Development Length Test G1C-East
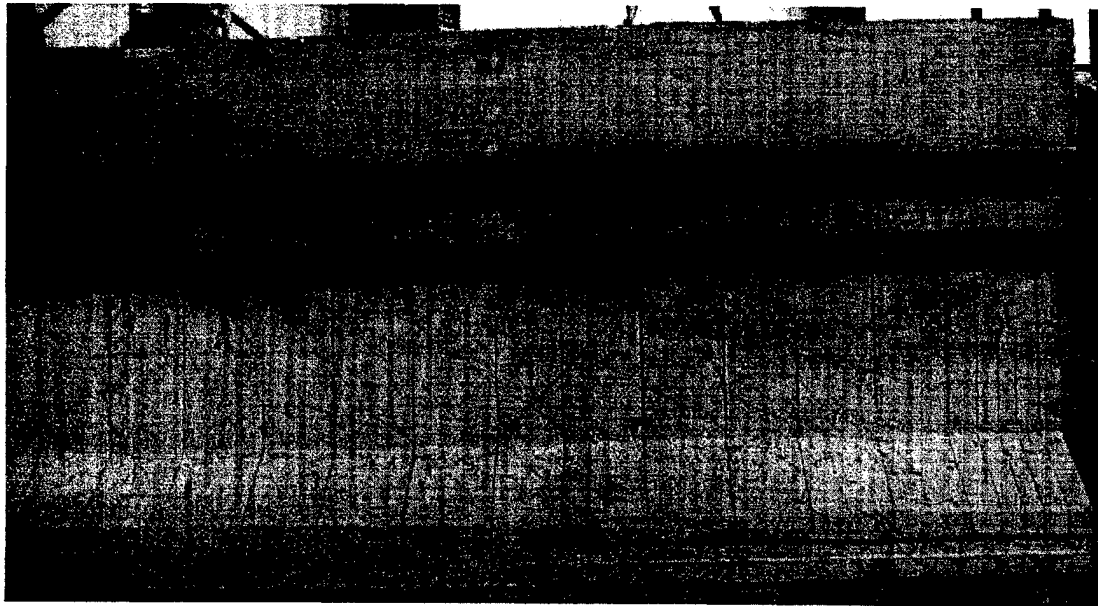
Figure Q.9 G1C-East Crack Patterns from Development Length Test
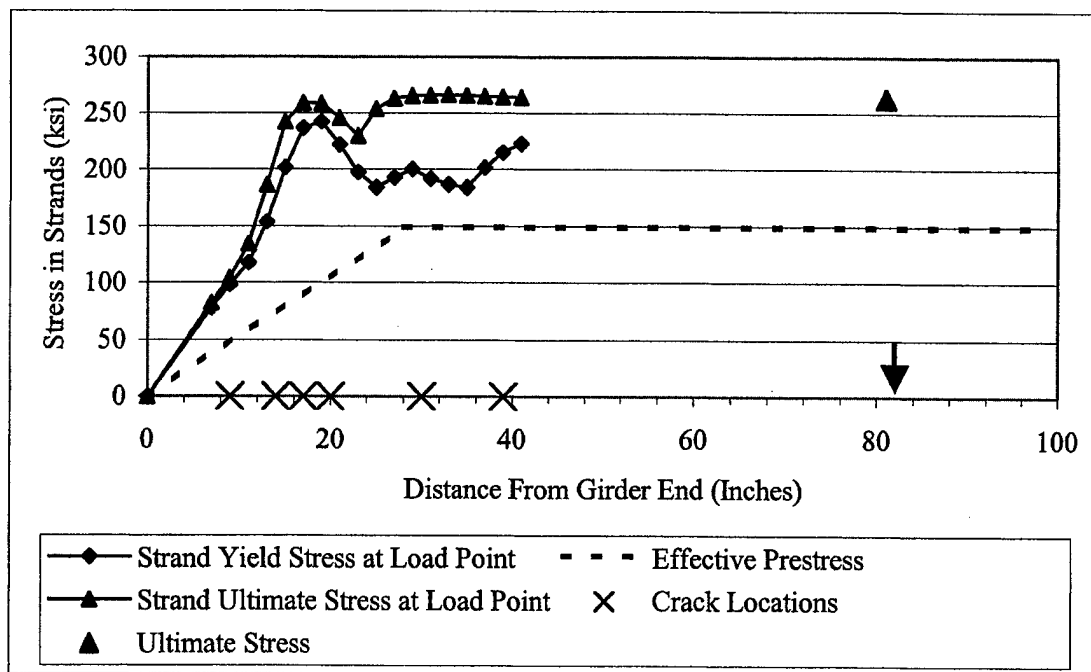
Figure Q.10 G1C-East Strand Stress vs Distance from Girder End

581

Q.6 Development Length Test G1C-West
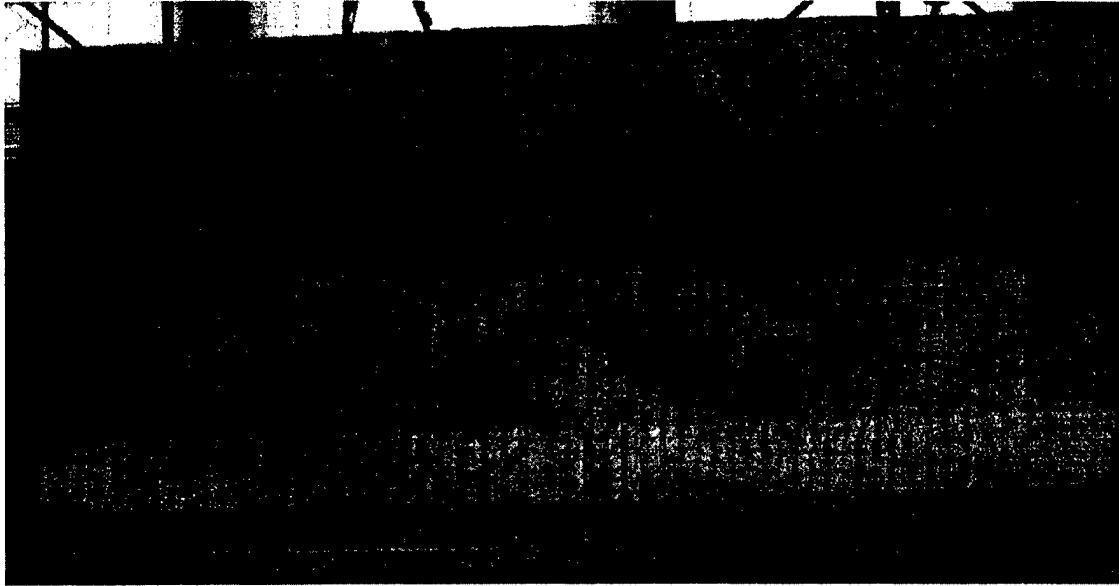
Figure Q.11 G1C-West Crack Patterns from Development Length Test
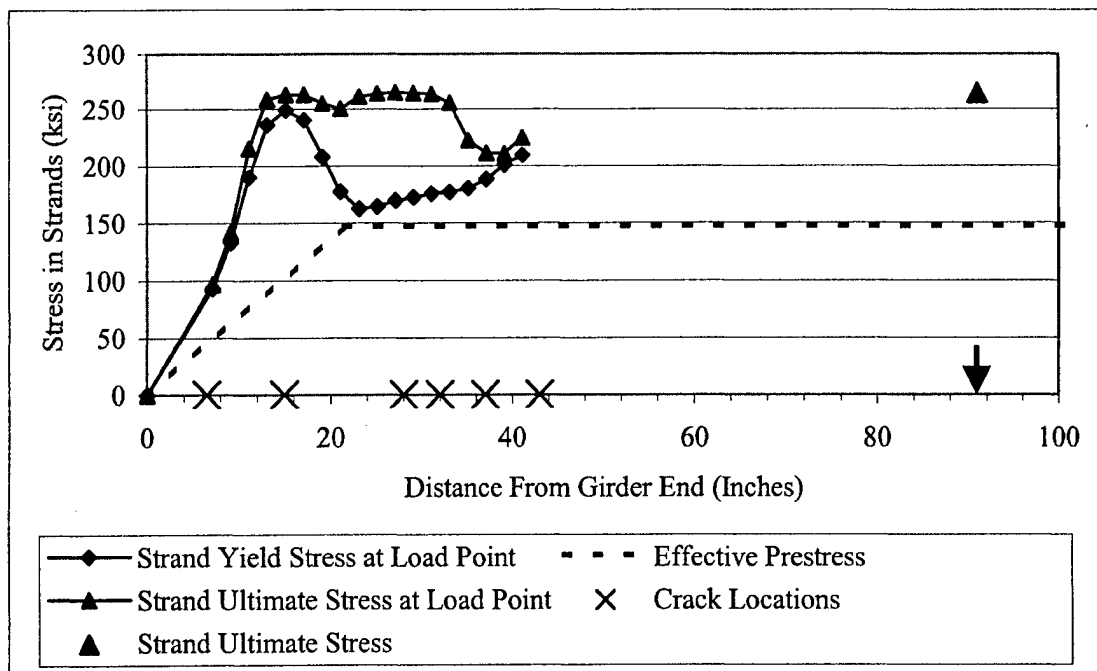
Figure Q.12 G1C-West Strand Stress vs Distance from Girder End

Q.7 Development Length Test G2A-East
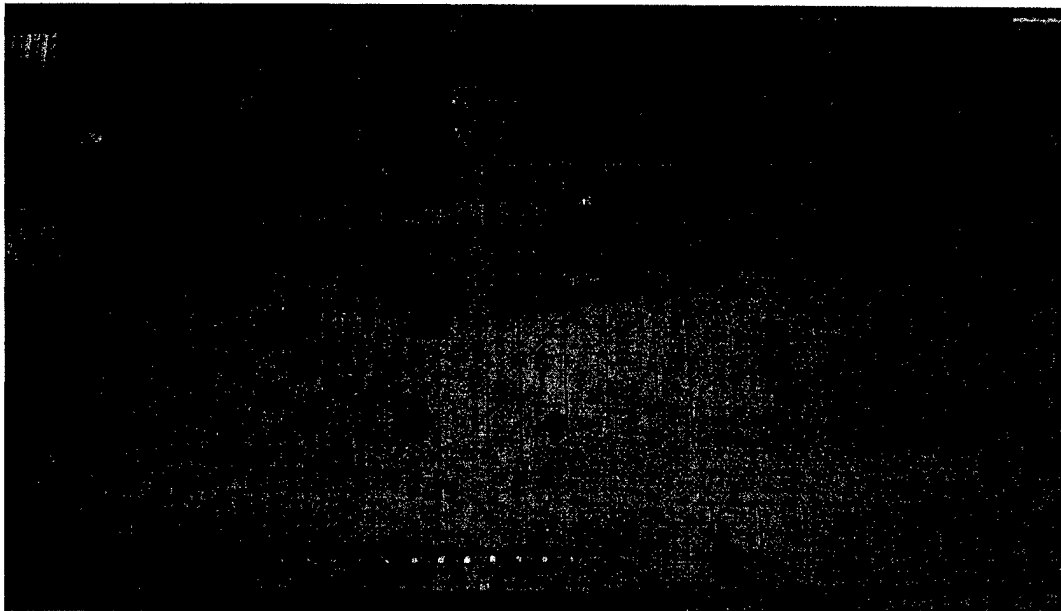
Figure Q.13 G2A-East Crack Patterns from Development Length Test
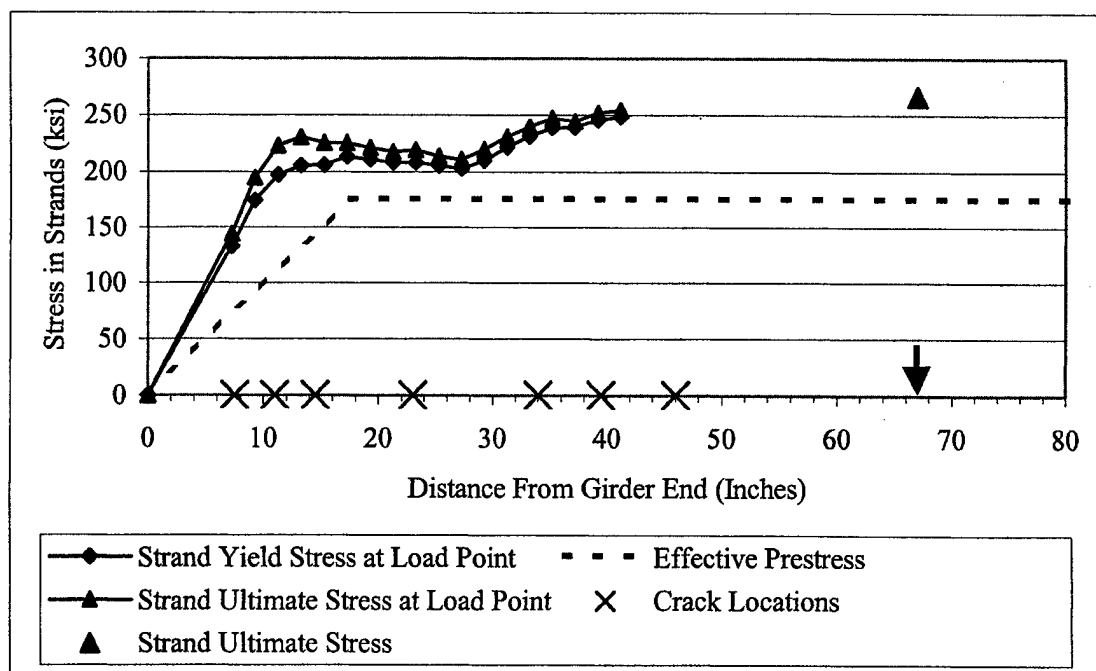
Figure Q.14 G2A-East Strand Stress vs Distance from Girder End

583

Q.8 Development Length Test G2A-West
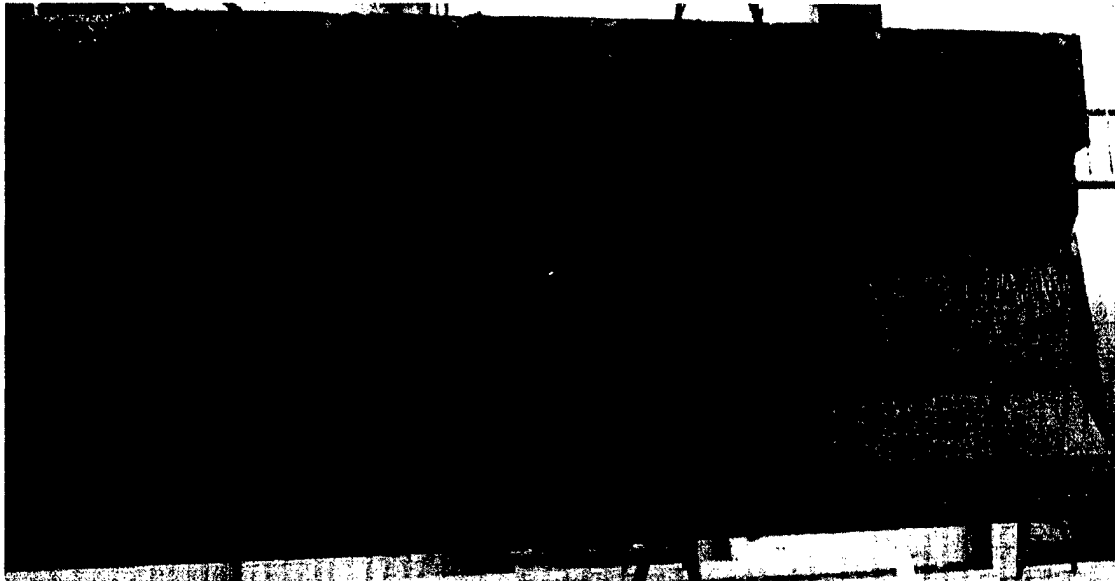
Figure Q.15 G2A-West Crack Patterns from Development Length Test
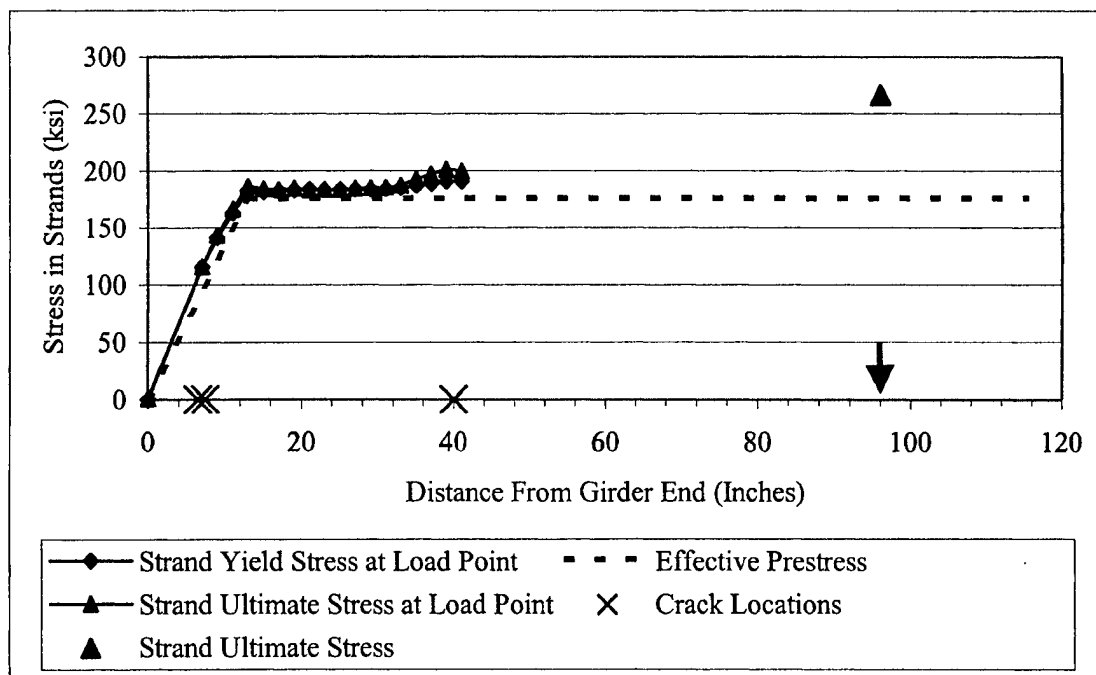
Figure Q.16 G2A-West Strand Stress vs Distance from Girder End

Q.9 Development Length Test G2B-East
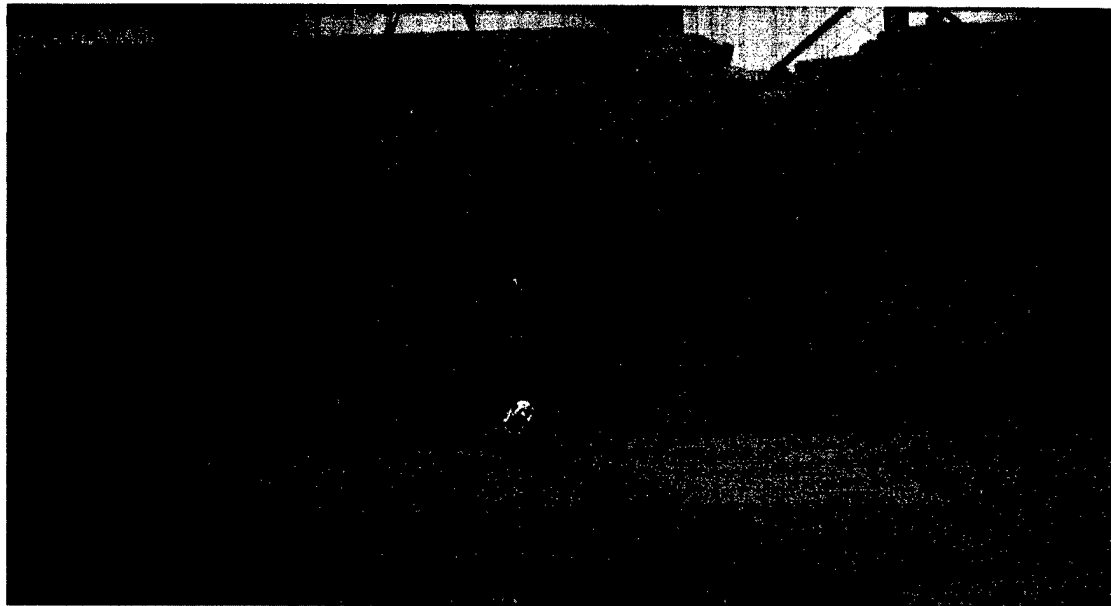
Figure Q.17 G2B-East Crack Patterns from Development Length Test
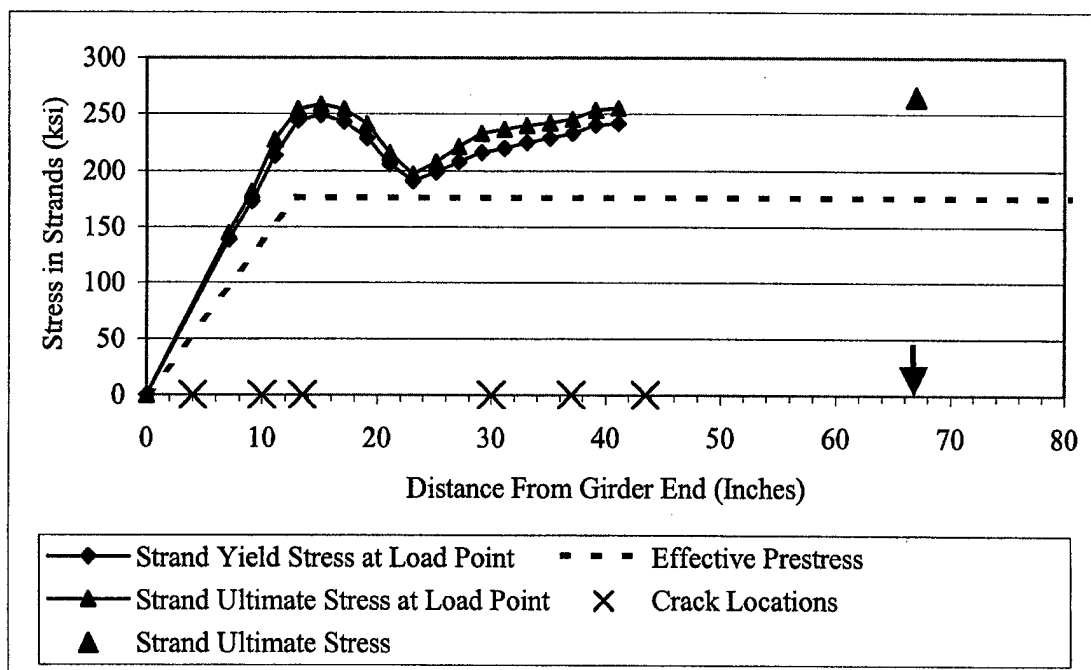
Figure Q.18 G2B-East Strand Stress vs Distance from Girder End

Q.10 Development Length Test G2B-West
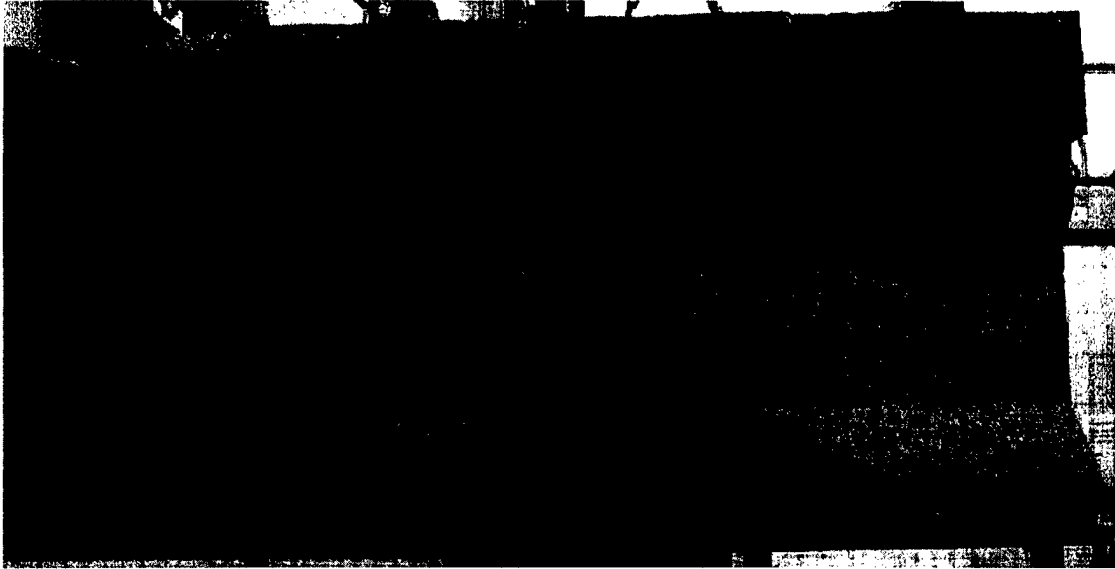
Figure Q.19 G2B-West Crack Patterns from Development Length Test
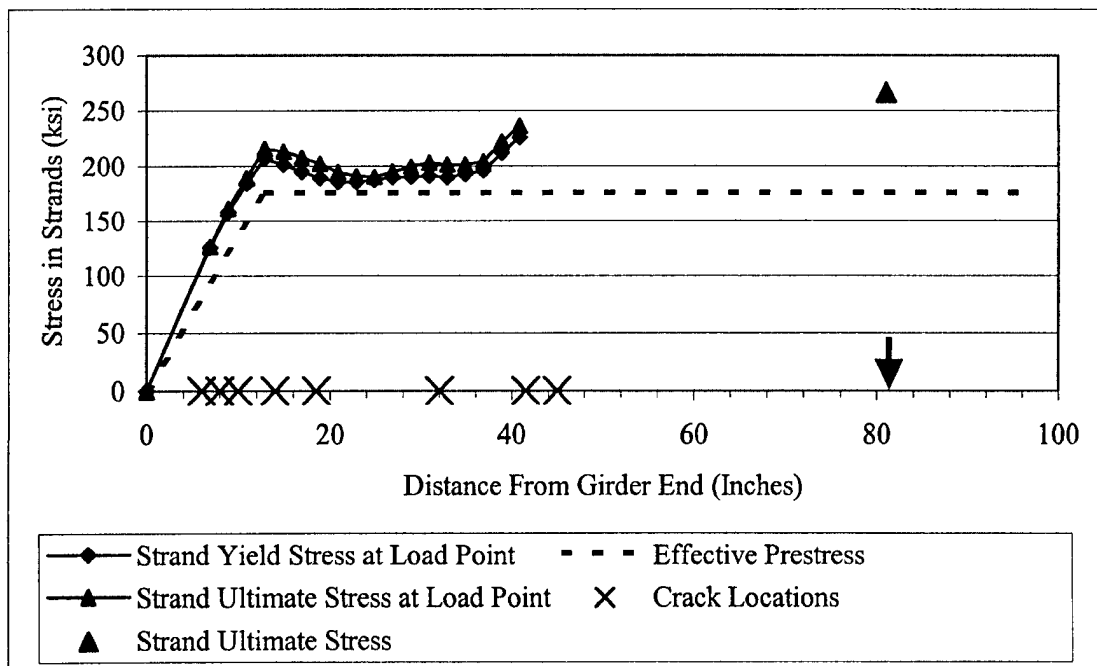
Figure Q.20 G2B-West Strand Stress vs Distance from Girder End

Q.11 Development Length Test G2C-East
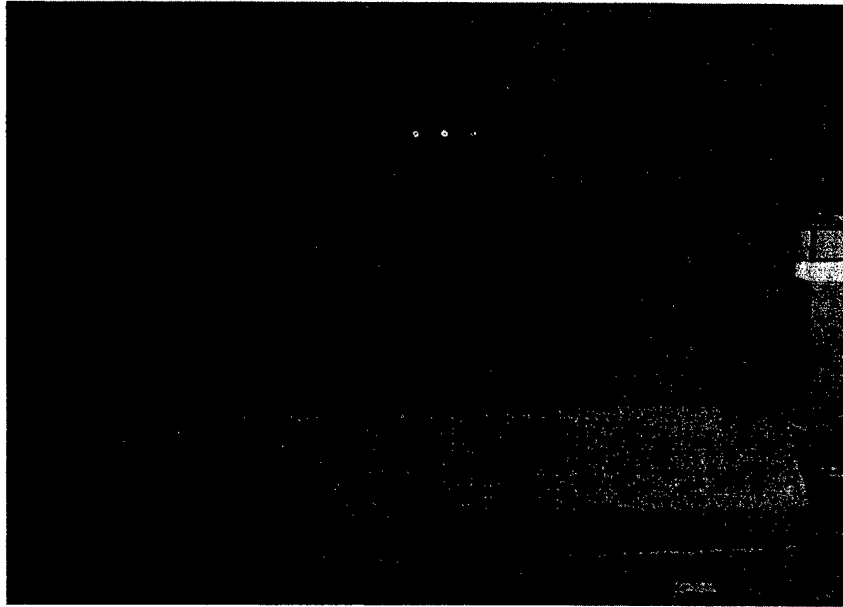
Figure Q.21 G2C-East Crack Patterns from Development Length Test
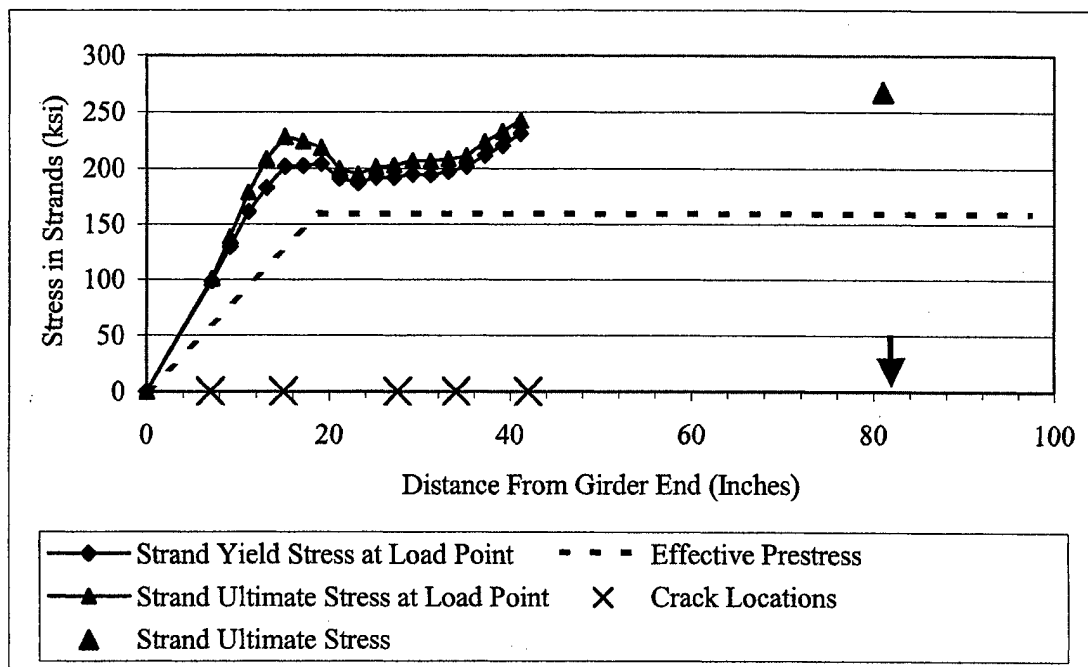
Figure Q.22 G2C-East Strand Stress vs Distance from Girder End

Q.12 Development Length Test G2C-West
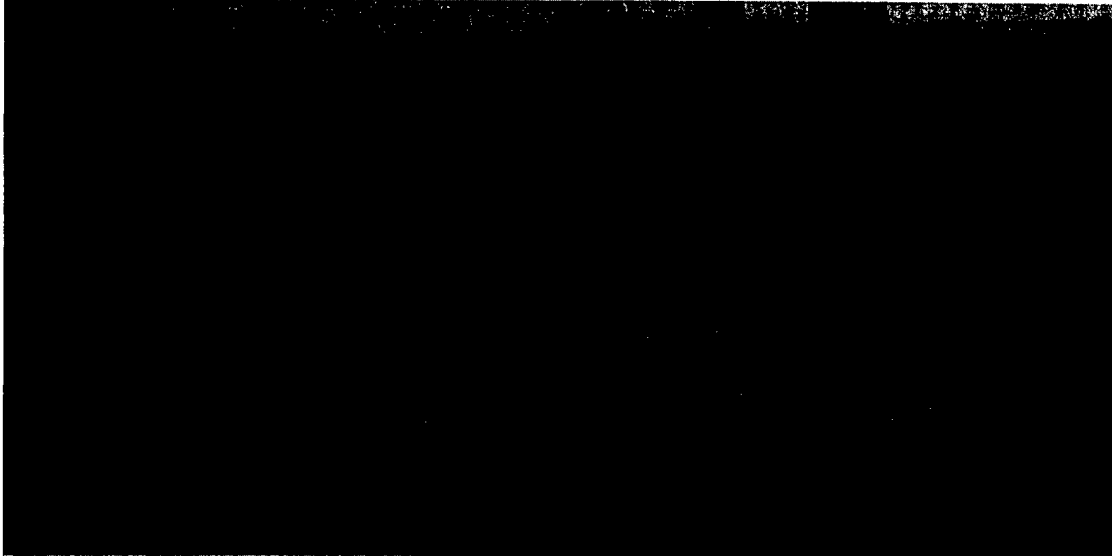
Figure Q.23 G2C-West Crack Patterns from Development Length Test
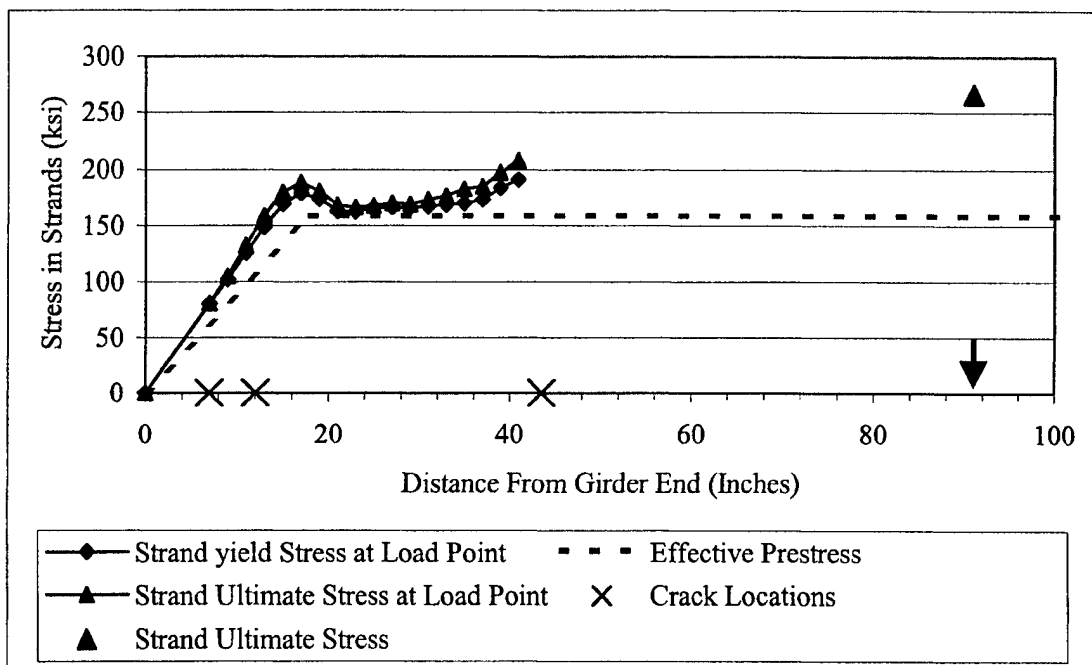
Figure Q.24 G2C-West Strand Stress vs Distance from Girder End

APPENDIX R

SHEAR vs. STRAND SLIP PLOTS
AND
CSS vs. DISTANCE FROM GIRDER END PLOTS
FROM
DEVELOPMENT LENGTH TESTS

Appendix R contains a plot comparing the applied shear vs. average strand slip and CSS vs. distance from girder ends for each development length test. For many of the applied shear vs. average strand slip plots, there is no definitive point where strand slip begins. The scatter of data on the graph as the applied shear increased due to variability in the data acquisition system and noise. In most cases, the variability of the data is less than 0.0006 inches, which essentially indicates "zero slip." On the CSS vs. distance from girder end plots, the CSS data were collected after each load step. Only the plots at applied shear levels where cracking occurred through the initial 48 inches of the girder at the lower strand level are shown. The sections correspond with the individual development length tests as follows:

Section R.1 – Test G1A-East

Section R.2 – Test G1A-West

Section R.3 – Test G1B-East

Section R.4 – Test G1B-West

Section R.5 – Test G1C-East

Section R.6 – Test G1C-West

Section R.7 – Test G2A-East

Section R.8 – Test G2A-West

Section R.9 – Test G2B-East

Section R.10 – Test G2B-West

Section R.11 – Test G2C-East

Section R.12– Test G2C-West

R.1 Development Length Test G1A-East
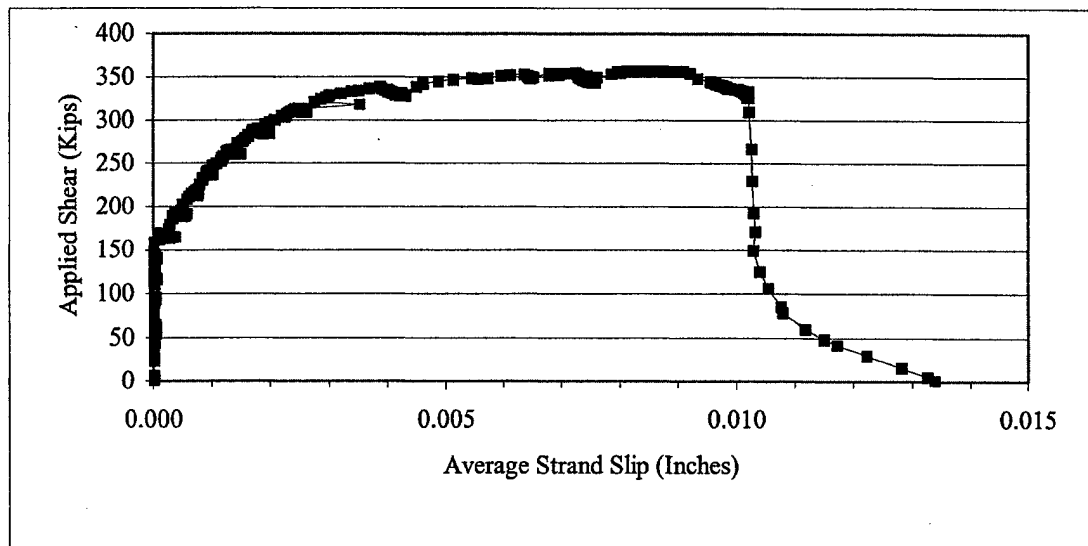
Figure R.1 G1A-East Applied Shear vs. Average Strand Slip
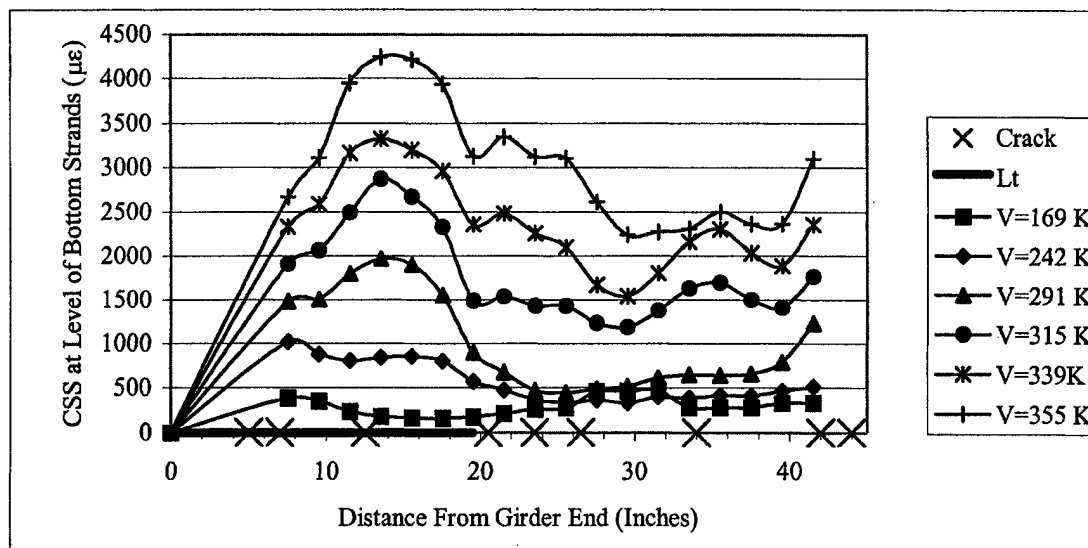
Shear Crack Data										
Distance From End (Inches)	5.0	7.0	12.5	20.5	23.5	26.5	34.0	42.0	44.0	47.5
Applied Shear at Cracking (Kips)	169	315	242	339	315	355	339	339	291	355

Figure R.2 G1A-East CSS and Shear Cracking vs. Distance from Girder End

591

R.2 Development Length Test G1A-West
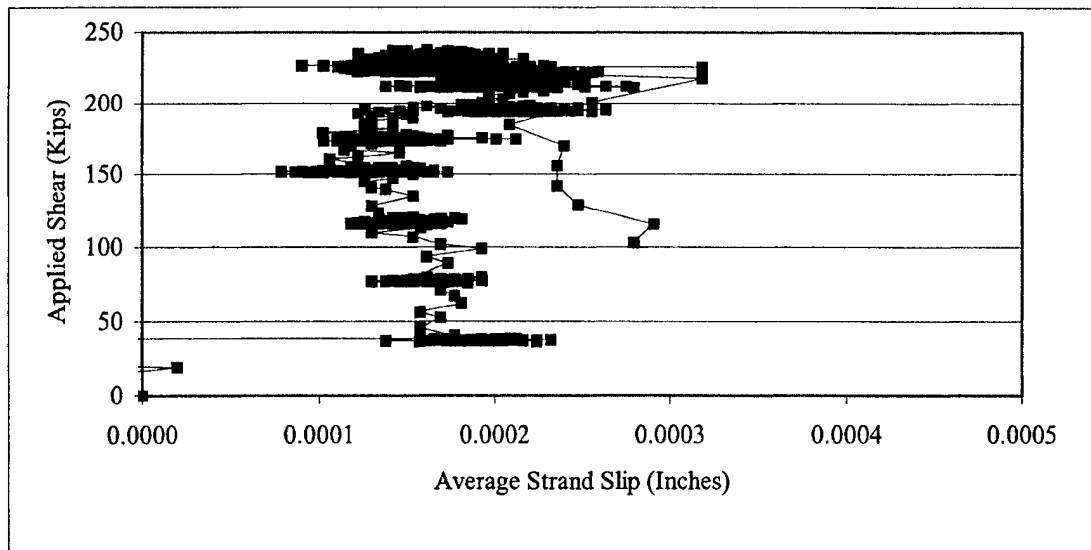
Figure R.3 G1A-West Applied Shear vs. Average Strand Slip
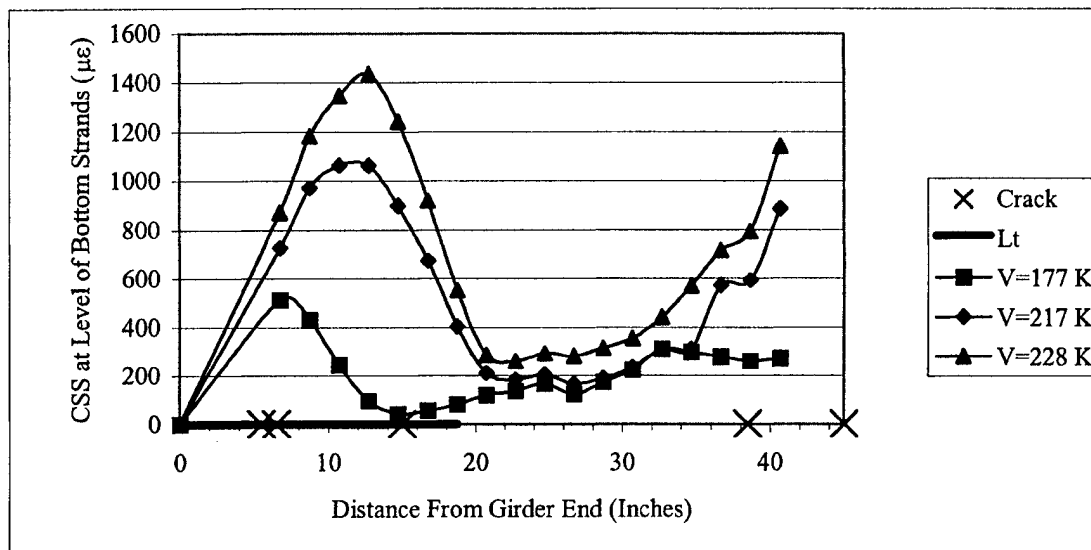
Shear Crack Data										
Distance From End (Inches)	5.5	6.5	15.0	38.5	45.0	46.5				
Applied Shear at Cracking (Kips)	177	177	217	228	228	217				

Figure R.4 G1A-West CSS and Shear Cracking vs. Distance from Girder End

592

R.3 Development Length Test G1B-East
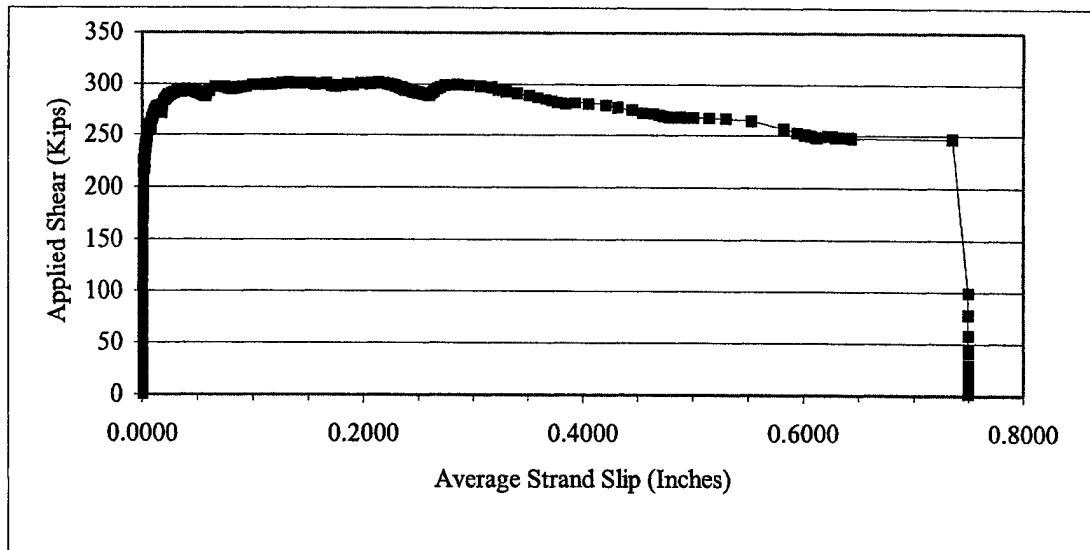
Figure R.5 G1B-East Applied Shear vs. Average Strand Slip
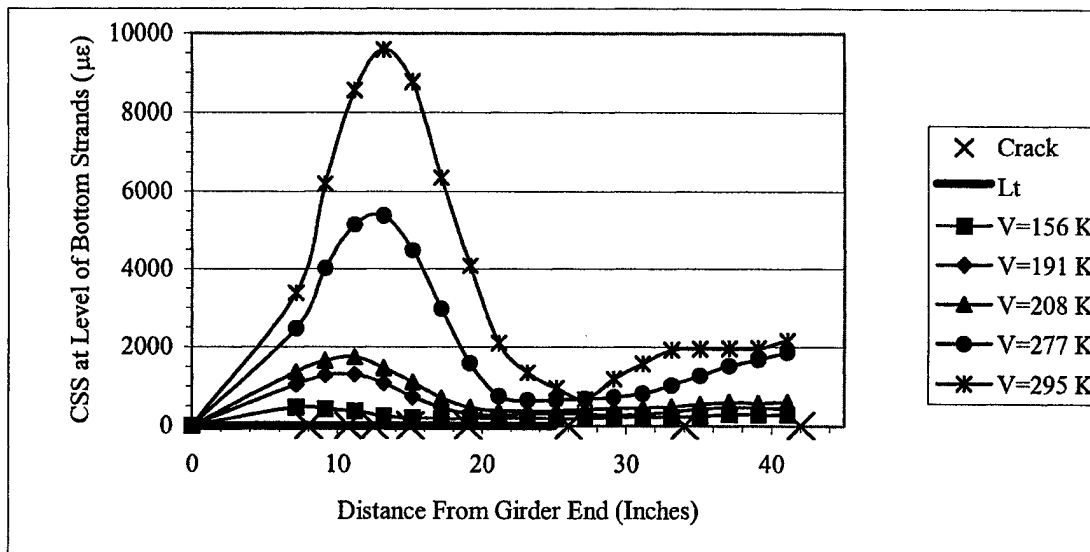
Shear Crack Data										
Distance From End (Inches)	8	10.75	12.5	15	19	26	34	42		
Applied Shear at Cracking (Kips)	156	191	208	295	295	295	295	277		

Figure R.6 G1B-East CSS and Shear Cracking vs. Distance from Girder End

R.4 Development Length Test G1B-West
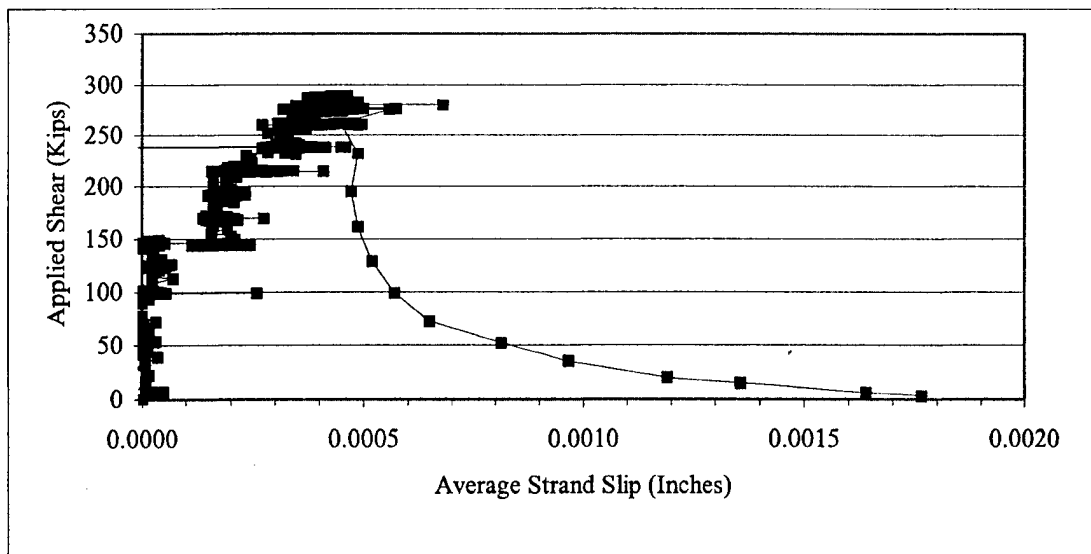
Figure R.7 G1B-West Applied Shear vs. Average Strand Slip
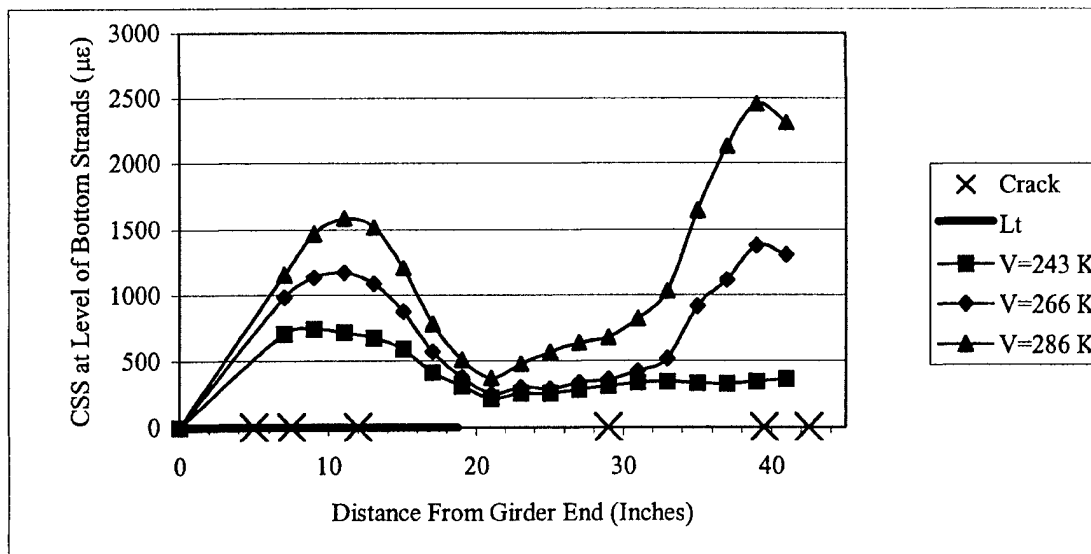
Shear Crack Data									
Distance From End (Inches)	5	7.5	12	29	39.5	42.5			
Applied Shear at Cracking (Kips)	243	266	266	286	286	286			

Figure R.8 G1B-West CSS and Shear Cracking vs. Distance from Girder End

594

R.5 Development Length Test G1C-East
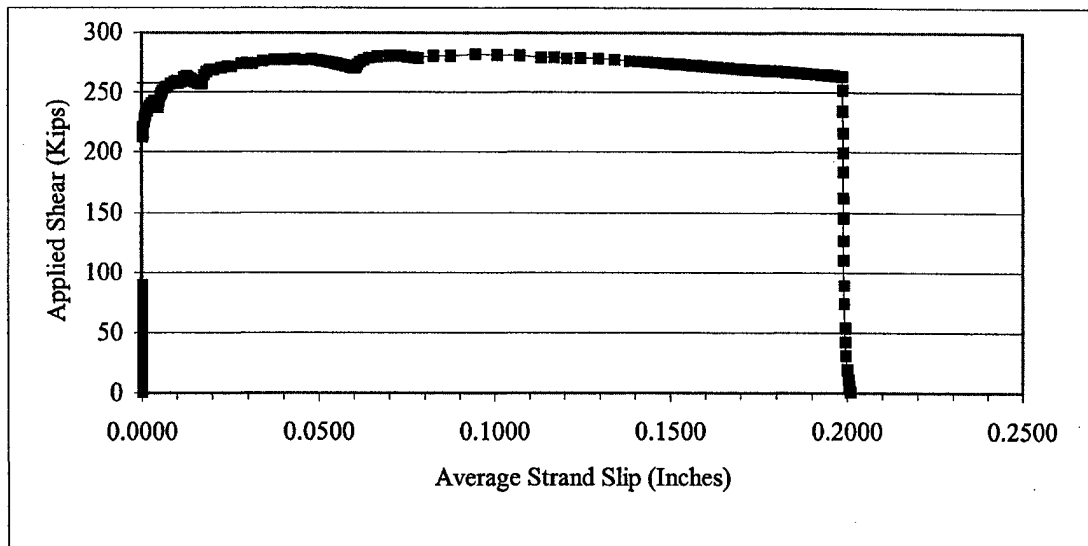
Figure R.9 G1C-East Applied Shear vs. Average Strand Slip
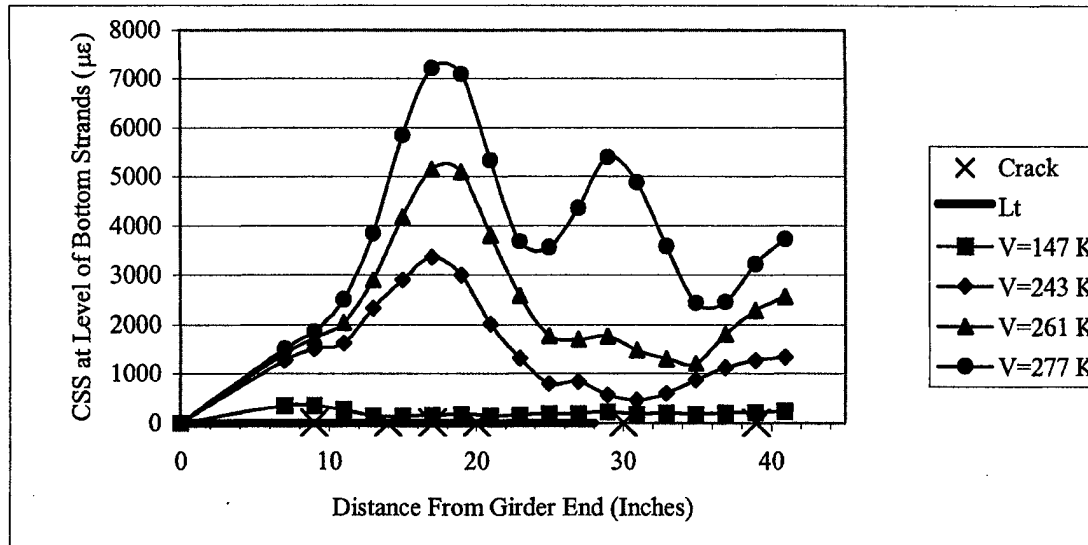
Shear Crack Data										
Distance From End (Inches)	9	14	17	20	30	39				
Applied Shear at Cracking (Kips)	147	261	243	261	261	277				

Figure R.10 G1C-East CSS and Shear Cracking vs. Distance from Girder End

595

R.6 Development Length Test G1C-West
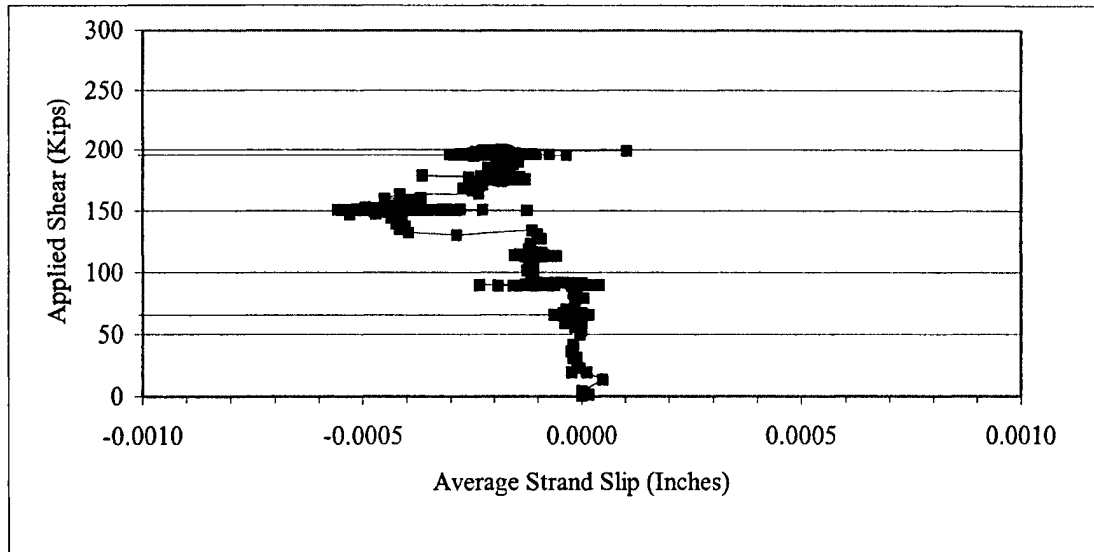
Figure R.11 G1C-West Applied Shear vs. Average Strand Slip
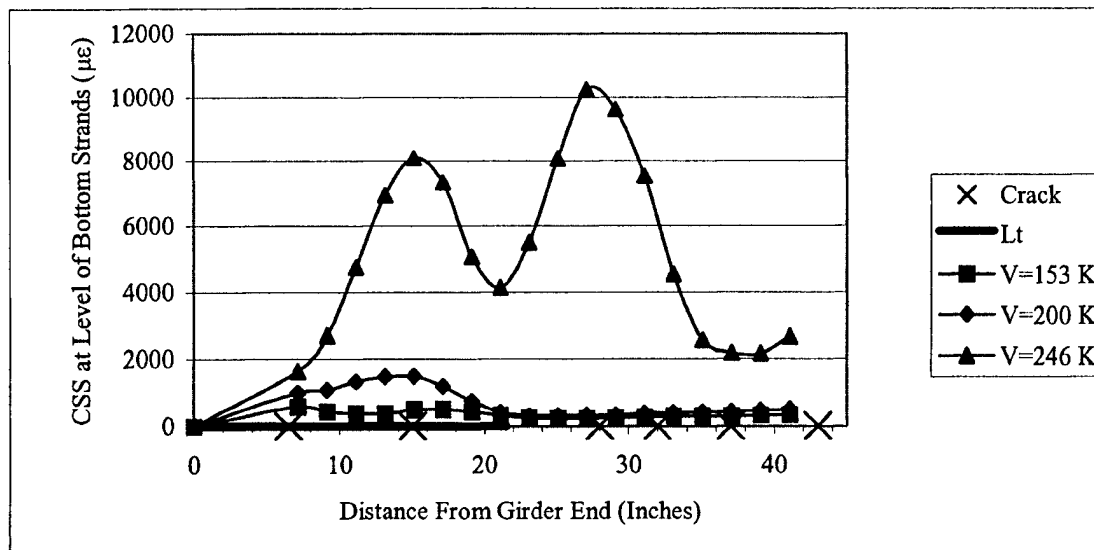
Shear Crack Data									
Distance From End (Inches)	6.5	15	28	32	37	43			
Applied Shear at Cracking (Kips)	153	153	246	246	200	246			

Figure R.12 G1C-West CSS and Shear Cracking vs. Distance from Girder End

R.7 Development Length Test G2A-East
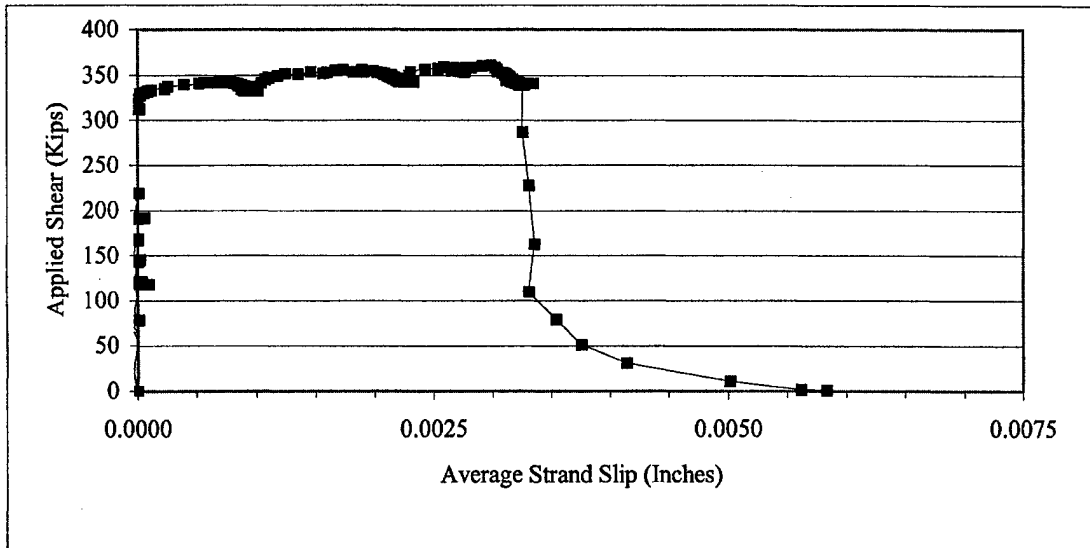
Figure R.13 G2A-East Applied Shear vs. Average Strand Slip
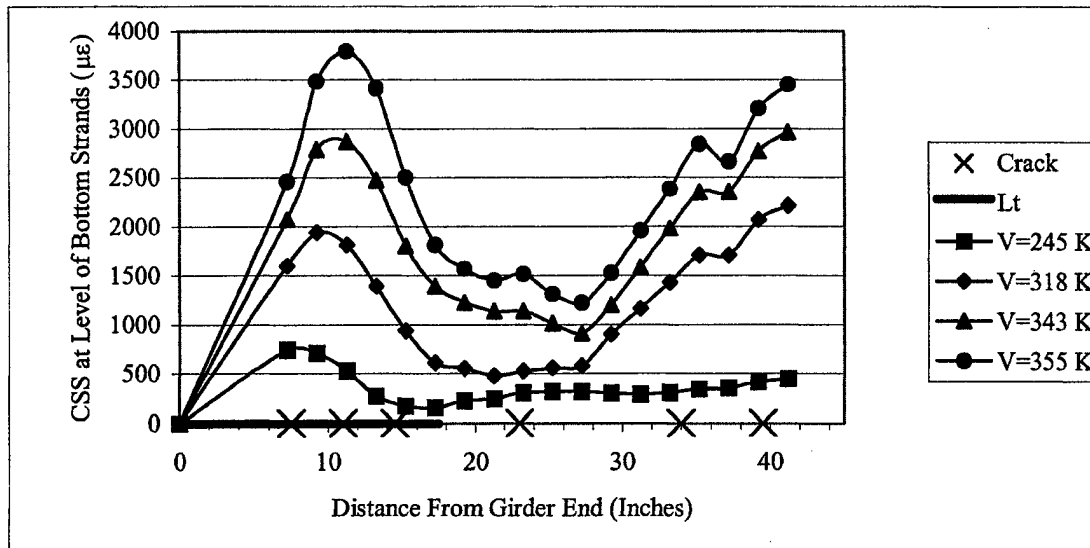
Shear Crack Data										
Distance From End (Inches)	7.5	11	14.5	23	34	39.5	46			
Applied Shear at Cracking (Kips)	245	355	343	343	318	318	355			

Figure R.14 G2A-East CSS and Shear Cracking vs. Distance from Girder End

597

R.8 Development Length Test G2A-West
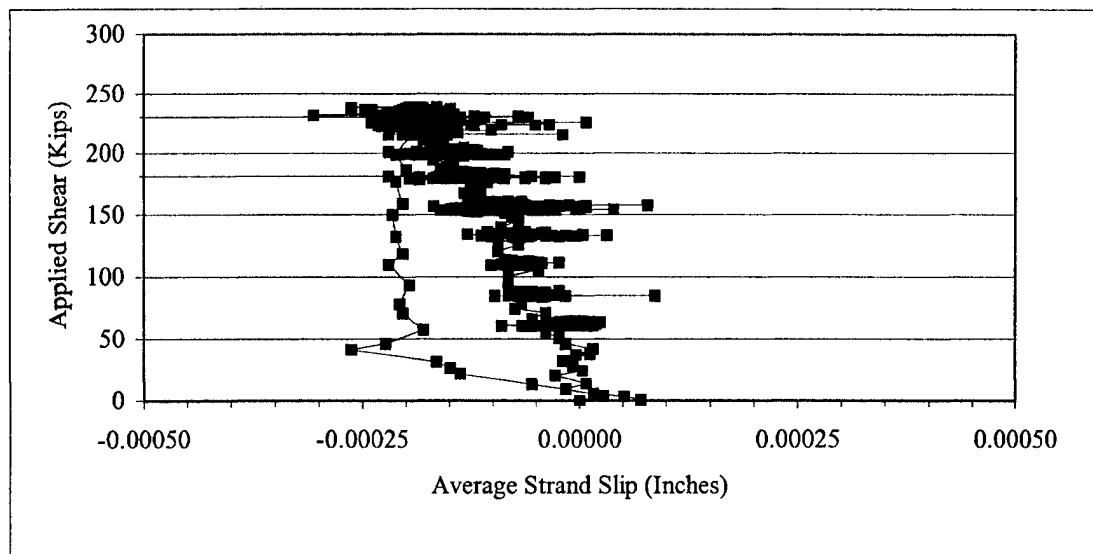
Figure R.15 G2A-West Applied Shear vs. Average Strand Slip
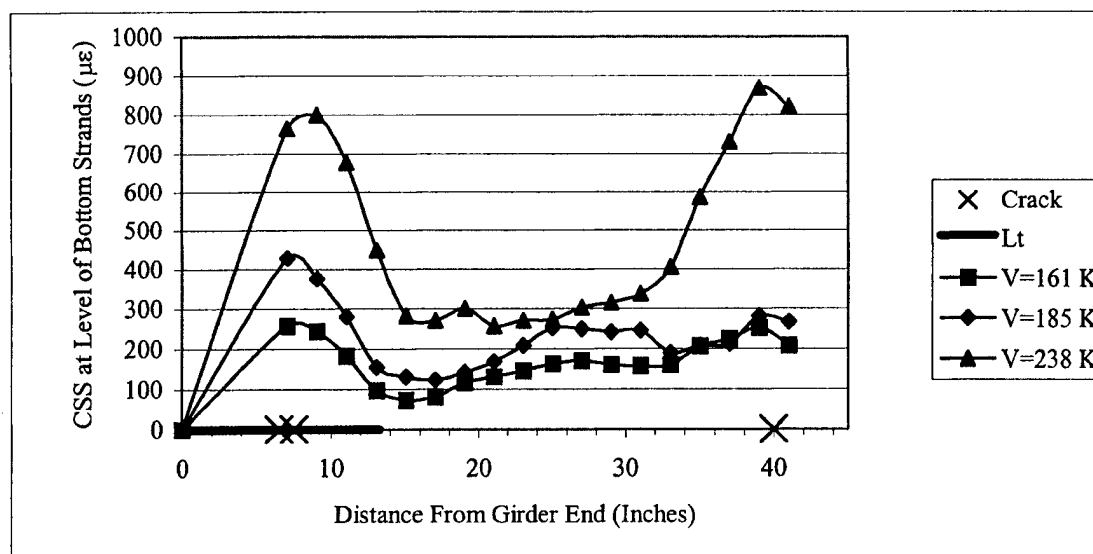
Shear Crack Data										
Distance From End (Inches)	6.5	7.5	40							
Applied Shear at Cracking (Kips)	161	185	238							

Figure R.16 G2A-West CSS and Shear Cracking vs. Distance from Girder End

598

R.9 Development Length Test G2B-East
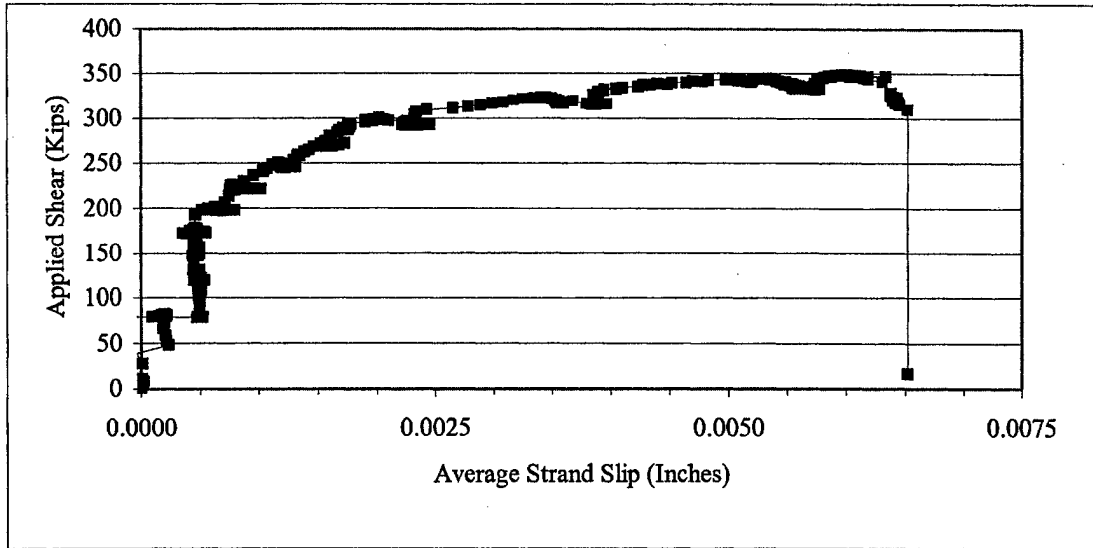
Figure R.17 G2B-East Applied Shear vs. Average Strand Slip
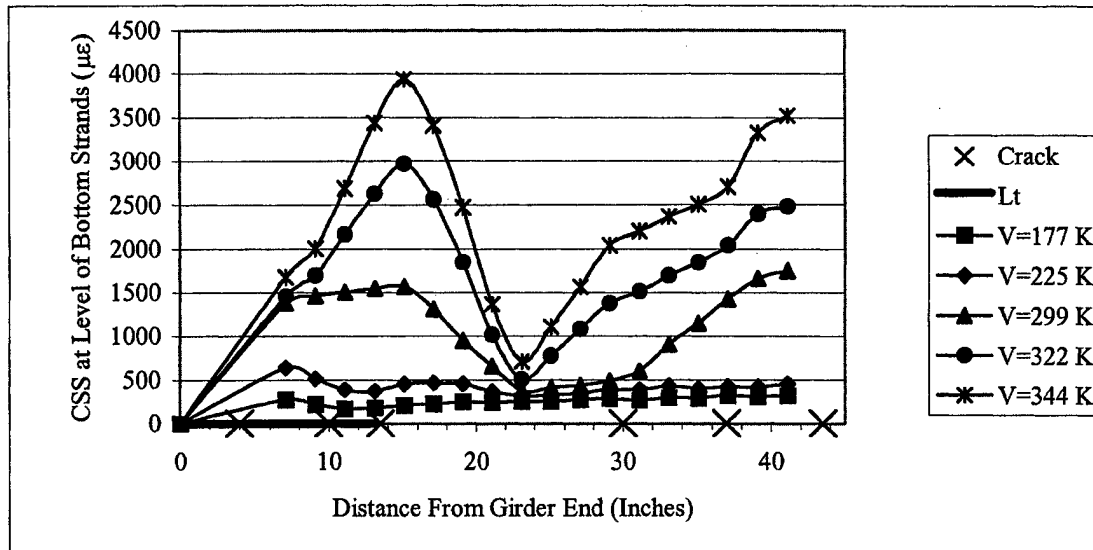
Shear Crack Data										
Distance From End (Inches)	4	10	13.5	30	37	43.5				
Applied Shear at Cracking (Kips)	177	225	322	344	299	299				

Figure R.18 G2B-East CSS and Shear Cracking vs. Distance from Girder End

R.10 Development Length Test G2B-West
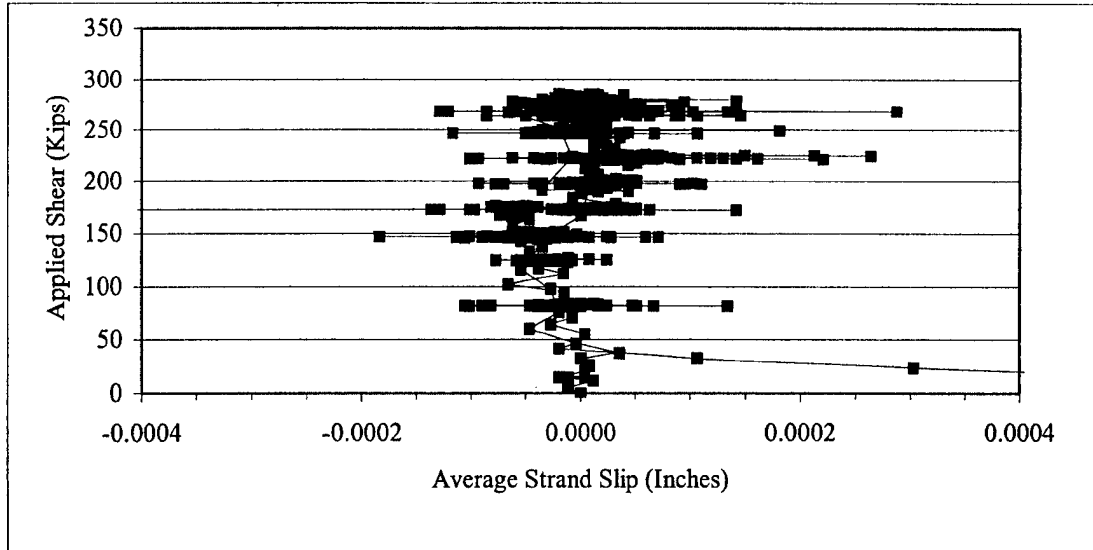
Figure R.19 G2B-West Applied Shear vs. Average Strand Slip
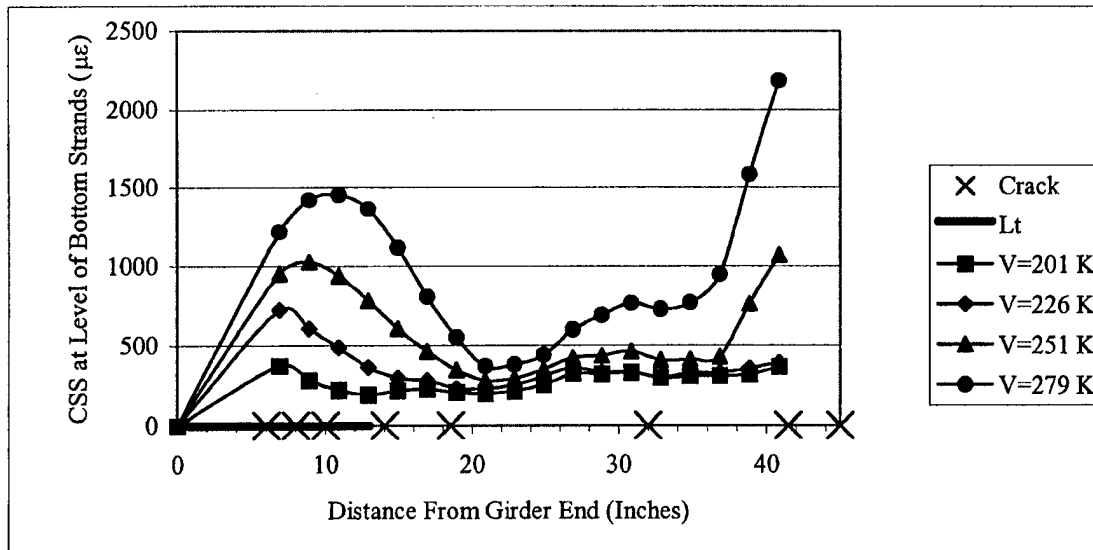
Shear Crack Data										
Distance From End (Inches)	6	8	10	14	18.5	32	41.5	45		
Applied Shear at Cracking (Kips)	201	226	251	251	279	279	279	251		

Figure R.20 G2B-West CSS and Shear Cracking vs. Distance from Girder End

R.11 Development Length Test G2C-East
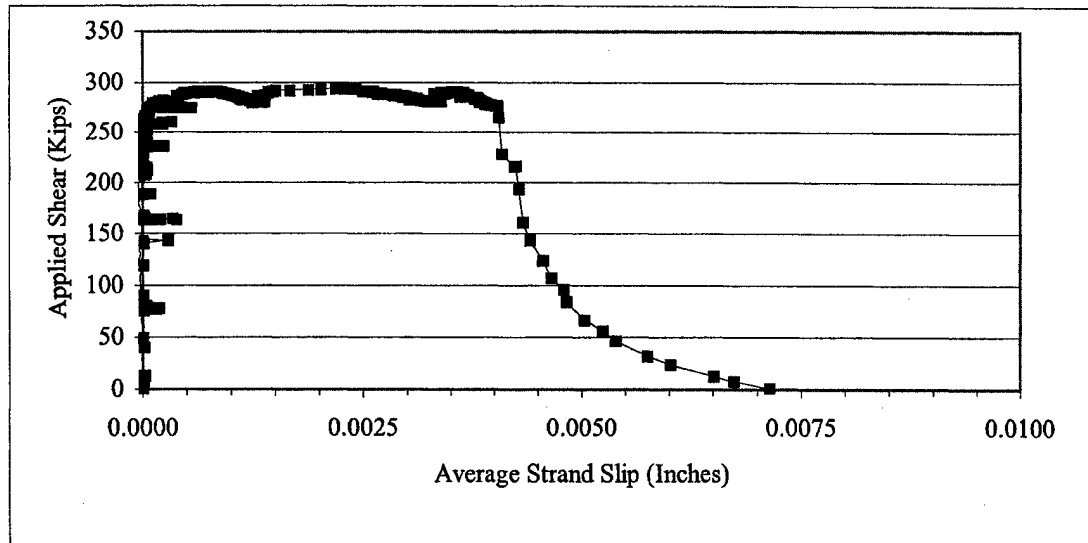
Figure R.21 G2C-East Applied Shear vs. Average Strand Slip
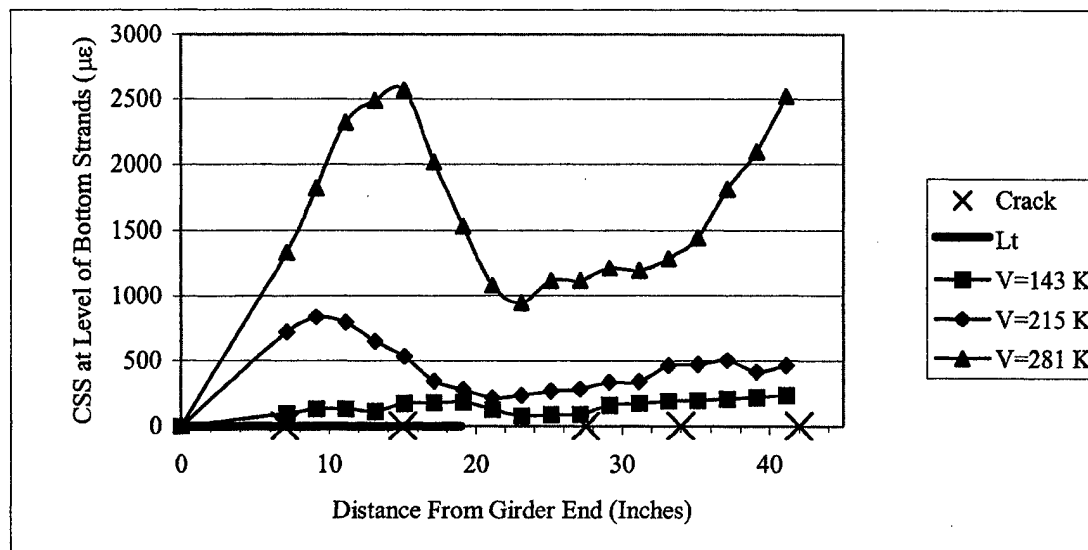
Shear Crack Data										
Distance From End (Inches)	7	15	27.5	34	42					
Applied Shear at Cracking (Kips)	143	215	281	281	281					

Figure R.22 G2C-East CSS and Shear Cracking vs. Distance from Girder End

R.12 Development Length Test G2C-West
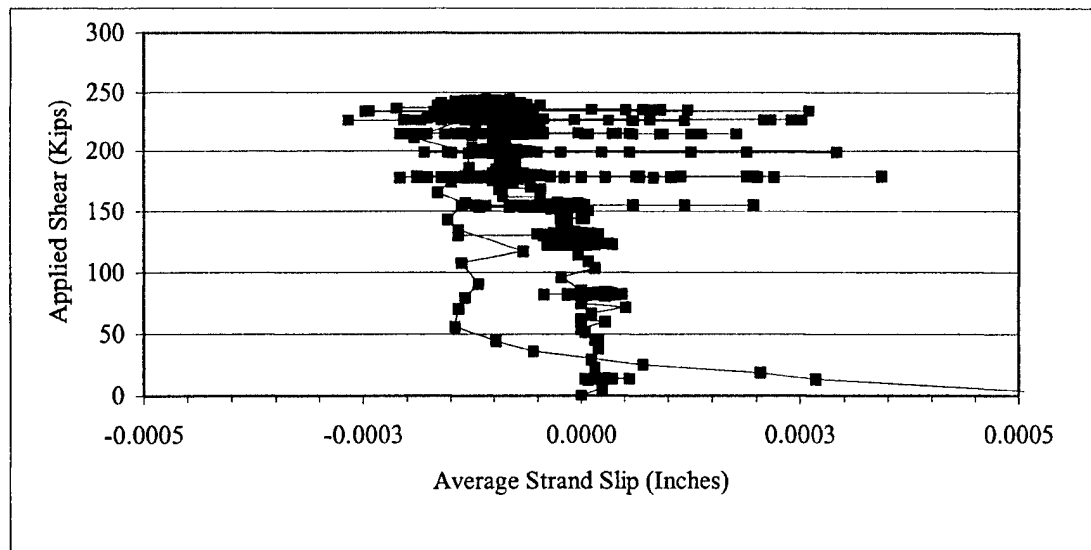
Figure R.23 G2C-West Applied Shear vs. Average Strand Slip
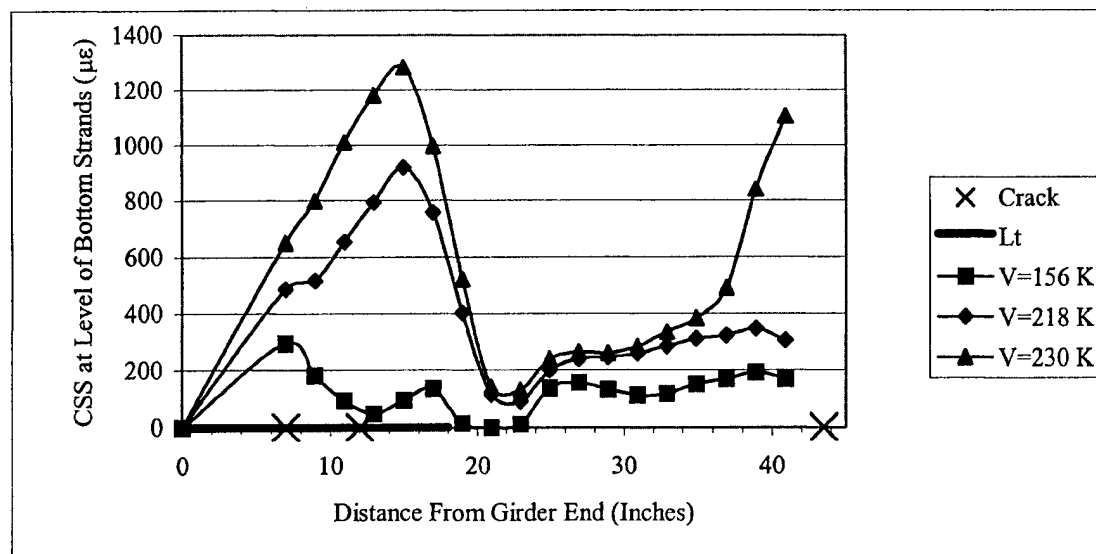
Shear Crack Data										
Distance From End (Inches)	7	12	43.5							
Applied Shear at Cracking (Kips)	156	218	230							

Figure R.24 G2C-West CSS and Shear Cracking vs. Distance from Girder End

602

APPENDIX S

VWSG AND CONCRETE SURFACE STRAIN DATA FROM DEVELOPMENT LENGTH TESTS

Appendix S contains raw data for each development length test. Prior to a test, values from the vibrating wire strain gage (VWSG) were recorded. During the test, CSS readings were taken at the tested end and at midspan at the level of the top and bottom strands. The sections correspond with the individual development length tests as follows

Section S.1 – Consolidated VWSG Data

Section S.2 – Test G1A-East

Section S.3 – Test G1A-West

Section S.4 – Test G1B-East

Section S.5 – Test G1B-West

Section S.6 – Test G1C-East

Section S.7 – Test G1C-West

Section S.8 – Test G2A-East

Section S.9 – Test G2A-West

Section S.10 – Test G2B-East

Section S.11 – Test G2B-West

Section S.12 – Test G2C-East

Section S.13 – Test G2C-West

S.1 Consolidated Vibrating Wire Strain Gage Data

Table S.1 Vibrating Wire Strain Gage Data From Development Length Tests

Development Length Test #	Vibrating Wire Strain Gage Reading (Hz)	Thermistor Reading (ohms)	Strain in Concrete At Bottom Strands (microstrains)	Effective Stress In Bottom Strands f_{se} (ksi)
G1A-East	774.77	3780	-378.9	153.7
G1A-West	763.93	3131	-343.7	152.3
G1B-East	762.59	3035	-353.8	151.2
G1B-West	754.38	3770	-360.4	149.7
G1C-East	718.33	3410	-359.4	149.0
G1C-West	708.37	3360	-329.2	147.6
G2A-East	836.69	3450	-418.9	175.8
G2A-West	836.12	3450	-387.4	175.7
G2B-East	817.63	3760	-418.6	176.2
G2B-West	813.30	3550	-393.9	175.6
G2C-East	801.33	Inoperative	-350.8	159.3
G2C-West	797.96	Inoperative	-327.2	158.8

S.2 G1A-East

Table S.2 Raw Concrete Surface Strains Data for Development Length Test G1A-East

Step	1	2	3	4	5	6	7	8	9	10	11	12	13
Load (Kips)	80	120	150	180	210	241	270	300	330	360	390	420	440

Gage	North Side CSS - microstrains												
1	113	113	113	138	363	564	965	1178	1253	1404	1742	2068	2319
2	94	181	181	206	457	632	995	1145	1183	1370	1733	1996	2246
3	113	125	150	150	188	163	363	800	1551	2239	3339	4565	5865
4	112	137	137	137	150	162	262	723	1509	2233	3056	3967	5251
5	119	169	169	181	181	181	306	756	1556	2419	3157	4044	5369
6	144	207	182	257	282	219	470	933	1773	2600	3427	4354	5795
7	125	125	150	175	175	175	225	213	301	376	426	1340	2831
8	94	219	232	269	282	219	194	320	470	457	1021	1923	2863
9	131	181	194	306	331	344	381	419	519	481	1281	2094	3044
10	113	163	188	238	276	263	288	338	363	413	1177	2142	4045
11	187	250	275	337	375	412	400	487	525	575	1312	1625	2500
12	112	162	237	287	350	337	337	412	387	512	787	1062	2087
13	150	163	200	250	225	275	363	388	401	388	601	864	2003
14	44	181	131	257	307	369	407	332	469	619	1608	2196	2459
15	100	201	213	288	326	313	389	426	426	527	1630	2320	2382
16	144	169	194	219	257	307	357	395	407	570	1560	2250	2287
17	132	182	207	294	332	357	407	445	470	620	1509	2211	2298
18	150	187	225	275	312	337	412	425	437	762	1137	1536	1998
19	188	175	263	313	363	388	463	550	563	1588	2326	3064	3914
20	157	194	244	294	369	407	457	570	607	1521	2248	3199	4238
Gage	South Side CSS - microstrains												
1	125	162	224	287	324	449	486	586	1134	2419	3154	4239	5286
2	87	112	437	475	362	387	450	487	487	525	587	700	1037
3	112	137	187	312	300	375	450	462	487	587	1137	1400	2100
4	138	113	213	275	300	363	438	413	438	663	1777	2403	2841
5	87	100	162	175	200	325	387	350	537	774	1861	2398	2648
6	106	106	293	206	293	468	355	480	443	717	1802	2264	2538
7	162	50	225	225	312	324	349	337	362	699	1322	1572	1559
8	94	81	181	231	1378	318	393	430	393	729	1265	1602	2724
9	231	144	131	306	218	393	368	106	343	181	1541	1941	2627
10	118	118	218	268	206	368	330	380	393	542	1876	2936	3722
11	68	255	143	193	243	305	342	305	392	479	1861	2882	3629
12	25	99	249	199	174	187	311	286	336	336	1069	1865	1790
13	81	131	180	193	-19	56	815	1213	1524	1910	2793	4000	4697
14	69	44	106	144	131	106	543	967	1279	1841	2340	2939	3525
15	81	144	231	119	94	231	681	1156	1518	2131	3968	3218	3930
16	13	88	75	138	113	138	525	1113	1488	2038	2700	3275	3800
17	25	212	300	312	287	300	387	387	549	387	936	1061	1286
18	6	168	156	68	492	616	953	1052	1326	1476	1774	2048	2123
19	107	194	232	357	545	758	871	1159	1172	1334	1560	1898	1886
20	63	88	113	50	289	577	728	778	929	1067	1305	1443	1606

S.3 G1A-West

Table S.3 Raw Concrete Surface Strains Data for Development Length Test G1A-West

Step	1	2	3	4	5	6	7	8	9	10	11
Load (Kips)	50	100	150	194	221	248	270	284	292	294	290

Gage	North Side CSS - microstrains										
1	94	144	207	307	370	495	1059	1987	1849	1949	1812
2	88	100	200	225	301	401	476	764	1565	1828	1778
3	88	75	163	250	301	388	1703	714	1540	1741	1728
4	63	113	163	226	276	338	439	765	1617	1855	1805
5	94	119	195	270	320	420	345	195	1525	1537	1512
6	88	138	164	239	252	340	315	340	378	466	491
7	188	201	239	289	364	402	389	490	502	615	628
8	69	81	106	182	182	269	282	332	370	382	395
9	38	75	100	138	176	251	238	276	301	313	288
10	81	81	119	243	281	343	343	381	443	443	406
11	119	157	207	257	244	332	307	407	432	357	395
12	44	82	107	157	157	194	207	220	257	232	270
13	75	63	88	75	213	276	376	326	288	288	451
14	0	50	38	113	138	301	890	1266	1530	1655	1655
15	37	37	12	62	62	287	923	1273	1535	1635	1647
16	31	94	81	157	144	407	959	1359	1547	1410	1673
17	38	63	113	88	125	651	1139	1690	1940	1815	1490
18	31	44	44	232	444	807	983	1020	995	995	945
19	0	50	63	251	790	752	840	865	840	865	990
20	12	37	12	187	399	648	499	785	773	785	773
Gage	South Side CSS - microstrains										
1	56	6	31	332	557	720	683	833	833	795	946
2	94	132	56	244	457	633	457	720	633	708	733
3	25	-12	-12	237	424	748	898	1010	1010	998	1048
4	19	-44	-31	143	343	842	1503	1790	1790	1728	1728
5	-13	-75	-138	-163	-13	325	888	1200	1463	1526	1601
6	-19	6	-56	-81	-81	319	956	1306	1556	1606	1656
7	50	0	-25	-38	0	351	777	1041	1542	1442	1780
8	56	19	-31	-19	6	56	119	306	556	731	818
9	69	-69	56	-19	-31	82	44	157	144	44	182
10	44	69	69	107	132	195	220	295	308	232	308
11	157	31	107	132	31	6	-19	107	144	56	282
12	82	120	132	107	132	196	145	284	360	322	423
13	169	219	132	69	-56	319	6	307	432	420	432
14	94	107	94	107	244	295	81	194	357	332	370
15	88	113	113	100	363	388	325	463	538	713	688
16	62	75	112	137	312	374	399	973	1559	1771	1808
17	62	25	112	62	262	225	37	686	1447	1347	1285
18	93	118	205	193	193	504	504	964	1599	1686	1736
19	249	374	237	249	224	411	399	872	1445	1495	1520
20	162	-37	174	162	237	349	1170	1544	1668	1606	1693

606

S.4 G1B-East

Table S.4 Raw Concrete Surface Strains Data for Development Length Test G1B-East

Step	1	2	3	4	5	6	7	8	9	10	11	12	13
Load (Kips)	100	120	140	160	180	200	220	240	260	280	300	320	340

Gage	North Side CSS - microstrains												
1	-31	-31	-44	-56	168	454	479	479	466	541	752	963	1187
2	-19	-31	-44	-118	193	642	1066	1514	1726	1789	2175	2973	3745
3	112	162	162	137	425	987	1524	1961	2586	3386	4098	5722	7696
4	106	94	119	106	319	1007	1483	1984	2697	3623	4436	6051	9129
5	-50	0	38	25	38	364	829	1344	1935	3154	4021	5817	9461
6	38	38	63	75	75	250	300	400	763	1951	2651	3939	6966
7	-94	-31	-31	-19	219	181	106	81	56	556	943	1443	5654
8	-25	-38	-13	-13	50	88	88	113	113	338	614	1077	4045
9	131	106	119	144	219	244	269	306	281	306	343	518	2841
10	94	81	106	144	181	207	219	257	257	294	344	507	2772
11	0	-25	38	50	-25	175	188	188	200	263	375	538	438
12	50	50	87	75	125	199	224	237	262	312	411	436	461
13	99	124	137	149	199	248	286	360	311	410	472	460	783
14	143	155	193	205	267	329	354	379	391	416	540	764	1361
15	75	62	99	137	75	236	286	323	286	385	447	559	1242
16	106	106	156	131	194	319	344	407	394	469	557	845	1445
17	107	94	69	119	119	295	270	333	370	496	634	1601	2216
18	19	82	119	157	207	282	333	383	408	533	621	1374	1563
19	132	169	194	219	269	382	370	432	482	645	808	1760	2224
20	88	113	163	175	200	300	300	388	363	538	1013	1875	2288
Gage	South Side CSS - microstrains												
1	220	321	321	321	396	572	522	937	786	723	1075	2597	3163
2	113	201	176	252	239	415	516	705	1032	793	768	1851	1737
3	264	352	326	377	427	515	615	778	979	866	916	1770	1958
4	340	302	327	365	390	504	617	818	1095	718	995	1699	2027
5	334	334	372	359	385	624	586	864	498	889	1255	1835	2566
6	227	240	164	328	265	492	467	505	821	606	644	1073	2159
7	126	139	126	38	177	215	38	442	1175	720	581	1112	2768
8	190	203	228	215	354	354	329	671	874	798	494	899	1165
9	139	164	113	76	151	340	340	567	617	529	277	655	554
10	145	182	233	170	295	270	459	471	735	773	446	1075	622
11	220	220	220	270	308	333	409	547	710	597	622	723	798
12	126	163	151	213	239	213	264	452	477	477	402	465	590
13	132	195	132	69	207	333	257	596	835	835	1337	1162	1526
14	56	94	119	69	182	620	821	1259	1911	2788	3677	4893	9804
15	94	106	144	131	307	758	1121	1697	2398	3212	4389	5278	10112
16	193	206	218	256	393	892	1203	1827	2326	3498	4046	5480	10680
17	112	199	212	125	312	1184	1583	1571	2593	3678	4613	5661	11184
18	336	-62	461	174	784	1195	1208	1755	1992	1992	2291	2141	3174
19	205	130	242	168	528	615	826	1174	1546	1745	1521	1571	2229
20	228	204	315	327	673	1118	1105	1315	1525	1575	1809	1402	2217

S.5 G1B-West

Table S.5 Raw Concrete Surface Strains Data for Development Length Test G1B-West

Step	1	2	3	4	5	6	7	8	9	10	11	12
Load (Kips)	77	130	160	190	220	250	280	310	340	360	365	367

Gage	North Side CSS - microstrains											
1	94	169	144	194	244	281	356	406	1144	1506	1731	1793
2	75	125	150	200	237	262	350	387	1437	1936	2224	2286
3	56	-6	56	219	281	269	343	443	1505	2317	2654	2741
4	63	113	125	150	213	225	275	338	1488	2175	2275	2313
5	50	113	125	163	200	250	301	388	864	1340	1440	1465
6	62	75	100	150	175	225	300	350	524	787	1099	1224
7	94	107	119	170	195	245	270	308	383	433	672	810
8	6	56	56	157	195	119	282	345	446	571	709	785
9	57	94	69	145	245	233	233	283	359	409	661	812
10	63	88	88	126	151	164	214	264	264	327	340	353
11	0	25	75	100	162	175	187	262	225	325	337	375
12	69	69	81	119	119	156	219	207	244	282	357	369
13	50	62	62	62	87	112	162	187	199	249	299	324
14	62	62	112	50	137	137	212	249	237	399	462	549
15	38	63	38	50	75	100	100	275	438	638	763	813
16	63	75	25	25	88	88	138	450	838	1150	1238	1375
17	50	63	50	75	113	100	138	700	1263	1588	1775	1850
18	25	37	25	50	75	75	87	699	1198	1435	1523	1585
19	6	31	19	81	181	306	468	1004	1353	1552	1627	542
20	56	69	56	143	218	330	480	791	953	1028	1052	1115
Gage	South Side CSS - microstrains											
1	-56	-94	-44	-19	44	294	457	545	707	720	707	695
2	-88	-326	-288	-163	75	213	426	476	539	639	652	601
3	-13	13	13	150	288	488	550	725	1163	1376	1376	1301
4	0	75	-12	-12	25	150	225	849	1312	1749	1861	1786
5	6	-69	-6	44	81	257	219	895	1271	1671	1721	1734
6	25	63	-25	-75	25	213	226	877	1416	1729	1729	1830
7	-13	-13	-38	25	63	251	263	814	1053	1341	1328	1341
8	125	50	50	63	113	63	25	100	88	113	125	125
9	232	132	182	169	207	257	219	320	457	345	507	545
10	19	31	94	44	194	144	207	244	294	382	607	645
11	38	63	50	63	201	138	163	238	314	289	728	778
12	19	-57	-19	69	233	107	195	245	283	258	723	823
13	44	69	144	182	220	220	295	320	358	395	684	722
14	63	75	150	75	176	50	251	364	326	326	639	652
15	0	-13	63	88	138	138	301	326	502	1003	1141	1192
16	225	75	150	188	225	275	325	338	526	1014	1202	1239
17	132	-6	257	82	220	232	144	245	1588	2505	2706	2794
18	101	-63	-25	176	252	289	201	214	717	2378	2504	2617
19	157	119	144	107	295	245	270	433	1511	2100	2364	2213
20	107	31	132	182	220	245	471	295	1538	2078	2392	2341

S.6 G1C-East

Table S.6 Raw Concrete Surface Strains Data for Development Length Test G1C-East

Step	1	2	3	4	5	6	7	8	9	10	11
Load (Kips)	81	112	152	185	215	245	275	305	328	348	349

Gage	North Side CSS - microstrains										
1	-119	-6	-19	256	431	568	606	856	693	681	681
2	-94	-44	31	319	482	607	720	920	1258	1445	1495
3	-25	113	88	414	627	689	652	1015	1341	1516	1579
4	31	82	132	420	633	696	872	1047	1398	1524	1612
5	-63	-50	13	75	88	50	75	125	638	1051	1288
6	-50	0	37	37	683	1566	2436	3890	4424	5431	5269
7	-12	37	62	124	757	1563	2432	3809	5149	7345	6849
8	25	62	112	149	808	1728	2562	3867	5135	7510	6938
9	12	-199	87	125	822	1719	2592	4386	5607	7600	6903
10	56	69	81	119	244	294	319	694	1307	2695	3233
11	50	163	175	200	275	325	488	1202	2654	5020	6434
12	44	6	69	181	156	193	356	1167	2852	5273	6471
13	69	81	169	232	257	282	407	758	2586	5104	6720
14	25	125	138	288	113	125	238	600	2501	5890	17432
15	0	38	-13	-25	150	138	326	414	714	1479	11557
16	38	38	113	251	264	289	402	1068	930	1457	11244
17	0	0	100	213	150	225	163	663	1051	2465	15578
18	-81	19	156	169	144	231	343	1205	2679	4265	8049
19	31	93	193	280	318	417	542	1663	2747	4492	8242
20	-69	44	118	181	218	280	492	1115	2410	4790	8265
Gage	South Side CSS - microstrains										
1	136	136	247	346	383	470	630	1113	2225	2905	7145
2	112	124	187	261	349	436	697	1556	2689	3038	7271
3	81	118	131	181	268	405	605	1378	2600	2912	7151
4	81	144	156	206	268	393	631	1143	1929	2179	11595
5	100	175	212	225	324	374	537	1236	1610	1435	7026
6	100	125	175	238	300	338	388	713	988	5603	16535
7	88	163	175	263	276	363	438	-438	1077	5661	16694
8	-19	157	169	107	245	232	433	709	960	5553	10334
9	138	226	289	302	390	452	578	628	616	4914	9991
10	88	126	151	151	239	365	428	566	503	302	428
11	119	107	145	208	233	296	396	522	2685	3188	2710
12	63	101	139	176	202	252	365	479	2759	3250	2797
13	-25	25	51	101	13	164	379	2061	5360	7749	7256
14	32	95	133	196	398	638	1534	3150	6370	8858	8378
15	0	50	101	126	379	593	1553	3131	4242	6148	6931
16	19	95	120	69	410	638	1496	3099	4021	6015	6015
17	82	132	170	522	1151	1830	2774	3013	3038	3277	3353
18	38	88	126	415	869	1284	1511	1775	2090	2014	2115
19	-6	19	57	383	735	1137	1375	1576	1551	1715	1802
20	-31	6	31	295	696	1072	1298	1474	1499	1637	1649

609

S.7 G1C-West

Table S.7 Raw Concrete Surface Strains Data for Development Length Test G1C-West

Step	1	2	3	4	5	6	7	8	9	10	11	12
Load (Kips)	80	110	140	155	184	215	240	261	276	287	295	296

Gage	North Side CSS - microstrains											
1	194	194	231	369	381	469	556	944	1769	2469	2694	3057
2	219	231	294	381	469	569	668	1056	1881	2693	2830	3043
3	219	243	268	368	418	518	581	1130	2042	2966	3153	3515
4	175	188	213	313	388	488	550	713	1013	1500	1600	1688
5	187	175	237	275	362	425	487	700	800	1049	1049	775
6	200	250	275	337	425	500	562	700	875	1450	1662	1700
7	207	207	220	320	383	408	483	533	496	973	1462	1789
8	182	107	220	295	333	358	446	496	496	1036	1965	10894
9	158	208	208	296	372	359	410	485	460	1002	1909	11211
10	138	164	189	277	352	340	440	466	528	617	1208	10532
11	156	194	194	281	394	381	456	506	556	594	844	10110
12	169	169	181	244	356	369	394	444	519	444	431	668
13	149	187	224	336	461	436	498	573	698	2952	5568	6054
14	143	143	118	218	330	368	405	443	555	3087	5967	6553
15	119	106	6	106	231	344	1132	1832	2583	5247	8586	9024
16	138	213	138	175	200	388	1088	1750	2513	5288	8589	9089
17	112	125	100	162	200	412	1062	1711	2410	2897	3547	3622
18	62	50	12	237	537	1048	1809	2533	3369	3594	4218	3968
19	131	268	118	305	605	1004	916	1054	1166	1315	1390	1365
20	175	137	162	362	661	948	1023	1060	1198	1223	1260	1310
Gage	South Side CSS - microstrains											
1	175	137	162	362	661	948	1023	1060	1198	1223	1260	1310
2	113	163	201	451	564	564	640	702	790	890	916	966
3	-6	132	94	445	520	533	596	646	746	871	934	947
4	88	63	75	100	213	963	1463	1976	2601	4940	5403	5390
5	75	62	25	100	674	1411	2047	2697	3296	5730	5630	5543
6	-13	50	75	150	751	1477	2115	2866	3918	6647	8837	9013
7	63	75	50	125	764	1540	2191	2904	3918	6672	9200	9363
8	106	106	144	169	570	695	820	1046	1346	1860	3901	4064
9	75	88	88	151	138	151	201	276	528	678	3467	3731
10	94	94	94	182	106	119	157	182	194	157	232	219
11	157	132	132	207	169	207	320	232	269	583	2137	7726
12	69	107	144	182	82	82	157	157	182	546	2531	8647
13	162	150	162	237	125	299	287	299	274	711	2645	12514
14	113	150	163	238	213	238	238	326	376	802	2869	12704
15	107	94	119	169	157	132	244	169	445	809	1147	5598
16	88	100	138	288	238	263	363	514	752	965	990	4725
17	95	120	158	233	208	221	271	460	662	952	1103	977
18	94	107	132	220	208	208	308	447	673	875	1064	1466
19	176	176	188	251	238	314	402	979	1443	1907	2133	2409
20	138	175	213	301	313	338	464	890	1328	1854	2118	2531

S.8 G2A-East

Table S.8 Raw Concrete Surface Strains Data for Development Length Test G2A-East

Step	1	2	3	4	5	6	7	8	9	10	11	12	13
Load (Kips)	100	151	181	211	244	274	304	334	364	394	425	439	440

Gage	North Side CSS - microstrains												
1	37	62	50	87	286	436	709	896	1058	1244	1356	1356	1419
2	-6	19	106	180	504	603	1114	1425	1785	2022	2408	2706	2793
3	106	119	156	219	493	606	1168	1567	2029	2416	2741	2966	3165
4	94	106	144	94	194	181	869	1394	2282	2920	4282	4995	5508
5	31	94	107	94	182	458	521	772	1374	1863	3093	3808	4222
6	44	94	69	69	119	144	169	356	844	1207	2183	2658	2971
7	50	100	100	150	200	262	250	399	811	1161	2247	2696	3021
8	69	94	106	131	169	219	219	244	319	419	1195	1370	1433
9	150	212	249	312	362	437	449	499	574	649	1272	1609	1659
10	100	125	113	138	225	275	263	288	426	501	1227	1402	1452
11	119	169	157	194	232	282	369	332	419	482	1196	1459	1596
12	106	156	193	243	268	380	405	417	455	442	442	479	579
13	62	62	-25	25	137	149	211	186	236	249	373	448	398
14	43	130	93	143	192	291	291	391	416	1209	1743	1991	2053
15	112	174	161	273	310	372	409	447	509	1278	1762	1985	2035
16	81	106	144	181	219	331	343	381	531	1268	1780	1980	2042
17	81	119	169	207	219	332	370	470	696	2325	3152	3640	3803
18	88	138	163	163	1027	388	426	451	576	1453	1842	2105	2205
19	113	125	150	213	263	363	438	463	789	1716	2204	2580	2642
20	50	137	212	225	312	387	425	425	1161	2510	3471	4045	4158
Gage	South Side CSS - microstrains												
1	119	107	182	195	270	408	571	848	2066	2995	3924	4640	4866
2	31	-44	-94	19	-207	207	508	609	1839	3119	4223	5177	5428
3	19	-44	94	82	56	194	320	458	859	1498	2113	2502	1398
4	63	88	101	176	201	226	452	427	905	2313	3067	3507	3771
5	57	-44	6	-6	145	82	221	271	447	1380	2199	2161	2741
6	76	38	50	189	189	215	290	353	416	1679	2158	2486	2650
7	63	63	63	190	164	291	316	455	544	1758	2277	2517	2795
8	51	13	38	165	241	114	228	329	228	798	1190	1431	1811
9	32	6	183	233	158	271	359	384	435	964	1178	1494	1531
10	-44	19	57	195	183	284	359	460	435	561	1103	1229	1418
11	19	107	44	107	157	220	182	258	345	408	948	1162	1300
12	-6	44	19	270	220	282	220	345	646	571	1073	1486	1650
13	56	19	107	44	69	119	157	257	282	345	1111	1312	1199
14	6	-44	69	81	56	119	94	169	131	181	457	494	444
15	0	-25	-63	50	-38	50	63	125	175	363	1165	1617	1805
16	-6	-31	-56	118	6	-19	-31	31	455	841	1676	2162	2549
17	-112	-12	-50	-37	-25	50	62	37	-274	1159	2442	3052	3426
18	100	162	149	162	336	261	622	796	1120	1692	2986	3683	3882
19	112	62	12	99	236	409	409	682	918	1426	1885	2245	2109
20	-111	-12	-86	86	173	284	432	518	296	790	1086	1345	1370

611

S.9 G2A-West

Table S.9 Raw Concrete Surface Strains Data for Development Length Test G2A-West

Step	1	2	3	4	5	6	7	8	9	10	11	12
Load (Kips)	80	110	140	170	200	230	254	275	288	293	297	297

Gage	North Side CSS - microstrains											
1	19	31	106	156	144	156	406	431	556	668	981	1043
2	125	125	162	237	325	362	462	600	650	737	1149	1249
3	131	169	169	194	306	306	431	518	581	606	1030	1105
4	200	250	300	350	375	275	499	562	475	712	1124	1236
5	163	150	150	200	250	325	363	463	450	475	588	725
6	131	131	169	169	244	319	381	431	431	469	406	494
7	82	82	94	132	182	257	358	332	332	420	420	408
8	88	100	175	175	213	251	389	338	363	389	338	351
9	101	113	113	163	239	251	302	327	339	339	339	365
10	88	75	138	126	214	251	289	289	314	314	302	314
11	81	119	131	144	219	293	256	256	356	293	231	281
12	44	44	81	69	156	156	231	219	244	257	219	369
13	37	50	75	87	187	187	262	249	311	311	311	299
14	25	37	62	100	162	175	225	262	374	424	437	437
15	-31	-56	-94	-19	44	69	106	156	269	406	381	344
16	44	44	81	81	131	144	169	194	319	382	382	382
17	-19	81	56	94	156	156	281	494	644	731	819	806
18	87	137	150	162	374	511	649	786	886	936	936	936
19	-12	125	87	150	312	387	561	699	798	811	798	786
20	25	62	62	112	262	399	511	623	711	773	760	760
Gage	South Side CSS - microstrains											
1	75	63	113	88	163	401	551	639	739	789	764	677
2	94	44	19	94	244	469	469	657	632	807	883	557
3	38	-13	38	0	188	400	526	613	676	763	888	876
4	56	6	81	-156	194	331	543	618	656	843	955	843
5	38	25	63	63	50	138	125	150	125	213	288	225
6	-6	-19	-6	19	6	94	81	119	-44	157	69	94
7	100	63	75	75	50	163	200	88	125	288	225	213
8	38	25	38	50	38	50	88	88	301	175	213	238
9	69	56	94	69	107	119	220	232	182	245	232	245
10	75	13	113	75	75	200	238	263	200	288	276	113
11	38	38	100	63	100	226	251	289	226	339	326	301
12	75	88	176	125	125	289	301	376	226	389	301	263
13	81	81	81	94	132	232	232	257	119	307	282	219
14	94	81	94	94	69	169	244	257	219	345	307	282
15	81	19	131	94	106	244	281	331	244	369	331	269
16	38	38	-13	63	113	-175	301	288	276	338	313	251
17	75	63	125	75	150	263	313	376	464	576	614	539
18	50	50	-251	75	151	276	301	402	402	515	565	528
19	119	107	169	132	207	207	383	458	445	533	621	558
20	82	56	144	107	119	295	345	433	408	533	496	445

S.10 G2B-East

Table S.10 Raw Concrete Surface Strains Data for Development Length Test G2B-East

Step	1	2	3	4	5	6	7	8	9	10	11
Load (Kips)	100	151	184	218	248	278	308	338	369	398	425

Gage	North Side CSS - microstrains										
1	69	94	19	257	507	620	557	683	833	1058	1321
2	25	75	100	237	475	799	1336	1861	2423	2360	2548
3	88	138	113	200	213	338	851	1251	1726	1614	1651
4	19	94	144	131	169	356	868	1268	1880	3403	4477
5	62	125	162	187	175	437	912	1399	2049	3798	5072
6	69	132	144	182	232	257	69	307	546	2478	3707
7	94	144	182	194	232	320	345	320	683	2675	3840
8	81	194	244	207	257	370	357	420	533	946	1247
9	100	163	213	263	313	376	338	364	426	426	539
10	94	131	181	219	306	343	318	368	456	468	581
11	87	150	237	275	350	275	362	412	387	500	587
12	38	75	113	163	250	300	325	325	350	1213	1851
13	69	144	181	256	331	381	381	381	456	1307	1944
14	144	169	219	269	432	445	482	557	595	1384	2110
15	75	113	176	238	313	364	301	401	915	2019	2959
16	225	288	325	413	525	550	600	650	1126	1613	2051
17	138	213	225	263	400	400	413	438	1026	1501	2077
18	162	250	262	337	425	437	462	575	1624	2287	3111
19	119	181	218	306	418	468	530	692	1628	2177	3350
20	200	213	213	301	401	438	451	601	1466	2042	3132
Gage	South Side CSS - microstrains										
1	150	225	287	362	449	499	537	849	1585	2147	2983
2	100	237	250	349	424	449	474	1011	2495	3818	5277
3	200	200	287	300	1000	437	450	537	1700	2450	3274
4	144	194	244	306	319	331	394	444	1481	2181	2843
5	156	231	293	318	356	406	406	480	1603	2202	2876
6	156	181	219	231	331	369	356	344	756	1581	2244
7	243	256	256	343	418	455	356	393	468	1403	1990
8	118	181	218	268	318	330	343	368	442	1377	1975
9	268	293	318	418	393	443	430	492	654	1602	2362
10	143	168	230	280	318	342	355	367	342	504	679
11	87	124	124	211	236	224	211	261	298	410	609
12	218	230	255	305	392	342	305	218	342	753	1275
13	131	231	218	255	305	555	1066	1290	1913	3134	3969
14	206	193	243	281	218	792	805	1241	1815	3137	3948
15	131	144	182	232	244	507	908	1208	2410	2985	3774
16	50	125	125	175	150	438	950	1388	1925	2763	3263
17	94	106	143	181	193	243	305	493	480	355	318
18	93	131	156	181	405	529	-44	815	977	1077	1338
19	138	150	188	413	700	813	888	1126	1288	1388	1688
20	125	88	150	364	690	740	740	740	1041	1254	1505

S.11 G2B-West

Table S.11 Raw Concrete Surface Strains Data for Development Length Test G2B-West

Step	1	2	3	4	5	6	7	8	9	10	11	12
Load (Kips)	100	150	180	210	240	270	300	322	334	341	342	328

Gage	North Side CSS - microstrains											
1	119	207	182	295	333	345	1174	1940	2417	2455	2505	2467
2	75	175	163	288	313	338	1215	1929	2392	2455	2429	2442
3	100	175	213	814	338	276	526	877	1140	1140	1178	1153
4	44	169	219	244	306	331	406	444	444	444	481	481
5	106	144	219	294	307	307	382	470	632	595	520	632
6	119	157	195	258	295	320	408	534	547	559	710	534
7	113	125	176	213	263	238	401	464	665	564	602	514
8	56	119	169	257	370	320	420	495	621	483	508	495
9	138	163	200	288	326	338	376	463	463	413	438	426
10	81	131	94	243	243	268	331	393	443	381	443	406
11	63	163	88	201	226	276	339	364	401	677	690	665
12	94	107	119	119	219	194	194	282	320	1085	1097	1110
13	94	132	132	169	232	232	307	383	408	1186	1161	1211
14	119	144	157	194	219	270	721	1097	1385	2063	2150	2000
15	106	106	106	156	193	306	717	1041	1303	1690	1653	1715
16	125	138	150	163	176	288	1154	1605	1931	1893	1806	1843
17	50	88	75	100	100	663	1402	1815	2065	2090	1977	1990
18	69	106	169	256	431	857	1257	1369	1294	1369	1219	1407
19	81	94	157	307	395	708	1122	1235	1322	1310	1285	1347
20	100	100	162	286	411	760	635	660	635	573	598	585
Gage	South Side CSS - microstrains											
1	50	125	113	301	401	840	966	1204	1442	1279	1204	1267
2	-19	69	56	206	332	594	870	1070	1145	1245	1107	1258
3	-50	-12	12	150	287	574	860	1210	1447	1609	1496	1596
4	31	69	143	168	168	243	643	1029	1254	1366	1341	1404
5	81	181	194	181	181	294	319	519	731	856	819	906
6	181	256	294	306	344	406	469	682	907	1007	1032	1119
7	88	138	138	188	201	226	276	376	439	439	439	464
8	81	106	106	131	194	256	294	356	394	406	381	431
9	31	69	107	144	182	220	295	320	358	295	282	307
10	31	82	94	94	170	207	257	295	345	283	257	295
11	50	213	151	188	251	377	352	339	414	377	377	427
12	101	164	201	214	327	390	466	516	579	730	768	793
13	100	225	250	338	438	476	601	638	1077	1390	1390	1365
14	82	144	119	157	207	245	370	420	746	1160	1160	1160
15	113	225	263	275	413	413	588	588	938	1276	1326	1251
16	87	187	137	237	312	300	312	412	837	1000	987	975
17	-50	50	150	62	212	299	399	998	1222	1272	1235	1247
18	87	236	199	274	398	485	559	957	1405	1417	1430	1442
19	162	249	237	299	336	423	1482	2416	2890	3039	2952	2989
20	149	274	274	348	485	485	1467	2437	2860	2909	2872	2897

614

S.12 G2C-East

Table S.12 Raw Concrete Surface Strains Data for Development Length Test G2C-East

Step	1	2	3	4	5	6	7	8	9	10	11	12
Load (Kips)	100	150	180	210	241	270	300	330	353	364	367	358

Gage	North Side CSS - microstrains											
1	-25	-25	-38	63	75	263	288	326	339	326	313	339
2	12	0	12	50	337	887	1349	1749	1986	2024	1924	1849
3	-63	-75	-13	-25	225	563	1126	1877	2415	2402	2628	2740
4	19	119	131	106	393	780	1342	2079	2778	3302	3814	3851
5	-19	6	44	6	306	744	1357	2044	2794	3257	3870	3957
6	0	75	63	100	75	175	389	677	1191	1629	2356	2381
7	-19	106	507	420	507	457	495	695	1033	1609	1935	2023
8	19	-19	132	31	194	107	370	483	708	871	984	1034
9	-13	100	63	125	175	225	238	438	726	864	989	876
10	56	94	144	156	219	256	306	519	1119	1444	1519	1482
11	-6	-344	-244	-6	31	131	131	331	631	656	781	756
12	-37	112	50	125	187	287	237	625	1112	1387	1399	1474
13	50	100	113	200	263	325	363	688	1138	1425	1538	1525
14	113	113	163	238	338	413	451	689	1077	1340	1528	1528
15	44	144	144	219	282	320	395	746	1585	1936	2087	2036
16	131	156	181	244	307	1020	419	907	1583	1821	2009	1971
17	94	194	169	257	307	432	532	1584	2585	2998	3161	3136
18	25	150	137	262	350	387	487	1425	2312	2650	2687	2675
19	94	194	181	319	419	469	569	1419	1920	2257	2320	2320
20	138	163	200	401	451	576	1352	2691	3267	3543	3693	3618
Gage	South Side CSS - microstrains											
1	212	299	312	362	412	512	711	1772	2895	3406	3681	3805
2	175	200	287	324	337	387	474	1297	2358	2857	3194	3281
3	150	213	288	338	375	450	513	1326	2377	2865	3165	3228
4	144	206	256	294	331	381	444	719	1031	1119	1194	1156
5	150	175	225	275	288	350	438	688	988	1113	1188	1163
6	112	125	200	250	262	325	425	612	887	999	1124	1187
7	175	175	237	300	325	362	462	924	1585	1835	2122	2122
8	131	168	193	255	255	293	330	579	916	1140	1265	1227
9	56	168	193	218	255	330	380	741	1451	1799	1949	1924
10	187	212	249	287	299	349	337	798	1471	1820	1970	1870
11	124	124	137	237	249	249	361	610	921	934	996	1008
12	99	99	124	162	211	211	311	559	821	945	995	982
13	125	149	174	262	249	237	672	1445	2192	2553	2727	2727
14	87	87	100	175	125	437	1673	2784	3708	4232	4606	4631
15	6	44	94	106	106	644	1469	2406	3256	3744	4069	4119
16	94	194	219	256	269	744	1632	2583	3433	3934	4271	4322
17	168	131	131	81	243	792	1154	1366	1466	1616	1803	1753
18	100	124	274	585	710	1145	884	959	1033	909	1145	1083
19	188	225	263	626	714	852	989	1127	1240	1302	1378	1353
20	-50	0	88	364	451	602	727	865	978	1053	1116	1040

S.13 G2C-West

Table S.13 Raw Concrete Surface Strains Data for Development Length Test G2C-West

Step	1	2	3	4	5	6	7	8	9	10
Load (Kips)	100	150	158	188	218	244	262	277	287	291

Gage	North Side CSS - microstrains									
1	157	-220	-144	69	19	94	144	1186	1838	1788
2	25	63	50	188	238	326	388	1504	2055	2018
3	81	94	219	244	307	395	395	1046	1410	1798
4	38	100	213	250	313	401	401	488	501	914
5	82	107	320	157	245	282	270	408	445	821
6	44	132	-44	82	182	257	195	282	395	697
7	-113	25	-25	50	125	163	301	326	376	313
8	13	100	125	75	251	238	188	225	463	576
9	0	75	38	163	150	275	150	225	350	275
10	25	125	187	237	299	299	312	412	449	462
11	-157	-69	-19	-56	6	-220	-82	31	220	94
12	628	703	653	778	828	916	929	941	954	1105
13	-38	163	489	188	339	238	389	301	564	502
14	-295	56	56	69	94	144	784	1097	846	1022
15	31	156	119	256	293	331	879	1254	1541	1690
16	-501	-38	-238	-50	125	225	476	914	1215	1352
17	-401	-263	-213	-226	150	-25	150	677	777	902
18	6	69	19	294	369	620	507	1058	1221	1334
19	-6	-31	-119	294	382	607	282	545	532	557
20	212	-12	-149	324	448	660	436	511	398	374
Gage	South Side CSS - microstrains									
1	44	44	56	257	433	596	496	534	559	571
2	75	25	75	275	463	613	525	550	538	563
3	69	81	94	330	518	692	667	705	692	667
4	13	-25	25	125	50	125	963	1263	1363	1413
5	56	44	56	94	144	206	1155	1455	1630	1792
6	31	44	56	94	119	132	1134	1523	1836	2024
7	38	63	75	113	138	188	1089	1453	1778	2004
8	75	87	87	100	162	225	275	362	550	675
9	31	69	56	94	132	169	194	220	358	470
10	50	75	125	151	163	238	238	238	326	339
11	50	63	63	113	138	201	213	201	264	289
12	101	38	88	227	227	252	365	328	403	416
13	-6	19	19	131	94	169	206	194	307	307
14	44	69	69	144	169	219	269	257	307	219
15	38	100	113	200	263	313	388	413	550	900
16	19	19	19	69	156	206	281	319	419	743
17	87	112	125	150	225	249	324	387	499	836
18	75	124	112	149	199	249	261	286	460	236
19	62	75	137	174	162	249	299	1331	1941	2103
20	62	112	149	199	211	273	336	1293	1926	2138

VITA

Lieutenant Colonel (LTC) Karl F. Meyer was born in San Diego, California on January 14, 1962. In 1984 he received a Bachelor of Science degree from the U.S. Military Academy at West Point and was commissioned a Second Lieutenant in the United States Army. He served as a platoon leader, company executive officer and battalion civil engineer in the 864th Engineer Battalion at Fort Lewis, Washington. While serving as a company commander in the 92nd Engineer Battalion at Fort Stewart, Georgia, LTC Meyer was deployed to the Persian Gulf region for Operations Desert Shield and Desert Storm where he was awarded the Bronze Star Medal. In 1993, he earned a Master of Science degree in Civil Engineering from the Georgia Institute of Technology. From 1993 through 1996, he served as an instructor and assistant professor in the Department of Civil and Mechanical Engineering at the U.S. Military Academy. In 1997, LTC Meyer graduated from the U.S. Army Command and General Staff College and was assigned to the 130th Engineer Brigade in Hanau, Germany where he served as the Brigade Executive Officer and Brigade S-3. In 1999, LTC Meyer was selected to be a permanent faculty member in the Department of Civil and Mechanical Engineering at the U.S. Military Academy and returned to the Georgia Institute of Technology to pursue a Doctor of Philosophy degree in civil engineering. LTC Meyer was awarded a Doctor of Philosophy in Civil Engineering in 2002. LTC Meyer holds a Professional Engineer license in the state of Virginia. He is married to the former Robin Carlene Heath of Stone Mountain, Georgia and has two children, Abigail and John.